

**A Thesis Submitted for the Degree of PhD at the University of Warwick**

**Permanent WRAP URL:**

<http://wrap.warwick.ac.uk/146803>

**Copyright and reuse:**

This thesis is made available online and is protected by original copyright.

Please scroll down to view the document itself.

Please refer to the repository record for this item for information to help you to cite it.

Our policy information is available from the repository home page.

For more information, please contact the WRAP Team at: [wrap@warwick.ac.uk](mailto:wrap@warwick.ac.uk)

**Rhodium and iridium phosphine complexes:**  
Approaches for studying the coordination chemistry  
of weakly interacting substrates

---

**Jack Emerson-King**

A thesis submitted in partial fulfilment of the requirements for the degree of  
Doctor of Philosophy in Chemistry

University of Warwick, Department of Chemistry

September 2019



## Table of contents

---

<i>Table of contents</i>	i
<i>Acknowledgements</i>	vi
<i>Declaration of collaborative and published work</i>	viii
<i>List of abbreviations</i>	ix
<i>Abstract</i>	x
 <i>Chapter 1: Introduction</i>	
1.1 Weak metal-substrate interactions	1
1.1.1 Motivation and scope	1
1.1.2 Energetic considerations	1
1.2 Coordination chemistry of alkanes	2
1.2.1 Bonding profile	2
1.2.2 Intramolecular M-H-C interactions	4
1.2.3 Alkane complexes by photolysis	6
1.2.4 Alkane complexes by protonation	11
1.2.5 Observations of alkane complexes in the solid state	12
1.2.6 Synthesis of alkane complexes in the solid state	13
1.3 Coordination chemistry of fluoroalkanes	13
1.3.1 Context and bonding profile	16
1.3.2 Crystallographically characterised examples	17
1.4 Dinitrogen complexes of late transition metals	19
1.4.1 Context and bonding profile	19
1.4.2 Crystallographically characterised examples	20
1.5 Coordination chemistry of noble gas elements	23
1.5.1 Characterisation in situ	23
1.5.2 Isolable complexes	25
1.6 Project aims	27



## ***Chapter 2: Rhodium and iridium 2,2'-biphenyl complexes***

2.1	The 2,2-biphenyl ligand	30
2.1.1	Properties and metallation	30
2.1.2	Reactivity	31
2.2	Intramolecular M-H-C interactions	33
2.2.1	Preamble	33
2.2.2	Synthesis of low-coordinate complexes	34
2.2.3	Solid state characterisation	35
2.2.4	Solution characterisation	41
2.2.5	Computational investigations	42
2.3	Intramolecular Rh-F-C interactions	45
2.3.1	Preamble	45
2.3.2	Preparation	45
2.3.3	Solid-state characterisation	46
2.3.4	Solution characterisation	48
2.4	Intermolecular reactivity	51
2.4.1	Preamble	51
2.4.2	Small molecule and solvent adducts	51
2.4.3	Hydrogenolysis of the 2,2'-biphenyl ligand	56
2.4.4	Carbonylation of the 2,2'-biphenyl ligand	57
2.4.5	Reactions with solvent	59
2.4.6	Substitution of phosphine	61
2.4.7	An unexpected result	63
2.5	Conclusions and future work	65

## ***Chapter 3: Complexes of a calixarene-based diphosphine***

3.1	Complexes of calixarene-based ligands	67
3.1.1	Host-guest complexes	67
3.1.2	Calixarenes	67
3.1.3	Calixarenes as ligands	68
3.1.4	Complexes of phosphine functionalised calixarenes	69
3.2	CxP <sub>2</sub>	72
3.2.1	Ligand synthesis	72

3.2.2	Complexes of simple cations	73
3.3	Synthesis of rhodium and iridium complexes of CxP <sub>2</sub>	77
3.3.1	Chloride complexes	77
3.3.2	Halide abstraction	79
3.3.3	The water complex	81
3.3.4	Solution dynamics	83
3.3.5	Synthesis via substitution	86
3.4	Ligand exchange reactions	89
3.4.1	Lability of the water ligand	89
3.4.2	Zirconocene reactions in dichloromethane	90
3.4.3	Zirconocene reactions in fluorobenzene	93
3.4.4	Returning to sieves	95
3.5	Preparation of water-free calixarene complexes	97
3.5.1	Practical considerations	97
3.5.2	The dihydrogen complex	98
3.5.3	The dichloromethane complex	100
3.5.4	The low-coordinate complex	101
3.5.5	The dinitrogen complex	102
3.6	Conclusions and future work	104

#### *Chapter 4: Rhodium and iridium 2,2'-bipyridyl complexes*

4.1	Complexes of 2,2'-bipyridyl	106
4.1.1	Preparation of dihydride salts	106
4.1.2	Comparison of structural metrics	107
4.2	Mechanistic investigations	109
4.2.1	Overall reaction profile	109
4.2.2	Hydrogenation reactions	109
4.2.3	Substitution reactions	112
4.2.4	Reactions of alternative precursors	114
4.2.5	Summary of mechanistic findings	114
4.3	Other reactivity of 2,2'-bipyridyl complexes	116
4.3.1	Dehydrogenation chemistry	116
4.3.2	Oxidative addition chemistry	116

4.3.3	Phosphine lability	118
4.4	Attempted preparation of a CxP <sub>2</sub> complex of 2,2'-bipyridyl	118
4.4.1	Attempted syntheses from 2,2'-bipyridyl precursors	118
4.4.2	Attempted syntheses from other precursors	120
4.5	Conclusions and future work	121

### ***Chapter 5: Complexes of a resorcinarene-based diphosphine***

5.1	Resorcinarenes as hosts and ligands	123
5.1.1	Preparation and properties	123
5.1.2	Walled resorcinarenes as alkane hosts	123
5.1.3	Tris-walled resorcinarenes	124
5.2	RcPOP	125
5.2.1	Ligand synthesis	125
5.3	Alkene complexes	127
5.3.1	Preparation	127
5.3.2	Solution characterisation	128
5.3.3	Solid state characterisation	129
5.4	Solution phase reactivity	132
5.4.1	Lability of alkene	132
5.4.2	Hydrogenation in dichloromethane and mesitylene	133
5.4.3	Hydrogenation in fluoroarenes	135
5.4.4	Hydrogenation in MTBE	138
5.5	Solid state reactivity	140
5.5.1	Approaching an alkane complex	140
5.6	Conclusions and future work	142

### ***Chapter 6: Experimental details***

6.1	General considerations	143
6.1.1	Practices	143
6.1.2	Solvents	143
6.1.3	Reagents	144
6.1.4	NMR spectroscopy	144
6.1.5	Other analyses	146

6.2	Biphenyl monophosphine systems	146
6.2.1	Preparation of metal biphenyl precursors	146
6.2.2	Preparation of $[M(2,2'\text{-biphenyl})(PR_3)_2Cl]$	148
6.2.3	Preparation of $[M(2,2'\text{-biphenyl})(PR_3)_2][\text{anion}]$	153
6.2.4	Preparation of $[M(2,2'\text{-biphenyl})(PPh_2Tol^F)_2(L)]$	159
6.2.5	Preparation of other triphenylphosphine complexes	165
6.2.6	Reactions of triphenylphosphine systems	172
6.3	CxP <sub>2</sub>	175
6.3.1	Ligand synthesis	175
6.3.2	Preparation of $M[CxP_2][\text{anion}]$	181
6.3.3	Preparation of dimeric CxP <sub>2</sub> complexes	186
6.3.4	Substitution reactions	188
6.3.5	Preparation of monomeric CxP <sub>2</sub> complexes	189
6.3.6	Ligand exchange reactions	198
6.4	Bipyridyl systems	199
6.4.1	Preparation of 2,2'-bipyridyl complexes	199
6.4.2	Mechanism probing reactions	208
6.4.3	Dehydrogenation reactions	211
6.4.4	Oxidative addition reactions	212
6.4.5	Substitution reactions	213
6.5	RcPOP	214
6.5.1	Ligand Synthesis	214
6.5.2	Preparation of $[Rh(\text{alkene})(RcPOP)][\text{anion}]$	219
6.5.3	Preparation of other RcPOP complexes	230
	<i>References</i>	235
	<i>Index of compounds</i>	253

## Acknowledgments

---

Huge thanks to Adrian for the diligent supervision, and for the significant personal, professional, and practical advice bestowed these past four years. Thanks for all the tasteful side projects, as well as putting up with my inability to not leave things till the last minute, and for all the help in proofing and fact checking in an outrageously prompt manner. I am really incredibly grateful.

Tremendous thanks to the former members of the Chaplin group, to Thibault, Lucero, Ruth, Rhiann and Rich collectively; for dealing with the totally inexperienced, fully feckless first year I was. You're all excellent humans who made me feel entirely welcome. Your guidance in chemistry and in life was invaluable and unforgettable. Though slightly more effective communication regarding meatballs wouldn't have gone amiss.

To Caroline, best PhD sibling ever, it was the best and worst of times and there's no one I'd rather have had to go through all that with. Naturally this is the very last thing I'm writing but I'm sure you'll understand the brevity. Words are hard. #inseparable.

Thanks CDMG for helping to start the most successful of Jack ideas; morning coffee. Also for showing me how to do proper organometallic chemistry, and not charging interest on overdue neutral currency wagers. Shockingly, I never learnt my lesson. Merci Baptiste for the amusement, and for those scrumptious... whatever they were. I feel more enriched as a human for having met you, both from the sugary goodness, and from being able to say mille-feeeuuuillle properly. Tom, Gemma, you were fine.

That was a joke, obviously, cheers for the company. Appreciations to Thomas for educating me on the price of Tanqueray, and to Gemma for the delicious, delicious quiche. They're great quiche. The best quiche. There are a lot of food related things in this aren't there? Scooting over to the rest of the group, Thursday coffee was always the highlight of the week, the company was always appreciated. Especially appreciated was New Matt's recently discovered talent for being able to tell jokes. Most amusing.

Good luck to Jennifer for the future resorcinarene adventures. Good luck to Sam in all your future endeavours too, and thanks for being a delight to have around this last year, for the probing questions and the grounded outlook; a pillar of stability amongst the chaos. Big thanks to Amy for just existing; I've never known anyone who works so hard on so many different things, your enthusiasm is infectious, and any research group should count itself lucky for having you in it.

Cheers to the Shipmen for the accommodation. Always fianchetto. Thanks to Ivan for all the words of wisdom, and patience in indulging excessive instrument times. Though apologies for the 600 breaking literally every time I touched it. Many appreciations to Steve for putting up with years of OPeRA debacles, to Rob for a common-sense approach to health and safety that made life so much easier, and all the rest of the people around the department who I never really got to know properly but were always happy to help and always had a smile on.

Of course, I wouldn't be here today without my dear friend, the sauce. No, not sweet chilli, though that's great too. Many appreciations to sambuca for the dramatic life choices, to finest reserve port for when you need to lose an hour, and to whatever drink it was that convinced me Hearsall common was flat, featureless, and entirely devoid of any ditch-like structure.

To all the non-chemists I've had the pleasure to meet along the way, thanks for being delightful. Cheers especially to the minty crowd, mostly for the mom's spaghetti incident of '16, and related antics. And to Roxanne and Katja for being the glowing rays of optimism you always are. Lastly, for putting up with me being a full mess and intolerably absent, and for being there for me the times I needed you the most, thanks Bean, I'll always appreciate it.

## Declaration of collaborative and published work

---

This thesis is submitted to the University of Warwick in support of my application for the degree of Doctor of Philosophy. It has been composed by myself and has not been submitted in any previous application for any degree. The work presented (including data generated and data analysis) was carried out by the author except in the cases outlined below:

- Dr Adrian B. Chaplin, Associate Professor, University of Warwick, conducted the crystallographic analysis of all compounds for which structures are described and performed the pseudo-Eyring analysis described in **Chapter 2, Section 3**.
- Dr Richard C. Knighton, Post-Doctoral Research Assistant, University of Warwick, prepared compounds **8, 9, 10, 17, 18, 19** and **20**, and collected the variable-temperature NMR data presented in **Chapter 2, Section 2**.
- Dr Jon P. Rourke, Reader, University of Warwick, collected the low-temperature NOE NMR data presented in **Chapter 2, Section 2**.
- Dr C. André Ohlin, Associate Professor, University of Umeå, performed the computational work presented in **Chapter 2, Section 2**.
- Dr Ivan Prokes, Senior NMR Technician, University of Warwick, collected the variable-temperature NMR data presented in **Chapter 2, Section 3**.
- Dr Matthew R. Gyton, Post-Doctoral Research Assistant, University of Warwick, collected the low-temperature NMR data presented in **Chapter 4**.
- Amy Kynman, MSc Student, University of Warwick, prepared compound **85**.

*Parts of this thesis have been published by the author:*

1. R. C. Knighton, J. Emerson-King, J. P. Rourke, C. A. Ohlin, and A. B. Chaplin, *Chem. Eur. J.*, 2018, **24**, 4927–4938.
2. J. Emerson-King, I. Prokes, and A. B. Chaplin, *Chem. Eur. J.*, 2019, **25**, 6317–6319.
3. J. Emerson-King, R. C. Knighton, M. R. Gyton, and A. B. Chaplin, *Dalton Trans.*, 2017, **46**, 11645–11655.

## List of abbreviations

---

acac	acetyl acetonato
COA	cyclooctane
COD	<i>cis,cis</i> -1,5-cyclooctadiene
COE	<i>cis</i> -cyclooctene
Ar <sup>F</sup>	3,5-bis(trifluoromethyl)phenyl
dtbpm	bis(di- <i>tert</i> -butyl)phosphanylmethane
fwhm	full-width at half-maximum
MTBE	methyl- <i>tert</i> -butylether
NBA	norbornane; bicyclo[2.2.1]heptane
NBD	norbornadiene; 2,5-bicyclo[2.2.1]heptadiene
NBO	natural bond orbital
QTAIM	quantum theory of atoms in molecules
R <sup>F</sup>	perfluoro- <i>tert</i> -butyl
TBE	<i>tert</i> -butyl-ethylene
Tol <sup>F</sup>	2-(trifluoromethyl)phenyl



## Abstract

---

This thesis documents the development of new synthetic approaches for the study of rhodium and iridium complexes featuring ligands that would be typically be considered weakly interacting at these metal centres; alkanes, fluoroalkanes, dinitrogen and xenon.

The coordination chemistry of complexes of the 2,2'-biphenyl ligand is explored first; the favourable donor properties of this ligand are exploited to prepare a range of well-defined derivatives featuring intramolecular M-H-C and M-F-C interactions. From this set, the solution phase reactivity of the complex  $[\text{Rh}(2,2'\text{-biphenyl})(\text{PPh}_3)_2]^+$  is investigated further, encompassing the isolation of solvent adducts, the hydrogenolysis and carbonylation of the 2,2'-biphenyl ligand, and the phosphine substitution chemistry.

Subsequently, procedures for enabling the synthesis of mononuclear complexes of the form  $[\text{Rh}(2,2'\text{-biphenyl})(\text{CxP}_2)\text{L}]^+$ , where  $\text{CxP}_2$  is a calix[4]arene-based *trans*-spanning diphosphine ligand, and where L is one of water, dihydrogen, dinitrogen, silver chloride, and dichloromethane are presented. Evidence for formation of a low coordinate species stabilised by interactions from fluorobenzene solvent is also discussed.

The synthesis of rhodium and iridium phosphine complexes using 2,2'-bipyridyl as a structurally similar ancillary ligand to 2,2'-biphenyl is then described. Mononuclear complexes of  $\text{CxP}_2$  were not formed under the conditions employed, however these studies provided useful mechanistic insights into the formation of dihydride complexes of the form  $[\text{M}(2,2\text{-bipyridyl})(\text{H})_2(\text{PPh}_3)_2]^+$ .

Finally, the preparation of a *cis*-chelating resorcinarene-based diphosphine ligand that enables complete incorporation of  $\{\text{M}(\text{diene})\}^+$  fragments within the interior of the cavity defined by the ligand scaffold is detailed. These complexes serve as precursors for the preparation of complexes featuring coordinated mesitylene, fluoroarenes, MTBE of alkane  $\sigma$ -complexes. The available solution and solid-state characterisation data are discussed, and the potential future utility of this ligand design are expanded upon.

# 1 Introduction

---

## 1.1 Weak metal-substrate interactions

### 1.1.1 Motivation and scope

Weak metal-substrate interactions underpin various pursuits of contemporary coordination chemistry, either by acting as stabilising influences on reactive metal fragments that enact challenging chemical transformations, or as direct intermediates in such transformations. A prototypical case is the interaction of a C-H bond with a late-transition metal; through intramolecular coordination – the so-called agostic interaction – the stabilisation of unsaturated metal centres is achieved, while the formation of intra- and intermolecular C-H adducts are recognised as critical intermediates in C-H bond cleavage reactions. In such contexts, a greater understanding of the structure of the pertinent interaction may inform the design of systems capable of ever more effective and selective transformations. The desire therefore arises to develop systems featuring adducts of weakly-coordinating substrates to an extent that are sufficiently stable that they may be interrogated by a range of analytical techniques, which in concert build a detailed understanding of the character of the interaction. This endeavour, by its nature, has further relevance in expanding the current scope of coordination chemistry to increasingly inert substrates; such as the noble gas elements.

### 1.1.2 Energetic considerations

A generalised reaction manifold, Figure 1.1, highlights the salient thermodynamic and kinetic issues associated with the isolation of complexes featuring weakly interacting substrates. Here the target complex of some hypothetical substrate ‘X<sub>2</sub>’, is taken to exist on a potential energy surface with low kinetic barriers to both substrate dissociation (**a**) and to some onward reaction (**b**) that results in a thermodynamically driven chemical transformation of the substrate (**c**). The transient unsaturated complex

[M] is also susceptible to the competing coordination (**d**) of a superior donor group, ‘Z’, which in solution may include the solvent itself, any counter-ion present, or a component of the supporting ligand periphery. The classical approaches to circumventing these issues tend to involve working at a low-temperature regime to kinetically trap the target system. Simultaneously, the design of the steric environment provided by supporting ligands, or otherwise, may serve to increase these kinetic barriers, exclude competitive donors, or offer supplementary stabilising interactions with the substrate. Moreover, the combination of the supporting ligand donor properties, the choice of metal, its oxidation state, and the overall charge imbued upon the system, serve to tune the electronics to stabilise the desired interaction.

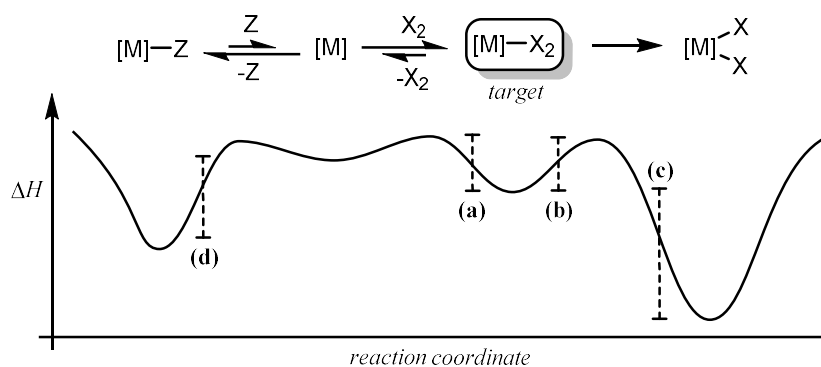


**Figure 1.1** Generalised reaction manifold involving a complex with a weakly interacting substrate of interest ( $X_2$ ) in solution, highlighting the pertinent energetic challenges (*see text*).

## 1.2 Coordination chemistry of alkanes

### 1.2.1 Bonding profile

Two primary modes are available by which the non-polar, poorly nucleophilic C-H bond may interact with a transition-metal centre, Figure 1.2. The archetypal  $\sigma$ -complex is composed of a three-centre-two-electron interaction comprising donation of the electron density of an intact C-H  $\sigma$ -bond to an unoccupied metal d-orbital, augmented by retro-donation from a filled metal d-orbital to the antibonding C-H  $\sigma^*$  orbital. Bonding of this sort is intermediate to concerted C-H oxidative addition,  $\sigma$ -complex assisted

metathesis, and electrophilic substitution processes.<sup>1-8</sup> A further differentiation may be made between an  $\eta^1$  and  $\eta^2$   $\sigma$ -complex,<sup>4</sup> an end-on or side-on interaction respectively, conforming to differing locality along the C-H activation trajectory.<sup>9</sup> An alternative bonding situation is described by the electrostatic interaction of a lone pair of electrons from a filled metal d-orbital to the hydrogen atom; a hydrogen bond. This arrangement allows for yet greater linearity in the M-H-C bond, and is anticipated at low oxidation state late-transition metals where there is a filled high-lying d-orbital, as is the case for square planar  $d^8$  complexes for example. In addition to orbital considerations, the overall metal-hydrocarbon interaction is supplemented by dispersive, and other electrostatic contributions. Indeed recent computational studies have indicated that the majority of the thermodynamic stability of M-H-C  $\sigma$ -complexes derives from dispersion.<sup>10,11</sup>

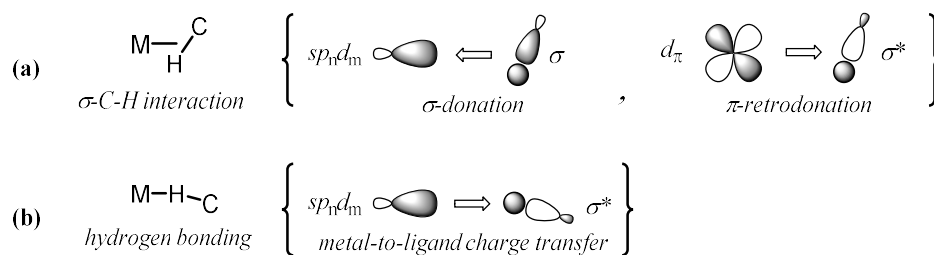


**Figure 1.2** Electronic description of two possible M-H-C interactions.

The  $\sigma$ -interaction and the hydrogen bond may be distinguished in solution through NMR spectroscopy by a downfield shift in the  $^1\text{H}$  resonance for a hydrogen bonding interaction, whereas a  $\sigma$ -complex  $^1\text{H}$  and  $^{13}\text{C}$  resonances are upfield relative to the free C-H bond. Additionally, with the  $\sigma$ -complex a significant increase in the C-H bond length is also apparent, inferred through a corresponding reduction of the  $^1J_{\text{CH}}$  coupling constant by NMR spectroscopy, a red-shifted C-H stretch in the IR spectrum, or observed directly in the solid state by neutron diffraction. By X-ray diffraction the two bonding modes may to some extent be differentiated by their respective coordination geometries, however there can be significant overlap in the ranges of bonding metrics for the two interactions. The most prevalent depositions of M-H-C interactions in the chemical literature come courtesy of tethering the C-H bond to the metal. Such

intramolecular systems are thus relatively convenient models for the scarcer, but arguably more intriguing, intermolecular  $\sigma$ -complexes.

### 1.2.2 Intramolecular M-H-C interactions

The intramolecular manifestations of M-H-C  $\sigma$ -interactions and hydrogen bonding are respectively termed the agostic and anagostic interaction.<sup>12</sup> The former are typically characterised by M-H contacts of 1.8 – 2.3 Å and M-H-C angles between 90° and 140°. The latter, meanwhile, tend to possess M-H contacts of 2.3 – 2.9 Å and M-H-C angles between 110° and 170°. For the relevance to concerted C-H bond activation reactions, the  $\sigma$ -bond interaction tends to be the more coveted of the two.

Complexes at Rh(I) and Ir(I) centres featuring agostic interactions are relatively rare, with some crystallographically characterised examples illustrated in Figure 1.3. Rhodium neopentyl complex **A1** possesses a  $\gamma$ -agostic with a Rh-C contact of 2.491(4) Å,<sup>13</sup> while the  $\beta$ -agostic of cationic tris(tri-*iso*-propylphosphine) **A2** is not significantly different at 2.494(12) Å.<sup>14</sup> A slightly closer approach is seen at propene complex **A3**, which is likely a consequence of the differing coordination geometry imposed by the alkene tethering group, as compared to the phosphine of **A2** for example. Iridium pincer complex **A4** brandishes a close  $\delta$ -agostic interaction of 2.394(5) Å.<sup>15</sup> Far lengthier contacts are observed with conformationally rigid ligands, as in the case of the double  $\delta$ -agostic interactions present in complex **A5**, bearing a sterically demanding cyclic alkyl amino carbene ligand, with Rh-C separations of 2.9306(13) and 3.0083(15) Å.<sup>16</sup> In solution, **A5** possesses a diagnostic upfield <sup>1</sup>H NMR resonance at  $\delta_{\text{H}}$  0.08 at 298 K.

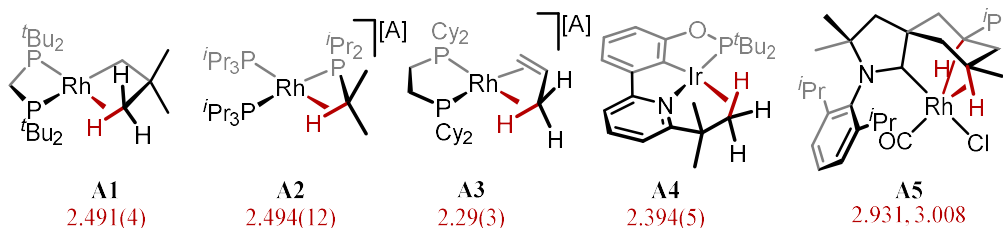


**Figure 1.3** Crystallographically characterised agostic interactions with Rh(I) and Ir(I) centres. Closest M-C contacts (Å) annotated. [A] = [BARF<sub>4</sub>].

Examples of agostic interactions at Rh(III) and Ir(III) centres are given in Figure 1.4, focussing on compounds which belong to structurally analogous series. All M-C contacts are found to be longer than those found with the T-shaped M(I) species just described, with the closest contacts belonging to metallocarborane complexes **A6** – **A9**,<sup>17–19</sup> varying from 2.515(3) Å in rhodium allyl complex **A6** to 2.313(4) Å for iridium complex **A9**. The series of Binor complexes **A10** – **A15** are notable in their own right as isolated intramolecular C-C  $\sigma$ -complexes,<sup>20</sup> which they possess in conjunction to alkyl phosphine  $\gamma$ -agostic interactions in the range 2.91 – 3.34 Å.<sup>21–24</sup> Bis(carbene) complexes **A16** – **A23** differ in the numbers of cyclometallated substituents.<sup>25–28</sup> Of the doubly cyclometallated **A16** – **A19**, only iridium chloride **A18** demonstrates a close M-C contact at 2.785 Å, which on halide abstraction to the cationic derivative is surprisingly elongated to 3.35 Å. Singly cyclometallated **A20** and **A21**, with their less restrained ligand environments, exhibit shorter contacts that are, within error, identical for both metal centres at 2.70 Å. The closest approach of all the carbenic systems is found with iridium dihydride **A23** at 2.653 Å, the phosphine analogues of which, **A24** – **A26**, all possess M-C distances that are seemingly independent of ligand framework at *ca.* 2.81 Å.<sup>29–31</sup>

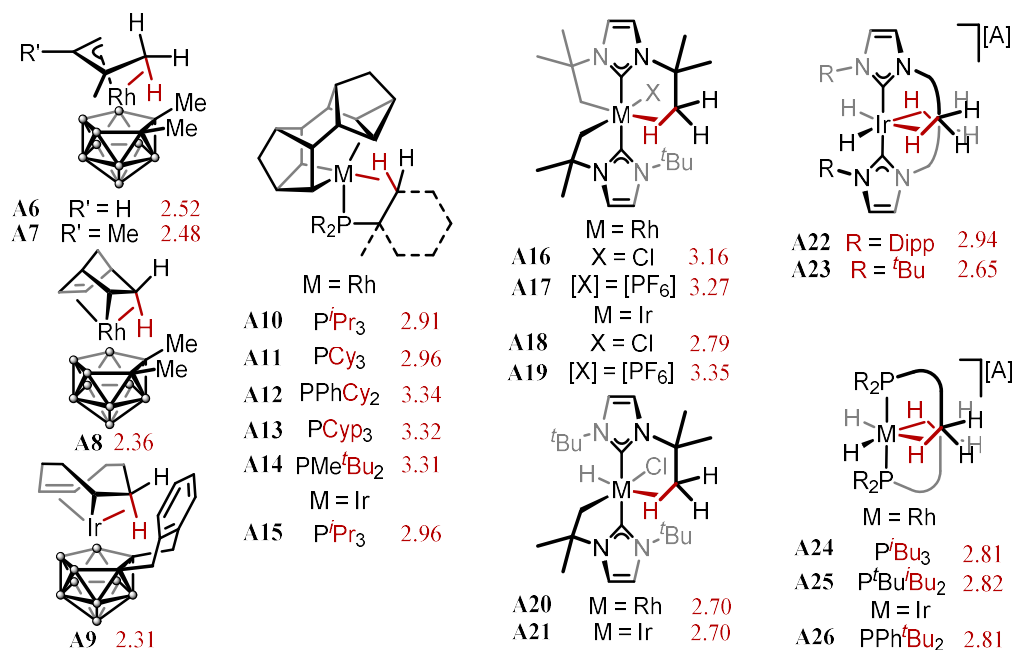
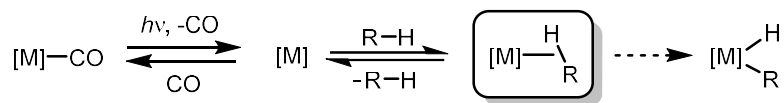


**Figure 1.4** Crystallographically characterised agostic interactions at Rh(III) and Ir(III) centres. Closest M-C contacts (Å) annotated. Grey spheres = BH; Complex **A22**: [A] = [PF<sub>6</sub>]; **A23** – **A26** [A] = [BARF<sub>4</sub>].

Aside from those just described, few late-transition metal agostic complexes belong to wider series that are structurally and electronically congruent. This makes extracting tangible information about the agostic interaction per se, challenging, as observations must be delineated across ligand bulk, flexibility of the ligating alkyl group, and other nuanced effects. A notable common feature of complexes **A10** – **A26** is the incorporation of strong *trans*-influencing ligands across the metal centre from the agostic interaction.

### 1.2.3 Alkane complexes by photolysis

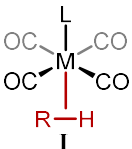
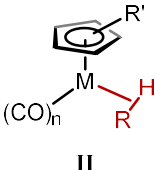
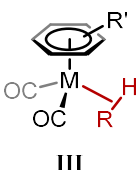
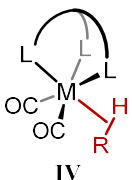
The first examples of intermolecular  $\sigma$ -complexes of alkanes were identified following the photolysis of metal carbonyl compounds in solid alkane matrices,<sup>32–36</sup> and in cyclohexane solution,<sup>37–39</sup> through observations of key shifts in the IR, visible and UV spectra of these complexes. The unsaturated complexes generated on CO photoejection endure for *ca.* 250 fs, prior to coordination of alkane, Figure 1.5.<sup>40</sup> The assignment of an alkane complex was first proposed by Perutz and Turner in 1975 during their work on the photolysis of the Group 6 hexacarbonyls.<sup>41</sup> Subsequent research, most notably involving the application of laser flash photolysis and ultra-fast time-resolved IR spectroscopy, with resolution down to the femtosecond, has enabled the elucidation of many metal alkane adducts and allowed for the quantification of the kinetic and thermodynamic behaviour of the M-H-C interaction, which are collated in Table 1.1.



**Figure 1.5** General synthesis of alkane  $\sigma$ -complexes by photolysis of metal carbonyl compounds. Loss of alkane  $\sigma$ -complex by recoordination of CO or onward reaction shown.

In general, and comparing within the same study (see Table 1.1 notes for a commentary on errors), higher dissociation enthalpies and slower decomposition kinetics correspond to the use of higher molecular weight alkanes, with cyclic alkanes tending to show improved stabilities over their linear counterparts. Across the transition series, stabilities consistently increase moving along a period or down a group.

**Table 1.1** Thermodynamic and kinetic data for alkane  $\sigma$ -complexes generated by CO photolysis

<div style="display: flex; justify-content: space-around; align-items: center;"> <div style="text-align: center;">  <p>I</p> </div> <div style="text-align: center;">  <p>II</p> </div> <div style="text-align: center;">  <p>III</p> </div> <div style="text-align: center;">  <p>IV</p> </div> </div>								
	M	L	alkane	$T / \text{K}$	$k_1^a$	$k_2^b$	BDE <sup>c</sup>	Ref
I	Cr	CO	methane	298 <sup>d</sup>	-	$7.8 \times 10^6$	30±2	42
		CO	pentane	-	-	-	37±13	43
		CO	heptane	298	$5.0 \times 10^3$	-	40±10	43-45
		CO	:	-	-	-	57±4	46
		CO	:	298	-	$9.3 \times 10^6$	21±2	47
		CO	decane	298	-	$1.2 \times 10^7$	23±2	47
		CO	dodecane	298	-	$2.4 \times 10^7$	24±2	47
		CO	<i>iso</i> -octane	-	-	-	46±9	43
		CO	cyclohexane	-	-	-	53±9	43
		CO	:	298	-	$2.3 \times 10^6$	22±2	47
		CO	MeCy	298	-	$3.5 \times 10^6$	24±2	47
	Mo	CO	heptane	-	-	-	37±11	43-46
		CO	:	-	-	-	64±4	46
		CO	:	298	-	$7.8 \times 10^6$	21±2	47
		CO	decane	298	-	$8.8 \times 10^6$	21±2	47
		CO	cyclohexane	298	-	$4.7 \times 10^6$	21±2	47
	W	CO	heptane	298	$6.7 \times 10^2$	$7.5 \times 10^5$	56±12	43,44
		CO	:	298	$1.0 \times 10^4$	-	-	48
		CO	:	298	-	$1.8 \times 10^6$	20±2	47
		CO	decane	298	-	$1.1 \times 10^6$	21±2	47
		CO	cyclohexane	298	-	$5.0 \times 10^5$	23±2	47
		CO	ethane <sup>e</sup>	-	-	-	31±8	49,50
		CO	propane <sup>e</sup>	-	-	-	34±8	50
		CO	butane <sup>e</sup>	-	-	-	38±13	50
		CO	pentane <sup>e</sup>	-	-	-	44±13	50
		CO	hexane <sup>e</sup>	-	-	-	45±13	50
		CO	<i>iso</i> -butane <sup>e</sup>	-	-	-	36±8	50
		CO	cyclopropane <sup>e</sup>	-	-	-	37±8	50
		CO	cyclopentane <sup>e</sup>	-	-	-	43±13	50
		CO	cyclohexane <sup>e</sup>	-	-	-	49±13	50
		PPh <sub>3</sub>	heptane	298	$1.4 \times 10^5$ <sup>f</sup>	-	-	48
		PPh <sub>3</sub>	:	298	$3.5 \times 10^4$	-	-	48
		P(O <sup>i</sup> Pr) <sub>3</sub>	heptane	298	$1.2 \times 10^5$ <sup>f</sup>	-	-	48
		P(O <sup>i</sup> Pr) <sub>3</sub>	:	298	$2.0 \times 10^4$	-	-	48
		P(OEt) <sub>3</sub>	heptane	298	$8.6 \times 10^4$ <sup>f</sup>	-	-	48
		P(OEt) <sub>3</sub>	:	298	$1.2 \times 10^4$	-	-	48
		dfepe <sup>g</sup>	hexane	298	$8.2 \times 10^5$	-	-	51
		dfepe <sup>g</sup>	cyclohexane	298	$3.5 \times 10^5$	-	-	51
	Mn	Me	cyclohexane	298	-	$2.2 \times 10^6$	-	52

*Continued overleaf*



	M	R' <sub>5</sub>	alkane	T / K	k <sub>1</sub> <sup>a</sup>	k <sub>2</sub> <sup>b</sup>	BDE <sup>c</sup>	Ref
II	V	H <sub>5</sub>	heptane	298	5.4×10 <sup>5</sup>	1.3×10 <sup>8</sup>	41±15	53,54
		Me <sub>5</sub>	heptane	298	4.7×10 <sup>5</sup>	-	-	53
	Nb	H <sub>5</sub>	heptane	298	-	7.0×10 <sup>6</sup>	-	53
	Ta	H <sub>5</sub>	heptane	298	5.9×10 <sup>3</sup>	5.0×10 <sup>6</sup>	-	53
	Mn	H <sub>5</sub>	methane	298 <sup>d</sup>	-	1.6×10 <sup>7</sup>	39±2	42
		H <sub>5</sub>	ethane	298 <sup>d</sup>	-	2.6×10 <sup>6</sup>	36±2	42
		H <sub>5</sub>	propane	298	-	2.4×10 <sup>6</sup>	33±3	55
		H <sub>5</sub>	heptane	298	-	8.0×10 <sup>5</sup>	39±2	56
		H <sub>5</sub>	cyclopentane	298	-	2.5×10 <sup>5</sup>	26±2	56
		H <sub>5</sub>	cyclohexane	295	-	3.4×10 <sup>5</sup>	-	57
		H <sub>5</sub>	methane	298 <sup>d</sup>	-	2.7×10 <sup>4</sup>	51±5	56
		H <sub>5</sub>	ethane	298 <sup>d</sup>	-	6.9×10 <sup>3</sup>	43±2	58
	Re	H <sub>5</sub>	propane	298	-	5.6×10 <sup>3</sup>	52±4	55
		H <sub>5</sub>	heptane	298	-	2.5×10 <sup>3</sup>	46±2	56,59
		H <sub>5</sub>	cyclopentane	298	-	1.1×10 <sup>3</sup>	32±2	56
		Me <sub>5</sub>	methane	298 <sup>d</sup>	-	5.0×10 <sup>4</sup>	47±2	42
		Me <sub>5</sub>	ethane	298 <sup>d</sup>	-	2.6×10 <sup>4</sup>	43±2	42
		Me <sub>5</sub>	cyclopentane	298	-	~6×10 <sup>3</sup>	-	56
		Ph <sub>5</sub>	cyclopentane	298	-	~4×10 <sup>3</sup>	-	56
		1,2- <sup>f</sup> Bu <sub>2</sub> H <sub>3</sub>	heptane	298	-	1.2×10 <sup>4</sup>	-	60
		1,2- <sup>f</sup> Bu <sub>2</sub> H <sub>3</sub>	cyclopentane	298	-	5.4×10 <sup>3</sup>	-	60
	M	R' <sub>6</sub>	alkane	T / K	k <sub>1</sub> <sup>a</sup>	k <sub>2</sub> <sup>b</sup>	BDE <sup>c</sup>	Ref
III	Cr	H <sub>6</sub>	heptane	298	-	2.0×10 <sup>6</sup>	38-45	61
		H <sub>6</sub>	decane	298	-	2.8×10 <sup>7</sup>	26±2	47
		H <sub>6</sub>	cyclohexane	298	-	9.8×10 <sup>6</sup>	22±2	47
		Me <sub>6</sub>	cyclohexane	298	-	1.5×10 <sup>7</sup>	25±2	47
	Mo	H <sub>6</sub>	cyclohexane	298	-	1.5×10 <sup>6</sup>	24±2	47
		1,4-Me <sub>2</sub> H <sub>4</sub>	cyclohexane	298	-	1.6×10 <sup>6</sup>	23±2	47
		1,3,5-Me <sub>3</sub> H <sub>3</sub>	heptane	298	-	2.0×10 <sup>6</sup>	23±2	47
		1,3,5-Me <sub>3</sub> H <sub>3</sub>	decane	298	-	2.5×10 <sup>6</sup>	25±2	47
		1,3,5-Me <sub>3</sub> H <sub>3</sub>	cyclohexane	298	-	1.8×10 <sup>6</sup>	23±2	47
		1,3,5-Me <sub>3</sub> H <sub>3</sub>	cyclohexane	298	-	2.1×10 <sup>6</sup>	23±2	47
	M	L <sub>3</sub>	alkane	T / K	k <sub>1</sub> <sup>a</sup>	k <sub>2</sub> <sup>b</sup>	BDE <sup>c</sup>	Ref
IV	Re	Kp <sup>h</sup>	cyclopentane	-	-	-	28±6	62
		Tp <sup>i</sup>	cyclopentane	-	-	-	45±2	63

<sup>a</sup> Pseudo first order rate constants (s<sup>-1</sup>) for alkane dissociation; <sup>b</sup> second order rate constant, (M<sup>-1</sup>·s<sup>-1</sup>), for recoordination of CO; <sup>c</sup> Empirical bond dissociation enthalpies (kJ·mol<sup>-1</sup>); <sup>d</sup> Supercritical alkane solution; <sup>e</sup> Gas-phase study; <sup>f</sup> rate for the *cis*-isomer; <sup>g</sup> Bis(bis(perfluoroethyl)phosphanyl)ethane, alkane dissociation by intramolecular recoordination; <sup>h</sup> cyclopentadienyltris(diethylphosphito)cobaltate; <sup>i</sup> hydro-tris(pyrazol-1-yl)borate. A note on error; wide ranging discrepancies in both rate constants and bond enthalpies have been found to arise from contrasting experimental technique, the sensitivity of these data to minute impurities present in the reaction mixtures, and the use in some studies of identical physical parameters (e.g. the quantum efficiency of photon absorption) – which are system specific – across a range of systems. The collated data should be viewed in that light, to provide a sense of the relative stabilities of each system, in cases where the rate constants differ by orders of magnitude, for example.

Of particular note are the high stabilities of the  $[\text{Re}(\text{C}_5\text{R}_5)(\text{alkane})]$  systems, for which substitution of heptane by ejected CO is approximately five orders of magnitude slower than otherwise analogous  $[\text{W}(\text{C}_5\text{R}_5)(\text{alkane})]$  systems. Indeed these rhenium systems are sufficiently stable that they may be characterised by NMR spectroscopy, a milestone reached in 1998 by Ball and Geftakis with the characterisation of  $[\text{Re}(\text{Cp})(\text{CO})_2(\text{cyclopentane})]$  in neat cyclopentane at 180 K, Figure 1.6, **A27**.<sup>64</sup> Four distinct pieces of data provided, for the first time, unambiguous evidence of a C-H  $\sigma$ -complex in solution; (1) an upfield shifted  $^1\text{H}$  resonance at  $\delta_{\text{IH}}$  -2.35, (2) an upfield shifted  $^{13}\text{C}$  resonance at  $\delta_{\text{13C}}$  -31.2, (3) a reduced  $^1J_{\text{CH}}$  coupling of 113 Hz (*cf.* free cyclopentane, 129 Hz), and (4) a shift in the cyclopentadienyl resonances on switching to *d*<sub>10</sub>-cyclopentane. A minimum bound to the binding energy was determined of  $\Delta G_{193\text{K}} = 34.8 \text{ kJ}\cdot\text{mol}^{-1}$ , with the complex persisting in solution for *ca.* 25 minutes at 200 K. The cyclohexane, pentane, neohexene, butane and propane  $[\text{Re}(\text{Cp})(\text{CO})_2(\text{alkane})]$  complexes, analogous of **A27** have all since been characterised by NMR spectroscopy.<sup>55,60,65</sup> Varying the cyclopentadienyl ligand to  $\text{C}_5\text{H}_4\text{Pr}$  and  $\text{C}_5\text{H}_3\text{Bu}_2$  has resulted in the observation of further alkane complexes.<sup>60,66</sup> The analogous manganese complexes  $[\text{Mn}(\text{Cp})(\text{CO})_2(\text{alkane})]$  are, expectedly, less stable, but NMR parameters have been extracted for the propane and butane complexes.<sup>55</sup>

Synthesised with a view to achieving a more idealised octahedral coordination environment than can be offered by a cyclopentadienyl ligand, tris(pyrazolyl)borate (Tp) complex **A28**,<sup>63</sup> and tris(diethylphosphito)cobaltate (Kp) complex **A29**,<sup>62</sup> proved similarly successful in forming complexes of cyclopentane, Figure 1.6. Upfield  $^1\text{H}$  resonances were recorded at  $\delta_{\text{IH}}$  -2.70 and -4.12 for **A28** and **A29** respectively, with which a minimum bound placed on cyclopentane dissociation of  $28.0 \pm 5.8 \text{ kJ}\cdot\text{mol}^{-1}$  for **A29**. Rhenium complex **A30** is impressive for being characterised in a non-alkane solvent; weakly coordinating fluorocarbon  $\text{CF}_3\text{CH}_2\text{CF}_3$ .<sup>67</sup> The cationic complex also employs a weakly coordinating perfluoro-alkoxy-aluminate anion developed by Krossing and co-workers,  $[\text{Al}(\text{OR}^{\text{F}})_4]$ .<sup>68,69</sup> The bound alkane is observed clearly, with characteristic resonances at  $\delta_{\text{IH}}$  -3.74 and  $\delta_{\text{13C}}$  -6.3, with a  $^1J_{\text{CH}}$  coupling constant of 113 Hz.

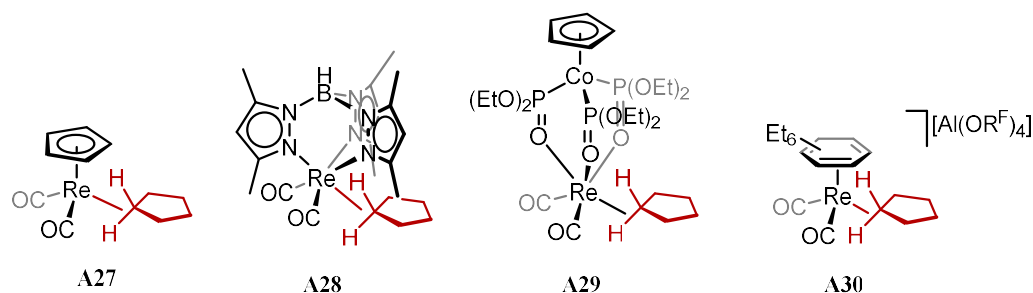


**Figure 1.6** Rhenium cyclopentane complexes characterised by NMR spectroscopy.

The characterisation of alkane  $\sigma$ -complexes by NMR spectroscopy has the advantage of allowing the determination of the regioselectivity of the alkane coordination, and to garner insight into dynamic exchange processes occurring between individual C-H bonds. For example in the cyclohexane analogue of **A27**, coordination of an axial C-H bond of cyclohexane is found to be favoured,<sup>70</sup> while at the  $\{\text{Re}(\text{Kp})(\text{CO})_2\}$  fragment (*cf.* **A29**) a time average composition of an axial and equatorial interaction is observed with cyclohexane. The lack of selectivity with the latter system, possibly a consequence of its less sterically imposing supporting ligand, extends to other alkanes. In  $[\text{Re}(\text{Kp})(\text{CO})_2(\text{pentane})]$  a statistical distribution of the three C-H environments is evident from the  $^1\text{H}$  NMR spectrum, as contrasts  $[\text{Re}(\text{Cp})(\text{CO})_2(\text{pentane})]$  where there is a 2:1 preference for a terminal  $\text{CH}_3$  interaction, which at  $[\text{Re}(\text{C}_6\text{Et}_6)(\text{CO})_2(\text{pentane})]$  (*cf.* **A30**) rises to 5:1. At the tungsten analogue  $[\text{W}(\text{C}_6\text{Et}_6)(\text{CO})_2(\text{pentane})]$  the  $\text{CH}_3$ -bound complex is exclusively observed. Excluding C-H activation equilibria, the chain-walking phenomenon is the primary dynamic process measurable in these systems by NMR spectroscopy. A relatively high energy process, barriers in  $[\text{Re}(\text{C}_5\text{H}_4\text{Pr})(\text{CO})_2(\text{alkane})]$  systems have been measured at 38 – 42  $\text{kJ}\cdot\text{mol}^{-1}$ .<sup>66</sup> Rhenium cyclopentane complex **A30** features the highest barrier measured to date; 50  $\text{kJ}\cdot\text{mol}^{-1}$ .<sup>67</sup>

The absence of alkane complexes of late transition metals such as rhodium or iridium prepared by photolytic means is a consequence of the tendency of the resulting fragment rapidly cleave the coordinated C-H bond.<sup>71–77</sup> Though in a stand out example, fast spectroscopic techniques have enabled direct observation of  $\sigma$ -complexes prior to C-H bond oxidative addition at rhodium cyclopentadienyl,<sup>78,79</sup> and Tp-based systems.<sup>80,81</sup>

### 1.2.4 Alkane complexes by protonation

A contrasting synthesis of rhodium  $\sigma$ -alkane complexes has been developed by Brookhart and co-workers. Protonation of a rhodium-methyl complex supported by a PONOP pincer ligand at  $-110\text{ }^{\circ}\text{C}$  in  $\text{CDCl}_2\text{F}$  solution afforded  $\sigma$ -methane complex **A31**, Figure 1.7.<sup>82</sup> This reaction is enabled by the similar free energies of the methane complex and the methyl hydride precursor and is kinetically stabilised by the low-temperature reaction conditions. Methane is eventually displaced by the dichlorofluoro-methane solvent with a half-life of 83 minutes at  $-87\text{ }^{\circ}\text{C}$ , and a corresponding activation energy of  $\Delta G^{\ddagger} = 61\text{ kJ}\cdot\text{mol}^{-1}$ . The  $^1\text{H}$  NMR spectrum of the methane complex comprises a broad doublet at  $\delta_{\text{IH}} -0.86$  ( $^1J_{\text{RhH}} = 6.3\text{ Hz}$ ) corresponding to the methane ligand (*cf.* a  $^2J_{\text{RhH}}$  of  $2.3\text{ Hz}$  for the methyl precursor). A downfield-shifted resonance in the  $^{13}\text{C}$  NMR spectrum is also noted at  $\delta_{13\text{C}} -41.7$ , observed as a quintet with a  $^1J_{\text{CH}}$  coupling constant of  $124\text{ Hz}$ , which on decoupling collapses to a broad singlet with a fwhm of  $6.7\text{ Hz}$ . This contrasts with free methane ( $^1J_{\text{CH}} = 125\text{ Hz}$ , fwhm =  $1.8\text{ Hz}$ ), the methyl precursor ( $\delta_{13\text{C}} -21.8$ ) and the related  $[\text{Ir}(\text{PONOP})(\text{H})\text{CH}_3][\text{BAR}^{\text{F}}_4]$  complex ( $\delta_{13\text{C}} -20.6$ ). Additional labelling studies involving protonation of  $\text{Rh-CD}_3$  and  $\text{Rh-}^{13}\text{CH}_3$  precursors concur with the assignment of a C-H  $\sigma$ -complex, rapidly exchanging across four C-H bonds.

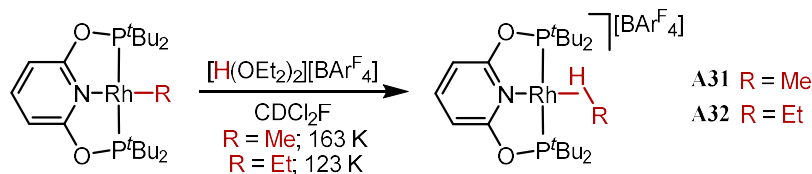


**Figure 1.7** Synthesis of a  $\sigma$ -methane and  $\sigma$ -ethane complex in solution.

The analogous ethane complex **A32** has been similarly prepared and characterised but was found to be much less stable in solution, observed at the lower temperature of  $-132\text{ }^{\circ}\text{C}$ .<sup>83</sup> Ethane was lost with a half-life of *ca.* 5.5 h at  $-132\text{ }^{\circ}\text{C}$ , with an activation energy of  $\Delta G^{\ddagger} = 46\text{ kJ}\cdot\text{mol}^{-1}$ . The ethane ligand is observed as two broad resonances in the  $^1\text{H}$  NMR spectrum at  $\delta_{\text{IH}} -0.83$  and  $1.13$ , and in the  $^{13}\text{C}$  spectrum at  $\delta_{13\text{C}} -31.6$  ( $^1J_{\text{CH}} = 124\text{ Hz}$ , fwhm =  $10.9\text{ Hz}$ ) and  $11.7$  ( $^1J_{\text{CH}} = 127\text{ Hz}$ , fwhm =  $7.5\text{ Hz}$ ), both resonances

are broadened compared to free ethane ( $\delta_{13\text{C}}$  7.0, fwhm = 2.5 Hz), attributed to unresolved rhodium and phosphorous coupling. The barrier to ethane chain walking was determined as  $\Delta G^\ddagger = 30 \text{ kJ}\cdot\text{mol}^{-1}$ . Neither a methane nor ethane complexes could be prepared with an iridium centre using the same approach. The iridium methyl hydride complex  $[\text{Ir}(\text{PONOP})(\text{H})(\text{CH}_3)][\text{BAr}^{\text{F}}_4]$  is remarkably stable to reductive elimination, while the ethyl variant  $[\text{Ir}(\text{PONOP})(\text{H})(\text{CH}_2\text{CH}_3)][\text{BAr}^{\text{F}}_4]$  eliminates ethane too rapidly to be detected even at low temperature.<sup>83,84</sup>

### 1.2.5 Observations of alkane complexes in the solid state

Contrasting the instability of alkane  $\sigma$ -complexes in solution, the issue of competitive solvent interactions is eliminated on moving to the solid state. Systems have been documented which on crystallisation are observed as metal-alkane adducts, Figure 1.8. While ostensibly serendipitous syntheses, the propensity for adduct formation with each system allowed for subsequent variation of the alkane in the latter studies. In the first instance, macrocyclic iron porphyrin complex **A33**, when crystallised from diffusion of heptane into fluorobenzene solutions, includes a heptane molecule in close proximity to the iron centre (2.5 – 2.8 Å, disordered) with the expected iron-porphyrin out-of-plane deformation associated with a square pyramidal coordination environment.<sup>85</sup> Notable here is the influence of the macrocycle of the system; apparently constraining the alkane, and possibly buttressing the interaction with supplementary host-guest interactions.

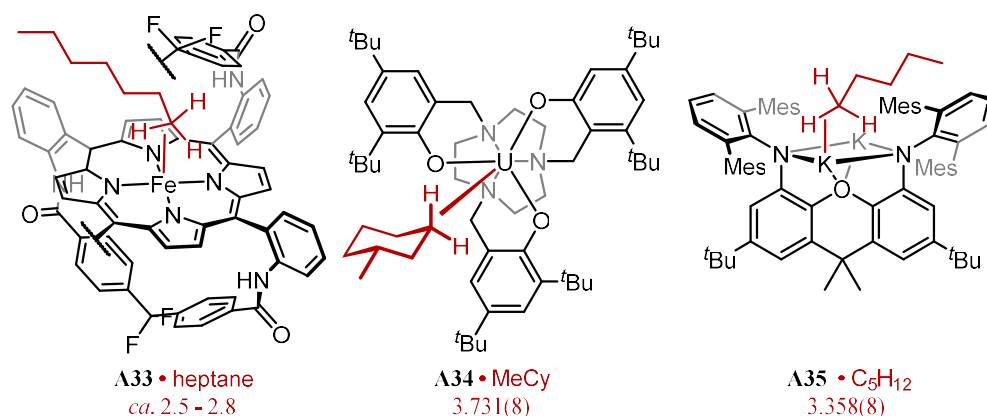


**Figure 1.8** Coordination of alkanes in the solid state. Closest M-C contacts (Å) annotated. Portion of the macrocycle of **A33** omitted for clarity (both macrocycles are identical).

Uranium complex **A34** has been crystallised with adducts of cyclohexane, cyclopentane, methylcyclohexane, methylcyclopentane, and neohexene.<sup>86</sup> All adducts are isomorphic and isostructural. The methylcyclohexane, methylcyclopentane and neohexene adducts are observed with M-C contacts of 3.864(7), 3.798(9) and 3.731(8) Å, respectively. These long contacts are (just) within the sum of uranium and carbon van der Waals radii (3.9 Å), suggestive of an orbital interaction. Close approach (2.12 – 2.71 Å) of the alkane to the *tert*-butyl groups of the ligand periphery is also noted.

In the sole example of an s-block-alkane interaction, potassium complex **A35** with the metal centre in proximity to hexane (K-C = 3.538(3) Å), pentane (K-C = 3.358(8) Å), 3-methylpentane (K-C = 3.215(5) Å), cyclopentane (K-C = 3.48 – 3.62 Å) and toluene (K-C = 3.39 – 3.31 Å) were prepared on recrystallisation from toluene-alkane mixtures or neat alkane.<sup>87</sup> Given the electronic situation at potassium and (consequently) the wildly divergent M-H-C bond angles (117° - 170°) this interaction is likely purely electrostatic between metal and alkane, supplemented by interactions with the mesityl groups decorating the flanks of the coordination site. Indeed, omitting dispersion corrections from DFT calculations here gives a 1 Å overestimation of the M-C distances.

### 1.2.6 Synthesis of alkane complexes in the solid state

Employing solid-gas reactivity,<sup>88</sup> the targeted synthesis of alkane  $\sigma$ -complexes by solid-state single-crystal to single-crystal hydrogenation of rhodium diene complexes has resulted in the most extensive and systematically characterised set of alkane  $\sigma$ -complexes, in any phase.<sup>89-94</sup> In the original preparation, Figure 1.9, hydrogenation of single crystals of rhodium norbornadiene complex **A36** resulted in the formation of  $\sigma$ -norbornane complex **A37**. The compound is characterised by (1) lengthened C-C contacts, (2) contracted Rh-P contacts by virtue of a diminished *trans*-influence, (3) Rh-C contacts of *ca.* 2.5 Å, and (4) a *ca.* 90° rotation of the hydrocarbon relative to the {RhP<sub>2</sub>} C<sub>2</sub> axis. Norbornane complex **A37** is unstable even in the solid-state above 253 K, ultimately giving rise to the zwitterionic **A38**, an amorphous solid material.

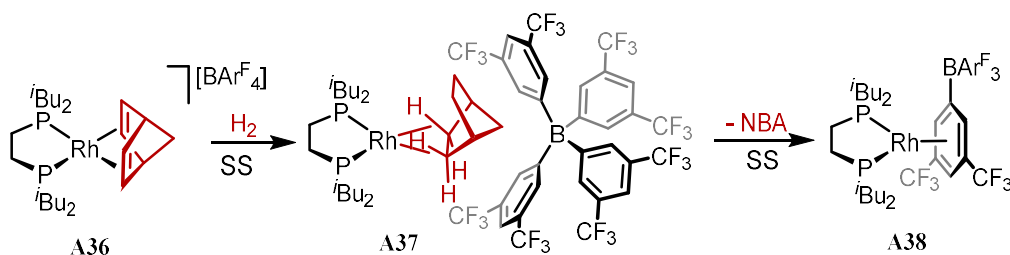


**Figure 1.9** Preparation of a  $\sigma$ -norbornane complex **A37** in the solid state.

The aromatic cavity defined by the  $[\text{BAR}^{\text{F}}_4]$  anion is critical to the stability of these complexes. In the solid state an octahedral microenvironment is established in which the cation-alkane complex is situated, through which supplementary dispersive and C-H- $\pi$ -interactions add to the thermodynamic stability of these systems. Dissolution in dichlorofluoromethane at  $-110^\circ\text{C}$  results in liberation of one equivalent of norbornene and a rhodium species assigned as either a complex stabilised by agostic interactions from the *iso*-butyl groups, or a solvent adduct. On warming to  $-20^\circ\text{C}$  complex **A38** is observed in solution.

Modification of the ancillary phosphine ligand to include cyclohexyl and cyclopropyl substituents lead to dramatically increased stabilities in the solid state, the former being stable for an indefinite period at ambient temperature. These changes, as well as variation in the length of the alkyl spacer in the chelating phosphine support have led to a vast proliferation in the number of alkane systems prepared using this approach, many of which are amenable to X-ray structure determination, Figure 1.10. The Rh(I) complexes **A37**, **A39** – **A46** all possess Rh-H-C interactions in the range  $2.36 - 2.62 \text{ \AA}$ , completing a square planar coordination geometry at rhodium. The two interactions established in each complex have essentially equivalent metrics to each other, with the exception of *iso*-butane complex **A41**, which features a shorter interaction with a terminal  $\text{CH}_3$  and a farther contact with the sterically encumbered tertiary centre. Across the norbornane complexes no substantial change in the M-C metrics is seen on variation of the diphosphine spacer. Much more dramatic variations in the recorded metrics result from altering the phosphine substituent (**A37** vs. **A39**), and on changing the anion (**A39** vs. **A44**), the latter eliciting a different norbornane coordination mode.

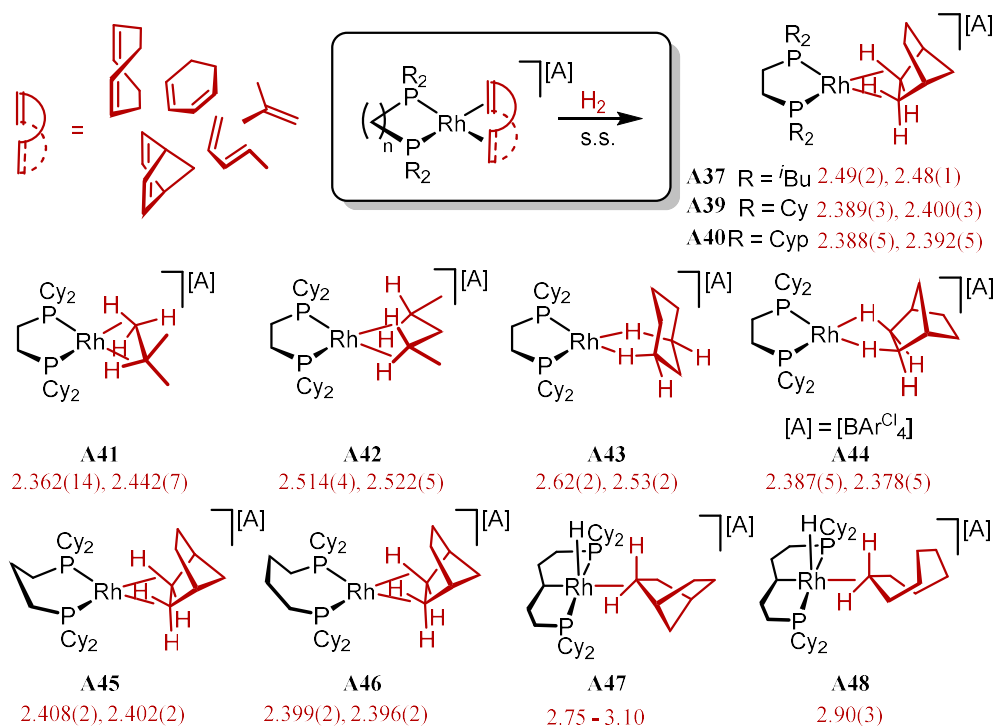


**Figure 1.10** Full set of crystallographically characterised alkane  $\sigma$ -complexes resulting from alkene hydrogenation. Annotated  $\underline{\text{M}}\text{-H}\text{-}\underline{\text{C}}$  contacts in Å. [A] = [BAr<sup>F</sup><sub>4</sub>] unless states. Ar<sup>Cl</sup> = 3,5-dichlorophenyl.

With longer diphosphine spacers, C-H bond oxidative addition was found to occur following hydrogenation of the diene, resulting in cyclometallated Rh(III) complexes **A47** and **A48**. A solitary Rh-H-C interaction is observed in these cases, with the remaining sterically encumbered coordination site on the metal remaining vacant, devoid even of agostic interactions with the accompanying cyclohexyl groups – the closest Rh-C(Cy) is 3.47 Å distant. The Rh-C separations associated with the alkane  $\sigma$ -complex interactions in these species are significantly increased in comparison to the Rh(I) variants, consistent with Rh(III) agostic precedents (*vide supra*, Figure 1.4).

Crystalline material of **A39** is appropriately disposed to allow for exchange of the hydrogenated alkane with freshly supplied small alkenes. This has been applied in the stoichiometric and catalytic hydrogenation and isomerisation of small alkenes,<sup>95,96</sup> and indeed allowed for the preparation of the isobutene precursor to complex **A41**. Further gas reactivity available to these systems include regioselective incorporation of deuterium.<sup>97,98</sup> These studies represent the first application of systems enacting



controlled catalytic and stoichiometric chemistry that rely explicitly on a stabilised alkane  $\sigma$ -complexes. The strategy of stabilising intermolecular M-H-C interactions by encapsulation is therefore a promising avenue that warrants further investigation.

### 1.3 Coordination chemistry of fluoroalkanes

#### 1.3.1 Context and bonding profile

Study of the coordination chemistry of C-F bonds is spurred by a desire to enact and control full cleavage of these robust linkages. Many systems have been investigated that are capable of such a reaction, driven by the formation of strong M-F bonds, although the vast majority are activation of aryl C-F bonds by electron rich centres,<sup>99–102</sup> enabled by the initial coordination of the intact C-F bond or an adjacent C=C bond, Figure 1.11, (a).<sup>103</sup> A stand out example of a reaction between a transition metal and an *alkyl* fluoride resulting in a cleaved C-F bond is that between an iridium PCP pincer complex and fluoromethane, Figure 1.11, (b).<sup>104</sup> Rather than direct C-F oxidative addition, a C-H bond is first broken, followed by an  $\alpha$ -fluoride migration to afford the iridium methyl fluoride complex. In this way the reaction bypasses the high activation barrier to direct C-F cleavage, calculated at 131 kJ·mol for this system. Other computational studies at rhodium and iridium put this barrier slightly lower when considering idealised model systems, and find the pre-coordination of fluoromethane and tetrafluoromethane to be favourable by 17 – 24 kJ·mol<sup>-1</sup> across the systems investigated.<sup>105,106</sup>

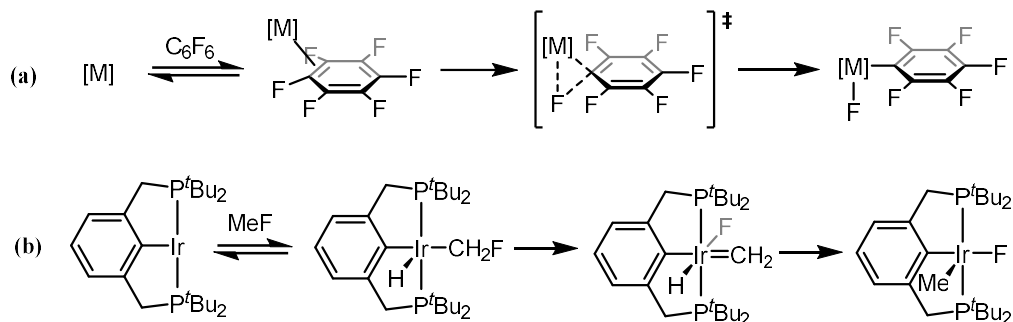


**Figure 1.11** C-F cleavage reactions; (a) general C-F activation of perfluorobenzene enabled by pre-coordination of the arene; (b) Net C-F cleavage of fluoromethane by an iridium pincer complex.

The challenge of preparing compounds featuring alkyl M-F-C interactions is further exacerbated by the reduction in the C-F bond polarity the more fluorine substituents are present. This is evidenced in gas phase studies of the bond dissociation enthalpies of fluoroalkanes with a tungsten pentacarbonyl fragment; the interactions with fluoroethane ( $51 \pm 13 \text{ kJ}\cdot\text{mol}^{-1}$ ) and fluoromethane ( $47 \pm 13 \text{ kJ}\cdot\text{mol}^{-1}$ ) – which are comparable in strength to the  $\{\text{W}(\text{CO})_5\}$ -(cyclohexane) interaction – are far stronger than interaction with trifluoromethane and perfluoromethane, which have dissociation enthalpies too small for this particular experiment to determine,  $< 21 \text{ kJ}\cdot\text{mol}^{-1}$ .<sup>50</sup>

### 1.3.2 Crystallographically characterised examples

Representative examples of M-F-C interactions characterised in the solid state are given in Figure 1.12. The shortest contacts are found with early metals; scandium,<sup>107</sup> titanium,<sup>107–109</sup> vanadium,<sup>110</sup> zirconium,<sup>111</sup> and hafnium.<sup>111</sup> The only intermolecular M-F-C interactions are characterised at scandium and titanium, forming complexes of fluorobenzene (**A49** – **A51**), 1,2-difluorobenzene (**A52**), and  $[\text{B}(\text{C}_6\text{F}_5)_4]^-$  (**A53**). The fluorobenzene complexes exhibit the closest approaches of any M-F interaction ( $2.113(7) - 2.2884(16) \text{ \AA}$ ). The M-F-C interaction is tolerant of a wide range of M-F-C bond angles, ranging from near linear in the fluorobenzene complexes ( $165.27(15)^\circ - 177.5(6)^\circ$ ), to the much more bent M-F-C angle found in the chelating complexes;  $118^\circ$  in vanadium complex **A55** for example. This is likely allowed for by the significant contribution to the interaction from a fluorine-centred lone pair.

Isolable complexes featuring interactions between C-F bonds and late transition metal centres are all intramolecular in nature. At ruthenium, C-F coordination has been applied in boosting the kinetics and selectivity of Grubbs-type catalysts,<sup>112,113</sup> for example complex **A56**, and have been observed arising from tight thione (**A57**) and imine (**A58**) based chelates, which possess close M-F contacts in the solid state at  $2.489(6)$  and  $2.367(3) \text{ \AA}$ , respectively.<sup>114–116</sup> Iridium complexes **A59**,<sup>117</sup> and palladium complex **A60**,<sup>118</sup> show M-F contacts of  $2.514(8)$  and  $2.4076(18) \text{ \AA}$  respectively. Here the

interaction is enforced through a rigid chelate, constraining the M-F-C interaction. With iridium complex **A61**,<sup>119</sup> and platinum complex **A62**,<sup>120</sup> the ligating C-F group is rather more flexible, and thus more representative of an intramolecular interaction. The M-F separations in these cases are 2.956(2) and 3.309(9) Å respectively. In all but one complex featuring multiple C-F bonds, the interacting C-F bond is elongated compared to the average length of the others by 0.02 - 0.04 Å. The notable exception is platinum complex **A62**, in which the C-F bond is contracted by 0.02 Å. Given the location of the fluorine atom – apical to a d<sup>8</sup> metal centre – a metal-to-fluorine charge transfer may well be implicated in this particular case.

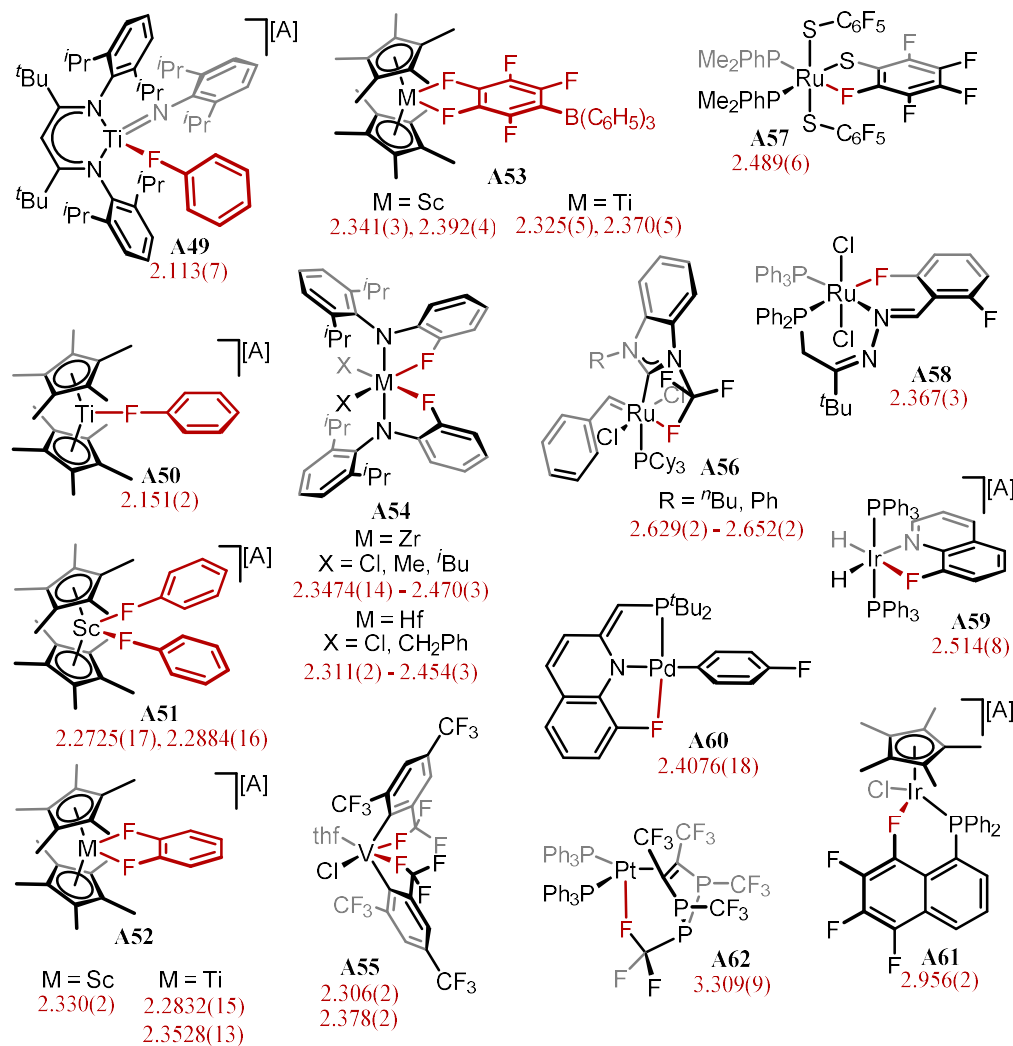


**Figure 1.12** Crystallographically characterised complexes with close  $\text{M-F-C}$  contacts; M-F contacts annotated (Å). [A] =  $[\text{B}(\text{C}_6\text{F}_5)_4]$ , **A49**;  $[\text{BPh}_4]$ , **A50** – **A52**;  $[\text{SbF}_6]$ , **A59**, **A61**.

## 1.4 Dinitrogen complexes of late transition metals

### 1.4.1 Context and bonding profile

The early transition metals have a well-established propensity for coordination and reduction of dinitrogen, with many studies motivated by the development of nitrogen fixation strategies.<sup>121–128</sup> Of the late transition-metal examples, while Group 8 is reasonably represented by a number of promising iron systems in particular, though within Group 9 the vast majority of examples are at cobalt, at which reduction chemistry is possible.<sup>129,130</sup> While a number of rhodium and iridium complexes have been characterised, these are not associated with activation of the dinitrogen bond, a consequence of the lower lying d-orbitals which are remote in energy from the frontier orbitals of dinitrogen.<sup>130,131</sup> Both the  $\sigma$ -donation from ligand to metal and the retrodonation to a high lying  $\pi^*$ -orbital are consequently weak; poorly stabilising, and poorly activating. End-on coordination of dinitrogen is typical, either in mononuclear systems or as bridging  $\mu$ -N<sub>2</sub> dimers. Side on coordination is rare in general and unprecedented at rhodium and iridium.

Rhodium and iridium dinitrogen complexes are thus often cited as latent sources of reactive low coordinate metal fragments. In many older reports authors candidly admit, or at least heavily imply, the serendipitous nature of some of these syntheses, resulting from working under dinitrogen atmospheres. The principal analytical techniques used for analysing these complexes are X-ray crystallography and NMR, IR and Raman spectroscopies. The <sup>15</sup>N chemical shift of dinitrogen is very sensitive to metal coordination, while <sup>1</sup>J<sub>NN</sub> coupling constants on the order of 4–7 Hz are typical across a range of metal centres.<sup>132</sup> IR and Raman spectroscopies provide a sensitive handle on the degree of activation of the dinitrogen ligand, though of note, it is documented that no correlation exists between the  $\nu(\text{N-N})$  stretching frequency and the N–N bond separation determined in a solid-state structure.<sup>130,133</sup> The most pertinent information from a solid-state structure therefore relate to the M–N contacts and the M–N–N angles, which are far more variable with the coordination environment and metal.

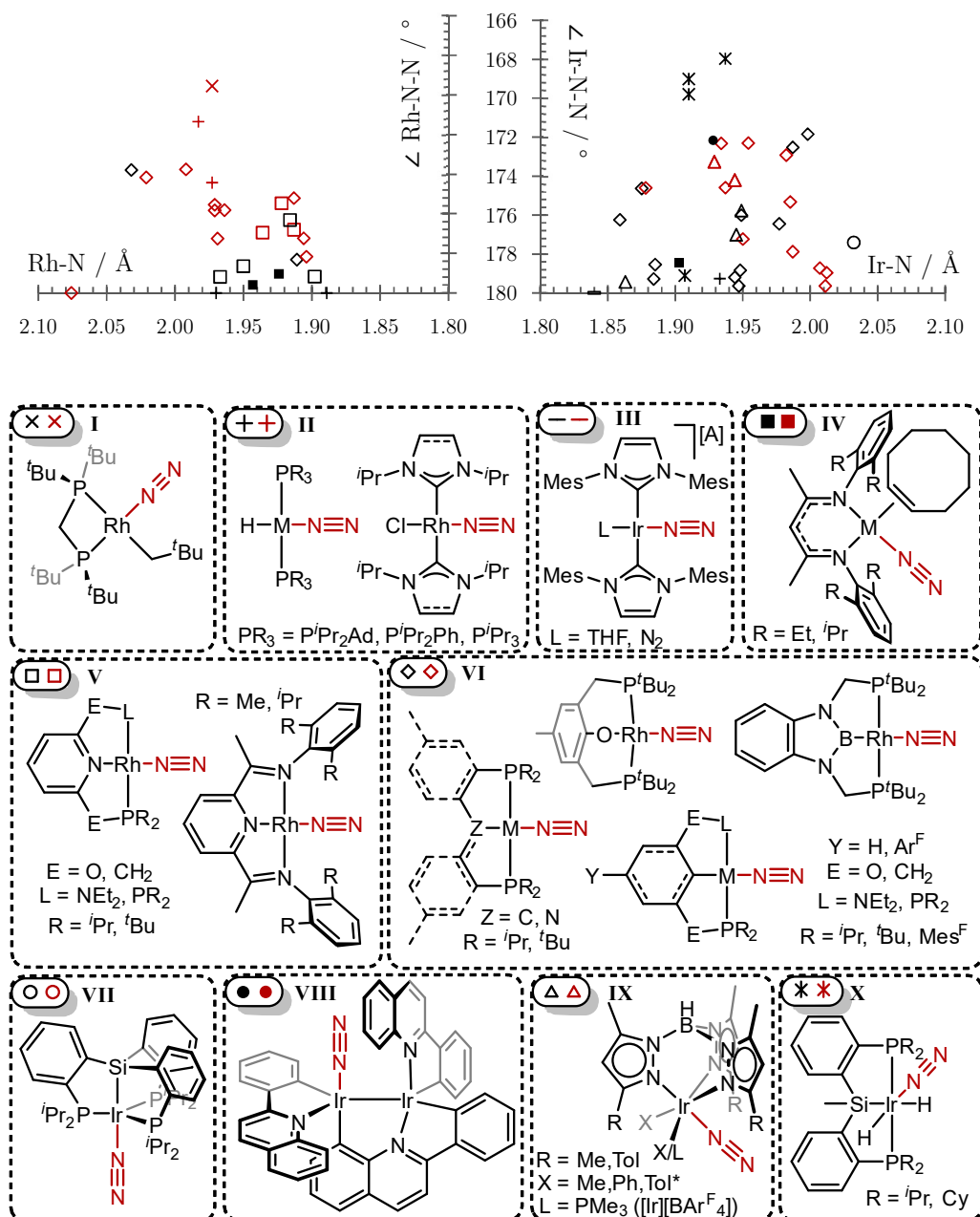
### 1.4.2 Crystallographically characterised examples

Figure 1.13 presents an overview of all rhodium and iridium dinitrogen complexes for which a solid-state structure has been deposited to the Cambridge Structural Database (v5.40, 2019). The data show a generally triangular distribution; there are a wider range of M-N bond distances the closer the M-N-N angle is to 180°. Across all the data, the average M-N bond length is in slightly closer approach with iridium at 1.939 Å as compared to 1.951 Å for rhodium. The spread of the data is equivalent for both metals. The complexes are delineated by supporting ligand architecture, each of which will now be summarised briefly. It should be noted that some compounds over-contribute to the data; structures with more than one molecule in the asymmetric unit for example.

$\kappa^1$ -N<sub>2</sub> and  $\mu$ -N<sub>2</sub> dimers are differentiated by black and red data points respectively, it can be generally observed that  $\mu$ -N<sub>2</sub> dimers tend to exhibit greater distortion of the M-N-N bond angle away from the idealised linear arrangement. This observation holds when comparing identical metal fragments isolated as both  $\kappa^1$ -N<sub>2</sub> and  $\mu$ -N<sub>2</sub> compounds. The distorted M-N-N geometries of these systems are possibly influenced by dispersive attraction between groups on the ligand peripheries of each metal fragment in the dimeric formulation, or may otherwise be perturbed by crystal packing effects.

At rhodium all examples are found in the +1 oxidation state. The  $\gamma$ -agostic interaction in neopentyl complex **A1** (Section 1.2.2, Figure 1.4), is readily displaced by dinitrogen affording a  $\mu$ -N<sub>2</sub> bridging dimer; Figure 1.13 (**I**).<sup>13</sup> Similarly with *trans*-bis(phosphine)<sup>133,134</sup> and *trans*-bis(carbene)<sup>135,136</sup> complexes (**II**), a dinitrogen complex is formed in preference to any potential agostic interaction. Within this set, the rhodium complex with a saturated carbene ligand has demonstrated an interesting solid-gas reaction is possible, where treatment of the dinitrogen complex with dioxygen results in a single-crystal to single crystal transformation to the  $\eta^2$ -dioxygen complex.<sup>135</sup> Neutral bis(phosphine) complexes (**II**) or have also been reported for iridium,<sup>137</sup> as have cationic iridium bis(carbene) complexes (**III**), particularly notable for the only characterised example of a bis(dinitrogen) complex with a Group 9 element.<sup>28</sup>

Diketiminato-supported dinitrogen complexes (**IV**) are known for rhodium,<sup>138,139</sup> and iridium,<sup>140</sup> with identical coordination environments. The iridium congener has the shorter M-N contact (1.90 Å compared to 1.94 Å), while the rhodium complex adopts a more linear M-N-N bond angle at 179.6° vs. 178.4° with iridium.



Dinitrogen complexes supported by pincer ligands are delineated by formally neutral (**V**) or anionic (**VI**) donor groups. With rhodium the various donor functionalities across the whole set are:  $\text{PN}_{\text{amido}}\text{P}$ ,<sup>141,142</sup>  $\text{PBP}$ ,<sup>143</sup>  $\text{PC}_{\text{aryl}}\text{P}$ ,<sup>144</sup>  $\text{PC}_{\text{alkyl}}\text{P}$ ,<sup>145,146</sup>  $\text{PCN}$ ,<sup>147</sup>  $\text{POCOP}$ ,<sup>148</sup>  $\text{POP}$ ,<sup>149</sup>  $\text{PNP}$ ,<sup>150,151</sup>  $\text{PNN}$ ,<sup>152</sup>  $\text{PONOP}$ ,<sup>153</sup> and  $\text{NNN}$ .<sup>154</sup> The only two rhodium examples with anionic pincers are monomeric  $\kappa^1\text{-N}_2$  complexes in the solid state. At iridium only dinitrogen complexes of anionic pincers (**VI**) are known with solid state characterisation, ranging across  $\text{PN}_{\text{amido}}\text{P}$ ,<sup>155–158</sup>  $\text{PC}_{\text{aryl}}\text{P}$ ,<sup>159–161</sup>  $\text{PC}_{\text{alkyl}}\text{P}$ ,<sup>162</sup> and  $\text{POCOP}$ <sup>163,164</sup> donors.

A trigonal bipyramidal iridium system (**VII**) was prepared as part of a systematic study of this ligand at various metal centres; the trend in  $\nu(\text{N-N})$  from 2008  $\text{cm}^{-1}$  to 2063  $\text{cm}^{-1}$  to 2122  $\text{cm}^{-1}$  for iron, cobalt and iridium respectively, reinforcing the notion of decreased dinitrogen activation along the transition series.<sup>165</sup> The Ir-N separation here is the largest of all the iridium complexes surveyed at 2.03 Å. A sole example with an Ir(II) centre exists (**VIII**), also in a trigonal bipyramidal field with the dinitrogen across from a high *trans*-influence ligand, and exhibiting an Ir-N bond length of 1.93 Å.<sup>166</sup>

Dinitrogen complexes at Ir(III) centres have been isolated, but are far scarcer than their lower oxidation state counterparts. The first thermally stable example was supported by a trispyrazolylhydroborate-based ligand,<sup>167,168</sup> and several related structures are known, both neutral and cationic in nature,<sup>169–171</sup> (**IX**). Ir(III) pincer complexes are also known, supported by a PSiP pincer ligand (**X**).<sup>172</sup> These examples span complexes with the PSiP pincer in both *fac*- and *mer*-coordination modes. In the *fac*-isomer, with the dinitrogen ligand *trans* to the silyl donor, the Ir-N bond length is determined to be 1.94 Å with an Ir-N-N bond angle of 168.0°; the furthest from linear of all compounds presented here. With the pincer in a *mer*-configuration the dinitrogen ligand becomes *trans* to hydride, wherein the Ir-N contact is contracted to 1.91 Å.

Group 9 dinitrogen complexes are reviewed in depth elsewhere, including extended discourse on their IR/Raman spectra.<sup>130</sup> To summarise,  $\nu(\text{N-N})$  values are reported in the range 2013 – 2203  $\text{cm}^{-1}$  at rhodium, and in the range 1926 – 2236  $\text{cm}^{-1}$  at iridium (*cf.* 2359  $\text{cm}^{-1}$  for free dinitrogen) with higher energy stretches found at Ir(III) centres.

## 1.5 Coordination chemistry of noble gas elements

### 1.5.1 Characterisation *in situ*

The early identification of noble gas coordination compounds closely parallels that of the alkane  $\sigma$ -complexes, with matrix dependant shifts in the IR and UV spectra of the Group 6 hexacarbonyls observed on photolysis in neon, argon, krypton and xenon at 20 K.<sup>41</sup> The bond strengths of the noble gas adducts were found to increase down Group 18, with M-Xe bond dissociation enthalpies at the Group 6 carbonyls measured in the gas phase as  $38 \pm 4 \text{ kJ}\cdot\text{mol}^{-1}$ ,  $34 \pm 4 \text{ kJ}\cdot\text{mol}^{-1}$  and  $35 \pm 4 \text{ kJ}\cdot\text{mol}^{-1}$  for chromium, molybdenum and tungsten respectively; generally similar to the dissociation enthalpies recorded for methane binding.<sup>173</sup> Parallel to this work, the krypton complexes  $[\text{Mn}(\text{CO})_5\text{Kr}]$  and  $[\text{Fe}(\text{CO})_5\text{Kr}]^+$  were observed by EPR spectroscopy at 77 K on  $\gamma$ -ray irradiated samples, with the respective spectra exhibiting distinctive  $^{83}\text{Kr}$  satellites.<sup>174</sup> Noble gas adducts of chromium fragments featuring more elaborate ligand architectures have been studied in matrix,<sup>34,175</sup> as have, much more recently, tungsten peroxide complexes  $[\text{WO}_3(\text{L})]$  and  $[\text{WO}_2\text{-}\eta^2\text{-(O}_2\text{)}(\text{L})]$  ( $\text{L} = \text{Ar, Xe}$ ).<sup>176</sup>

Kinetic studies of metal carbonyl photolysis in liquid xenon were initially hindered by dinitrogen contamination; 20 ppm of dinitrogen was found to be sufficient to fully outcompete the vast excess of xenon present during the photolysis of chromium hexacarbonyl.<sup>177,178</sup> In the absence of dinitrogen, FTIR interferometry allowed for characterisation of  $[\text{Cr}(\text{CO})_5\text{Xe}]$  in liquid krypton (5% Xe added) at 151 K and in neat xenon at 175 K. In both regimes the xenon complex was observed to have a half-life of about two seconds.<sup>179</sup> The analogous tungsten complex was also prepared in solution and a binding strength was found of  $35 \pm 1 \text{ kJ}\cdot\text{mol}^{-1}$ ,<sup>180</sup> in excellent agreement with the gas phase data.

Studies in supercritical krypton or xenon of the Group 6 systems have allowed for the characterisation of  $[\text{M}(\text{CO})_5(\text{L})]$  complexes ( $\text{M} = \text{chromium, molybdenum and tungsten}$ ) for  $\text{L} = \text{xenon, krypton and (tungsten only) argon}$ , at room temperature,<sup>181</sup> with a



barrier to xenon dissociation in  $[\text{W}(\text{CO})_5\text{Xe}]$  again found to be  $35 \pm 1 \text{ kJ}\cdot\text{mol}^{-1}$ . The agreement of the solution data with the gas phase data is indicative of a dissociative mechanism in these media. Beyond Group 6, noble gas interactions with transition metals have to date been observed in a supercritical medium at vanadium,<sup>182</sup> niobium,<sup>182</sup> tantalum,<sup>182</sup> manganese,<sup>183–185</sup> rhenium,<sup>56,59,185,186</sup> iron,<sup>36,187,188</sup> ruthenium,<sup>189,190</sup> and rhodium,<sup>78,191,192</sup> across a multitude of ligand topologies, with reactivities following the trend  $\text{Re} < \text{W} < \text{Mn} < \text{Mo} \approx \text{Cr} \approx \text{Nb} \approx \text{Ta}$ .<sup>193</sup> The rhenium fragment  $\{\text{Re}(\text{Cp})(\text{CO})_2\}$ , in addition to the alkane coordination noted previously, has been observed to interact with xenon and krypton in supercritical solutions.<sup>59</sup>  $[\text{Re}(\text{Cp})(\text{CO})_2\text{Xe}]$  was found to be *ca.* 400 times less reactive to CO recoordination than  $[\text{W}(\text{CO})_5\text{Xe}]$ , and *ca.* 2000 times slower than the same process with  $[\text{Re}(\text{Cp})(\text{CO})_2\text{Kr}]$ .<sup>56</sup>

A solitary example exists of an NMR characterised noble gas complex arrived at via a photolytic synthesis, achieved on photolysis of  $[\text{Re}(\text{C}_5\text{H}_4\text{Pr})(\text{CO})_2(\text{PF}_3)]$  in liquid xenon at 163 K.<sup>186</sup> The trifluorophosphine ligand here serves both to aid solubilisation this complex and to provide useful NMR handles for observing the products of photolysis. Using isotopically enriched  $^{129}\text{Xe}$  as solvent a shift at  $\delta_{\text{Xe}}$  -6179 relative to  $\text{XeOF}_4$  is located, with  $^3J_{\text{XeF}}$  coupling of  $5.1 \pm 0.8 \text{ Hz}$  and  $^2J_{\text{XeP}}$  coupling of  $42 \pm 1 \text{ Hz}$ .

Computational investigations into the bonding of  $[\text{Re}(\text{C}_5\text{H}_4\text{Pr})(\text{CO})(\text{PF}_3)\text{Xe}]$ , which obtain metrics in excellent agreement with experimental data, indicate that the interaction between the rhenium fragment and xenon is overwhelmingly dominated by interactions between xenon and cyclopentadienyl, carbonyl, and trifluorophosphine ligands, with minimal contribution from metal centred orbitals.<sup>194</sup> An in-depth computational study on  $[\text{M}(\text{CO})_5\text{L}]$  ( $\text{M} = \text{Cr}, \text{Mo}, \text{W}$ ;  $\text{L} = \text{Ar}, \text{Kr}, \text{Xe}$ ) draws the same conclusion, demonstrating a significant contribution of carbonyl-based orbitals to the interaction with the noble gas atom.<sup>195</sup> Other computational work on  $[\text{CoH}(\text{CO})_3\text{Xe}]$ , however, describes a topological analysis which only determines the occurrence of metal-xenon bond critical points, with the Co-Xe interaction comprising  $\sigma$ -donation from a xenon p-orbital to the metal, as determined by NBO analysis.<sup>196</sup>

In an interesting recent development, X-ray absorption fine structure spectroscopy has found application in probing the interaction of the  $\{\text{W}(\text{CO})_5\}$  fragment with alkanes, fluoroalkanes, and xenon.<sup>197</sup> This technique allows for structural characterisation of these species, specifically  $\text{W-H-C}$ ,  $\text{W-F-C}$  and  $\text{W-Xe}$  bond distances which show excellent agreement with DFT calculations of these structures. The  $\text{W-Xe}$  bond length is determined as  $3.10 \pm 0.02 \text{ \AA}$ .

Without the issue of onward reactivity, a number of rhodium xenon complexes have been prepared, Figure 1.14. This includes characterisation of a  $\text{Tp}^*$  (**A63**) and  $\text{Bp}^*$  (**A64**) system in liquid xenon at 223 K, which demonstrated a half-life of *ca.* 50  $\mu\text{s}$ ,<sup>71</sup> and of  $[\text{Rh}(\text{Cp}^*)(\text{CO})\text{Xe}]$  (**A65**) by time resolved IR methods.<sup>191</sup> The reactive  $\{\text{Rh}(\text{Cp}^*)(\text{CO})\}$  fragment here targeted for applicability to C-H activation, a reaction which proceeds well when making use of liquid krypton as a reaction medium, but is heavily attenuated in liquid xenon, in line with all previous observations of the relative interaction strength of these two elements.<sup>192</sup> No NMR spectroscopic characterisation of a molecular rhodium-xenon interaction has yet been reported.

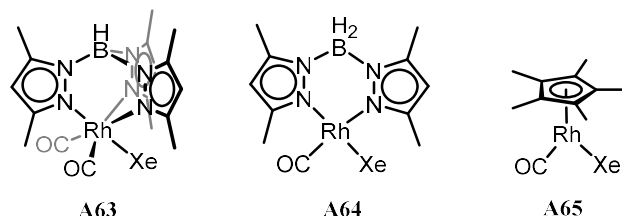


**Figure 1.14** Xenon complexes of rhodium.

### 1.5.2 Isolable complexes

Isolable metal complexes of xenon are scarce.<sup>198</sup> The first such examples were gold complexes, the most electronegative transition metal. The  $\text{Au}^+-\text{Xe}$  bond strength had previously been determined in the gas phase as  $127 \text{ kJ}\cdot\text{mol}^{-1}$ .<sup>199</sup> Originally targeting the synthesis of  $\text{AuF}$  by reduction of  $\text{AuF}_3$  in  $\text{HF}/\text{SbF}_5$ ,<sup>200</sup> utilisation of xenon as a mild reductant arrived at the  $\text{Au}(\text{II})$  species  $[\text{AuXe}_4][\text{Sb}_2\text{F}_{11}]$ , Figure 1.15, **A66**.<sup>201</sup> Crystalline samples of this material could be prepared at 195 K, analysis of which revealed a square

planar coordination mode with Au-Xe contacts in the range 2.7330(6) – 2.7456(5) Å. The coordination sphere is augmented with three close Au-F contacts with two antimonate anions. The compound is stable in the solid state below 233 K, above which the material liquifies with associated loss of gaseous xenon and a noticeable colour change from deep red to light orange. The compound is stable in HF/SbF<sub>5</sub> solution under xenon at 233 K, and can be stabilised at room temperature with a 10 bar overpressure of xenon.

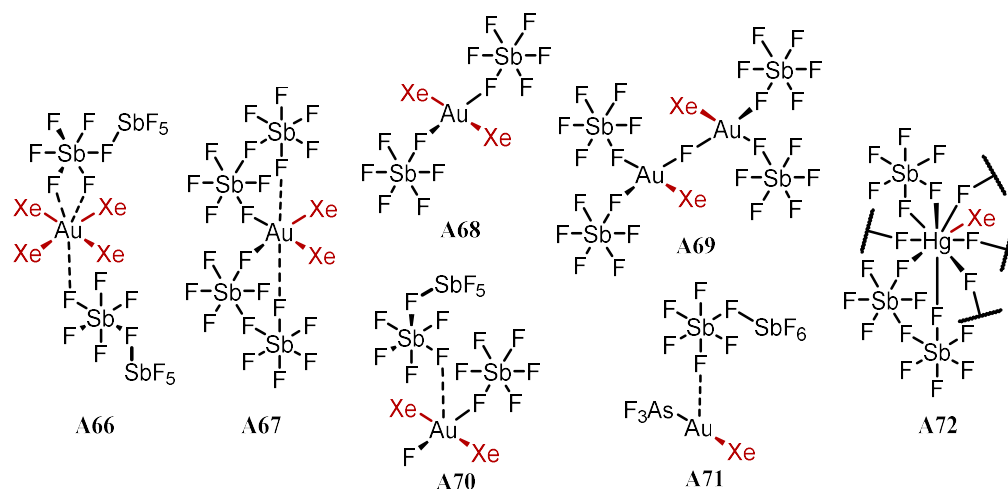


**Figure 1.15** Complexes of xenon isolated in the solid state.

In follow up work the crystallisation of [AuXe<sub>2</sub>]<sup>2+</sup> was reported;<sup>202</sup> the *cis*-isomer **A67** was prepared as the [Sb<sub>2</sub>F<sub>11</sub>]<sup>−</sup> salt by slight modification of the original reaction conditions, possessing Au-Xe bond lengths of 2.658(1) and 2.671(1) Å. *trans*-[AuXe<sub>2</sub>]<sup>2+</sup>, **A68**, was prepared as the [SbF<sub>6</sub>]<sup>−</sup> salt by oxidation of elemental gold with XeF<sub>2</sub> in HF/SbF<sub>5</sub> solution under an overpressure of xenon, and in the solid state exhibited Au-Xe contacts of 2.709(1) Å. Attempted preparation of the *trans*-isomer under a lower xenon pressure results in the mono-xenon dimer, **A69** (Au-Xe = 2.647(1) Å). The shortest Au-Xe bond so far reported belongs to a Au(III) complex, **A70**, which possesses two xenon ligands separated from the gold centre by 2.619(1) and 2.593(1) Å. A Au(I) complex, **A71**, was finally prepared by treating [Au(AsF<sub>3</sub>)] [SbF<sub>6</sub>] in HF/SbF<sub>5</sub> solution with xenon.<sup>203</sup> The compound is stable at room temperature, and in the solid state shows a Au-Xe contact of 2.6072(6) Å, comparable to the Au(III) species. **A71** was

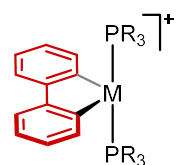
interrogated further by  $^{129}\text{Xe}$  NMR spectroscopy; at 253 K a multiplet resonance is elicited at  $\delta_{^{129}\text{Xe}}$  -5149.9 – -5150.3 (relative to  $\text{XeOF}_4$ ), slightly downfield of free xenon ( $\delta_{^{129}\text{Xe}}$  -5180.7). Concurrently a xenon complex of mercury was reported, **A72**, prepared from  $\text{HgF}_2$  and  $\text{SbF}_5$  under xenon at 80 °C, crystallising as the mono-xenon complex stabilised by six interactions with the anion fluorine atoms.

While the preparations of xenon complexes **A66** – **A72** are impressive, the harsh reaction conditions necessary for these syntheses limits the extent to which the ligand environment or indeed the metal centre may be varied further. An alternative strategy to preparing persistent metal-xenon complexes must be developed if the objective is to study and proliferate the M-Xe interaction in systems which may be isolated in the solid state and examined in solution.

## 1.6 Project aims

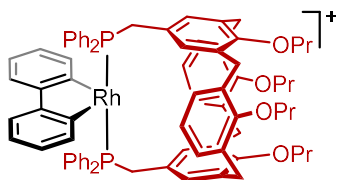
The overarching objective of this project is to prepare rhodium and iridium complexes of dinitrogen, alkanes, fluoroalkanes, and noble gas atoms, that persist sufficiently for their structure and properties to be thoroughly interrogated in solution and in the solid state. The work is divided into four interrelated lines of enquiry:

### Electronic stabilisation



Few rhodium and iridium complexes featuring agostic interactions belong to well-populated homologous families, and no rhodium complexes featuring persistent Rh-F-C interactions have been characterised. Noting the prevalence of strong  $\sigma$ -donors in Group 9 systems which exhibit agostic interactions, the 2,2'-biphenyl ligand was identified as a prospective ancillary ligand to support phosphine-tethered M-H-C and M-F-C interactions. A synthesis of *trans*-[M(2,2'-biphenyl)( $\text{PR}_3$ ) $_2$ ] $^+$  that is tolerant to a range of phosphines is targeted, from which the M-H-C and M-F-C interactions may be systematically interrogated. These systems will serve as models for coveted intermolecular complexes of alkanes and fluoroalkanes.

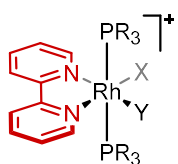
### Encapsulation of small substrates



Complexes of alkanes and noble gas elements have limited stability in solution as a consequence of competing coordination of the solvent, anion, or extraneous substance generated during the synthesis.

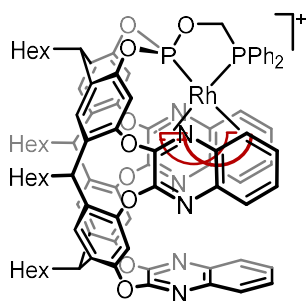
Seeking to circumvent these kinetic issues and to provide supplementary thermodynamic stabilisation, the use of mononuclear complexes of a calixarene-based chelating diphosphine ligand is proposed. The cavity-shaped ligand provides a sterically demanding enclosure, within which the metal can interact with small substrates – such as methane, dinitrogen, and xenon – unimpeded by the exterior solution environment.

### Relevance to bond cleaving processes



Rhodium and iridium complexes of 2,2'-bipyridyl are potentially interesting structural and functional analogues of 2,2'-biphenyl complexes. To this end, complexes of the form *trans*-[M(2,2'-bipyridyl)(H)<sub>2</sub>(PR<sub>3</sub>)<sub>2</sub>]<sup>+</sup> will be prepared, and the +1/+3 redox couple investigated, with a view to preparing variants that feature a calixarene-based diphosphine.

### Encapsulation of large substrates



Single-crystal to single-crystal hydrogenation of rhodium diene complexes has been shown to be effective approach for characterising alkane  $\sigma$ -complexes in the solid state. In these systems the metal-alkane interaction is stabilised within a well-defined molecular microenvironment defined by the anion, a cavity which is necessarily lost on

dissolution. By incorporating a pre-formed cavity within the ligand scaffold itself, the associated stabilising influences may be preserved on dissolution, permitting characterisation of an alkane  $\sigma$ -complex not only in the solid-state, but in solution. A resorcinarene-based diphosphine ligand has been designed for this purpose and its organometallic chemistry will be explored.

## 2 Rhodium and iridium 2,2'-biphenyl complexes

---

This chapter describes rhodium and iridium complexes bearing the 2,2'-biphenyl ligand. The syntheses of compounds featuring a series of phosphine ligands are described, exploiting the electronic properties of the 2,2'-biphenyl ligand to enforce a *trans*-phosphine coordination geometry and stabilise coordinatively unsaturated M(III) centres. The use of aryl and alkyl phosphines enabled structural characterisation – in solution and the solid state – of a collection of complexes of the form  $[M(2,2'\text{-biphenyl})(PR_3)_2][\text{anion}]$  ( $M = \text{Rh}, \text{Ir}$ ;  $R = \text{Ph}, \text{Cy}, \text{'Pr}, \text{'Bu}$ ;  $[\text{anion}]^- = [\text{BAr}^{\text{F}}_4]^-$ ,  $[\text{Al}(\text{OR}^{\text{F}})_4]^-$ ) stabilised by agostic interactions. Rhodium complexes  $[\text{Rh}(2,2'\text{-biphenyl})(\text{PPh}_2\text{Tol}^{\text{F}})(\text{L}_n)]^{0/+}$  ( $\text{L}_n = \text{Cl}, \text{PPh}_2\text{Tol}^{\text{F}}, 2,2'\text{-bipyridyl}, \text{acac}$ ) featuring a partially fluorinated phosphine ligand, and exhibiting Rh-F-C interactions in solution and the solid state are then described. The chapter closes with an examination of the intermolecular reactivity of  $[\text{Rh}(2,2'\text{-biphenyl})(\text{PPh}_3)_2]^+$ , underpinning work described in the following chapter exploring the use a cavitand-based diphosphine ligand.

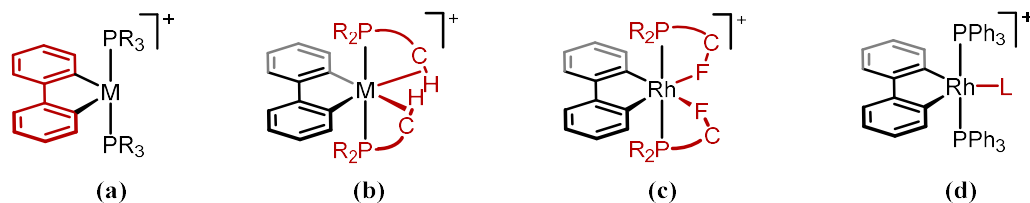


**Figure 2.1** Chapter 2 targets; **(a)** the synthesis of complexes of the form  $[M(\text{biphenyl})(\text{PR}_3)_2][\text{anion}]$ ; **(b)** alkyl phosphine systems for characterising agostic interactions; **(c)**, fluorinated phosphines for characterising intramolecular M-F-C interactions; **(d)**, intermolecular reactivity.

*Publications resulting from work described in this chapter:*

1. R. C. Knighton, J. Emerson-King, J. P. Rourke, C. A. Ohlin, and A. B. Chaplin, *Chem. Eur. J.*, 2018, **24**, 4927–4938.
2. J. Emerson-King, I. Prokes, and A. B. Chaplin, *Chem. Eur. J.*, 2019, **25**, 6317–6319.

## 2.1 The 2,2-biphenyl ligand

### 2.1.1 Properties and metallation

The 2,2'-biphenyl ligand is well-applied in organometallic chemistry as a rigid chelate. Resistant to auto-reductive elimination, and possessing an unimposing steric profile, the 2,2'-biphenyl ligand has found excellent utility in supporting high-oxidation state metal centres. The strong  $\sigma$ -donor and competent  $\pi$ -acceptor is correspondingly an effective *trans*-influencing ligand, enabling the formation of complexes with two weakly-occupied or formally vacant coordination sites. The incorporation of the 2,2'-biphenyl ligand into metal complexes may be accomplished by a range of syntheses, Figure 2.2.

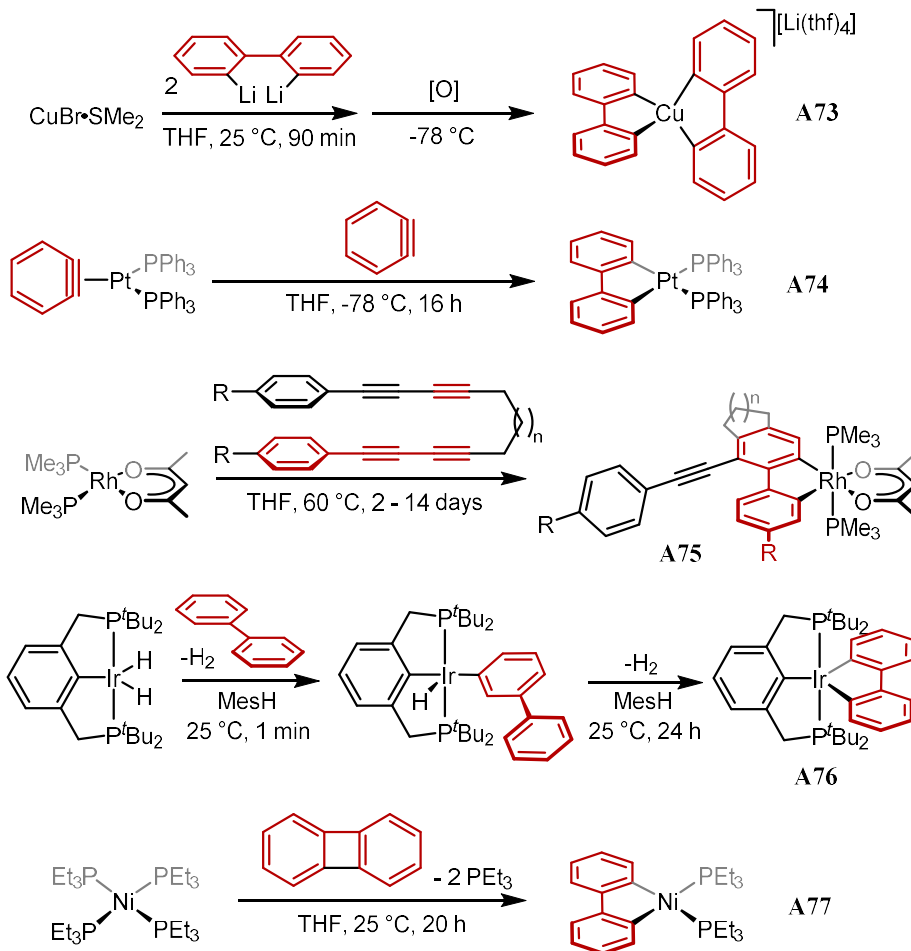


**Figure 2.2** Installation of the 2,2'-biphenyl ligand: (a) by transmetalation of dilithiated biphenyl; (b) by oxidative benzyne insertion; (c) by oxidative diene coupling; (d) by sequential C-H bond oxidative addition of biphenyl; (e) by C-C cleavage of biphenylene.

Transmetallation from dilithium salts of biphenyl is a versatile methodologies,<sup>204–209</sup> here exemplified with the preparation of cuprate spirocycle **A73**, Figure 2.2; an unusual example of a stable Cu(III) complex. Somewhat more niche syntheses include the oxidative coupling of benzyne,<sup>210</sup> or bis(diyne)s,<sup>211</sup> leading to complexes **A74** and **A75**, respectively, the latter exhibiting extended functionality on the 2,2'-biphenyl ligand. Sequential oxidative addition of two biphenyl C-H bonds has been enacted by iridium pincer complex via an Ir(V) intermediate leading to complex **A76**,<sup>212,213</sup> and at platinum centres through both Pt(0)/Pt(II) and Pt(II)/Pt(IV) redox couples.<sup>214–216</sup> The most common route to 2,2'-biphenyl complexes proceeds through the oxidative addition of the central C-C bond of biphenylene. Whilst C-H bond cleavage of biphenylene is kinetically favoured, the formation of the metallocycle is preferred thermodynamically by the relief of the incumbent ring strain – weakening the C-C bond to 275 kJ·mol<sup>-1</sup> (*cf.* 482 kJ·mol<sup>-1</sup> for the central C-C bond of biphenyl)<sup>217</sup> – and by the establishment of two strong M-aryl bonds. Zero-valent nickel centres were the first to achieve biphenylene C-C bond cleavage; the first example of which arriving at complex **A77**.<sup>218</sup>

### 2.1.2 Reactivity

The desire to prepare functionalised biphenyl moieties has inspired an array of catalytic inquiries, which are reviewed in depth elsewhere.<sup>217,219–221</sup> Of relevance to the work described herein is the onward reactivity (or lack thereof) of the 2,2'-biphenyl ligand that has emerged from these investigations. Such reactions typically involve insertion of some substrate into one of the M-C bonds, representative examples of which are given in Figure 2.3. The viability of each of these transformations depends heavily on the metal centre and the ligand environment. The first-row transition metals are particularly prone to elimination of the 2,2'-biphenyl ligand,<sup>205,206,222–224</sup> a decomposition which occurs at [Ni(2,2'-biphenyl)(PEt<sub>3</sub>)<sub>2</sub>] in the absence of added substrate; this compound dimerises with loss of phosphine before eliminating tetraphenylene via a bimetallic reductive elimination. The reactivity of nickel 2,2'-biphenyl complexes is attenuated by the use of bulkier phopshines,<sup>225–227</sup> or N-heterocyclic carbenes.<sup>228–232</sup>



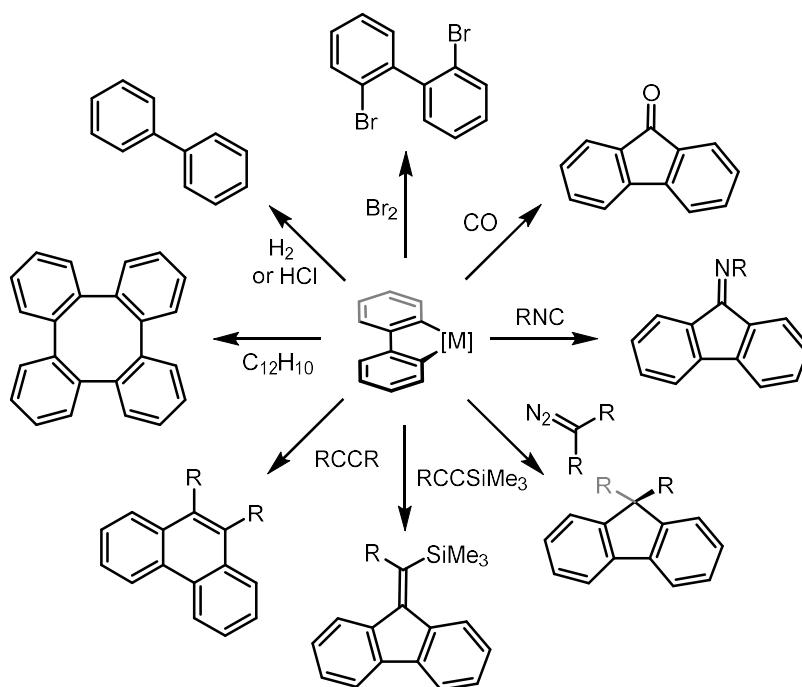


**Figure 2.3** Typical onward reactivity of the  $\{M(2,2'\text{-biphenyl})\}$  fragment.

The stability of the  $\{M(2,2'\text{-biphenyl})\}$  fragment increases moving down Group 10, with a variety of palladium and platinum complexes having been prepared, usually as models for the more coveted nickel chemistry.<sup>233–236</sup> The use of chelating phosphine ligands results in more stable biphenyl species throughout the group, presumably by mitigating phosphine dissociation.<sup>237–239</sup> The majority of these systems are  $M(\text{II})$   $d^8$  complexes, though  $\text{Pt}(\text{IV})$  dihydrides and dibromides are isolable, the former of which only slowly undergoes a migratory insertion of the hydride ligand ( $t_{1/2} \approx 300$  h at  $65^\circ\text{C}$ ).<sup>234,236</sup> The propensity of the 2,2'-biphenyl ligand to stabilise higher oxidation states is also demonstrated in Group 11 by a string of work on 2,2'-biphenyl-supported  $\text{Au}(\text{III})$  catalysis.<sup>240–244</sup> While in many of these complexes the 2,2'-biphenyl ligand is thermally stable to a range of substrates,<sup>245</sup> reactive carbenes can insert into the  $\text{Au-C}$  bond.<sup>246</sup>

The reactivity of Group 9 metal biphenyl fragments is similarly greatest with the first-row member and decreases moving down the group. Comparing across structurally analogous  $[M(2,2'\text{-biphenyl})(\text{Cp}^*)\text{L}]$  compounds **A78** – **A81**, Figure 2.4, at cobalt trimethylphosphine complex **A78** is isolable, while attempted synthesis of the carbonyl

analogue results in immediate elimination of fluorenone.<sup>247</sup> Rhodium trimethylphosphine complex **A79** is stable to hydrogenation (130 °C, 0.66 bar H<sub>2</sub>),<sup>248</sup> and both rhodium (**A80**) and iridium (**A81**) carbonyl complexes are stable to the insertion of carbonyl.<sup>249</sup> These compounds are presumably fortified by virtue of their saturated coordination spheres. At conformationally flexible rhodium and iridium centres insertion reactions are possible. Rhodium complex **1** is thermally stable, but reacts rapidly with carbon monoxide, *tert*-butylisocyanide, as well as a variety of alkenes and alkynes.<sup>250</sup> The structurally related iridium complex **2** possesses a robust M-biphenyl linkage, which is only cleavable by the addition elemental bromine.<sup>251–253</sup> Reaction of **2** with CO or acetylene leads only to substitution of the cyclooctadiene ligand.

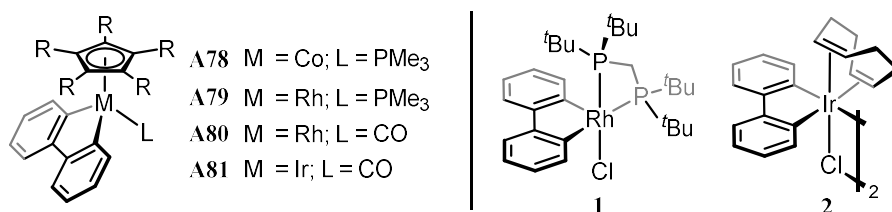


**Figure 2.4** Isolable Group 9 2,2'-biphenyl complexes. **A78** – **A80**: R = Me, **A81**: R = H.

## 2.2 Intramolecular M-H-C interactions

### 2.2.1 Preamble

The latent  $\{\text{Rh}(\text{P}^i\text{Pr}_3)_2\}^+$  fragment enacts the C-C bond cleavage of biphenylene under moderate conditions (40 °C, 5 days) to afford complex **13**, Figure 2.5, a coordinatively unsaturated complex stabilised by the adoption of agostic interactions with the pendant *iso*-propyl groups.<sup>254</sup> Reasoning that structural analogues of **13**;  $\text{trans}-[\text{M}(2,2'\text{-biphenyl})(\text{PR}_3)_2]^+$ , would likely also exhibit agostic stabilisation, rhodium and iridium complexes featuring a range of phosphine ligands were sought to enable systematic investigation of the M-H-C (agostic) interaction.<sup>¶</sup>

<sup>¶</sup> Work presented in this section is part of a collaborative venture. Dr R. C. Knighton prepared complexes **8**, **9**, **10**, **17**, **18**, **19**, **20**, conducted the crystallographic analysis together with Dr A. B. Chaplin, and collected the bulk of the variable temperature NMR data. The low-temperature NOE experiments were performed by Dr Jon Rourke and the computational work by Dr C. A. Óhlin. See page viii for affiliations.

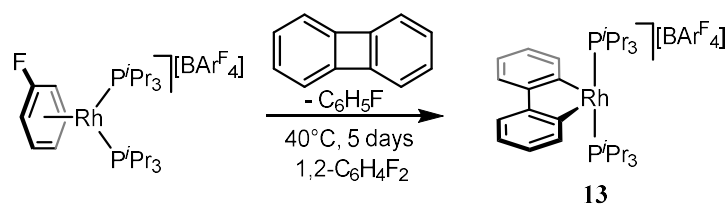


**Figure 2.5** Previous preparation of low-coordinate rhodium tri-*iso*-propylphosphine complex **13**.

In order to prepare an extended series of complexes analogous to **13** an alternative synthetic protocol was mandated that would be tolerant to a variety of phosphines and amenable to iridium chemistry. Noting that complexes **1** and **2** (Figure 2.4) react with triphenylphosphine to afford *trans*-bis(phosphine) chloride complexes, simple adaption of these procedures to alternative phosphines followed by halide abstraction could afford the desired analogues of **13**. Complexes of rhodium and iridium with a set of phosphine ligands with varying flexibilities were targeted, ranging from a rigid  $sp^2$  case (triphenylphosphine), to a saturated variant (tricyclohexylphosphine), to the acyclic tri-*iso*-propylphosphine and finally to tri-*iso*-butylphosphine.

### 2.2.2 Synthesis of low-coordinate complexes

The full synthetic route to the target low coordinate systems is detailed in Scheme 2.6, with precursors **1** and **2** prepared per literature procedures.<sup>250,252</sup> No solution data has previously been reported for **2**; the compound is, however, sufficiently soluble in dichloromethane that with modern spectrometers it may be characterised by  $^1\text{H}$  NMR spectroscopy as a 3:2 mixture of  $C_i$  and  $C_s$  symmetric components, assigned as a dimeric and solvent-cleaved monomeric complex respectively. Substitution of dtbpm (**1**) or COD (**2**) with tricyclohexyl-, tri-*iso*-propyl- and tri-*iso*-butylphosphine afforded the desired phosphine chlorides **3** – **10** in 37% – 83% yield; the lower yields of the *iso*-propyl and *iso*-butyl variants are a consequence of the high solubility of these species in alkanes.

With chlorides **3** – **10** in hand, reaction with either  $\text{Na}[\text{BAr}^{\text{F}}_4]$  or  $\text{Li}[\text{Al}(\text{OR}^{\text{F}})_4]$  at ambient temperature for 18 h in dichloromethane solution afforded the corresponding low-coordinate complexes **11** – **20** in 32% – 80% yield, with only the halide abstraction of

iridium triphenylphosphine complex **7** requiring a slightly elevated temperature of 50 °C to proceed at a satisfactory rate. Only iridium triphenylphosphine complex **16** is unstable in dichloromethane solution on timescales relevant to these syntheses, limiting the isolated yield in this case. A more detailed discussion of the solution stabilities of some of these compounds is presented in Section 2.4.5.

Compounds **11** – **20** were isolated as crystalline solids following diffusion of pentane into concentrated dichloromethane solutions of the respective metal salt. Material prepared in this way was amenable to X-ray diffraction studies, though *iso*-butyl complexes **14** and **19** – featuring the  $[\text{BAr}^{\text{F}}_4]^-$  anion – exhibited extensive disorder in the phosphine ligand, and so precluded meaningful interpretation of the solid-state metrics. As such the  $[\text{Al}(\text{OR}^{\text{F}})_4]^-$  analogues **15** and **20** were prepared, both of which are non-disordered with respect to the alkyl substituent in close approach to the metal centre.

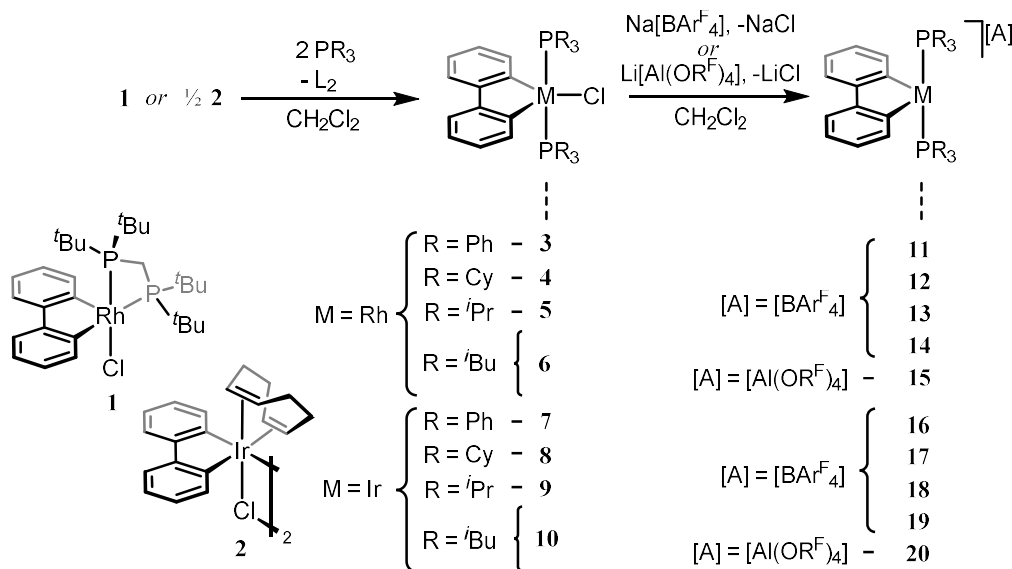


**Figure 2.6** Synthesis of  $[\text{M}(2,2'\text{-biphenyl})(\text{PR}_3)_2]^+$  compounds **11** – **20**. Conditions: Compound **16** from **7**: 50 °C, 18 hours; all other preparations: ambient temperature, 18 hours.

### 2.2.3 Solid state characterisation

In the solid state triphenylphosphine complexes **11** and **16** are observed as  $\kappa^1$ -dichloromethane adducts in pseudo-square pyramidal geometries, Figure 2.7, **11**·**dcm**:  $\angle \text{C4-Rh1-Cl8} = 174.33(8)^\circ$ ; **16**·**dcm**:  $\angle \text{C4-Ir1-Cl8} = 175.25(11)^\circ$ . The M–Cl contacts

are 2.6067(8) Å and 2.5567(12) Å for **11·dcm** and **16·dcm**, respectively, and in good agreement with literature precedents for other  $\kappa^1$ -dichloromethane adducts of rhodium,<sup>255–259</sup> and iridium,<sup>260–262</sup> which share the commonality of the dichloromethane bound *trans* to a strong  $\sigma$ -donor. Compounds **11·dcm** and **16·dcm** are the first crystallographically characterised homologous series of platinum-group dichloromethane complexes. The remaining coordination site is patently vacant, with the closest available carbon atom of the phosphine phenyl moiety displaced by 3.271(4) Å and 3.349(5) Å for **11** and **16** respectively. Only a solitary example of a solid-state  $\kappa^2$ -dichloromethane adduct is known, characterised at a ruthenium centre.<sup>263</sup>

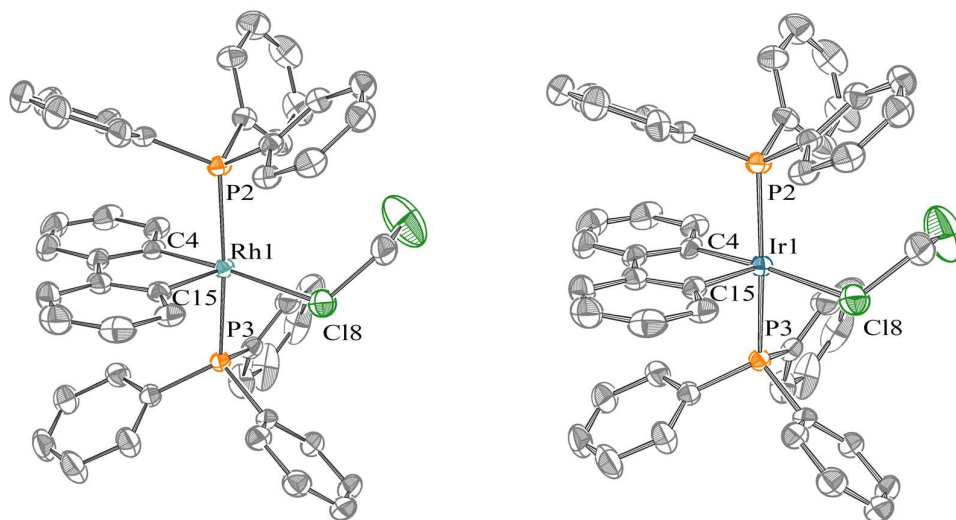


**Figure 2.7** Solid state structures of **11·dcm** (left) and **16·dcm** (right). Co-crystallised dichloromethane molecule (uncoordinated) and [BAR<sup>F</sup>]<sub>4</sub> anion omitted. Selected bond lengths (Å) and angles (°): **11·dcm**; Rh1-Cl8, 2.6067(8); Rh1-P2, 2.3648(7); Rh1-P3, 2.3437(7); Rh1-C4, 2.007(3); Rh1-C15, 2.000(3); P2-Rh-cent(rhodacycle), 88.66(4); P3-Rh1-cent(rhodacycle), 87.63(4); C4-Rh1-Cl8, 174.33(8). **16·dcm**; Ir1-Cl8, 2.5567(12); Ir1-P2, 2.3513(9); Ir1-P3, 2.3421(9); Ir1-C4, 2.000(4); Ir1-C4, 2.012(4); P2-Ir1-cent(iridacycle), 88.31(5); P3-Ir1-cent(iridacycle), 89.74(5); C8-Ir-Cl = 175.25(11).

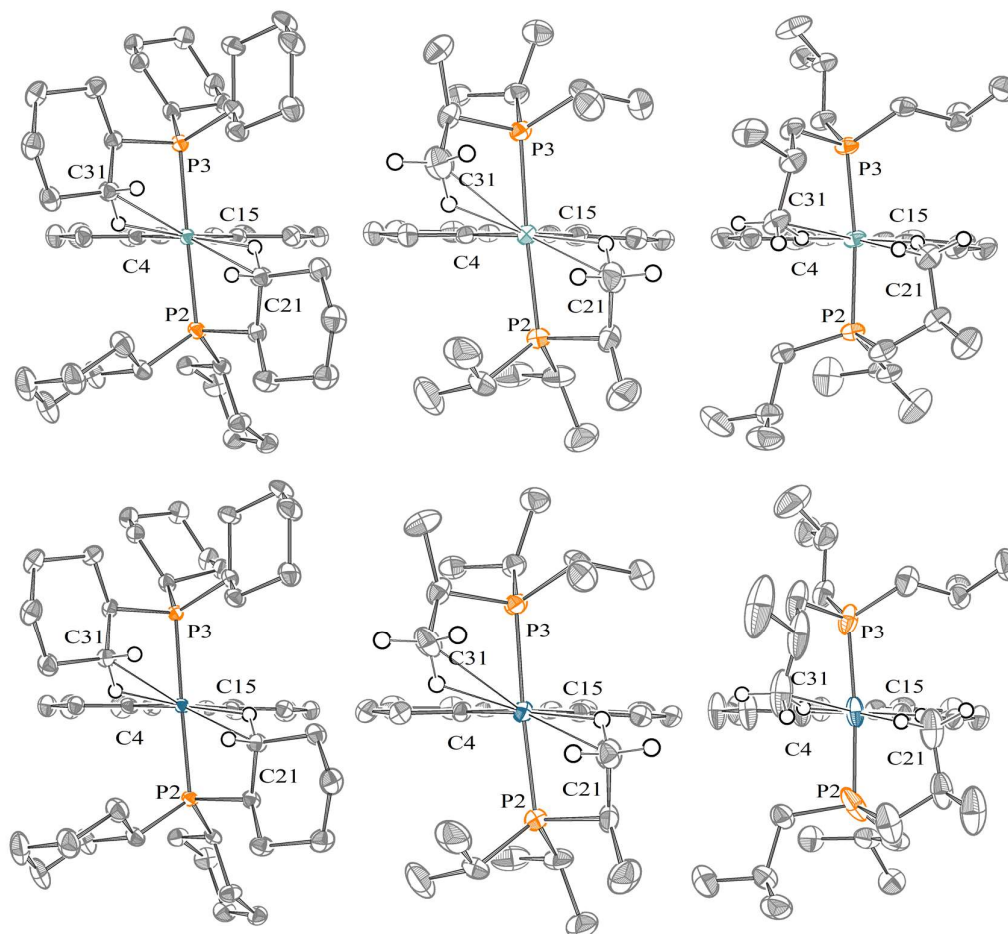
Proceeding to the trialkylphosphine species, these are observed in the solid state devoid of solvent adducts, and instead the metal centre is stabilised by the adoption of two  $\gamma$ - or  $\delta$ -agostic interactions, Table 2.1. Complexes of tricyclohexylphosphine **12** and **17** each possess a single cation in the asymmetric unit, co-crystallised with a molecule of dichloromethane remote from the metal centre. One of the non-interacting cyclohexyl components in each structure is found to be disordered and modelled over two sites

with occupancies of the major disordered component of 0.542(3) and 0.741(3) for **12** and **17**, respectively. The cyclohexyl units interacting with the metal show no substantial disorder. Tri-*iso*-propylphosphine compounds **13** and **18** crystallise with two distinct cations in the asymmetric unit, one of which at both metals possesses a substantially disordered phosphine ligand and is consequently omitted from this analysis. Tri-*iso*-butylphosphine compounds **15** and **20** featuring the  $[\text{Al}(\text{OR}^{\text{F}})_4]^-$  anion crystallise with slightly different conformations to their  $[\text{BAr}^{\text{F}}_4]^-$  analogues, **14** and **19**. The structure of **15** contains a single cation which is well ordered, while the structure of **20** is refined with two molecules in the asymmetric unit, of which the cation with closest agreement to the conformation of **15** is discussed in this analysis. The variety of conformations observed demonstrates the flexibility of the *iso*-butyl group.

The trialkylphosphine systems all adopt see-saw metal geometries with respect to the phosphine and biphenyl ligands, with agostic interactions completing the remainder of an octahedral coordination sphere. Each structure possesses generally equivalent metal-biphenyl related structural metrics, with M-C4 and M-C15 contacts in the narrow range 1.99 – 2.00 Å for the rhodium complexes and 2.01 – 2.02 Å for iridium, and with the exception of complex **13** the metal-biphenyl bond lengths are the same within error for each compound. The metal-phosphine bond lengths are longer in the order cyclohexyl > *iso*-propyl > *iso*-butyl, though of note: in all but two cases the M-P2 and M-P3 distances are not equivalent (*vide infra*).

The agostic carbon atoms C21 and C31 are separated from the metal centre in the tricyclohexylphosphine systems by 2.877(3) Å and 2.899(3) Å for rhodium complex **12**, and at 2.857(3) Å and 2.875(3) Å for iridium complex **17**. Within each complex the two interactions are thus observed to be inequivalent, with a major (closer) and minor interaction. This asymmetry is seen across the series, and is particularly pronounced for the tri-*iso*-propylphosphine systems with a  $\sim 0.3$  Å difference; 2.836(3) Å and 3.185(3) Å for the rhodium complex **13** and 2.810(8) Å and 3.115(9) Å for the heavier congener **18**. The tri-*iso*-butylphosphine systems show a  $\sim 0.2$  Å difference; 2.863(5) Å and 2.979(4) Å with rhodium, **15**, 2.781(7) Å and 2.956(6) Å with iridium, **20**.

**Table 2.1** Selected bond lengths (Å) and angles (°) of rhodium complexes **12**, **13** and **15** (top) and iridium complexes **17**, **18** and **20** (bottom) at 150 K. Thermal ellipsoids at 50%. Minor disorder and anions omitted.



	<b>12</b> R = Cy	<b>13</b> <sup>a</sup> R = <sup>t</sup> Pr	<b>15</b> R = <sup>t</sup> Bu	<b>17</b> R = Cy	<b>18</b> R = <sup>t</sup> Pr	<b>20</b> <sup>b</sup> R = <sup>t</sup> Bu
<b>M-C21</b>	2.877(3)	2.836(3)	2.863(5)	2.857(3)	2.810(8)	2.780(7)
<b>M-C31</b>	2.899(3)	3.185(3)	2.979(4)	2.875(3)	3.115(9)	2.957(6)
<b>M-P2</b>	2.3755(7)	2.3593(7)	2.3301(10)	2.3614(7)	2.352(2)	2.3301(15)
<b>M-P3</b>	2.3636(7)	2.3542(7)	2.3545(10)	2.3608(7)	2.347(2)	2.3501(15)
<b>M-C4</b>	1.996(3)	1.989(2)	1.992(4)	2.016(3)	2.021(7)	2.017(6)
<b>M-C15</b>	1.994(3)	1.995(2)	2.003(4)	2.010(3)	2.015(8)	2.024(6)
<b>P2-M-cent</b> <sup>c</sup>	95.33(4)	95.54(4)	94.50(6)	96.07(4)	96.89(12)	95.69(10)
<b>P3-M-cent</b> <sup>c</sup>	93.75(5)	91.32(5)	90.50(6)	93.95(5)	91.55(12)	90.98(10)
<b>P2-npln</b> <sup>d</sup>	8.04(6)	9.00(6)	5.28(7)	8.88(6)	10.35(17)	6.71(10)
<b>P3-npln</b> <sup>d</sup>	5.97(6)	4.16(7)	6.61(11)	6.41(7)	4.4(2)	6.28(16)
<b>C4-M-C21</b>	160.63(11)	160.86(10)	170.80(17)	161.49(11)	161.9(3)	172.4(2)
<b>C15-M-C31</b>	157.20(11)	151.20(10)	174.05(16)	158.01(11)	152.5(3)	174.0(2)

<sup>a</sup> Data for non-disordered cations only; <sup>b</sup> Selected cation; <sup>c</sup> Centroid of the biphenyl metallacycle; <sup>d</sup> angle between the M-P vector and the normal vector to the plane defined by the metallacycle.

Across the series the iridium species consistently demonstrate closer interactions by *ca.* 0.05 Å. The overall trend in the major agostic bond length seems driven by an increase in ligand flexibility, from phenyl- to cyclohexyl- to *iso*-propyl- to *iso*-butyl substituents. The structures in Table 2.1 illustrate this point visually, with only the *iso*-butyl complexes possessing agostic interactions in the plane of the 2,2'-biphenyl ligand, while with tricyclohexylphosphine and tri-*iso*-propylphosphine the interactions are markedly above and below the plane, as quantified by the C4-M-C21 and C15-M-C31 angles which range from 151.2° for the minor agostic in rhodium *iso*-propyl complex **13** to 174.1° for rhodium *iso*-butyl complex **15**. Also observed is an increased linearity of the M-H-C interaction with the *iso*-butyl complexes, approaching 160° for **15** and 140° for **20** (calculated hydrogen positions) as contrasting the *ca.* 125° for **13** and **18**.

The deviation of the metal-phosphine geometry away from an idealised octahedron can be used to garner further information pertaining to the agostic interaction. This property is quantified here by the angle  $\angle \text{P-npln}$ ; that between the M-P vector and the normal vector to the plane described by the biphenyl metallocycle. Looking solely at the major agostic interaction in each complex, this metric shows the *iso*-butyl systems to be the least distorted (5.28(7)° and 6.71(10)° for **15** and **20**, respectively), the *iso*-propyl systems the most distorted (9.00(6)° and 10.35(17)° for **13** and **18**, respectively), with the cyclohexyl systems as the intermediate case (8.04(6)° and 8.88(6)° for **12** and **17** respectively). The phosphines bearing the minor agostic interaction are not distorted by more than *ca.* 6.6°, and in all cases the directionality of the distortion is away from the biphenyl moiety, facilitating a closer approach of the agostic C-H bond to the metal centre for the tri-*iso*-propyl and tricyclohexyl complexes. The *iso*-butyl substituent meanwhile is suitably flexible and possesses a long enough carbon chain to satisfy a stabilising agostic interaction without distortion of the metal-phosphine geometry.

The inclusion of solvent in the unit cell of tricyclohexyl complexes **12** and **17** opens an avenue for the interrogation of the effect of crystal packing on the solid-state metrics associated with agostic interactions. Diffusion of pentane into solutions of **12** and **17** in 1,2-difluorobenzene afforded crystalline solids found to contain a molecule of



1,2-difluorobenzene in place of dichloromethane. The cell volumes of these crystals are *ca.* 2% larger, but not as large as would be expected for the increase in solvent volume; the dichloromethane solvent void comprises 5.5% – 6.0% of the unit cell, while the fluorobenzene void represents 8.6% – 8.9% of the unit cell (Mercury 3.9, 1.2 Å probe radius, 0.2 Å grid). That is to say, the contents of the cell are relatively more compressed with the larger solvent.

Normalising for the solvent void, a compression of the unit cell by 1.1% for **12** resulted in shorter Rh-C contacts by 0.013(11) Å (Rh-C21) and 0.022(11) Å (Rh-C31); while a compression of 1.2% for **17** resulted in Ir-C contractions of 0.015(13) Å (Ir1-C21) and 0.019(11) Å (Ir1-C31). Additional data was obtained by cooling the four samples to 25 K, affording further compression of the lattice. Again, normalised for the solvent void, compressions of 1.5% (**12**, CH<sub>2</sub>Cl<sub>2</sub>), 1.3% (**12**, 1,2-difluorobenzene), 1.8% (**17**, CH<sub>2</sub>Cl<sub>2</sub>), and 1.0% (**17**, 1,2-difluorobenzene) were achieved, resulted in shorter M-C contacts, the most dramatic changes expressed by the dichloromethane included structures of 0.023(15) and 0.020(13) Å for **12** and **17** respectively. Plotting these data, Figure 2.8, a positive correlation may be drawn between cell volume and the observed M-C contact. Similar conclusions has been made with uranium complexes featuring agostic interactions, in which the cell volume mas modulated via variable-pressure X-ray crystallography.<sup>264</sup>

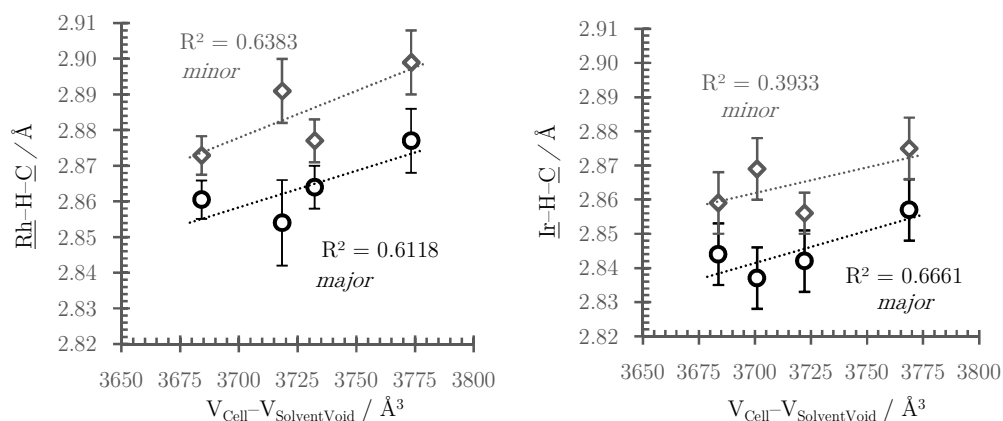


**Figure 2.8** Changes in  $\text{M-H-C}$  bond length tricyclohexylphosphine complexes **12** ( $\text{M} = \text{Rh}$ , left) and **17** ( $\text{M} = \text{Ir}$ , right) with solid-state molecular volume.

## 2.2.4 Solution characterisation

In dichloromethane solution complexes **11** – **20** are all  $C_{2v}$  symmetric at 298 K, and there is no indication of any upfield resonance characteristic of a static agostic interaction. Incremental cooling to 185 K of trialkylphosphine complexes **12** – **14** and **17** – **19** results in the onset of signal decoalescence of the alkyl  $^1\text{H}$  resonances, Figure 2.9, though in no case is the slow-exchange regime reached within the working temperature range of the solvent, precluding a quantitative analysis of the data. Despite this, qualitative trends are extractable by inspection of the developing line shapes of the alkyl resonances on cooling. The observed line broadening begins to occur at higher temperatures for the iridium complexes, comparing respective phosphines. For example, with the tri-*iso*-butyl complexes, the onset of decoalescence of the terminal  $\text{CH}_3$  resonance occurs at 200 K with the rhodium congener **14**, but at 225 K with iridium complex **19**. This holds for all phosphines and is consistent with the solid-state data. Comparing across the phosphine ligands, the onset of decoalescence occurs in the order tri-*iso*-butylphosphine > tricyclohexylphosphine > tri-*iso*-propylphosphine. This trend is not wholly in line with the conclusions drawn from the solid-state data, however mitigating factors such as phosphine distortion and the greater rigidity of the tricyclohexylphosphine ligand may serve to expedite the approach to a slow-exchange regime.

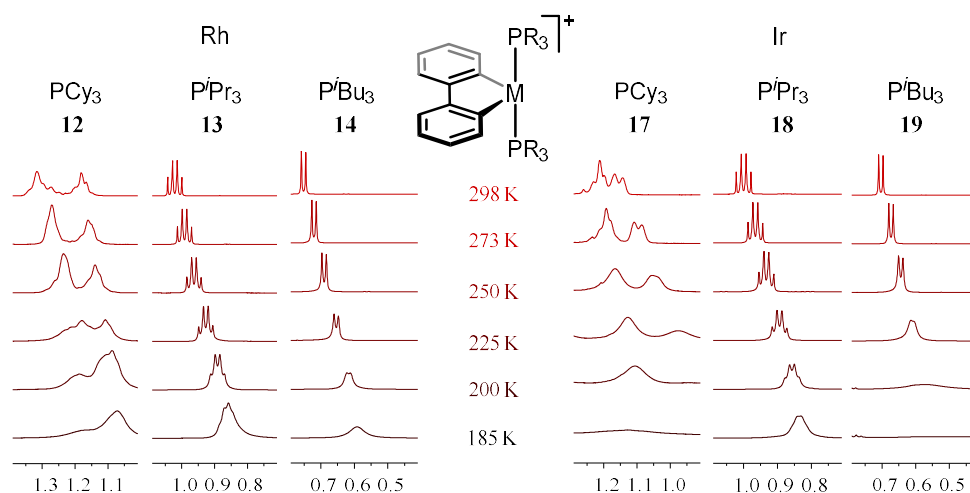


**Figure 2.9**  $^1\text{H}$  NMR spectra ( $\text{CD}_2\text{Cl}_2$ , 500 MHz) focussing on the terminal alkyl signals of rhodium complexes **12** – **14** and iridium complexes **17** – **19** at 298 – 185 K.

No dichloromethane binding was noted with triphenylphosphine complexes **11** and **16** through the 298 – 185 K temperature range. At 185 K decoalescence of the phenyl  $^1\text{H}$  resonances was observed, attributed to hindered rotation of the P-Ph bond, with the most profound change present for rhodium complex **11** where a 3H upfield signal at  $\delta_{\text{IH}}$  6.02 assigned as an *ortho*-phenyl proton resonance is detected. A significant NOE correlation with the 6,6'-biphenyl<sup>¶</sup> resonance suggest that these phenyl protons are in proximity to the metal centre, possibly associated with a transient agostic interaction.

## 2.2.5 Computational investigations

Calculations were performed on the cationic components of complexes **11** – **20** (DFT, PBE0/def2-TZVP). With  $[\text{M}(2,2'\text{-biphenyl})(\text{PPh}_3)_2]^+$  the binding of dichloromethane was found to be entropically disfavoured, in line with experimental observations, with  $\Delta H = -21.8$  and  $-25.1 \text{ kJ}\cdot\text{mol}^{-1}$  and  $\Delta G_{298\text{K}} = +38.7$  and  $+39.3 \text{ kJ}\cdot\text{mol}^{-1}$  for rhodium and iridium, respectively. Optimised geometries of the triphenylphosphine complexes in the absence of bound dichloromethane indicate distortion of the phosphine;  $\angle\text{P-M-P} = 166.3^\circ$  and  $164.8^\circ$  for rhodium and iridium, respectively, projecting the C-H bonds towards the metal, though the M-C contacts remain distant at 3.1833 Å and 3.2721 Å for rhodium and at 3.2430 Å and 3.2449 Å for iridium respectively.

NBO analysis of the M-H-C interactions substantiated a three-centre-two-electron bonding interaction by considerable 2<sup>nd</sup> order perturbation energies corresponding to the typical donation - retrodonation analysis. Figure 2.10 illustrates an example of the component orbitals analysed, Table 2.2 collates the perturbation energies. The energies associated with the triphenylphosphine cations and with the minor interaction in rhodium tri-*iso*-propylphosphine cation are small, again consistent with the weak agostic interactions indicated by the solution and solid-state data. The trend of higher

---

<sup>¶</sup> The C-H group adjacent to the metal-carbon linkage. The biphenyl ligand is numbered throughout such that 1-biphenyl is the metal-bound carbon, 2-biphenyl is the C-C linkage, and so on. This is at odds with some literature conventions, but was chosen for consistency with the 2,2'-bipyridyl ligand employed later.

perturbation energies associated with the iridium systems and with phosphine substituents in the order cyclohexyl < *iso*-propyl < *iso*-butyl is also reaffirmed.

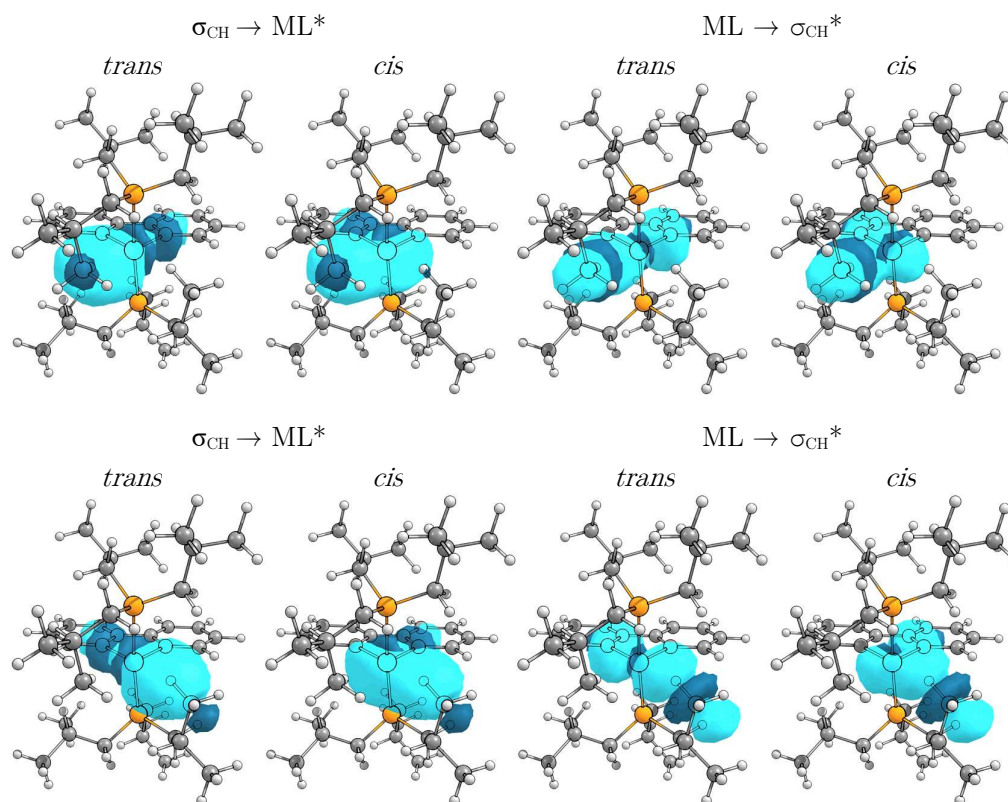


**Figure 2.10** Exemplar NBO orbital overlaps (isosurface value 0.04) for interactions of M(2,2'-biphenyl) based orbitals ML and ML\* with  $\sigma$ -CH and  $\sigma^*$ -CH orbitals for the  $[\text{Rh}(2,2'\text{-biphenyl})(\text{P}^t\text{Bu}_3)_2]^+$  cation: top row, the major interaction; bottom row, the minor interaction.

**Table 2.2** NBO perturbation energies <sup>a</sup> / kJ·mol<sup>-1</sup> for  $[\text{M}(2,2'\text{-biphenyl})(\text{PR}_3)_2]^+$

M	R	Major interaction		Minor interaction		Total
		$\sigma_{\text{CH}} \rightarrow \text{ML}^*$	$\text{ML} \rightarrow \sigma_{\text{CH}}^*$	$\sigma_{\text{CH}} \rightarrow \text{ML}^*$	$\text{ML} \rightarrow \sigma_{\text{CH}}^*$	
Rh	Ph	4.50	2.11	4.88	<0.2	11.5
	Cy	34.1	15.2	25.8	16.8	91.8
	<i><sup>t</sup></i> Pr	37.6	12.3	8.21	8.00	66.2
	<i><sup>t</sup></i> Bu	62.8	30.2	48.7	39.9	181.6
Ir	Ph	6.95	2.7	6.90	7.2	23.8
	Cy	44.8	25.6	42.3	28.5	141.3
	<i><sup>t</sup></i> Pr	49.5	14.2	13.9	15.0	92.6
	<i><sup>t</sup></i> Bu	80.8	45.5	71.3	70.3	267.9

<sup>a</sup> Perturbation energies resulting from the interactions of  $\sigma$ -CH and  $\sigma^*$ -CH orbitals with M(2,2'-biphenyl) based orbitals ML and ML\*, summed over *cis* and *trans* contributions (*cf.* Figure 2.10).

Analysis of the topology of the electron density via the QTAIM approach elicits the characteristic curved bond path associated with agostic interactions.<sup>265</sup> At least one (of a possible two) M–H bond and M–P–C(–C)–C–H–M ring critical points are located for all trialkylphosphine complexes, with corresponding electron densities,  $\rho_{\text{MH}}$ , ranging from 0.027 – 0.051 au for the major interactions and 0.017 – 0.041 au for the minor interaction, Table 2.3. For frame of reference, an electron density of 0.035 corresponds roughly to a bond order of *ca.* 0.15 by a QTAIM delocalisation index approach.<sup>266</sup> The chemical literature generally associates densities greater than 0.035 au with agostic interactions,<sup>267–269</sup> and those less 0.035 au for a hydrogen bond set up.<sup>270</sup> This has the effect of conflating weak agostic interaction with the hydrogen bond, indeed major interactions of the rhodium *iso*-propyl, rhodium and iridium *iso*-butyl, and the minor agostic of the iridium *iso*-butyl fit this criterion. Across the series the iridium complexes possess greater M–H electron densities, and the trend in alkyl group proceeds cyclohexyl < *iso*-propyl < *iso*-butyl, in line with the solid-state experimental data. The electron density of the corresponding C–H bond itself is reduced following a parallel trend, which may be used to extrapolate the strength of the minor *iso*-propyl interaction intermediate to that cyclohexyl and phenyl.

**Table 2.3** QTAIM bond critical point properties <sup>a</sup> for [M(2,2'-biphenyl)(PR<sub>3</sub>)<sub>2</sub>]<sup>+</sup>

M	R	Major interaction				Minor interaction			
		$\rho_{\text{MH}}$	$\nabla^2\rho_{\text{MH}}$	$\rho_{\text{CH}}$	$\nabla^2\rho_{\text{CH}}$	$\rho_{\text{MH}}$	$\nabla^2\rho_{\text{MH}}$	$\rho_{\text{CH}}$	$\nabla^2\rho_{\text{CH}}$
Rh	Ph	-	-	0.282	-0.994	-	-	0.282	-0.991
	Cy	0.027	+0.102	0.261	-0.847	0.024	+0.081	0.263	-0.856
	Pr	0.027	+0.107	0.261	-0.846	-	-	0.270	-0.898
	Bu	0.039	+0.158	0.254	-0.795	0.032	+0.124	0.256	-0.807
Ir	Ph	-	-	0.283	-0.998	-	-	0.280	-0.978
	Cy	0.034	+0.118	0.254	-0.802	0.033	+0.113	0.254	-0.800
	Pr	0.035	+0.130	0.255	-0.805	0.017	+0.049	0.267	-0.878
	Bu	0.051	+0.167	0.246	-0.749	0.041	+0.139	0.249	-0.766

<sup>a</sup> Data in atomic units.

## 2.3 Intramolecular Rh-F-C interactions

### 2.3.1 Preamble

Capitalising on the established utility of the 2,2'-biphenyl ancillary ligand to stabilise agostic interactions, it was reasoned that by introducing a fluorinated phosphine ligand the 2,2'-biphenyl supported systems could serve as a useful platform on which to study the M-F-C interaction. This work exclusively deals with rhodium chemistry, a metal with which interactions with alkyl fluorides has not been documented previously. Rhodium also offers the benefit of being a 100% spin  $\frac{1}{2}$  nuclei, providing a helpful NMR handle in concert with fluorine and phosphorous for gauging the Rh-F-C interaction.<sup>¶</sup> The known phosphine  $\text{PPh}_2\text{Tol}^{\text{F}}$  ( $\text{Tol}^{\text{F}}$  = 2-trifluoromethylphenyl) was selected as the ligand in this study, deemed to offer sufficient conformational flexibility so as not to enforce an interaction, and possessing a similar steric profile to triphenylphosphine.

### 2.3.2 Preparation

The fluorinated phosphine  $\text{PPh}_2\text{Tol}^{\text{F}}$  was reacted with  $[\text{Rh}(2,2\text{-biphenyl})(\text{dtbpm})\text{Cl}]$  **1** in dichloromethane per the procedure set out in Section 2.2. Unexpectedly, this resulted in an equilibrium mixture of precursor **1**, dimeric  $[\{\text{Rh}(2,2'\text{-biphenyl})(\text{PPh}_2\text{Tol}^{\text{F}})\text{Cl}\}_2]$ , **21**, and a species formulated as bis(phosphine) chloride **22**, in a 1.0 : 2.7 : 1.6 ratio, when two equivalents of fluorinated phosphine were used (Figure 2.11). This equilibrium is driven in favour of **22** by the addition of excess phosphine. Dimer **21** is poorly soluble in dichloromethane, precipitating as a microcrystalline solid, and isolated in 82% yield. Use of isolated dimer **21** allowed access to coordination compounds with donor functionality featuring contrasting electronic and steric profiles; reaction with  $\text{PPh}_2\text{Tol}^{\text{F}}$ , 2,2'-bipyridyl, Na[acac] or Na[Cp] (with a halide abstracting agent as appropriate) in dichloromethane solution afforded compounds **23** – **26**, isolated in 87%, 85%, 75% and 13% yields, respectively, as crystalline solids suitable for X-ray analysis.

---

<sup>¶</sup> Dr I. Prokes collected the low-temperature NMR data discussed in this section. See page viii for affiliation.

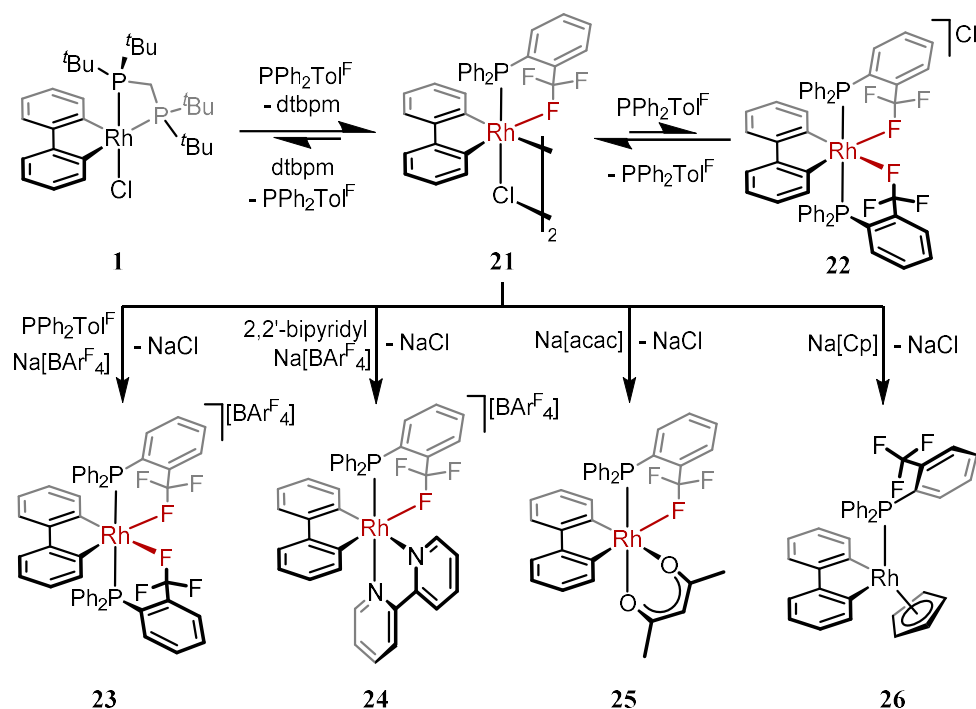
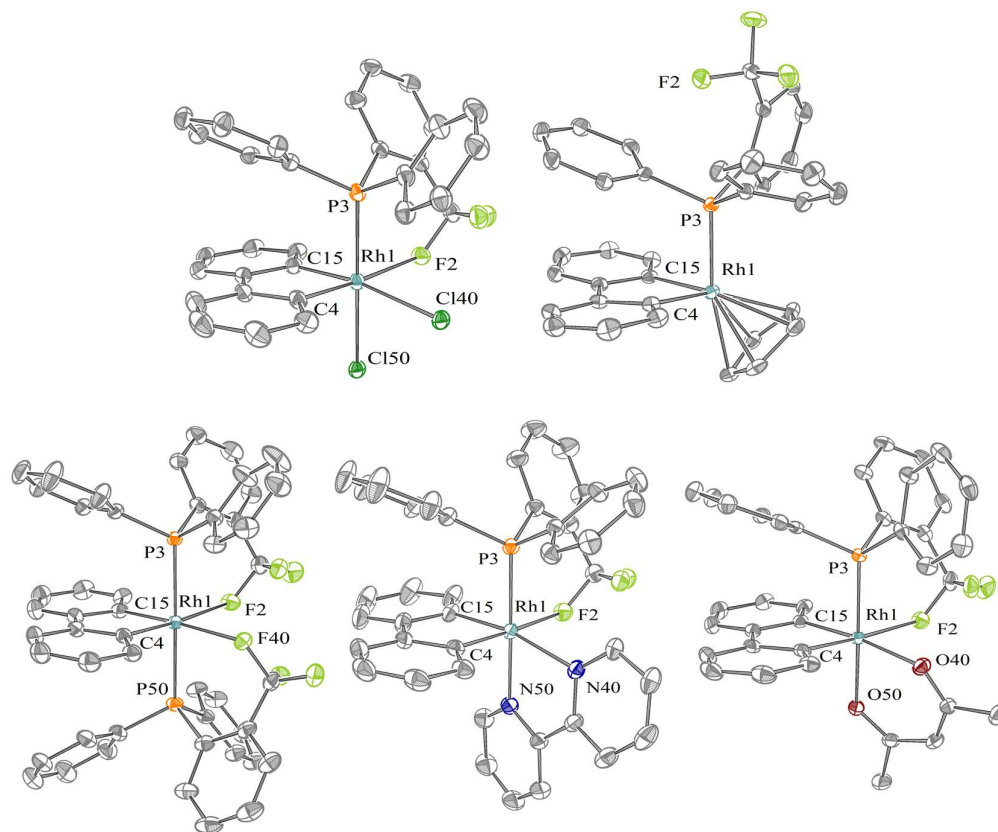


**Figure 2.11** Preparation of complexes of PPh<sub>2</sub>Tol<sup>F</sup>. Conditions: CH<sub>2</sub>Cl<sub>2</sub>, ambient temperature, 18 hours.

### 2.3.3 Solid-state characterisation

The solid-state structures of compounds **21**, **23**, **24** and **25**, Table 2.4, all exhibit coordination of the pendant CF<sub>3</sub> group in a  $\kappa^1$ -F manner. The fluorine atom completes an octahedral coordination sphere, with C-Rh-F bond angles close to linear ( $173.00(9)^\circ$  –  $177.53(6)^\circ$ ) and the phosphorous atom near perpendicular with respect to rhodacycle plane. Rh-F contacts are in the range  $2.362(2) - 2.450(1)$  Å, *cf.*  $2.367(3) - 3.309(9)$  Å for the intramolecular platinum group M-F-C interactions summarised in Section 1.3.2. The closest Rh-F contacts are exhibited by cationic complexes **23** and **24**, which are  $0.05 - 0.10$  Å shorter than the Rh-F contact present in neutral complexes **21** and **25**. An elongation of  $0.04$  Å of the C-F bond of the interacting fluorine atom compared to the two non-interacting C-F bonds is also noteworthy, and consistent with literature precedents for other platinum group metals (Section 1.3.2). With saturated compound **26** the CF<sub>3</sub> group is projected entirely away from the metal, demonstrating the propensity for free rotation about the P-Tol<sup>F</sup> bond, such that the interactions observed in **21**, **23**, **24** and **25** are shown to not be enforced by the ligand environment.

**Table 2.4** Selected bond lengths (Å) and angles (°) of **21**, **23** – **25** at 150 K. Thermal ellipsoids at 30%. Unique component of centrosymmetric **21** only. minor disordered components, and [BARF<sub>4</sub>] anions omitted.



	<b>21</b> L = Cl	<b>23</b> L = P	<b>24</b> L <sub>2</sub> = bipy	<b>25</b> L <sub>2</sub> = acac	<b>26</b> L <sub>3</sub> = Cp
<b>Rh1-F2</b>	2.459(2)	2.402(1)	2.362(2) 2.370(2) <sup>b</sup>	2.426(1) 2.450(1) <sup>b</sup>	5.4334(9)
<b>Rh1-C4</b>	1.992(3)	1.991(2)	1.993(3) 1.994(3) <sup>b</sup>	1.977(2) 1.979(2) <sup>b</sup>	2.0307(14)
<b>Rh1-C15</b>	2.004(3)	1.992(2)	2.012(3) 2.013(3) <sup>b</sup>	2.000(2) 2.003(2) <sup>b</sup>	2.0372(16)
<b>Rh1-P3</b>	2.2492(9)	2.3625(8)	2.2777(7) 2.2771(7) <sup>b</sup>	2.2325(5) 2.2419(5) <sup>b</sup>	2.2692(5)
<b>Rh1-L40</b>	2.4999(9)	2.408(1)	2.215(2) 2.212(2) <sup>b</sup>	2.127(1) 2.133(1) <sup>b</sup>	-
<b>Rh1-L50</b>	2.4032(8)	2.3665(8)	2.115(2) 2.116(2) <sup>b</sup>	2.086(1) 2.078(1) <sup>b</sup>	-
<b>F-Rh1-C</b>	175.9(1)	176.16(7) 175.87(7) <sup>c</sup>	173.47(9) 173.00(9) <sup>b</sup>	177.53(6) 177.40(6) <sup>b</sup>	-
<b>P-Rh1-cent<sup>a</sup></b>	89.90(4)	88.86(4) 90.49(4) <sup>c</sup>	87.92(4) 88.37(4) <sup>b</sup>	88.97(3) 90.21(3) <sup>b</sup>	88.02(3)

<sup>a</sup> Centroid of the five-membered biphenyl rhodacycle; <sup>b</sup> alternate cation (Z' = 2); <sup>c</sup> relating to closer C-F.



### 2.3.4 Solution characterisation

In solution compounds **21** – **25** exhibit time-averaged Rh-F interactions, such that in each complex all fluorine atoms are magnetically equivalent. Accordingly, the  $^{31}\text{P}\{^1\text{H}\}$  NMR spectra of the mono-phosphine complexes **21**, **24** and **25** appear as a doublet of quartets, and bisphosphine **23** as a doublet of heptets, all with  $^1J_{\text{RhP}}$  coupling in the range 124 – 170 Hz and  $^2J_{\text{PF}}$  coupling of 4 – 6 Hz. The corresponding  $^{19}\text{F}\{^1\text{H}\}$  resonances are resolved as apparent triplets (**21**, **24**, **25**) or an apparent quartet (**23**) each with approximately equal  $^1J_{\text{RhF}}$  and  $^2J_{\text{PF}}$  coupling of *ca.* 5 Hz. Cyclopentadienyl complex **26** is expectedly devoid of any variety of P-F or Rh-F coupling, while chloride salt **22** exhibits spectra analogous to its  $[\text{BAr}^{\text{F}}_4]$  analogue **23**, though with reduced  $^2J_{\text{PF}}$  and  $^1J_{\text{RhF}}$  coupling constants, likely a consequence of access to additional exchange processes involving the coordinating chloride anion.

At room temperature, the coordination spheres of complexes **21** – **26** are dynamic on the NMR time scale (400 – 500 MHz), expressing  $C_{2v}$  (**23**) or  $C_s$  (**21**, **24** – **26**) symmetry in their respective  $^1\text{H}$  NMR spectra, implying that the  $\text{CF}_3$  moiety is undergoing rapid dissociation-association with the rhodium centre via a conformationally fluxional 5-coordinate intermediate, Figure 2.12, (a) and (b). In complex **25** each side of the acac ligand is equivalent at room temperature (see also Figure 2.13), suggesting the it is able to rotate via an intermediate in which the acac component is co-planar with the 2,2'-biphenyl ligand, Figure 2.12, (c). By contrast, in complex **24** each pyridyl unit is inequivalent at room temperature, and the 2,2-biphenyl moiety elicits broad  $^1\text{H}$  resonances. Two interpretations of these data are possible, that the Rh-F-C interaction is particularly strong in **24**, or more likely that the steric bulk of the 2,2'-bipyridyl ligand is presenting an obstacle to interconversion of the square pyramidal intermediates following Rh-F dissociation. A final dynamic process to consider is the rapid pinwheeling of the  $\text{CF}_3$  moiety, Figure 2.12, (d), which is reasonably hypothesised as the lowest energy process of those outlined. Not considered here are any exchange events involving full dissociation of the relatively electron-poor phosphine ligand.

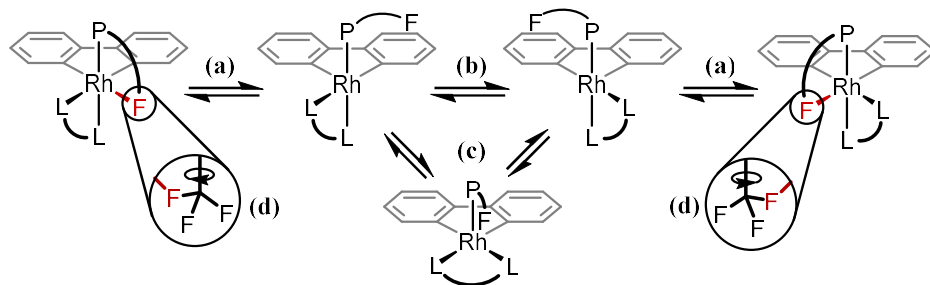


**Figure 2.12** Pertinent dynamic exchange processes accessible to complexes **21** – **25** (*see text*).

To garner insight into the aforementioned dynamics, and to seek some quantification of the thermodynamic parameters associated with fluorine coordination, solutions of complexes **23** – **26** in dichloromethane were incrementally cooled to 185 K. The resulting  $^1\text{H}$  NMR spectra (400 MHz) of **24** and **25**, Figure 2.13, both show full signal decoalescence to  $C_1$  symmetric structures. With acac system **25** the onset of signal decoalescence occurs between 250 and 225 K. In spectra of 2,2'-bipyridyl complex **24** this decoalescence is fully realised by 225 K, with further cooling resulting in substantial broadening of the phenyl resonances of bisphosphine **23**.

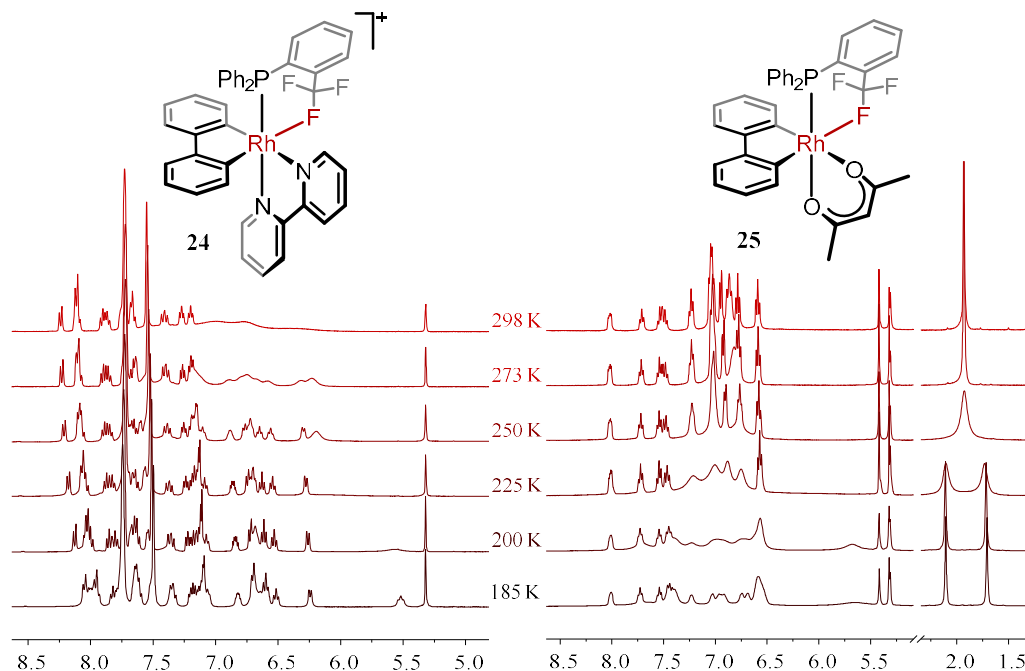


**Figure 2.13**  $^1\text{H}$  NMR spectra ( $\text{CD}_2\text{Cl}_2$ , 400 MHz) of **24** and **25** at 298 – 185 K.

Through the same temperature course, the  $^{19}\text{F}\{^1\text{H}\}$  resonances of all systems examined begin to exhibit notable and system-specific line broadening, Figure 2.14. While in no instance is the slow-exchange regime reached, the enthalpy barriers to the exchange events can be estimated via a pseudo-Eyring analysis. By such analysis, the barriers to exchange are determined to be smallest for **26**, then increasing in the order **25** < **23** < **24** with corresponding enthalpies of  $\Delta H^\ddagger = 9.6(11)$ ,  $12.6(13)$ ,  $17.6(14)$  and  $21.4(7)$   $\text{kJ}\cdot\text{mol}^{-1}$ , respectively. These parameters quantify the perturbation in the pinwheeling rotation barriers of the  $\text{CF}_3$  group, ostensibly due to the interaction with the rhodium centre. Markedly stronger M-F-C interactions are therefore indicated for cationic complexes **23** and **24**, consistent with the solid-state data. Indeed the trend in estimated enthalpies shows a direct correlation with the Rh-F contacts determined in the solid state.

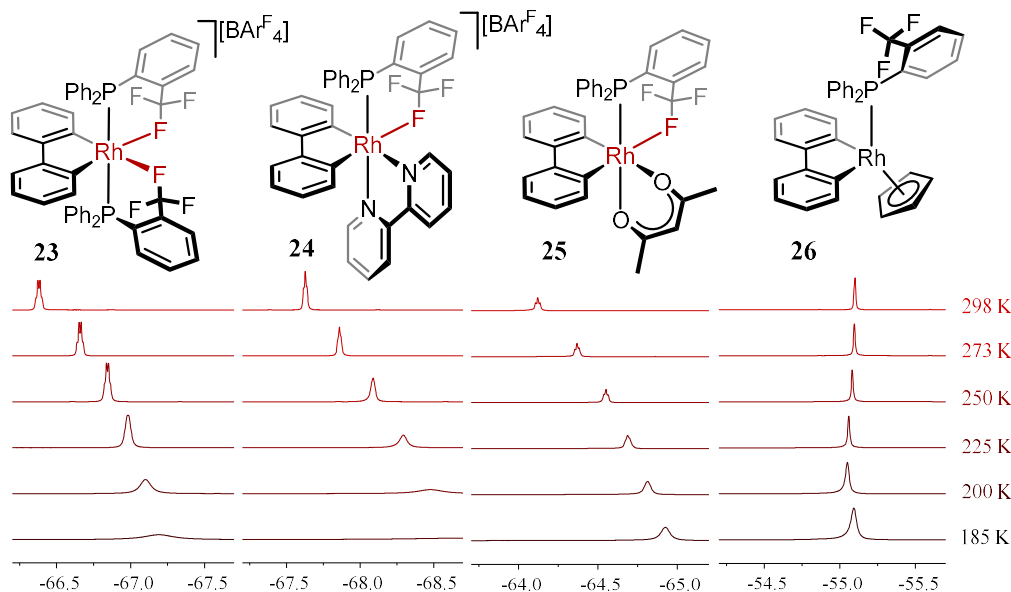


**Figure 2.14**  $^{19}\text{F}\{^1\text{H}\}$  NMR spectra ( $\text{CD}_2\text{Cl}_2$ , 376 MHz) of **23** – **26** at 298 – 185 K.

## 2.4 Intermolecular reactivity

### 2.4.1 Preamble

It has been demonstrated in the preceding section that  $[M(2,2'\text{-biphenyl})(PPh_3)_2][BAr^F_4]$  complexes, **11** ( $M = Rh$ ) and **16** ( $M = Ir$ ), exhibit only very weak agostic stabilisation from the ligand periphery, such that in the solid state these systems are observed as  $\kappa^1$ -dichloromethane complexes. Investigations into the intermolecular behaviour of the 2,2'-biphenyl based systems will thus centre on triphenylphosphine-based compounds. The requisite information for informing the work in subsequent chapters involves determining: (1) which substrates elicit a persistent interaction with  $[M(2,2'\text{-biphenyl})(PPh_3)_2]^+$ ; (2) the behaviour of  $[M(2,2'\text{-biphenyl})(PPh_3)_2]^+$  in a range of solvents; (3) how chemically robust the 2,2'-biphenyl ligand is; and (4) the lability of the phosphine ligands.

### 2.4.2 Small molecule and solvent adducts

The dichloromethane adducts of **11** and **16** have been discussed in Section 2.2. The dichloromethane ligand is determined to be labile in solution with no persistent coordination observed spectroscopically, while a solitary molecule of dichloromethane is coordinated on isolation of **11** and **16** as either crystalline or amorphous material. Further to these findings, isolated solid material of **11** when dissolved in fluorobenzene is observed by  $^1H$  NMR spectroscopy with a stoichiometric quantity of free dichloromethane. Fluorobenzene is a far poorer donor than dichloromethane in these systems; and it is worth reinforcing that given the nature of the constituent ligands of **11** and **16** that any fluorobenzene interaction is necessarily either  $\kappa^1$ -F,  $\kappa^2$ -F-C or  $\eta^2$ -arene in nature, of which there are no reported Group 9 examples.<sup>102</sup>

If insufficiently anhydrous solvents are used in the preparation of **11** or **16** these systems will preferentially form mono(aqua) complexes;  $[M(2,2'\text{-biphenyl})(PPh_3)_2(OH_2)][BAr^F_4]$ , **27** ( $M = Rh$ ) and **28** ( $M = Ir$ ), Figure 2.15. Analogous to the dichloromethane adducts,

these compounds adopt near-idealised square pyramidal coordination geometries; with C4-M-O80 bond angles of 176.03(9)° and 174.8(1)° for **27** and **28** respectively, and P-M-cnt(rhodacycle) angles in the range 89.4° – 92.6°. The M-P and M-O distances are only slightly elongated with the iridium congener, by *ca.* 0.01 Å in both cases.

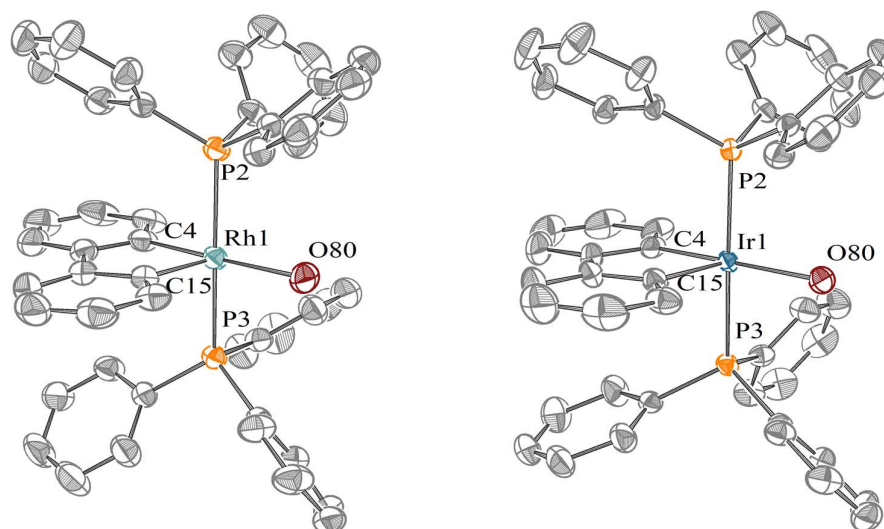


**Figure 2.15** Solid-state structures of water adducts **27** (left, M = Rh) and **28** (right, M = Ir). Data at 150 K, thermal ellipsoids drawn at 50%, [BAr<sup>F</sup><sub>4</sub>] anions omitted. Selected bond lengths (Å) and angles (°): **27**; Rh1-O80, 2.244(2); Rh1-P2, 2.3401(6), Rh1-P3, 2.3339(5); Rh-C4, 2.000(3); Rh-C15, 1.991(2); O80-Rh1-C4, 176.03(9); P2-Rh1-cnt(rhodacycle), 91.59(4); P3-Rh1-cnt(rhodacycle), 89.48(4). **28**; Ir1-O80, 2.232(3); Ir1-P2, 2.3329(7); Ir1-P3, 2.3225(7); Ir-C4, 2.009(3); Ir-C15, 2.006(3); O-Ir-C4, 174.8(1); P2-Ir1-cnt(iridacycle), 92.20(5); P2-Ir1-cnt(iridacycle) 89.38(5).

The coordinated water in **27** and **28** is observed in dichloromethane solution at room temperature by <sup>1</sup>H NMR spectroscopy courtesy of distinctive resonances at  $\delta_{\text{IH}}$  2.44 and  $\delta_{\text{IH}}$  2.34 for the rhodium and iridium complexes, respectively, consistent with the high relative binding strength of the aqua ligand; *cf.* the absence of any characteristic bound dichloromethane signal at low temperature or in alternative solvent for complexes **11** or **16**. The water ligand is demonstrated to be in fast exchange in solution, with the resulting <sup>31</sup>P{<sup>1</sup>H} resonance shifted depending on the concentration of water in solution. Removal of the bound water is thus a facile procedure; brief agitation (< 5 minutes) over 3 Å molecular sieves is sufficient to revert the system to exclusively low-coordinate compounds **11** and **16**.

Rhodium water complex **27** may be prepared in near quantitative yield by the addition of excess water to dichloromethane solutions of **11**, or by deliberate use of undried solvents. Under these conditions the iridium congener demonstrated unidentified onward reactivity, resulting in intractable reaction mixtures. This, coupled with the instability of iridium complex **16** in dichloromethane solution, restricted subsequent investigations solely to complexes of rhodium. For the purposes of comparison and for synthetic purtenance to compounds described in Chapter 3, the  $[\text{Al}(\text{OR}^{\text{F}})_4]^-$  salt **29** was prepared using  $\text{Li}[\text{Al}(\text{OR}^{\text{F}})_4]$  in place of  $\text{Na}[\text{BAr}^{\text{F}}_4]$ , and allowed to proceed to the analogous water complex **30** in either a one or two pot procedure, Figure 2.16. Salts of the two anions are spectroscopically similar with respect to the cation  $^1\text{H}$ ,  $^{31}\text{P}$  and  $^{13}\text{C}$  resonances. Water complex **30** is visibly  $C_{2v}$  symmetric, associated with rapid interconversion of the square pyramidal configurations, and possesses a  $^{31}\text{P}\{^1\text{H}\}$  NMR spectrum with a downfield shifted doublet resonance at  $\delta_{^{31}\text{P}}$  22.7 ( $^1J_{\text{RhP}} = 119$  Hz), relative to **29** at  $\delta$  20.3 ( $^1J_{\text{RhP}} = 118$  Hz).

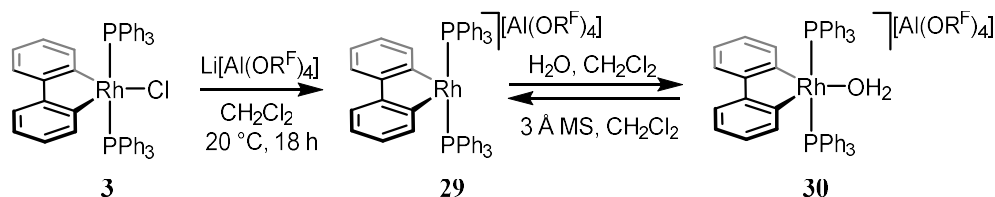


**Figure 2.16** Preparation of complexes **29** and **30** and their interconversion.

Irreversible water abstraction presents an opportunity to use alternative solvent environments in the absence of a stoichiometric amount of dichloromethane. In fluorobenzene under an argon atmosphere the loss of water from complex **30** was found to be slow, progressing to 80% completion after one hour of agitation over 1000 wt% 3 Å molecular sieves, *cf.* the essentially instantaneous desiccation that results in dichloromethane. A species devoid of bound water and assigned as complex **29** was prepared within 5 hours via this method. The  $^1\text{H}$ ,  $^{19}\text{F}\{^1\text{H}\}$  and  $^{31}\text{P}\{^1\text{H}\}$  NMR spectra are generally unremarkable, aside from minor chemical shift changes in the  $^1\text{H}$  NMR of the biphenyl resonances. Cooling a sample of **29** in fluorobenzene solution to 230 K results in subtle line broadening of the biphenyl and phenyl resonances. At 230 K

additional broad signals in the range  $\delta_{\text{H}}$  5.4 – 6.4 begin to appear; these presumably originate from the beginnings of hindered rotation of the phenyl moiety, a consequence of transient agostic interaction much like those described in dichloromethane solution for  $[\text{BAr}^{\text{F}}_4]^-$  salt **11** (Section 2.2.4), though here observed at a much higher temperature by virtue of the use of a less strongly competing solvent.

Removal of the water ligand from **30** in fluorobenzene by 3 Å molecular sieves is greatly accelerated when conducting the reaction under an atmosphere of dinitrogen, progressing to 100% conversion within an hour under the same conditions as those just described. Solutions of low-coordinate **29** in fluorobenzene under argon and under dinitrogen are indistinguishable down to 230 K, suggesting only a transient coordination of dinitrogen, but one that is sufficient to facilitate accelerated substitution of the aqua ligand of complex **30**. Based on these findings, a mechanism for ligand substitution mechanism is proposed, Figure 2.17. In this regime dissociative ligand substitution is disfavoured, and instead dynamic water exchange proceeds either associatively via a transient 6-coordinate intermediate, or in a concerted manner. In fluorobenzene alone the weak donor properties of the solvent results in a slow water exchange, while with access to a stronger donor, be this dinitrogen or dichloromethane, the rate of water substitution and by extension the desiccation of the system by 3 Å molecular sieves is accelerated. This manifold thus provides a lower energy path for the substitution while maintaining the water adduct as the resting state of the system.

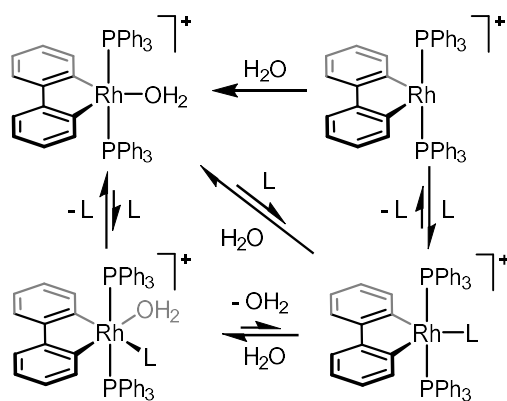


**Figure 2.17** Proposed ligand exchange pathway for biphenyl-based systems.

Switching to the stronger donor solvent THF, water substitution is observed in the absence of 3 Å molecular sieves, resulting within 5 minutes in a 3 : 17 equilibrium mixture of water complex **30** and a species assigned as THF adduct **31**. A corresponding equilibrium constant of  $7.8 \times 10^{-3}$  is thus determined in favour of the water complex, placing THF at an intermediate binding strength to water and dichloromethane. Addition of sieves drives the equilibrium to THF complex **31**, which was isolated and fully characterised. Crystalline material suitable for X-ray diffraction was prepared by the diffusion of hexane into THF solutions **31**, though extensive disorder of the  $[\text{Al}(\text{OR}^{\text{F}})_4]^-$  anion precluded the determination of precise structural metrics, Figure 2.18. The complex is in the archetypal square pyramidal coordination geometry, with contacts and bond angles generally similar to those of water complex **30**.

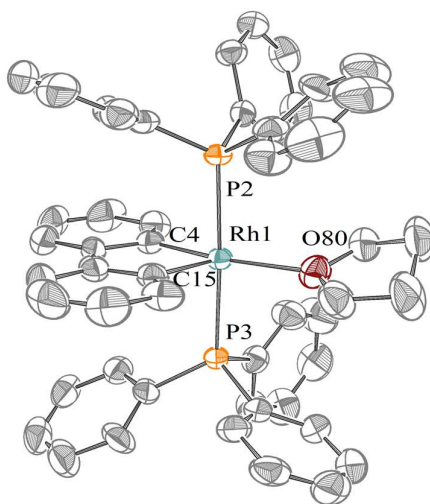


**Figure 2.18** Crystal structure of THF adduct **31**. Data at 150 K, thermal ellipsoids drawn at 50%. Extensive disorder of the  $[\text{Al}(\text{OR}^{\text{F}})_4]^-$  anion (omitted) precludes the determination of precise structural metrics. Selected approximate bond lengths (Å) and angles (°): Rh1-O80, 2.32; Rh1-P2, 2.35; Rh1-P3 2.34; Rh-C4, 2.00; Rh-C15, 2.00; O-Rh-C4, 169; P-Rh-cent(rhodacycle), 88.3, 89.2.

THF complex **31** is amenable to characterisation in both THF and dichloromethane solution. In the former the resultant NMR spectra are sharp, consistent with an equilibrium saturated towards THF coordination. The aromatic resonances are all well-defined in the  $^1\text{H}$  NMR spectrum, though signals associated with bound THF are not observed, potentially obscured by the dominating signals of the proteosolvent. In the  $^{31}\text{P}\{^1\text{H}\}$  NMR spectrum in THF solution a doublet resonance is observed at  $\delta_{31\text{P}}$  22.2



with a  $^1J_{\text{RhP}}$  coupling constant of 120 Hz. The signal is broad, with a line width of 16 Hz in the proton decoupled spectrum compared to, for example, 6 Hz for water complex **30**. In dichloromethane solution the line broadening of **31** is even more pronounced at 60 Hz, with the aromatic  $^1\text{H}$  resonances similarly broadened, especially those of the 2,2'-biphenyl ligand. These observations may be manifestations of some increased phosphine lability in the presence of THF, or indicative of dynamic THF - dichloromethane ligand exchange. Bound THF is evident in the  $^1\text{H}$  NMR spectrum in dichloromethane solution, though several additional THF-resembling signals are present as a minor component of the mixture (<10%) that are not convincingly assigned.

### 2.4.3 Hydrogenolysis of the 2,2'-biphenyl ligand

Reaction of **29** with dihydrogen was found to cleave the 2,2'-biphenyl ligand in a reaction which proceeded to completion within 4 hours, affording Rh(I) complex **32** featuring an  $\eta^6$ -coordinated biphenyl ligand, Figure 2.19. The reaction presumably proceeds initially via a  $\sigma$ -complex assisted metathesis rather than invoking a Rh(V) intermediate, though effective establishment of the four-membered transition state required for such a process would favour the dihydrogen ligand in an apical coordination site with respect to the biphenyl plane, Figure 2.19. Some degree of coordinative flexibility may be essential for this reaction to proceed, *vide infra*. Calculations on an imposed side on hydride insertion, carried out elsewhere for an iridium pincer complex, found the insertion to proceed through a highly distorted transition state.<sup>212</sup>

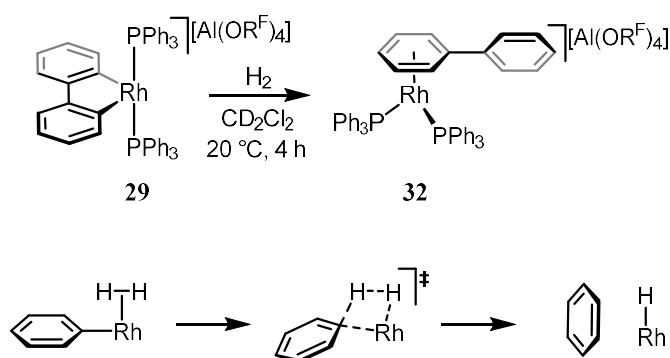


**Figure 2.19** Reaction of **29** with dihydrogen and an illustration of a hydride insertion transition state.

In solution the  $\eta^6$ -phenyl component of **32** is identifiable by a set of upfield resonances in the  $^1\text{H}$  NMR spectrum in the range  $\delta_{\text{IH}}$  5.64 – 5.29. The  $^{31}\text{P}\{^1\text{H}\}$  NMR spectrum diagnoses both the equivalency of the phosphine ligands and the Rh(I) oxidation state, courtesy of the 206 Hz  $^1J_{\text{RhP}}$  coupling constant. The preference for forming a Rh(I)  $\eta^6$ -aryl complex over a rhodium *trans*-phosphine *cis*-dihydride is a noted phenomenon,<sup>271,272</sup> and will be discussed in more detail in the Chapter 4. The solid-state structure of biphenyl complex **32**, Figure 2.20, illustrates the *cis*-phosphine coordination (P-Rh-P = 93.87(3)°), and the  $\eta^6$ -coordination of the biphenyl ligand, Rh-cnt = 1.8645(11).

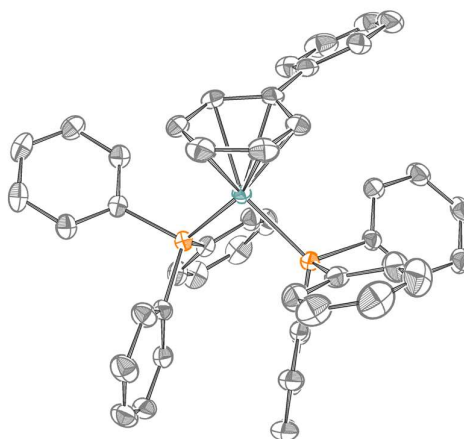


**Figure 2.20** Solid-state structure of  $\eta^6$ -biphenyl complex **32**. Data at 150 K, thermal ellipsoids drawn at 50%, [Al(OR<sup>F</sup>)<sub>4</sub>] anion and co-crystallised dichloromethane molecule omitted. Selected bond lengths (Å) and angles (°): Rh-P, 2.2627(5), 2.2462(9); Rh-cnt(biphenyl), 1.8645(11); P-Rh-P, 93.87(3); P-Rh-cnt(biphenyl), 131.25(5), 134.80(4); torsion(Ph-Ph) = 30.1(4).

#### 2.4.4 Carbonylation of the 2,2'-biphenyl ligand

Reaction of low-coordinate **29** or water complex **30** with carbon monoxide immediately affords a species characterised as bis(carbonyl) **33**, Figure 2.21. The  $^{31}\text{P}$  NMR spectrum comprises a solitary doublet at  $\delta_{31\text{P}}$  19.2 ( $^1J_{\text{RhP}}$  = 93 Hz), consistent with an electron poor Rh(III) species. The coordinated CO ligands are equivalent, appearing in the  $^{13}\text{C}\{^1\text{H}\}$  NMR spectrum as a relatively intense downfield doublet of triplets;  $\delta_{13\text{C}}$  185.9,  $^1J_{\text{RhC}}$  = 42 Hz,  $^2J_{\text{PC}}$  = 8 Hz. The rhodium-bound biphenyl carbons present with a drastically reduced  $^1J_{\text{RhC}}$  coupling constant of 23 Hz *cf.* a coupling constant of *ca.* 40 Hz for all other 2,2'-biphenyl complexes described thus far.

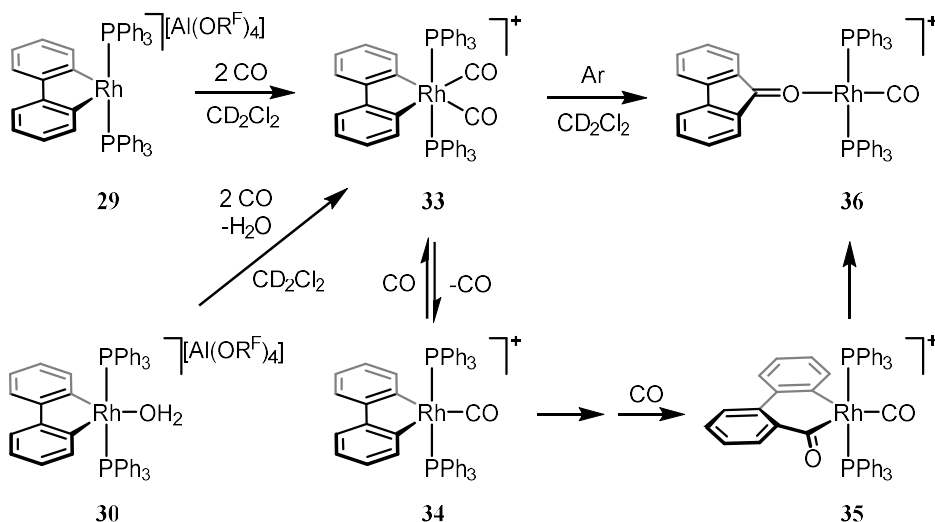


**Figure 2.21** Reaction of **29** with carbon monoxide and onward reactivity of the resultant bis carbonyl complex **33** in the absence of a carbon monoxide atmosphere to afford fluorenone adduct **34**.

Bis(carbonyl) **33** is only stable in solution under an atmosphere of carbon monoxide; under argon it begins to slowly decompose ( $t_{1/2} \approx 3$  days) to a species with similar  $^{31}\text{P}$  NMR metrics ( $\delta_{31\text{P}}$  19.9, doublet,  $^1J_{\text{RhP}} = 106$  Hz), assigned as monocarbonyl derivative **34**, Figure 2.20. Soon thereafter two new doublets at  $\delta_{31\text{P}}$  26.3 ( $^1J_{\text{RhP}} = 107$  Hz, fwhm = 18 Hz) – assigned as Rh(III) monocarbonyl **35** – and  $\delta_{31\text{P}}$  32.1 ( $^1J_{\text{RhP}} = 125$  Hz) were seen to appear in the  $^{31}\text{P}\{^1\text{H}\}$  NMR spectrum, coinciding with the depletion of signals assigned to **33** and **34**. The signal at  $\delta_{31\text{P}}$  32.1 continued to increase in concentration over the following 15 days, concurrent with the depletion of all other phosphorous containing compounds. The increased  $^1J_{\text{RhP}}$  coupling of 125 Hz is consistent with a Rh(I) carbonyl, and the  $^1\text{H}$  NMR spectrum shows the complex to be highly symmetric in solution. This compound was isolated via crystallisation as fluorenone complex **36**. The  $^{13}\text{C}\{^1\text{H}\}$  NMR spectrum is devoid of the characteristic rhodium coupled biphenyl resonances, and instead the aryl protons show a HMBC correlation with a downfield resonance at  $\delta_{13\text{C}}$  202.6. The major ion in the ESI-mass spectrum is  $[\text{Rh}(\text{PPh}_3)_2(\text{CO})]^+$ ,  $m/z = 655.0842$  (calcd 655.0821). Crystalline material obtained of **36** was suitable for X-ray diffraction analysis, Figure 2.22, though the data presented is a preliminary refinement. Evident nonetheless is the square planar coordination geometry at rhodium, with overall  $C_s$  symmetry by virtue of the bent Rh1-O6-C7 angle at and a *ca.* 135°.

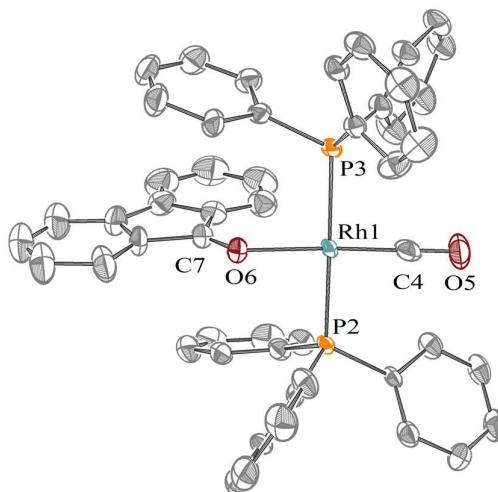


**Figure 2.22** Solid-state structure of fluorenone complex **36**. Data at 150 K, thermal ellipsoids drawn at 50%,  $[\text{Al}(\text{OR}^{\text{F}})_4]$  anion and co-crystallised dichloromethane molecule omitted. Preliminary refinement. Selected bond lengths ( $\text{\AA}$ ) and angles ( $^\circ$ ): Rh1-P2, 2.34; Rh1-P3, 2.33; Rh1-C4, 1.79; Rh1-O6, 2.10; C4-O5, 1.16; O6-C7, 1.22; Rh1-C4-O6, 178; Rh1-O6-C7, 135; P2-Rh1-P3, 178; C4-Rh1-O5, 175; P3-Rh1-C4, 89; torsion(P3-Rh1-O6-C7), 82.

#### 2.4.5 Reactions with solvent

In dichloromethane solution low coordinate complex **29** is stable for weeks at ambient temperature, and is indefinitely stable stored in the solid state as an adduct of dichloromethane. However, in the presence of a weak nucleophile in the form of triphenylphosphine, **29** reacts near-instantaneously with dichloromethane, abstracting a chloride to reform complex **3** with concomitant formation of [(chloromethyl)-triphenylphosphonium] $[\text{Al}(\text{OR}^{\text{F}})_4]$ , Figure 2.23.

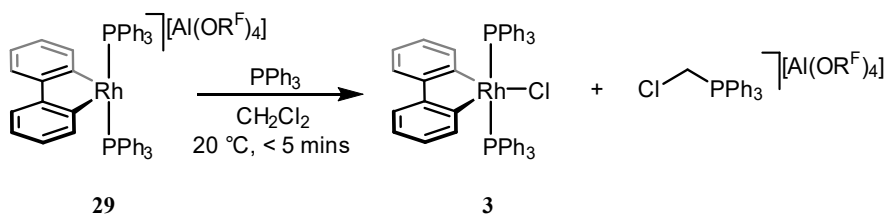


**Figure 2.23** Reaction of low-coordinate **29** with dichloromethane in the presence of triphenylphosphine.

In THF an analogous reaction occurs, though at a considerably slower rate,  $t_{1/2} \approx 6$  days at  $85^\circ\text{C}$ , resulting in two new signals in the  $^{31}\text{P}\{^1\text{H}\}$  NMR spectrum coinciding with the consumption of triphenylphosphine; a 2P doublet resonance at  $\delta_{31\text{P}}$  28.8 that is

resolved as a 119 Hz doublet with a generally comparable shift to rhodium chloride **3** (*cf.*  $\delta_{31\text{P}}$  28.7,  $^1J_{\text{RhP}} = 119$  Hz), and a 1P singlet resonance at  $\delta_{31\text{P}}$  24.2, a similar shift to [(chloromethyl)triphenylphosphonium][Al(OR<sup>F</sup>)<sub>4</sub>]. These data are tentatively assigned to the anticipated ring-opened alkoxide complex, **37**, Figure 2.24.

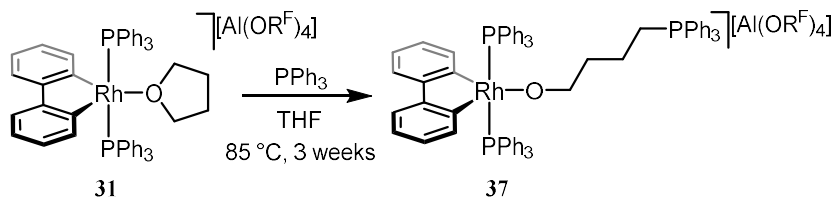


**Figure 2.24** Reaction of THF complex **31** with triphenylphosphine.

The crude reaction mixture was layered with excess hexane in an attempt to crystallise **37**. After a period of weeks, the precipitated material was isolated and extracted into dichloromethane solution. Two  $^{31}\text{P}\{^1\text{H}\}$  resonances were observed, again in a 1:2 ratio at  $\delta_{31\text{P}}$  28.2 ( $^1J_{\text{RhP}} = 119$  Hz) and 23.9, shifted compared to the *in situ* reaction mixture, but by an acceptable margin given the change of solvent. However, the  $^1\text{H}$  and  $^{13}\text{C}$  NMR spectra recorded for this compound are not consistent with alkoxide **37**; this solution is instead assigned as carboxylate **38**, Figure 2.25. Only three methylene signals are observed in the  $^1\text{H}$  NMR spectrum, one of which possesses a HMBC correlation with a carbon resonance at  $\delta_{13\text{C}}$  180.7, a drastically downfield shift, in good agreement with reported data for a closely related platinum carboxylate complex ( $\delta_{13\text{C}}$  180.5).<sup>273</sup> Analysis of the crude reaction mixture by low-resolution mass spectrometry registered a strong signal at 1127.2 *m/z*, corresponding to the mass of carboxylate **38**.

A mechanism accounting for the occurrence of **38** is proposed in Figure 2.25, invoking a facile  $\beta$ -hydride elimination of alkoxide **37**. The resulting activated aldehyde is then prone to attack from adventitious water, providing the supplementary oxygen atom. A second  $\beta$ -hydride elimination and loss of dihydrogen then affords carboxylate **38**. Regardless of mechanism, these results determine that the ring opening of THF by additional phosphine is sufficiently slow that THF can be used as the solvent in reactions investigating phosphine substitution at rhodium 2,2'-biphenyl systems.

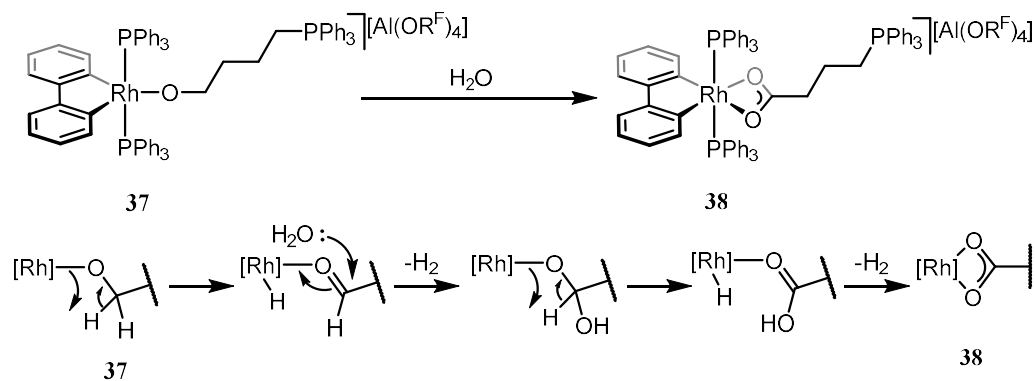


**Figure 2.25** Onward reaction of 37 with water, proposed mechanism for the formation of carboxylate **38**.

## 2.4.6 Substitution of phosphine

The phosphine substitution kinetics of neutral chlorides **3** ( $M = \text{Rh}$ ) and **7** ( $M = \text{Ir}$ ) and cationic **11** ( $M = \text{Rh}$ ) and **16** ( $M = \text{Ir}$ ) were investigated using an excess of the more electron rich ligand, tricyclohexylphosphine, Figure 2.26. In light of the observed reactivity of  $[\text{Rh}(2,2'\text{-biphenyl})(\text{PPh}_3)_2]^+$  with dichloromethane, THF was selected as solvent for these investigations, and the reactions monitored at room temperature for up to 48 hours. Reactions of iridium compounds **7** and **16** under these conditions produce a common product, assigned as mixed phosphine complex **39** – with either chloride or  $[\text{BAr}^{\text{F}}_4]$  as counter anion. The cation of **39** is identifiable in the mass spectrum of the crude reaction mix at  $887.5\ m/z$ , and is observed in the  $^{31}\text{P}\{^1\text{H}\}$  NMR spectrum as two doublet resonances with strong phosphorous-phosphorous coupling, at  $\delta_{31\text{P}}$  12.9 and 5.3 ( $^2J_{\text{PP}} = 365\ \text{Hz}$ ). The displacement of the chloride ligand is presumably facilitated by the use of a relatively polar solvent in combination with the agostic stabilisation of low-coordinate **39** courtesy of the tricyclohexylphosphine ligand. Attempts to isolate **39** were unsuccessful.

The substitution of rhodium chloride **3** proceeds in a similar, stepwise manner, though with far faster kinetics. **3** is consumed within 3 hours, initially giving rise to a compound formulated as mixed phosphine chloride **40**, identified in the  $^{31}\text{P}\{^1\text{H}\}$  NMR spectrum by two heavily roofed doublet of doublet resonances at  $\delta_{31\text{P}}$  24.8 ( $^2J_{\text{PP}} = 395\ \text{Hz}$ ,

$^1J_{\text{RhP}} = 111 \text{ Hz}$ ) and 21.6 ( $^2J_{\text{PP}} = 395 \text{ Hz}$ ,  $^1J_{\text{RhP}} = 115 \text{ Hz}$ ). Onward substitution to tricyclohexylphosphine complex **4** proceeds to completion over the following 45 hours. Determination of accurate kinetics parameters here were hampered by the poor solubility of **4**, which precipitated during the course of the reaction. At the cationic rhodium centre of **11** substitution to bis(tricyclohexylphosphine) complex **12** proceeds to completion within 5 minutes. A coordinating solvent is not required for this reaction; in fluorobenzene solution the substitution of **29** is also complete within 5 minutes. These experiments demonstrate the overall trend of faster substitution reaction at rhodium compared to iridium, and at low coordinate, cationic metal centres.

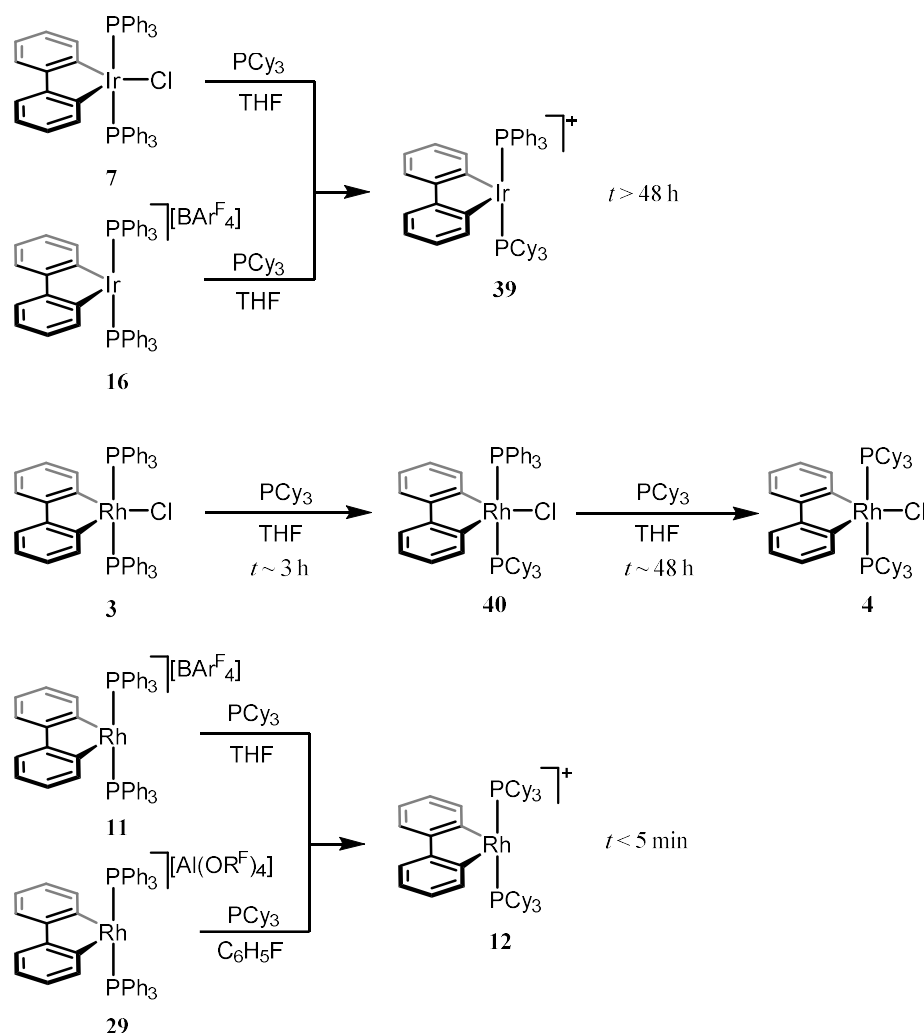


**Figure 2.26** Substitution of triphenylphosphine complexes with tricyclohexyl phosphine. Conditions: ambient temperature, 5.0 equivalents of PCy<sub>3</sub>.

### 2.4.7 An unexpected result

As part of related phosphine substitution studies in dichloromethane / THF mixtures, attempted isolation of the substitution product resulted in the crystallisation of a small quantity of bright red blocks. X-ray diffraction analysis of this material results in structural data modelled as a trimer of the  $\{\text{Rh}(2,2'\text{-biphenyl})(\text{PPh}_3)\}$  fragment, compound **41**, Figure 2.27 and 2.28. The complex is mono-cationic, with two distinct cations present in the unit cell. Each cation is three-fold symmetric with each unique cation comprising a single component in the asymmetric unit. Rhodium-rhodium separations of 2.8065(5) - 2.8070(7) Å are noted across the two cations, with Rh-C contacts subtly elongated over the 2,2'-biphenyl complexes characterised so far; 2.009(5) – 2.036(4) Å. The Rh-P contacts are in line with the Rh(III) species collated previously in this chapter, though at 2.330(1) and 2.3310(8) Å they are at the lower end of the range.

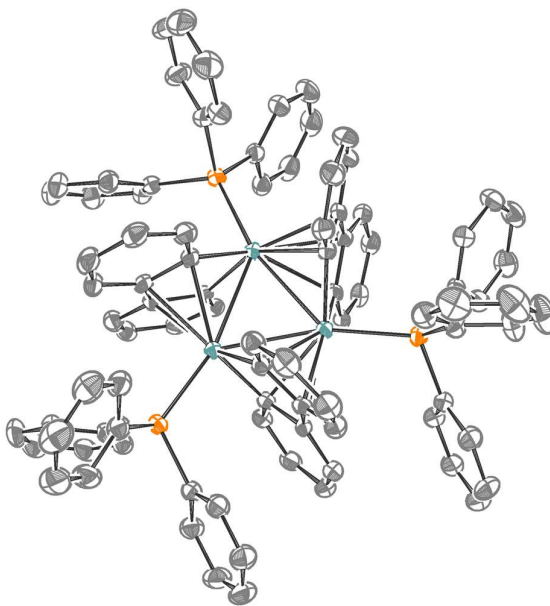


**Figure 2.27** Crystal structure of rhodium 2,2'-biphenyl trimer **41**. Data at 150 K, thermal ellipsoids drawn at 50%,  $Z' = 2$ , one of the two unique cations shown,  $[\text{Al}(\text{OR}^F)_4]$  anion omitted. Each cation is three-fold symmetric. Selected bond lengths (Å) and angles (°) for both cations: Rh-Rh, 2.8065(5) & 2.8070(7); Rh-P, 2.330(1) & 2.3310(8); Rh-C, 2.009(5), 2.035(5) & 2.011(4), 2.036(4); Rh-cnt( $\eta^5$ -rhodacycle), 2.067(2) & 2.086(2); P-Rh-cnt(rhodacycle), 87.60(7) & 88.71(6); P-Rh-cnt( $\eta^5$ -rhodacycle), 126.21(4) & 133.73(6).



Each rhodium centre is asserted to be 6-coordinate, comprising the phosphine ligand, the 2,2'-biphenyl ligand, and the  $\eta^5$  coordination of another metallocycle. Although arguments could be made for coordination in an  $\eta^4$  fashion; the observation that the 5-membered metallocycle remains planar seems more indicative of the  $\eta^5$  mode. Such a motif has been observed elsewhere; coordination of a second metal to a biphenyl-defined is known for rhodium, Figure 2.28, **A82**,<sup>247</sup> cobalt, **A82** and **A83**,<sup>247,274</sup> and throughout Group 8 with iron, ruthenium and osmium carbonyl compounds, **A84**.<sup>275</sup> Comparing rhodium complexes, the contacts of trimetallic **41** are elongated over bimetallic **A82**, which exhibits intermetallic contacts of 2.683(2) Å, and rhodium-biphenyl contacts of 1.991(8) – 2.015(8) Å. Complexes **A82** possesses time-averaged  $C_{2v}$  symmetry in THF solution, consequent of interconversion of the metal centres. This exchange process is viable for complex **41**, and would be associated with an accent in symmetry from the  $C_{3h}$  of the solid-state structure to time averaged  $D_{3h}$ .

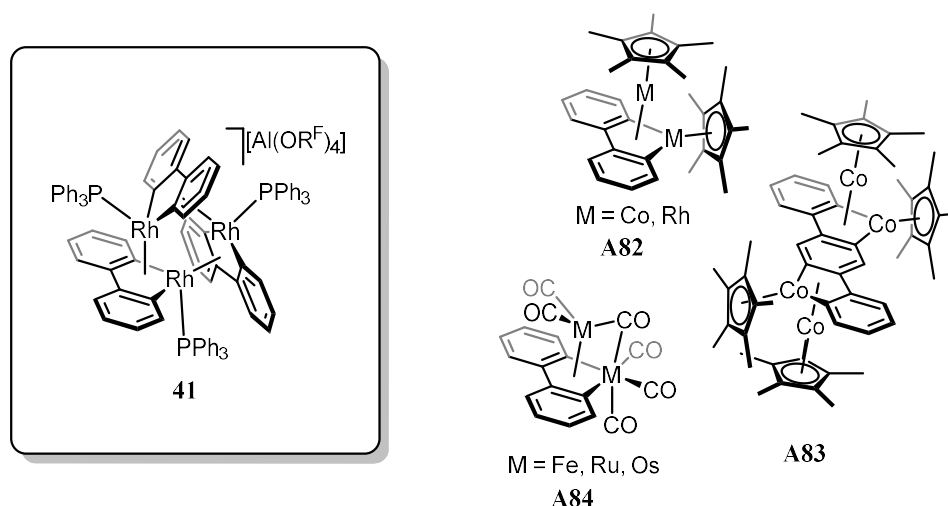


**Figure 2.28** Compound **41** and related examples featuring an equivalent bonding motif.

Regrettably, a synthesis of **41** remains elusive. Attempts to reproduce the original reaction conditions failed to afford additional material, and efforts to prepare the compound by some rational synthesis, using  $\text{Na}[\text{BH}_4]$  or cobaltocene as a reductant, have all proved unsuccessful, giving rise to new, unstable, and thus far unidentified products. The use of a very mild reductant seems to be indicated; in the original

serendipitous preparation it is possible that the additional phosphine served as the reducing agent. procedure which sequesters an equivalent of phosphine from the reaction mixture would also be desirable. In that mind set, and given previously discussed results, this may involve concurrent formation of an oxidizable phosphonium salt.

## 2.5 Conclusions and future work

Overall the 2,2'-biphenyl ligand has been shown to have great utility in the pursuit of isolating complexes featuring weak metal substrate interactions. In this context there is ample scope for further variation of the incorporated phosphine ligands. The M-F-C interaction is particularly interesting; the systems presented herein sought to vary the metal electronics with a range of ancillary ligands, the orthogonal approach of maintaining a consistent ligand sphere and systematically modifying the phosphine with alternative fluorinated groups, may be yet more informative. Systems that simultaneously offer proximal hydrocarbon and fluorocarbon groups such that an intramolecular competition experiment can be conducted would be intriguing.

In the absence of viable intramolecular stabilising interactions, as is the case when employing the triphenylphosphine ligand, the systems are shown to seek out intermolecular stabilisation in the form of solvent and small molecule adducts. The rhodium 2,2'-biphenyl system is shown to be reasonably stable in solution, in isolation, but exhibits interesting reactivity with carbon monoxide, dihydrogen, and also dichloromethane and THF when in the presence of a mild nucleophile. Phosphine substitution is found to be facile at a cationic, low coordinate rhodium centre. The combination of these metal electronics with a cavitand-based ligand that is capable of size excluding the relatively strong intermolecular interactions observed here is therefore a promising avenue for isolating adducts of weakly coordinating substrates, and will be the focus of the next chapter.

### 3 Complexes of a calixarene-based diphosphine

---

This chapter describes the preparation and coordination chemistry of the  $\{M(\text{biphenyl})\}^+$  fragment ligated by a calixarene-based diphosphine. Building directly on the chemistry previously explored with monodentate phosphine complexes, synthetic protocols for the preparation of a well-defined mononuclear rhodium aqua complex are described. The exchange of the aqua ligand for less strongly coordinating substrates is then explored. Despite the extreme hydrophilicity of the calixarene system, synthetic procedures are developed that are applicable to the isolation of a range of small molecule adducts. Stable adducts of silver chloride, dichloromethane, dinitrogen and dihydrogen are characterised in solution, and the dinitrogen complex further characterised in the solid state. Evidence is presented of a transient interaction with fluorobenzene serving to stabilise a formally 14-electron metal complex.

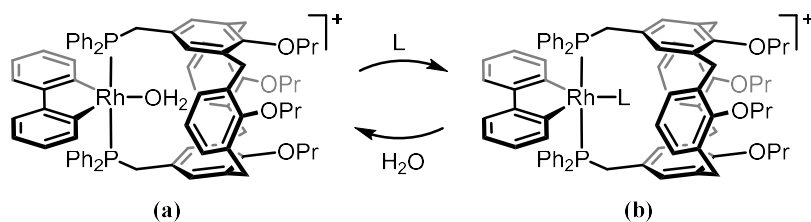


**Figure 3.1** Mononuclear rhodium calixarene complexes.

*Manuscripts resulting from work described in this chapter are in preparation.*

### 3.1 Complexes of calixarene-based ligands

#### 3.1.1 Host-guest complexes

Cavitands are bowl-shaped molecules, able to form supramolecular host-guest complexes courtesy of an array of intramolecular interactions between a suitable substrate and the interior surface of the cavitand molecule, Figure 3.2. The host cavitand is typically highly discriminatory with respect to the size and shape of the guest substrate. These inclusion complexes have shown excellent application in, for example, the stabilisation of reactive guest molecules,<sup>276</sup> and in gas sensing.<sup>277</sup> Of particular relevance to this work, inclusion complexes of methane,<sup>278,279</sup> higher alkanes,<sup>280–288</sup> and xenon,<sup>278,289–294</sup> have been documented across a variety of cavitand architectures.

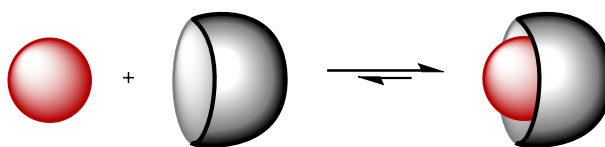


**Figure 3.2** Abstract representation of a favourable host-guest complex.

#### 3.1.2 Calixarenes

One particular cavitand topology which attracts substantial attention is the calixarene. First described by Gutsche,<sup>295–299</sup> the condensation products of *para*-phenols and formaldehyde are well applied in supramolecular chemistry.<sup>300–303</sup> The calix[4]arene, exemplified by the ubiquitous starting material *tert*-butylcalix[4]arene, Figure 3.3, may be functionalised at both upper- and lower-rims, allowing access to a multitude of cavitand architectures, with functionalisation serving to supplement the host-guest interactions, or enforce specific conformations of the calixarene in solution.

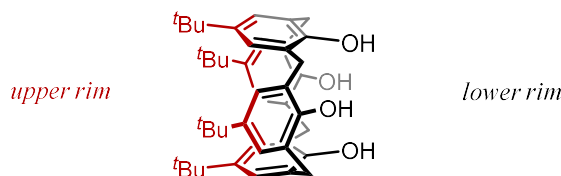


**Figure 3.3** *tert*-butylcalix[4]arene.

The base calix[4]arene, henceforth simply calixarene, has access to a number of conformations in solution, Figure 3.4, (a). The inversion processes (*i.e.* rotation of the arene units) that convert between these conformers is arrested by lower-rim functionalisation, and syntheses have been designed which selectively afford one particular conformation. The cone conformation is the most synthetically convenient to trap, and offers the most sterically inaccessible cavity. The ground-state of the cone conformation is described as a pinched-cone, Figure 3.4, (b). These  $C_{2v}$  symmetric structures rapidly interconvert, giving rise to the time averaged  $C_{4v}$  symmetry. Coordination of guest molecules may slow the pinched cone interconversion process,<sup>304,305</sup> while the relative energies of the two conformations are made non-degenerate by difunctionalisation of opposing arenes. In the pinched-cone the apex carbons of the splayed aryl unit can be in excess of 10 Å separated, compared to *ca.* 5 Å for the other arene rings, which tend to be near-coplanar.<sup>306-308</sup>

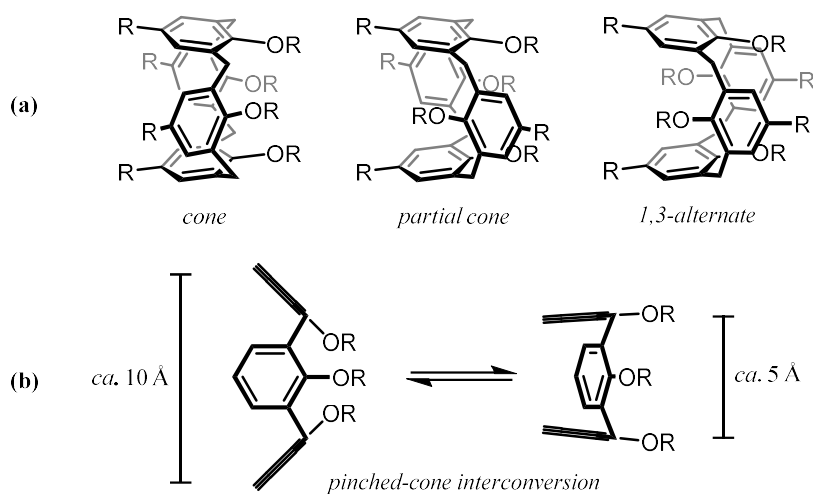


**Figure 3.4** Conformations of calix[4]arenes.

### 3.1.3 Calixarenes as ligands

Research into the application of calixarenes as ligands in coordination chemistry is primarily motivated by the desire to exploit the unique steric properties of the calixarene to effect a selective transformation, and have been investigated with metals across the periodic table for use in a range of catalytic processes.<sup>309,310</sup> Unfunctionalised calixarenes

may serve as ligands in their own right, complexing hard metal atoms courtesy of the hydroxyl groups at the lower rim, or in the formation of arene complexes with the main body of the calixarene.<sup>311,312</sup> The true utility of the calixarene scaffold in coordination chemistry is realised upon functionalisation with an appropriate donor groups.<sup>313–315</sup> Expectedly, with late-transition metals N-heterocyclic carbene or phosphine functionalisation feature heavily, and are predominantly investigated at palladium centres in the context of catalytic cross-coupling reactions. Carbene functionalised calixarenes demonstrate a rich variety of coordination chemistry,<sup>316–325</sup> and have been the focus of previous enquiries within the Chaplin group, Figure 3.5. Notable results from those studies are the preparation of an unusual dirhodium complex **A85**,<sup>326</sup> and the characterisation of di-cationic rhodium and iridium complexes **A86** featuring close cation-cation approaches, facilitated by the inclusion properties of the calixarene.<sup>327</sup> Departing from these enquiries, the work described in this thesis is interested in pursuing the chemistry of phosphine functionalised calixarenes.

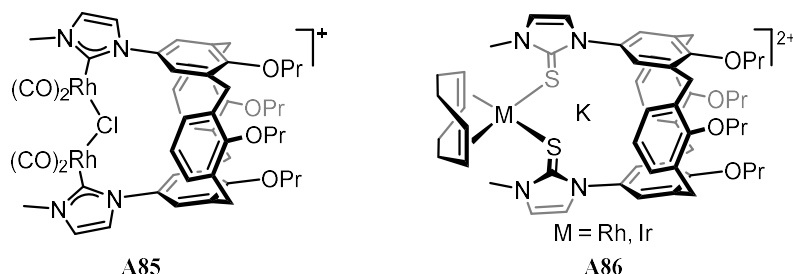


**Figure 3.5** Previous outcomes of work on calixarenes in the Chaplin group.

### 3.1.4 Complexes of phosphine functionalised calixarenes

Three considerations are key to fully utilising the interior microenvironment defined by a calixarene-based ligand; (1) proximity of the donor group to the calixarene, (2) the ability to coordinate in a manner which leaves an available coordination site directed at the cavity, and (3) retaining the metal fragment above the cavity. A number of well-defined complexes of mono-dentate phosphine calixarenes have been characterised for example,<sup>328–335</sup> though with few exceptions,<sup>330,332</sup> the metal fragments are free to exist in the less sterically demanding environment *exo* the calixarene.

Examples of chelating complexes of lower-rim functionalised calixarenes are given in Figure 3.6. Phosphorous donors may be installed directly at the arene as in complexes **A87**, here projecting an acetonitrile ligand directly into the calixarene cavity.<sup>336</sup> Lower rim phosphites are a common motif, though these tend to form *cis*-chelates across a wide variety of metal fragments,<sup>337–340</sup> for example with the palladium dichloride complex **A88**.<sup>341</sup> Phosphine functionalisation with a single methylene spacer between oxygen and phosphorous atoms permit *trans*-chelates with platinum, gold and silver.<sup>342,343</sup> Platinum complex **A89** directs a hydride ligand towards the calixarene cavity, though with only a two element spacer here the metal is already fairly remote from the cavitand. The importance of the selection of metal precursor in achieving a desired coordination motif becomes apparent here; the combination of hydride and bulky triphenylphosphine in **A89** facilitates the *trans*-coordination mode. By contrast the use of platinum alkene, palladium allyl, rhodium norbornadiene, or ruthenium arene fragments elicits a *cis*-coordination mode at the same ligand.<sup>343,344</sup>

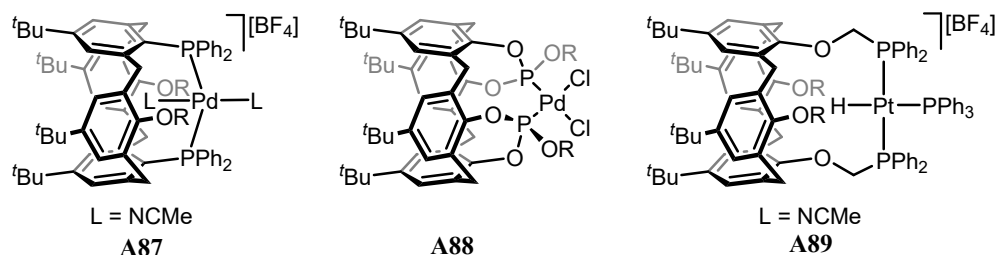


**Figure 3.6** Lower-rim functionalised calixarenes as metal chelates.

At the upper-rim, the establishment of a chelating coordination mode with any donor functionality is – perhaps unexpectedly – a difficult proposition. Phosphines directly affixed to the arene units give rise to *cis*-chelates,<sup>345–349</sup> as for example in nickel cyclopentadienyl complex **A90**, Figure 3.7. Crucially, in this coordination mode the functionalised arenes are projected towards each other, constricting the calixarene cavity. Complexes with *trans*-chelation at  $\alpha$ -phosphines are known, featuring platinum, palladium and ruthenium fragments,<sup>350</sup> for example platinum hydride **A91**. With a lengthier ethylene spacer as in **A92**, *cis*-chelation again results for the palladium and molybdenum fragments trailed.<sup>351</sup>





## 3.2 CxP<sub>2</sub>

### 3.2.1 Ligand synthesis

The known bis(phosphine) functionalised calixarene 5,17-bis(diphenylphosphinomethy)-25,26,27,28-tetrapropoxycalix[4]arene,<sup>353</sup> **50**, henceforth **CxP<sub>2</sub>**, was synthesised in 17% yield over eight steps from *tert*-butylcalixarene via intermediates **42** – **49**, Figure 3.9. The compound was accessed in the final step by reaction of synthetically convenient bromomethyl calixarene **49** with potassium diphenylphosphide in preference to the previous literature protocol proceeding through chloromethyl calixarene **48**. The solid-state structure of **CxP<sub>2</sub>** has been reported previously, and shows the calixarene in a pinched-cone conformation with the close contact, coplanar arenes (*cf.* Figure 3.4) bearing the phosphine functionalisation.

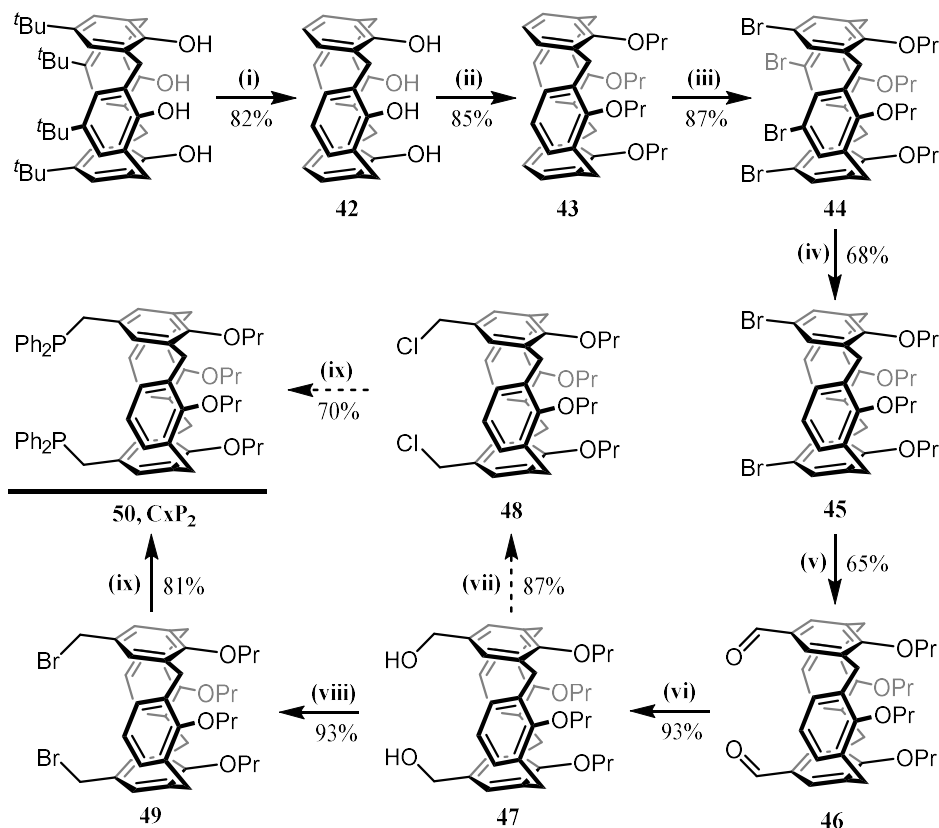


**Figure 3.9** Synthesis of **CxP<sub>2</sub>**. (i) AlCl<sub>3</sub>, PhOH, toluene, 20 °C, 5 h; (ii) PrI, NaH, DMF, 80 °C 18 h; (iii) N-bromosuccinamide, THF, 20 °C, 24 h; (iv) <sup>n</sup>BuLi, THF, -78 °C, 20 min, MeOH; (v) <sup>n</sup>BuLi, THF, -78 °C, 20 min, DMF; (vi) NaBH<sub>4</sub>, EtOH, 90 min; (vii) SOCl<sub>2</sub>, CH<sub>2</sub>Cl<sub>2</sub>, -78 °C, 2 h; (viii) PBr<sub>3</sub>, CH<sub>2</sub>Cl<sub>2</sub>, 20 °C, 10 min; (ix) KPPH<sub>2</sub>, THF, -78 °C, 18 h.

The **CxP<sub>2</sub>** ligand is observed by <sup>1</sup>H NMR spectroscopy with overall *C*<sub>2v</sub> symmetry, Figure 3.10. The axial and equatorial proton resonances of the lower rim methylene linker are observed at δ<sub>1H</sub> 4.31 and 2.96 respectively, with a geminal coupling of 13.3 Hz. The methylene group linking the phosphine and calixarene, CH<sub>2</sub>P, is observed as a relatively broad resonance at δ<sub>1H</sub> 3.37 with no appreciable <sup>31</sup>P coupling. The three distinct upper rim aryl proton resonances are observed at δ<sub>1H</sub> 5.88, 6.17 and 6.75, with the furthest downfield resonance of the three belonging to the protons on the functionalised arene. A solitary phosphorous environment is observed in the <sup>31</sup>P{<sup>1</sup>H} NMR spectrum of **CxP<sub>2</sub>**; the singlet resonance residing at δ<sub>31P</sub> -10.6.

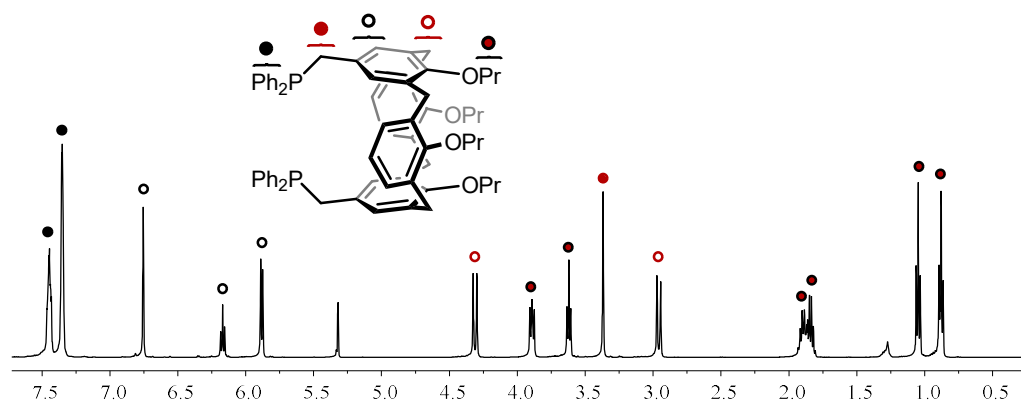
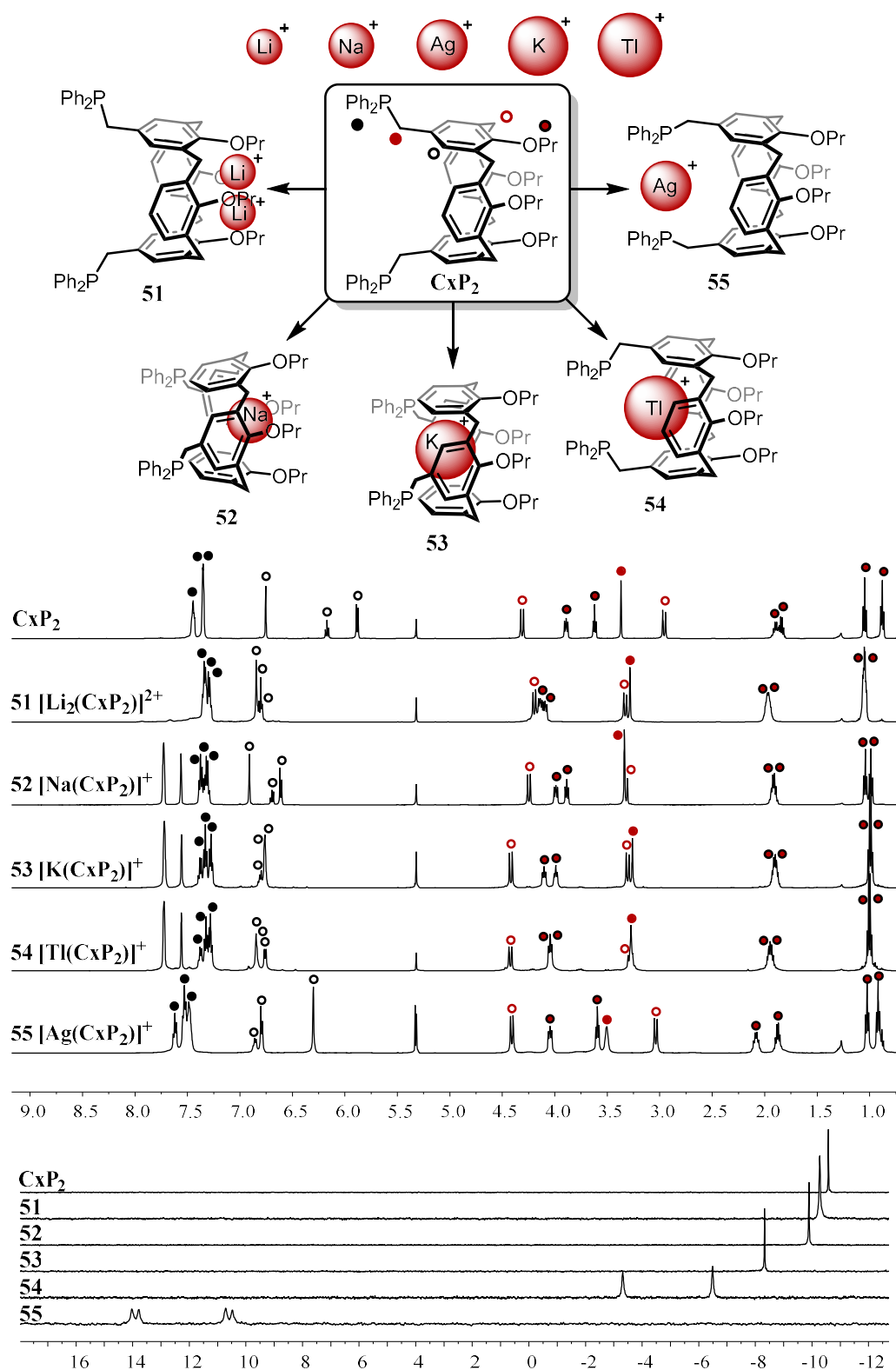


Figure 3.10 <sup>1</sup>H NMR spectrum (CD<sub>2</sub>Cl<sub>2</sub>, 500 MHz) of **CxP<sub>2</sub>**.

### 3.2.2 Complexes of simple cations

Three distinct regions exist in the **CxP<sub>2</sub>** molecule capable of interacting with a given metal atom; these being the phosphine, the arene surface of the cavity, and alkoxy groups at lower rim. Prior to attempted coordination of rhodium and iridium fragments, the complexation of **CxP<sub>2</sub>** to a range of monoatomic cations; Li<sup>+</sup>, Na<sup>+</sup>, K<sup>+</sup>, Tl<sup>+</sup>, and Ag<sup>+</sup> was investigated. Suspensions of **CxP<sub>2</sub>** and Li[Al(OR<sup>F</sup>)<sub>4</sub>], Na[BAr<sup>F</sup><sub>4</sub>], K[BAr<sup>F</sup><sub>4</sub>], Tl[BAr<sup>F</sup><sub>4</sub>] or Ag[Al(OR<sup>F</sup>)<sub>4</sub>] were agitated for *ca.* 5 minutes to afford, quantitatively, the corresponding metal adducts **51** – **55**. Figure 3.11 presents the <sup>1</sup>H and <sup>31</sup>P{<sup>1</sup>H} NMR spectra of **51** – **55** with a proposed location within the calixarene framework for the cation binding in each compound.



**Figure 3.11** Cation adducts of **CxP<sub>2</sub>**. Top: Synthesis and proposed cation locations in solution. **51**, **55**: anion =  $[\text{Al}(\text{OR}^{\text{F}})_4]^-$ ; **52** – **54**: anion =  $[\text{BAr}^{\text{F}}_4]^-$ ; Middle:  $^1\text{H}$  NMR spectra ( $\text{CD}_2\text{Cl}_2$ , 500 MHz) of **51** – **55**; Bottom:  $^{31}\text{P}\{^1\text{H}\}$  NMR spectra ( $\text{CD}_2\text{Cl}_2$ , 162 MHz) of **51** – **55**.

Reaction of **CxP<sub>2</sub>** with stoichiometric Li[Al(OR<sup>F</sup>)<sub>4</sub>] results in the immediate formation of a 1:1 mixture of **CxP<sub>2</sub>** and [Li<sub>2</sub>(C<sub>x</sub>P<sub>2</sub>)] [Al(OR<sup>F</sup>)<sub>4</sub>]<sub>2</sub>, **51**. Addition of a further equivalent of Li[Al(OR<sup>F</sup>)<sub>4</sub>] progresses the mixture to exclusively **51**, with no further reactivity on addition of excess Li[Al(OR<sup>F</sup>)<sub>4</sub>]. The strong preference for the uptake of two lithium cations implies a strong interaction with degenerate binding sites, here proposed to be at the lower rim alkoxides. The oxygen-based functionality serves to adequately separate the two cations, of which there is precedent.<sup>355</sup> The propyl <sup>1</sup>H resonances of **51** are all downfield shifted relative to free ligand, and the <sup>31</sup>P{<sup>1</sup>H} resonance is only very slightly downfield shifted at δ<sub>31P</sub> -10.3, from δ<sub>31P</sub> -10.6 for **CxP<sub>2</sub>**, consistent with this interpretation.

Reaction of **CxP<sub>2</sub>** with Na[BAr<sup>F</sup><sub>4</sub>] and K[BAr<sup>F</sup><sub>4</sub>] proceeded directly to the monometallic [Na(C<sub>x</sub>P<sub>2</sub>)] [BAr<sup>F</sup><sub>4</sub>], **52** and [K(C<sub>x</sub>P<sub>2</sub>)] [BAr<sup>F</sup><sub>4</sub>], **53**, respectively. The <sup>31</sup>P{<sup>1</sup>H} NMR spectra of both compounds show a downfield shift, greater than that observed for dilithium salt **51**, at δ<sub>31P</sub> -9.9 and δ<sub>31P</sub> -8.3 for **52** and **53**, respectively. Crystals of **53** suitable for XRD analysis were grown by slow diffusion of hexane into a dichloromethane solution, and while the collected data is not of reportable quality, it does indicate that the potassium ion is binding to two opposing arenes of the calixarene, Figure 3.12. Both **52** and **53** are thus assigned as arene bound adducts.

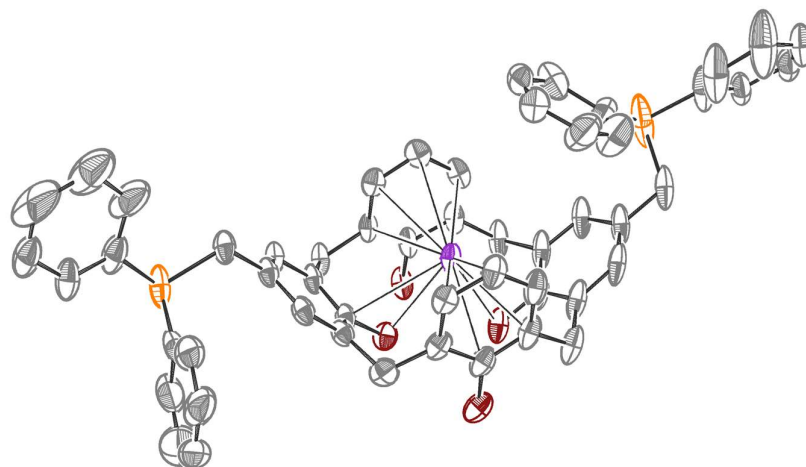


**Figure 3.12** Solid-state structure of **53**. Data at 150 K, thermal ellipsoids at 30%. Poor diffraction data precludes the determination of precise structural metrics. [BAr<sup>F</sup><sub>4</sub>] anion and propyl groups omitted. Selected bond lengths (Å) and angles (°): K1-cnt, 2.77, 2.74; K1-O, 2.75; C60-C80, 9.66; C70-C90, 5.62; cnt-K-cnt, 177.

Reaction of **CxP<sub>2</sub>** with stoichiometric Tl[BAr<sup>F</sup><sub>4</sub>] results in immediate formation of [Tl(CxP<sub>2</sub>)] [BAr<sup>F</sup><sub>4</sub>], **54**, assigned as an arene complex. The <sup>1</sup>H NMR spectrum of **54** is remarkably similar to that of potassium salt **53**, and the <sup>13</sup>C{<sup>1</sup>H} NMR spectrum exhibits arene resonances with large *J*<sub>TIC</sub> coupling constants of 50 – 60 Hz. A tandem interaction with the phosphine is indicated from the <sup>31</sup>P{<sup>1</sup>H} NMR data, with a downfield-shifted, thallium coupled resonance at δ<sub>31P</sub> -4.9, *J*<sub>TIP</sub> = 386 Hz. Addition of a further equivalent of Tl[BAr<sup>F</sup><sub>4</sub>] proceeds to increase the complexity of the <sup>1</sup>H NMR spectrum. Additional calixarene containing signals are observed, and the <sup>31</sup>P{<sup>1</sup>H} spectrum becomes increasingly broad on the addition of greater quantities of thallium salt. Binding of a second thallium ion to the phosphine is therefore implicated; indeed crystalline material obtained of such a compound was found by X-ray diffraction to contain both an arene bound thallium ion and a second on the phosphine, forming an extended 1D coordination polymer, Figure 3.13.

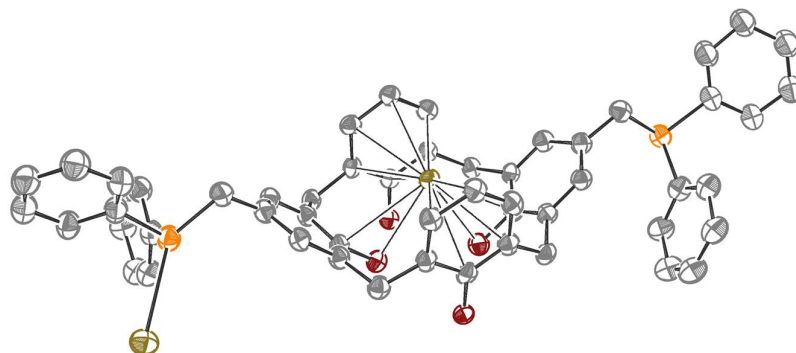


**Figure 3.12** Solid-state structure of a dithallium coordination polymer derived from **54**. Data at 150 K, thermal ellipsoids at 30%. Poor diffraction data precludes the determination of precise structural metrics. [BAr<sup>F</sup><sub>4</sub>] anion and propyl groups omitted. Selected bond lengths (Å) and angles (°): Tl1-cnt, 2.81, 2.82; Tl1-O, 2.87, 3.06; Tl2-P, 3.00, 3.03; C60-C80, 9.74; C70-C90, 5.87; cnt-Tl-cnt, 175; P-Tl-P, 86.

The silver adduct, [Ag(CxP<sub>2</sub>)] [Al(OR<sup>F</sup>)<sub>4</sub>] **55**, exhibits a very distinct <sup>1</sup>H NMR spectra to the other cation adducts discussed. The CH<sub>2</sub>P signal is broadened, suggestive of some imposed rigidity in the phosphine beginning to elicit diastereotopic methylene protons resonances. The chemical shift of all the <sup>1</sup>H resonances is very similar to the free ligand, with three significant exceptions; the upper-rim aryl signals are in a different order, with a greatly upfield aryl signal at δ<sub>1H</sub> 6.30, is noted. This implies that the conformation

of the calixarene is the opposite pinch-cone conformation to that adopted by the free ligand. Ag-P coordination is substantiated by the clear  $^{107}\text{Ag}$  and  $^{109}\text{Ag}$  coupling observed in the  $^{31}\text{P}\{^1\text{H}\}$  NMR spectrum;  $\delta_{31\text{P}}$  12.2,  $^1J_{107\text{AgP}} = 575$  Hz and  $^1J_{109\text{AgP}} = 497$  Hz. In the absence of phosphine functionality on the calixarene silver is known to interact with two opposing arenes in an  $\eta^1$ -fashion only.<sup>304</sup> Silver is thus adjudged to form an interaction exclusively with the phosphine moiety in a chelating manner.

### 3.3 Synthesis of rhodium and iridium complexes of $\text{CxP}_2$

#### 3.3.1 Chloride complexes

Proceeding analogously to the systems prepared in Chapter 2, reaction of  $\text{CxP}_2$  with  $[\text{Rh}(2,2'\text{-biphenyl})(\text{dtbpm})\text{Cl}]$  **1** or  $[\{\text{Ir}(2,2'\text{-biphenyl})(\text{cod})(\text{Cl})\}_2]$  **2** in dichloromethane results immediately in yellow and red solution respectively, which on addition of excess diethyl ether precipitate as amorphous solids. The solid materials in both cases were found to be reasonably soluble in dichloromethane, but initiating dissolution required substantial agitation. Rather than the intended mononuclear metal chlorides, these compounds are assigned as dimeric species **56** ( $\text{M} = \text{Rh}$ ) and **57** ( $\text{M} = \text{Ir}$ ), Figure 3.12.

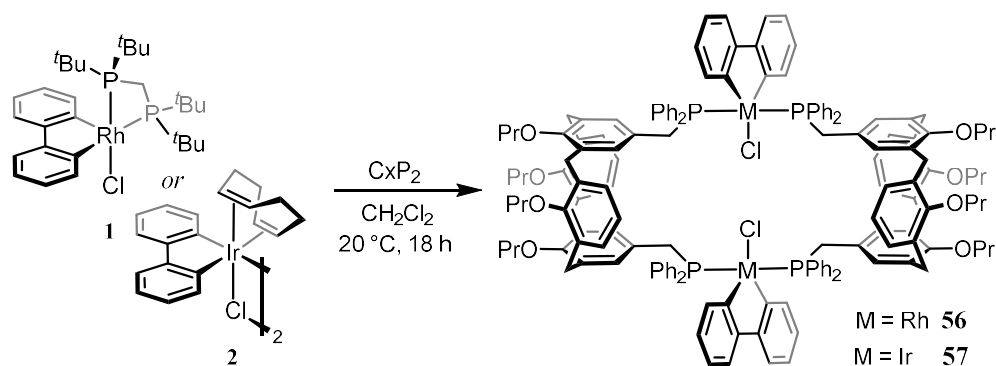
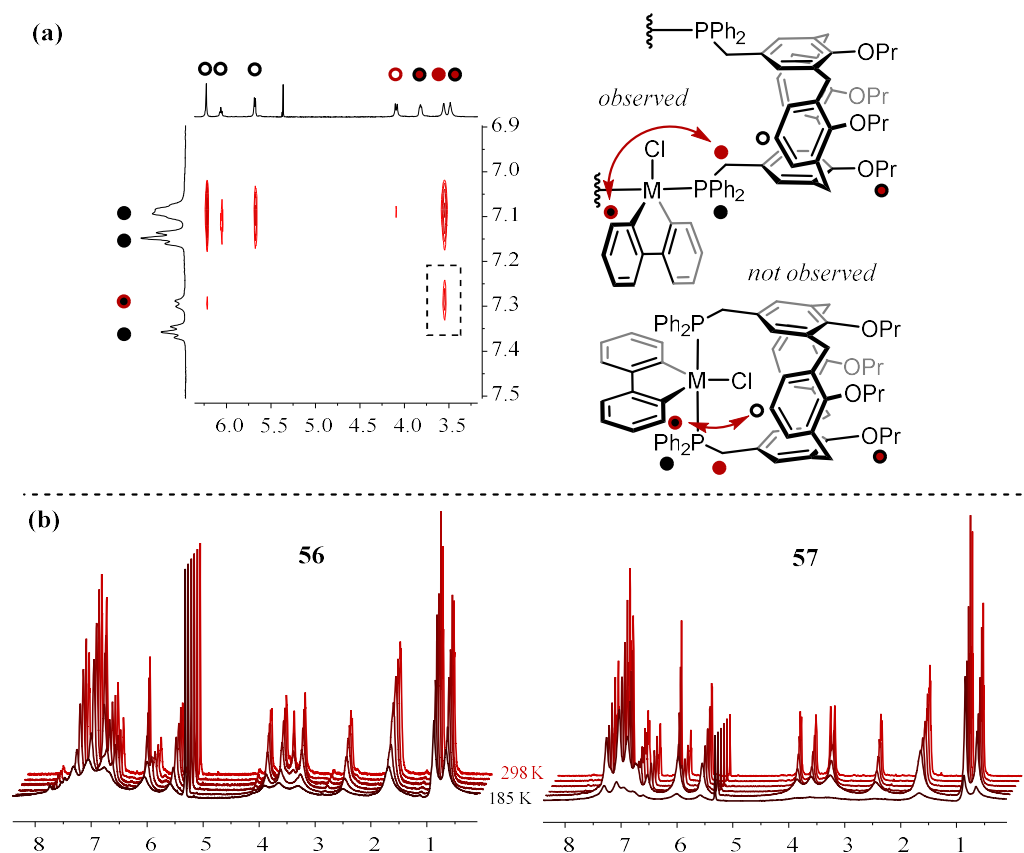


Figure 3.12 Synthesis of chloride complexes **56** and **57**.

Resonances in the  $^{31}\text{P}\{^1\text{H}\}$  NMR spectrum at  $\delta_{31\text{P}}$  29.9 ( $^1J_{\text{RhP}} = 114$  Hz) for **56** and at  $\delta_{31\text{P}}$  20.3 for **57** are observed, consistent with a *trans*-bis(phosphine) chloride compound by comparison to chlorides **3** – **10**. The  $^1\text{H}$  NMR spectra indicate a 1:1 correspondence of biphenyl and calixarene resonances, and are notably broadened compared to the free

ligand, but aside from an upfield shift of *ca.* 0.3 ppm, the spectra are very similar to that of free **CxP<sub>2</sub>**. Analysis of the NOESY spectrum of **57** is consistent with a dimeric formulation in solution. Figure 3.13, (a), reveals a correlation between the CH<sub>2</sub>P protons and the 6-biphenyl resonance (expected for a dimeric configuration, not consistent with a monomeric configuration) while no cross peak is observed between 6-biphenyl signal and the indicated aryl proton resonances (expected for a monomeric configuration, not consistent with dimeric configuration). Additionally, the <sup>1</sup>H NMR spectra of **56** and **57** species maintain a *C<sub>2v</sub>* symmetry on cooling to 185 K, though substantial line broadening of all resonances is observed following the temperature decrease, Figure 3.13, (b). This is the expected behaviour of multi-metallic calixarene complexes with a relatively unconstrained calixarene ligand, but is not in any way consistent with the behaviour of mononuclear calixarene complexes, *vide infra*.



**Figure 3.13** Evidence for dimeric formulation of **56** and **57**: (a) NOESY spectra of **57**, with illustration of the expected correlations for a monomeric vs. dimeric formulation, pertinent cross peak highlighted; (b) <sup>1</sup>H NMR spectra (CD<sub>2</sub>Cl<sub>2</sub>, 600 MHz) of **56** and **57** at 298 – 185 K.

Crystals of **56** suitable for X-ray diffraction were obtained upon standing in a mixed solvent system of dichloromethane and diethyl ether over a period of several months, and demonstrates a dimeric structure in the solid state, Figure 3.14. Two unique molecules are present in the asymmetric unit, each of which is centrosymmetric. Speaking broadly, owing to poor data quality, the calixarene core of **56** is shown to exist in a pinched-cone conformation with the phosphine functionalised arenes coplanar. The rhodium coordination geometry is intermediate between square pyramidal and trigonal bipyramidal, in line with other 2,2'-biphenyl chloride systems,<sup>250,252</sup> while the P-Rh-P bond angle is near-linear at *ca.* 176°. The two metal centres are fairly remote, separated by *ca.* 7.5 Å. The chloride atoms are separated by *ca.* 5.3 Å.

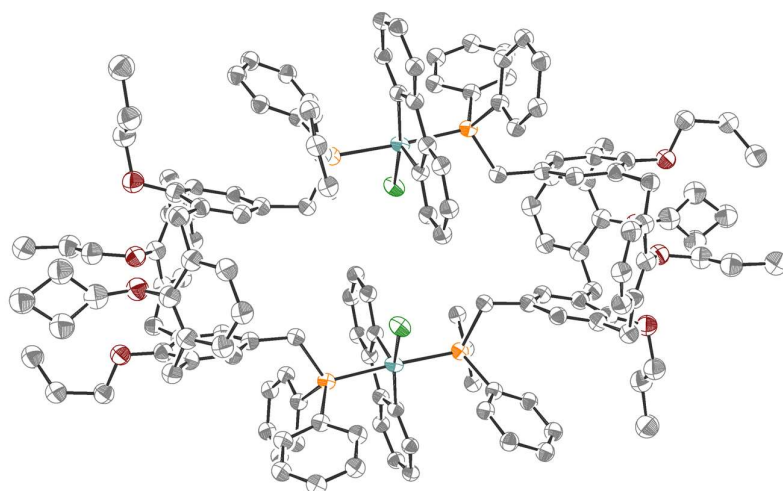


**Figure 3.14** Solid-state structure of **56**, selected molecule. Data at 150 K, thermal ellipsoids at 30%. Poor diffraction data precludes the determination of precise structural metrics. Selected bond lengths (Å) and angles (°): Rh1-Rh1', 7.52; Cl4-Cl4', 5.33; C60-C80, 4.45; C70-C90, 9.72; C-Rh-Cl, 164; P2-Rh1-P3, 176.

### 3.3.2 Halide abstraction

Given the earlier demonstration, Section 2.4.6, that phosphine substitution has been demonstrated to be much more facile at cationic rhodium 2,2'-biphenyl centres than the respective chloride, efforts proceeded to abstract the chloride ligand to facilitate an isomerisation to the target low coordinate compound. All attempted halide abstraction reactions of iridium chloride **57** either did not progress or gave rise to intractable reaction mixtures. Similarly, reaction of rhodium chloride **56** with Na[Bar<sup>F</sup><sub>4</sub>] or K[Bar<sup>F</sup><sub>4</sub>]



resulted in multiple new rhodium-coupled signals in the  $^{31}\text{P}\{^1\text{H}\}$  NMR spectra. Employing a stronger halophile, the reaction of **56** with a stoichiometric quantity of  $\text{Ti}[\text{BAR}^{\text{F}}_4]$  resulted immediately in the formation of a solitary new species in the  $^{31}\text{P}\{^1\text{H}\}$  NMR spectrum at  $\delta_{31\text{P}}$  27.4 ( $^1J_{\text{RhP}} = 116$  Hz), however the  $^1\text{H}$  NMR spectrum showed substantial line broadening on the chloride starting material. This material was consumed on heating, giving rise to uninterpretable  $^{31}\text{P}\{^1\text{H}\}$  and  $^1\text{H}$  NMR spectra.

By striking contrast, the reaction of rhodium chloride **56** with  $\text{Ag}[\text{Al}(\text{OR}^{\text{F}})_4]$  proceeds within two hours at ambient temperature to one compound, characterised as mononuclear silver chloride adduct **58**, Figure 3.15. The new compound is observed in the  $^{31}\text{P}\{^1\text{H}\}$  NMR spectrum at  $\delta_{31\text{P}} = 13.9$ ,  $^1J_{\text{RhP}} = 120$  Hz, far upfield of the chloride starting material, consistent with a cationic rhodium biphenyl compound, such as those described previously.

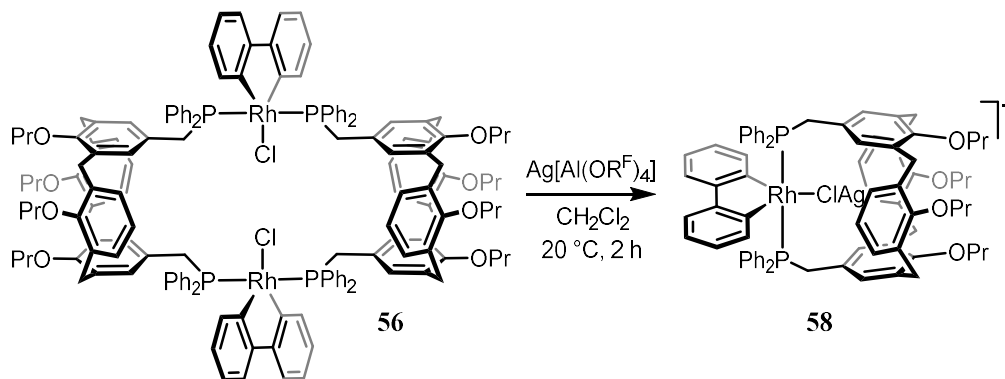
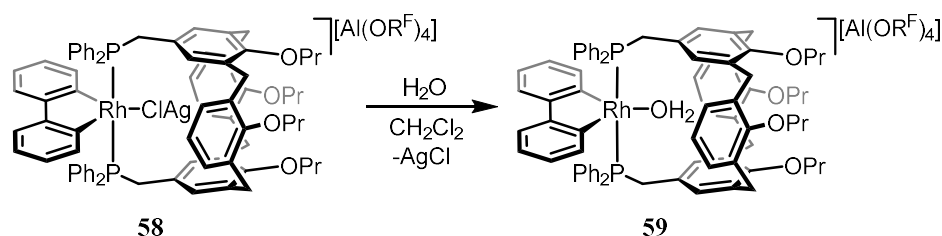


Figure 3.15 Synthesis of silver chloride adduct **58**.

The preparation of **58** was found to be highly sensitive to the stoichiometry of the silver reagent. Reaction with excess  $\text{Ag}[\text{Al}(\text{OR}^{\text{F}})_4]$  resulted in  $[\text{Ag}(\text{CxP}_2)][\text{Al}(\text{OR}^{\text{F}})_4]$ , **55**, as the only  $\text{CxP}_2$  containing component of the reaction mixture, while with sub-stoichiometric  $\text{Ag}[\text{Al}(\text{OR}^{\text{F}})_4]$  a highly dynamic system was recorded. These observations, coupled with the failure of the previously trialled abstracting agents, point to a critical silver containing intermediate in the isomerisation of dimeric **56** to monomeric **58**. Silver chloride adduct **58** is enormously sensitive to water. Addition of a stoichiometric quantity of water displaces the silver chloride in its entirety, resulting in a white

precipitate, and a yellow solution of a new species; water complex **59**, Figure 3.16. To emphasise this point by experimental anecdote: a glass microfibre filter pad wedged into a glass pipette that had been oven dried at 150 °C for 72 hours, was taken without delay into an argon atmosphere glovebox, and rinsed immediately with rigorously dried solvents. Passing a dichloromethane solution of **58** directly from one J. Young's NMR tube, through this filter into a second NMR tube that had been flamed under high vacuum prior to use, resulted in a 5% increase in the concentration of **59** as gauged by  $^1\text{H}$  and  $^{31}\text{P}$  NMR spectroscopy.



**Figure 3.16** Displacement of silver chloride from **58** resulting in water complex **59**.

### 3.3.3 The water complex

Water complex **59** was found to be an extremely useful precursor for entry into studying the small molecule coordination chemistry of mononuclear rhodium calixarene systems. It is stable to air, moisture, alumina, and persists under high vacuum ( $10^{-3}$  mbar) indefinitely at temperatures below 120 °C (above which it irrevocably decomposes). The compound is also highly amenable to crystallisation, with material suitable for XRD analysis readily prepared by diffusion of hexane into solutions of **59** in dichloromethane, emerging as orange blocks with dimensions up to *ca.* 5 mm, co-crystallising with 1.5 equivalents of hexane.

The solid-state structure of water complex **59** is illustrated in Figure 3.17. The compound is observed with  $C_s$  symmetry in the solid state, with the ubiquitous square pyramidal coordination geometry of the  $\{\text{Rh}(2,2'\text{-biphenyl})\}^+$  fragment. The Rh-O bond distance of 2.205(2) Å is contracted by 0.04 Å relative to the triphenylphosphine analogue **27** (2.244(2) Å). A C15-Rh1-O2 bond angle of 172.18(8)° is measured, slightly

further from linear than is found with **27** ( $176.03(9)^\circ$ ). This angle places the water ligand closer to the nearest arene moiety, and may perhaps be consequent of establishing favourable O-H- $\pi$  interactions between the water molecule and the calixarene. The final coordination site on the metal is seemingly vacant; while the **CxP<sub>2</sub>** phenyl groups are ideally situated such that they might offer agostic stabilisation, the M-C contacts are very distant at 3.485(2) and 3.503(2) Å. Despite this, the phenyl units are orientated in such a way so as to seemingly maximise any interaction with the metal centre. The phenyl units serve to complete the encapsulation of the water ligand, which is contained within an almost uninterrupted van der Waals surface defined by the calixarene, the biphenyl ligand and the phenyl groups acting in concert.

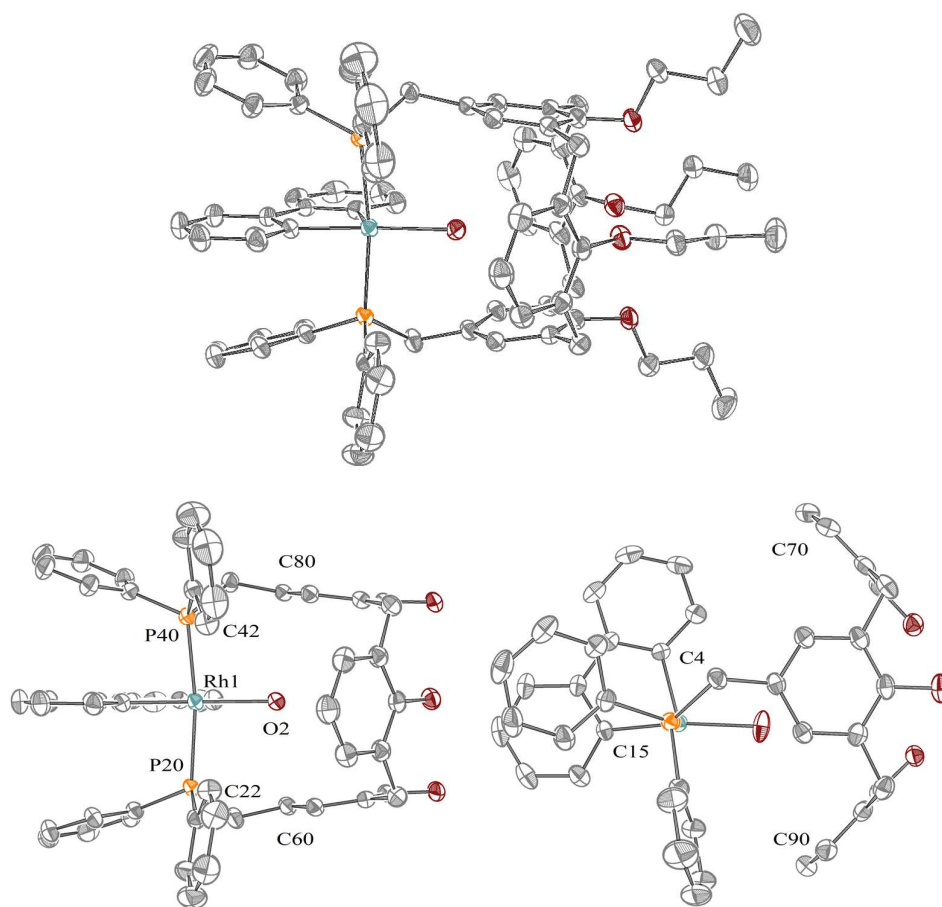


**Figure 3.17** Top: Crystal structure of water complex **59**; Data at 150 K, thermal ellipsoids drawn at 50%, [Al(OR<sup>F</sup>)<sub>4</sub>] anion and co-crystallised hexane omitted. Bottom: orthogonal views with labelled atoms of interest, truncated for clarity. Selected bond lengths (Å) and angles (°): Rh1-O2, 2.205(2); Rh1-P20, 2.3505(5); Rh1-P40, 2.3405(6); Rh1-C4, 1.982(2); Rh1-C15, 1.996(2); Rh1-C22, 3.503(2); Rh1-C42, 3.485(2); C60-C80, 5.945(3); C70-C90, 9.465(3); O2-Rh1-C15, 172.18(8); P20-Rh1-cent(rhodacycle), 86.85(3); P40-Rh1-cent(rhodacycle), 86.73(3); pln(C60)-pln(C80), 13.07(6); pln(C90)-pln(C70), 92.75(9).

Inspecting the calixarene core, the pinch-cone conformation is quantified by the distance between opposing apical carbons (C60-C80/C70-C90) of 5.945(3) and 9.465(3) Å. The angle between the planes defined by opposing arene units are slightly off parallel for the functionalised arenes (containing C60 and C80; 13.07(6)°) and near perpendicular for the splayed arenes (containing C70 and C90; 92.75(9)°). The metal fragment is positioned off-centre with respect to the calixarene, a necessity born of establishing a reasonable rhodium-phosphine interaction; a P-Rh-P angle approaching 180° is only viable with the calixarene contorting to either a  $C_s$  symmetric structure (as here), or one with  $C_2$  symmetry.

Water complex **59** exhibits time-averaged  $C_{2v}$  symmetry in the  $^1\text{H}$  NMR spectra recorded in  $\text{CD}_2\text{Cl}_2$  and  $\text{C}_6\text{D}_5\text{F}$  solution at 298 K. The spectra are notable for broad aromatic signals, resulting from conformational dynamics occurring at the  $^1\text{H}$  NMR timescale (600 MHz). The bound water is clearly detected at  $\delta_{\text{IH}}$  0.9 ppm in dichloromethane solution (*cf.*  $\delta_{\text{IH}}$  2.5 for complex **27**) though is coincident with a terminal propyl resonance in fluorobenzene solution at 298 K. The upfield shift is consistent with the encapsulation of the water protons by the aromatic cavity of the calixarene. This signal is static, and is entirely unaffected by the addition of excess water to the system; that is to say the rhodium centre does not persistently bind two water molecules.

### 3.3.4 Solution dynamics

Seeking to better understand the dynamics of complex **59**, solutions of the compound in dichloromethane and fluorobenzene were examined by NMR spectroscopy (400 – 600 MHz) across the full temperature range available to these solvents; 313 – 185 K and 353 – 230 K respectively, Figure 3.18. The dynamics are on first inspection qualitatively independent of solvent. Only in fluorobenzene solution at 353 K is full coalescence of the aromatic resonances of **59** achieved in the  $^1\text{H}$  NMR spectrum (600 MHz). At this temperature the bound water resonance becomes discernible at  $\delta_{\text{IH}}$  0.94.

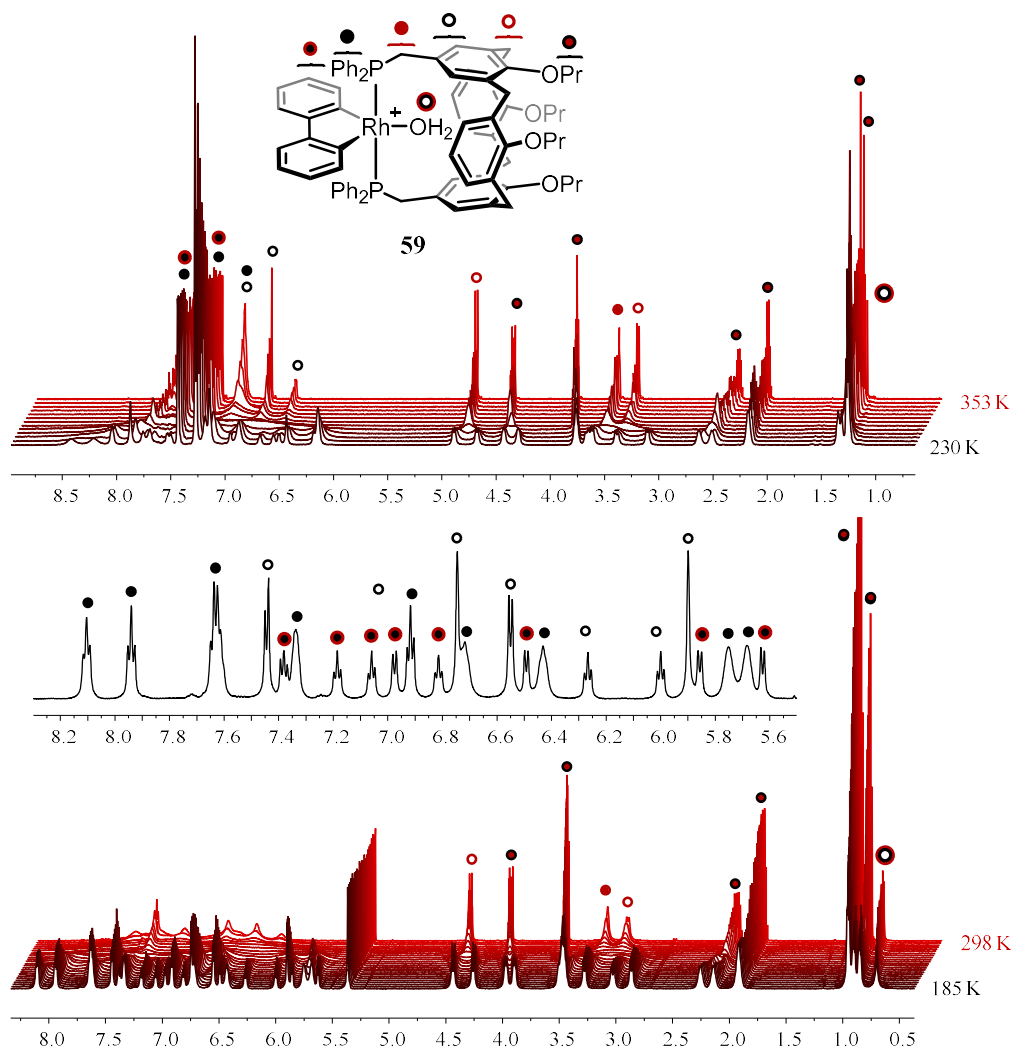


**Figure 3.18**  $^1\text{H}$  NMR spectra of water complex **59** (600 MHz) at 353 – 185 K in (top)  $\text{C}_6\text{D}_5\text{F}$  and (bottom)  $\text{CD}_2\text{Cl}_2$ . Inset: enlargement of the aromatic region of the  $\text{CD}_2\text{Cl}_2$  185 K spectrum.

At low temperature the  $^1\text{H}$  NMR signals of **59** decoalesce to a system with  $C_s$  symmetry, with a decoalescence temperature of *ca.* 255 K. By 210 K in dichloromethane solution the calixarene and biphenyl resonances are fully resolved. The offset nature of the calixarene evident in the solid state is also the case in low temperature solution, as evidenced by the two  $\text{CH}_2\text{P}$  protons having become inequivalent, observed at 185 K at  $\delta_{\text{H}}$  3.46 and 2.98 with a geminal coupling of *ca.* 16 Hz. The phenyl resonances remain broad at 210 K, though they are resolved as two distinct phenyl units per the conformation imposed by the calixarene (two moieties adjacent the metal, two projected

away from the complex, *cf.* the solid-state structure, Figure 3.17). Further cooling to 185 K decoalesces these resonances into two sets of signals for the *ortho* and *meta* positions, indicative of fully abated rotation of the phenyl moiety, ascribed to the steric environment of the system, as opposed to any persistent rhodium-phenyl interaction.

At least three relevant dynamic processes are implicated for complex **59**, and indeed mononuclear calixarene biphenyl systems in general; biphenyl pseudorotation, calixarene rocking, and phenyl rotation. The former two processes have a degenerate outcome; the interconversion of the two  $C_s$  symmetric forms of the system. For the purposes of studying the dynamics by  $^1\text{H}$  NMR spectroscopy, these processes are indistinguishable and are thus treated as a singular process, simply termed ‘inversion’.

The calixarene methylene resonances were modelled in gNMR (v4.1.2) in the temperature range 210 – 298 K with starting parameters determined from the 210 K experimental  $^1\text{H}$  NMR spectrum; a base line width of 3.64 and 4.18 Hz for the axial and equatorial protons respectively, and  $^2J_{\text{HH}}$  coupling constants of 12.84 and 13.17 Hz. Figure 3.19 summarises the simulation results. Using these data the thermodynamic parameters  $\Delta G^\ddagger_{298\text{K}} = 49.9(12) \text{ kJ}\cdot\text{mol}^{-1}$ ,  $\Delta H^\ddagger = 51.2(8) \text{ kJ}\cdot\text{mol}^{-1}$  and  $\Delta S^\ddagger = 5(3) \text{ J}\cdot\text{K}^{-1}\cdot\text{mol}^{-1}$  are extracted. Performing an equivalent analysis using the fluorobenzene solution data returns values that are the same, within error;  $\Delta G^\ddagger_{298\text{K}} = 50(3) \text{ kJ}\cdot\text{mol}^{-1}$ ,  $\Delta H^\ddagger = 48(2) \text{ kJ}\cdot\text{mol}^{-1}$  and  $\Delta S^\ddagger = -9(7) \text{ J}\cdot\text{K}^{-1}\cdot\text{mol}^{-1}$ . The entropy term is negligible in both instances with the free energy barrier largely comprised of enthalpic contributions.

The barrier to phenyl rotation was similarly evaluated via an Eyring analysis, modelling the experimental spectra in the range 185 K – 210 K, taking the starting line widths (3.70 Hz) and  $^3J_{\text{HH}}$  coupling constant (7.50 Hz) from the fully coalesced 353 K data. Parameters of  $\Delta G^\ddagger_{298\text{K}} = 43(3) \text{ kJ}\cdot\text{mol}^{-1}$ ;  $\Delta H^\ddagger = 33.8(12) \text{ kJ}\cdot\text{mol}^{-1}$  and  $\Delta S^\ddagger = -32(9) \text{ J}\cdot\text{K}^{-1}\cdot\text{mol}^{-1}$  were obtained. Here a not-insignificant negative entropy term is noted.

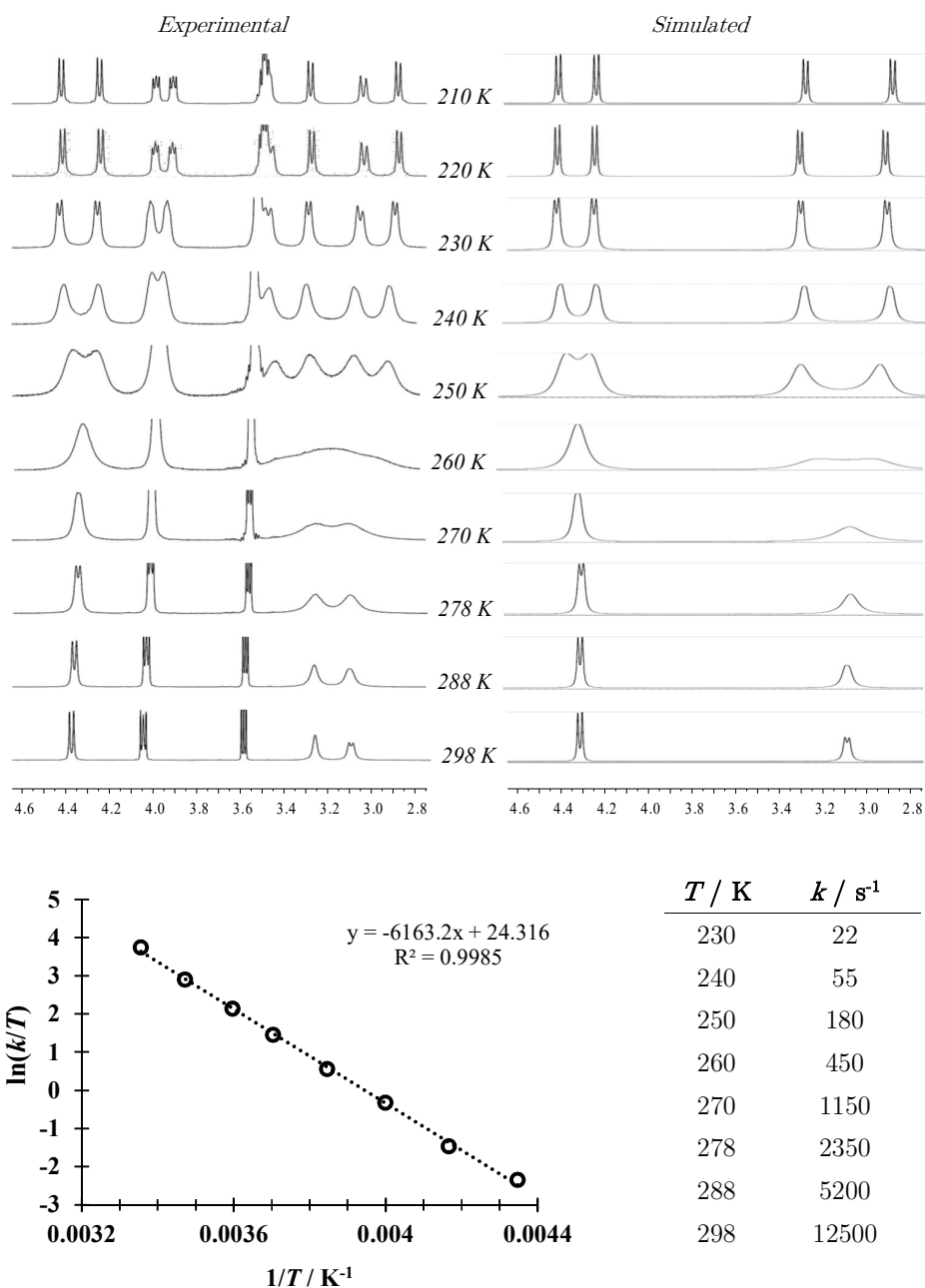


**Figure 3.19** Simulated methylene resonances of **59** in the range 210 – 298 K and Eyring analysis.

### 3.3.5 Synthesis via substitution

Preparation of water complex **59** via a salt metathesis of dimeric chloride **57** offers some undesirable synthetic limitations, particularly in the requirement for the precise stoichiometry of  $\text{Ag}[\text{Al}(\text{OR}^{\text{F}})_4]$  as described previously. This is further exacerbated when working at scale by inconsistent bulk purity of the silver salt, presumably in the most

part due to the photosensitivity of the reagent. It is also time consuming to fully eradicate the resultant silver chloride in its entirety, requiring several repeats of the purification procedures. Not content with these limitations, and building on prior knowledge of the phosphine substitution reactions of the triphenylphosphine complexes described in Section 2.4.6, it was determined that the reaction of  $[\text{Rh}(2,2'\text{-biphenyl})(\text{PPh}_3)_2][\text{Al}(\text{OR}^{\text{F}})_4]$  **30** with  $\text{C}_x\text{P}_2$  in THF converts cleanly within five hours to a solution of water complex **59**, Figure 3.20.

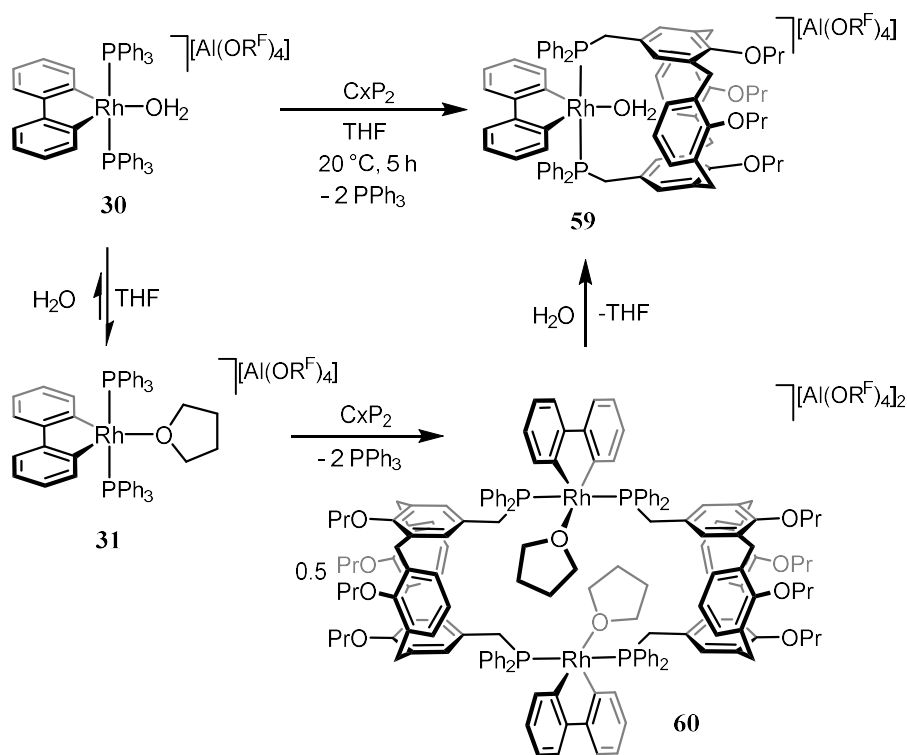


**Figure 3.20** Preparation of water complex **59** via phosphine substitution.

The reaction is found to proceed via an intermediate characterised as dimeric THF complex **60**, possessing a clear  $[\text{M}]^{2+}$  molecular ion peak in the mass spectrum. The  $^1\text{H}$  and  $^{31}\text{P}$  NMR spectra of **60** are notably broad at 298 K, precluding assignment in the first instance, and of the latter, a single broad doublet resonance is resolved at  $\delta_{31\text{P}}$  22.8 (fwhm = 45 Hz,  $^1J_{\text{RhP}} = 128$  Hz). Interestingly, the rate determining step in the substitution of triphenylphosphine complex **30** with  $\text{C}_x\text{P}_2$  appears to be the rearrangement-substitution of THF complex **60** to water complex **59**. The other steps



performed in isolation (establishment of the equilibrium between **30** and **31**, and phosphine substitution) are instantaneous processes. The rearrangement is found to proceed to completion irreversibly in NMR-scale syntheses, with the solitary equivalent of water from **30** sufficient to progress the transformation to completion. The resulting spectra are identical to those of an authentic sample of water complex **59** dissolved in THF.

While the synthesis of water complex **59** by substitution proceeds quantitatively on the scale of an NMR reaction, when performing a preparative scale reaction residual THF complex **60** persists in the reaction mixture, even with the supplementation of a vast excess of additional water (up to 1000 equivalents). In a curious observation: the initial appearance of the bulk reaction is a red solution, characteristic of the THF complex. Addition of excess water gives rise to a yellow solution. Leaving this solution for a period of hours returns the solution to an orange colour. The nuances of this reaction have not yet been exhaustively determined. Per the reactivity described in Section 2.4.5, the triphenylphosphine must be removed in its entirety prior to working with dichloromethane lest the sample revert to a chloride complex.

The viability of a substitution approach to the preparation of mononuclear rhodium calixarene complexes begs the question of whether a low-coordinate calixarene complex could be approached directly by substitution of anhydrous triphenylphosphine complex **29** prepared in fluorobenzene solution. Unfortunately, while in fluorobenzene substitution does occur near instantaneously on dissolution, the product is an ill-defined oligomeric species. This implies that the calixarene ligand at these rhodium biphenyl systems is kinetically inert in weakly coordinating solvents. It also carries the further implication that the water ligand itself is intrinsic to establishing the chelate; augmenting the thermodynamics of the system through the supply of two O-H- $\pi$  interactions with the calixarene. Computational work is ongoing elsewhere to explore the energetic contributions of such interactions.

### 3.4 Ligand exchange reactions

#### 3.4.1 Lability of the water ligand

Exposing a dichloromethane solution of water complex **59** to an atmosphere of carbon monoxide results in an immediate decolouration of the initially yellow solution. Inspection of the  $^1\text{H}$  and  $^{31}\text{P}\{^1\text{H}\}$  NMR spectra collected within 5 minutes indicated the clean conversion to a new  $\text{C}_x\text{P}_2$ -containing compound with associated liberation of one equivalent of water. The product of this reaction is characterised as calixarene bis(carbonyl) **61**, Figure 3.21. The compound is spectroscopically very similar to triphenylphosphine bis(carbonyl) **33** (*vide supra*, Section 2.4.4).  $^1\text{H}$  NMR signals express a  $C_{2v}$  symmetry, while the  $^{31}\text{P}\{^1\text{H}\}$  NMR spectra consists of a doublet resonance at  $\delta_{31\text{P}}$  15.3 ( $^1J_{\text{RhP}} = 97$  Hz). Compound **61** exhibits a similar stability profile to **33**; specifically that **61** begins to decompose to a new calixarene-based species on removing the carbon monoxide atmosphere. This reaction was not investigated in any great detail, but these results serve to indicate that the water ligand is kinetically labile in the presence of a stronger donor, and by extension that exchange of the water ligand should be possible under appropriate conditions.

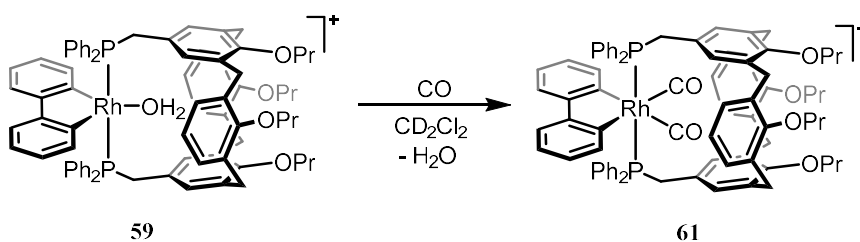
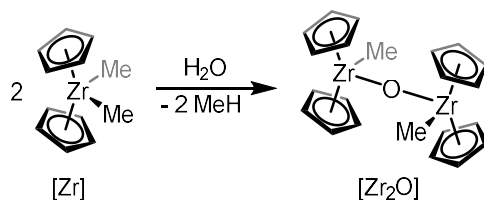


Figure 3.21 Reaction of water complex **59** with carbon monoxide.

In contrast to triphenylphosphine analogue **30**, standing dichloromethane solutions of water complex **59** over 3 Å molecular sieves under argon results in no detectable chemical change. This is proposed to be an equilibrium effect; given the previously observed water-sensitivity of silver chloride adduct **58** it can be reasonably posited that the thermodynamic favourability of water coordination to rhodium calixarene system exceeds the stabilisation offered by the interaction of water with the 3 Å zeolite, *i.e.*

that  $[\text{Rh}(2,2'\text{-biphenyl})(\text{CxP}_2)]^+$  is the superior molecular sieve. With that in mind, an alternative desiccating agent was sought. Dimethylzirconocene is known to rapidly and irreversibly react with water, Figure 3.22,<sup>356-358</sup> and has been used effectively as a drying agent in various organometallic preparations,<sup>359-362</sup> and also as a quantitative probe of the water content of weakly coordinating anions.<sup>363</sup> The by-product of this reaction is methane, which may be useful given the ultimate aim of this research endeavour.



**Figure 3.22** Reaction of dimethylzirconocene with water.

### 3.4.2 Zirconocene reactions in dichloromethane

Reaction of water complex **59** with 2.5 equivalents of dimethylzirconocene in dichloromethane solution at ambient temperature resulted in the steady conversion to one new calixarene-containing compound by  $^1\text{H}$  and  $^{31}\text{P}\{^1\text{H}\}$  NMR spectroscopy, Figure 3.23. The reaction proceeded to completion in 12 hours, consuming *ca.* 2 equivalents of dimethylzirconocene with concomitant formation of a methane and oxo-bridged zirconocene. The new calixarene compound is assigned as dichloromethane complex **62**, which by  $^{31}\text{P}\{^1\text{H}\}$  NMR spectroscopy is observed upfield of **59** as a relatively broad doublet resonance at  $\delta_{31\text{P}}$  4.4 ( $^1J_{\text{RhP}} = 115$  Hz). The  $^1\text{H}$  NMR spectrum of **62** is by contrast sharp; with a fully-coalesced  $C_{2v}$  symmetry. These observations are proposed to be consequent of a relatively persistent interaction between dichloromethane and the rhodium centre, but that consequent of the steric demands of the **CxP<sub>2</sub>** ligand is binding *exo* the cavitand. The association-dissociation is proposed to be fast on the  $^1\text{H}$  NMR time scale (400-600 MHz). The broad  $^{31}\text{P}$  resonance is suggested to be consequent of a strained or otherwise perturbed P-Rh-P chelate to accommodate an interaction with the bulky dichloromethane ligand; analogously to how the significant distortion in the

M-P bonding is energetically permissible to establish a closer agostic interaction in the trialkylphosphine complexes described previously (*vide supra*, Section 2.2.3).

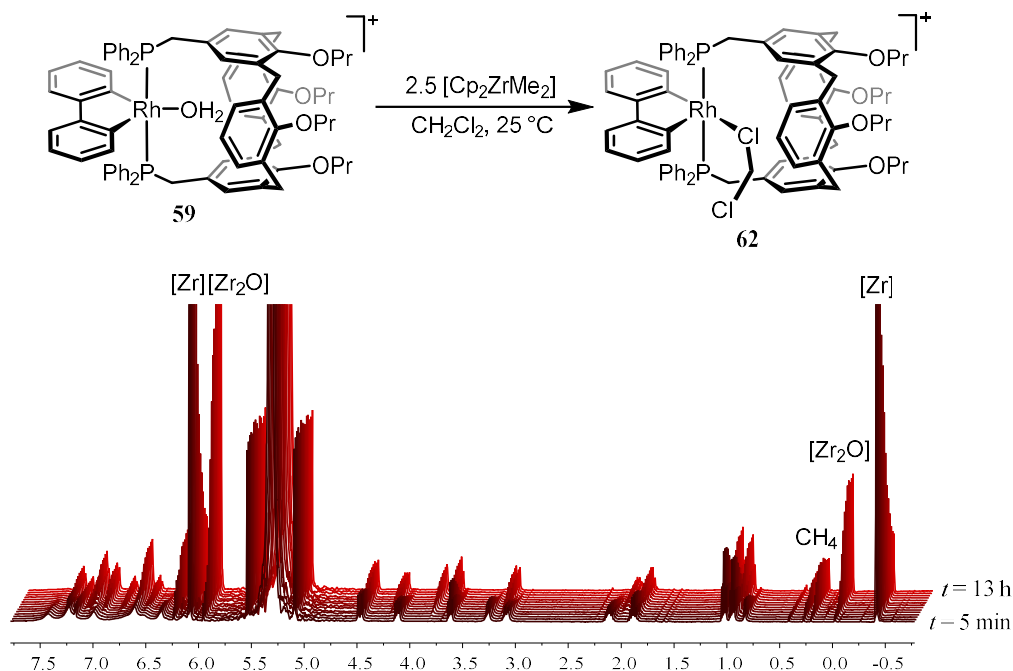


**Figure 3.23** Reaction of water complex **59** with dimethylzirconocene in dichloromethane. Time-resolved  $^1\text{H}$  NMR spectra (400 MHz) at hourly intervals for the 13 hours.

Given that dichloromethane is proposed to be excluded from an ideal binding pocket, introduction of a suitably sized substrate that is able to exist *endo* the calixarene should show a preferential binding. To this end the reaction was repeated under an atmosphere of dinitrogen. This was found to result in the formation of dichloromethane complex **62**, in addition to a new species, observed in the  $^{31}\text{P}\{^1\text{H}\}$  NMR spectrum as a sharp doublet resonance at  $\delta_{31\text{P}}$  16.1 ( $^1J_{\text{RhP}} = 117\text{ Hz}$ ), ascribed to dinitrogen complex **63**, Figure 3.24. The relative proportion of **62** and **63** are independent on reaction progress, remaining at a roughly constant 48:52 ratio throughout. Consistent with this formulation, freeze-pump-thaw degassing the solution transitions the mixture to exclusively dichloromethane complex **62**.

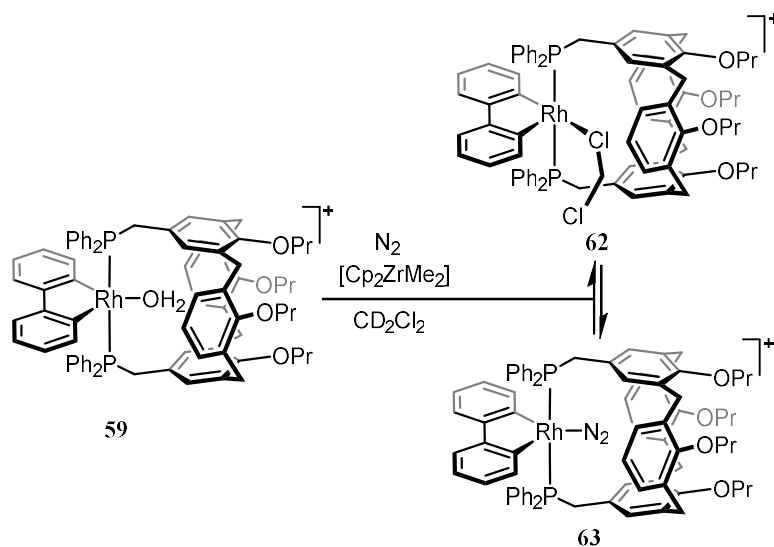


**Figure 3.24** Reaction of **59** with dimethylzirconocene in dichloromethane under dinitrogen.

Reaction of water complex **59** with dimethylzirconocene under dihydrogen affords another new compound, characterised as dihydrogen complex **64**, Figure 3.25, observed by  $^{31}\text{P}\{^1\text{H}\}$  NMR spectroscopy as a downfield-shifted doublet resonance at  $\delta_{31\text{P}}$  25.1 ( $^1J_{\text{RhP}} = 113$  Hz). No dichloromethane complex **62** is observed, suggesting a stronger interaction with dihydrogen compared to dinitrogen and dichloromethane. Dimethylzirconocene will react with dihydrogen,<sup>364–371</sup> however this process is slow enough that increasing the amount of zirconocene used in these reactions to 5.0 equivalents is sufficient to progress the reaction to completion. Alternatively, the compound may be prepared by replacing the atmosphere of a sample of dichloromethane complex **62** with dihydrogen. The occurrence of a dihydrogen complex is particularly significant given the known hydrogenolysis of the 2,2'-biphenyl ligand which occurs with triphenylphosphine complex **29** (*vide supra*, Section 2.4.3).

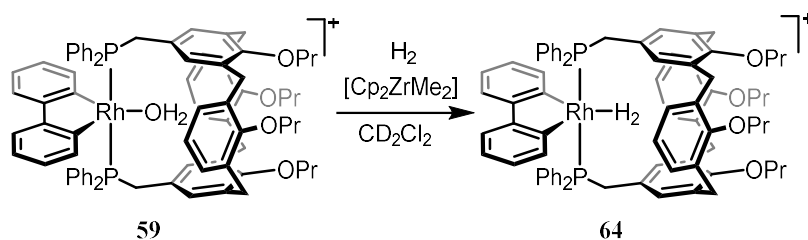


**Figure 3.25** Reaction of **59** with dimethylzirconocene in dichloromethane under dihydrogen.

A more in-depth discussion of dichloromethane, dinitrogen and dihydrogen complexes **62** – **64** follows in Section 3.5. These compounds all exhibit limited stability when synthesised via a reaction with dimethylzirconocene. After several days in the reaction media a new, very broad, but certainly calixarene-containing compound is observed by  $^1\text{H}$  NMR spectroscopy. Over time a red-brown precipitate is also observed in the reaction vessel. This material has thus far eluded identification, though is probably an oligomeric calixarene-based complex. While the material is soluble in polar solvents the resultant NMR spectra are generally uninformative.

### 3.4.3 Zirconocene reactions in fluorobenzene

Given that dichloromethane is observed to interact competitively with the metal centre, in the interest of preparing adducts of substrates with anticipated interactions weaker than those with dinitrogen, a change to a less coordinating solvent was mandated. Investigations proceeded into the use of fluorobenzene in reactions of water complex **59** with dimethylzirconocene.

Reaction of water complex **59** with dimethylzirconocene in fluorobenzene under argon resulted in complete decomposition over a period of 16 hours, to a compound with a similar spectroscopic and visual signature to the decomposition observed in dichloromethane. During the course of this reaction however, a new species is observed is the  $^{31}\text{P}\{^1\text{H}\}$  spectrum as a doublet resonance at  $\delta_{31\text{P}}$  17.2 ( $^1J_{\text{RhP}} = 122$  Hz). This new signal is rapidly consumed concurrently to the water complex, and is proposed to belong to formally 14 electron, 4-coordinate  $[\text{Rh}(2,2'\text{-biphenyl})(\text{CxP}_2)]^+$ , **65**, stabilised by transient interactions with the fluorobenzene solvent. As with dichloromethane, the size exclusion demanded by the **CxP<sub>2</sub>** cavity mandates this interaction is at an *exo* coordination site, though unlike with dichloromethane, no significant line broadening of the  $^{31}\text{P}\{^1\text{H}\}$  NMR signal of **65** is observed, suggesting a weaker, transient interaction.

In the presence of a coordinating gas, under the same conditions with a headspace of dinitrogen or dihydrogen, these reactions elicited full conversion to complexes **63** and

**64**, respectively. Both complexes possess similar  $^{31}\text{P}$  NMR data in fluorobenzene as compared to dichloromethane solution, with **63** and **64** resolved as doublet resonances at  $\delta_{31\text{P}}$  16.0 ( $^1J_{\text{RhP}} = 116$  Hz) and  $\delta_{31\text{P}}$  25.1 ( $^1J_{\text{RhP}} = 113$  Hz), respectively. The stability of these complexes under these conditions differ, with dihydrogen complex **64** exhibiting a protracted lifetime.

The reaction of water complex **59** with 2.5 equivalents of dimethylzirconocene under dinitrogen was examined under two temperature regimes, Figure 3.26. The reaction is observed to proceed to dinitrogen complex **63**, with complete consumption of **59** in 20 hours at 25 °C, and in 2 hours at 50 °C. At the higher temperature, the decomposition event is also accelerated, with the dinitrogen complex **63** only accounting for 60% of the starting concentration by the time the water complex is consumed.

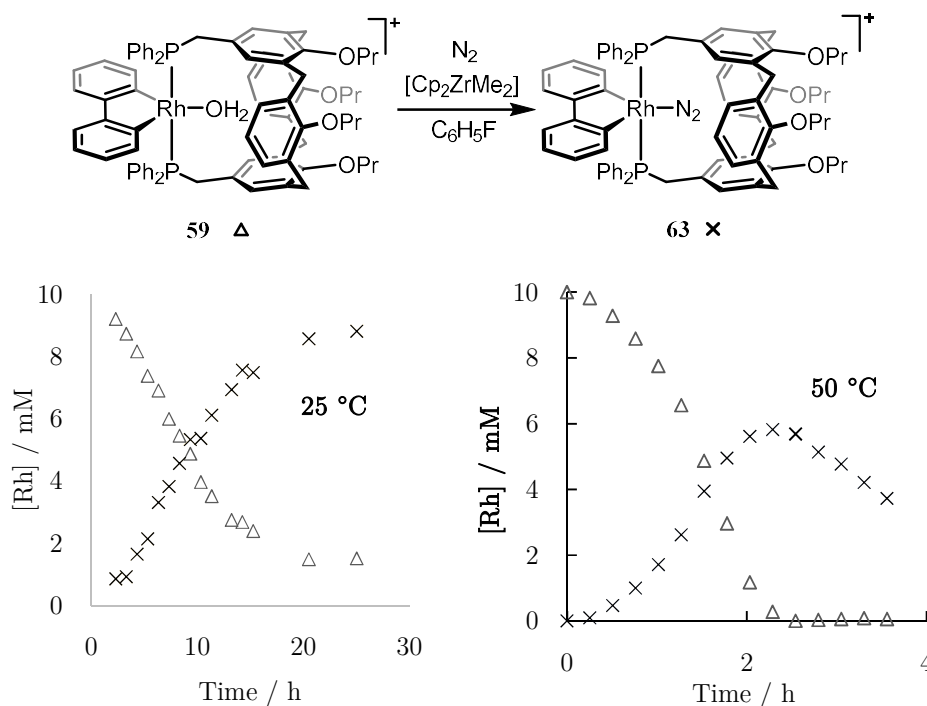


**Figure 3.26** Reaction of water complex **59** with dimethylzirconocene in fluorobenzene under dinitrogen, plots of absolute concentrations of **59** and **63** in solution at two reaction temperatures, as derived from integration of  $^1\text{H}$ ,  $^{31}\text{P}$  and  $^{31}\text{P}\{^1\text{H}\}$  NMR resonances.

Investigation commenced into introducing methane and xenon into these systems. Unfortunately, neither under methane nor xenon did these reaction conditions result in the observation of any new signals in the  $^{31}\text{P}\{^1\text{H}\}$  NMR spectra, with the only product

signal observed spectroscopically indistinguishable from previous recordings of the proposed low coordinate **65**. With both gasses the reaction kinetics are observed to be roughly equivalent to reactions performed under argon,

Quantitative analyses of the zirconocene drying reaction kinetics are hampered by a general lack of reproducibility. There are several mitigating factors which may account for this; for example the highly variable starting concentration of dimethylzirconocene due to the initial reaction with any available free water, both residual water adhered to the inner surface of the glassware and within the solvents themselves. The reactions are also found to be highly pressure sensitive; when performed with a higher over pressure of dinitrogen, dihydrogen (*ca.* 3 bar) or indeed xenon (*ca.* 5 bar) the reaction is dramatically slowed, with only limited consumption of water complex **59** observed after a 24-hour time frame.

In terms of isolating the complexes **62** – **65**, removing the zirconocene-derived products and reagents from the reaction mixtures is challenging without reverting the calixarene containing species to water complex **59**, with crystallisation attempts hampered by the ongoing decomposition reaction. During the course of attempting to purify the products of the zirconocene drying reactions, it was determined that complexes **62** - **65** are, in fact, indefinitely stable in isolation. Either dimethylzirconocene or one of the zirconium-containing products of the drying reaction, are causing the irreversible decomposition of the mononuclear calixarene complexes.

#### 3.4.4 Returning to sieves

It was earlier remarked that 3 Å molecular sieves are ineffective at eliminating water from these systems in dichloromethane under argon. Having now become reasonably convinced of the persistent interaction of the rhodium calixarene system with dinitrogen and dihydrogen, the assertion was made that the equilibrium in which water thermodynamically favours the calixarene over a 3 Å molecular sieve, might be perturbed sufficiently by the introduction of a competent donor substrate. This is indeed



the case, and the results of these investigations, covering dichloromethane and fluorobenzene solvent, under argon, dinitrogen and dihydrogen atmospheres are collated in Table 3.1. The reactions proceed with high order kinetics, potentially rationalised by the multiple water binding sites available within the 3 Å zeolite.<sup>372,373</sup> The kinetics are again challenging to quantify, largely because of inconsistencies in solution mixing, and variable size, shape and activation of the 3 Å molecular sieves.

**Table 3.1** Product distributions of 3 Å molecular sieves drying reactions.<sup>a</sup>

	solvent	atm	P / bar	3 Å MS <sup>b</sup>	t / h	59	62	63	64	65
1	CD <sub>2</sub> Cl <sub>2</sub>	Ar	1	200	108	1.00				
2	CD <sub>2</sub> Cl <sub>2</sub>	Ar	1	2000	66	0.65	0.35			
3	CD <sub>2</sub> Cl <sub>2</sub>	N <sub>2</sub>	1	2000	48	0.42	0.37	0.21		
4	CD <sub>2</sub> Cl <sub>2</sub>	N <sub>2</sub>	3	2000	120	0.61	0.11	0.28		
5	CD <sub>2</sub> Cl <sub>2</sub>	H <sub>2</sub>	1	2000	12	0.00				1.00
6	CD <sub>2</sub> Cl <sub>2</sub>	H <sub>2</sub>	3	2000	3	0.00				1.00
7	C <sub>6</sub> H <sub>5</sub> F	N <sub>2</sub>	1	200	16	0.85		0.15		
8					144	0.72		0.28		
9				200 <sup>d</sup>	24	0.64		0.36		
10				5000 <sup>d</sup>	0	0.72		0.28		
11					24	0.67		0.33		
12					48	0.25		0.75		
13	C <sub>6</sub> H <sub>5</sub> F	N <sub>2</sub>	3	2000	48	0.57		0.43		
14					168	0.51		0.49		
15	C <sub>6</sub> H <sub>5</sub> F	H <sub>2</sub>	1	200	24	0.37				0.63
16					48	0.31				0.69
17					72	0.29				0.71
18				200 <sup>d</sup>	24	0.13				0.87
19					48	0.13				0.87
20	C <sub>6</sub> H <sub>5</sub> F	Ar	1	200	96	1.00				0.00

<sup>a</sup> product ratios determined by NMR integration, with <sup>1</sup>H, <sup>31</sup>P and <sup>31</sup>P{<sup>1</sup>H} data all in excellent agreement;  
<sup>b</sup> wt%; <sup>c</sup> sieves replaced with a fresh batch after the preceding time point.

Speaking qualitatively; the more sieves, the longer the agitation time, the higher the pressure, and the more coordinating the substrate, the lower the concentration of water complex **59** in solution. Replacing the sieves for a fresh batch once the equilibrium has been reached is a potential avenue to eliminate water entirely, however the benefits of the fresh sieves were often counterbalanced by ingress of adventitious water, even during the most careful of manipulations. Crucially, however, under dihydrogen in dichloromethane, dihydrogen complex **64** may be prepared as the exclusive organometallic component of the solution. Significantly, through careful sample manipulation, this grants access to dinitrogen and dichloromethane adducts **63** and **64**, and the low coordinate complex **65**.

### 3.5 Preparation of water-free calixarene complexes

#### 3.5.1 Practical considerations

The syntheses of complexes **62** – **65** had to address the following challenges: (1) The system is an equilibrium perturbed by a gas, thus if the solution is in contact with the 3 Å molecular sieves that contain a stoichiometric quantity of water, removal of the coordinating atmosphere will swiftly restore the water molecule to its thermodynamic minimum in the calixarene. (2) Simple manipulations such as cannular transfer are sufficient to provide a stoichiometric amount of water to the system. (3) The ligand exchange reactions are themselves equilibria, such that multiple repeat manipulations are demanded to achieve full conversion from one complex to another.

The experimental design devised to circumvent these issues was as follows. An NMR tube was fitted with a glass pedestal (a glass capillary with an engorged end that is only slightly narrower than the inner diameter of the NMR tube). The 3 Å molecular sieves are added above the capillary, such that in a vertical configuration the solution is below, and not in contact with, the sieves. By rotating the NMR tube the sieves and solution are free to mix. The solvent may thereby be degassed or evaporated *in vacuo*, and the sieves easily replaced. This approach also has the added advantage of keeping

the solid desiccant out of the probe of the NMR spectrometer so as not to negatively affect the spectrum quality. The approach is however limited by losses of material to the surfaces of the sieves and the accumulation of not insignificant amounts of pulverised molecular sieves, precluding meaningful determinations of yield.

### 3.5.2 The dihydrogen complex

Per Table 3.1, agitation of a solution of water complex **59** in dichloromethane over 2000 wt% 3 Å molecular sieves under 3 bar of dihydrogen for 3 hours is sufficient to afford a >95% clean sample of dihydrogen complex **64**. Spectra in fluorobenzene were obtained by removing the dichloromethane solvent *in vacuo*, dissolving the residues in fluorobenzene, removing the solvent once more and finally dissolving the compound in *d*<sub>5</sub>-fluorobenzene and restoring the dihydrogen atmosphere. The dihydrogen complex is found to be indefinitely stable under dihydrogen, with no evidence of any onward reactivity. As noted, the chemical robustness exhibited here is in sharp contrast to the facile hydrogenolysis of bis(triphenylphosphine) analogue **29**. This is an alternative and unanticipated stabilisation vector of the calixarene ligand; rather than bolstering the thermodynamics of the binding interaction or sterically shielding the metal centre, in this instance the rigid *trans*-chelate hinders the establishment of a suitable coordination mode in which biphenyl hydrogenolysis can occur.

The 298 K <sup>1</sup>H NMR spectrum (600 MHz) of **64** is highly dynamic, even more so than water complex **59**, with no resolution possible of any aromatic <sup>1</sup>H resonances. The non-aromatic calixarene signals are very much in line with those of **59**. The dihydrogen ligand is not observed in the range  $\delta_{\text{H}}$  20 – -90. Similarly, no additional coupling is observed comparing the <sup>31</sup>P and <sup>31</sup>P{<sup>1</sup>H} NMR spectra. Given the dynamic nature of the system the assignment of a dihydrogen complex is not necessarily in doubt as a consequence of this observation. Aside from the dynamics of the calixarene framework, with a substrate as coordinating and as small as dihydrogen, dihydrogen complex **64** likely has access to additional ligand exchange dynamics, such as ligand tumbling, and access to a stable *exo*-only binding mode.

To better explore the dynamic processes, and to attempt to locate a bound dihydrogen ligand, solutions of **64** in fluorobenzene and dichloromethane were progressively cooled to 230 K and 185 K respectively. The recorded spectra are generally similar to that of water complex **59** down to *ca.* 215 K, progressing to a  $C_s$  symmetric structure. Notably, Below the  $C_{2v}$  /  $C_s$  decoalescence temperature, a second species appears in the  $^1\text{H}$  and  $^{31}\text{P}$  NMR spectra. This compound is bis(dihydrogen) complex **66**, Figure 3.27, observed upfield of the dihydrogen complex at *ca.*  $\delta_{31\text{P}}$  20.3 (185 K) with a slightly smaller  $^1J_{\text{RhP}}$  coupling constant of 107 Hz. The low-temperature  $^1\text{H}$  NMR spectrum is found to contain a slightly offset duplication of all the  $C_s$  symmetric calixarene signals of dihydrogen complex **64**. Additionally, two very broad signals are observed upfield at  $\delta_{1\text{H}}$  -0.10 (fwhm = 177 Hz) and -1.79 (fwhm = 395 Hz), in a 1:1 ratio with each other and with the new set of calixarene containing signals, assigned as the *exo*-H<sub>2</sub> and *endo*-H<sub>2</sub> ligands, respectively. No additional signal for the bound dihydrogen ligand of **64** is observed.

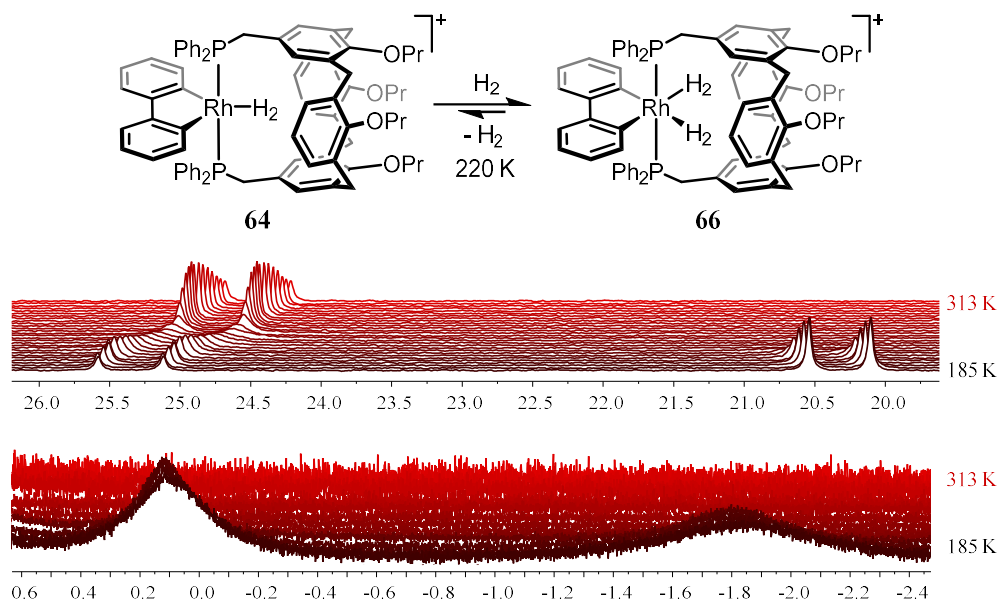


**Figure 3.27**  $^{31}\text{P}\{^1\text{H}\}$  (top) and  $^1\text{H}$  (bottom) NMR spectrum of the dihydrogen system **64** / **66** ( $\text{CD}_2\text{Cl}_2$ , 162 MHz), 313 – 185 K.

Substantiating this assignment, below the temperature at which bis(dihydrogen) **66** appears in the spectra, free dihydrogen is apparent at *ca.* 4.2 ppm, indicating slow dynamic dihydrogen exchange, brought about by the establishment of a saturated

bis(dihydrogen complex). Cycling above and below the decoalescence temperature repeatedly causes the signals assigned to **66** to appear and disappear, and repeating the variable temperature NMR study with a sub-stoichiometric quantity of dihydrogen results in cooling through to 185 K without the appearance of complex **66**. A variable delay experiment was unable to locate any resonance with an appropriate  $T_1$  relaxation time for a bound dihydrogen ligand.

### 3.5.3 The dichloromethane complex

Cooling a dichloromethane solution of dihydrogen complex **64** to -78 °C and slowly, over a period of hours, remove the solvent *in vacuo*, followed by redissolving the sample in dichloromethane, is the least taxing method of removing the dihydrogen ligand and achieving a sample of dichloromethane complex **62**. The spectra obtained are in agreement with those recorded *in situ* during the zirconocene drying reactions; a broad doublet in the  $^{31}\text{P}\{^1\text{H}\}$  NMR spectrum at  $\delta_{31\text{P}} = 4.4$ , and a room temperature  $^1\text{H}$  NMR spectrum with well defined, sharp resonances of a  $C_{2v}$  symmetric calixarene complex. Incremental cooling of the solution to 185 K results in the same decoalesce behaviour observed for the other calixarene complexes described, Figure 3.28. Samples prepared with proteo-dichloromethane and deuterio-dichloromethane are indistinguishable even at 185 K, indicative of a weak interaction between solvent and metal.

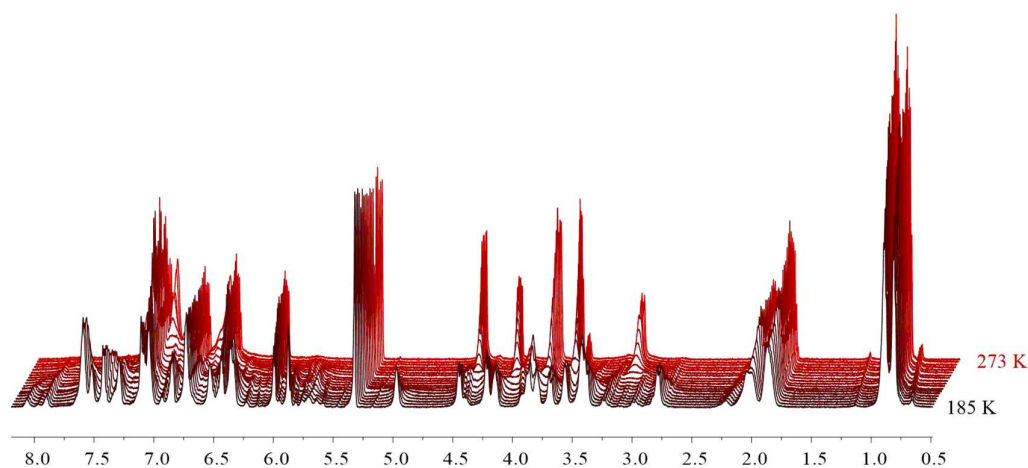


**Figure 3.28**  $^1\text{H}$  NMR spectrum of dichloromethane complex **62** ( $\text{CD}_2\text{Cl}_2$ , 600 MHz), 273 – 185 K.

### 3.5.4 The low-coordinate complex

Dissolution of dichloromethane complex **62** in fluorobenzene results in the liberation of one equivalent of dichloromethane, and a single calixarene containing complex, low-coordinate **65**. The dichloromethane molecule may be removed entirely by removing the fluorobenzene solvent *in vacuo* and re-dissolving the residues in fluorobenzene. Exposure of **65** to an atmosphere of xenon results in no appreciable change in either the  $^1\text{H}$  or the  $^{31}\text{P}\{^1\text{H}\}$  NMR spectrum. Given how sensitive the later nuclei has proved to be in probing the metal coordination sphere, the conclusion must be drawn that no persistent interaction with xenon is occurring, despite the availability of a highly reactive metal fragment.

It may well be the case that the calixarene cavity is simply too small to house the xenon atom. In a previously crystallographically characterised calixarene-xenon host-guest complex, *tert*-butylcalixarene is observed in a cone conformation, offering a large internal surface to the included xenon atom, with interactions supplemented by the upper rim *tert*-butyl groups.<sup>294</sup> With rhodium complex **65**, the anticipated pinched-cone conformation severely limits the size of substrates that may bind inside the cavity.

### 3.5.5 The dinitrogen complex

Dinitrogen complex **63** may be prepared either by multiple freeze-pump-thaw degas cycles of dihydrogen complex **64**, replacing the dihydrogen atmosphere with dinitrogen, or, unsurprisingly, by taking isolated low-coordinate complex **65** and introducing dinitrogen. This latter approach was taken to prepare the  $^{15}\text{N}_2$  labelled dinitrogen complex, however within the working temperature range of the fluorobenzene solvent used, the bound dinitrogen ligand was not observed spectroscopically, either with an overpressure of  $^{15}\text{N}_2$  or a sub-stoichiometric quantity. Experiments at lower temperature in dichloromethane may resolve the bound ligand once the slow-exchange regime of the calixarene ligand dynamics is reached, but this approach will be further hampered by the dinitrogen-dichloromethane equilibrium.

Pleasingly however, crystalline material of dinitrogen complex **63** was forthcoming, obtained through slow diffusion of hexane into dichloromethane solutions of **63** derived from a dimethylzirconocene reaction, Figure 3.28. The dinitrogen complex is isomorphic and isostructural with the water complex, again co-crystallising with 1.5 equivalents of hexane. The dinitrogen ligand is seen not to significantly impact the calixarene structure; and generally all bonding metrics are in line with water complex **59**. The calixarene is in approximately the same configuration, with a slightly reduced pinch angle; C60-C80 = 6.150(3) Å, C70-C90 = 9.355(4) Å, pln(C60)-pln(C80) = 15.81(8)°, and pln(C90)-pln(C70) = 90.16(11)° (**63**) compared to C60-C80 = 5.945(3) Å, C70-C90 = 9.465(3) Å, pln(C60)-pln(C80) = 13.07(6)°, and pln(C90)-pln(C70) = 92.75(9)° (**59**). The Rh-P separations are slightly elongated with complex, at 2.3733(7) and 2.3628(7) Å (**63**) compared to 2.3505(5) and 2.3405(6) Å (**59**). The same is true of the biphenyl carbon separations, here at 2.000(2) and 2.009(3) Å.

Regarding the dinitrogen ligand; the N2-Rh1-C15 bond angle is measured at 176.7(2)°, closer to linear with respect to the 2,2'-biphenyl ligand that is the case with the water ligand (O2-Rh1-C15 = 172.18(8)°). The Rh-N2 bond itself is also close to linear; Rh1-N2-N3 = 179.4(1)°, and long; at 2.160(3) Å the Rh-N bond length is far in excess of the previously documented maximum of Rh-N contacts, the previous longest being *ca.* 2.076(2) Å at a PBP pincer complex,<sup>143</sup> (*cf.* Section 1.4.2). This difference is perhaps is not unexpected given that this is the first crystallographically characterised Rh(III) dinitrogen complex, and given the unique ligand environment.

The N-N bond length in complex **63** of 1.091(4) Å is only slightly shorter than free dinitrogen, 1.0976(2),<sup>374</sup> though as noted previously there is a disconnect between solid-state bond lengths and the extent of dinitrogen activation, which is much better probed by IR techniques.<sup>133</sup> Unfortunately, at the time of writing no satisfactory IR spectrum of complex **63** featuring a definitive  $\nu(\text{N-N})$  stretching band has been obtained, owing predominantly to the extreme hydrophilicity of this compound. Efforts towards satisfying this endeavour are ongoing.

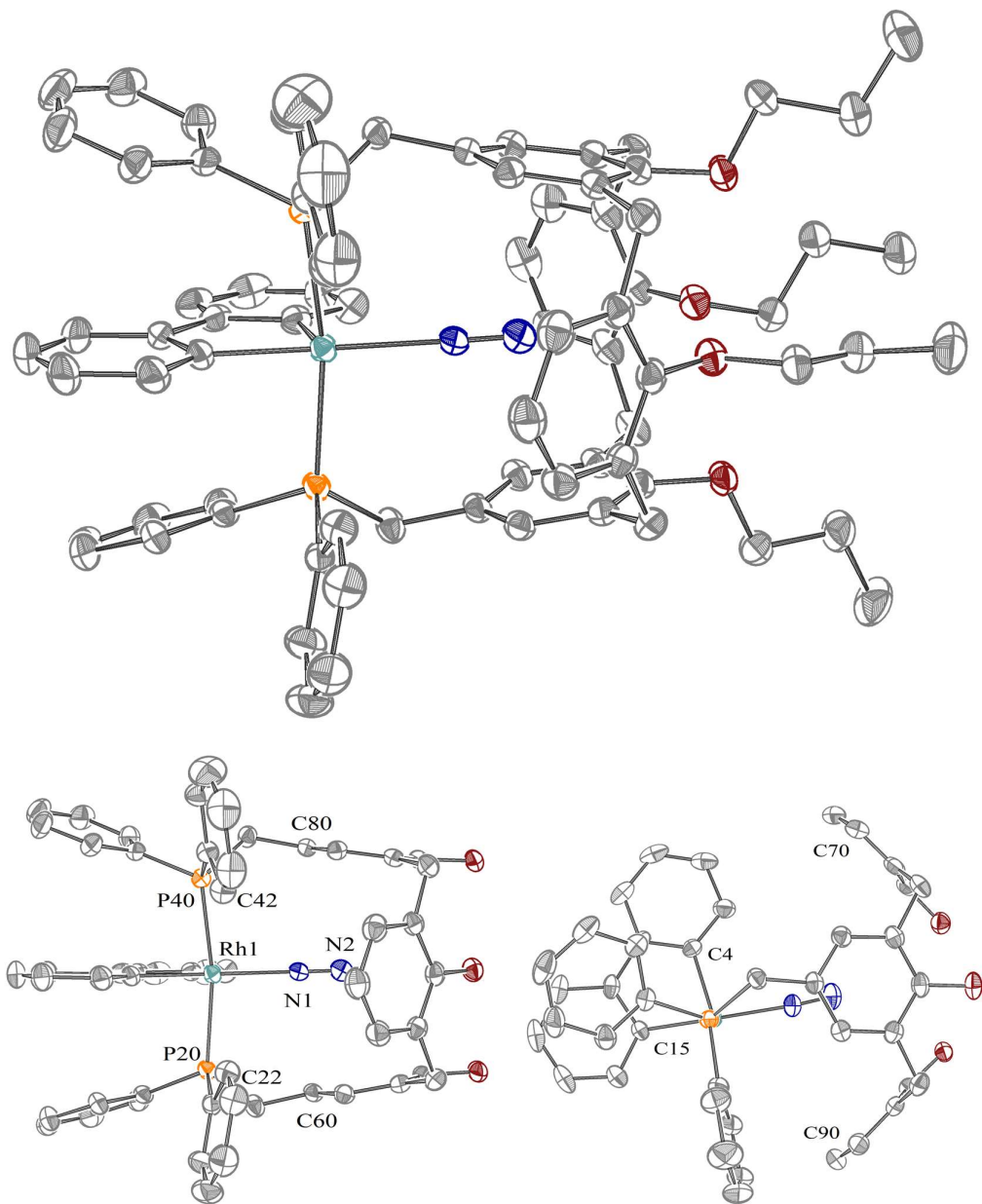


**Figure 3.29** Top: Crystal structure of dinitrogen complex 63; Data at 150 K, thermal ellipsoids drawn at 50%,  $[\text{Al}(\text{OR}^{\text{F}})_4]$  anion and co-crystallised hexane omitted. Bottom: orthogonal views with labelled atoms of interest, rear half of calixarene and propyl groups omitted for clarity. Selected bond lengths (Å) and angles (°): Rh1-N2 = 2.160(3), N2-N3 = 1.091(4), Rh1-P20 = 2.3733(7), Rh1-P40 = 2.3628(7), Rh1-C4 = 2.000(2), Rh1-C15 = 2.009(3), Rh1-C22 = 3.515(2), Rh1-C42 = 3.470(3), C60-C80 = 6.150(3), C70-C90 = 9.355(4), Rh1-N2-N3 = 179.4(1), N2-Rh1-C15 = 176.7(2), P20-Rh1-cnt(rhodacycle) = 86.42(4), P40-Rh1-cnt(rhodacycle) = 86.26(4), pln(C60)-pln(C80) = 15.81(8), pln(C90)-pln(C70) = 90.16(11).



### 3.6 Conclusions and future work

This chapter has described two successful methodologies for the synthesis of mononuclear complexes of a calixarene-based diphosphine. The resulting rhodium calixarene systems form extremely robust mono-aqua complexes, which is both a great convenience with respect to isolating and working with the calixarene water complex, but also presents a sizable synthetic challenge with respect to irreversibly extricating the water ligand in order to install a more chemically interesting substrate. This has been achieved with the preparation of dinitrogen, dihydrogen and dichloromethane complexes, and through establishing a route to the formally unsaturated complex, from which complexes featuring alternative small substrates should be synthetically viable. Unfortunately no evidence of a persistent methane or xenon complex was forthcoming, potentially hindered in the latter case by the size constraints of the cavity.

This work has succeeded in, for the first time, preparing a persistent Rh(III) dinitrogen complex that is amenable to solid-state characterisation. Though despite the expected degeneracy of the solid-state structures of the adducts presented – defined as they are by the exterior surface of the complexes – only the water and dinitrogen complex have been isolated as crystalline materials suitable for study by X-ray diffraction thus far. With more sustained efforts in this regard complexes of other substrates should be isolable, though research into larger, more accommodating cavitand-based ligands is perhaps be a more promising endeavour. This avenue will be explored in Chapter 5.

The use of an encapsulating ligand architecture to stabilise weak interactions is vindicated as a strategy, though the inherent dynamics of this particular ligand scaffold are somewhat problematic; obfuscating the interrogation of the dihydrogen and dinitrogen interactions by NMR spectroscopy. The best prospects for future enquiries with these systems would require a redesign of the ligand environment to perturb the flexible molecular motion of the system. This could involve adding additional bulky functionality to the calixarene, tethering the arenes of the calixarene into a rigid conformation, or conversely by installing bulky components on the 2,2'-biphenyl ligand.

This chapter describes the preparation and characterisation of cationic rhodium and iridium phosphine complexes supported a 2,2'-bipyridyl ligand as a structural analogue of the 2,2'-biphenyl ligand previously explored, with the view to accessing M(I)/M(III) redox chemistry, and ultimately targeting the preparation of a mononuclear complex featuring **CxP<sub>2</sub>** paired with the 2,2'-bipyridyl ancillary ligand. The syntheses of complexes of the form  $[M(2,2'\text{-bipyridyl})(H)_2(PPh_3)_2]^+$  ( $M = Rh, Ir$ ) from simple organometallic precursors are described, with mechanistic insight garnered by the identification of key intermediates in competitive reaction pathways. A synthetic route to one of these intermediates,  $[Rh(2,2'\text{-bipyridyl})(PPh_3)_2]^+$ , was identified in the course of these investigations, and investigated for its propensity to engage in oxidative addition chemistry. The chapter closes with efforts to incorporate the **CxP<sub>2</sub>** ligand in a *trans*-chelating manner, spanning a  $\{M(2,2'\text{-bipyridyl})\}$  fragment, though the synthetic methodology proved unsuitable to this particular application.

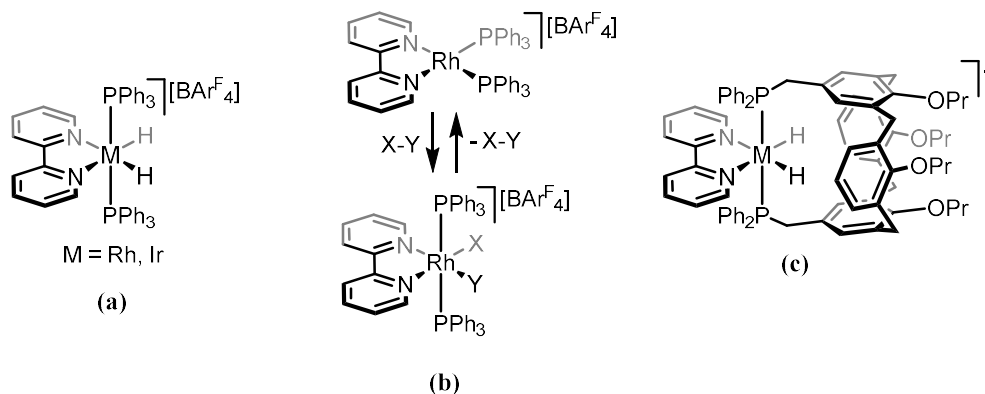


**Figure 4.1** Work involving complexes supported by the 2,2'-bipyridyl ligand: (a) in depth mechanistic understanding of the synthesis of *trans*-bis(phosphine) rhodium and iridium dihydride complexes of the 2,2'-bipyridyl ligand; (b) investigation of the redox chemistry of the systems; (c) targeted synthesis of a mononuclear complex featuring **CxP<sub>2</sub>**.

*Publications resulting from work described in this chapter:*

3. J. Emerson-King, R. C. Knighton, M. R. Gyton, and A. B. Chaplin, *Dalton Trans.*, 2017, **46**, 11645-11655.

## 4.1 Complexes of 2,2'-bipyridyl

### 4.1.1 Preparation of dihydride salts

In parallel to the work described in the previous chapter, efforts were undertaken to synthesize rhodium and iridium 2,2'-bipyridyl fragments of  $C_xP_2$ , both as structural models, and for exploring potential oxidative addition chemistry. Rhodium and iridium complexes of the form  $[M(2,2'\text{-bipyridyl})H_2(PPh_3)_2]^+$  were targeted in this pursuit, and have been previously reported with the counter ions  $[Cl]^-$ ,<sup>375</sup>  $[BF_4]^-$ ,<sup>375-377</sup>  $[PF_6]^-$ ,<sup>375,377,378</sup>  $[N(CN)_2]^-$ ,<sup>375</sup>  $[OTf]^-$ ,<sup>377,379</sup> and  $[BPh_4]^-$ ,<sup>377</sup> for iridium, and as the  $[ClO_4]^-$ ,<sup>380,381</sup>  $[B_9H_{12}S]^-$ ,<sup>382</sup> and  $[BPh_4]^-$ ,<sup>383</sup> salts at rhodium. A range of synthetic procedures are employed across these examples, here adapted and standardised for the synthesis of  $[BAR^F_4]^-$  salts in dichloromethane solution.

Synthesis of the complexes  $[M(2,2'\text{-bipyridyl})H_2(PPh_3)_2][BAR^F_4]$  ( $M = Rh$ , **67**;  $M = Ir$ , **68**) was undertaken by reaction of stoichiometric mixtures of  $[M(cod)(PPh_3)_2][BAR^F_4]$ , ( $M = Rh$ , **69**;  $M = Ir$ , **70**) and 2,2'-bipyridyl in dichloromethane under an atmosphere of dihydrogen, Figure 4.2. With both metals the reactions proceeded to the desired dihydride, however the rhodium congener reacts markedly slower; 18 hours at 50 °C, or 8 days at 25 °C, compared to the essentially immediate preparation of iridium complex **68**, apparent from a striking colour change from deep red to pale yellow associated with the hydrogenation. Both **67** and **68** are characteristically identified by upfield hydride resonances at  $\delta_{1H}$  -15.66 (app. q,  $^1J_{RhH} \approx {}^2J_{PH} \approx 14$  Hz) and -19.48 (t,  $^2J_{PH} = 17$  Hz), and  $^{31}P\{^1H\}$  resonances at  $\delta_{31P}$  47.1 (d,  $^1J_{RhP} = 115$  Hz) and 20.1, respectively. All data are in good agreement with reported metrics for compounds with alternative anions.

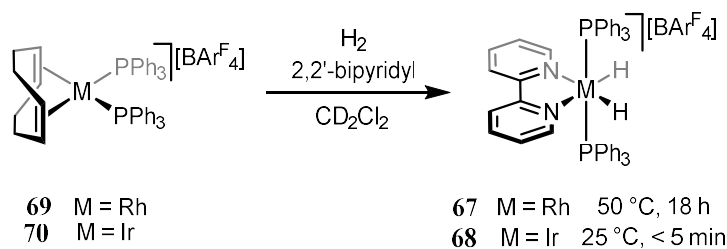


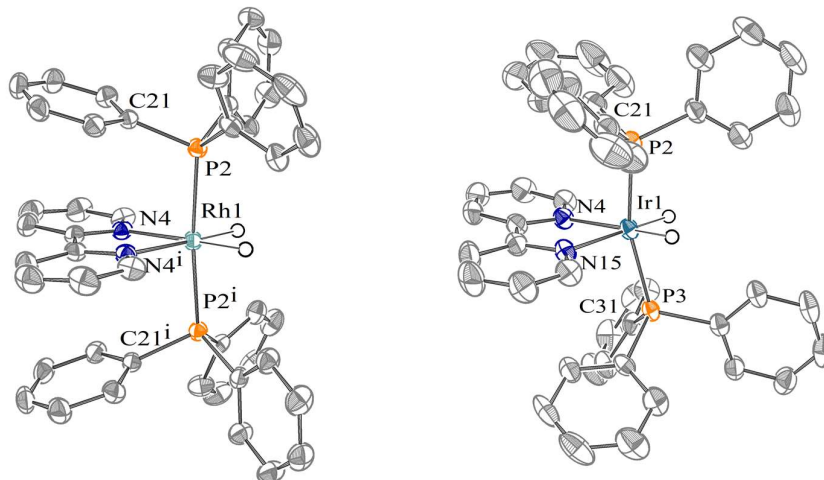
**Figure 4.2** Synthesis of rhodium and iridium dihydrides **67** and **68**.

#### 4.1.2 Comparison of structural metrics

Crystals of  $[M(2,2'\text{-bipyridyl})H_2(PPh_3)_2][BAr^F_4]$  suitable for crystallographic analysis were obtained on slow diffusion of hexane into dichloromethane solutions of **67** and **68**. A single polymorph of **67** and two of **68** were studied. Table 4.1 collates these metrics together with the solid-state data for their literature counterparts with alternative counter anions. The cationic components in each instance all exhibit the anticipated pseudo-octahedral geometries, though with varying distortion of the phosphine ligands away from the bipyridyl unit. At the extreme, iridium  $[BAr^F_4]$  **68**, rhodium  $[B_9H_{12}S]$  **A93** and iridium  $[PF_6]$  **A94** salts all possess a P-M-cent angle in excess of  $101^\circ$ . This bend in P-M-P bond angle away from linear is a known structural feature with iridium, found in complexes with various ancillary ligands aside from 2,2'-bipyridyl, including complexes of DCE,<sup>384</sup> and  $[HCB_{11}H_5I_6]$ .<sup>385</sup>

A wide range of conformations of the phosphine moieties is apparent, most overtly in their relative orientations. These range between near-eclipsed with rhodium complex **67** and one of the morphologies of **68**, as quantified by a C21-P2-P3-C41 torsion angle of  $11.5^\circ$  and  $118.0^\circ$  respectively, to the staggered conformation of triflate salt **A95**, in which the P-C bonds are  $56.9^\circ$  offset. The phosphine orientations relative to the bipyridyl ligand are also fairly varied across these eight compounds. These torsion metrics do not seem to correlate with P-M-P angle or M-P separation, and are also variable even within structures bearing the same anion, as for the three distinct cations of iridium complex **68** studied. The various orientations are potentially due to the influence of nuanced crystal packing effects, however it is worth pointing out that such variety of phosphine conformations is not observed with the triphenylphosphine 2,2'-biphenyl complexes characterised in Chapter 2. These compounds all exhibit conformations analogous to rhodium bipyridyl complex **67**. It is possible that this orientation is facilitated in some way by interactions between the biaryl ligand and the phenyl group on the phosphine.

**Table 4.1** – Comparison of structural metrics across a range of anions. Left: **67** (M = Rh); Right: **68** (M = Ir)<sup>b</sup>. Data at 150 K, thermal ellipsoids drawn at 50%, [BAr<sup>F</sup><sub>4</sub>] anions omitted. Selected bond lengths (Å) and angles (°) for **67**, **68** and published analogues with alternative anions.



<i>This work</i>	<b>67</b> <sup>a</sup>	<b>68</b> <sup>b</sup>	<b>68</b> <sup>c</sup>	<b>68</b> <sup>c</sup>
M-P2	2.3119(6)	2.2924(8)	2.3048(7)	2.3000(11)
M-P3	-	2.3009(7)	2.3035(7)	2.2944(10)
M-N4	2.154(2)	2.118(2)	2.115(2)	2.138(2)
M-N15	-	2.121(2)	2.145(2)	2.129(3)
P2-M-P3	174.05(4)	166.53(3)	166.40(3)	164.08(3)
P1-M1-cent <sup>d</sup>	92.98(6)	96.79(5)	97.97(5)	94.05(5)
P2-M1-cent <sup>d</sup>	-	96.49(6)	94.73(5)	101.87(5)
C21-P2-P3-C31	11.53(15)	36.72(15)	92.03(15)	118.02(16)
C21-P2-M-cent <sup>d</sup>	5.65(8)	14.98(11)	37.45(10)	53.86(10)
C31-P3-M-cent <sup>d</sup>	-	19.87(11)	49.76(11)	57.65(13)
<i>Lit.</i>	<b>A93</b> <sup>382</sup>	<b>A94</b> <sup>375</sup>	<b>A95</b> <sup>379</sup>	<b>A96</b> <sup>375</sup>
M/[anion]	Rh/[B <sub>9</sub> H <sub>12</sub> S]	Ir/[PF <sub>6</sub> ]	Ir/[OTf]	Ir/[Cl]
M-P2	2.3004(9)	2.2975(5)	2.3197(9)	2.310(3)
M-P3	2.2941(9)	2.2907(5)	2.3050(9)	2.297(3)
M-N4	2.164(3)	2.1301(16)	2.146(3)	2.119(8)
M-N15	2.146(3)	2.1644(15)	2.177(3)	2.136(8)
P2-M-P3	159.75(3)	161.986(16)	167.32(3)	168.04(11)
P1-M1-cent <sup>d</sup>	101.45(4)	101.53(2)	98.13(4)	95.90(5)
P2-M1-cent <sup>d</sup>	98.76(4)	96.00(2)	94.54(4)	96.07(15)
C21-P2-P3-C31	91.44(18)	20.11(10)	56.87(18)	75.1(6)
C21-P2-M-cent <sup>d</sup>	36.26(12)	35.47(6)	19.75(13)	14.1(4)
C31-P3-M-cent <sup>d</sup>	47.49(12)	55.56(7)	34.24(12)	57.6(4)

<sup>a</sup> Centrosymmetric cation; <sup>b</sup> Polymorph with Z' = 1; <sup>c</sup> Polymorph with Z' = 2; <sup>d</sup> centroid of the 2,2'-bipyridyl metallocycle

## 4.2 Mechanistic investigations

### 4.2.1 Overall reaction profile

As noted, the preparations of dihydrides **67** and **68** from bis(phosphine) precursors  $[M(\text{cod})(\text{PPh}_3)_2][\text{BAR}^{\text{F}}_4]$ , **69** and **70**, proceed at highly disparate rates. Additionally, a distribution of hydrocarbon side products is observed that varies between metal and shows dependence on the reaction temperature, Figure 4.3. Preparation of iridium complex **68** gives rise to a 14 : 86 mixture of cyclooctane (COA) and *cis*-cyclooctene (COE). With rhodium non-hydrogenated COD is also observed, with COA : COE : COD ratios of 14 : 23 : 63 and 6 : 36 : 58 arising from reactions at 25 °C and 50 °C, respectively, as determined by gas chromatographic analysis of the crude reaction mixtures and in good agreement with values derived from *in situ* ratios divined by NMR spectroscopy. In control reactions, dihydrides **67** and **68** were found not to catalyse the hydrogenation of COD beyond trace quantities on timescales appropriate to these reactions. The presence of COD and COE in the reaction mixtures therefore points to a substitutional mechanism occurring simultaneously to the loss of alkane by hydrogenation. A more detailed understanding of the mechanism was thus desired.

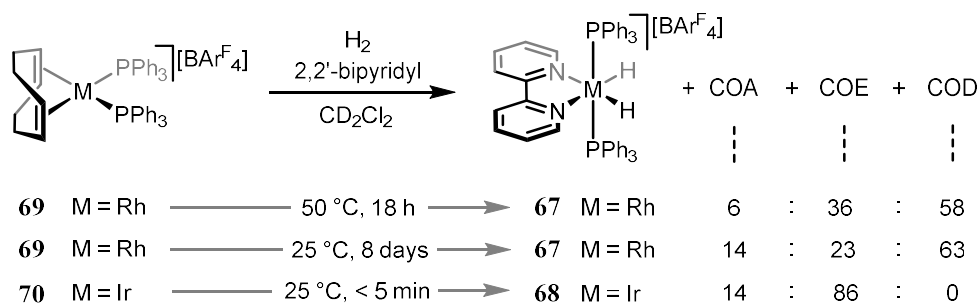


**Figure 4.3** Reaction forming dihydrides **67** and **68** and hydrocarbon by-products, ratios by GC analysis.

### 4.2.2 Hydrogenation reactions

In the absence of 2,2'-bipyridyl, hydrogenation of  $[\text{Rh}(\text{cod})(\text{PPh}_3)_2][\text{BAR}^{\text{F}}_4]$  **69** in dichloromethane solution affords bimetallic  $[\{\text{Rh}(\text{PPh}_3)_2\}_2][\text{BAR}^{\text{F}}_4]_2$ , **71**, Figures 4.4 and 4.5, in *ca.* 4 hours at room temperature with concomitant formation of COA. While the

rhodium dihydride bis(solvate)  $[\text{Rh}(\text{solv})_2\text{H}_2(\text{PR}_3)_2]^+$  is the favoured outcome of similar reactions in coordinating polar solvent,<sup>386,387</sup> or in dichloromethane when employing an alkyl phosphine,<sup>388</sup> here the bimetallic formulation is preferred, evident by the upfield shifted phenyl resonances at  $\delta_{\text{IH}}$  6.87, 6.37 and 5.51 corresponding to the bound arene component, and the two distinct phosphorous resonances, resolved at  $\delta_{\text{31P}}$  45.9 (ddd,  $^1J_{\text{RhP}} = 216$  Hz,  $^2J_{\text{PP}} = 36$ ,  $^2J_{\text{RhP}} = 7$  Hz) and 43.2 (dd,  $^1J_{\text{RhP}} = 197$  Hz,  $^2J_{\text{PP}} = 38$  Hz). These metrics are in agreement with previous reports of this di-cation paired with the  $[\text{HCB}_{11}\text{H}_5\text{Br}_6]^-$  anion.<sup>272</sup>

Crystals of **71** suitable for X-ray diffraction analysis were obtained from diffusion of hexane into dichloromethane solutions of **71**, Figure 4.3. The structure is centrosymmetric per the  $[\text{HCB}_{11}\text{H}_5\text{Br}_6]^-$  analogue. The bonding metrics are in expected good agreement, with only slightly exaggerated Rh1-P2, Rh1-P3 and P2-Rh1-P3 parameters of 2.248(2) Å, 2.262(3) Å, and 95.96(8)° respectively, compared to 2.2594(7), 2.2548(7), and 93.19(2)° for **71**. The rhodium-phenyl metrics are not significantly different, with a Rh1-cent separation of 1.852(2) Å compared to 1.8547(18) Å for **71**.

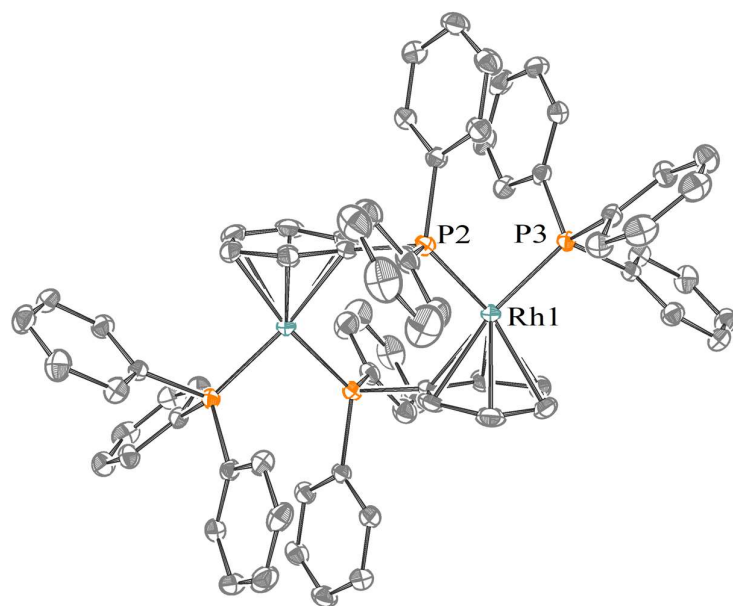


**Figure 4.4** Crystal structure of **71**; Data at 150 K, thermal ellipsoids drawn at 50%,  $[\text{BAr}^{\text{F}}_4]$  anion and co-crystallised hexane omitted. Selected bond lengths (Å) and angles (°): Rh1-P2, 2.2594(7), Rh1-P3, 2.2548(7). Rh1-cent = 1.8547(18), P2-Rh1-P3, 93.19(2).

In the absence of hydrogen, bimetallic **71** reacts cleanly with 2,2'-bipyridyl to give  $[\text{Rh}(2,2'\text{-bipyridyl})(\text{PPh}_3)_2][\text{BAr}^{\text{F}}_4]$  **73**, within 5 minutes at room temperature, Figure 4.5. Complex **73** may be isolated by precipitation from excess hexane, though material suitable for crystallographic analysis was not forthcoming. The  $^{31}\text{P}\{^1\text{H}\}$  NMR spectrum of **73** shows a very similar shift to that found with dihydride **67**, but is clearly differentiated by the larger rhodium coupling of the Rh(I) compound;  $\delta_{31\text{P}}$  46.6 ( $^1J_{\text{RhP}} = 182$ ) (**73**) vs. 47.3 ( $^1J_{\text{RhP}} = 115$ ) (**67**). Placing solutions of **73** in dichloromethane under an atmosphere of dihydrogen affords dihydride **67** within 5 minutes.

Hydrogenation of  $[\text{Ir}(\text{cod})(\text{PPh}_3)_2][\text{BAr}^{\text{F}}_4]$  **70** in dichloromethane in the absence of 2,2'-bipyridyl proceeds to completion within 5 minutes with the elimination of COA, resulting in a complex mixture, formulated as an equilibrium of species formulated  $[\text{Ir}(\text{H})_2(\text{L})_2(\text{PPh}_3)_2][\text{BAr}^{\text{F}}_4]$ , **72**, where L = dichloromethane or dihydrogen. A solitary broad resonance is observed in the  $^{31}\text{P}\{^1\text{H}\}$  NMR spectrum at  $\delta_{31\text{P}}$  23.4, which on cooling to 185 K is resolved into three distinct signals at  $\delta_{31\text{P}}$  27.0, 23.2 and 15.2, assigned as the bis(solvato), bis(dihydrogen) and solvato-dihydrogen system, respectively. Similarly in the  $^1\text{H}$  NMR spectra; a single broad hydridic resonance at  $\delta_{1\text{H}}$  -26.24 is resolved on cooling to 185 K to six resonances in the range  $\delta_{1\text{H}}$  -1.75 – -26.72 with  $T_1$  times in line with the proposed formulation.<sup>¶</sup>

This description is in step with previous characterisation of related iridium dihydride systems:  $[\text{Ir}(\text{H})_2(\text{ClCH}_2\text{CH}_2\text{Cl})(\text{PPh}_3)_2][\text{BAr}^{\text{F}}_4]$  ( $\delta_{1\text{H}}$  -23.84;  $\delta_{31\text{P}}$  19.4),<sup>384</sup>  $[\text{Ir}(\text{H})_2(1\text{-}closo\text{-CB}_{11}\text{H}_6\text{X}_6)(\text{PPh}_3)_2]$  (X = Cl, Br, I;  $\delta_{1\text{H}}$  -21.7 – -27.7;  $\delta_{31\text{P}}$  20.6 – 12.1),<sup>385,389</sup> and  $[\text{Ir}(\text{H})_2(1,2\text{-C}_6\text{H}_4\text{X}_2)(\text{PPh}_3)_2][\text{BAr}^{\text{F}}_4]$  (X = Cl, Br, I;  $\delta_{1\text{H}}$  -16.5 – -20.8).<sup>390</sup> Further upfield  $^1\text{H}$  shifts correlate with stronger metal-ligand interactions here, and with more coordinating O-donor ligands.<sup>391</sup> The room temperature data of **72** has been reported previously, and has been noted as having limited stability in solution; dimerising to a compound characterised as  $[(\text{PPh}_3)_2\text{HIrH}_3\text{IrH}(\text{PPh}_3)_2][\text{BAr}^{\text{F}}_4]$ .<sup>389,392</sup> Reaction of **72** with 2,2'-bipyridyl proceeds immediately to dihydride **68**.

---

<sup>¶</sup> Dr M. R. Gyton collected the low-temperature NMR data in this section. See page viii for affiliation.



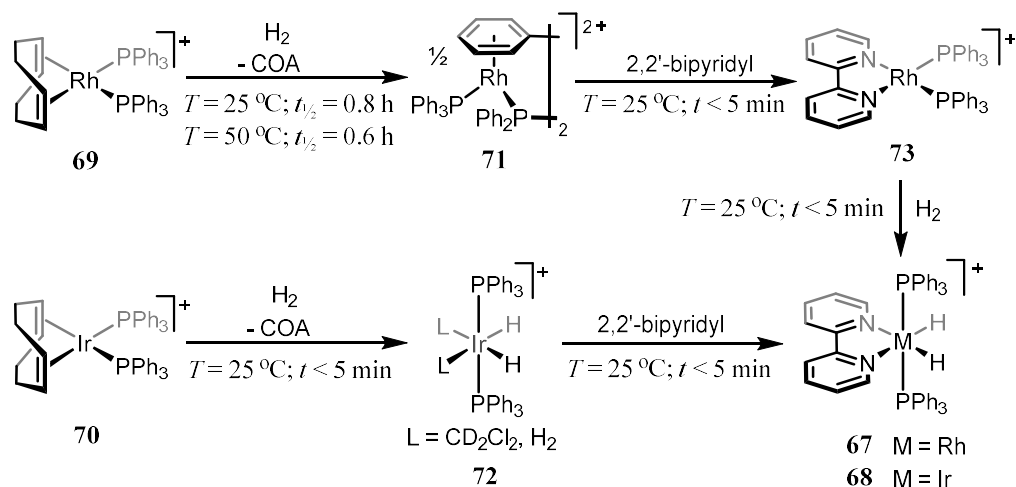


**Figure 4.5** Hydrogenation of  $[\text{M}(\text{cod})(\text{PPh}_3)_2][\text{BAR}^{\text{F}}_4]$  followed by reaction with 2,2'-bipyridyl in dichloromethane solution. Anion =  $[\text{BAR}^{\text{F}}_4]$  throughout.

### 4.2.3 Substitution reactions

Reaction of **69** and **70** with 2,2'-bipyridyl in the absence of dihydrogen results in substitution of one of the phosphine ligands, giving rise to coordinatively saturated  $[\text{M}(2,2'\text{-bipyridyl})(\text{cod})(\text{PPh}_3)][\text{BAR}^{\text{F}}_4]$  ( $\text{M} = \text{Rh}$ , **74**;  $\text{M} = \text{Ir}$ , **75**), Figure 4.6. These reactions proceed at disparate rates, with rhodium system exhibiting the faster kinetics of the two ( $t_{1/2} = 1.3\text{ h}$  at  $25\text{ }^{\circ}\text{C}$ ,  $0.5\text{ h}$  at  $50\text{ }^{\circ}\text{C}$ ) compared to the iridium analogue ( $t_{1/2} = 34\text{ h}$  at  $25\text{ }^{\circ}\text{C}$ ). Iridium compound **75** is itself entirely resistant to either hydrogenation or further substitution even under forcing conditions (weeks at  $50\text{ }^{\circ}\text{C}$ ), while the rhodium analogue **74** slowly and reversibly experiences full substitution of the COD ligand in solution, giving rise to an equilibrium mixture of **74** and bis(phosphine) **73** ( $25\text{ }^{\circ}\text{C}$ :  $t_{1/2} = 110\text{ h}$ ,  $K_{\text{eq}} = 2.4$ ;  $50\text{ }^{\circ}\text{C}$ :  $t_{1/2} = 1.8\text{ h}$ ,  $K_{\text{eq}} = 2.1$ ).

An alternative synthesis of the 5-coordinate intermediates **74** and **75** was carried out using  $[\text{M}(2,2'\text{-bipyridyl})(\text{cod})][\text{BAR}^{\text{F}}_4]$  ( $\text{M} = \text{Rh}$ , **76**;  $\text{M} = \text{Ir}$ , **77**) as starting material in combination with triphenylphosphine. These reactions proceed rapidly to completion, allowing a for more detailed characterisation of the rhodium congener prior to COD substitution.

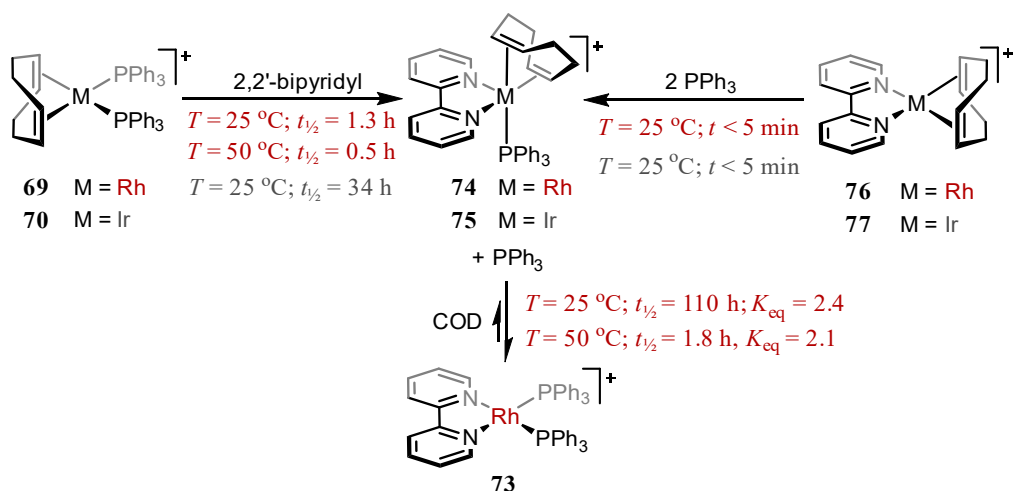


**Figure 4.6** Substitution chemistry of  $[M(\text{cod})(\text{PPh}_3)_2][\text{Bar}^{\text{F}}_4]$ .

A stoichiometric mixture of **74** and triphenylphosphine are observed in dynamic exchange at a rate close to the  $^{31}\text{P}$  NMR time scale (162 – 202 MHz), giving rise to a single broad resonance in the  $^{31}\text{P}\{^1\text{H}\}$  spectrum at  $\delta$  10.6, which decoalesces at 200 K to a sharp doublet at  $\delta_{31\text{P}}$  33.3 and free triphenylphosphine in a 1:1 ratio. Both compounds **74** and **75** are  $C_s$  symmetric in solution. Crystals of **74** and **75** suitable for X-ray analysis were obtained by layering dichloromethane solutions of **76** or **77** with a stoichiometric amount of triphenylphosphine with excess hexane. Both structures, Figure 4.7, adopt a square pyramidal geometry, with phosphines near perpendicular to the plane of the bipyridyl metallocycle.

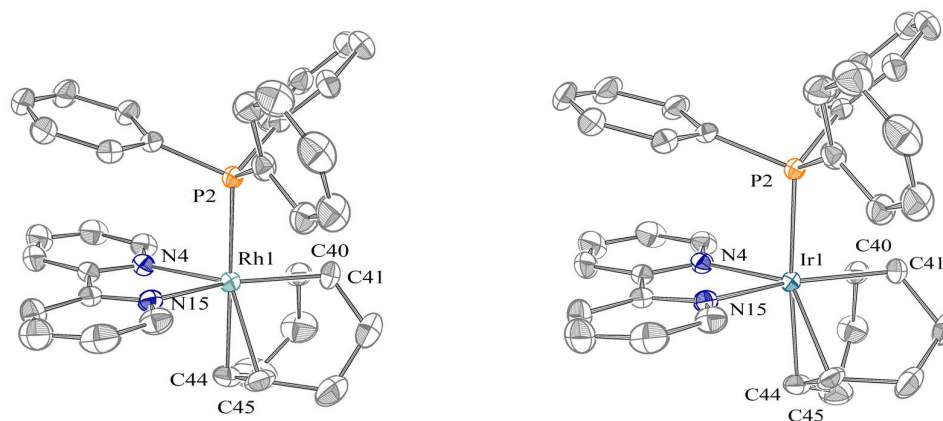


**Figure 4.7** Solid-state structures of **74** (left) and **75** (right). Data at 150 K, thermal ellipsoids drawn at 50%,  $[\text{Bar}^{\text{F}}_4]$  anions omitted. Selected bond lengths (Å) and angles ( $^\circ$ ): **74**, Rh1-P2, 2.3306(7); Rh1-N4, 2.262(2); Rh1-N15, 2.161(2); Rh1-cent(C40,C41), 1.996(3); Rh1-cent(C44,C45), 2.072(3). **75**, Ir1-P2, 2.3426(6); Ir1-N4, 2.213(2); Ir1-N15, 2.121(2); Ir1-cent(C40,C41), 2.013(2); Ir1-cent(C44,C45), 2.017(2).

#### 4.2.4 Reactions of alternative precursors

A bulk scale preparation of dihydride **67** was carried out in dichloromethane solution under dihydrogen utilising **76** as starting material, Figure 4.8, which proceeded to completion on timescales appropriate to the kinetic parameters determined for the substitution of COD with two equivalents of triphenylphosphine; *ca.* 1 week at ambient temperature. Reaction of the perchlorate analogue of **76** with triphenylphosphine followed by dihydrogen in methanol/ether mixtures has been described previously and characterised by IR methods. This early report conjectured a cation such as that in **73** as intermediate to the reaction.<sup>381</sup>

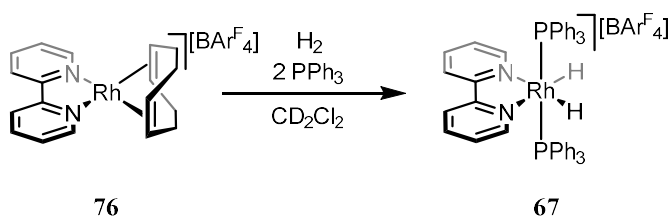


**Figure 4.8** Synthesis of **67** from  $[\text{Rh}(2,2'\text{-bipyridyl})(\text{cod})][\text{BARF}_4]$ .

For completeness, **76** and **77** were confirmed as non-intermediate to the overall synthesis of **67** and **68**, with only **77** showing any reaction under hydrogenation conditions, giving rise to an equilibrium mixture **77** and a species assigned as the dihydride  $[\text{Ir}(2,2'\text{-bipyridyl})(\text{cod})\text{H}_2][\text{BARF}_4]$ , **78** in a 5:1 ratio, Figure 4.9.

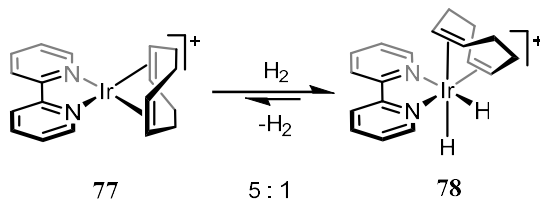


**Figure 4.9** Reversible oxidative addition of dihydrogen by **77**.

#### 4.2.5 Summary of mechanistic findings

The overall reaction manifold is presented in Figure 4.10. The slow reaction of  $[\text{Rh}(\text{cod})(\text{PPh}_3)_2][\text{BARF}_4]$  **69** and 2,2'-bipyridyl under dihydrogen is thus rationalised by the competitive irreversible formation of 5-coordinate **74**, which proceeds at a

comparable rate to the direct hydrogenation of COD, and only slowly proceeds to fully substituted  $[\text{Rh}(\text{cod})(\text{PPh}_3)_2][\text{BAR}^{\text{F}_4}]$ , **73**, a species with which oxidative addition of dihydrogen is possible. The substitution route is not competitive for the iridium congener; the initial hydrogenation is a substantially faster reaction compared to substitution with 2,2'-bipyridyl. The occurrence of COE in the synthesis of rhodium and iridium dihydrides **67** and **68** is rationalised by the fast substitution of an intermediate to hydrogenation,  $\{\text{M}(\text{coe})\text{L}(\text{PPh}_3)_2\}^+$ , with 2,2'-bipyridyl. An optimised, one pot synthesis of rhodium dihydride **67** is thus realised; hydrogenation of precursor **69**, at ambient temperature for 5 hours, followed by addition of 2,2'-bipyridyl.

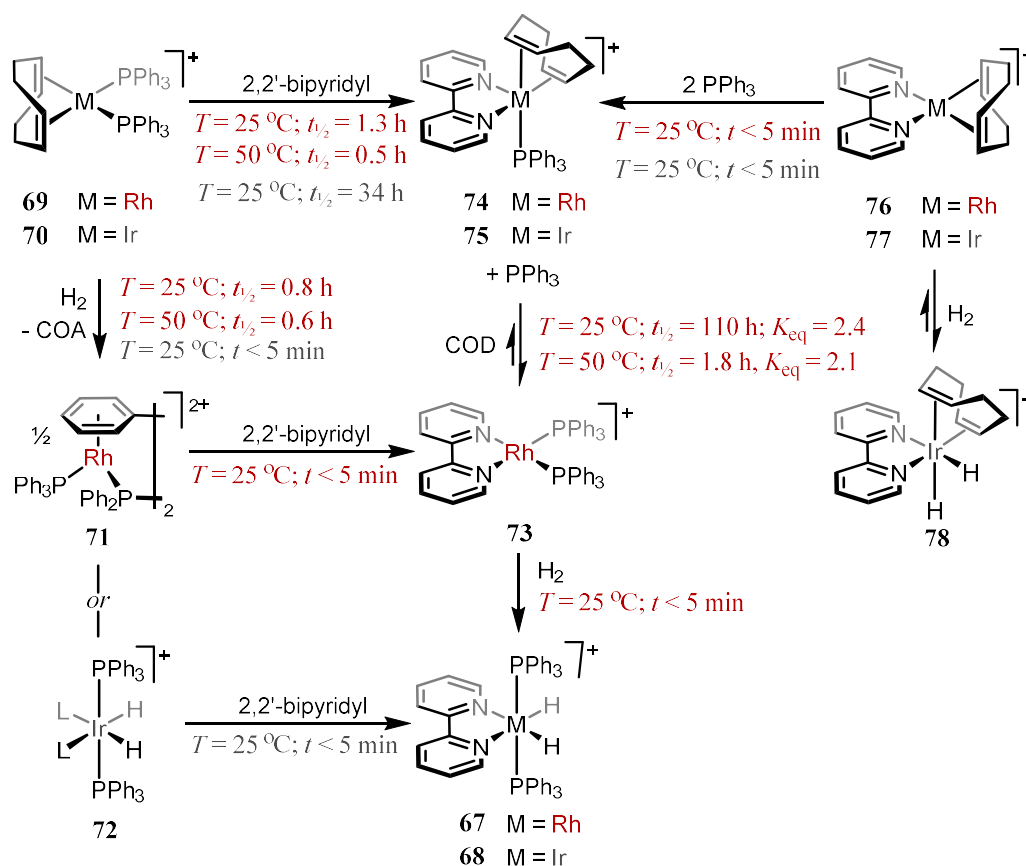


**Figure 4.10** Intermediates in the formation of **67** and **68** and other relevant compounds. Conditions: 20 mM solutions in  $\text{CD}_2\text{Cl}_2$ , 1 bar argon or dihydrogen as appropriate. anion =  $[\text{BAR}^{\text{F}_4}]^-$  throughout.

### 4.3 Other reactivity of 2,2'-bipyridyl complexes

#### 4.3.1 Dehydrogenation chemistry

The dehydrogenation of dihydrides **67** and **68** was attempted by reaction with 10 equivalents of *tert*-butylethylene (TBE) in dichloromethane, Figure 4.11. These reactions were unsuccessful, with no conversion observed for the iridium congener, and only a 15% conversion seen with rhodium after 7 weeks at 50 °C. This is perhaps unsurprising given that **67** and **68** are coordinatively saturated, necessitating either a phosphine dissociation or dihydride/dihydrogen equilibrium to facilitate coordination of TBE. A commentary on phosphine lability follows in Section 4.3.3.

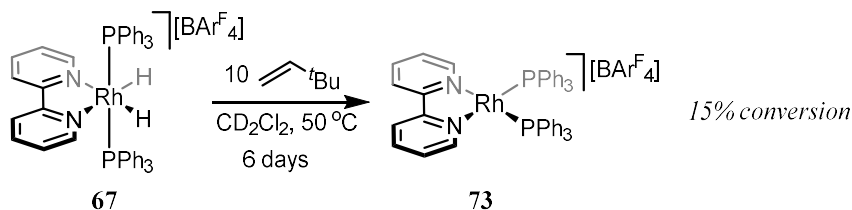
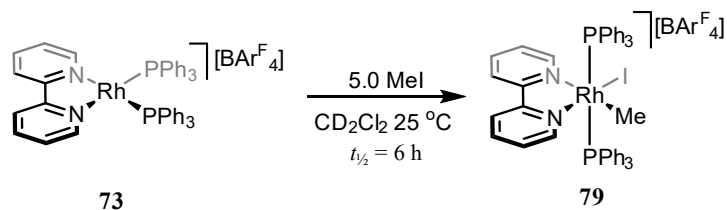


Figure 4.11 Reaction of dihydride **67** with TBE.

#### 4.3.2 Oxidative addition chemistry

Despite the inaccessibility of  $[\text{Rh}(2,2'\text{-bipyridyl})(\text{PPh}_3)_2][\text{BARF}_4]$  **73** via a dehydrogenation reaction, this species may be readily prepared directly from  $[\text{Rh}(\text{cod})(\text{PPh}_3)_2][\text{BARF}_4]$  **69** as described earlier. The oxidative addition chemistry of this species (beyond that with dihydrogen) was first assessed with iodomethane. The reaction, Figure 4.12, proceeds at a moderate rate forming methyl iodide complex **79** within 24 hours. The methyl component is evident at  $\delta_{\text{IH}}$  1.68 ( $^3J_{\text{PH}} = 5.7$  Hz,  $^2J_{\text{RhH}} = 2.0$  Hz), with the  $^{31}\text{P}\{^1\text{H}\}$  NMR spectrum consisting of a solitary doublet resonance at  $\delta_{31\text{P}}$  16.1 ( $^1J_{\text{RhP}} = 96$  Hz), in good agreement with a structurally related *cis,cis,trans*- $[\text{Rh}(\text{acac})(\text{Me})(\text{I})(\text{PPh}_3)_2]$ ,<sup>393</sup> and *trans*- $[\text{Rh}(\text{Me})(\text{I})_2(\text{PPh}_3)_2]$ .<sup>394,395</sup> Attempted reaction of bis(phosphine) **73** with methane under similar conditions proved entirely unsuccessful.



**Figure 4.12** Reaction of **73** with iodomethane.

Crystals of methyl iodide **79** suitable for X-ray diffraction analysis were prepared by diffusion of hexane into concentrated dichloromethane solution of **79**, Figure 4.13. The cationic component is disordered over two components related by a  $C_2$  rotation. The phosphines are found to be near linear with respect to each other;  $\angle \text{P30-Rh-P50} = 176.63(3)^\circ$ , and indeed the overall structure is fairly close to an idealised octahedral coordination environment. The Rh-P distances are elongated as compared to the corresponding dihydride **67** (2.3910(7) Å and 2.4034(7) Å compared to 2.3119(6) Å for **67**), and the phosphines themselves are once again found to be in an eclipsed conformation, though rotated through *ca.* 60° as compared to **67**.

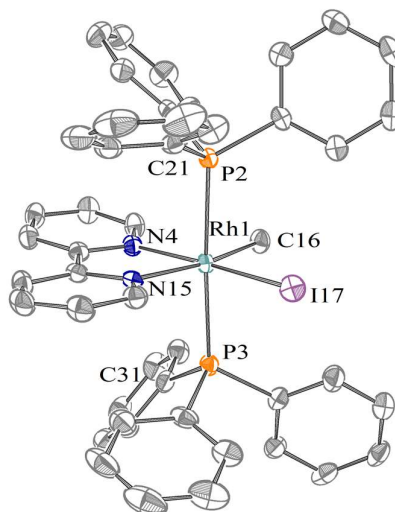


**Figure 4.13** Solid-state structure of **79**. One of two disordered components. Data at 150 K, thermal ellipsoids drawn at 50%, [BARF<sub>4</sub>] anion omitted. Selected bond lengths (Å) and angles (°): Rh1-P2, 2.3910(7), Rh1-P3, 2.4034(7), Rh1-N4, 2.153(3), Rh1-N15, 2.080(2), Rh1-C16, 2.084(5), Rh1-I17, 2.6492(3), P2-Rh1-P3, 176.63(3), P2-Rh1-cent(Rh1,N4,N15), 2.831(18), P3-Rh1-cent(Rh1,N4,N15), 90.447(18), C16-Rh1-I17, 93.84(17), C16-Rh1-N4, 91.43(18), N4-Rh1-N15 78.22(9), N4-Rh1-I17, 96.51(6), |C21-P2-P3-C31|, 115.83(16), |C21-P2-Rh1-cent|, 51.31(11), |C31-P3-Rh1-cent|, 56.46(10).

### 4.3.3 Phosphine lability

The lability of the triphenylphosphine ligand was probed by the reaction of rhodium and iridium dihydrides **67** and **68** with five equivalents of tricyclohexylphosphine, Figure 4.14. With the rhodium congener, no reaction was observed after 6 days at ambient temperature, and only on heating to 50 °C did dihydride **67** begin to be consumed, giving rise over a period of 16 weeks to a mixture of **67**, and two new species with diagnostic hydride signals at  $\delta_{\text{IH}} -16.69$  ( $^1J_{\text{RhH}} \approx ^2J_{\text{PH}} \approx 15.0$ ) and  $\delta_{\text{IH}} -17.71$  ( $^1J_{\text{RhH}} \approx ^2J_{\text{PH}} \approx 15.45$ ) with corresponding signals in the  $^{31}\text{P}\{^1\text{H}\}$  NMR spectrum at  $\delta_{31\text{P}} 46.9$  ( $^1J_{\text{RhP}} = 111$ ) and  $42.1$  ( $^1J_{\text{RhP}} = 108$ ) assigned respectively as the monosubstituted  $[\text{Rh}(2,2'\text{-bipyridyl})\text{H}_2(\text{PPh}_3)(\text{PCy}_3)][\text{BAr}^{\text{F}}_4]$ , **80**, and bis-substituted  $[\text{Rh}(2,2'\text{-bipyridyl})\text{H}_2(\text{PCy}_3)_2][\text{BAr}^{\text{F}}_4]$  **81**, respectively, Figure 4.14. Analysis of the crude reaction mixture by mass spectrometry indicated strong molecular ion signals at  $m/z$  803.4, consistent with such a formulation of **80**. No reaction is observed after 6 weeks at 50 °C for the equivalent reaction of iridium dihydride **68**. These results rule out installation of **CxP<sub>2</sub>** via a substitution approach.

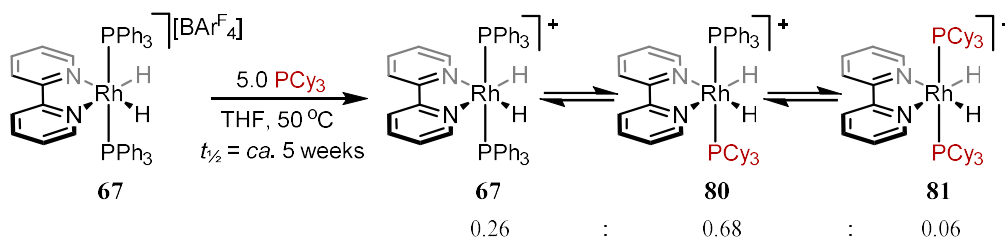


**Figure 4.14** Reaction of dihydride **67** with five equivalents of tricyclohexylphosphine.

## 4.4 Attempted preparation of a CxP<sub>2</sub> complex of 2,2'-bipyridyl

### 4.4.1 Attempted syntheses from 2,2'-bipyridyl precursors

From the outset, the investigations described thus far on the monophosphine systems indicate that a successful synthesis of a mononuclear **CxP<sub>2</sub>** complex would likely be unsuccessful, owing to the slow substitution kinetics, and exclusively *cis*-intermediates for the rhodium reaction pathway.

The one pot reaction of  $[\text{Rh}(2,2'\text{-bipyridyl})(\text{cod})][\text{BAr}^{\text{F}}_4]$  **76** with **CxP<sub>2</sub>** under dihydrogen in dichloromethane was examined, seeking to directly prepare a mononuclear rhodium dihydride complex of **CxP<sub>2</sub>**. In 18 hours the reaction is seen to have given rise to a  $^1\text{H}$  NMR spectrum featuring a quartet resonance at  $\delta_{\text{IH}} -15.91$  ( $^1J_{\text{RhH}} \approx ^2J_{\text{PH}} \approx 13.8$  Hz) and a doublet resonance in the  $^{31}\text{P}\{^1\text{H}\}$  spectrum at  $\delta_{31\text{P}} 42.6$  ( $^1J_{\text{RhP}} = 112$  Hz). In the ensuing 4 days four additional signals grow in, in both spectra, with similar metrics. The new hydridic signals are observed in the range  $\delta_{\text{IH}} -13.1 - -16.6$  with corresponding  $^1J_{\text{RhH}}$  and  $^2J_{\text{PH}}$  values in the range 13.8 – 16 Hz. Attempts to isolate individual components of this mixture by crystallisation or chromatographic methods were unsuccessful. All of these compounds are assigned as oligomeric dihydride calixarene complexes, Figure 4.15 (a), supported by analysis of the crude reaction mixtures by mass spectrometry, in which the spectrum is dominated by a high intensity signal spanning a 4-5  $m/z$  range centred at  $m/z$  1249.5, correct for the formulation of  $[\text{M}]^+ = [\text{Rh}(2,2'\text{-bipyridyl})(\text{Cxp}_2)(\text{H})_2]^+$ , but evidently composed of multiple different oligomers,  $[\text{nM}]^{n+}$ .

Performing an otherwise equivalent reaction in the absence of hydrogen, immediately a dynamic system is established with a broad  $^{31}\text{P}\{^1\text{H}\}$  resonance at  $\delta_{31\text{P}} 10.2$  (fwhm = 291 Hz), characterised as 5-coordinate  $[\text{Rh}(2,2'\text{-bipyridyl})(\text{cod})(\text{Cxp}_2)]^+$ , Figure 4.15 (b), undergoing self-exchange of pendant and coordinated phosphine groups at rates approaching the  $^{31}\text{P}$  NMR time scale (162 MHz), Figure 4.14. After 96 hours at 50 °C the  $^{31}\text{P}\{^1\text{H}\}$  NMR spectrum is found to contain at least eight distinct doublet resonances in the range  $\delta_{31\text{P}} 21.0 - 17.0$ , assigned as the various oligomers of  $[\{\text{Rh}(2,2'\text{-bipyridyl})(\text{Cxp}_2)_n\}_m]^{m+}$ , Figure 4.15 (c). Interestingly, exposure of this mixture to dihydrogen does not immediately result in the occurrence of the characteristic dihydride signals observed in the previous experiment performed under dihydrogen from the outset. Over a timeframe of days at 50 °C upfield signals are observed in the  $^1\text{H}$  NMR spectrum, but these are distinct to those observed for the previously described reaction in the presence of dihydrogen from the outset. No evidence is seen of any sort of rearrangement event of the dihydrides prepared in this reaction on protracted heating to 50 °C in dichloromethane solution.



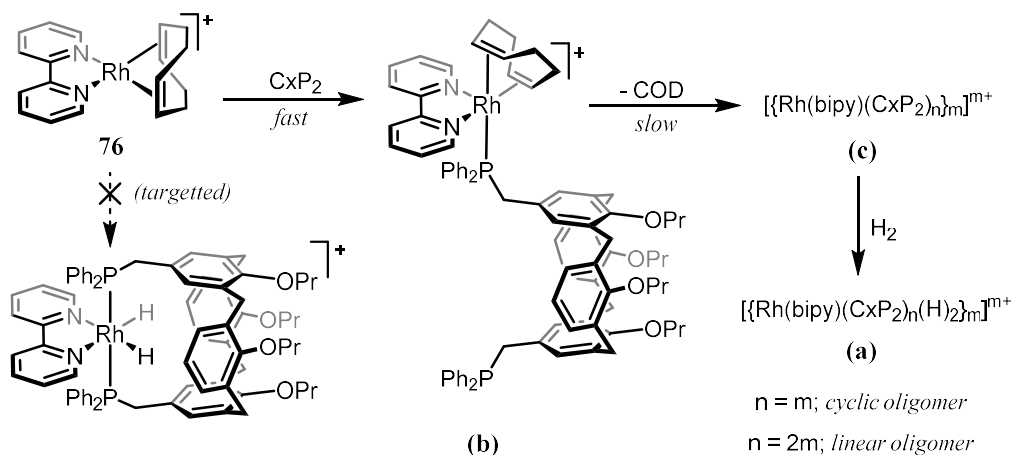


**Figure 4.15** Targeted synthesis of mononuclear dihydride, and the proposed reaction products and intermediates of the reaction of **76** with **CxP<sub>2</sub>** under dihydrogen.

#### 4.4.2 Attempted syntheses from other precursors

Finally, an attempt was made to access the synthesis of target dihydride by hydrogenation of mixtures of **CxP<sub>2</sub>** and metal diene  $[\text{M}(\text{cod})_2][\text{BAr}^{\text{F}}_4]$  ( $\text{M} = \text{Rh}, \text{Ir}$ ), followed by addition of 2,2'-bipyridyl, thereby accessing the hydrogenation mechanism outlined previously, which with iridium is known to proceed through a *trans* intermediate. Reaction of **CxP<sub>2</sub>** with  $[\text{Rh}(\text{cod})_2][\text{BAr}^{\text{F}}_4]$  gives rise to a new doublet resonance in the  $^{31}\text{P}\{^1\text{H}\}$  spectrum at  $\delta_{31\text{P}} 20.0$  ( $^1J_{\text{RhP}} = 143$  Hz) assigned as a some rapidly exchanging species of the form  $\{\text{Rh}(\text{cod})(\text{CxP}_2)\}_n^{n+}$ . One equivalent of COD is liberated in this reaction. Exposure of the solution to dihydrogen immediately results in a new species, expressing a very broad downfield resonance at  $\delta_{31\text{P}} 43.5$  (fwhm = 425 Hz), with concomitant formation of COA as evident from the  $^1\text{H}$  NMR spectrum. Addition of 2,2'-bipyridyl to this solution under dihydrogen affords a mixture of compounds consistent with a phosphine ligated  $\{\text{Rh}(2,2'\text{-bipyridyl})(\text{H})_2\}^+$  fragment; at  $\delta_{31\text{P}} 43.2 - 40.9$ , with four hydridic proton signals between  $\delta_{\text{H}} -15.5$  and  $-16.0$ .

A similar case is observed with  $[\text{Ir}(\text{cod})_2][\text{BAr}^{\text{F}}_4]$ ; a new  $^{31}\text{P}\{^1\text{H}\}$  resonance at  $\delta_{31\text{P}} 9.4$  is formed on initial mixing, which on hydrogenation immediately gives a new species at  $\delta_{31\text{P}} 3.9$  with liberation of COA and several upfield  $^1\text{H}$  resonances. Trapping the reaction with the addition of bipyridyl results in a  $^1\text{H}$  NMR spectrum containing at least two

triplet resonances at  $\delta_{\text{IH}}$  -19.6 ( $^2J_{\text{PH}} = 16.3$ ) and -19.7 ( $^2J_{\text{PH}} = 15.8$ ). The  $^{31}\text{P}\{^1\text{H}\}$  NMR spectrum contains a multitude of closely related signals. Analysis of the crude reaction mixture by high-resolution mass spectrometry indicates the presence of the  $[\text{M}]^+$ ,  $[2\text{M}]^{2+}$ ,  $[3\text{M}]^{3+}$  and trace detection of the  $[4\text{M}]^{4+}$  molecular ions at  $m/z$  1339.5. The reaction is thus asserted to have formed mixtures of cyclic oligomers. Attempts at isolate individual component of this mixture by chromatography or recrystallisation were unsuccessful.

## 4.5 Conclusions and future work

This chapter has investigated in depth the synthesis of rhodium and iridium complexes featuring the 2,2'-bipyridyl ligand in dichloromethane solvent. While ultimately found to not be appropriate to the synthesis of complexes featuring a *trans*-spanning diphosphine, the knowledge gained from this study was applied elsewhere in the Chaplin Group in the synthesis of a [2]rotaxane containing an analogous coordination sphere.

In terms of achieving a **CxP<sub>2</sub>** complex, the 2,2'-bipyridyl ligand is obstructive. The synthetic routes investigated demand the installation of the 2,2'-bipyridyl ligand early in the overall synthesis, thus from the outset the coordination sphere of the metal is coordinatively saturated with *cis*-chelating ligands; a setup which is not conducive to introducing a *trans*-chelating diphosphine calixarene, with a known propensity to form dimeric or higher oligomeric coordination compounds. A more viable synthon may have been a simple *trans*-bis(phosphine) metal dihydride bis(solvate). In many ways it seems that the true link between the 2,2'-biphenyl and 2,2'-bipyridyl systems discussed herein is not the planar biaryl ligand, but the strong  $\sigma$ -donating biphenyl and hydride ligands. Indeed, if only the 2,2'-biphenyl **CxP<sub>2</sub>** dihydrogen complex was less stable to hydrogenation, a natural link between the 2,2'-biphenyl and 2,2'-bipyridyl work would emerge. A mononuclear calixarene complex featuring a  $\{\text{M}(\text{H})_2(\text{L})_2\}^+$  fragment chelated by **CxP<sub>2</sub>** would be an interesting system to study.

Having explored the **CxP<sub>2</sub>** ligand in some depth, work in the final chapter now moves on to a larger cavitand-based ligand, with a return to the pursuit of alkane  $\sigma$ -complexes.

## 5 Complexes of a resorcinarene-based diphosphine

This chapter describes the preparation and reactivity of rhodium complexes ligated by a *cis*-chelating phosphine-phosphite functionalised cavitand; **RcPOP**. Based on a tris(quinoxaline) ‘walled’ resorcin[4]arene, the deep-cavitand is suitably sized to encompass  $\{\text{Rh}(\text{diene})\}^+$  fragments. The preparation of complexes  $[\text{Rh}(\text{diene})(\text{RcPOP})][\text{A}]$  (diene = COD, NBD;  $[\text{A}] = [\text{Al}(\text{OR}^{\text{F}})_4]$ ,  $[\text{BAr}^{\text{F}}_4]$ ,  $[\text{HCB}_{11}\text{Me}_5\text{I}_6]$  and  $[\text{SbF}_6]$ ) with two straightforward methodologies is described, and the hydrogenation chemistry of these complexes investigated.

Hydrogenation of  $[\text{Rh}(\text{diene})(\text{RcPOP})][\text{Al}(\text{OR}^{\text{F}})_4]$  in fluoroarenes, mesitylene or methyl-*tert*-butyl ether (MTBE) solution results in the formation of solvent adducts, of which  $[\text{Rh}(\text{C}_6\text{H}_5\text{F})(\text{RcPOP})][\text{Al}(\text{OR}^{\text{F}})_4]$ ,  $[\text{Rh}(1,2\text{-C}_6\text{H}_4\text{F}_2)(\text{RcPOP})][\text{Al}(\text{OR}^{\text{F}})_4]$  and  $[\text{Rh}(1,3,5\text{-C}_6\text{H}_3\text{Me}_3)(\text{RcPOP})][\text{Al}(\text{OR}^{\text{F}})_4]$  were isolated. In all cases the solvent ligand is weakly bound, and evidence is presented that it may, under certain conditions, be displaced by excess alkane in solution. In the solid state, hydrogenation of crystalline samples of  $[\text{Rh}(\text{diene})(\text{RcPOP})][\text{A}]$  results in complexes formulated as  $[\text{Rh}(\text{alkane})(\text{RcPOP})][\text{A}]$  (alkane = NBA, COA), though attempts to characterise these compounds crystallographically are hindered by weak diffraction and a potential loss of sample crystallinity following hydrogenation.

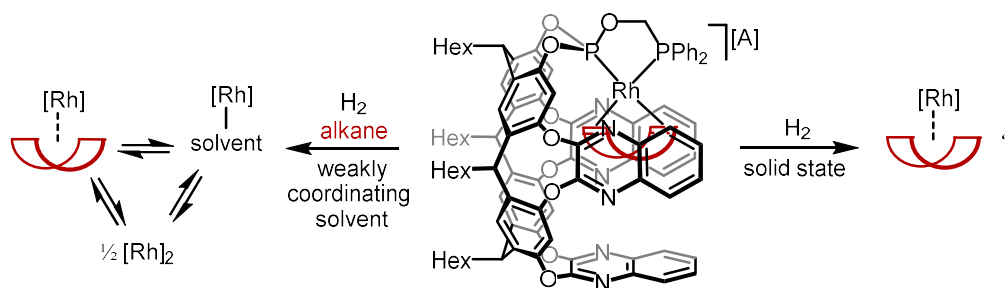


**Figure 5.1** Rhodium diene complexes encapsulated by a resorcinarene-based diphosphine ligand and the hydrogenation chemistry thereof.

*Manuscripts resulting from work described in this chapter are in preparation.*

## 5.1 Resorcinarenes as hosts and ligands

### 5.1.1 Preparation and properties

Resorcinarenes are a variety of calixarene. Formed through the condensation of aldehydes and resorcinol, Figure 5.2 (a),<sup>396</sup> they differ from those calixarenes described in Chapter 3 in that the hydroxyl functionalisation is at the upper rim of the cavitand, and the methylene units are axially substituted with alkyl or aryl groups.<sup>397,398</sup> The base resorcinarene has access to a wide variety of conformations with relatively similar energies, though many functionalised resorcinarenes have been designed to confine the molecule flexibility. Taking advantage of the positioning of the upper rim hydroxyl groups, the introduction of short chemical linkages joining adjacent arenes results in resorcinarenes with rigid cone-shaped conformations, Figure 5.2 (b).<sup>280</sup>

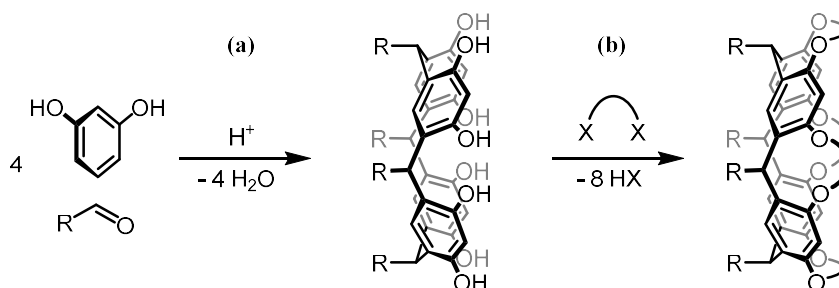


**Figure 5.2** Synthesis of resorcinarene, tethering into a rigid cone-shaped conformation.

### 5.1.2 Walled resorcinarenes as alkane hosts

Resorcinarenes functionalised with molecular panels, or ‘walls’, are well-noted for their inclusion complexes,<sup>276,281,399</sup> and notably have demonstrated an excellent propensity for alkane binding in organic solvents. Bis(quinoxaline)-bis(diazaphthalimide) cavitand **A97** (Figure 5.3) has shown a high affinity for the binding of cyclohexane ( $K_a = 3.6 \pm 0.8 \times 10^3 \text{ M}^{-1}$  in *d*<sub>12</sub>-mesitylene),<sup>400</sup> while capsules composed of two hydrogen bonded tetra-(diazaphthalimide)-walled cavitands; **A98**,<sup>287</sup> and related structures,<sup>284–286,401</sup> form persistent inclusion complexes of linear alkanes, which are found to coil within the cavitand, maximising contact with the interior surface defined by the arene walls.

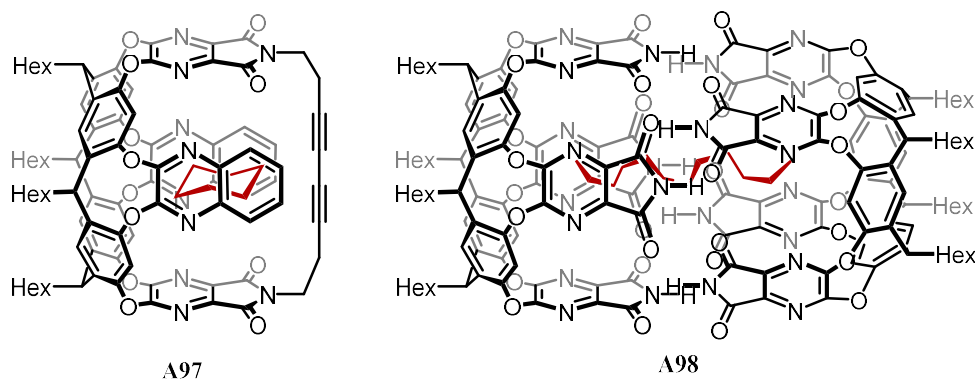


**Figure 5.3** Alkane inclusion complexes of resorcinarenes in mesitylene solution.

### 5.1.3 Tris-walled resorcinarenes with phosphite functionalisation

As with other calixarenes, resorcinarenes functionalised with various donor moieties have been explored in coordination chemistry, primarily in catalytic enquiries seeking to exploit the molecular topology of the ligand.<sup>310,313–315,402</sup> The first catalytic application of a resorcinarene ligand in regioselective allylic substitution made use of a tris-walled resorcinarene systems featuring phosphite functionalisation on the fourth side of the cavitand, with which palladium allyl complex **A99**, Figure 5.4, was isolated.<sup>403</sup> More recently, tris(quinoxaline)-walled systems with simpler monodentate phosphorous-based ligating groups have been employed in selective gold catalysis, **A100**.<sup>404</sup> The ligand architecture in **A100** is particularly compelling, not least for its straightforward synthesis and the relatively unobtrusive donor properties of the quinoxaline walls, but also for the potential derivatisation of the phosphine donor functionality.

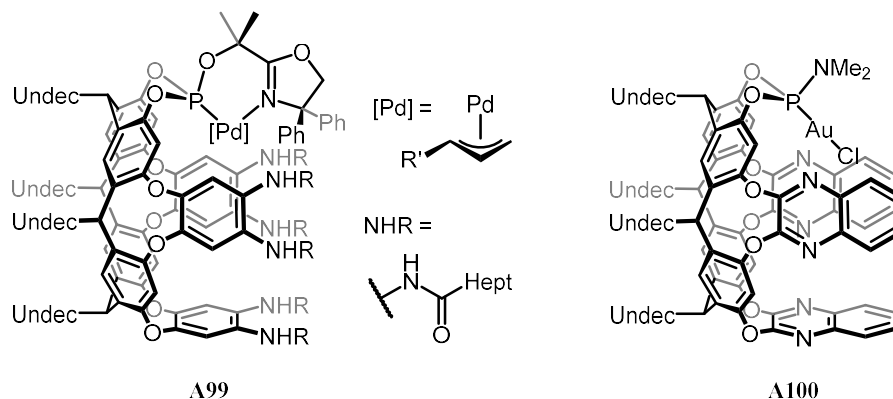


**Figure 5.4** Complexes of tris-walled resorcinarenes.

Preliminary work in the Chaplin Group has demonstrated the viability of coordinating a tris-walled resorcinarene ligand with a  $\{M(\text{diene})\}$  fragment, Figure 5.5.<sup>¶</sup> A straightforward reaction of phosphoramidite **86** with  $[\{\text{Ir}(\text{cod})\text{Cl}\}_2]$  cleaves the metal dimer to afford iridium chloride complex **82**. The COD ligand was found to be persistently located within the resorcinarene cavity, with characteristic upfield resonances in the  $^1\text{H}$  NMR spectrum (*vide infra*) and a confirmatory solid-state structure. The stereochemistry of the phosphite is responsible for projecting the metal centre towards the cavity, though a solitary phosphite does allow for rotation about the P-M bond, and thus permits interactions between metal and substrate outside of the resorcinarene enclosure. Pre-empting this issue, a diphosphine chelate was sought.

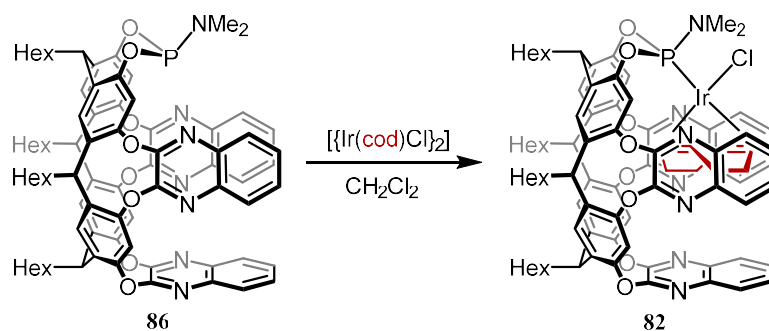


**Figure 5.5** Preliminary investigations into cavitand-based ligands with metal diene fragments.

## 5.2 RcPOP

### 5.2.1 Ligand synthesis

For synthetic convenience, a mixed phosphine-phosphite chelating was targeted. The full ligand synthesis is given in Figure 5.6. Phosphoramidite **86** was prepared according to adapted literature procedures for a variant featuring undecyl alkyl chains in place of hexyl.<sup>404</sup> Scission of the phosphoramidite with ethereal hydrogen chloride yielded phosphite chloride **87** quantitatively, and in a stereospecific manner. Reaction of **87** with (hydroxymethyl)diphenylphosphine then affords the chelating diphosphine **88**, henceforth **RcPOP**, which in dichloromethane possesses two doublets resonances at  $\delta_{31\text{P}}$

<sup>¶</sup> Synthesis of phosphoramidite **86** and metallation carried out by Amy Kynman. See page viii for affiliation.

127.5 and -14.5 for the phosphite and phosphine components respectively, with a  $^3J_{\text{PP}}$  of 5 Hz. The  $^1\text{H}$  NMR spectrum demonstrates overall  $C_s$  molecular symmetry.

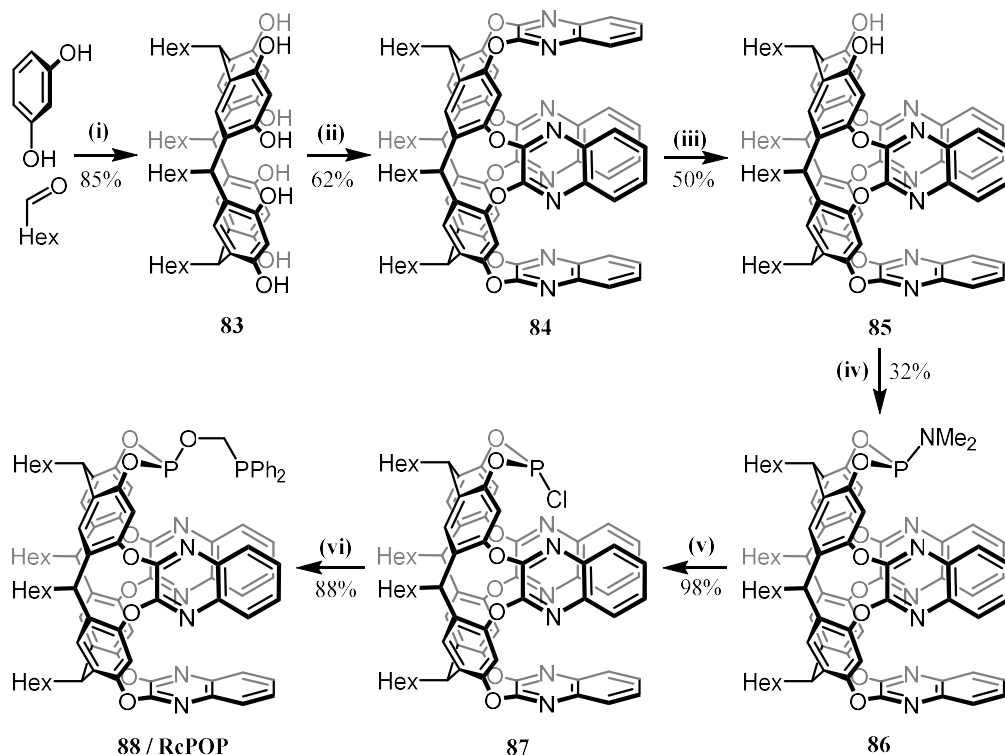


**Figure 5.6** Synthesis of **RcPOP**. (i)  $\text{HCl(aq)}$ ,  $\text{EtOH}/\text{H}_2\text{O}$ ,  $80\text{ }^\circ\text{C}$ , 18 h; (ii) 2,3-dichloroquinoxaline,  $\text{K}_2\text{CO}_3$ ,  $\text{DMSO}$ ,  $60\text{ }^\circ\text{C}$ , 18 h; (iii)  $\text{CsF}$ , pyrocatechol,  $\text{DMF}$ ,  $80\text{ }^\circ\text{C}$ , 1 h; (iv)  $\text{P}(\text{NMe}_2)_3$ ,  $\text{NEt}_3$ , toluene,  $20\text{ }^\circ\text{C}$ , 1.5 h; (v)  $\text{HCl}$  in  $\text{Et}_2\text{O}$ ,  $\text{THF}$ ,  $20\text{ }^\circ\text{C}$ , 1 h; (vi)  $\text{HOCH}_2\text{PPh}_2$ ,  $\text{NEt}_3$ ,  $\text{CH}_2\text{Cl}_2$ ,  $20\text{ }^\circ\text{C}$ , 1 h.

Slow diffusion of methanol into concentrated dichloromethane solutions of **RcPOP** afforded crystalline material suitable for determination of a solid-state structure, Figure 5.7. The phosphine unit is orientated away from the resorcinarene, however critically the stereochemistry of the phosphite moiety is correct for the adoption of a chelate with the metal fragment directed into the cavitand. The quinoxaline wall opposite the diphosphine is angled slightly outward from the cavity, with a  $\text{pln(Rc)}\text{-pln(Q)}$  angle of  $99.54(6)^\circ$ .<sup>†</sup> One of the flanking quinoxaline units is observed near perpendicular to the

<sup>†</sup> The metric  $\text{pln(Rc)}\text{-pln(Q)}$  is here defined as the angle between the plane described by a quinoxaline unit and the plane described by the centroids of the four aryl units of the resorcinarene.  $\text{cnt(Q)}$  is the centroid of the nitrogen containing ring of a quinoxaline unit. The quinoxaline unit opposite the phosphine is abbreviated Q and the two adjacent the phosphine as Q'.

resorcinarene ( $\angle \text{pln(Rc)}-\text{pln(Q')} = 93.62(5)^\circ$ ) while the other is directed inwards; ( $\angle \text{pln(Rc)}-\text{pln(Q')} = 78.59(6)^\circ$ ). Inspection of the extended packing of the structure shows the quinoxaline unit described as perpendicular to be interacting intermolecularly with its counterpart in an adjacent molecule, with the formation of an interpenetrating self-inclusion complex of two **RcPOP** molecules. The interacting quinoxalines are separated by *ca.* 3.97 Å; a much closer contact than that observed in previous reports of this phenomenon with bis(quinoxaline)-walled resorcinarenes (4.55 – 4.34 Å).<sup>405,406</sup>

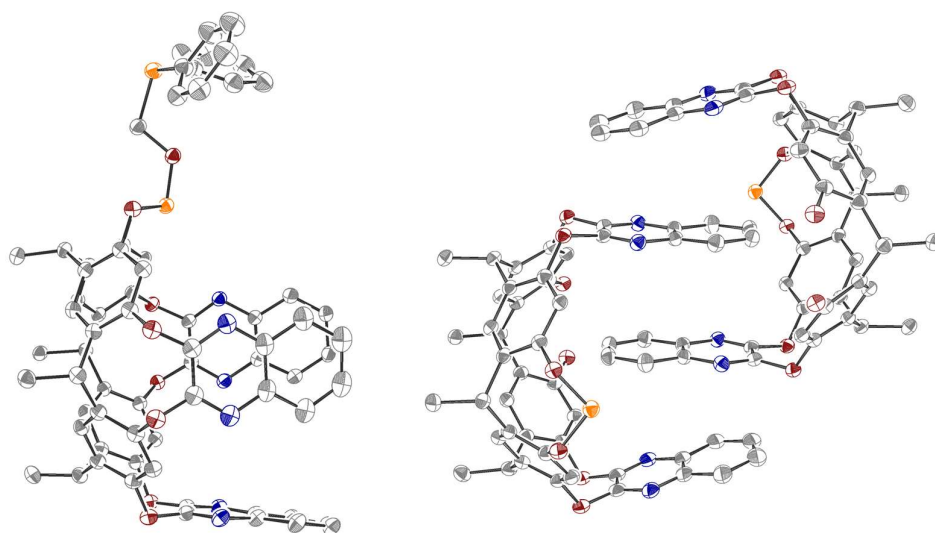


**Figure 5.7** Solid state structure of **RcPOP**; Left: asymmetric unit, hexyl chains truncated; Right: intermolecular packing, structure truncated for clarity. Data at 150 K, thermal ellipsoids drawn at 15%, Selected bond lengths (Å) and angles ( $^\circ$ ):  $\text{cnt(Q')} - \text{cnt(Q')}$ , 8.2190(1);  $\text{pln(Rc)} - \text{pln(Q)}$ , 99.54(6);  $\text{pln(Rc)} - \text{pln(Q')}$ , 78.59(6), 93.62(5). Intermolecular contacts (Å):  $\text{pln(Q')} - \text{pln(Q')}$ , 3.974(3).<sup>e</sup>

## 5.3 Alkene complexes

### 5.3.1 Preparation

Two approaches have been developed for the ligation of **RcPOP** to metal diene fragments; (1) reaction of **RcPOP** with  $[\{\text{Rh}(\text{diene})\text{Cl}\}_2]$  and a suitable halide abstracting agent, and (2) substitution reactions using  $[\text{Rh}(\text{diene})_2][\text{anion}]$ , Figure 5.7. Here the diene is COD or NBD throughout, though these procedures could reasonably be extendable to a range of dienes (or mono-enes) of interest. With a view to modulating the solid-state properties of the targeted alkane complexes (*vide infra*), the



$[\text{Rh}(\text{diene})(\text{RcPOP})]^+$  cations were prepared partnered with  $[\text{Al}(\text{OR}^{\text{F}})_4]^-$ ,  $[\text{BAR}^{\text{F}}_4]^-$ ,  $[\text{HCB}_{11}\text{Me}_5\text{I}_6]^-$  and  $[\text{SbF}_6]^-$  anions; **89** – **95**, Figure 5.8. The compounds were isolated by precipitation or crystallisation as orange solids in 34% – 87% yield, the range of yields owing to the variable solubilities of **89** – **95**. While COD complexes **92** – **95** are air stable, exposure of NBD analogues **93** – **95** to air results in rapid decomposition, in both solution and the solid state.

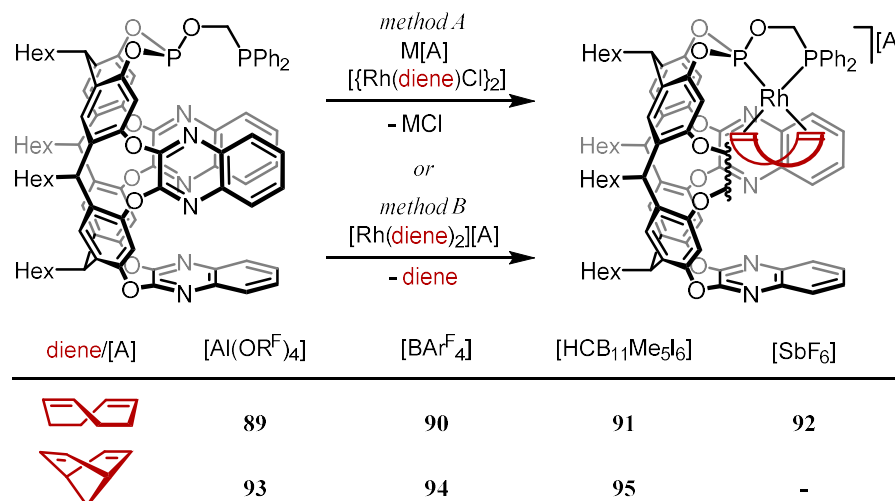


**Figure 5.8** Synthesis of rhodium diene complexes of **RcPOP**. Conditions: dichloromethane solution, 18 hours, ambient temperature. Front quinoxaline wall omitted for clarity here and throughout.  $\text{M}[\text{A}] = \text{Li}[\text{Al}(\text{OR}^{\text{F}})_4]$ ,  $\text{Na}[\text{BAR}^{\text{F}}_4]$ ,  $\text{Cs}[\text{HCB}_{11}\text{Me}_5\text{I}_6]$ ,  $\text{Ag}[\text{SbF}_6]$ .

### 5.3.2 Solution characterisation

By  $^1\text{H}$  NMR spectroscopy, diene complexes **89** – **95** exhibit overall  $C_s$  symmetry. While similar, there are anion-dependent differences in the  $^1\text{H}$  NMR spectra, largely pertaining to the chemical shift of the quinoxaline resonances. Distortion of the quinoxaline units to accommodate closer ion pairs, or interaction of the quinoxaline with the arene surfaces of  $[\text{BAR}^{\text{F}}_4]^-$  or the iodine atoms of  $[\text{HCB}_{11}\text{Me}_5\text{I}_6]^-$  may account for this observation. The diene ligands of complexes **89** – **95** are demonstrably within the cavitand as evident by the upfield-shifted resonances at  $\delta_{\text{H}}$  *ca.* 3.7 and 2.5 for the two CH environments, and at  $\delta_{\text{H}}$  *ca.* -0.9, -1.0 and -1.5 for the  $\text{CH}_2$  environments of COD complexes **89** – **92**, and similarly at  $\delta_{\text{H}}$  *ca.* 3.6, 1.9, -0.3, -2.2 and -2.7 for NBD complexes **96** – **98**, Figure 5.9. The phenomenon of a greater upfield shift the ‘deeper’ a guest

proton resides in a walled cavitand is well described by work on linear alkane encapsulation,<sup>284–287,401</sup> and is manifested here by the inequivalent COD and NBD methylene signals, and by the notable differentiation in the alkene CH signals themselves, differing by 1.2 and 1.7 ppm for COD and NBD respectively. This disparity is far greater than the chemical shift difference that arises from the distinct electronic situation of being *trans* to a phosphite *vs.* a phosphine (*ca.* 0.3 ppm).<sup>407–409</sup> The  $^{31}\text{P}\{^1\text{H}\}$  NMR spectra are independent of anion, expressed as two doublet of doublet resonances downfield of the free ligand; for COD complexes **89** – **92**  $\delta_{31\text{P}}$  *ca.* 154 ( $^1J_{\text{RhP}} \approx 250$  Hz) for the phosphite and  $\delta_{31\text{P}}$  *ca.* 66 ( $^1J_{\text{RhP}} \approx 150$  Hz) for the phosphine ( $^2J_{\text{PP}} \approx 40$  Hz). For NBD complexes **93** – **95**, resonances of *ca.*  $\delta_{31\text{P}}$  161 ( $^1J_{\text{RhP}} \approx 260$  Hz) and  $\delta_{31\text{P}}$  66 ( $^1J_{\text{RhP}} \approx 150$  Hz) for the phosphite and phosphine resonances, respectively ( $^2J_{\text{PP}} \approx 50$  Hz), are observed.

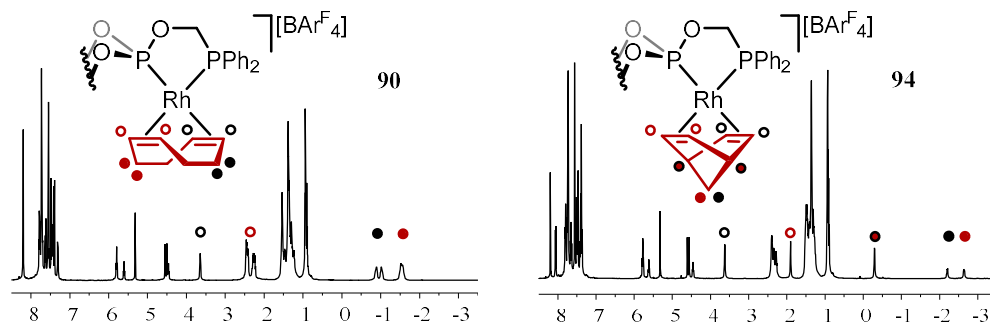


**Figure 5.9**  $^1\text{H}$  NMR spectra (298 K 500 MHz) of COD complex **90** and NBD complex **94**. Diene signals indicated. Structures truncated for clarity.

### 5.3.3 Solid state characterisation

Crystalline material suitable for X-ray diffraction analysis may be prepared of complexes **89** – **95** by slow diffusion of hexane into dichloromethane or fluorobenzene solutions of the particular compound. Material derived from fluorobenzene is found to consistently co-crystallise with one or two molecules of fluorobenzene, located in the cleft between the hexyl chains at the base of the cavitand. For brevity, a solitary example of each diene is discussed here. The solid-state structures of COD complex **91** and NBD complex **95** are presented in Figures 5.10 and 5.11, respectively.

The rhodium-centric metrics of COD complex **91** are in good agreement with a reported structure for a rhodium COD complex of a non-cavitand-based but structurally and electronically analogous diphenylphosphine-diarylphosphite ligand.<sup>408</sup> The interior angles of the rhodium phosphine-phosphite chelate, at 80.92(7)°, 107.1(3)° and 113.6(2)° for the P2-Rh1-P5, Rh1-P2-C3 and Rh1-P5-O4 angles, respectively, are all within 1° of the previous report, indicating the cavitand is having no appreciable affect on this aspect of the coordination. The Rh-cnt(alkene) contacts in **94** are near equidistant, at 2.1834(5) and 2.1806(5) Å, values intermediate to the 2.209 and 2.171 Å contacts for the non-cavitand system. The cavitand itself appears fairly deformed, though it is unclear if this is due to the system attempting to maximise the quinoxaline-COD CH- $\pi$  interactions or an effect of crystal packing. The quinoxaline moiety on the underside of the COD ligand deflects toward the metal ( $\angle\text{pln(Rc)}\text{-pln(Q)} = 76.07(10)^\circ$ ), while the flanking quinoxaline units, separated by *ca.* 10.0 Å, are close to perpendicular with respect to the resorcinarene plane ( $\angle\text{pln(Rc)}\text{-pln(Q')} = 85.61(10)^\circ, 89.03(10)^\circ$ ).

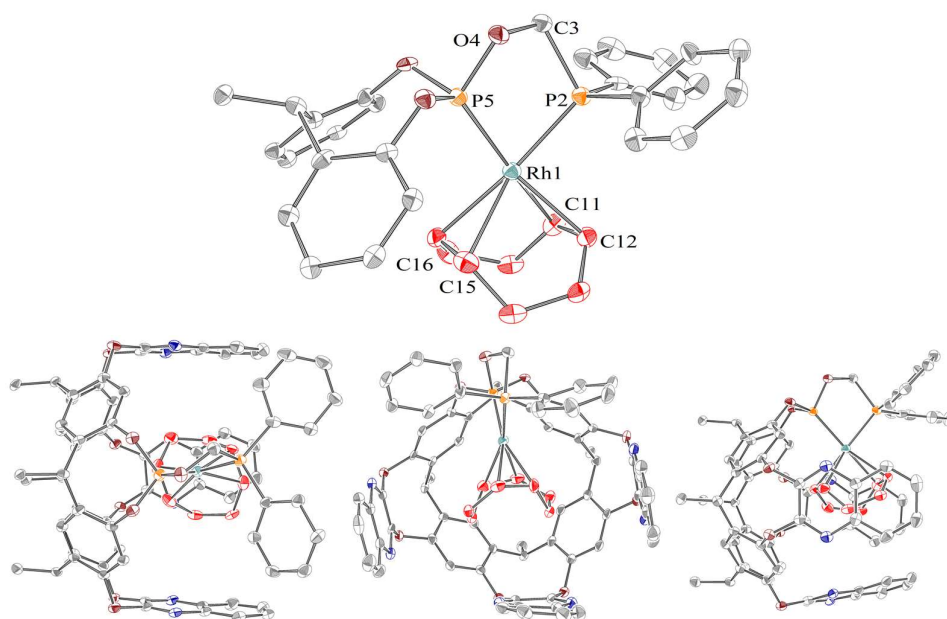


**Figure 5.10** Solid state structure of COD complex **91**. Top: truncated view of the organometallic component. Bottom: views along the principal axes of the molecule with; hexyl chains truncated and [HCB<sub>11</sub>Mes<sub>16</sub>] anion omitted. Data at 150 K, thermal ellipsoids drawn at 30%, Selected bond lengths (Å) and angles (°): Rh1-P2, 2.258(2); Rh1-P3, 2.221(2); Rh1-cnt(C11,C12), 2.1834(5); Rh1-cnt(C15,C16), 2.1806(5); C11-C12, 1.372(13); C15-C16, 1.368(14); cnt(Q')-cnt(Q'), 10.0059(1); P2-Rh1-P5, 80.92(7); cnt(C11,C12)-Rh1-cnt(C15,C16), 83.892(19); Rh1-P2-C3, 107.1(3); Rh1-P5-O4, 113.6(2); pln(Rc)-pln(Q), 76.07(10); pln(Rc)-pln(Q'), 85.61(10), 89.03(10); torsion(O4-C3-P2-P5), 30.3(5).

The geometry of the rhodium phosphine-phosphite chelate of NBD complex **98** is generally similar to that of the COD analogue **91**, though the slightly larger P2-Rh1-P5 angle of 82.12(5)° facilitates a reduced torsion of the C3-O4 linker out of the P2-Rh1-P5 plane; 17.8(3)° for **95** vs. 30.3(5) for **91**. Rhodium-alkene contacts measured as 2.1249(4) Å and 2.1685(4) Å are shorter than those to the COD ligand of **91**, consistent with other systems for which NBD and COD analogues have been prepared.<sup>93</sup> The cavitand of **95** adopts a visibly less distorted conformation than that seen with **91**, potentially a consequence of (or permitted because) the NBD ligand is less spatially imposing than COD in the direction parallel to the C=C bonds. The angles of the quinoxaline units with respect to the resorcinarene base remain consistent with **91**; the opposing quinoxaline is still deflected towards the metal ( $\angle \text{pln(Rc)-pln(Q)} = 77.78(6)^\circ$ ) and the flanking components are still near perpendicular ( $\angle \text{pln(Rc)-pln(Q')} = 91.72(7)^\circ$ ,  $93.49(6)^\circ$ ) however the separation of the latter two arenes is reduced to *ca.* 9.40 Å.

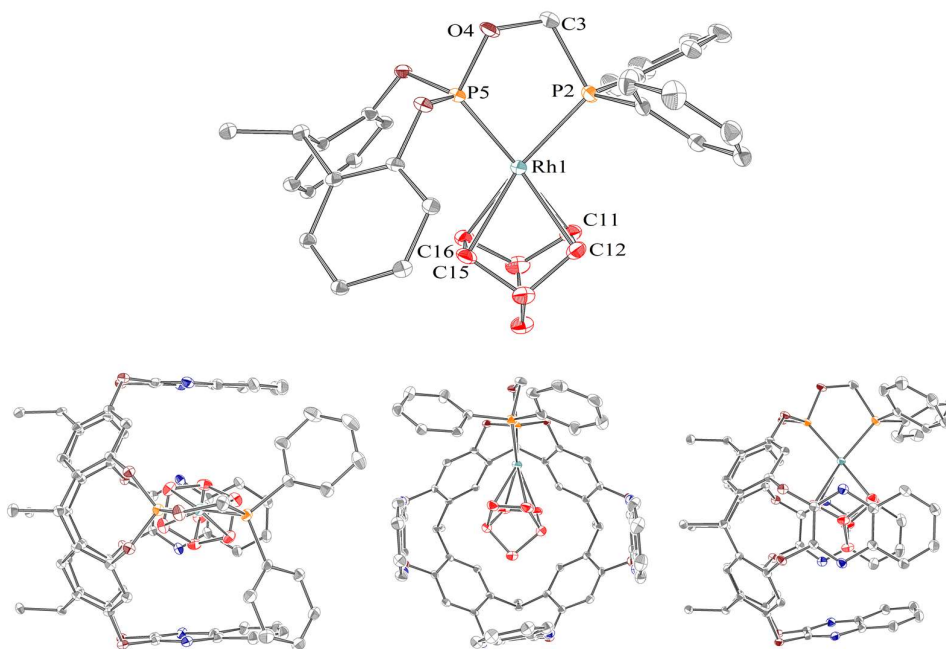


**Figure 5.11** Solid state structure of NBD complex **95**. Top: truncated view of the organometallic component. Bottom: views along the principal axes of the molecule with; hexyl chains truncated and [HCB<sub>11</sub>Me<sub>5</sub>I<sub>6</sub>] anion and two co-crystallising molecules of fluorobenzene omitted. Data at 150 K, thermal ellipsoids drawn at 30%, Selected bond lengths (Å) and angles (°): Rh1-P2, 2.2632(13); Rh1-P3, 2.2116(13); Rh1-cnt(C11,C12), 2.1249(4); Rh1-cnt(C15,C16), 2.1685(4); C11-C12, 1.367(9); C15-C16, 1.353(9); cnt(Q')-cnt(Q'), 9.4005(2); P2-Rh1-P5, 82.12(5); cnt(C11,C12)-Rh1-cnt(C15,C16), 68.572(11); Rh1-P2-C3, 107.54(18); Rh1-P5-O4, 115.27(16); pln(Rc)-pln(Q), 77.78(6); pln(Rc)-pln(Q'), 91.72(7), 93.49(6); torsion(O4-C3-P2-P5), 17.8(3).

## 5.4 Solution phase reactivity

### 5.4.1 Lability of alkene

The dienes of complexes **89** and **93** are retained on dissolution in dichloromethane, fluorobenzene, 1,2-difluorobenzene, mesitylene and MTBE.<sup>†</sup> In acetonitrile the dienes are fully substituted within 5 minutes as gauged by <sup>1</sup>H NMR spectroscopy, resulting in the formation of bis(acetonitrile) complex **96**, Figure 5.12. Visual inspection of the dissolution event suggests that this reaction can occur in the solid state as well as solution; the orange diene complexes immediately take on a yellow colouration on addition of acetonitrile, prior to dissolution. Bis(acetonitrile) complex **96** is indefinitely stable in acetonitrile solution, however isolated material has limited stability in dichloromethane, decomposing over a period of days to an intractable mixture.

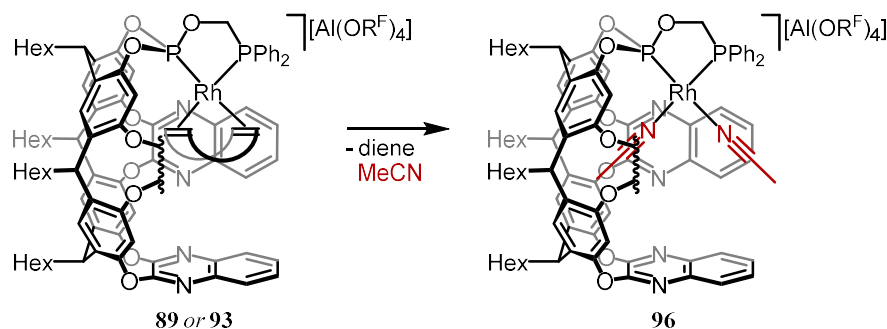


**Figure 5.12** Reaction of diene complexes **89** and **93** with neat acetonitrile.

In dichloromethane solution the two bound acetonitrile ligands of **96** are evident in the <sup>1</sup>H NMR and <sup>13</sup>C{<sup>1</sup>H} NMR spectra at  $\delta_{\text{1H}}$  -2.55 and  $\delta_{\text{13C}}$  -4.6 and  $\delta_{\text{1H}}$  1.05 and  $\delta_{\text{13C}}$  2.5. The phosphite resonance in the <sup>31</sup>P{<sup>1</sup>H} NMR spectrum is fairly close in chemical shift to that of dienes **89** and **93**, though an increase in both the <sup>1</sup>*J*<sub>RhP</sub> and the <sup>2</sup>*J*<sub>PP</sub> coupling constants (by *ca.* 50 and 10 Hz, respectively) compared to the diene complexes is noted;  $\delta_{\text{31P}}$  159.9 (<sup>1</sup>*J*<sub>RhP</sub> = 294 Hz, <sup>2</sup>*J*<sub>PP</sub> = 63 Hz). The phosphine resonance meanwhile is shifted downfield by *ca.* 20 ppm relative to the diene complexes, at  $\delta_{\text{31P}}$  83.4 (<sup>1</sup>*J*<sub>RhP</sub> = 165 Hz).

<sup>†</sup> For solution chemistry of these systems only the [Al(OR<sup>F</sup>)<sub>4</sub>] salts are discussed. The chemistry is anticipated to be equivalent for other non-coordinating anions, though some disparate reactivity is observed when employing the [HCB<sub>11</sub>Me<sub>5</sub>I<sub>6</sub>] anion, presumably due to the coordinating iodide functionality.

### 5.4.2 Hydrogenation in dichloromethane and mesitylene

Placing solutions of COD complex **89** or NBD complex **93** under an atmosphere of dihydrogen in dichloromethane solution results in the rapid precipitation of a pale-orange gel. Attempts to solubilise this material, for example by dissolution in acetonitrile, were unsuccessful. This points to an irreversible reaction with dichloromethane by the reactive fragment generated on alkane liberation, presumably an oxidative addition reaction, which is known at dppe rhodium chlorides for example.<sup>410</sup> A more chemically robust solvent was therefore mandated.

Mesitylene is a commonly employed solvent for performing guest titration experiments on walled resorcinarenes (*cf.* Section 5.1.2) with the solvent being sufficiently bulky that it does not form a persistent host-guest complexes with tetra-walled resorcinarenes. Reaction of **89** or **93** with dihydrogen in mesitylene results immediately in a red solution, which by NMR spectroscopy is associated with the formation of one new RcPOP-containing compound, common to both starting materials, assigned as  $\eta^6$ -mesitylene complex **97**, Figure 5.13. Concomitant liberation of COA or NBA is observed in these reactions by  $^1\text{H}$  NMR spectroscopy, so too is a broad resonance in the  $^1\text{H}$  NMR spectra at  $\delta_{\text{H}} -0.4$ . Several additional low-intensity, upfield signals in the range  $\delta_{\text{H}} -1.6 - -3.2$  are noted in the crude reaction mixture, which are as yet unidentified. The  $^{31}\text{P}\{^1\text{H}\}$  NMR spectra of the reaction mixture exhibits resonances at  $\delta_{31\text{P}} 152.8$  ( $^1J_{\text{RhP}} = 329$  Hz) and  $84.1$  ( $^1J_{\text{RhP}} = 194$  Hz) with a  $^2J_{\text{PP}}$  of *ca.* 58 Hz, and assigned to mesitylene complex **97**.

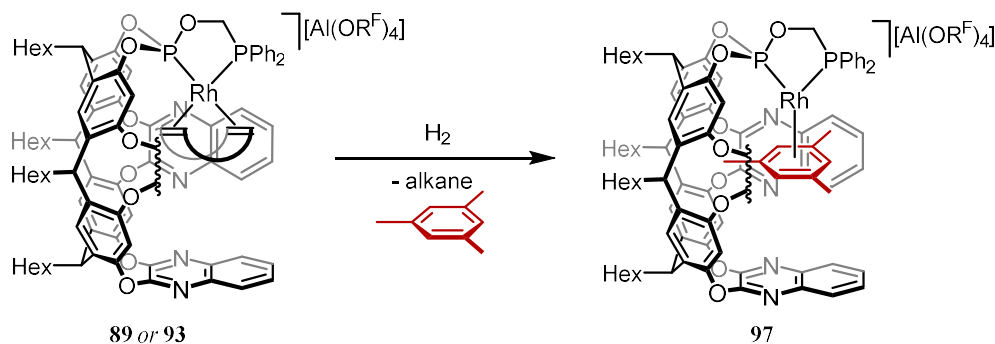


**Figure 5.13** Reaction of diene complexes **89** and **93** with dihydrogen in mesitylene.

Diffusion of hexane into the crude reaction mixture generated from COD complex **89** afforded crystalline material suitable for X-ray diffraction analysis, Figure 5.14. While the data is particularly low quality, the structural distortions required to include a mesitylene ligand within the cavity are evident, with the flanking quinoxaline walls projected dramatically outward. The mesitylene ligand has the expected minimum-energy orientation, with the majority of the bulk directed to the top of the cavity.

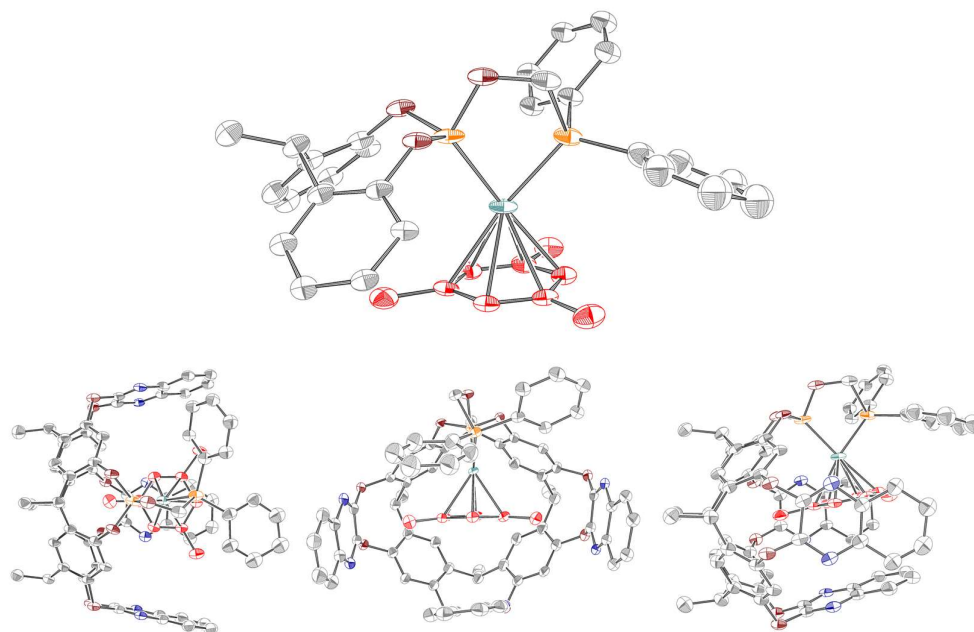


**Figure 5.14** Solid state structure of mesitylene complex **97**. Selected cation. Top: truncated view of the organometallic component. Bottom: views along the principal axes of the molecule with; hexyl chains truncated and  $[\text{Al}(\text{OR}^{\text{F}})_4]$  anion omitted. Data at 150 K, thermal ellipsoids drawn at 30%. The data is of insufficient quality to report any meaningful information besides connectivity.

Dissolution of crystallised material of **97** in 1,2-difluorobenzene results in a sample possessing a  $^{31}\text{P}\{^1\text{H}\}$  NMR spectrum very similar (chemical shift within 1 ppm, coupling within 0.1 Hz) to the *in situ* reaction mixture. The corresponding  $^1\text{H}$  NMR spectrum contains signals typical of the **RcPOP** ligand, in addition to two broad resonances at  $\delta_{\text{H}}$  1.41 (fwhm = 27 Hz) and -0.09 (fwhm = 53 Hz), in a 2:1 ratio, which may reasonably be assigned to two inequivalent methyl groups of a mesitylene ligand. This assignment would imply hindered rotation with a preferred orientation of the mesitylene that directs two methyl groups towards the top of the cavitand, consistent with the solid-state structure.





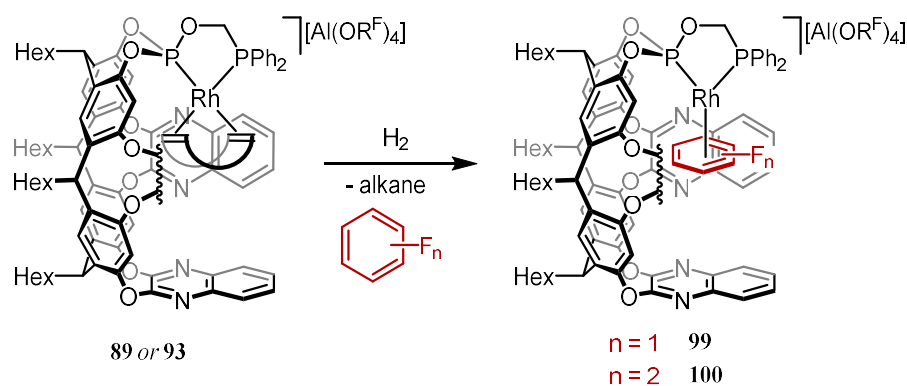


**Figure 5.16** Hydrogenation of diene complexes in fluorobenzene and 1,2-difluorobenzene.

Bound fluorobenzene in complex **99** is clearly observed in the  $^{19}\text{F}\{^1\text{H}\}$  NMR spectrum recorded in fluorobenzene solvent at  $\delta_{19\text{F}}$  -117.30; upfield of the free fluoroarene ( $\delta_{19\text{F}}$  -113.15). The bound arene is also apparent in the  $^1\text{H}$  NMR spectrum, with upfield-shifted resonances at  $\delta_{1\text{H}}$  3.29, 2.84 and 2.01 for the *ortho*-, *meta*- and *para*-protons, respectively, with a  $^3J_{\text{HH}}$  coupling constant of *ca.* 6 Hz. The trend in nuclear shielding experienced the fluorobenzene ligand is suggestive of a favoured orientation with the fluorine atom directed out of the cavity. The  $^{31}\text{P}\{^1\text{H}\}$  NMR chemical shift is generally similar to that of acetonitrile complex **96**, while the strong  $^1J_{\text{RhP}}$  coupling is closer to that of mesitylene complex **97**;  $\delta_{31\text{P}}$  164.5 ( $^1J_{\text{RhP}} = 323$  Hz) and 82.5 ( $^1J_{\text{RhP}} = 194$  Hz) for the phosphite and phosphine resonance, respectively ( $^2J_{\text{PP}} \approx 55$  Hz). Very similar data is obtained of isolated **99** in dichloromethane solution;  $\delta_{19\text{F}}$  -116.96,  $\delta_{1\text{H}}$  3.78, 3.41 and 2.4 for the *ortho*-, *meta*- and *para*-protons of the bound arene, respectively.

The bound 1,2-difluorobenzene of complex **100** is similarly observable in 1,2-difluorobenzene solution; in the  $^1\text{H}$  NMR spectrum as two broad multiplets at  $\delta_{1\text{H}}$  3.42 and 2.03, and in the  $^{19}\text{F}\{^1\text{H}\}$  NMR spectrum at  $\delta_{19\text{F}}$  -141.45. The  $^{31}\text{P}\{^1\text{H}\}$  NMR spectrum is very to that of fluorobenzene complex **99**;  $\delta_{31\text{P}}$  161.9 ( $^1J_{\text{RhP}} = 328$  Hz) for the phosphite resonance, and 82.6 ( $^1J_{\text{RhP}} = 195$  Hz) for the phosphine resonance ( $^2J_{\text{PP}} = 57$  Hz). Complex **100** is unstable in dichloromethane solution, immediately forming a gelatinous orange precipitate similar to the material observed on attempting to hydrogenate diene complex **89** or **93** in neat dichloromethane. Fluorobenzene complex **99** also exhibits instability in dichloromethane, to a lesser extent, fully decomposing within 72 hours.

Crystalline material suitable for X-ray diffraction analysis of the fluorobenzene adduct was obtained through slow diffusion of hexane into a fluorobenzene solution of **99**, Figure 5.17. The rhodium-phosphine geometry, specifically the angles pertaining to the diphosphine chelate, are generally similar to that of COD complex **91** and NBD complex **95**, and the Rh-cnt(arene) distance of 1.8810(5) is in line with previously reported structurally analogous rhodium *cis*-diphosphine  $\eta^6$ -fluorobenzene complexes; 1.86 - 1.88 Å.<sup>411,412</sup> The fluoroarene is orientated with the fluorine atom projected out of the cavity; the C-F torsion angle with respect to the P2-Rh1 bond is 1.3(3)°. Deflection of the opposing quinoxaline unit towards the metal is to a greater extent than is the case with **91** or **95**, with a pln(Rc)-pln(Q) angle of 69.54(13)°, possibly a consequence of the reduced steric bulk of the fluoroarene relative to the diene ligands. The flanking walls are again coplanar and perpendicular to the plane of the resorcinarene (pln(Rc)-pln(Q') = 91.61(12)°, 91.08(16)°). With a quinoxaline separation comparable to COD complex **91** of 9.91 Å.

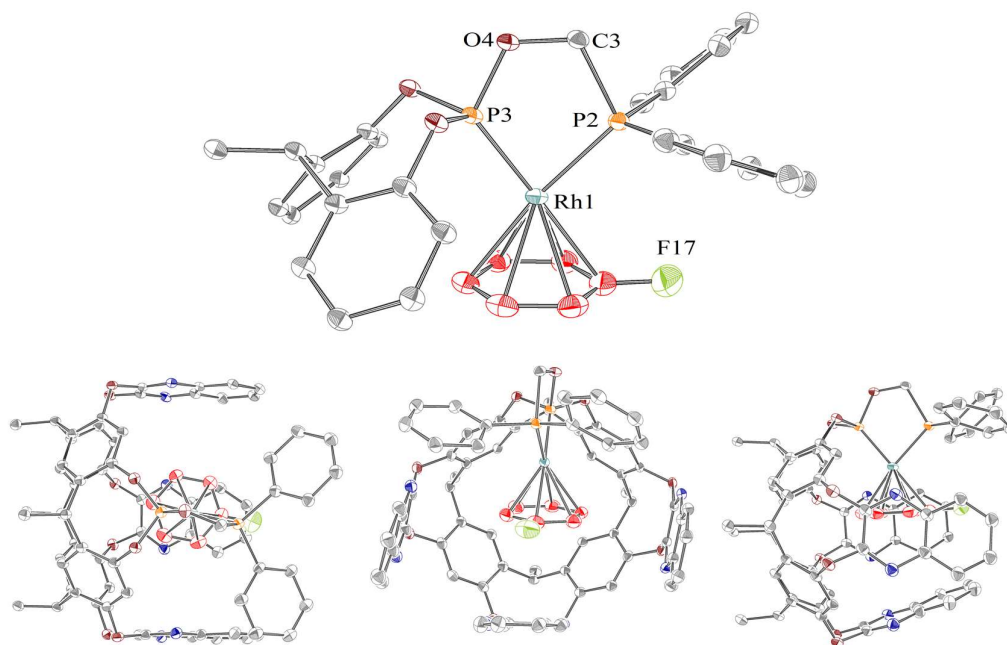


**Figure 5.17** Solid-state structure of fluorobenzene complex **99**. Top: truncated view of the organometallic component. Bottom: views along the principal axes of the molecule with, hexyl chains and [Al(OR<sup>F</sup>)] anion omitted. Data at 150 K, thermal ellipsoids drawn at 15%, Selected bond lengths (Å) and angles (°): Rh1-P2, 2.239(2); Rh1-P3, 2.168(2); Rh1-cnt(arene), 1.8810(5); cnt(Q')-cnt(Q'), 9.9084(1); P2-Rh1-P5, 82.18(7); Rh1-P2-C3, 107.9(3); Rh1-P5-O4, 115.7(2); pln(Rc)-pln(Q), 69.54(13); pln(Rc)-pln(Q'), 91.61(12), 91.08(16); torsion(O4-C3,P2-P5), 16.2(5); torsion(P2-Rh1-cnt(arene)-F17), 1.3(3).

Neither fluoroarene complex **99** nor **100** enact the dehydrogenation of NBA or COA in their respective fluoroarene solution on time scales up to 2 weeks. The diene complex may be regenerated by addition of fresh diene, however with fluorobenzene complex **102** this reaction is relatively slow; with 5 equivalents of NBD added a 10 mM solution of **99**, after 1 hour only 25% conversion to NBD complex **93** was observed by  $^1\text{H}$  NMR spectroscopy. This is not a surprising result given the vast excess of fluorobenzene present, and the necessarily dissociative substitution mechanism. Attempts to extend the series of fluoroarene complexes to the weaker coordinating 1,3-bis(trifluoromethyl)benzene or 1,3,5-trifluorobenzene, were unsuccessful; NBD complex **93** is very poorly soluble in the former, and investigations on the latter were hampered by what are believed to be batch impurities in the 1,3,5-trifluorobenzene, resulting in the formation of competitive adducts.

#### 5.4.4 Hydrogenation in MTBE

The behaviour of the resorcinarene system following hydrogenation of NBD complex **93** in MTBE solvent is complicated. Within 5 minutes **93** is fully consumed with concomitant liberation of NBD as gauged by  $^1\text{H}$  NMR spectroscopy. An additional upfield signal at  $\delta_{\text{IH}}$  -2.2 and a corresponding signal at  $\delta_{\text{IH}}$  3.0 is observed initially, Figure 5.18 (a), which are themselves consumed within 30 minutes. Over a 3 hour time period from the start of the reaction, new signals at  $\delta_{\text{IH}}$  3.33 and 1.36 are observed which seem to be in some way related to MTBE, Figure 5.17 (b). These signals are not consistent with the standard metal catalysed decomposition products of MTBE; *iso*-butene (or under these conditions, *iso*-butane) and methanol. By integration relative to an internal benzene capillary, assuming each signal corresponds to 3:9 protons, 20 equivalents have been produced; the resorcinarene proton resonances are highlighted for comparison, Figure 5.17 (c). In this reaction the  $^{31}\text{P}\{^1\text{H}\}$  NMR spectrum becomes immediately broad and remains that way for the duration. Analogous to the hydrogenation reactions performed in mesitylene, from *ca.* 24 hours into the reaction a precipitate, characterised as dimer **98**, is observed in the reaction vessel.

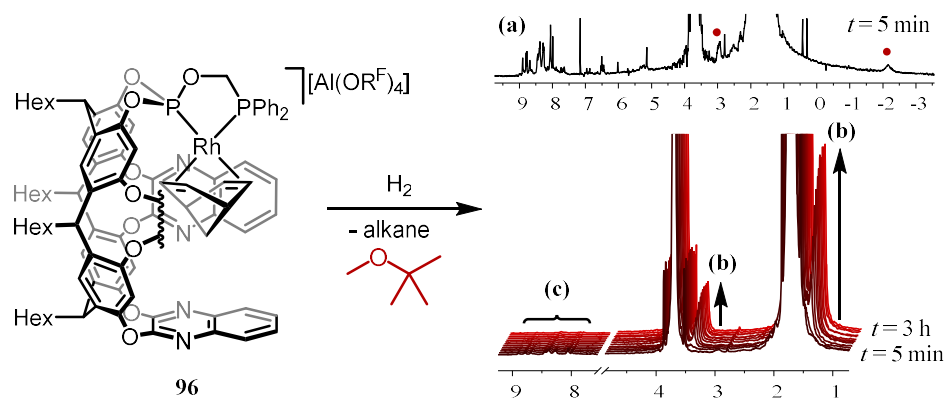


**Figure 5.18** Hydrogenation of NBD complex in MTBE, resulting  $^1\text{H}$  NMR spectra (400 MHz) (*see text*).

The reactivity just described is entirely suppressed by the addition of excess alkane to the system. Separately, the effect of the addition of *ca.* 250 equivalents of cyclohexane, NBA and adamantane prior to the introduction of dihydrogen were examined. With all three hydrocarbons the MTBE-related signals (Figure 5.18 (b)) are not observed in the respective  $^1\text{H}$  NMR spectra, and the precipitation of dimer **98** is slowed. With 250 equivalents of NBA or adamantane several low intensity **RcPOP**-derived  $^1\text{H}$  NMR signals are observed that are alkane dependant. No signals are apparent in the  $^{31}\text{P}\{^1\text{H}\}$  NMR spectrum in these cases, and no upfield signals characteristic of an alkane interaction are observed.

In the hydrogenation of NBD complex **93** in MTBE with 250 equivalents of cyclohexane results in clean conversion to a solitary **RcPOP**-containing compound as determined by  $^1\text{H}$  NMR spectroscopy, featuring the upfield resonances at  $\delta_{\text{H}}$  2.93 and -2.14 detected previously (Figure 5.18, a). This compound is assigned as an MTBE complex, with the upfield signals assigned as the *tert*-butyl and methyl signals, respectively. Only very broad signals are observed in the  $^{31}\text{P}\{^1\text{H}\}$  NMR spectrum during this reaction, indicative of dynamic exchange processes occurring on the NMR time scale (162 MHz). The reason the MTBE complex is not persistently observed in the absence of cyclohexane, or why cyclohexane stabilises the MTBE complex, is unclear.

## 5.5 Solid state reactivity

### 5.5.1 Approaching an alkane complex

To gauge whether hydrogenation proceeds in the solid state, crystalline material of NBD  $[\text{Al}(\text{OR}^{\text{F}})_4]$  complex **96** was treated with dihydrogen, resulting in an immediate colour change from orange to red. After 10 minutes the atmosphere was returned to argon by multiple gas-vacuum cycles not exceeding a vacuum of  $10^{-1}$  mbar and the material dissolved in fluorobenzene. The result was a solution of analytically pure fluorobenzene complex **99** with *ca.* 1 equivalent of free NBA, placing an upper bound on the solid-state reaction time of *ca.* 10 minutes. In an attempt to observe the bound alkane prior to displacement with solvent, dichloromethane was vacuum distilled onto a sample of hydrogenated **93**, the solvent thawed and the sample placed directly into the probe of an NMR spectrometer pre-cooled to 185 K. A standard 16 scan spectrum was obtained within 2 minutes but no signals consistent with a bound alkane were apparent.

The exposure of single crystals of diene complexes **89** – **95** to dihydrogen results in a similar red material with each complex. The material which results appears crystalline on visual inspection, but elicits negligible X-ray diffraction, with longer delays between hydrogenation and mounting the crystals on the goniometer exacerbating the issue. This occurs for all anions trialled, across several experiments, with one exception. The  $[\text{HCB}_{11}\text{Me}_5\text{I}_6]^-$  anion was selected specifically to improve the quality of the diffraction data with the high atomic weight iodine atoms, and in one hydrogenation experiment, of NBD complex **95**, crystallised from fluorobenzene, with a short hydrogenation time, enough diffraction data was obtained to determine a very low-quality structure. The full unit cell, Figure 5.19, contains two cations, two anions and four fluorobenzene molecules. In one cation, a difference peak close to the rhodium centre is modelled as a coordinated water molecule. In neither cation is the hydrocarbon component orientated in a way consistent with the starting material of this reaction, though insufficient data is available to draw any conclusions about the nature of the bonding.

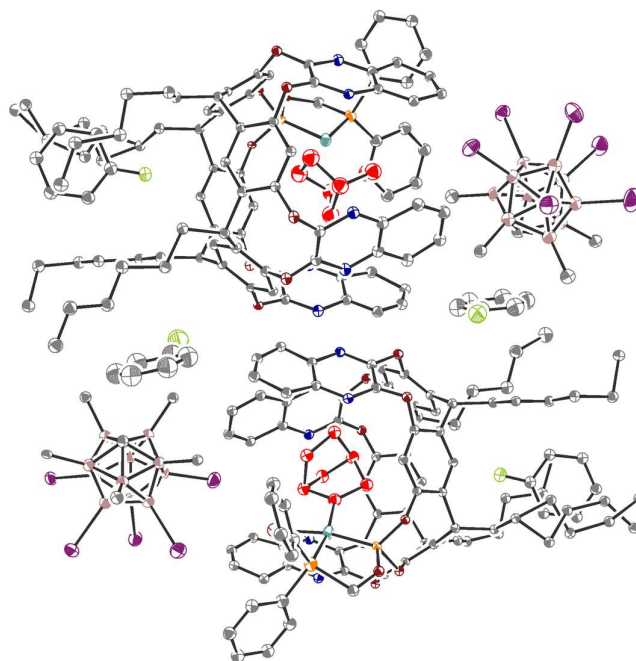


**Figure 5.19** Solid state structure resulting from the hydrogenation of fluorobenzene-derived crystals of **95**. Data at 150 K, thermal ellipsoids drawn at 15%.

In the event that the issue of weak diffraction is due to the loss of crystallinity in these systems, this is likely a consequence of the flexibility of the cavitand ligand. As has been observed, the quinoxaline walls are able to contort to accommodate various molecular topologies, most notably with mesitylene complex **97**. Given the fairly substantial changes in coordination geometry that have been previously observed elsewhere in single-crystal to single-crystal diene hydrogenation of rhodium diphosphine  $[\text{BAR}^{\text{F}}_4]$  systems (*cf.* Section 1.2.6), particularly the *ca.*  $90^\circ$  rotation of the hydrocarbon observed with the NBD/NBA ligands, it is reasonable to assume that on hydrogenation, the steric demands within the quinoxaline-defined cavity change, such that a change of the resorcinarene framework results, which then percolates through the lattice.

## 5.6 Conclusions and future work

This chapter has demonstrated a synthetically straightforward procedure for the preparation of rhodium COD and NBD complexes in which the diene is encapsulated by a cavitand-based ligand architecture. Adducts of weakly interacting solvent have been synthesised, with the potential for further diversification of this series. The ultimate aim of characterising an alkane within the cavity has not yet been realised, although the hydrogenation chemistry is viable and formation of an alkane complexes are indirectly implicated, the solution behaviour of this system is not yet well understood. Recently in the Chaplin Group it has been demonstrated that bound fluoroarenes may be displaced by the addition of alkane in non-fluoroarene solvent. This is an ongoing line of enquiry, as is the design of related ligand architectures which should feasibly perturb some of the suggested dynamic processes.

A great deal of scope exists for modification to the ligand system in order to perturb some of the undesired properties of the system. If the crystallographic issues are indeed a consequence of the flexible quinoxaline units, then efforts to rigidify the system by chemically bonding neighbouring quinoxaline walls, for example, may be a worthwhile investigation. A modified ligand design could similarly abate the adduct exchange processes observed in solution; even a slight increase in bulk at the top of the cavity may serve to disfavour the dimerisation of the complex, and remove one convolution to the complicated dynamic picture. Many exciting avenues are open to the resorcinarene based cavitand systems.

Investigations continue.

## 6 Experimental details

---

### 6.1 General considerations

#### 6.1.1 Practices

All manipulations were performed under argon using standard Schlenk line and glove box techniques unless otherwise stated. Glassware was oven dried at 150 °C overnight and flamed under vacuum prior to use unless the reaction was performed in air or liberates water as a by-product. 3 Å molecular sieves were activated by heating at 300 °C *in vacuo* overnight prior to use. Argon, dihydrogen, dinitrogen, carbon monoxide, methane and xenon were purchased from BOC and used as supplied unless prefixed as ‘*dry*’; *dry* gasses were passed through a column of activated 3 Å molecular sieves. The system pressure was 1 atm unless otherwise stated.

#### 6.1.2 Solvents

DMSO, DMF, THF, MeOH, EtOH, MeCN, CHCl<sub>3</sub>, CH<sub>2</sub>Cl<sub>2</sub>, toluene, mesitylene, Et<sub>2</sub>O, hexane, and pentane, were purchased anhydrous from Acros, Aldrich or Alfa-Aesar and used as received when working under dinitrogen, or otherwise freeze-pump-thaw degassed before being placed under argon over activated 3 Å molecular sieves, except in the following cases: *dry* hexane, *dry* pentane and *dry* heptane were dried over Na/K<sub>2</sub> alloy, vacuum-distilled, and freeze-pump-thaw degassed before being placed under *dry* argon over a potassium mirror. *Dry* CH<sub>2</sub>Cl<sub>2</sub> was stirred over CaH<sub>2</sub> overnight, vacuum-distilled, and freeze-pump-thaw degassed three times before being placed under argon over activated 3 Å molecular sieves. THF and MTBE were dried over Na/benzophenone, vacuum-distilled, and freeze-pump-thaw degassed three times before being placed under argon over activated 3 Å molecular sieves. C<sub>6</sub>H<sub>5</sub>F and 1,2-C<sub>6</sub>H<sub>4</sub>F<sub>2</sub> were purchased undried from Fluorochem, stirred over neutral alumina for 4-6 h, filtered, stirred over CaH<sub>2</sub> overnight, vacuum-distilled, and freeze-pump-thaw



degassed three times before being placed under argon over activated 3 Å molecular sieves. CD<sub>2</sub>Cl<sub>2</sub> was placed over activated 3 Å molecular sieves and freeze–pump–thaw degassed three times before being placed under argon. C<sub>6</sub>D<sub>5</sub>F was stirred over neutral alumina for 1 h, filtered, dried over CaH<sub>2</sub>, vacuum-distilled, being placed under argon over activated 3 Å molecular sieves. All other solvents were purchased undried and used benchtop, in air. Where noted, solvents prefixed as ‘*wet*’ are benchtop solvents, contained dissolved atmospheric water, which have been freeze–pump–thaw degassed three times and placed under argon prior to use.

### 6.1.3 Reagents

[{Ir(cod)Cl}<sub>2</sub>],<sup>413</sup> [{Rh(dtbpm)Cl}<sub>2</sub>],<sup>414</sup> [{Rh(coe)<sub>2</sub>Cl}<sub>2</sub>],<sup>415</sup> [{Rh(cod)Cl}<sub>2</sub>],<sup>416</sup> [{Rh(nbd)Cl}<sub>2</sub>],<sup>417</sup> Li[Al(OR<sup>F</sup>)<sub>4</sub>],<sup>68</sup> Na[BAr<sup>F</sup><sub>4</sub>],<sup>418</sup> K[BAr<sup>F</sup><sub>4</sub>],<sup>418</sup> Tl[BAr<sup>F</sup><sub>4</sub>],<sup>419</sup> Cs[HCB<sub>11</sub>Me<sub>5</sub>I<sub>6</sub>],<sup>420</sup> Na[acac],<sup>421</sup> Na[Cp],<sup>422</sup> and PPh<sub>2</sub>Tol<sup>F</sup>,<sup>421</sup> were synthesised according to adapted literature procedures. [Rh(cod)<sub>2</sub>][Al(OR<sup>F</sup>)<sub>4</sub>], [Rh(cod)<sub>2</sub>][BAr<sup>F</sup><sub>4</sub>], [Rh(cod)<sub>2</sub>][SbF<sub>6</sub>] and [Rh(nbd)<sub>2</sub>][Al(OR<sup>F</sup>)<sub>4</sub>] were synthesised using a common procedure based on that for [Rh(cod)<sub>2</sub>][BAr<sup>F</sup><sub>4</sub>].<sup>423</sup> All other reagents are commercial products and were used as received, except in the following cases: NBD, COD and TBE were and freeze–pump–thaw degassed three times before being placed under argon over activated 3 Å molecular sieves. NEt<sub>3</sub> was stirred over CaH<sub>2</sub>, vacuum-distilled, and freeze–pump–thaw degassed three times before being placed under argon.

### 6.1.4 NMR spectroscopy

NMR spectra were recorded on Bruker Avance spectrometers (300 – 600 MHz) at 298 K unless otherwise stated. Variable temperature measurements were performed on samples equilibrated to the target temperature for 5 minutes (5 K increment) or 10 minutes (25 K increment) prior to data collection. Chemical shifts are quoted in ppm and coupling constants in Hz. Signal descriptors are abbreviated as: app., apparent; br, broad; vbr, very broad; obsc., obscured; m, multiplet; s, singlet; d, doublet; t, triplet;

q, quartet; pent, pentet; and so on. vbr signals are quoted with an associated line width (fwhm) in Hz. Where a resonance is only observed via a 2D NMR experiment, this is noted at the start of the assignment.

$^1\text{H}$  and  $^{13}\text{C}\{^1\text{H}\}$  NMR spectra recorded in  $\text{CD}_2\text{Cl}_2$ ,  $\text{CDCl}_3$ , and  $d_6$ -DMSO are referenced to the residual solvent signal.<sup>424</sup>  $^1\text{H}$  and  $^{13}\text{C}\{^1\text{H}\}$  NMR spectra recorded in proteosolvents were locked to, and are referenced with, an internal sealed capillary of  $\text{C}_6\text{D}_6$ .  $^1\text{H}$  NMR spectra recorded in 1,2- $\text{C}_6\text{H}_4\text{F}_2$  were referenced using the highest intensity peak of the highest frequency fluoroarene multiplet ( $\delta_{\text{IH}}$  6.865).  $^1\text{H}$  NMR spectra recorded in  $\text{C}_6\text{H}_5\text{F}$  were referenced using the highest intensity peak of the highest frequency fluoroarene multiplet ( $\delta_{\text{IH}}$  6.865).  $^1\text{H}$  NMR spectra recorded in  $\text{C}_6\text{D}_5\text{F}$  are referenced to residual proton signals at 7.09 (d,  $^4J_{\text{FH}} = 5.7$ , *m*-FB), 6.92 (s, *p*-FB), and 6.90 (d,  $^3J_{\text{FH}} = 9.1$ , *o*-FB).  $^{13}\text{C}\{^1\text{H}\}$  NMR spectra recorded in  $\text{C}_6\text{D}_5\text{F}$  are referenced to carbon resonances at 163.1 (d,  $^1J_{\text{FC}} = 245$ , *i*-FB), 129.5 (td,  $^1J_{\text{CD}} = 25$ ,  $^3J_{\text{FC}} = 8$ , *m*-FB), 123.5 (t,  $^1J_{\text{CD}} = 25$ , *p*-FB), 114.9 (dt,  $^2J_{\text{FC}} = 28$ ,  $^1J_{\text{CD}} = 25$ , *o*-FB).  $^{31}\text{P}$  NMR spectra are where possible referenced to an internal sealed capillary of a 25 mM solution of trimethylphosphate in  $\text{C}_6\text{D}_6$  ( $\delta_{31\text{P}} = 3.7$ ).<sup>425</sup> Spectra are otherwise referenced to an external standard, noted with a † after the assignment.  $^{19}\text{F}$  NMR spectra are referenced to an external standard.

NMR assignments of cavitand-based ligands are recorded through a standard notation outlined in Figure 6.1. The  $\underline{\text{C}}(\text{CF}_3)_3$  carbon resonance of the  $[\text{Al}(\text{OR}^{\text{F}})_4]^-$  anion is not observed in any  $^{13}\text{C}\{^1\text{H}\}$  spectra described here in, a consequence of quadrupolar relaxation from the Al nuclei.

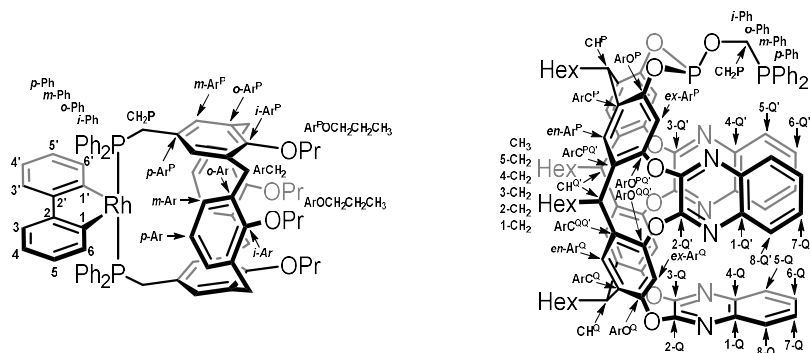


**Figure 6.1** Assignment notation for cavitand-based ligands.

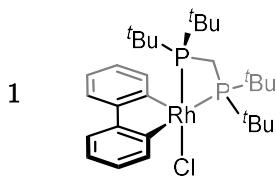
### 6.1.5 Other analyses

Crystallographic data were collected on either an Oxford Diffraction Agilent SuperNova AtlasS2 CCD diffractometer equipped with a microfocus SuperNova Mo K $\alpha$  or Cu K $\alpha$  x-ray source, or on an Oxford Diffraction Xcalibur Gemini Ruby CCD diffractometer equipped with an Enhance Mo K $\alpha$  x-ray source and a graphite monochromator. The data was collected and reduced using CrysAlisPro. All non-hydrogen atoms were refined anisotropically using SHELXL as implemented through the Olex2 interface. Gas chromatographic analyses were performed on an Agilent 7820A GC system fitted with a 7693A auto-injector. High-resolution ESI mass spectra were recorded on a Bruker Maxis Plus instrument. Low-resolution ESI mass spectra were recorded on an Agilent 6130B single Quad instrument. IR spectroscopy was performed on a Bruker ALPHA FT-IR instrument (ATR mode). Microanalyses were performed by Stephen Boyer at London Metropolitan University.

## 6.2 Biphenyl monophosphine systems

### 6.2.1 Preparation of metal biphenyl precursors

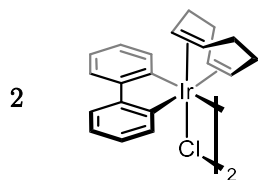
#### 6.2.1.1 [Rh(2,2'-biphenyl)(dtbpm)Cl]



A solution of [ $\{\text{Rh}(\text{dtbpm})\text{Cl}\}_2$ ] (374 mg, 0.422 mmol) and biphenylene (321 mg, 2.11 mmol) in  $\text{CH}_2\text{Cl}_2$  (20 mL) was stirred at 85 °C for 18 h. The solvent was removed *in vacuo*, the residues washed with  $\text{Et}_2\text{O}$  ( $3 \times ca.$  10 mL), and the crude material dissolved in  $\text{CH}_2\text{Cl}_2$  (*ca.* 5 mL). Slow diffusion of excess  $\text{Et}_2\text{O}$  (*ca.* 45 mL) at -30 °C over 72 h precipitated the title compound. The supernatant was decanted, and the solid material dried *in vacuo*. Yield: 343 mg (68%, orange crystalline solid).

**$^1\text{H}$  NMR** (400 MHz,  $\text{CD}_2\text{Cl}_2$ ):  $\delta$  7.55 (d,  $^3J_{\text{HH}} = 7.2$ , 2H, 6-biph), 7.30 (d,  $^3J_{\text{HH}} = 7.3$ , 2H, 3-biph), 6.95 (t,  $^3J_{\text{HH}} = 7.2$ , 2H, 4-biph), 6.86 (t,  $^3J_{\text{HH}} = 7.3$ , 2H, 5-biph), 3.19 (dd,  $^2J_{\text{PH}} = 8.5$ ,  $^2J_{\text{PH}} = 5.9$ , 2H,  $\text{CH}_2$ ), 1.57 (d,  $^3J_{\text{PH}} = 12.8$ , 18H,  $t\text{-Bu}$ ), 1.07 (d,  $^3J_{\text{PH}} = 13.6$ , 18H,  $t\text{-Bu}$ ).  **$^{31}\text{P}\{^1\text{H}\}$  NMR** (121 MHz,  $\text{CD}_2\text{Cl}_2$ ):  $\delta$  20.0 (dd,  $^1J_{\text{RhP}} = 135$ ,  $^2J_{\text{PP}} = 11$ , *trans*-Cl), -12.2 (dd,  $^1J_{\text{RhP}} = 56$ ,  $^2J_{\text{PP}} = 11$ , *trans*-biph). **LR ESI-MS** (positive ion): 559.2 ( $[\text{M}-\text{Cl}]^+$ , calcd 559.2)  $m/z$ . Data consistent with previous reports.<sup>250</sup>

#### 6.2.1.2 [ $\{\text{Ir}(2,2'\text{-biphenyl})(\text{cod})\text{Cl}\}_2$ ]

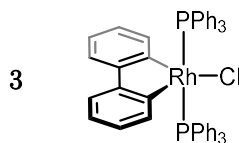


A solution of  $[\{\text{Ir}(\text{cod})\text{Cl}\}_2]$  (200 mg, 0.298 mmol) and biphenylene (90.6 mg, 0.596 mmol) in  $\text{CH}_2\text{Cl}_2$  (5 mL) was stirred at 90 °C for 2 h. The solid material precipitated from the reaction was collected by filtration, washed with  $\text{CH}_2\text{Cl}_2$  ( $3 \times ca.$  5 mL), and dried *in vacuo*. Yield: 166 mg (57%, yellow microcrystalline solid).

A saturated  $\text{CD}_2\text{Cl}_2$  solution (*ca.* 0.1 mM) of the title compound is observed by  $^1\text{H}$  NMR spectroscopy as a 2:3 mixture of  $C_1$  and  $C_s$  symmetric biphenyl and diene resonances, formulated as the dimer and solvent cleaved monomer, respectively. Normalised integrals:  **$^1\text{H}$  NMR** (400 MHz,  $\text{CD}_2\text{Cl}_2$ ):  $\delta$  8.12 (d,  $^3J_{\text{HH}} = 7.4$ , 1H,  $C_1$  biph), 7.70 (d,  $^3J_{\text{HH}} = 7.0$ , 2H,  $C_s$  biph), 7.56 – 7.49 (m, 3H,  $C_1$  biph &  $C_s$  biph), 7.46 (d,  $^3J_{\text{HH}} = 7.0$ , 1H,  $C_1$  biph), 7.38 (d,  $^3J_{\text{HH}} = 7.7$ , 1H,  $C_1$  biph), 7.15 – 7.10 (m, 3H,  $C_1$  biph &  $C_s$  biph), 7.03 – 6.86 (m, 4H,  $C_1$  biph &  $C_s$  biph), 6.72 (t,  $^3J_{\text{HH}} = 7.2$ , 1H,  $C_1$  biph), 5.81 (q,  $^3J_{\text{HH}} = 7.9$ , 2H,  $C_s$  cod), 5.51 – 5.43 (m, 2H,  $C_1$  cod), 5.42 – 5.31 (m, 2H,  $C_1$  cod), 4.00 – 3.93 (m, 2H,  $C_1$  cod), 3.57 – 3.51 (m, 2H,  $C_s$  cod), 3.37 – 3.21 (m, 2H,  $C_s$  cod). Insufficient data is available for a full assignment. **Anal.** Calcd for  $\text{C}_{40}\text{H}_{40}\text{Cl}_2\text{Ir}$  (488.05  $\text{g}\cdot\text{mol}^{-1}$ ): C, 49.22; H, 4.13; N, 0.00. Found: C, 49.10; H, 4.26; N, 0.00.

## 6.2.2 Preparation of [M(2,2'-biphenyl)(PPh<sub>3</sub>)<sub>2</sub>Cl]

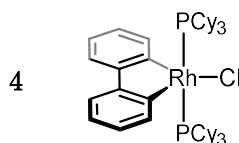
### 6.2.2.1 [Rh(2,2'-biphen)(PPh<sub>3</sub>)<sub>2</sub>Cl]



A solution of **1** (297.5 mg, 500.0  $\mu\text{mol}$ ) and PPh<sub>3</sub> (263.6 mg, 1050  $\mu\text{mol}$ ) in CH<sub>2</sub>Cl<sub>2</sub> (5 mL) was stirred at ambient temperature for 3 h. The product was precipitated by addition of excess Et<sub>2</sub>O (*ca.* 20 mL) and isolated by filtration. Yield: 360.0 mg (88%, microcrystalline yellow solid).

**<sup>1</sup>H NMR** (500 MHz, CD<sub>2</sub>Cl<sub>2</sub>):  $\delta$  7.42 (d,  $^3J_{\text{HH}} = 7.8$ , 2H, 6-biph), 7.32 (t,  $^3J_{\text{HH}} = 7.4$ , 6H, *p*-Ph), 7.27 (vbr, fwhm = 30 Hz, 12H, *o*-Ph), 7.17 (app. t,  $^3J_{\text{HH}} = 7.6$ , 12H, *m*-Ph), 6.57 (t,  $^3J_{\text{HH}} = 7.3$ , 2H, 4-biph), 6.45 (td,  $^3J_{\text{HH}} = 7.5$ ,  $^4J_{\text{HH}} = 1.6$ , 2H, 5-biph), 6.34 (dd,  $^3J_{\text{HH}} = 7.5$ ,  $^4J_{\text{HH}} = 1.6$ , 2H, 3-biph). **<sup>1</sup>H NMR** (400 MHz, THF):  $\delta$  7.75 (d,  $^3J_{\text{HH}} = 7.7$ , 2H, 6-biph), 7.66 (vbr, fwhm = 20 Hz, 12H, *o*-Ph), 7.57 (t,  $^3J_{\text{HH}} = 7.2$ , 6H, *p*-Ph), 7.43 (app. t,  $^3J_{\text{HH}} = 7.2$ , 12H, *m*-Ph), 6.81 (t,  $^3J_{\text{HH}} = 7.1$ , 2H, 4-biph), 6.70 (t,  $^3J_{\text{HH}} = 7.0$ , 2H, 5-biph), 6.60 (d,  $^3J_{\text{HH}} = 7.2$ , 2H, 3-biph). **<sup>13</sup>C{<sup>1</sup>H} NMR** (126 MHz, CD<sub>2</sub>Cl<sub>2</sub>):  $\delta$  163.7 (dt,  $^1J_{\text{RhC}} = 33$ ,  $^2J_{\text{PC}} = 10$ , 2-biph), 153.9 (s, 1-biph), 135.0 (t,  $J_{\text{PC}} = 5$ , *o*-Ph), 133.1 (s, 6-biph), 130.7 (t,  $J_{\text{PC}} = 23$ , *i*-Ph), 130.4 (s, *p*-Ph), 128.2 (t,  $J_{\text{PC}} = 5$ , *m*-Ph), 123.8 (s, 5-biph), 122.9 (s, 4-biph), 122.1 (s, 3-biph). **<sup>31</sup>P{<sup>1</sup>H} NMR** (162 MHz, CD<sub>2</sub>Cl<sub>2</sub>):  $\delta$  29.3 (d,  $^1J_{\text{RhP}} = 119$ ). **<sup>31</sup>P{<sup>1</sup>H} NMR** (162 MHz, THF):  $\delta$  29.3 (d,  $^1J_{\text{RhP}} = 119$ ). **LR ESI-MS** (positive ion): 779.1 ([M-Cl]<sup>+</sup>, calcd 779.1) *m/z*. Data consistent with previous reports.<sup>250</sup>

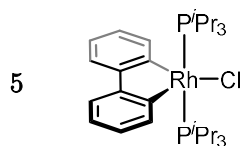
### 6.2.2.2 [Rh(2,2'-biphenyl)(PCy<sub>3</sub>)<sub>2</sub>Cl]



A solution of **1** (50.0 mg, 84.0  $\mu\text{mol}$ ) and PCy<sub>3</sub> (47.4 mg, 169  $\mu\text{mol}$ ) in CH<sub>2</sub>Cl<sub>2</sub> (5 mL) was stirred at ambient temperature for 16 h. The resulting precipitate was filtered and washed with cold (0 °C) CH<sub>2</sub>Cl<sub>2</sub> (3  $\times$  5 mL). Yield: 59.3 mg (83%, yellow solid).

**<sup>1</sup>H NMR** (500 MHz, CD<sub>2</sub>Cl<sub>2</sub>): δ 7.70 (d, <sup>3</sup>J<sub>HH</sub> = 8.0, 2H, 6-biph), 7.32 (dd, <sup>3</sup>J<sub>HH</sub> = 7.6, <sup>4</sup>J<sub>HH</sub> = 1.6, 2H, 3-biph), 6.92 (t, <sup>3</sup>J<sub>HH</sub> = 7.3, 2H, 4-biph), 6.76 (dt, <sup>3</sup>J<sub>HH</sub> = 7.5, <sup>4</sup>J<sub>HH</sub> = 1.6, 2H, 5-biph), 2.03 (app. t, *J* = 12, 6H, Cy), 1.53 – 1.66 (m, 30H, Cy), 1.26 (app. q, *J* = 12, 14H, Cy), 0.99 – 1.18 (m, 16H, Cy). **<sup>1</sup>H NMR** (400 MHz, THF): δ 8.09 (d, <sup>3</sup>J<sub>HH</sub> = 7.9, 2H, 6-biph), 7.66 (d, <sup>3</sup>J<sub>HH</sub> = 7.9, 2H, 3-biph), 7.23 (t, <sup>3</sup>J<sub>HH</sub> = 7.8, 2H, 4-biph), 7.07 (t, <sup>3</sup>J<sub>HH</sub> = 7.7, 2H, 5-biph). **<sup>13</sup>C{<sup>1</sup>H} NMR** (126 MHz, CD<sub>2</sub>Cl<sub>2</sub>): δ 162.4 (dt, <sup>1</sup>J<sub>RhC</sub> = 37, <sup>2</sup>J<sub>PC</sub> = 9, 1-biph), 153.2 (s, 2-biph), 137.2 (s, 6-biph), 124.6 (s, 5-biph), 122.6 (s, 4-biph), 120.2 (s, 3-biph), 35.3 (t, *J*<sub>PC</sub> = 9, Cy), 30.6 (s, Cy), 28.4 (t, *J*<sub>PC</sub> = 5, Cy), 26.9 (s, Cy). **<sup>31</sup>P{<sup>1</sup>H} NMR** (162 MHz, CD<sub>2</sub>Cl<sub>2</sub>): δ 13.8 (d, <sup>1</sup>J<sub>RhP</sub> = 108). **<sup>31</sup>P{<sup>1</sup>H} NMR** (162 MHz, THF): δ 13.7 (d, <sup>1</sup>J<sub>RhP</sub> = 109). **HR ESI-MS** (positive ion): 815.4309 ([M-Cl]<sup>+</sup>, calcd 815.4315) *m/z*. Cy <sup>1</sup>H signals in THF are obscured by proteo-solvent.

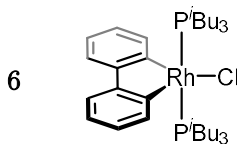
### 6.2.2.3 [Rh(2,2'-biphenyl)(P<sup>*i*</sup>Pr<sub>3</sub>)<sub>2</sub>Cl]



To solution of **1** (17.8 mg, 30.0 μmol) in CH<sub>2</sub>Cl<sub>2</sub> (5 mL) was added P<sup>*i*</sup>Pr<sub>3</sub> (0.84 M in pentane, 71.8 μL, 60.3 μmol) and the resulting solution stirred at ambient temperature for 3 h. The volatiles were removed *in vacuo* and the residue extracted with CH<sub>2</sub>Cl<sub>2</sub> (5 mL) through a short plug of neutral Al<sub>2</sub>O<sub>3</sub>. The solvent was then removed *in vacuo*. Yield: 6.8 mg (37%, yellow solid).

**<sup>1</sup>H NMR** (500 MHz, CD<sub>2</sub>Cl<sub>2</sub>): δ 7.77 (d, <sup>3</sup>J<sub>HH</sub> = 7.9, 2H, 6-biph), 7.30 (dd, <sup>3</sup>J<sub>HH</sub> = 7.5, <sup>4</sup>J<sub>HH</sub> = 1.6, 2H, 3-biph), 6.94 (t, <sup>3</sup>J<sub>HH</sub> = 7.3, 2H, 4-biph), 6.76 (td, <sup>3</sup>J<sub>HH</sub> = 7.6, <sup>4</sup>J<sub>HH</sub> = 1.6, 2H, 5-biph), 2.36 – 2.44 (m, 6H, CH), 0.98 (app. q, *J* = 7, 36H, CH<sub>3</sub>). **<sup>13</sup>C{<sup>1</sup>H} NMR** (126 MHz, CD<sub>2</sub>Cl<sub>2</sub>): δ 160.7 (dt, <sup>1</sup>J<sub>RhC</sub> = 35, <sup>2</sup>J<sub>PC</sub> = 9, 1-biph), 154.4 (s, 2-biph), 136.8 (s, 6-biph), 124.7 (s, 5-biph), 123.1 (s, 4-biph), 120.3 (s, 3-biph), 24.1 (t, *J*<sub>PC</sub> = 10, CH), 20.3 (s, CH<sub>3</sub>). **<sup>31</sup>P{<sup>1</sup>H} NMR** (121 MHz, CD<sub>2</sub>Cl<sub>2</sub>): δ 23.0 (d, <sup>1</sup>J<sub>RhP</sub> = 109). **HR ESI-MS** (positive ion): 575.2436 ([M-Cl]<sup>+</sup>, calcd 575.2437) *m/z*. **Anal.** Calcd for C<sub>30</sub>H<sub>50</sub>ClP<sub>2</sub>Rh (611.03 g·mol<sup>-1</sup>): C, 58.97; H, 8.25; N, 0.00. Found: C, 58.82; H, 8.09; N, 0.00.

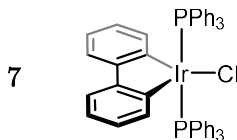
#### 6.2.2.4 [Rh(2,2'-biphenyl)(P<sup>t</sup>Bu<sub>3</sub>)<sub>2</sub>Cl]



To a solution of **1** (17.8 mg, 30.0  $\mu$ mol) in CH<sub>2</sub>Cl<sub>2</sub> (5 mL) was added P<sup>t</sup>Bu<sub>3</sub> (15.1  $\mu$ L, 60.3  $\mu$ mol) and the resulting solution stirred at ambient temperature for 3 h. The volatiles were removed *in vacuo* and the resulting residue extracted with CH<sub>2</sub>Cl<sub>2</sub> (5 mL) and passed through a short plug of neutral Al<sub>2</sub>O<sub>3</sub>. The solvent was then removed *in vacuo*. Yield: 11.6 mg (56%, yellow solid).

**<sup>1</sup>H NMR** (500 MHz, CD<sub>2</sub>Cl<sub>2</sub>):  $\delta$  7.53 (d, <sup>3</sup>*J*<sub>HH</sub> = 7.8, 2H, 6-biph), 7.34 (dd, <sup>3</sup>*J*<sub>HH</sub> = 7.5, <sup>4</sup>*J*<sub>HH</sub> = 1.6, 2H, 3-biph), 6.96 (t, <sup>3</sup>*J*<sub>HH</sub> = 7.3, 2H, 4-biph), 6.79 (td, <sup>3</sup>*J*<sub>HH</sub> = 7.5, <sup>4</sup>*J*<sub>HH</sub> = 1.6, 2H, 5-biph), 1.75 – 1.87 (m, 6H, CH), 1.43 (app. dt, *J* = 6, *J* = 3, 12H, CH<sub>2</sub>), 0.78 (d, <sup>3</sup>*J*<sub>HH</sub> = 6.7, 36H, CH<sub>3</sub>). **<sup>13</sup>C{<sup>1</sup>H} NMR** (126 MHz, CD<sub>2</sub>Cl<sub>2</sub>):  $\delta$  163.3 (dt, <sup>1</sup>*J*<sub>RhC</sub> = 36, <sup>2</sup>*J*<sub>PC</sub> = 10, 1-biph), 152.6 (s, 2-biph), 134.5 (s, 6-biph), 125.4 (s, 5-biph), 122.9 (s, 4-biph), 120.7 (s, 3-biph), 32.6 (t, *J*<sub>PC</sub> = 11, CH<sub>2</sub>), 26.1 (t, *J*<sub>PC</sub> = 3, CH), 25.1 (s, CH<sub>3</sub>). **<sup>31</sup>P{<sup>1</sup>H} NMR** (162 MHz, CD<sub>2</sub>Cl<sub>2</sub>):  $\delta$  12.9 (d, <sup>1</sup>*J*<sub>RhP</sub> = 109).<sup>†</sup> **HR ESI-MS** (positive ion): 659.3378 ([M-Cl]<sup>+</sup>, calc. 659.3376) *m/z*. **Anal.** Calcd for C<sub>36</sub>H<sub>62</sub>ClP<sub>2</sub>Rh (695.20 g·mol<sup>-1</sup>): C, 62.20; H, 8.99; N, 0.00. Found: C, 61.89; H, 8.84; N, 0.00.

#### 6.2.2.5 [Ir(2,2'-biphenyl)(PPh<sub>3</sub>)<sub>2</sub>Cl]

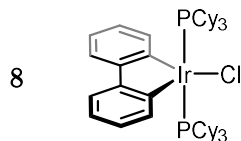


A solution of **2** (50.0 mg, 51.2  $\mu$ mol) and PPh<sub>3</sub> (54.0 mg, 206  $\mu$ mol) in CH<sub>2</sub>Cl<sub>2</sub> (5 mL) was stirred at ambient temperature for 18 h. The product was precipitated by addition of excess Et<sub>2</sub>O (*ca.* 20 mL) and isolated by filtration. Yield: 64.1 mg (83%, yellow solid).

**<sup>1</sup>H NMR** (500 MHz, CD<sub>2</sub>Cl<sub>2</sub>):  $\delta$  7.34 (d, <sup>3</sup>*J*<sub>HH</sub> = 8, 2H, 6-biph), 7.32 (t, <sup>3</sup>*J*<sub>HH</sub> = 7.5, 6H, *p*-Ph), 7.25 (br, fwhm = 40 Hz, 12H, *o*-Ph), 7.18 (app. t, <sup>3</sup>*J*<sub>HH</sub> = 7.5, 12H, *m*-Ph), 6.47 (t, <sup>3</sup>*J*<sub>HH</sub> = 7.3, 2H, 4-biph), 6.28 (td, <sup>3</sup>*J*<sub>HH</sub> = 7.6, <sup>4</sup>*J*<sub>HH</sub> = 1.6, 2H, 5-biph), 6.26 (dd,

$^3J_{\text{HH}} = 7.5$ ,  $^4J_{\text{HH}} = 1.6$ , 2H, 3-biph).  **$^1\text{H}$  NMR** (400 MHz, THF):  $\delta$  7.67 (d,  $^3J_{\text{HH}} = 7.8$ , 2H, 6-biph), 7.62 (vbr, fwhm = 30 Hz, 12H, *o*-Ph), 7.57 (t,  $^3J_{\text{HH}} = 7.4$ , 6H, *p*-Ph), 7.43 (t,  $^3J_{\text{HH}} = 6.9$ , 12H, *m*-Ph), 6.70 (t,  $^3J_{\text{HH}} = 7.2$ , 2H, 4-biph), 6.52 (t,  $^3J_{\text{HH}} = 7.6$ , 2H, 5-biph), 6.50 (d,  $^3J_{\text{HH}} = 7.2$ , 2H, 3-biph).  **$^{13}\text{C}\{^1\text{H}\}$  NMR** (126 MHz,  $\text{CD}_2\text{Cl}_2$ ):  $\delta$  155.6 (s, 2-biph), 138.4 (t,  $^2J_{\text{PC}} = 7$ , 1-biph), 135.1 (t,  $J_{\text{PC}} = 5$ , *o*-Ph), 132.8 (t,  $^3J_{\text{PC}} = 2$ , 6-biph), 130.4 (s, *p*-Ph), 130.1 (t,  $J_{\text{PC}} = 27$ , *i*-Ph), 128.2 (t,  $J_{\text{PC}} = 5$ , *m*-Ph), 123.8 (s, 5-biph), 122.3 (s, 4-biph), 121.4 (s, 3-biph).  **$^{31}\text{P}\{^1\text{H}\}$  NMR** (162 MHz,  $\text{CD}_2\text{Cl}_2$ ):  $\delta$  21.7 (s).<sup>†</sup>  **$^{31}\text{P}\{^1\text{H}\}$  NMR** (162 MHz, THF):  $\delta$  22.3 (s).<sup>†</sup> **LR ESI-MS** (positive ion): 869.2 ( $[\text{M}-\text{Cl}]^+$ , calcd 869.2) *m/z*. Data consistent with previous reports.<sup>252</sup>

#### 6.2.2.6 $[\text{Ir}(\text{2,2'}$ -biphenyl) $(\text{PCy}_3)_2\text{Cl}]$

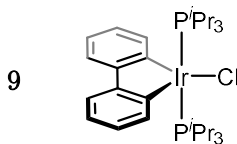


A solution of **2** (60.0 mg, 61.5  $\mu\text{mol}$ ) and  $\text{PCy}_3$  (69.3 mg, 247  $\mu\text{mol}$ ) in  $\text{CH}_2\text{Cl}_2$  (5 mL) was stirred at ambient temperature for 16 h. The resulting precipitate was filtered and washed with  $\text{CH}_2\text{Cl}_2$  ( $3 \times 5$  mL). Yield: 93.0 mg (80%, orange solid).

**$^1\text{H}$  NMR** (500 MHz,  $\text{CD}_2\text{Cl}_2$ ):  $\delta$  7.53 (d,  $^3J_{\text{HH}} = 7.8$ , 2H, 6-biph), 7.25 (dd,  $^3J_{\text{HH}} = 7.6$ ,  $^4J_{\text{HH}} = 1.5$ , 2H, 3-biph), 6.83 (t,  $^3J_{\text{HH}} = 7.3$ , 2H, 4-biph), 6.64 (td,  $^3J_{\text{HH}} = 7.3$ ,  $^4J_{\text{HH}} = 1.5$ , 2H, 5-biph), 2.15 (app. t,  $J = 12$ , 6H, Cy), 1.56 – 1.69 (m, 18H, Cy), 1.56 – 1.42 (m, 12H, Cy), 1.27 (app. q,  $J = 12$ , 12H, Cy), 1.18 – 0.97 (m, 18H, Cy).  **$^1\text{H}$  NMR** (400 MHz, THF):  $\delta$  7.90 (d,  $^3J_{\text{HH}} = 7.6$ , 2H, 6-biph), 7.57 (d,  $^3J_{\text{HH}} = 7.7$ , 2H, 3-biph), 7.11 (d,  $^3J_{\text{HH}} = 7.6$ , 2H, 4-biph), 6.93 (d,  $^3J_{\text{HH}} = 7.7$ , 2H, 5-biph).  **$^{13}\text{C}\{^1\text{H}\}$  NMR** (126 MHz,  $\text{CD}_2\text{Cl}_2$ ):  $\delta$  154.4 (s, 2-biph), 137.2 (t,  $^2J_{\text{PC}} = 7$ , 1-biph), 135.9 (s, 6-biph), 124.8 (s, 5-biph), 121.9 (s, 4-biph), 119.8 (s, 3-biph), 35.0 (t,  $J_{\text{PC}} = 12$ , Cy), 30.6 (s, Cy), 28.4 (t,  $J_{\text{PC}} = 5$ , Cy), 26.9 (s, Cy).  **$^{31}\text{P}\{^1\text{H}\}$  NMR** (162 MHz,  $\text{CD}_2\text{Cl}_2$ ):  $\delta$  -5.4 (s).<sup>†</sup>  **$^{31}\text{P}\{^1\text{H}\}$  NMR** (162 MHz, THF):  $\delta$  -4.0 (s).<sup>†</sup> **HR ESI-MS** (positive ion): 905.4904 ( $[\text{M}-\text{Cl}]^+$ , calcd 905.4893) *m/z*. **Anal.** Calcd for  $\text{C}_{48}\text{H}_{74}\text{ClIrP}_2$  (940.73  $\text{g}\cdot\text{mol}^{-1}$ ): C, 61.28; H, 7.93; N, 0.00. Found: C, 61.17; H, 8.01; N, 0.00. Cy  $^1\text{H}$  signals in THF are obscured by proteo-solvent.



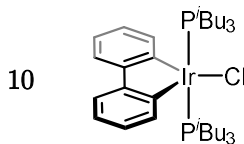
#### 6.2.2.7 [Ir(2,2'-biphenyl)(P<sup>*i*</sup>Pr<sub>3</sub>)<sub>2</sub>Cl]



To a solution of **2** (60.0 mg, 61.5  $\mu$ mol) in CH<sub>2</sub>Cl<sub>2</sub> (5 mL) was added P<sup>*i*</sup>Pr<sub>3</sub> (0.84 M in pentane, 293  $\mu$ L, 247  $\mu$ mol) and the resulting solution stirred at ambient temperature for 16 h. The solution was concentrated to *ca.* 2 mL, diluted with pentane (5 mL), and filtered. The volatiles were removed *in vacuo* and the resulting residue washed with pentane (2 mL) at -78 °C. Yield: 59.0 mg (69%, orange solid).

**<sup>1</sup>H NMR** (500 MHz, CD<sub>2</sub>Cl<sub>2</sub>):  $\delta$  7.62 (dd, <sup>3</sup>*J*<sub>HH</sub> = 7.9, 2H, 6-biph), 7.23 (dd, <sup>3</sup>*J*<sub>HH</sub> = 7.5, <sup>4</sup>*J*<sub>HH</sub> = 1.6, 2H, 3-biph), 6.84 (t, <sup>3</sup>*J*<sub>HH</sub> = 7.3, 2H, 4-biph), 6.61 (td, <sup>3</sup>*J*<sub>HH</sub> = 7.5, <sup>4</sup>*J*<sub>HH</sub> = 1.6, 5-biph), 2.48 – 2.56 (m, 6H, CH), 0.98 (app. q, <sup>3</sup>*J*<sub>HH</sub> = 7, 36H, CH<sub>3</sub>). **<sup>13</sup>C{<sup>1</sup>H} NMR** (126 MHz, CD<sub>2</sub>Cl<sub>2</sub>):  $\delta$  155.8 (s, 2-biph), 135.8 (t, <sup>2</sup>*J*<sub>PC</sub> = 7, 1-biph), 135.7 (s, 6-biph), 124.7 (s, 5-biph), 122.5 (s, 4-biph), 120.0 (s, 3-biph), 23.7 (t, *J*<sub>PC</sub> = 13, CH), 20.3 (s, CH<sub>3</sub>). **<sup>31</sup>P{<sup>1</sup>H} NMR** (121 MHz, CD<sub>2</sub>Cl<sub>2</sub>):  $\delta$  5.8 (s).<sup>†</sup> **HR ESI-MS** (positive ion): 665.3012 ([M-Cl]<sup>+</sup>, calcd 665.3013) *m/z*. **Anal.** Calcd for C<sub>30</sub>H<sub>50</sub>ClIrP<sub>2</sub> (700.34 g·mol<sup>-1</sup>): C, 51.45; H, 7.20; N, 0.00. Found: C, 51.45; H, 7.39; N, 0.00.

#### 6.2.2.8 [Ir(2,2'-biphenyl)(P<sup>*t*</sup>Bu<sub>3</sub>)<sub>2</sub>Cl]



To a solution of **2** (60.0 mg, 61.5  $\mu$ mol) in CH<sub>2</sub>Cl<sub>2</sub> (5 mL) was added P<sup>*t*</sup>Bu<sub>3</sub> (61.6  $\mu$ L, 247  $\mu$ mol) and the resulting solution stirred at ambient temperature for 16 h. The solution was concentrated to *ca.* 2 mL, diluted with pentane (5 mL), and filtered. The filtrate was dried *in vacuo*. Yield = 78.0 mg (81%, orange solid).

**<sup>1</sup>H NMR** (500 MHz, CD<sub>2</sub>Cl<sub>2</sub>):  $\delta$  7.43 (d, <sup>3</sup>*J*<sub>HH</sub> = 7.7, 2H, 6-biph), 7.27 (dd, <sup>3</sup>*J*<sub>HH</sub> = 7.5, <sup>4</sup>*J*<sub>HH</sub> = 1.5, 2H, 3-biph), 6.88 (t, <sup>3</sup>*J*<sub>HH</sub> = 7.3, 2H, 4-biph), 6.66 (td, <sup>3</sup>*J*<sub>HH</sub> = 7.6, <sup>4</sup>*J*<sub>HH</sub> = 1.5, 2H, 5-biph), 1.75 – 1.85 (m, 6H, CH), 1.52 (app. dt, *J* = 6, *J* = 3, 12H, CH<sub>2</sub>), 0.76 (d,

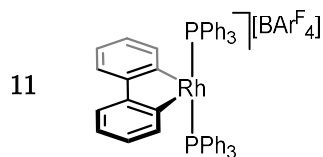
$^3J_{\text{HH}} = 6.7$ , 36H, CH<sub>3</sub>).  **$^{13}\text{C}\{^1\text{H}\}$  NMR** (126 MHz, CD<sub>2</sub>Cl<sub>2</sub>):  $\delta$  154.1 (s, 2-biph), 138.2 (t,  $^2J_{\text{PC}} = 7$ , 1-biph), 134.1 (s, 6-biph), 125.5 (s, 5-biph), 122.3 (s, 4-biph), 120.2 (s, 3-biph), 32.1 (t,  $J_{\text{PC}} = 14$ , CH<sub>2</sub>), 26.1 (t,  $J_{\text{PC}} = 4$ , CH), 25.0 (s, CH<sub>3</sub>).  **$^{31}\text{P}\{^1\text{H}\}$  NMR** (202 MHz, CD<sub>2</sub>Cl<sub>2</sub>):  $\delta$  0.6 (s).<sup>†</sup> **HR ESI-MS** (positive ion): 749.3954 ([M – Cl]<sup>+</sup>, calcd 749.3952) *m/z*. **Anal.** Calcd for C<sub>36</sub>H<sub>62</sub>ClIrP<sub>2</sub> (784.51 g·mol<sup>-1</sup>): C, 55.12; H, 7.97; N, 0.00. Found: C, 55.26; H, 8.05; N, 0.00.

## 6.2.3 Preparation of [M(2,2'-biphenyl)(PPh<sub>3</sub>)<sub>2</sub>][anion]

### 6.2.3.1 General procedure

Suspensions of chlorides **3** – **10** (1.0 equiv.) and Na[BAr<sup>F</sup><sub>4</sub>] or Li[Al(OR<sup>F</sup>)<sub>4</sub>] (1.1 equiv.) in CH<sub>2</sub>Cl<sub>2</sub> (*ca.* 10 mM) were stirred at ambient temperature for 18 h, diluted with minimal pentane and filtered. Slow diffusion of excess pentane precipitated the title compounds as crystalline materials, which were isolated by filtration and dried *in vacuo*.

### 6.2.3.2 [Rh(2,2'-biphenyl)(PPh<sub>3</sub>)<sub>2</sub>][BAr<sup>F</sup><sub>4</sub>]

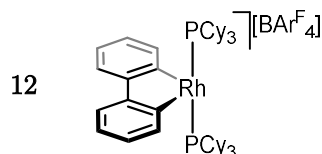


Prepared from **3** (20.0 mg, 24.5  $\mu\text{mol}$ ) and Na[BAr<sup>F</sup><sub>4</sub>] (23.9 mg, 27.0  $\mu\text{mol}$ ) using *dry* solvents. Yield: 33.9 mg (80%, orange crystals).

**$^1\text{H}$  NMR** (500 MHz, CD<sub>2</sub>Cl<sub>2</sub>):  $\delta$  7.71 – 7.76 (m, 8H, *o*-Ar<sup>F</sup>), 7.56 (br, 4H, *p*-Ar<sup>F</sup>), 7.50 (t,  $^3J_{\text{HH}} = 7.5$ , 6H, *p*-Ph), 7.32 (t,  $^3J_{\text{HH}} = 7.7$ , 12H, *m*-Ph), 6.99 – 7.05 (m, 14H, *o*-Ph & 6-biph), 6.87 (t,  $^3J_{\text{HH}} = 7.3$ , 2H, 4-biph), 6.76 (td,  $^3J_{\text{HH}} = 7.7$ ,  $^3J_{\text{HH}} = 1.6$ , 2H, 5-biph), 6.65 (dd,  $^3J_{\text{HH}} = 7.5$ ,  $^3J_{\text{RhH}} = 1.6$ , 2H, 3-biph).  **$^{13}\text{C}\{^1\text{H}\}$  NMR** (126 MHz, CD<sub>2</sub>Cl<sub>2</sub>):  $\delta$  162.3 (q,  $^1J_{\text{CB}} = 50$ , *i*-Ar<sup>F</sup>), 154.8 (dt,  $^1J_{\text{RhC}} = 39$ ,  $^2J_{\text{PC}} = 10$ , 1-biph), 150.0 (s, 2-biph), 135.4 (s, *o*-Ar<sup>F</sup>), 134.0 (t,  $J_{\text{PC}} = 6$ , *o*-Ph), 132.4 (s, *p*-Ph), 131.7 (s, 6-biph), 129.7 (t,  $J_{\text{PC}} = 5$ , *m*-Ph), 129.4 (qq,  $^2J_{\text{FC}} = 32$ ,  $^3J_{\text{BC}} = 3$ , *m*-Ar<sup>F</sup>), 126.9 (t,  $J_{\text{PC}} = 24$ , *i*-Ph), 126.5 (s, 5-biph), 125.3 (s, 4-biph), 125.2 (q,  $^1J_{\text{FC}} = 272$ , CF<sub>3</sub>), 123.6 (s, 3-biph), 118.0 (sept,

$^3J_{\text{FC}} = 4$ ,  $p\text{-Ar}^{\text{F}}$ ).  **$^{31}\text{P}\{\text{H}\}$  NMR** (202 MHz,  $\text{CD}_2\text{Cl}_2$ ):  $\delta$  19.7 (d,  $^1J_{\text{RhP}} = 118$ ).<sup>†</sup> **HR ESI-MS** (positive ion): 779.1507 ( $[\text{M}]^+$ , calcd 779.1498)  $m/z$ . **Anal.** Calcd for  $\text{C}_8\text{H}_{50}\text{BF}_{24}\text{P}_2\text{Rh}\cdot\text{CH}_2\text{Cl}_2$  (1727.83  $\text{g}\cdot\text{mol}^{-1}$ ): C, 56.31; H, 3.03; N, 0.00. Found: C, 56.42; H, 3.03; N, 0.00.

### 6.2.3.3 $[\text{Rh}(2,2'\text{-biphenyl})(\text{PCy}_3)_2][\text{BAR}^{\text{F}}_4]$



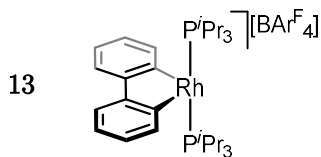
Prepared from **4** (30.0 mg, 35.2  $\mu\text{mol}$ ) and  $\text{Na}[\text{BAR}^{\text{F}}_4]$  (34.3 mg, 38.8  $\mu\text{mol}$ ). Yield: 42.4 mg (71%, yellow crystals).

**$^1\text{H}$  NMR** (500 MHz,  $\text{CD}_2\text{Cl}_2$ ):  $\delta$  7.71 – 7.75 (m, 8H,  $o\text{-Ar}^{\text{F}}$ ), 7.56 (br, 4H,  $p\text{-Ar}^{\text{F}}$ ), 7.48 (dd,  $^3J_{\text{HH}} = 7.5$ ,  $^4J_{\text{HH}} = 1.6$ , 2H, 3-biph), 7.16 (t,  $^3J_{\text{HH}} = 7.3$ , 2H, 4-biph), 7.11 (d,  $^3J_{\text{HH}} = 8.1$ , 2H, 6-biph), 7.01 (td,  $^3J_{\text{HH}} = 7.7$ ,  $^4J_{\text{HH}} = 1.6$ , 2H, 5-biph), 1.95 – 2.05 (m, 6H, Cy), 1.67 – 1.77 (m, 18H, Cy), 1.24 – 1.38 (m, 24H, Cy), 1.13 – 1.24 (m, 18H, Cy).

**$^1\text{H}$  NMR** (400 MHz, THF):  $\delta$  8.13 – 8.07 (m, 8H,  $o\text{-Ar}^{\text{F}}$ ), 7.90 (obsc., 2H, 3-biph), 7.88 (br, 4H,  $p\text{-Ar}^{\text{F}}$ ), 7.58 (d,  $^3J_{\text{HH}} = 8.0$ , 2H, 3-biph), 7.49 (t,  $^3J_{\text{HH}} = 7.3$ , 2H, 4-biph), 7.33 (t,  $^3J_{\text{HH}} = 7.5$ , 2H, 6-biph).  **$^{13}\text{C}\{\text{H}\}$  NMR** (126 MHz,  $\text{CD}_2\text{Cl}_2$ ):  $\delta$  162.3 (q,  $^1J_{\text{CB}} = 50$ ,  $i\text{-Ar}^{\text{F}}$ ), 153.8 (dt,  $^1J_{\text{RhC}} = 44$ ,  $^2J_{\text{PC}} = 8$ , 1-biph), 148.8 (d,  $^2J_{\text{RhC}} = 4$ , 2-biph), 135.4 (s,  $o\text{-Ar}^{\text{F}}$ ), 129.8 (s, 6-biph), 129.4 (qq,  $^2J_{\text{FC}} = 32$ ,  $^3J_{\text{CB}} = 3$ ,  $m\text{-Ar}^{\text{F}}$ ), 128.0 (s, 5-biph), 125.5 (s, 4-biph), 125.2 (q,  $^1J_{\text{FC}} = 272$ ,  $\text{CF}_3$ ), 122.1 (d,  $^2J_{\text{RhC}} = 2$ , 3-biph), 118.0 (sept,  $^3J_{\text{FC}} = 4$ ,  $p\text{-Ar}^{\text{F}}$ ), 35.1 (t,  $J_{\text{PC}} = 10$ , Cy), 30.4 (s, Cy), 27.9 (t,  $J_{\text{PC}} = 5$ , Cy), 26.3 (s, Cy).

**$^{31}\text{P}\{\text{H}\}$  NMR** (202 MHz,  $\text{CD}_2\text{Cl}_2$ ):  $\delta$  13.4 (d,  $^1J_{\text{RhP}} = 109$ ).<sup>†</sup>  **$^{31}\text{P}\{\text{H}\}$  NMR** (162 MHz, THF):  $\delta$  13.0 (d,  $^1J_{\text{RhP}} = 109$ ).<sup>†</sup> **HR ESI-MS** (positive ion): 815.4325 ( $[\text{M}]^+$ , calcd 815.4315)  $m/z$ . **Anal.** Calcd for  $\text{C}_{80}\text{H}_{86}\text{BF}_{24}\text{P}_2\text{Rh}$  (1679.19  $\text{g}\cdot\text{mol}^{-1}$ ): C, 57.22; H, 5.16; N, 0.00. Found: C, 57.38; H, 5.26; N, 0.00. Cy  $^1\text{H}$  signals in THF are obscured by proteo-solvent.

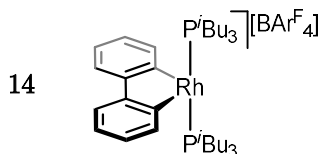
#### 6.2.3.4 [Rh(2,2'-biphenyl)(P<sup>t</sup>Pr<sub>3</sub>)<sub>2</sub>][BAr<sup>F</sup><sub>4</sub>]



Prepared from **5** (20.0 mg, 32.7  $\mu$ mol) and Na[BAr<sup>F</sup><sub>4</sub>] (31.9 mg, 36.0  $\mu$ mol). Yield: 27.1 mg (58%, orange crystals).

**<sup>1</sup>H NMR** (500 MHz, CD<sub>2</sub>Cl<sub>2</sub>):  $\delta$  7.70 – 7.75 (m, 8H, *o*-Ar<sup>F</sup>), 7.56 (br, 4H, *p*-Ar<sup>F</sup>), 7.46 (dd, <sup>3</sup>*J*<sub>HH</sub> = 7.6, <sup>4</sup>*J*<sub>HH</sub> = 1.6, 2H, 3-biph), 7.24 (d, <sup>3</sup>*J*<sub>HH</sub> = 8.1, 2H, 6-biph), 7.15 (t, <sup>3</sup>*J*<sub>HH</sub> = 7.4, 2H, 4-biph), 6.98 (td, <sup>3</sup>*J*<sub>HH</sub> = 7.8, <sup>4</sup>*J*<sub>HH</sub> = 1.6, 2H, 5-biph), 2.24 – 2.36 (m, 6H, CH), 1.02 (app. q, *J* = 7, 36H, CH<sub>3</sub>). **<sup>13</sup>C{<sup>1</sup>H} NMR** (126 MHz, CD<sub>2</sub>Cl<sub>2</sub>):  $\delta$  162.3 (q, <sup>1</sup>*J*<sub>CB</sub> = 50, *i*-Ar<sup>F</sup>), 152.1 (dt, <sup>1</sup>*J*<sub>RhC</sub> = 44, <sup>2</sup>*J*<sub>PC</sub> = 8, 1-biph), 148.6 (d, <sup>2</sup>*J*<sub>RhC</sub> = 5, 2-biph), 135.4 (s, *o*-Ar<sup>F</sup>), 129.6 (s, 6-biph), 129.4 (qq, <sup>2</sup>*J*<sub>FC</sub> = 32, <sup>3</sup>*J*<sub>CB</sub> = 3, *m*-Ar<sup>F</sup>), 128.0 (s, 5-biph), 125.8 (s, 4-biph), 125.2 (q, <sup>1</sup>*J*<sub>FC</sub> = 272, CF<sub>3</sub>), 122.5 (s, 3-biph), 118.0 (sept, <sup>3</sup>*J*<sub>FC</sub> = 4, *p*-Ar<sup>F</sup>), 24.3 (t, *J*<sub>PC</sub> = 11, CH), 19.7 (s, CH<sub>3</sub>). **<sup>31</sup>P{<sup>1</sup>H} NMR** (202 MHz, CD<sub>2</sub>Cl<sub>2</sub>):  $\delta$  25.7 (d, <sup>1</sup>*J*<sub>RhP</sub> = 112).<sup>†</sup> **LR ESI-MS** (positive ion): 575.2 ([M]<sup>+</sup>, calcd 575.2) *m/z*. Data consistent with previous reports.<sup>254</sup>

#### 6.2.3.5 [Rh(2,2'-biphenyl)(P<sup>t</sup>Bu<sub>3</sub>)<sub>2</sub>][BAr<sup>F</sup><sub>4</sub>]

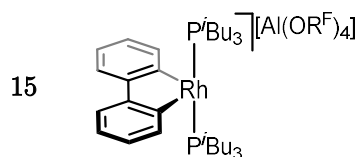


Prepared from **6** (25.1 mg, 36.1  $\mu$ mol) and Na[BAr<sup>F</sup><sub>4</sub>] (35.2 mg, 39.7  $\mu$ mol). Yield: 39.3 mg (71%, orange crystals).

**<sup>1</sup>H NMR** (500 MHz, CD<sub>2</sub>Cl<sub>2</sub>):  $\delta$  7.71 – 7.75 (m, 8H, *o*-Ar<sup>F</sup>), 7.56 (br, 4H, *p*-Ar<sup>F</sup>), 7.52 (dd, <sup>3</sup>*J*<sub>HH</sub> = 7.5, <sup>4</sup>*J*<sub>HH</sub> = 1.6, 2H, 3-biph), 7.17 (t, <sup>3</sup>*J*<sub>HH</sub> = 7.4, 2H, 4-biph), 7.08 (d, <sup>3</sup>*J*<sub>HH</sub> = 8.0, 2H, 6-biph), 6.98 (td, <sup>3</sup>*J*<sub>HH</sub> = 7.7, <sup>4</sup>*J*<sub>HH</sub> = 1.6, 2H, 5-biph), 1.57 – 1.71 (m, 6H, CH), 1.43 (app. dt, *J* = 6, *J* = 3, 12H, CH<sub>2</sub>), 0.75 (d, <sup>3</sup>*J*<sub>HH</sub> = 6.6, 36H, CH<sub>3</sub>). **<sup>13</sup>C{<sup>1</sup>H} NMR** (126 MHz, CD<sub>2</sub>Cl<sub>2</sub>):  $\delta$  162.3 (q, <sup>1</sup>*J*<sub>CB</sub> = 50, *i*-Ar<sup>F</sup>), 156.6 (dt, <sup>1</sup>*J*<sub>RhC</sub> = 43, <sup>2</sup>*J*<sub>PC</sub> = 9,

1-biph), 148.7 (d,  $^2J_{\text{RhC}} = 4$ , 2-biph), 135.4 (s,  $\sigma\text{-Ar}^{\text{F}}$ ), 130.2 (s, 6-biph), 129.4 (qq,  $^2J_{\text{FC}} = 32$ ,  $^3J_{\text{CB}} = 3$ ,  $m\text{-Ar}^{\text{F}}$ ), 128.0 (s, 5-biph), 125.6 (4-biph), 125.2 (q,  $^1J_{\text{FC}} = 272$ ,  $\text{CF}_3$ ), 123.1 (s, 3-biph), 118.0 (sept,  $^3J_{\text{FC}} = 4$ ,  $p\text{-Ar}^{\text{F}}$ ), 33.2 (t,  $J_{\text{PC}} = 12$ ,  $\text{CH}_2$ ), 25.9 (t,  $J_{\text{PC}} = 3$ , CH), 25.6 (s,  $\text{CH}_3$ ).  **$^{31}\text{P}\{^1\text{H}\}$  NMR** (202 MHz,  $\text{CD}_2\text{Cl}_2$ ):  $\delta$  18.5 (d,  $^1J_{\text{RhP}} = 110$ ).<sup>†</sup> **HR ESI-MS** (positive ion): 659.3383 ( $[\text{M}]^+$ , calcd 659.3376)  $m/z$ . **Anal.** Calcd for  $\text{C}_{68}\text{H}_{74}\text{BF}_{24}\text{P}_2\text{Rh}$  (1522.96  $\text{g}\cdot\text{mol}^{-1}$ ): C, 53.63; H, 4.90; N, 0.00. Found: C, 53.76; H, 4.81; N, 0.00.

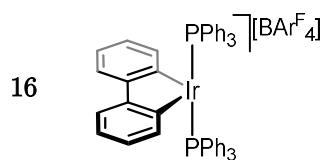
#### 6.2.3.6 $[\text{Rh}(2,2'\text{-biphenyl})(\text{P}^i\text{Bu}_3)_2][\text{Al}(\text{OR}^{\text{F}})_4]$



Prepared from **6** (5.0 mg, 7.2  $\mu\text{mol}$ ) and  $\text{Li}[\text{Al}(\text{OR}^{\text{F}})_4]$  (7.7 mg, 7.9  $\mu\text{mol}$ ). Yield: 4.4 mg (38%, orange crystals).

**$^1\text{H}$  NMR** (300 MHz,  $\text{CD}_2\text{Cl}_2$ ):  $\delta$  7.52 (d,  $^3J_{\text{HH}} = 7.6$ , 2H, 3-biph), 7.18 (t,  $^3J_{\text{HH}} = 7.6$ , 2H, 4-biph), 7.08 (d,  $^3J_{\text{HH}} = 8.1$ , 2H, 6-biph), 6.99 (t,  $^3J_{\text{HH}} = 7.6$ , 2H, 5-biph), 1.56 – 1.74 (m, 6H, CH), 1.44 (vbr, fwhm = 12 Hz, 12H,  $\text{CH}_2$ ), 0.77 (d,  $^3J_{\text{HH}} = 6.3$ , 36H,  $\text{CH}_3$ ).  **$^{31}\text{P}\{^1\text{H}\}$  NMR** (121 MHz,  $\text{CD}_2\text{Cl}_2$ ):  $\delta$  18.5 (d,  $^1J_{\text{RhP}} = 110$ ).<sup>†</sup> **LR ESI-MS** (positive ion): 659.3 ( $[\text{M}]^+$ , calcd 659.3)  $m/z$ .

#### 6.2.3.7 $[\text{Ir}(2,2'\text{-biphenyl})(\text{PPh}_3)_2][\text{BAr}^{\text{F}}_4]$

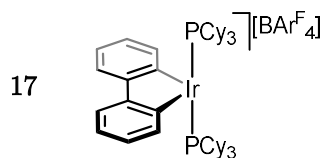


Prepared from **7** (20.0 mg, 22.1  $\mu\text{mol}$ ) and  $\text{Na}[\text{BAr}^{\text{F}}_4]$  (21.6 mg, 24.3  $\mu\text{mol}$ ) using *dry* solvents according to a modification of general procedure: the suspension was heated at 50  $^\circ\text{C}$  for 18 h. Yield: 12.7 mg (32%, burgundy crystals).

**$^1\text{H}$  NMR** (500 MHz,  $\text{CD}_2\text{Cl}_2$ ):  $\delta$  7.71 – 7.76 (m, 8H,  $\sigma\text{-Ar}^{\text{F}}$ ), 7.56 (br, 4H,  $p\text{-Ar}^{\text{F}}$ ), 7.50 (t,  $^3J_{\text{HH}} = 7.5$ , 6H,  $\sigma\text{-Ph}$ ), 7.33 (t,  $^3J_{\text{HH}} = 7.7$ , 12H,  $p\text{-Ph}$ ), 7.04 (app q,  $^3J_{\text{HH}} = 6$ , 12H,  $m\text{-Ph}$ ), 6.85 (d,  $^3J_{\text{HH}} = 7.9$ , 2H, 6-biph), 6.77 (t,  $^3J_{\text{HH}} = 7.4$ , 2H, 4-biph), 6.61 (td,

$^3J_{\text{HH}} = 7.7, ^4J_{\text{HH}} = 1.6$ , 2H, 5-biph), 6.57 (dd,  $^3J_{\text{HH}} = 7.6, ^4J_{\text{HH}} = 1.6$ , 2H, 3-biph).  **$^{13}\text{C}\{^1\text{H}\}$  NMR** (126 MHz,  $\text{CD}_2\text{Cl}_2$ ):  $\delta$  162.3 (q,  $^1J_{\text{CB}} = 50$ ,  $i\text{-Ar}^{\text{F}}$ ), 150.8 (s, 2-biph), 135.4 (s,  $o\text{-Ar}^{\text{F}}$ ), 134.1 (t,  $J_{\text{PC}} = 6$ ,  $o\text{-Ph}$ ), 132.4 (s,  $p\text{-Ph}$ ), 130.5 (s, 6-biph), 129.7 (t,  $J_{\text{PC}} = 5$ ,  $m\text{-Ph}$ ), 129.4 (qq,  $^2J_{\text{FC}} = 32, ^3J_{\text{CB}} = 3$ ,  $m\text{-Ar}^{\text{F}}$ ), 127.0 (t,  $^2J_{\text{PC}} = 7$ , 1-biph), 126.5 (t,  $J_{\text{PC}} = 28$ ,  $i\text{-Ph}$ ), 126.1 (s, 4-biph), 125.2 (s, 5-biph), 125.2 (q,  $^1J_{\text{FC}} = 272$ ,  $\text{CF}_3$ ), 122.6 (s, 3-biph), 118.0 (sept,  $^3J_{\text{FC}} = 4$ ,  $p\text{-Ar}^{\text{F}}$ ).  **$^{31}\text{P}\{^1\text{H}\}$  NMR** (202 MHz,  $\text{CD}_2\text{Cl}_2$ ):  $\delta$  11.6 (s).<sup>†</sup> **HR ESI-MS** (positive ion): 869.2088 ( $[\text{M}]^+$ , calcd 869.2076)  $m/z$ . **Anal.** Calcd for  $\text{C}_{81}\text{H}_{52}\text{BCl}_2\text{F}_{24}\text{P}_2\text{Ir}$  (1817.14  $\text{g}\cdot\text{mol}^{-1}$ ): C, 53.54; H, 2.88; N, 0.00. Found: C, 53.67; H, 3.01; N, 0.00.

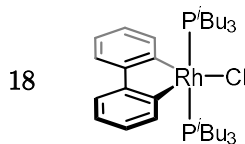
#### 6.2.3.8 $[\text{Ir}(2,2'\text{-biphenyl})(\text{PCy}_3)_2][\text{BAr}^{\text{F}}_4]$



Prepared from **8** (30.0 mg, 30.3  $\mu\text{mol}$ ) and  $\text{Na}[\text{BAr}^{\text{F}}_4]$  (28.2 mg, 38.8  $\mu\text{mol}$ ). Yield: 42.0 mg (75%, orange crystals).

**$^1\text{H}$  NMR** (500 MHz,  $\text{CD}_2\text{Cl}_2$ ):  $\delta$  7.70 – 7.75 (m, 8H,  $o\text{-Ar}^{\text{F}}$ ), 7.56 (br, 4H,  $p\text{-Ar}^{\text{F}}$ ), 7.43 (dd,  $^3J_{\text{HH}} = 7.6, ^4J_{\text{HH}} = 1.6$ , 2H, 3-biph), 7.07 (t,  $^3J_{\text{HH}} = 7.4$ , 2H, 4-biph), 6.92 (d,  $^3J_{\text{HH}} = 7.9$ , 2H, 6-biph), 6.83 (td,  $^3J_{\text{HH}} = 7.6, ^4J_{\text{HH}} = 1.6$ , 2H, 5-biph), 2.06 – 2.16 (m, 6H, Cy), 1.68 – 1.81 (m, 18H, Cy), 1.34 – 1.46 (m, 12H, Cy), 1.10 – 1.29 (m, 30H, Cy).  **$^{13}\text{C}\{^1\text{H}\}$  NMR** (126 MHz,  $\text{CD}_2\text{Cl}_2$ ):  $\delta$  162.3 (q,  $^1J_{\text{CB}} = 50$ ,  $i\text{-Ar}^{\text{F}}$ ), 149.5 (s, 2-biph), 135.4 (s,  $o\text{-Ar}^{\text{F}}$ ), 129.4 (qq,  $^2J_{\text{FC}} = 32, ^3J_{\text{CB}} = 3$ ,  $m\text{-Ar}^{\text{F}}$ ), 129.0 (s, 6-biph), 127.5 (s, 5-biph), 125.8 (t,  $^2J_{\text{PC}} = 6$ , 1-biph), 125.2 (q,  $^1J_{\text{FC}} = 272$ ,  $\text{CF}_3$ ), 125.1 (s, 4-biph), 121.6 (s, 3-biph), 118.0 (sept,  $^3J_{\text{FC}} = 4$ ,  $p\text{-Ar}^{\text{F}}$ ), 36.3 (t,  $J_{\text{PC}} = 12$ , Cy), 30.4 (s, Cy), 27.8 (t,  $J_{\text{PC}} = 5$ , Cy), 26.3 (s, Cy).  **$^{31}\text{P}\{^1\text{H}\}$  NMR** (202 MHz,  $\text{CD}_2\text{Cl}_2$ ):  $\delta$  3.0 (s).<sup>†</sup> **HR ESI-MS** (positive ion): 905.4912 ( $[\text{M}]^+$ , calcd 905.4893)  $m/z$ . **Anal.** Calcd for  $\text{C}_{80}\text{H}_{86}\text{BF}_{24}\text{IrP}_2$  (1768.50  $\text{g}\cdot\text{mol}^{-1}$ ): C, 54.33; H, 4.90; N, 0.00. Found: C, 54.34; H, 5.01; N, 0.00.

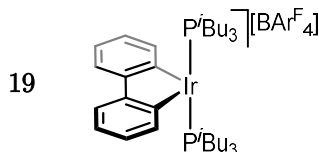
### 6.2.3.9 [Ir(2,2'-biphenyl)(P<sup>t</sup>Pr<sub>3</sub>)<sub>2</sub>][BAr<sup>F</sup><sub>4</sub>]



Prepared from **9** (30.0 mg, 42.8  $\mu$ mol) and Na[BAr<sup>F</sup><sub>4</sub>] (41.8 mg, 47.2  $\mu$ mol). Yield: 27.8 mg (64%, red crystals).

**<sup>1</sup>H NMR** (600 MHz, CD<sub>2</sub>Cl<sub>2</sub>):  $\delta$  7.71 – 7.75 (m, 8H, *o*-Ar<sup>F</sup>), 7.56 (br, 4H, *p*-Ar<sup>F</sup>), 7.41 (dd, <sup>3</sup>*J*<sub>HH</sub> = 7.6, <sup>4</sup>*J*<sub>HH</sub> = 1.6, 2H, 3-biph), 7.05 (t, <sup>3</sup>*J*<sub>HH</sub> = 7.4, 2H, 4-biph), 6.99 (d, <sup>3</sup>*J*<sub>HH</sub> = 8.0, 2H, 6-biph), 6.79 (dt, <sup>3</sup>*J*<sub>HH</sub> = 7.7, <sup>4</sup>*J*<sub>HH</sub> = 1.6, 2H, 5-biph), 2.41 – 2.51 (m, 6H, CH), 1.00 (app. q, *J* = 7, 36H, CH<sub>3</sub>). **<sup>13</sup>C{<sup>1</sup>H} NMR** (151 MHz, CD<sub>2</sub>Cl<sub>2</sub>):  $\delta$  162.3 (q, <sup>1</sup>*J*<sub>CB</sub> = 50, *i*-Ar<sup>F</sup>), 149.3 (s, 2-biph), 135.4 (s, *o*-Ar<sup>F</sup>), 129.4 (qq, <sup>2</sup>*J*<sub>FC</sub> = 32, <sup>3</sup>*J*<sub>CB</sub> = 3, *m*-Ar<sup>F</sup>), 128.3 (s, 6-biph), 127.3 (s, 5-biph), 125.6 (s, 4-biph), 125.2 (q, <sup>1</sup>*J*<sub>FC</sub> = 272, CF<sub>3</sub>), 123.4 (t, <sup>2</sup>*J*<sub>PC</sub> = 6, 1-biph), 122.0 (s, 3-biph), 118.0 (sept, <sup>3</sup>*J*<sub>FC</sub> = 4, *p*-Ar<sup>F</sup>), 25.3 (t, *J*<sub>FC</sub> = 13, CH), 19.7 (s, CH<sub>3</sub>). **<sup>31</sup>P{<sup>1</sup>H} NMR** (202 MHz, CD<sub>2</sub>Cl<sub>2</sub>):  $\delta$  17.8 (s).<sup>†</sup> **HR ESI-MS** (positive ion): 665.3021 ([M]<sup>+</sup>, calcd 665.3013) *m/z*. **Anal.** Calcd for C<sub>62</sub>H<sub>62</sub>BF<sub>24</sub>IrP<sub>2</sub> (1528.11 g·mol<sup>-1</sup>): C, 48.73; H, 4.09; N, 0.00. Found: C, 48.81; H, 4.09; N, 0.00.

### 6.2.3.10 [Ir(2,2'-biphenyl)(P<sup>t</sup>Bu<sub>3</sub>)<sub>2</sub>][BAr<sup>F</sup><sub>4</sub>]

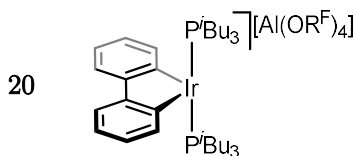


Prepared from **10** (22.7 mg, 28.9  $\mu$ mol) and Na[BAr<sup>F</sup><sub>4</sub>] (28.2 mg, 31.8  $\mu$ mol). Yield: 27.0 mg (59%, yellow crystals).

**<sup>1</sup>H NMR** (500 MHz, CD<sub>2</sub>Cl<sub>2</sub>):  $\delta$  7.70 – 7.75 (m, 8H, *o*-Ar<sup>F</sup>), 7.56 (br, 4H, *p*-Ar<sup>F</sup>), 7.46 (dd, <sup>3</sup>*J*<sub>HH</sub> = 7.7, <sup>4</sup>*J*<sub>HH</sub> = 1.6, 2H, 3-biph), 7.10 (t, <sup>3</sup>*J*<sub>HH</sub> = 7.4, 2H, 4-biph), 6.97 (d, <sup>3</sup>*J*<sub>HH</sub> = 7.8, 2H, 6-biph), 6.84 (td, <sup>3</sup>*J*<sub>HH</sub> = 7.6, <sup>4</sup>*J*<sub>HH</sub> = 1.6, 2H, 5-biph), 1.59 – 1.72 (m, 6H, CH), 1.54 (app. dt, *J* = 7, *J* = 3, 12H, CH<sub>2</sub>), 0.71 (d, <sup>3</sup>*J*<sub>HH</sub> = 6.5, 36H, CH<sub>3</sub>). **<sup>13</sup>C{<sup>1</sup>H} NMR** (126 MHz, CD<sub>2</sub>Cl<sub>2</sub>):  $\delta$  162.3 (q, <sup>1</sup>*J*<sub>CB</sub> = 50, *i*-Ar<sup>F</sup>), 149.4 (s, 2-biph), 135.4 (s, *o*-Ar<sup>F</sup>), 130.3 (t, <sup>2</sup>*J*<sub>PC</sub> = 7, 1-biph), 129.6 (s, 6-biph), 129.4 (qq, <sup>2</sup>*J*<sub>FC</sub> = 32, <sup>3</sup>*J*<sub>CB</sub> = 3,

*m*-Ar<sup>F</sup>), 127.7 (s, 5-biph), 125.3 (s, 4-biph), 125.2 (q, <sup>1</sup>*J*<sub>FC</sub> = 272, CF<sub>3</sub>), 122.4 (s, 3-biph), 118.0 (sept, <sup>3</sup>*J*<sub>FC</sub> = 4, *p*-Ar<sup>F</sup>), 34.0 (t, *J*<sub>PC</sub> = 14, CH<sub>2</sub>), 25.8 – 26.0 (m, CH & CH<sub>3</sub>). **<sup>31</sup>P{<sup>1</sup>H} NMR** (202 MHz, CD<sub>2</sub>Cl<sub>2</sub>): δ 14.5 (s).<sup>†</sup> **HR ESI-MS** (positive ion): 749.3952 ([M]<sup>+</sup>, calcd 749.3952) *m/z*. **Anal.** Calcd for C<sub>68</sub>H<sub>74</sub>BF<sub>24</sub>IrP<sub>2</sub> (1612.28 g·mol<sup>-1</sup>): C, 50.66; H, 4.63; N, 0.00. Found: C, 50.80; H, 4.72; N, 0.00.

#### 6.2.3.11 [Ir(2,2'-biphenyl)(P<sup>*i*</sup>Bu<sub>3</sub>)<sub>2</sub>][Al(OR<sup>F</sup>)<sub>4</sub>]

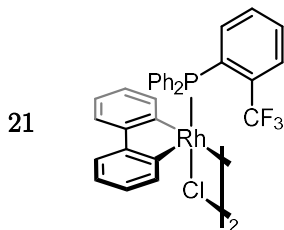


Prepared from **10** (5.0 mg, 7.2 μmol) and Li[Al(OR<sup>F</sup>)<sub>4</sub>] (7.7 mg, 7.9 μmol). Yield: 4.0 mg (34%, yellow crystals).

**<sup>1</sup>H NMR** (400 MHz, CD<sub>2</sub>Cl<sub>2</sub>): δ 7.46 (dd, <sup>3</sup>*J*<sub>HH</sub> = 7.6, <sup>4</sup>*J*<sub>HH</sub> = 1.6, 2H, 3-biph), 7.11 (t, <sup>3</sup>*J*<sub>HH</sub> = 7.3, 2H, 4-biph), 6.98 (d, <sup>3</sup>*J*<sub>HH</sub> = 7.8, 2H, 6-biph), 6.84 (td, <sup>3</sup>*J*<sub>HH</sub> = 7.6, <sup>4</sup>*J*<sub>HH</sub> = 1.6, 2H, 5-biph), 1.59 – 1.74 (m, 6H, CH), 1.54 (app. dt, *J* = 7, *J* = 3, 12H, CH<sub>2</sub>), 0.72 (d, <sup>3</sup>*J*<sub>HH</sub> = 6.5, 36H, CH<sub>3</sub>). **<sup>31</sup>P{<sup>1</sup>H} NMR** (162 MHz, CD<sub>2</sub>Cl<sub>2</sub>): δ 13.8 (s).<sup>†</sup> **LR ESI-MS** (positive ion): 749.5 ([M]<sup>+</sup>, calcd 749.4) *m/z*.

### 6.2.4 Preparation of [M(2,2'-biphenyl)(PPh<sub>2</sub>Tol<sup>F</sup>)<sub>2</sub>(L)]

#### 6.2.4.1 [{Rh(2,2'-biphenyl)(PPh<sub>2</sub>Tol<sup>F</sup>)Cl]<sub>2</sub>]



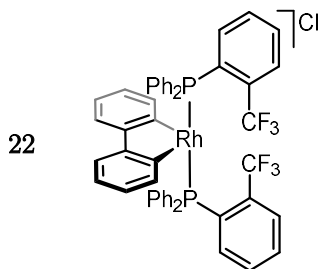
A solution of **1** (297.5 mg, 0.500 mmol) and PPh<sub>2</sub>Tol<sup>F</sup> (412.9 mg, 1.250 mmol) in CH<sub>2</sub>Cl<sub>2</sub> (3 mL) was stirred at ambient temperature for 18 h. The resulting yellow microcrystalline precipitate was isolated by filtration, washed with CH<sub>2</sub>Cl<sub>2</sub> (3 × 5 mL), and dried *in vacuo*. Concentration of the combined filtrate and washings to *ca.* 5 mL



afforded additional product on cooling to 4 °C, which was isolated by filtration, washed with CH<sub>2</sub>Cl<sub>2</sub> (3 × 5 mL), and dried *in vacuo*. Yield: 253.7 mg (82%, yellow solid).

**<sup>1</sup>H NMR** (500 MHz, CD<sub>2</sub>Cl<sub>2</sub>): δ 8.06 (dd, <sup>3</sup>J<sub>HH</sub> = 8.0, <sup>3</sup>J<sub>PH</sub> = 3.9, 2H, 6-Tol<sup>F</sup>), 7.74 (t, <sup>3</sup>J<sub>HH</sub> = 7.8, 2H, 5-Tol<sup>F</sup>), 7.50 (t, <sup>3</sup>J<sub>HH</sub> = 7.7, 2H, 4-Tol<sup>F</sup>), 7.45 – 7.37 (m, 6H, 3-Ar<sup>F</sup> & 6-biph), 7.20 (t, <sup>3</sup>J<sub>HH</sub> = 7.5, 4H, *p*-Ph), 7.02 – 6.94 (m, 12H, 3-biph & *m*-Ph), 6.82 (t, <sup>3</sup>J<sub>HH</sub> = 7.3, 4H, 4-biph), 6.64 (br, 8H, *o*-Ph), 6.62 (t, <sup>3</sup>J<sub>HH</sub> = 7.5, 4H, 5-biph). **<sup>13</sup>C{<sup>1</sup>H} NMR** (126 MHz, CD<sub>2</sub>Cl<sub>2</sub>): δ 158.7 (HMBC, 1-biph), 151.5 (s, 2-biph), 137.3 (s, 3-Tol<sup>F</sup>), 135.4 (s, 6-biph), 133.8 (d, <sup>2</sup>J<sub>PC</sub> = 10, *o*-Ph), 134 (obsc., 2-Ar<sup>F</sup>), 132.2 (d, <sup>4</sup>J<sub>PC</sub> = 7, 4-Ar<sup>F</sup>), 132.0 (s, 5-Tol<sup>F</sup>), 130.6 (d, <sup>4</sup>J<sub>PC</sub> = 2, *p*-Ph), 129.2 (d, <sup>1</sup>J<sub>PC</sub> = 42, 1-Tol<sup>F</sup>), 128.6 (br, 6-Tol<sup>F</sup>), 128 (obscured, *i*-Ph), 127.8 (d, <sup>3</sup>J<sub>PC</sub> = 11, *m*-Ph), 125.2 (s, 5-biph), 124.7 (q, <sup>1</sup>J<sub>FC</sub> = 277, α-Tol<sup>F</sup>), 123.5 (s, 4-biph), 121.3 (s, 3-biph). **<sup>31</sup>P{<sup>1</sup>H} NMR** (162 MHz, CD<sub>2</sub>Cl<sub>2</sub>): δ 39.1 (dq, <sup>1</sup>J<sub>RhP</sub> = 170, <sup>2</sup>J<sub>PF</sub> = 4). **<sup>19</sup>F{<sup>1</sup>H} NMR** (376 MHz, CD<sub>2</sub>Cl<sub>2</sub>): δ -62.80 (vbr, fwhm = 15.5 Hz). Use of sine bell apodization resolved the broad CF<sub>3</sub> signal into an apparent triplet resonance with <sup>1</sup>J<sub>RhF</sub> ≈ <sup>2</sup>J<sub>PF</sub> ≈ 3 Hz. **HR ESI-MS** (positive ion): 626.0718 ([<sup>1</sup>/<sub>2</sub>M-Cl+MeCN]<sup>+</sup>, calcd 626.0726) *m/z*. **Anal.** calcd for C<sub>62</sub>H<sub>44</sub>Cl<sub>2</sub>F<sub>6</sub>P<sub>2</sub>Rh<sub>2</sub> (1241.68 g·mol<sup>-1</sup>): C, 59.97; H, 3.57; N, 0.00. Found: C, 59.90; H, 3.64; N, 0.00.

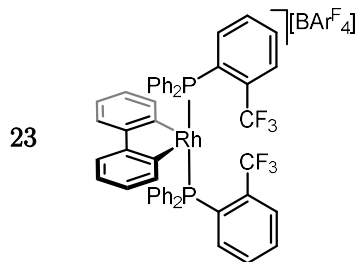
#### 6.2.4.2 [Rh(2,2'-biphenyl)(PPh<sub>2</sub>Tol<sup>F</sup>)<sub>2</sub>][Cl]



A solution of **1** (11.9 mg, 20.0 μmol) and PPh<sub>2</sub>Tol<sup>F</sup> (13.3 mg, 40.2 μmol) in CD<sub>2</sub>Cl<sub>2</sub> (0.5 mL) was left to stand at ambient temperature for 18 h. The resulting solution was analysed again by NMR spectroscopy and found to contain an equilibrium mixture of precursor **1**, dimer **21**, and the title compound in a 1.0 : 2.7 : 1.6 ratio. Addition of further PPh<sub>2</sub>Tol<sup>F</sup> (13.3 mg, 40.2 μmol) and leaving the solution to stand for 18 h resulted in the precipitation of dimer **21** and a solution of the title compound and PPh<sub>2</sub>Tol<sup>F</sup>.

**$^1\text{H}$  NMR** (300 MHz,  $\text{CD}_2\text{Cl}_2$ ), selected signals:  $\delta$  8.40 (app q,  $^3J_{\text{HH}} \approx ^3J_{\text{PH}} \approx 7.3$ , 2H, 6-Tol<sup>F</sup>), 6.68 (t,  $^3J_{\text{HH}} = 7.1$ , 2H, 4-biph), 6.58 (d,  $^3J_{\text{HH}} = 7.3$ , 2H, 3-biph), .47 (t,  $^3J_{\text{HH}} = 7.7$ , 2H, 5-biph).  **$^{31}\text{P}\{^1\text{H}\}$  NMR** (162 MHz,  $\text{CD}_2\text{Cl}_2$ ):  $\delta$  39.1 (dh,  $^1J_{\text{RhP}} = 120$ ,  $^2J_{\text{PF}} = 2$ ).  **$^{19}\text{F}\{^1\text{H}\}$  NMR** (376 MHz,  $\text{CD}_2\text{Cl}_2$ ):  $\delta$  -55.99 (td,  $^1J_{\text{RhF}} = 2.0$ ,  $^2J_{\text{RhF}} = 0.7$ ).

#### 6.2.4.3 $[\text{Rh}(\text{2,2'-biphenyl})(\text{PPh}_2\text{Tol}^{\text{F}})_2][\text{BAr}^{\text{F}}_4]$

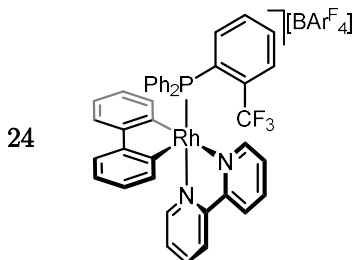


A suspension of dimer **21** (62.1 mg, 50.0  $\mu\text{mol}$ ),  $\text{Na}[\text{BAr}^{\text{F}}_4]$  (97.5 mg, 110  $\mu\text{mol}$ ), and  $\text{PPh}_2\text{Tol}^{\text{F}}$  (36.3 mg, 110  $\mu\text{mol}$ ) in  $\text{CH}_2\text{Cl}_2$  (5 mL) was stirred at ambient temperature for 18 h. The resulting pale-yellow solution was filtered, and the product crystallised by the addition of excess hexane (*ca.* 20 mL). Yield: 153.9 mg (87%, pale yellow solid).

**$^1\text{H}$  NMR** (500 MHz,  $\text{CD}_2\text{Cl}_2$ ):  $\delta$  8.13 (d,  $^3J_{\text{HH}} = 7.8$ , 2H, 6-Tol<sup>F</sup>), 7.87 (t,  $^3J_{\text{HH}} = 7.8$ , 2H, 5-Tol<sup>F</sup>), 7.75 – 7.70 (m, 8H, *o*-Ar<sup>F</sup>), 7.69 (t,  $^3J_{\text{HH}} = 7.8$ , 2H, 4-Tol<sup>F</sup>), 7.55 (br, 4H, *p*-Ar<sup>F</sup>), 7.49 (dt,  $^3J_{\text{HH}} = 7.8$ ,  $^3J_{\text{PH}} = 5.0$ , 2H, 5-Tol<sup>F</sup>), 7.36 (t,  $^3J_{\text{HH}} = 7.5$ , 4H, *p*-Ph), 7.10 (t,  $^3J_{\text{HH}} = 7.8$ , 8H, *m*-Ph), 7.03 (d,  $^3J_{\text{HH}} = 8.0$ , 2H, 6-biph), 6.78 (t,  $^3J_{\text{HH}} = 7.4$ , 2H, 4-biph), 6.66 (t,  $^3J_{\text{HH}} = 7.6$ , 2H, 5-biph), 6.56 (vbr, fwhm = 22.5 Hz, 8H, *o*-Ph), 6.50 (d,  $^3J_{\text{HH}} = 7.4$ , 3-biph).  **$^{13}\text{C}\{^1\text{H}\}$  NMR** (126 MHz,  $\text{CD}_2\text{Cl}_2$ ):  $\delta$  162.3 (q,  $^1J_{\text{CB}} = 50$ , *i*-Ar<sup>F</sup>), 152.5 (br d,  $^1J_{\text{RhC}} = 42$ , 1-biph), 150.0 (s, 2-biph), 137.4 (s, 3-Tol<sup>F</sup>), 135.3 (s, *o*-Ar<sup>F</sup>), 134.1 (t,  $^3J_{\text{PC}} = 3$ , 4-Tol<sup>F</sup>), 133.5 (t,  $J_{\text{PC}} = 6$ , *o*-Ph), 133.1 (s, 5-Tol<sup>F</sup>), 131.9 (s, *p*-Ph), 131.7 (obscured, 2-Tol<sup>F</sup>), 129.9 (s, 6-biph), 129.4 (qq,  $^2J_{\text{FC}} = 32$ ,  $^3J_{\text{CB}} = 3$ , *m*-Ar<sup>F</sup>), 129.1 (obscured m, 6-Tol<sup>F</sup>), 128.9 (t,  $J_{\text{PC}} = 5$ , *m*-Ph), 126.7 (t,  $J_{\text{PC}} = 19$ , 1-Tol<sup>F</sup>), 126.1 (s, 5-biph), 125.9 (q,  $^1J_{\text{FC}} = 276$ , *o*-Tol<sup>F</sup>), 125.2 (q,  $^1J_{\text{FC}} = 272$ ,  $\text{CF}_3$ ), 125.0 (obscured, *i*-Ph), 124.9 (s, 4-biph), 123.7 (s, 3-biph), 118.0 (sept,  $^3J_{\text{FC}} = 4$ , *p*-Ar<sup>F</sup>).  **$^{31}\text{P}\{^1\text{H}\}$  NMR** (162 MHz,  $\text{CD}_2\text{Cl}_2$ ):  $\delta$  20.1 (dh,  $^1J_{\text{RhP}} = 124$ ,  $^2J_{\text{PF}} = 5$ ).  **$^{19}\text{F}\{^1\text{H}\}$  NMR** (376 MHz,  $\text{CD}_2\text{Cl}_2$ ):  $\delta$  -62.89 (s, Ar<sup>F</sup>), -66.39 (app. q,  $^1J_{\text{RhF}} \approx ^2J_{\text{RhF}} \approx 5$ , Tol<sup>F</sup>). **HR ESI-MS** (positive ion):

915.1222 ( $[M]^+$ , calcd 915.1246)  $m/z$ . **Anal.** calcd for  $C_{82}H_{48}BF_{30}P_2Rh$  (1778.90  $g \cdot mol^{-1}$ ): C, 55.37; H, 2.72; N, 0.00. Found: C, 55.56; H, 2.62; N, 0.0.

#### 6.2.4.4 $[Rh(2,2'\text{-biphenyl})(2,2'\text{-bipyridyl})(PPh_2Tol^F)][BAR^F_4]$

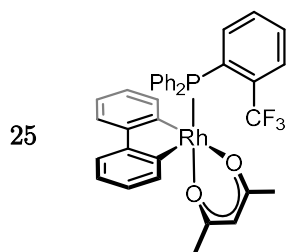


A suspension of dimer **21** (62.1 mg, 50.0  $\mu$ mol),  $Na[BAR^F_4]$  (97.5 mg, 110  $\mu$ mol), and 2,2'-bipyridyl (17.2 mg, 110  $\mu$ mol) in  $CH_2Cl_2$  (5 mL) was stirred at ambient temperature for 18 h. The resulting yellow solution was filtered, and the product crystallised by the addition of excess hexane (*ca.* 20 mL). Yield: 137.2 mg (85%, yellow solid).

**$^1H$  NMR** (500 MHz,  $CD_2Cl_2$ ):  $\delta$  8.24 (d,  $^3J_{HH} = 8.1$ , 1H, 3'-bipy), 8.14 – 8.07 (m, 3H, 6-Tol $^F$  & 3-bipy & 4'-bipy), 8.00 – 5.80 (br m, 18 H, biph + Ph). 7.90 (t,  $^3J_{HH} = 7.8$ , 1H, 4-bipy), 7.87 (t,  $^3J_{HH} = 7.8$ , 1H, 5-Tol $^F$ ), 7.78 – 7.75 (m, 1H, 6-bipy), 7.75 – 7.70 (m, 8H, *o*-Ar $^F$ ), 7.69 – 7.63 (m, 2H, 4-Tol $^F$  & 6'-bipy), 7.55 (br, 4H, *p*-Ar $^F$ ), 7.41 (dd,  $^3J_{PH} = 10.9$ ,  $^3J_{HH} = 8.0$ , 1H, 3-Tol $^F$ ), 7.27 (t,  $^3J_{HH} = 6.6$ , 1H, 5'-bipy), 7.20 (t,  $^3J_{HH} = 6.7$ , 1H, 5-bipy),  **$^{13}C\{^1H\}$  NMR** (126 MHz,  $CD_2Cl_2$ ):  $\delta$  162.3 (q,  $^1J_{CB} = 50$ , *i*-Ar $^F$ ), 155.94 (d,  $^2J_{RhC} = 2$ , 2/2'-bipy), 155.92 (d,  $^2J_{RhC} = 1$ , 2'/2-bipy), 152.9 (d,  $^2J_{RhC} = 2$ , 6'-bipy), 151.7 (app. t,  $^2J_{RhC} \approx ^3J_{PC} \approx 2$ , 6-bipy), 151.3 (br, tentatively assigned to 1-biph), 140.7 (s, 4'-bipy), 140.5 (s, 4-bipy), 138.5 (d,  $^3J_{PC} = 2$ , 3-Tol $^F$ ), 135.4 (*o*-Ar $^F$ ), 134.1 (br, tentatively assigned to *o*-Ph), 133.7 (d,  $^4J_{PC} = 7$ , 4-Tol $^F$ ), 133.2 (d,  $^3J_{PC} = 2$ , 5-Tol $^F$ ), 132.8 (qd,  $^2J_{FC} = 29$ ,  $^2J_{PC} = 11$ , 2-Tol $^F$ ), 129.4 (qq,  $^2J_{FC} = 32$ ,  $^3J_{CB} = 3$ , *m*-Ar $^F$ ), 128.8 (app p,  $^4J_{FC} \approx ^2J_{PC} \approx 6$ , 6-Tol $^F$ ), 127.59 (br, 5-bipy), 127.57 (d,  $^1J_{PC} = 42$ , 1-Tol $^F$ ), 127.0 (s, 5'-bipy), 126.9 (s, tentatively assigned to *p*-Ph), 125.5 (qd,  $^1J_{FC} = 275$ ,  $^3J_{PC} = 2$ ,  $\alpha$ -Tol $^F$ ), 125.3 (br, tentatively assigned to *m*-Ph), 125.2 (q,  $^1J_{FC} = 272$ , CF $_3$ ), 123.4 – 123.5 (m, 3-bipy & 3'-bipy), 118.0 (sept,  $^3J_{FC} = 4$ , *p*-Ar $^F$ ). Due to structural dynamics on the NMR time scale the signals for biph and Ph are either

not observed or not unambiguously assigned.  $^{31}\text{P}\{^1\text{H}\}$  NMR (162 MHz,  $\text{CD}_2\text{Cl}_2$ ):  $\delta$  32.6 (dq,  $^1J_{\text{RhP}} = 150$ ,  $^2J_{\text{PF}} = 5$ ). $^\dagger$   $^{19}\text{F}\{^1\text{H}\}$  NMR (376 MHz,  $\text{CD}_2\text{Cl}_2$ ):  $\delta$  -62.89 (s,  $\text{Ar}^\text{F}$ ), -67.61 (app t,  $^1J_{\text{RhF}} \approx ^2J_{\text{RhP}} \approx 4.0$ ,  $\text{Tol}^\text{F}$ ). **HR ESI-MS** (positive ion): 741.1144 ( $[\text{M}]^+$ , calcd 741.1148)  $m/z$ . **Anal.** calcd for  $\text{C}_{73}\text{H}_{42}\text{BF}_{27}\text{N}_2\text{PRh}$  (1604.80  $\text{g}\cdot\text{mol}^{-1}$ ): C, 54.64; H, 2.64; N, 1.75. Found: C, 54.49; H, 2.80; N, 1.74.

#### 6.2.4.5 $[\text{Rh}(\text{acac})(2,2'\text{-biphenyl})(\text{PPh}_2\text{Tol}^\text{F})]$

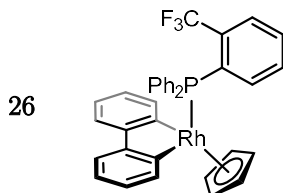


A suspension of dimer **21** (62.1 mg, 50.0  $\mu\text{mol}$ ),  $\text{Na}[\text{acac}]$  (13.4 mg, 110  $\mu\text{mol}$ ) in  $\text{CH}_2\text{Cl}_2$  (5 mL) was stirred at ambient temperature for 18 h. The resulting yellow solution was filtered, and the product crystallised by the addition of excess hexane (*ca.* 20 mL). Yield: 48.4 mg (75%, yellow solid).

$^1\text{H}$  NMR (500 MHz,  $\text{CD}_2\text{Cl}_2$ ):  $\delta$  8.03 (dd,  $^3J_{\text{HH}} = 8.0$ ,  $^3J_{\text{PH}} = 4.1$ , 1H, 6- $\text{Tol}^\text{F}$ ), 7.72 (t,  $^3J_{\text{HH}} = 7.6$ , 1H, 5- $\text{Tol}^\text{F}$ ), 7.55 (t,  $^3J_{\text{HH}} = 7.6$ , 1H, 4- $\text{Tol}^\text{F}$ ), 7.50 (t,  $^3J_{\text{HH}} = 8.8$ , 1H, 3- $\text{Tol}^\text{F}$ ), 7.25 (t,  $^3J_{\text{HH}} = 7.3$ , 2H, *p*-Ph), 7.08 – 7.01 (m, 6H, 6-biph & *m*-Ph), 6.96 (dd,  $^3J_{\text{HH}} = 7.5$ ,  $^4J_{\text{HH}} = 1.6$ , 2H, 3-biph), 6.88 (app. t,  $^3J_{\text{HH}} \approx ^3J_{\text{PH}} \approx 10$ , 4H, *o*-Ph), 6.79 (t,  $^3J_{\text{HH}} = 7.4$ , 2H, 4-biph), 6.60 (td,  $^3J_{\text{HH}} = 7.5$ ,  $^4J_{\text{HH}} = 1.6$ , 2H, 5-biph), 5.43 (s, 1H, CH), 1.94 (s, 6H,  $\text{CH}_3$ ).  $^{13}\text{C}\{^1\text{H}\}$  NMR (126 MHz,  $\text{CD}_2\text{Cl}_2$ ):  $\delta$  187.5 (s, CO), 160.8 (br d,  $^1J_{\text{RhC}} = 37$ , 1-biph), 152.4 (s, 2-biph), 135.8 (s, 3- $\text{Tol}^\text{F}$ ), 134.5 (d,  $^2J_{\text{PC}} = 10$ , *o*-Ph), 134.2 (s, 6-biph), 132.7 (qd,  $^2J_{\text{FC}} = 30$ ,  $^2J_{\text{PC}} = 11$ , 2- $\text{Tol}^\text{F}$ ), 132.3 (d,  $^4J_{\text{PC}} = 6$ , 4- $\text{Tol}^\text{F}$ ), 131.5 (d,  $^3J_{\text{PC}} = 2$ , 5- $\text{Tol}^\text{F}$ ), 131.1 (d,  $^1J_{\text{PC}} = 40$ , 1- $\text{Tol}^\text{F}$ ), 130.4 (d,  $^4J_{\text{PC}} = 2$ , *p*-Ph), 129.0 (d,  $^1J_{\text{PC}} = 54$ , *i*-Ph), 128.5 (app. p,  $^2J_{\text{PC}} \approx ^4J_{\text{FC}} \approx 7$ , 6- $\text{Tol}^\text{F}$ ), 127.6 (d,  $^3J_{\text{PC}} = 11$ , *m*-Ph), 125.2 (qd,  $^1J_{\text{FC}} = 275$ ,  $^3J_{\text{PC}} = 2$ ,  $\alpha$ - $\text{Tol}^\text{F}$ ), 124.9 (s, 5-biph), 123.4 (s, 4-biph), 121.2 (s, 3-biph), 99.2 (s, CH), 28.40 (s,  $\text{CH}_3$ ), 28.38 (s,  $\text{CH}_3$ ).  $^{31}\text{P}\{^1\text{H}\}$  NMR (162 MHz,  $\text{CD}_2\text{Cl}_2$ , 298 K):  $\delta$  38.9 (dq,  $^1J_{\text{RhP}} = 162$ ,  $^2J_{\text{PF}} = 6$ ). $^\dagger$   $^{19}\text{F}\{^1\text{H}\}$  NMR (376 MHz,  $\text{CD}_2\text{Cl}_2$ ):  $\delta$  -64.13

(app. t,  $^1J_{\text{RhF}} \approx ^2J_{\text{PF}} \approx 5$ ). **HR ESI-MS** (positive ion): 684.0905 ( $[\text{M}]^{+\bullet}$ , calcd 684.0907)  $m/z$ . **Anal.** calcd for  $\text{C}_{36}\text{H}_{29}\text{F}_3\text{O}_2\text{PRh}$  (684.50  $\text{g}\cdot\text{mol}^{-1}$ ): C, 63.17; H, 4.27; N, 0.00. Found: C, 63.10; H, 4.25; N, 0.00.

#### 6.2.4.6 $[\text{Rh}(\text{2,2'-biphenyl})(\text{Cp})(\text{PPh}_2\text{Tol}^{\text{F}})]$

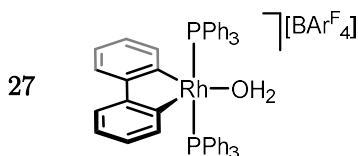


A suspension of dimer **21** (62.1 mg, 50.0  $\mu\text{mol}$ ),  $\text{Na}[\text{Cp}]$  (9.7 mg, 110  $\mu\text{mol}$ ) in  $\text{CH}_2\text{Cl}_2$  (5 mL) was stirred at ambient temperature for 18 h. The resulting pale-yellow solution was filtered, and the product crystallised by the addition of excess hexane (*ca.* 20 mL). Yield: 9.1 mg (13%, yellow solid).

**$^1\text{H}$  NMR** (500 MHz,  $\text{CD}_2\text{Cl}_2$ ):  $\delta$  9.09 (dd,  $^3J_{\text{PH}} = 16.3$ ,  $^3J_{\text{HH}} = 7.8$ , 1H, 6-Tol<sup>F</sup>), 7.89 (t,  $^3J_{\text{HH}} = 7.7$ , 1H, 5-Tol<sup>F</sup>), 7.71 (t,  $^3J_{\text{HH}} = 7.8$ , 1H, 4-Tol<sup>F</sup>), 7.64 (d,  $^3J_{\text{HH}} = 8.0$ , 1H, 3-Tol<sup>F</sup>), 7.59 (d,  $^3J_{\text{HH}} = 7.5$ , 2H, 6-biph), 7.19 (td,  $^3J_{\text{HH}} = 7.5$ ,  $^5J_{\text{PH}} = 1.8$ , 2H, *p*-Ph), 7.02 (td,  $^3J_{\text{HH}} = 7.8$ ,  $^4J_{\text{PH}} = 2.5$ , 4H, *m*-Ph), 6.95 (dd,  $^3J_{\text{HH}} = 7.4$ ,  $^4J_{\text{HH}} = 1.5$ , 2H, 3-biph), 6.86 (dd,  $^3J_{\text{HH}} = 8.0$ ,  $^3J_{\text{PH}} = 11.2$ , 4H, *o*-Ph), 6.77 (t,  $^3J_{\text{HH}} = 7.4$ , 2H, 4-biph), 6.67 (td,  $^3J_{\text{HH}} = 7.8$ ,  $^4J_{\text{HH}} = 2.5$ , 2H, 5-biph), 5.22 (s, 5H, Cp).  **$^{13}\text{C}\{^1\text{H}\}$  NMR** (126 MHz,  $\text{CD}_2\text{Cl}_2$ ):  $\delta$  162.8 (dd,  $^1J_{\text{RhC}} = 35$ ,  $^2J_{\text{PC}} = 17$ , 1-biph), 155.3 (s, 2-biph), 144.2 (d,  $^2J_{\text{PC}} = 25$ , 6-Tol<sup>F</sup>), 141.3 (d,  $^3J_{\text{RhC}} = 2$ , 6-biph), 134.9 (d,  $^1J_{\text{PC}} = 50$ , *i*-Ph), 132.7 (q,  $^2J_{\text{FC}} = 33$ , 2-Tol<sup>F</sup>), 132.0 (d,  $^4J_{\text{PC}} = 2$ , 4-Tol<sup>F</sup>), 131.6 (d,  $^2J_{\text{PC}} = 10$ , *o*-Ph), 131.3 (d,  $^3J_{\text{PC}} = 14$ , 5-Tol<sup>F</sup>), 130.3 (d,  $^1J_{\text{PC}} = 38$ , 1-Tol<sup>F</sup>), 129.4 (obsc., 3-Tol<sup>F</sup>), 129.4 (d,  $^4J_{\text{PC}} = 3$ , *p*-Ph), 127.4 (d,  $^3J_{\text{PC}} = 10$ , *m*-Ph), 124.0 (s, 5-biph), 123.8 (q,  $^1J_{\text{FC}} = 274$ ,  $\alpha$ -Tol<sup>F</sup>), 122.7 (s, 4-biph), 121.9 (s, 3-biph), 93.1 (app. t,  $^1J_{\text{RhC}} \approx ^2J_{\text{PC}} \approx 3$ , Cp).  **$^{31}\text{P}\{^1\text{H}\}$  NMR** (162 MHz,  $\text{CD}_2\text{Cl}_2$ ):  $\delta$  55.9 (d,  $^1J_{\text{RhP}} = 167$ ).<sup>†</sup>  **$^{19}\text{F}\{^1\text{H}\}$  NMR** (376 MHz,  $\text{CD}_2\text{Cl}_2$ ):  $\delta$  -55.12 (s). **HR ESI-MS** (positive ion): 650.0847 ( $[\text{M}]^{+\bullet}$ , calcd 684.0852)  $m/z$ . **Anal.** calcd for  $\text{C}_{36}\text{H}_{27}\text{F}_3\text{PRh}$  (650.49  $\text{g}\cdot\text{mol}^{-1}$ ): C, 66.47; H, 4.18; N, 0.00. Found: C, 66.39; H, 4.35; N, 0.00.

## 6.2.5 Preparation of other triphenylphosphine complexes

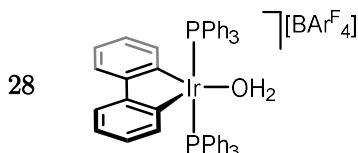
### 6.2.5.1 [Rh(2,2'-biphenyl)(PPh<sub>3</sub>)<sub>2</sub>(OH<sub>2</sub>)] [BAr<sup>F</sup><sub>4</sub>]



Addition of *wet* hexane (*ca.* 19 mL) to a solution of **11** · CH<sub>2</sub>Cl<sub>2</sub> (34.5 mg, 20.0 μmol) in *wet* CH<sub>2</sub>Cl<sub>2</sub> (1 mL) precipitated the title compound which was isolated by filtration and dried *in vacuo*. Yield: 22.6 mg (68%, orange solid).

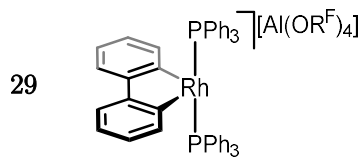
**<sup>1</sup>H NMR** (500 MHz, CD<sub>2</sub>Cl<sub>2</sub>): δ 7.75 – 7.70 (m, 8H, *o*-Ar<sup>F</sup>), 7.55 (br, 4H, *p*-Ar<sup>F</sup>), 7.50 (t, <sup>3</sup>*J*<sub>HH</sub> = 7.4, 6H, *p*-Ph), 7.33 (t, *J* = 7.6, 12H, *m*-Ph), 7.06 – 6.93 (m, 14H, *o*-Ph & 6-biph), 6.89 (t, <sup>3</sup>*J*<sub>HH</sub> = 7.3, 2H, 4-biph), 6.79 (d, <sup>3</sup>*J*<sub>HH</sub> = 7.2, 2H, 3-biph), 6.74 (t, <sup>3</sup>*J*<sub>HH</sub> = 7.5, 2H, 5-biph), 2.57 (s, 2H, OH<sub>2</sub>). **<sup>13</sup>C{<sup>1</sup>H} NMR** (126 MHz, CD<sub>2</sub>Cl<sub>2</sub>): δ 162.3 (q, <sup>1</sup>*J*<sub>CB</sub> = 50, *i*-Ar<sup>F</sup>), 154.3 (dt, <sup>1</sup>*J*<sub>RhC</sub> = 40, <sup>2</sup>*J*<sub>PC</sub> = 8, 1-biph), 150.6 (s, 2-biph), 135.4 (s, *o*-Ar<sup>F</sup>), 133.9 (t, <sup>2</sup>*J*<sub>PC</sub> = 6, *o*-Ph), 132.4 (s, *p*-Ph), 131.9 (s, 6-biph), 129.8 (t, <sup>3</sup>*J*<sub>PC</sub> = 5, *m*-Ph), 129.4 (qq, <sup>2</sup>*J*<sub>FC</sub> = 32, <sup>3</sup>*J*<sub>CB</sub> = 3, *m*-Ar<sup>F</sup>), 126.5 (t, <sup>1</sup>*J*<sub>PC</sub> = 24, *i*-Ph), 126.2 (s, 5-biph), 125.2 (q, <sup>1</sup>*J*<sub>FC</sub> = 272, CF<sub>3</sub>), 125.1 (s, 4-biph), 123.3 (s, 3-biph), 118.0 (sept, <sup>3</sup>*J*<sub>FC</sub> = 4, *p*-Ar<sup>F</sup>). **<sup>31</sup>P{<sup>1</sup>H} NMR** (162 MHz, CD<sub>2</sub>Cl<sub>2</sub>): δ 20.8 (d, <sup>1</sup>*J*<sub>RhP</sub> = 119).<sup>†</sup> **HR ESI-MS** (positive ion): 779.1492 ([M-OH<sub>2</sub>]<sup>+</sup>, calcd 779.1498) *m/z*.

### 6.2.5.2 [Ir(2,2'-biphenyl)(PPh<sub>3</sub>)<sub>2</sub>(OH<sub>2</sub>)] [BAr<sup>F</sup><sub>4</sub>]



Prepared per water-free **16** using insufficiently dry solvents, resulting in an additional upfield signal in the <sup>1</sup>H spectrum. Attempts to prepare this compound preparatively proved unsuccessful. *In situ* characterisation: **<sup>1</sup>H NMR** (500 MHz, CD<sub>2</sub>Cl<sub>2</sub>), selected signals: δ 2.34 (s, OH<sub>2</sub>). **LR ESI-MS** (positive ion): 869.1 ([M-OH<sub>2</sub>]<sup>+</sup>, calcd 869.1) *m/z*.

### 6.2.5.3 [Rh(2,2'-biphenyl)(PPh<sub>3</sub>)<sub>2</sub>][Al(OR<sup>F</sup>)<sub>4</sub>]



**Method A:** A suspension of chloride **3** (326.1 mg, 400.0  $\mu$ mol) and Li[Al(OR<sup>F</sup>)<sub>4</sub>] (409.1 mg, 420.0  $\mu$ mol) in *dry* CH<sub>2</sub>Cl<sub>2</sub> (5 mL) over activated 3 Å molecular sieves (*ca.* 100 mg) was stirred at ambient temperature for 18 h. The reaction was filtered, and the compound precipitated by the addition of excess *dry* hexane (*ca.* 40 mL). The solvent was decanted and the material dried *in vacuo*, isolating the compound as the CH<sub>2</sub>Cl<sub>2</sub> adduct, **29** · CH<sub>2</sub>Cl<sub>2</sub>. Yield: 628.1 mg (96%, orange solid).

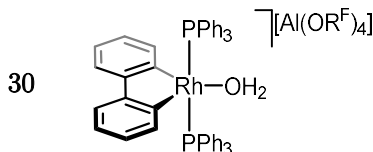
**Method B:** Where generated *in situ* for the purposes of NMR scale reactions and characterisation, a solution of water complex **30** (17.6 mg, 10.0  $\mu$ mol) in CH<sub>2</sub>Cl<sub>2</sub>, CD<sub>2</sub>Cl<sub>2</sub>, C<sub>6</sub>H<sub>5</sub>F or C<sub>6</sub>D<sub>5</sub>F (0.5 mL) was agitated over activated 3 Å molecular sieves (*ca.* 25 mg) for 18 h, resulting in the quantitative conversion to water-free **30**, whereupon the sieves were removed. Where desired, this material could be isolated as CH<sub>2</sub>Cl<sub>2</sub> adduct, **29** · CH<sub>2</sub>Cl<sub>2</sub>, by removing the solvent *in vacuo*. Yield: 18.3 mg (99%, orange solid).

Crystals suitable for X-ray analysis were prepared by diffusion of *dry* hexane (*ca.* 6 mL) into *dry* CH<sub>2</sub>Cl<sub>2</sub> solutions of the title compound (0.5 mL, *ca.* 20 mM).

**<sup>1</sup>H NMR** (500 MHz, CD<sub>2</sub>Cl<sub>2</sub>):  $\delta$  7.51 (t, <sup>3</sup>J<sub>HH</sub> = 7.5, 6H, *p*-Ph), 7.33 (app. t, <sup>3</sup>J<sub>HH</sub> = 7.7, 12H, *m*-Ph), 7.07 - 6.99 (m, 14H, *o*-Ph & 6-biph), 6.87 (t, <sup>3</sup>J<sub>HH</sub> = 7.3, 2H, 4-biph), 6.76 (t, <sup>3</sup>J<sub>HH</sub> = 7.7, 2H, 5-biph), 6.65 (d, <sup>3</sup>J<sub>HH</sub> = 7.5, 2H, 3-biph). **<sup>1</sup>H NMR** (500 MHz, C<sub>6</sub>D<sub>5</sub>F):  $\delta$  7.51 (t, <sup>3</sup>J<sub>HH</sub> = 7.5, 6H, *p*-Ph), 7.36 (app. t, <sup>3</sup>J<sub>HH</sub> = 7.7, 12H, *m*-Ph), 7.26 - 7.21 (obsc. m, 12H, *o*-Ph), 7.06 - 7.00 (obsc. m, 4H, 6-biph & 3-biph), 6.78 - 6.74 (m, 4H, 5-biph & 4-biph). **<sup>13</sup>C{<sup>1</sup>H} NMR** (126 MHz, CD<sub>2</sub>Cl<sub>2</sub>):  $\delta$  154.8 (dt, <sup>1</sup>J<sub>RhC</sub> = 39, <sup>2</sup>J<sub>PC</sub> = 10, 1-biph), 150.0 (s, 2-biph), 134.0 (t, *J*<sub>PC</sub> = 6, *o*-Ph), 132.4 (s, *p*-Ph), 131.7 (s, 6-biph), 129.6 (t, *J*<sub>PC</sub> = 5, *m*-Ph), 127.0 (t, *J*<sub>PC</sub> = 24, *i*-Ph), 126.5 (s, 5-biph), 125.3 (s, 4-biph), 123.6 (s, 3-biph), 121.8 (q, <sup>1</sup>J<sub>FC</sub> = 294, CF<sub>3</sub>). **<sup>13</sup>C{<sup>1</sup>H} NMR** (126 MHz, C<sub>6</sub>D<sub>5</sub>F):  $\delta$  153.1 (dt, <sup>1</sup>J<sub>RhC</sub> = 42, <sup>2</sup>J<sub>PC</sub> = 8, 1-biph), 148.3 (s, 2-biph), 133.1 (t, *J*<sub>PC</sub> = 6, *o*-Ph), 132.2 (s, *p*-Ph),

129.6 – 129.5 (m, 6-biph & *m*-Ph), 126.3 (s, 5-biph), 125.9 (t,  $J_{\text{FC}} = 24.4$ , *i*-Ph), 125.0 (s, 4-biph), 122.6 (s, 3-biph) 121.8 (q,  $^1J_{\text{FC}} = 294$ ,  $\text{CF}_3$ ).  **$^{31}\text{P}\{^1\text{H}\}$  NMR** (202 MHz,  $\text{CD}_2\text{Cl}_2$ ):  $\delta$  20.3 (d,  $^1J_{\text{RHP}} = 118$ ).  **$^{31}\text{P}\{^1\text{H}\}$  NMR** (202 MHz,  $\text{C}_6\text{D}_5\text{F}$ ):  $\delta$  23.4 (d,  $^1J_{\text{RHP}} = 120$ ). **HR ESI-MS** (positive ion): 779.1493 ( $[\text{M}]^+$ , calcd 779.1498) *m/z*.

#### 6.2.5.4 $[\text{Rh}(\text{2,2'-biphenyl})(\text{PPh}_3)_2(\text{OH}_2)][\text{Al}(\text{OR}^{\text{F}})_4]$



**Method A:** A suspension of chloride **3** (360 mg, 442  $\mu\text{mol}$ ) and  $\text{Li}[\text{Al}(\text{OR}^{\text{F}})_4]$  (475 mg, 486  $\mu\text{mol}$ ) in  $\text{CH}_2\text{Cl}_2$  (5 mL) was stirred at ambient temperature for 18 h. The reaction was filtered, and to the supernatant was added  $\text{H}_2\text{O}$  (7.0  $\mu\text{L}$ , 4.4 mmol). The compound was precipitated by the addition of excess hexane (*ca.* 40 mL) and isolated by filtration. The residues were extracted into  $\text{CH}_2\text{Cl}_2$  (*ca.* 10 mL), filtered, and the solvent removed *in vacuo*. Yield: 725.5 mg (93%, orange solid).

**Method B:** To a solution of **29**  $\cdot \text{CH}_2\text{Cl}_2$  (200 mg, 112  $\mu\text{mol}$ ) in  $\text{CH}_2\text{Cl}_2$  (1 mL) was added excess of  $\text{H}_2\text{O}$  (*ca.* 0.1 mL). The solution was agitated briefly, and the compound precipitated by the addition of excess hexane (*ca.* 19 mL), isolated by filtration and dried *in vacuo*. Yield: 189.6 mg (96%, orange solid).

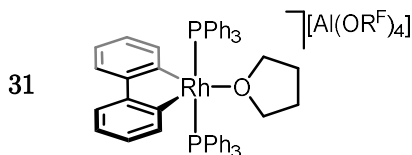
Crystals suitable for X-ray analysis were prepared by diffusion of hexane (6 mL) into  $\text{CH}_2\text{Cl}_2$  solutions of the title compound (0.5 mL, *ca.* 20 mM).

**$^1\text{H}$  NMR** (500 MHz,  $\text{CD}_2\text{Cl}_2$ ):  $\delta$  7.52 (t,  $^3J_{\text{HH}} = 7.4$ , 6H, *p*-Ph), 7.35 (app. t,  $^3J_{\text{HH}} = 7.5$ , 12H, *m*-Ph), 6.98 (app. q,  $^3J_{\text{HH}} \approx ^3J_{\text{PH}} \approx 5.7$ , 12H, *o*-Ph), 6.93 (d,  $^3J_{\text{HH}} = 7.7$ , 2H, 6-biph), 6.91 (t,  $^3J_{\text{HH}} = 7.5$ , 2H, 5-biph), 6.83 (d,  $^3J_{\text{HH}} = 7.3$ , 2H, 4-biph), 6.74 (t,  $^3J_{\text{HH}} = 7.5$ , 2H, 3-biph), 2.44 (s, 2H,  $\text{OH}_2$ ).  **$^1\text{H}$  NMR** (400 MHz,  $\text{C}_6\text{D}_5\text{F}$ ):  $\delta$  7.29 (t,  $^3J_{\text{HH}} = 7.4$ , 6H, *p*-Ph), 7.16 (app. t,  $^3J_{\text{HH}} = 7.6$ , 12H, *m*-Ph), 6.96 (app q,  $^3J_{\text{HH}} \approx ^3J_{\text{PH}} \approx 6.5$ , 12H, *o*-Ph), 6.85 (obsc., 4H, 6-biph & 3-biph), 6.69 – 6.60 (m, 5-biph & 4-biph).  **$^{13}\text{C}\{^1\text{H}\}$  NMR** (126 MHz,  $\text{CD}_2\text{Cl}_2$ ):  $\delta$  154.0 (dt,  $^1J_{\text{RhC}} = 39$ ,  $^2J_{\text{PC}} = 9$ , 1-biph), 151.0 – 150.7 (m, 2-biph),



133.8 (t,  $J_{\text{FC}} = 6$ , *o*-Ph), 132.4 (s, *p*-Ph), 132.0 (s, 3-biph), 129.9 (t,  $J_{\text{FC}} = 5$ , *m*-Ph), 126.4 (t,  $J_{\text{FC}} = 24$ , *i*-Ph), 126.1 (s, 5-biph), 125.0 (s, 4-biph), 123.2 (s, 6-biph), 121.8 (q,  $^1J_{\text{FC}} = 294$ ,  $\text{CF}_3$ ).  **$^{31}\text{P}\{^1\text{H}\}$  NMR** (162 MHz,  $\text{CD}_2\text{Cl}_2$ ):  $\delta$  22.7 (d,  $^1J_{\text{RhP}} = 119$ ).  **$^{31}\text{P}\{^1\text{H}\}$  NMR** (202 MHz,  $\text{C}_6\text{D}_5\text{F}$ ):  $\delta$  22.7 (d,  $^1J_{\text{RhP}} = 119$ ).<sup>†</sup> **HR ESI-MS** (positive ion): 779.1492 ( $[\text{M-OH}_2]^+$ , calcd 779.1498) *m/z*. **Anal.** Calcd for  $\text{C}_{64}\text{H}_{40}\text{AlF}_{36}\text{O}_5\text{P}_2\text{Rh}$  (1764.80  $\text{g}\cdot\text{mol}^{-1}$ ): C, 43.56; H, 2.28; N, 0.00. Found: C, 43.65; H, 2.44; N, 0.00.

#### 6.2.5.5 $[\text{Rh}(2,2'\text{-biphenyl})(\text{PPh}_3)_2(\text{thf})][\text{Al}(\text{OR}^{\text{F}})_4]$

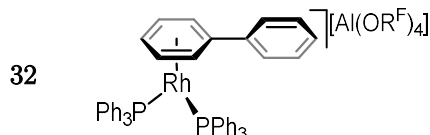


A solution of **30** (176.4 mg, 100.0  $\mu\text{mol}$ ) in THF (1 mL) was agitated over activated 3 Å molecular sieves (*ca.* 100 mg) for 1 h. The solution was filtered and the compound crystallised by the addition of excess hexane (*ca.* 19 mL). The supernatant was decanted and the compound dried *in vacuo*. Yield: 154.6 mg (85%, orange-red solid).

**$^1\text{H}$  NMR** (500 MHz,  $\text{CD}_2\text{Cl}_2$ ), major component:  $\delta$  7.49 (t,  $^3J_{\text{HH}} = 7.1$ , 6H, *p*-Ph), 7.31 (app. t,  $^3J_{\text{HH}} = 7.3$ , 12H, *o*-Ph), 7.17 – 7.09 (br m, 2H, 6-biph), 7.02 (br, 12H, *o*-Ph), 6.91 – 6.80 (br m, 2H, 4-biph), 6.77 – 6.69 (br m, 2H, 5-biph), 6.70 – 6.62 (br m, 2H, 3-biph), 3.59 – 3.42 (m, 4H, thf), 1.70 – 1.59 (m, 4H, thf).  **$^1\text{H}$  NMR** (500 MHz, THF):  $\delta$  7.89 (t,  $^3J_{\text{HH}} = 7.4$ , 6H, *p*-Ph), 7.73 (t,  $^3J_{\text{HH}} = 7.6$ , 12H, *m*-Ph), 7.08 – 7.00 (m, 12, *o*-Ph), 7.21 (t,  $^3J_{\text{HH}} = 7.3$ , biph), 7.10 (t,  $^3J_{\text{HH}} = 6.8$ , biph). The biphenyl resonances could not be satisfactorily assigned with the available data.  **$^{13}\text{C}\{^1\text{H}\}$  NMR** (126 MHz,  $\text{CD}_2\text{Cl}_2$ ):  $\delta$  134.1 (br t,  $J_{\text{FC}} = 6$ , *o*-Ph), 132.1 (br, *p*-Ph), 129.4 (br, *m*-Ph), 127.4 (br t,  $J_{\text{FC}} = 24$ , *i*-Ph), 121.83 (d,  $J = 293.5$ ). The biph resonances could not be unambiguously assigned due to exchange on the NMR time scale.  **$^{13}\text{C}\{^1\text{H}\}$  NMR** (126 MHz, THF):  $\delta$  154.8 (dt,  $^1J_{\text{RhC}} = 38$ ,  $^2J_{\text{FC}} = 10$ , 1-biph), 151.4 (s, 2-biph), 134.2 (t,  $J_{\text{FC}} = 6$ , *o*-Ph), 132.4 (s, *p*-Ph), 131.8 (s, 6-biph), 129.3 (t,  $J_{\text{FC}} = 5$ , *m*-Ph), 128.3 (t,  $J_{\text{FC}} = 24$ , *i*-Ph), 125.7 (s, 5-biph), 124.6 (s, 4-biph), 123.0 (s, 3-biph), 121.8 (q,  $^1J_{\text{FC}} = 293$ ,  $\text{CF}_3$ ).  **$^{31}\text{P}\{^1\text{H}\}$  NMR** (162 MHz,  $\text{CD}_2\text{Cl}_2$ ):  $\delta$  20.7 (br d,  $^1J_{\text{RhP}} = 118$ ,

fwhm = 60).  **$^{31}\text{P}\{^1\text{H}\}$  NMR** (162 MHz, THF):  $\delta$  22.2 (d,  $^1J_{\text{RhP}} = 120$ , fwhm = 16). **HR ESI-MS** (positive ion): 779.1495 ( $[\text{M} - \text{THF}]^+$ , calcd 779.1498)  $m/z$ . **Anal.** Calcd for  $\text{C}_{68}\text{H}_{46}\text{AlF}_{36}\text{O}_5\text{P}_2\text{Rh}$  (1818.89  $\text{g}\cdot\text{mol}^{-1}$ ): C, 44.90; H, 2.55; N, 0.00. Found: C, 44.73; H, 2.64; N, 0.00.

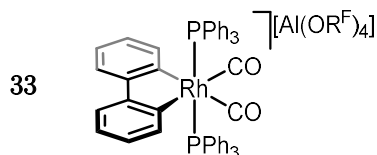
#### 6.2.5.6 $[\text{Rh}(\eta^6\text{-biphenyl})(\text{PPh}_3)_2][\text{Al}(\text{OR}^{\text{F}})_4]$



A solution of **29** ·  $\text{CH}_2\text{Cl}_2$  (35.2 mg, 20.0  $\mu\text{mol}$ ) in  $\text{CD}_2\text{Cl}_2$  (0.5 mL) was freeze-pump-thaw degassed three times and placed under dihydrogen for 5 h with intermittent agitation. The solution was freeze-pump-thaw degassed and placed under argon. The compound was crystallised by the diffusion of excess hexane (*ca.* 9 mL), which was isolated by filtration and dried *in vacuo*. Yield: 24.8 mg (71%, orange crystalline solid).

**$^1\text{H}$  NMR** (500 MHz,  $\text{CD}_2\text{Cl}_2$ ):  $\delta$  7.70 – 7.59 (m, 3H, *m*-Ph-Ph & *p*-Ph-Ph), 7.58 – 7.53 (m, 2H, *o*-Ph-Ph), 7.44 (t,  $^3J_{\text{HH}} = 6.2$ , 1H, *p*- $\eta^6$ -Ph-Ph), 7.36 (t,  $^3J_{\text{HH}} = 7.5$ , 2H, *p*-Ph), 7.30 – 7.23 (m, 12H, *o*-Ph), 7.18 (t,  $^3J_{\text{HH}} = 7.3$ , 12H, *m*-Ph), 5.64 (d,  $^3J_{\text{HH}} = 6.5$ , 2H, *o*- $\eta^6$ -Ph-Ph), 5.34 – 5.29 (m, 2H, *m*- $\eta^6$ -Ph-Ph).  **$^{13}\text{C}\{^1\text{H}\}$  NMR** (126 MHz,  $\text{CD}_2\text{Cl}_2$ ):  $\delta$  134.3 (t,  $J_{\text{FC}} = 17$ , *i*-Ph), 134.2 (t,  $J_{\text{FC}} = 6$ , *o*-Ph), 133.9 (s, *i*- $\eta^6$ -Ph-Ph), 131.3 (s, *p*-Ph), 130.9 (s, *p*-Ph-Ph), 130.3 (s, *m*-Ph-Ph), 128.8 (t,  $J_{\text{FC}} = 5$ , *m*-Ph), 127.5 (s, *o*-Ph-Ph), 126.0 (s, *i*-Ph-Ph), 121.8 (q,  $^1J_{\text{FC}} = 293$ ,  $\text{CF}_3$ ), 107.1 (d,  $^1J_{\text{RhC}} = 2.0$ , *p*- $\eta^6$ -biph), 101.2 (q,  $^1J_{\text{RhC}} \approx ^2J_{\text{PC}} \approx 2.8$ , *m*- $\eta^6$ -Ph-Ph), 100.6 (q,  $^1J_{\text{RhC}} \approx ^2J_{\text{PC}} \approx 2.7$ , *o*- $\eta^6$ -Ph-Ph).  **$^{31}\text{P}\{^1\text{H}\}$  NMR** (121 MHz,  $\text{CD}_2\text{Cl}_2$ ):  $\delta$  43.0 (d,  $^1J_{\text{RhP}} = 206$ ).<sup>†</sup> **HR ESI-MS** (positive ion): 627.0865 ( $[\text{M}-\text{Ph}_2]^+$ , calcd 672.0872)  $m/z$ .

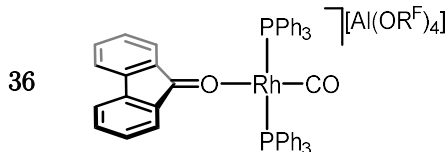
#### 6.2.5.7 $[\text{Rh}(2,2'\text{-biphenyl})(\text{PPh}_3)_2(\text{CO})_2][\text{Al}(\text{OR}^{\text{F}})_4]$



A solution of **29** in CD<sub>2</sub>Cl<sub>2</sub> (0.5 mL), prepared from water complex **30** (17.6 mg, 10 μmol), was freeze-pump-thaw degassed three times and placed under CO. The resulting colourless solution showed quantitative conversion to the title compound, characterised *in situ* owing to the instability of the compound in the absence of CO.

**<sup>1</sup>H NMR** (500 MHz, CD<sub>2</sub>Cl<sub>2</sub>): δ 7.43 (t, <sup>3</sup>*J*<sub>HH</sub> = 7.4, 6H, *p*-Ph), 7.25 (app. t, <sup>3</sup>*J*<sub>HH</sub> = 7.6, 12H, *m*-Ph), 7.18 (d, <sup>3</sup>*J*<sub>HH</sub> = 7.6, 2H, 6-biph), 7.01 – 6.94 (m, 14H, *o*-Ph & 4-biph), 6.89 (d, <sup>3</sup>*J*<sub>HH</sub> = 7.6, 2H, 3-biph), 6.85 (t, <sup>3</sup>*J*<sub>HH</sub> = 7.4, 2H, 5-biph). **<sup>13</sup>C{<sup>1</sup>H} NMR** (126 MHz, CD<sub>2</sub>Cl<sub>2</sub>): δ 185.9 (dt, <sup>1</sup>*J*<sub>RhC</sub> = 42, <sup>2</sup>*J*<sub>PC</sub> = 8, CO), 158.8 (dt, <sup>1</sup>*J*<sub>RhC</sub> = 23, <sup>2</sup>*J*<sub>PC</sub> = 8, 1-biph), 153.0 (t, <sup>2</sup>*J*<sub>RhC</sub> = 3, 2-biph), 139.4 (t, <sup>2</sup>*J*<sub>PC</sub> = 2, 6-biph), 134.2 (t, *J*<sub>PC</sub> = 5, *o*-Ph), 132.3 (s, *p*-Ph), 129.1 (t, *J*<sub>PC</sub> = 5, *m*-Ph), 128.7 (s, 5-biph), 128.6 (t, *J*<sub>PC</sub> = 27, *i*-Ph), 126.5 (s, 4-biph), 124.4 (s, 3-biph), 121.8 (q, <sup>1</sup>*J*<sub>FC</sub> = 293, CF<sub>3</sub>). **<sup>31</sup>P{<sup>1</sup>H} NMR** (202 MHz, CD<sub>2</sub>Cl<sub>2</sub>): δ 19.2 (d, <sup>1</sup>*J*<sub>RhP</sub> = 93).

#### 6.2.5.8 [Rh(κ<sup>1</sup>-O-fluorenone)(CO)(PPh<sub>3</sub>)<sub>2</sub>][Al(OR<sup>F</sup>)<sub>4</sub>]

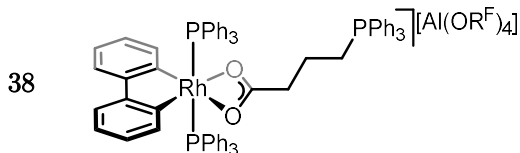


A solution of bis(carbonyl) **33**, prepared as described above from water complex **30** (17.6 mg, 10 μmol), in CD<sub>2</sub>Cl<sub>2</sub> (0.5 mL) was freeze-pump-thaw degassed three times, placed under argon (1 bar) and left to stand at ambient temperature for 2 weeks. The compound was precipitated by slow diffusion of excess hexane (*ca.* 19 mL), the supernatant decanted and the solid dried *in vacuo*. Yield: 5.1 mg (28%, orange crystalline solid).

**<sup>1</sup>H NMR** (500 MHz, CD<sub>2</sub>Cl<sub>2</sub>): δ 7.63 – 7.50 (m, 14H, *o*-Ph & 6-fluor), 7.41 – 7.36 (m, 8H, *p*-Ph & 4-fluor), 7.32 (t, <sup>3</sup>*J*<sub>HH</sub> = 7.4, 12H, *m*-Ph), 7.18 (d, <sup>3</sup>*J*<sub>HH</sub> = 7.3, 2H, 3-fluor), 7.07 (d, <sup>3</sup>*J*<sub>HH</sub> = 7.3, 2H, 5-fluor). **<sup>13</sup>C{<sup>1</sup>H} NMR** (126 MHz, CD<sub>2</sub>Cl<sub>2</sub>): δ 202.6 (HMBC, fluorCO), 144.8 (s, 6-fluor), 138.3 (s, 4-fluor), 134.6 (t, *J*<sub>PC</sub> = 6, *o*-Ph), 132.1 (s, *p*-Ph), 129.7 (t, *J*<sub>PC</sub> = 24, *i*-Ph), 129.6 (t, *J*<sub>PC</sub> = 4, *m*-Ph), 129.4 (s, 5-fluor), 126.1 (s, 6-fluor),

121.5 (s, 3-fluor), 121.8 (q,  $^1J_{\text{FC}} = 295.7$ ,  $\text{CF}_3$ ).  **$^{31}\text{P}\{^1\text{H}\}$  NMR** (162 MHz,  $\text{CD}_2\text{Cl}_2$ ):  $\delta$  32.9 (d,  $^1J_{\text{RhP}} = 125$ ). **HR ESI-MS** (positive ion): 655.0842 ( $[\text{M-fluorenone}]^+$ , calcd 655.0821)  $m/z$ . The CO and 1-fluor  $^{13}\text{C}$  resonances could not be unambiguously located.

#### 6.2.5.9 $[\text{Rh}(\text{2,2'-biphenyl})(\text{PPh}_3)_2(\text{O}_2\text{CCH}_2\text{CH}_2\text{CH}_2\text{PPh}_3)][\text{Al}(\text{OR}^{\text{F}})_4]$



A solution of THF complex **31** (18.2 mg, 10.0  $\mu\text{mol}$ ) and  $\text{PPh}_3$  (5.2 mg, 20  $\mu\text{mol}$ ) in THF (0.5 mL) was left to stand at 85  $^\circ\text{C}$  for 4 weeks. Addition of excess hexane (*ca.* 19 mL) precipitated the title compound, which was isolated by filtration and dried *in vacuo*. Yield: 10.1 mg (49%, off-white crystalline solid).

**$^1\text{H}$  NMR** (500 MHz,  $\text{CD}_2\text{Cl}_2$ ):  $\delta$  7.96 (t,  $^3J_{\text{HH}} = 7.5$ , 3H, *p*-Ph\*), 7.78 (td,  $^3J_{\text{HH}} = 7.9$ ,  $^4J_{\text{PH}} = 3.4$ , 6H, *m*-Ph\*), 7.72 – 7.67 (m, 2H, 6-biph), 7.53 (dd,  $^2J_{\text{PH}} = 12.7$ ,  $^3J_{\text{HH}} = 7.7$ , 2H, *o*-Ph\*), 7.18 – 7.09 (m, 18H, *o*-Ph & *p*-Ph), 7.02 (app. t,  $^3J_{\text{HH}} = 7.5$ , 12H, *m*-Ph), 6.62 – 6.54 (m, 4H, 4-biph & 5-biph), 6.52 – 6.46 (m, 2H, 3-biph), 2.27 (td,  $^1J_{\text{PH}} = 12.6$ ,  $^3J_{\text{HH}} = 8.8$ , 2H,  $\text{PCH}_2$ ), 1.54 – 1.42 (m, 2H,  $\text{PCH}_2\text{CH}_2$ ), 1.22 – 1.11 (m, 2H,  $\text{PCH}_2\text{CH}_2$ ).  **$^{13}\text{C}\{^1\text{H}\}$  NMR** (126 MHz,  $\text{CD}_2\text{Cl}_2$ ):  $\delta$  180.7 (s,  $\text{O}_2\text{C}$ ), 159.0 (dt,  $^1J_{\text{RhC}} = 31$ ,  $^2J_{\text{PC}} = 10$ , 1-biph), 154.2 (s, 2-biph), 136.4 (d,  $^2J_{\text{RhC}} = 3$ , 6-biph), 135.0 (t,  $J_{\text{PC}} = 5$ , *o*-Ph), 134.6 (s, *p*-Ph\*), 134.0 (d,  $^3J_{\text{PC}} = 10$ , *m*-Ph\*), 131.2 (d,  $^2J_{\text{PC}} = 13$ , *o*-Ph\*), 130.24 (s, *p*-Ph), 130.22 (obsc. t,  $J_{\text{PC}} = 22$ , *i*-Ph), 127.9 (t,  $J_{\text{PC}} = 5$ , *m*-Ph), 123.8 (s, 5-biph), 122.5 (s, 4-biph), 121.8 (s, 3-biph), 121.2 (q,  $^1J_{\text{FC}} = 290$ ,  $\text{CF}_3$ ), 118.0 (d,  $^1J_{\text{PC}} = 86$ , *i*-Ph\*), 36.0 (d,  $^2J_{\text{PH}} = 18$ ,  $\text{PCH}_2\text{CH}_2$ ), 22.8 (d,  $^1J_{\text{PH}} = 52$ ,  $\text{PCH}_2$ ), 18.5 (s,  $\text{CH}_2$ ).  **$^{31}\text{P}\{^1\text{H}\}$  NMR** (162 MHz,  $\text{CD}_2\text{Cl}_2$ ):  $\delta$  28.2 (d,  $^1J_{\text{RhP}} = 119$ , 2P,  $\text{PPh}_3$ ), 23.9 (s, 1P,  $\text{PPh}_3^*$ ). **LR ESI-MS** (positive ion): 1127.2 ( $[\text{M}]^+$ , calcd 1127.3)  $m/z$ .

## 6.2.6 Reactions of triphenylphosphine systems

### 6.2.6.1 Dissolution of $[\text{Rh}(\text{2,2'-(biphenyl)})(\text{PPh}_3)_2(\text{OH}_2)][\text{Al}(\text{OR}^{\text{F}})_4]$ in THF

Water complex **30** (11.8 mg, 6.67  $\mu\text{mol}$ ) was dissolved in THF (0.33 mL), resulting in a mixture of **30** and THF complex **31** in the ratio 0.15 : 0.85 ( $K_{\text{eq}} = 7.8 \times 10^{-3}$ , taking  $[\text{THF}] = 12.3 \text{ M}$ ) as determined by  $^{31}\text{P}$  NMR spectroscopy.  $^{31}\text{P}\{^1\text{H}\}$  NMR (162 MHz, THF):  $\delta$  29.3 (d,  $^1J_{\text{RhP}} = 119$ , fwhm = 6.6, **30**), 23.0 (d,  $^1J_{\text{RhP}} = 119$ , fwhm = 16.5, **31**).

### 6.2.6.2 Dissolution of $[\text{Rh}(\text{2,2'-(biphenyl)})(\text{PPh}_3)_2(\text{dcm})][\text{Al}(\text{OR}^{\text{F}})_4]$ in $\text{C}_6\text{H}_5\text{F}$

Dichloromethane adduct **29**  $\cdot$   $\text{CH}_2\text{Cl}_2$  (17.6 mg, 10.0  $\mu\text{mol}$ ) was dissolved in  $\text{C}_6\text{H}_5\text{F}$  (0.5 mL), resulting in a mixture of **29** and  $\text{CH}_2\text{Cl}_2$  in a 1:1 ratio as determined by  $^1\text{H}$  NMR spectroscopy.  $^1\text{H}$  NMR (400 MHz,  $\text{CD}_2\text{Cl}_2$ ), selected signals:  $\delta$  4.97 (s,  $\text{CH}_2\text{Cl}_2$ ).

### 6.2.6.3 Reactions of $[\text{Rh}(\text{2,2'-(biphenyl)})(\text{PPh}_3)_2(\text{OH}_2)][\text{Al}(\text{OR}^{\text{F}})_4]$ **30** with 3 Å MS

**General procedure:** A solution of water complex **30** (17.6 mg, 10.0  $\mu\text{mol}$ ) in the given solvent (0.5 mL) under the given gas was agitated over 3 Å molecular sieves (1000 wt%) with intermittent monitoring by  $^1\text{H}$  and  $^{31}\text{P}\{^1\text{H}\}$  NMR spectroscopy. The reaction was deemed complete by the absence of the  $^1\text{H}$  NMR resonance at *ca.*  $\delta_{\text{H}}$  2.4 of bound  $\text{OH}_2$ .

**In  $\text{CD}_2\text{Cl}_2$  under argon:** Within 1 h 100% conversion to low coordinate **29** was observed. Use of a smaller amount of 3 Å molecular sieves (down to 100 wt%) resulted in the same conversion over a period of 6 – 18 h, dependant on batch of 3 Å molecular sieves.

**In  $\text{C}_6\text{H}_5\text{F}$  under argon:** After 1 h 80% conversion to **29** was observed. Within 5 h the reaction had proceeded to 100% conversion.

**In  $\text{C}_6\text{H}_5\text{F}$  under dinitrogen:** Within 1 h 100% conversion to **29** was observed.

**In THF under argon:** Within 5 min the sample contained exclusively THF adduct **31**

#### 6.2.6.4 Decomposition of $[\text{Rh}(2,2'\text{-biphenyl})(\text{PPh}_3)_2(\text{CO})_2][\text{Al}(\text{OR}^{\text{F}})_4]$ under argon

A solution of water complex **30** in  $\text{CD}_2\text{Cl}_2$  (0.5 mL) was freeze-pump-thaw degassed three times and placed under CO. The solution became immediately colourless with quantitative conversion to the **33**. The solution was freeze-pump-thaw degassed three times and placed under argon. The solution was left to stand at ambient temperature with intermittent monitoring by  $^1\text{H}$  and  $^{31}\text{P}$  NMR spectroscopy. Over the following 6 days **33** was converted into a mixture of Rh(I) monocarbonyl **34** and Rh(III) monocarbonyl **35**. These compounds were themselves converted over the following 15 days to a solution of exclusively fluorenone complex **36**.  $^{31}\text{P}\{^1\text{H}\}$  NMR (162 MHz,  $\text{CD}_2\text{Cl}_2$ ):  $\delta$  19.9 (d,  $^1J_{\text{RhP}} = 106$ , **34**), 26.3 (d,  $^1J_{\text{RhP}} = 107$ , **35**), 32.1 (d,  $^1J_{\text{RhP}} = 125$ , **36**).

#### 6.2.6.5 Reaction of $[\text{Rh}(2,2'\text{-biphenyl})(\text{PPh}_3)_2][\text{Al}(\text{OR}^{\text{F}})_4]$ with $\text{PPh}_3$ in $\text{CD}_2\text{Cl}_2$

To a solution of **29** in  $\text{CH}_2\text{Cl}_2$  (0.5 mL), prepared from water complex **30** (18.2 mg, 10.0  $\mu\text{mol}$ ), was added  $\text{PPh}_3$  (5.2 mg, 20  $\mu\text{mol}$ ). Within 5 mins compound **29** was consumed with concomitant formation of equal quantities of chloride **3** and  $[\text{Ph}_3\text{PCH}_2\text{Cl}][\text{Al}(\text{OR}^{\text{F}})_4]$  as gauged by  $^1\text{H}$  and  $^{31}\text{P}$  NMR spectroscopy.  $^1\text{H}$  NMR (400 MHz,  $\text{CD}_2\text{Cl}_2$ ) selected signals:  $\delta$  4.74 (d,  $^2J_{\text{PH}} = 6.00$ ,  $\text{PCH}_2$ ).  $^{31}\text{P}\{^1\text{H}\}$  NMR (162 MHz,  $\text{CD}_2\text{Cl}_2$ ):  $\delta$  29.3 (d,  $^1J_{\text{RhP}} = 118$ , **3**), 23.3 (s,  $[\text{Ph}_3\text{PCH}_2\text{Cl}]^+$ ), -5.08 (s,  $\text{PPh}_3$ ). Data consistent with the analogous  $[\text{Ph}_3\text{PCH}_2\text{Cl}][\text{B}(\text{C}_6\text{F}_5)_4]$ .<sup>426</sup>

#### 6.2.6.6 Reaction of $[\text{Rh}(2,2'\text{-biphenyl})(\text{PPh}_3)_2(\text{thf})][\text{Al}(\text{OR}^{\text{F}})_4]$ with $\text{PPh}_3$ in THF

A solution of THF complex **31** (18.2 mg, 10.0  $\mu\text{mol}$ ) and  $\text{PPh}_3$  (5.2 mg, 20  $\mu\text{mol}$ ) in THF (0.5 mL) was left to stand at 85 °C with intermittent monitoring by  $^1\text{H}$  and  $^{31}\text{P}$  NMR spectroscopy. Slow conversion ( $t_{1/2} = 6$  days) to alkoxide **37** was observed with a corresponding consumption of  $\text{PPh}_3$ . Selected data for **37**:  $^{31}\text{P}\{^1\text{H}\}$  NMR (162 MHz, THF):  $\delta$  28.8 (d,  $^1J_{\text{RhP}} = 119$ ,  $\text{PPh}_3$ ), 24.2 (s,  $\text{PPh}_3^*$ ).

### 6.2.6.7 Substitution reactions

**General procedure:** A solution of a given metal salt (6.7  $\mu\text{mol}$ ) in THF of  $\text{C}_6\text{H}_5\text{F}$  (0.3 mL) was transferred via cannula to an NMR tube containing  $\text{PCy}_3$  (9.4 mg, 33.3  $\mu\text{mol}$ ). The tube was sealed and left to stand at ambient temperature for up to 48 h with intermittent monitored by  $^1\text{H}$  and  $^{31}\text{P}\{^1\text{H}\}$  NMR spectroscopy.

**$[\text{Ir}(\text{2,2'}$ -biphenyl)( $\text{PPh}_3$ ) $_2\text{Cl}]$  in THF:** Complex **7** was slowly consumed with concomitant liberation of  $\text{PPh}_3$  and mixed phosphine complex **39** ( $[\text{Cl}]^-$  salt);  $^{31}\text{P}\{^1\text{H}\}$  NMR (162 MHz, THF):  $\delta$  12.9 (d,  $^2J_{\text{PP}} = 365$ ,  $\text{PCy}_3$ ), 5.3 (d,  $^2J_{\text{PP}} = 365$   $\text{PPh}_3$ ).

**$[\text{Ir}(\text{2,2'}$ -biphenyl)( $\text{PPh}_3$ ) $_2][\text{BAr}^{\text{F}}_4]$  in THF:** Complex **16** in THF forms a dynamic mixture with a featureless  $^{31}\text{P}\{^1\text{H}\}$  NMR spectrum. Signals for complex **39** ( $[\text{BAr}^{\text{F}}_4]^-$  salt) and  $\text{PPh}_3$  increased in intensity over the following two days.

**$[\text{Rh}(\text{2,2'}$ -biphenyl)( $\text{PPh}_3$ ) $_2\text{Cl}]$  in THF:** Complex **3** is converted over a period of *ca.* 3 h with concomitant liberation of  $\text{PPh}_3$  to mixed phosphine chloride **40**;  $^{31}\text{P}\{^1\text{H}\}$  NMR (162 MHz, THF):  $\delta$  24.8 (dd,  $^2J_{\text{PP}} = 395$ ,  $^1J_{\text{RhP}} = 111$ ,  $\text{PCy}_3$ ) and 21.6 (dd,  $^2J_{\text{PP}} = 395$ ,  $^1J_{\text{RhP}} = 115$ ,  $\text{PPh}_3$ ).

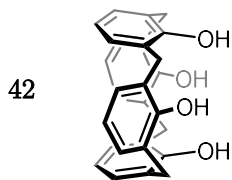
**$[\text{Rh}(\text{2,2'}$ -biphenyl)( $\text{PPh}_3$ ) $_2][\text{BAr}^{\text{F}}_4]$  in THF:** Complex **11** was converted to bis(tricyclohexylphosphine) complex **12** within 5 minutes.

**$[\text{Rh}(\text{2,2'}$ -biphenyl)( $\text{PPh}_3$ ) $_2][\text{Al}(\text{OR}^{\text{F}})_4]$  in  $\text{C}_6\text{H}_5\text{F}$ :** Complex **29** was converted to the  $[\text{Al}(\text{OR}^{\text{F}})_4]^-$  analogue of bis(tricyclohexylphosphine) complex **12** within 5 minutes.

## 6.3 $\text{C}_x\text{P}_2$

### 6.3.1 Ligand synthesis

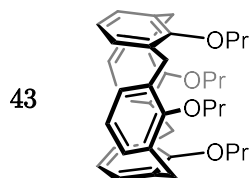
#### 6.3.1.1 25,26,27,28-tetrahydroxycalix[4]arene



Under dinitrogen; a suspension of *tert*-butylcalix[4]arene (30.0 g, 46.2 mmol), AlCl<sub>3</sub> (46.3 g, 347 mmol) and phenol (21.8 g, 231 mmol) in toluene (1 L) was stirred at ambient temperature for 5 h. In air; the reaction mixture was poured onto HCl<sub>(aq)</sub> (2 M, 800 mL), and extracted into CH<sub>2</sub>Cl<sub>2</sub> (800 mL), washed with H<sub>2</sub>O (3 × 400 mL), dried over Mg[SO<sub>4</sub>], and the solvent removed *in vacuo*. The crude residue was dissolved in CH<sub>2</sub>Cl<sub>2</sub> (50 mL) and the compound precipitated by the addition of MeOH (400 mL), which was isolated by filtration and dried *in vacuo*. Yield: 16.0 g (82%, white solid).

**<sup>1</sup>H NMR** (400 MHz, CDCl<sub>3</sub>): δ 10.19 (s, 4H, OH), 7.05 (d, <sup>3</sup>J<sub>HH</sub> = 7.6, 8H, *m*-Ar), 6.73 (t, <sup>3</sup>J<sub>HH</sub> = 7.6, 4H, *p*-Ar), 4.26 (br, 4H, CH<sub>2(ax)</sub>), 3.55 (br, 4H, CH<sub>2(eq)</sub>). **LR ESI-MS** (negative ion): 423.2 ([M-H]<sup>-</sup>, calcd 423.2) *m/z*. Data consistent with previous reports.<sup>296</sup>

#### 6.3.1.2 25,26,27,28-tetrapropoxycalix[4]arene

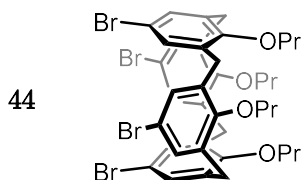


Under dinitrogen; to a solution of calix[4]arene **42** (16.0 g, 37.7 mmol) in DMF (1 L) was added PrI (29.4 mL, 302 mmol) and NaH (10.9 g, 452 mmol) and the reaction stirred for 18 h at 80 °C. In air, the suspension was poured onto H<sub>2</sub>O (1 L), extracted into CH<sub>2</sub>Cl<sub>2</sub> (1 L), washed with HCl<sub>(aq)</sub> (2 M, 2 × 1 L), dried over Mg[SO<sub>4</sub>], and the solvent removed *in vacuo*. and the crude residue dissolved in CH<sub>2</sub>Cl<sub>2</sub> (50 mL) and the compound precipitated by the addition of MeOH (400 mL), and the material isolated by filtration and dried *in vacuo*. Yield: 17.6 g (85%, white solid).

**<sup>1</sup>H NMR** (300 MHz, CDCl<sub>3</sub>): δ 6.68 – 6.49 (m, 12H, *m*-Ar & *p*-Ar), 4.46 (d, <sup>2</sup>J<sub>HH</sub> = 13.3, 4H, CH<sub>2(ax)</sub>), 3.85 (dd, <sup>3</sup>J<sub>HH</sub> = 8.0, 7.0, 8H, ArOCH<sub>2</sub>CH<sub>2</sub>CH<sub>3</sub>), 3.15 (d, <sup>2</sup>J<sub>HH</sub> = 13.4, 4H, CH<sub>2(eq)</sub>), 1.93 (app. h, <sup>3</sup>J<sub>HH</sub> = 7.5, 8H, ArOCH<sub>2</sub>CH<sub>2</sub>CH<sub>3</sub>), 1.00 (t, <sup>3</sup>J<sub>HH</sub> = 7.5, 12H, ArOCH<sub>2</sub>CH<sub>2</sub>CH<sub>3</sub>). **LR ESI-MS** (positive ion): 615.5 ([M+Na]<sup>+</sup>, calcd 615.3) *m/z*. Data consistent with previous reports.<sup>427</sup>



### 6.3.1.3 5,11,17,23-tetrabromo-25,26,27,28-tetrapropoxycalix[4]arene

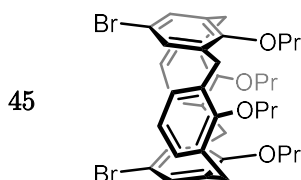


Under dinitrogen; a solution of **43** (4.10 g, 6.92 mmol) and N-bromosuccinamide (11.1 g, 62.2 mmol) in THF (250 mL) was stirred at ambient temperature for 24 h. The reaction mixture was poured onto  $\text{NaHSO}_3(\text{aq})$  (10 wt%, 250 mL), extracted into  $\text{CH}_2\text{Cl}_2$  (250 mL), washed with  $\text{H}_2\text{O}$  ( $2 \times 250$  mL) and dried over  $\text{Mg}[\text{SO}_4]$ . The solution was concentrated to 50 mL and the compound precipitated by the addition of MeOH (400 mL), isolated by filtration and dried *in vacuo*. Yield: 5.44 g (87%, white solid).

**$^1\text{H}$  NMR** (300 MHz,  $\text{CDCl}_3$ ):  $\delta$  6.80 (s, 8H, *m*-Ar), 4.35 (d, 4H,  $^2J_{\text{HH}} = 13.5$ ,  $\text{CH}_{2(\text{ax})}$ ), 3.80 (t,  $^3J_{\text{HH}} = 7.5$  8H,  $\text{ArOCH}_2\text{CH}_2\text{CH}_3$ ), 3.08 (d, 4H,  $^2J_{\text{HH}} = 13.5$ ,  $\text{CH}_{2(\text{eq})}$ ), 1.87 (app. h,  $^3J_{\text{HH}} = 7.4$ , 8H,  $\text{ArOCH}_2\text{CH}_2\text{CH}_3$ ), 0.96 (t,  $^3J_{\text{HH}} = 7.4$ , 12H,  $\text{ArOCH}_2\text{CH}_2\text{CH}_3$ ).

**LR ESI-MS** (positive ion): 931.1 ( $[\text{M}+\text{Na}]^+$ , calcd 931.0) *m/z*. Data consistent with previous reports.<sup>428</sup>

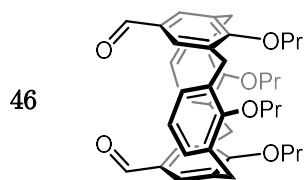
### 6.3.1.4 5,17-dibromo-25,26,27,28-tetrapropoxycalix[4]arene



Under dinitrogen; to a solution of **44** (22.0 g, 24.2 mmol) in THF (750 mL) cooled to  $-78^\circ\text{C}$  was added  $n\text{BuLi}$  (38.0 mL, 1.6 M in hexanes, 60.8 mmol) and the reaction stirred for 20 mins, then quenched with the addition of MeOH (100 mL). The mixture was warmed to ambient temperature, poured onto ice-cold  $\text{HCl}(\text{aq})$  (2 M, 750 mL), extracted into  $\text{CH}_2\text{Cl}_2$  (500 mL), washed with  $\text{H}_2\text{O}$  ( $2 \times 500$  mL), dried over  $\text{Mg}[\text{SO}_4]$ , and the solvent removed *in vacuo*. and the crude residue dissolved in  $\text{CH}_2\text{Cl}_2$  (50 mL) and the compound precipitated by the addition of MeOH (400 mL), and the material isolated by filtration and dried *in vacuo*. Yield: 12.4 g (68%, white solid).

**$^1\text{H}$  NMR** (300 MHz,  $\text{CDCl}_3$ ):  $\delta$  6.77 (s, 4H, *m*-Ar<sup>Br</sup>), 6.64 (s, 6H, *m*-Ar & *p*-Ar), 4.40 (d,  $^2J_{\text{HH}} = 13.4$ , 4H, ArCH<sub>2(ax)</sub>Ar<sup>Br</sup>), 3.82 (app. q,  $^3J_{\text{HH}} = 6.9$ , ArOCH<sub>2</sub>CH<sub>2</sub>CH<sub>3</sub> & Ar<sup>Br</sup>OCH<sub>2</sub>CH<sub>2</sub>CH<sub>3</sub>), 3.11 (d,  $^2J_{\text{HH}} = 13.4$ , 4H, ArCH<sub>2(eq)</sub>Ar<sup>Br</sup>), 1.91 (app. h,  $^3J_{\text{HH}} = 7.9$ , 8H, ArOCH<sub>2</sub>CH<sub>2</sub>CH<sub>3</sub> & Ar<sup>Br</sup>OCH<sub>2</sub>CH<sub>2</sub>CH<sub>3</sub>), 1.11 – 0.85 (m, 12H, ArOCH<sub>2</sub>CH<sub>2</sub>CH<sub>3</sub> & Ar<sup>Br</sup>OCH<sub>2</sub>CH<sub>2</sub>CH<sub>3</sub>). **LR ESI-MS** (positive ion): 773.3 ( $[\text{M}+\text{Na}]^+$ , calcd 773.2) *m/z*. Data consistent with previous reports.<sup>428</sup>

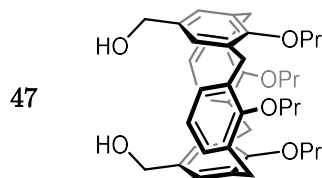
#### 6.3.1.5 5,17-diformyl-25,26,27,28-tetrapropoxycalix[4]arene



Under dinitrogen; to a solution of **45** (11.4 g, 15.2 mmol) in THF (500 mL) cooled to -78 °C was added *n*BuLi (38.0 mL, 1.6 M in hexanes, 60.8 mmol) and the reaction stirred for 15 mins, then quenched with the addition of DMF (25 mL, 304 mmol). The mixture was warmed to ambient temperature, poured onto ice-cold HCl<sub>(aq)</sub> (2 M, 500 mL), extracted into CH<sub>2</sub>Cl<sub>2</sub> (500 mL), washed with H<sub>2</sub>O (2 × 500 mL), dried over Mg[SO<sub>4</sub>], and the solvent removed *in vacuo*. The crude residue was dissolved in hot EtOH (100 mL), cooled to 4 °C and the precipitated material isolated by filtration and dried *in vacuo*. Yield: 6.40 g (65%, white solid).

**$^1\text{H}$  NMR** (300 MHz,  $\text{CDCl}_3$ ):  $\delta$  9.47 (s, 2H, CHO), 7.00 (s, 4H, *m*-Ar<sup>CHO</sup>), 6.85 – 6.61 (m, 6H, *m*-Ar & *p*-Ar), 4.47 (d,  $^2J_{\text{HH}} = 13.6$ , 4H, ArCH<sub>2(ax)</sub>Ar<sup>CHO</sup>), 4.01 – 3.68 (m, 8H, ArOCH<sub>2</sub>CH<sub>2</sub>CH<sub>3</sub> & Ar<sup>CHO</sup>OCH<sub>2</sub>CH<sub>2</sub>CH<sub>3</sub>), 3.23 (d,  $^2J_{\text{HH}} = 13.6$ , 4H, ArCH<sub>2(eq)</sub>Ar<sup>CHO</sup>), 2.00 – 1.84 (m, ArOCH<sub>2</sub>CH<sub>2</sub>CH<sub>3</sub> & Ar<sup>CHO</sup>OCH<sub>2</sub>CH<sub>2</sub>CH<sub>3</sub>), 1.11 – 1.90 (m, ArOCH<sub>2</sub>CH<sub>2</sub>CH<sub>3</sub> & Ar<sup>CHO</sup>OCH<sub>2</sub>CH<sub>2</sub>CH<sub>3</sub>). **LR ESI-MS** (positive ion): 671.4 ( $[\text{M}+\text{Na}]^+$ , calcd 671.3) *m/z*. Data consistent with previous reports.<sup>428</sup>

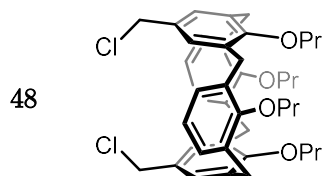
#### 6.3.1.6 5,17-bis(hydroxymethyl)-25,26,27,28-tetrapropoxycalix[4]arene



Under dinitrogen, to a solution of **46** (6.48 g, 10.0 mmol) in EtOH (200 mL) was added Na[BH<sub>4</sub>] (0.378 g, 10 mmol) and the reaction stirred at ambient temperature for 1.5 h. The solvent was removed in vacuo, and the crude mixture extracted into CH<sub>2</sub>Cl<sub>2</sub> (100 mL), washed with HCl<sub>(aq)</sub> (2 M, 2 × 100 mL), H<sub>2</sub>O (2 × 100 mL), dried over Mg[SO<sub>4</sub>] and the solvent removed *in vacuo*. The compound was purified by flash column chromatography (SiO<sub>2</sub>; 2:2:3 CH<sub>2</sub>Cl<sub>2</sub>:EtOAc:hexane). Yield: 6.11 g (93%, white solid).

**<sup>1</sup>H NMR** (300 MHz, CDCl<sub>3</sub>): δ 6.92 (d, <sup>3</sup>J<sub>HH</sub> = 7.3, 4H, *m*-Ar), 6.79 (t, <sup>3</sup>J<sub>HH</sub> = 7.2, 2H, *p*-Ar), 6.38 (s, 4H, *m*-Ar<sup>OH</sup>), 4.46 (d, <sup>2</sup>J<sub>HH</sub> = 13.2, 4H, ArCH<sub>2(ax)</sub>Ar<sup>OH</sup>), 4.16 (s, 4H, CH<sub>2</sub>OH), 3.98 (t, <sup>3</sup>J<sub>HH</sub> = 7.8, 4H, ArOCH<sub>2</sub>CH<sub>2</sub>CH<sub>3</sub>), 3.73 (t, <sup>3</sup>J<sub>HH</sub> = 6.8, 4H, Ar<sup>OH</sup>OCH<sub>2</sub>CH<sub>2</sub>CH<sub>3</sub>), 3.15 (d, <sup>2</sup>J<sub>HH</sub> = 13.3, 4H, ArCH<sub>2(eq)</sub>Ar<sup>OH</sup>), 2.06 – 1.83 (m, 8H, ArOCH<sub>2</sub>CH<sub>2</sub>CH<sub>3</sub> & Ar<sup>OH</sup>OCH<sub>2</sub>CH<sub>2</sub>CH<sub>3</sub>), 1.59 (s, 2H, OH), 1.05 (t, <sup>3</sup>J<sub>HH</sub> = 7.3, 6H, Ar<sup>OH</sup>OCH<sub>2</sub>CH<sub>2</sub>CH<sub>3</sub>), 0.94 (t, <sup>3</sup>J<sub>HH</sub> = 7.4, 6H, ArOCH<sub>2</sub>CH<sub>2</sub>CH<sub>3</sub>). **LR ESI-MS** (positive ion): 675.5 ([M+Na]<sup>+</sup>, calcd 675.4) *m/z*. **LR ESI-MS** (negative ion): 651.4 ([M-H]<sup>-</sup>, calcd 651.4) *m/z*. Data consistent with previous reports.<sup>429,430</sup>

#### 6.3.1.7 5,17-bis(chloromethyl)-25,26,27,28-tetrapropoxycalix[4]arene

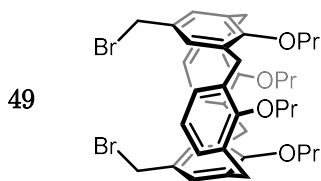


Under dinitrogen, to a solution of **47** (1.31 g, 2.00 mmol) in CH<sub>2</sub>Cl<sub>2</sub> (25 mL) cooled to -78 °C was added SOCl<sub>2</sub> (0.44 mL, 6.0 mmol) dropwise. The reaction was stirred for 30 mins while warming to ambient temperature and then stirred for a further 2 h. The volatiles were removed *in vacuo* and the crude material washed with ice cold pentane

(10 mL) and purified by crystallisation from hot pentane (*ca.* 250 mL), with additional material obtained by concentrating the supernatant. Yield: 1.20 g (87%, white solid).

**$^1\text{H}$  NMR** (300 MHz,  $\text{CDCl}_3$ ):  $\delta$  6.71 – 6.61 (m, 6H. *m*-Ar and *p*-Ar), 6.58 (s, 4H, m-Ar<sup>Cl</sup>), 4.43 (d,  $^2J_{\text{HH}} = 13.3$ , 4H,  $\text{CH}_{2(\text{ax})}$ ), 4.24 (s, 4H,  $\text{CH}_2\text{Cl}$ ), 3.87 (t,  $^3J_{\text{HH}} = 7.5$ , 4H,  $\text{ArOCH}_2\text{CH}_2\text{CH}_3$ ), 3.82 (t,  $^3J_{\text{HH}} = 7.5$ , 4H,  $\text{Ar}^{\text{Cl}}\text{OCH}_2\text{CH}_2\text{CH}_3$ ), 3.14 (d,  $^2J_{\text{HH}} = 13.4$ , 4H,  $\text{CH}_{2(\text{eq})}$ ), 1.91 (app. h,  $^3J_{\text{HH}} = 7.3$ , 8H,  $\text{ArOCH}_2\text{CH}_2\text{CH}_3$  &  $\text{Ar}^{\text{Cl}}\text{OCH}_2\text{CH}_2\text{CH}_3$ ), 0.99 (app. q,  $^3J_{\text{HH}} = 7.6$ , 12H,  $\text{ArOCH}_2\text{CH}_2\text{CH}_3$  &  $\text{Ar}^{\text{Cl}}\text{OCH}_2\text{CH}_2\text{CH}_3$ ). **LR ESI-MS** (positive ion): 711.5 ( $[\text{M}+\text{Na}]^+$ , calcd 711.3) *m/z*. Data consistent with previous reports.<sup>353</sup>

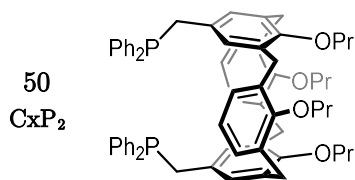
#### 6.3.1.8 5,17-bis(bromomethyl)-25,26,27,28-tetrapropoxycalix[4]arene



Under dinitrogen, to a solution of **47** (2.00 g, 3.06 mmol) in  $\text{CH}_2\text{Cl}_2$  (250 mL) was added  $\text{PBr}_3$  (0.316 mL, 63.4 mmol) dropwise. The reaction was stirred for 10 mins, then washed with  $\text{NaHCO}_{3(\text{aq})}$  (satd.,  $3 \times 250$  mL), extracted into additional  $\text{CH}_2\text{Cl}_2$  ( $3 \times 50$  mL), washed with  $\text{H}_2\text{O}$  ( $3 \times 250$  mL), dried over  $\text{Mg}[\text{SO}_4]$  and dried *in vacuo*. Yield: 2.25 g (93%, white solid).

**$^1\text{H}$  NMR** (300 MHz,  $\text{CDCl}_3$ ):  $\delta$  6.69 – 6.61 (m, 6H. *m*-Ar and *p*-Ar), 6.59 (s, 4H, m-Ar<sup>Br</sup>), 4.41 (d,  $^2J_{\text{HH}} = 13.5$ , 4H,  $\text{CH}_{2(\text{ax})}$ ), 4.17 (s, 4H,  $\text{CH}_2\text{Br}$ ), 3.83 (app. q,  $^3J_{\text{HH}} = 7.8$ , 8H,  $\text{ArOCH}_2\text{CH}_2\text{CH}_3$  &  $\text{Ar}^{\text{Br}}\text{OCH}_2\text{CH}_2\text{CH}_3$ ), 3.13 (d,  $^2J_{\text{HH}} = 13.4$ , 4H,  $\text{CH}_{2(\text{eq})}$ ), 2.03 – 1.80 (m, 8H,  $\text{ArOCH}_2\text{CH}_2\text{CH}_3$  &  $\text{Ar}^{\text{Br}}\text{OCH}_2\text{CH}_2\text{CH}_3$ ), 0.98 (app. q,  $^3J_{\text{HH}} = 7.5$ , 12H,  $\text{ArOCH}_2\text{CH}_2\text{CH}_3$  &  $\text{Ar}^{\text{Br}}\text{OCH}_2\text{CH}_2\text{CH}_3$ ). **LR ESI-MS** (positive ion): 801.3 ( $[\text{M}+\text{Na}]^+$ , calcd 801.2) *m/z*. Data consistent with previous reports.<sup>429</sup>

### 6.3.1.9 5,17-bis(diphenylphosphinomethyl)-25,26,27,28-tetrapropoxycalix[4]arene



**Method A:** To a solution of **48** (1.0 g, 1.5 mmol) in THF (25 mL) cooled to -78 °C was added a solution of KPPH<sub>2</sub> (0.5 M in THF, 8.7 mL) dropwise with stirring. The reaction was warmed to ambient temperature overnight then refluxed at 70 °C for 2 h. The resulting suspension was washed with [NH<sub>4</sub>]Cl<sub>(aq)</sub> (satd., 3 × 30 mL, argon-sparged), H<sub>2</sub>O (3 × 30 mL, argon-sparged), then dried over Mg[SO<sub>4</sub>] and filtered. The solution volume was reduced to *ca.* 5 mL *in vacuo* and the compound precipitated by slow diffusion of excess hexane (*ca.* 100 mL). Additional material was obtained by concentrating the supernatant to *ca.* 50 mL *in vacuo*. The compound was isolated by filtration and the combined batches dried *in vacuo*. Yield = 1.00 g (70%, white crystalline solid)

**Method B:** To solution of **49** (0.45 g, 0.58 mmol) in THF (15 mL) cooled to -78 °C was added a solution of KPPH<sub>2</sub> (0.5 M in THF, 3.5 mL) dropwise with stirring. The reaction was warmed to ambient temperature overnight and the resulting suspension washed with [NH<sub>4</sub>]Cl<sub>(aq)</sub> (satd., 3 × 20 mL, argon-sparged), H<sub>2</sub>O (3 × 20 mL, argon-sparged), then dried over Mg[SO<sub>4</sub>] and filtered. The solution volume was reduced to *ca.* 5 mL *in vacuo* and the compound precipitated by slow diffusion of excess hexane (*ca.* 100 mL). Additional material was obtained by concentrating the supernatant to *ca.* 50 mL *in vacuo*. The compound was isolated by filtration and the combined batches dried under high vacuum. Yield = 463 mg (81%, white microcrystalline solid)

**<sup>1</sup>H NMR** (500 MHz, CDCl<sub>3</sub>): δ 7.47 – 7.41 (m, 8H, *o*-Ph), 7.37 – 7.33 (m, 12H, *m*-Ph & *p*-Ph), 6.75 (s, 4H, *m*-Ar<sup>P</sup>), 6.17 (t, <sup>3</sup>J<sub>HH</sub> = 7.5, 2H, *p*-Ar), 5.88 (d, <sup>3</sup>J<sub>HH</sub> = 7.6, 4H, *m*-Ar), 4.31 (d, <sup>2</sup>J<sub>HH</sub> = 13.2, 4H, ArCH<sub>2(ax)</sub>Ar<sup>P</sup>), 3.89 (t, <sup>3</sup>J<sub>HH</sub> = 6.8, 4H, Ar<sup>P</sup>OCH<sub>2</sub>CH<sub>2</sub>CH<sub>3</sub>), 3.62 (t, <sup>3</sup>J<sub>HH</sub> = 6.8, 4H, ArOCH<sub>2</sub>CH<sub>2</sub>CH<sub>3</sub>), 3.37 (s, 4H, CH<sub>2</sub>P), 2.96 (d, <sup>2</sup>J<sub>HH</sub> = 13.3, 4H, ArCH<sub>2(eq)</sub>Ar<sup>P</sup>), 1.89 (app. sex, <sup>3</sup>J<sub>HH</sub> = 8.0, 4H, Ar<sup>P</sup>OCH<sub>2</sub>CH<sub>2</sub>CH<sub>3</sub>),

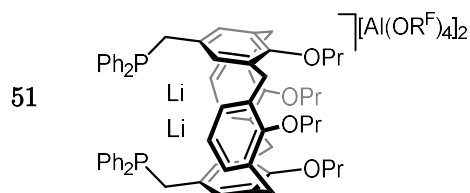
1.84 (app. sex,  $^3J_{\text{HH}} = 7.2$ , 4H,  $\text{ArOCH}_2\text{CH}_2\text{CH}_3$ ), 1.05 (t,  $^3J_{\text{HH}} = 7.4$ , 6H,  $\text{Ar}^{\text{P}}\text{OCH}_2\text{CH}_2\text{CH}_3$ ), 0.88 (t,  $^3J_{\text{HH}} = 7.5$ , 6H,  $\text{ArOCH}_2\text{CH}_2\text{CH}_3$ ).  $^{13}\text{C}\{\text{H}\}$  NMR ( $\text{CD}_2\text{Cl}_2$ , 126 MHz):  $\delta$  156.5 (s,  $i\text{-Ar}^{\text{P}}$ ), 155.9 (s,  $i\text{-Ar}$ ), 139.4 (d,  $^1J_{\text{PC}} = 16$ ,  $i\text{-Ph}$ ), 137.0 (s,  $o\text{-Ar}^{\text{P}}$ ), 133.9 (s,  $o\text{-Ar}$ ), 133.5 (d,  $^2J_{\text{PC}} = 19$ ,  $o\text{-Ph}$ ), 130.6 (d,  $^2J_{\text{PC}} = 7$ ,  $p\text{-Ar}^{\text{P}}$ ), 130.2 (d,  $^3J_{\text{PC}} = 7$ ,  $m\text{-Ar}^{\text{P}}$ ), 129.1 (s,  $p\text{-Ph}$ ), 128.9 (d,  $^2J_{\text{PC}} = 6$ ,  $m\text{-Ph}$ ), 127.9 (s,  $p\text{-Ar}$ ), 122.4 (s,  $m\text{-Ar}$ ), 77.4 (s,  $\text{ArOCH}_2\text{CH}_2\text{CH}_3$ ), 77.0 (s,  $\text{Ar}^{\text{P}}\text{OCH}_2\text{CH}_2\text{CH}_3$ ), 35.4 (d,  $^1J_{\text{PC}} = 15$ ,  $\text{CH}_2\text{P}$ ), 31.3 (s,  $\text{ArCH}_2\text{Ar}^{\text{P}}$ ), 24.0 (s,  $\text{ArOCH}_2\text{CH}_2\text{CH}_3$ ), 23.6 (s,  $\text{Ar}^{\text{P}}\text{OCH}_2\text{CH}_2\text{CH}_3$ ), 11.1 (s,  $\text{ArOCH}_2\text{CH}_2\text{CH}_3$ ), 10.3 (s,  $\text{Ar}^{\text{P}}\text{OCH}_2\text{CH}_2\text{CH}_3$ ).  $^{31}\text{P}\{\text{H}\}$  NMR ( $\text{CD}_2\text{Cl}_2$ , 162 MHz):  $\delta$  -10.6 (s). **LR ESI-MS** (positive ion): 1097.2 ( $[\text{M}+\text{Ag}]^+$ , calcd 1097.4)  $m/z$ . Data consistent with previous reports.<sup>353</sup>

### 6.3.2 Preparation of $\text{M}[\text{CxP}_2][\text{anion}]$

#### 6.3.2.1 General procedure

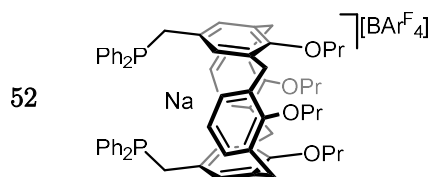
A suspension of  $\text{CxP}_2$  (9.9 mg, 10.0  $\mu\text{mol}$ ) of  $\text{M}[\text{anion}]$  (10.0  $\mu\text{mol}$ ) in  $\text{CH}_2\text{Cl}_2$  was mixed for 10 mins and dried *in vacuo* to afford the title compounds quantitatively as white solids. A stoichiometric mixture of  $\text{Li}[\text{Al}(\text{OR}^{\text{F}})_4]$  (9.8 mg, 10.0  $\mu\text{mol}$ ) and  $\text{CxP}_2$  (9.9 mg, 10.0  $\mu\text{mol}$ ) in  $\text{CH}_2\text{Cl}_2$  was found after 18 h to have converted to a 1:1 mixture of  $\text{CxP}_2$  and the title compound. Addition of a second equivalent of  $\text{Li}[\text{Al}(\text{OR}^{\text{F}})_4]$  afforded the title compound quantitatively. In separate reactions, addition of excess salts (up to 5.0 equivalents) resulted in no appreciable uptake of second cation, with the exception of thallium salt **54**, where limited spectroscopic and solid-state evidence exists for the formation of a di-cation. Addition of 10 equivalents of  $\text{Tl}[\text{BAr}^{\text{F}}_4]$  results in partial conversion (*ca.* 25%) to a third species, speculatively formulated as the tri-cation.

#### 6.3.2.2 $[\text{Li}_2(\text{CxP}_2)][\text{Al}(\text{OR}^{\text{F}})_4]_2$



**$^1\text{H}$  NMR** (500 MHz,  $\text{CDCl}_3$ ):  $\delta$  7.38 – 7.31 (m, 12H, *o*-Ph & *p*-Ph), 7.31 – 7.25 (m, 8H, *m*-Ph), 6.84 (s, 4H, *m*-Ar<sup>P</sup>), 6.84 – 6.77 (m, 4H, *p*-Ar & *m*-Ar), 4.19 (d,  $^2J_{\text{HH}} = 12.9$ , 4H ArCH<sub>2(ax)</sub>Ar<sup>P</sup>), 4.17 – 4.06 (m, 8H, Ar<sup>P</sup>OCH<sub>2</sub>CH<sub>2</sub>CH<sub>3</sub> & ArOCH<sub>2</sub>CH<sub>2</sub>CH<sub>3</sub>), 3.33 (d,  $^2J_{\text{HH}} = 12.9$ , 4H, ArCH<sub>2(eq)</sub>Ar<sup>P</sup>), 3.28 (s, 4H, CH<sub>2</sub>P), 2.03 – 1.92 (m, 12H, Ar<sup>P</sup>OCH<sub>2</sub>CH<sub>2</sub>CH<sub>3</sub> & ArOCH<sub>2</sub>CH<sub>2</sub>CH<sub>3</sub>), 1.10 – 1.10 (m, 12H, ArOCH<sub>2</sub>CH<sub>2</sub>CH<sub>3</sub> & Ar<sup>P</sup>OCH<sub>2</sub>CH<sub>2</sub>CH<sub>3</sub>).  **$^{13}\text{C}\{^1\text{H}\}$  NMR** ( $\text{CD}_2\text{Cl}_2$ , 126 MHz):  $\delta$  150.2 (s, *i*-Ar), 148.5 (s, *i*-Ar<sup>P</sup>), 138.4 (d,  $^1J_{\text{PC}} = 14$ , *i*-Ph), 137.4 (d,  $^2J_{\text{PC}} = 8$ , *p*-Ar<sup>P</sup>), 135.9 (s, *o*-Ar<sup>P</sup>), 135.7 (s, *o*-Ar), 133.4 (d,  $^2J_{\text{PC}} = 19$ , *o*-Ph), 131.2 (d,  $^3J_{\text{PC}} = 7$ , *m*-Ar<sup>P</sup>), 130.2, (s, *m*-Ar), 129.5, (s, *p*-Ph), 129.0 (d,  $^3J_{\text{PC}} = 7$ , *m*-Ph), 127.6 (s, *p*-Ar), 121.8 (q,  $^1J_{\text{FC}} = 293$ , CF<sub>3</sub>), 79.5 (s, ArOCH<sub>2</sub>CH<sub>2</sub>CH<sub>3</sub>), 79.4 (s, Ar<sup>P</sup>OCH<sub>2</sub>CH<sub>2</sub>CH<sub>3</sub>), 35.3 (d,  $^1J_{\text{PC}} = 17$ , CH<sub>2</sub>P), 31.8 (s, ArCH<sub>2</sub>Ar<sup>P</sup>), 23.5 (s, ArOCH<sub>2</sub>CH<sub>2</sub>CH<sub>3</sub>), 23.3 (s, Ar<sup>P</sup>OCH<sub>2</sub>CH<sub>2</sub>CH<sub>3</sub>), 9.9 (s, ArOCH<sub>2</sub>CH<sub>2</sub>CH<sub>3</sub>), 9.8 (s, Ar<sup>P</sup>OCH<sub>2</sub>CH<sub>2</sub>CH<sub>3</sub>).  **$^{31}\text{P}\{^1\text{H}\}$  NMR** ( $\text{CD}_2\text{Cl}_2$ , 162 MHz):  $\delta$  -10.3 (s).<sup>†</sup>

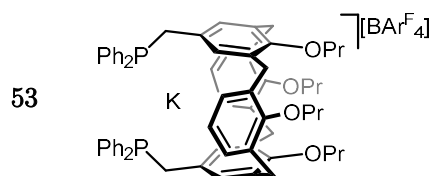
### 6.3.2.3 $[\text{Na}(\text{C}_x\text{P}_2)][\text{BAr}^{\text{F}}_4]$



**$^1\text{H}$  NMR** (500 MHz,  $\text{CD}_2\text{Cl}_2$ ):  $\delta$  7.75 – 7.70 (m, 8H, *o*-Ar<sup>F</sup>), 7.55 (br, 4H, *p*-Ar<sup>F</sup>), 7.38 (t,  $J = 7.4$ , 8H, *o*-Ph), 7.36 – 7.28 (m, 12H, *p*-Ph & *m*-Ph), 6.91 (s, 4H, *m*-Ar<sup>P</sup>), 6.70 (t,  $^3J_{\text{HH}} = 7.5$ , 2H, *p*-Ar), 6.61 (d,  $^3J_{\text{HH}} = 7.6$ , 4H, *m*-Ar), 4.25 (d,  $^2J_{\text{HH}} = 13.3$ , 4H, ArCH<sub>2(ax)</sub>Ar<sup>P</sup>), 4.02 – 3.95 (m, 4H, ArOCH<sub>2</sub>CH<sub>2</sub>CH<sub>3</sub>), 3.93 – 3.84 (m, 4H, Ar<sup>P</sup>OCH<sub>2</sub>CH<sub>2</sub>CH<sub>3</sub>), 3.34 (s, 4H, CH<sub>2</sub>P), 3.32 (d,  $^2J_{\text{HH}} = 13.4$ , 4H, ArCH<sub>2(eq)</sub>Ar<sup>P</sup>), 1.96 – 1.86 (m, 8H, Ar<sup>P</sup>OCH<sub>2</sub>CH<sub>2</sub>CH<sub>3</sub> & ArOCH<sub>2</sub>CH<sub>2</sub>CH<sub>3</sub>), 1.04 (t,  $^3J_{\text{HH}} = 7.4$ , 6H, ArOCH<sub>2</sub>CH<sub>2</sub>CH<sub>3</sub>), 0.99 (t,  $^3J_{\text{HH}} = 7.4$ , 6H, Ar<sup>P</sup>OCH<sub>2</sub>CH<sub>2</sub>CH<sub>3</sub>).  **$^{13}\text{C}\{^1\text{H}\}$  NMR** ( $\text{CD}_2\text{Cl}_2$ , 126 MHz):  $\delta$  162.3 (q,  $^1J_{\text{CB}} = 50$ , *i*-Ar<sup>F</sup>), 152.3 (s, *i*-Ar), 149.7 (s, *i*-Ar<sup>P</sup>), 138.5 (d,  $^1J_{\text{PC}} = 15$ , *i*-Ph), 136.6 (d,  $^2J_{\text{PC}} = 8$ , *p*-Ar<sup>P</sup>), 136.4 (s, *o*-Ar<sup>P</sup>), 135.8 (s, *o*-Ar), 135.4 (s, *o*-Ar<sup>F</sup>), 133.4 (d,  $^2J_{\text{PC}} = 14$ , *o*-Ph), 131.5 (d,  $^3J_{\text{PC}} = 7$ , *m*-Ar<sup>P</sup>), 129.8 (s, *p*-Ph), 129.5 (s, *m*-Ar), 129.4 (qq,  $^2J_{\text{FC}} = 32$ ,  $^3J_{\text{CB}} = 3$ , *m*-Ar<sup>F</sup>), 128.9 (d,  $^3J_{\text{PC}} = 7$ , *m*-Ph), 126.4 (s, *p*-Ar), 125.2 (q,  $^1J_{\text{FC}} = 272$ , CF<sub>3</sub>), 118.0 (sept,  $^3J_{\text{FC}} = 4$ , *p*-Ar<sup>F</sup>), 79.7 (s,

ArOCH<sub>2</sub>CH<sub>2</sub>CH<sub>3</sub>), 79.5 (s, Ar<sup>P</sup>OCH<sub>2</sub>CH<sub>2</sub>CH<sub>3</sub>), 35.3 (d, <sup>2</sup>J<sub>PC</sub> = 16, CH<sub>2</sub>P), 30.7 (s, ArCH<sub>2</sub>Ar<sup>P</sup>), 23.9 (s, ArOCH<sub>2</sub>CH<sub>2</sub>CH<sub>3</sub>), 23.6 (s, Ar<sup>P</sup>OCH<sub>2</sub>CH<sub>2</sub>CH<sub>3</sub>), 10.2 (s, ArOCH<sub>2</sub>CH<sub>2</sub>CH<sub>3</sub>), 9.8 (s, Ar<sup>P</sup>OCH<sub>2</sub>CH<sub>2</sub>CH<sub>3</sub>). **<sup>31</sup>P{<sup>1</sup>H} NMR** (CD<sub>2</sub>Cl<sub>2</sub>, 162 MHz): δ -9.9 (s). **HR ESI-MS** (positive ion): 1011.4629 ([M]<sup>+</sup>, calcd 1011.4642) *m/z*. **Anal.** Calcd for C<sub>98</sub>H<sub>82</sub>BF<sub>24</sub>NaO<sub>4</sub>P<sub>2</sub> (1875.44 g·mol<sup>-1</sup>): C, 62.76; H, 4.41; N, 0.00. Found: C, 62.68; H, 4.50; N, 0.00.

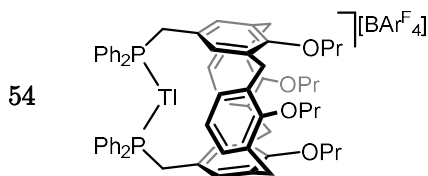
#### 6.3.2.4 [K(CxP<sub>2</sub>)] [BAr<sup>F</sup><sub>4</sub>]



**<sup>1</sup>H NMR** (500 MHz, CD<sub>2</sub>Cl<sub>2</sub>): δ 7.75 – 7.70 (m, 8H, *o*-Ar<sup>F</sup>), 7.55 (br, 4H, *p*-Ar<sup>F</sup>), 7.38 (t, <sup>3</sup>J<sub>HH</sub> = 7.2, 4H, *p*-Ph), 7.33 (t, <sup>3</sup>J<sub>HH</sub> = 7.3, 8H, *m*-Ph), 7.28 (app. t, <sup>3</sup>J<sub>HH</sub> = 7.3, 8H, *o*-Ph), 6.83 – 6.79 (m, 4H, *p*-Ar), 6.78 – 7.73 (m, 8H, *m*-Ar & *m*-Ar<sup>P</sup>), 4.42 (d, <sup>2</sup>J<sub>HH</sub> = 13.4, 4H, ArCH<sub>2(ax)</sub>Ar<sup>P</sup>), 4.13 – 4.08 (m, 4H, ArOCH<sub>2</sub>CH<sub>2</sub>CH<sub>3</sub>), 4.02 – 3.96 (m, 4H, Ar<sup>P</sup>OCH<sub>2</sub>CH<sub>2</sub>CH<sub>3</sub>), 3.31 (d, <sup>2</sup>J<sub>HH</sub> = 13.4, 4H, ArCH<sub>2(eq)</sub>Ar<sup>P</sup>), 3.26 (s, 4H, CH<sub>2</sub>P), 1.96 – 1.85 (m, 8H, Ar<sup>P</sup>OCH<sub>2</sub>CH<sub>2</sub>CH<sub>3</sub> & ArOCH<sub>2</sub>CH<sub>2</sub>CH<sub>3</sub>), 0.99 (app. q, <sup>3</sup>J<sub>HH</sub> = 7.5, Ar<sup>P</sup>OCH<sub>2</sub>CH<sub>2</sub>CH<sub>3</sub> & ArOCH<sub>2</sub>CH<sub>2</sub>CH<sub>3</sub>). **<sup>13</sup>C{<sup>1</sup>H} NMR** (CD<sub>2</sub>Cl<sub>2</sub>, 126 MHz): δ 162.3 (q, <sup>1</sup>J<sub>CB</sub> = 50, *i*-Ar<sup>F</sup>), 155.6 (s, *i*-Ar), 142.8 (s, *i*-Ar<sup>P</sup>), 138.1 (d, <sup>1</sup>J<sub>PC</sub> = 14, *i*-Ph), 136.5 (d, <sup>2</sup>J<sub>PC</sub> = 9, *p*-Ar<sup>P</sup>), 136.0 (s, *o*-Ar<sup>P</sup>), 135.7 (s, *o*-Ar), 135.4 (s, *o*-Ar<sup>F</sup>), 133.3 (d, <sup>2</sup>J<sub>PC</sub> = 19, *o*-Ph), 131.5 (d, <sup>3</sup>J<sub>PC</sub> = 6, *m*-Ar<sup>P</sup>), 130.6 (s, *p*-Ph), 129.7 (s, *m*-Ar), 129.4 (qq, <sup>2</sup>J<sub>FC</sub> = 32, <sup>3</sup>J<sub>CB</sub> = 3, *m*-Ar<sup>F</sup>), 129.2 (d, <sup>3</sup>J<sub>PC</sub> = 7, *m*-Ph), 125.8 (s, *p*-Ar), 125.2 (q, <sup>1</sup>J<sub>FC</sub> = 272, CF<sub>3</sub>), 118.0 (sept, <sup>3</sup>J<sub>FC</sub> = 4, *p*-Ar<sup>F</sup>), 78.7 (s, ArOCH<sub>2</sub>CH<sub>2</sub>CH<sub>3</sub>), 78.2 (s, Ar<sup>P</sup>OCH<sub>2</sub>CH<sub>2</sub>CH<sub>3</sub>), 35.5 (d, <sup>2</sup>J<sub>PC</sub> = 16, CH<sub>2</sub>P), 31.4 (s, ArCH<sub>2</sub>Ar<sup>P</sup>), 23.5 (s, ArOCH<sub>2</sub>CH<sub>2</sub>CH<sub>3</sub>), 23.3 (s, Ar<sup>P</sup>OCH<sub>2</sub>CH<sub>2</sub>CH<sub>3</sub>), 10.4 (s, ArOCH<sub>2</sub>CH<sub>2</sub>CH<sub>3</sub>), 10.3 (s, Ar<sup>P</sup>OCH<sub>2</sub>CH<sub>2</sub>CH<sub>3</sub>). **<sup>31</sup>P{<sup>1</sup>H} NMR** (CD<sub>2</sub>Cl<sub>2</sub>, 162 MHz): δ -8.3 (s). **HR ESI-MS** (positive ion): 989.4814 ([M-K+H]<sup>+</sup>, calcd 989.4822) *m/z*. **Anal.** Calcd for C<sub>98</sub>H<sub>82</sub>BF<sub>24</sub>KO<sub>4</sub>P<sub>2</sub> (1891.55 g·mol<sup>-1</sup>): C, 62.23; H, 4.37; N, 0.00. Found: C, 61.99; H, 4.28; N, 0.00.



### 6.3.2.5 [Tl(CxP<sub>2</sub>)] [BAr<sup>F</sup><sub>4</sub>]

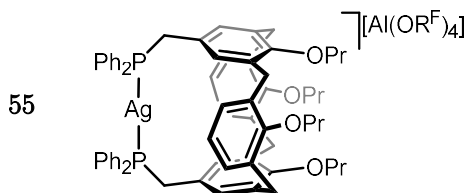


**<sup>1</sup>H NMR** (500 MHz, CD<sub>2</sub>Cl<sub>2</sub>): δ 7.75 – 7.70 (m, 8H, *o*-Ar<sup>F</sup>), 7.55 (br, 4H, *p*-Ar<sup>F</sup>), 7.38 (t, <sup>3</sup>*J*<sub>HH</sub> = 6.5, 4H, *p*-Ph), 7.32 (t, <sup>3</sup>*J*<sub>HH</sub> = 7.2, 8H, *m*-Ph), 7.28 (t, <sup>3</sup>*J*<sub>HH</sub> = 7.1, 8H, *o*-Ph), 6.87 – 6.81 (m, 6H, *p*-Ar & *m*-Ar<sup>P</sup>), 6.76 (d, <sup>3</sup>*J*<sub>HH</sub> = 8.0, 4H, *m*-Ar), 4.42 (d, <sup>2</sup>*J*<sub>HH</sub> = 13.0, 4H, ArCH<sub>2(ax)</sub>Ar<sup>P</sup>), 4.07 – 4.02 (m, 8H, Ar<sup>P</sup>OCH<sub>2</sub>CH<sub>2</sub>CH<sub>3</sub> & ArOCH<sub>2</sub>CH<sub>2</sub>CH<sub>3</sub>), 3.33 – 3.22 (m, 8H, CH<sub>2</sub>P & ArCH<sub>2(eq)</sub>Ar<sup>P</sup>), 2.03 – 1.85 (m, 12H, Ar<sup>P</sup>OCH<sub>2</sub>CH<sub>2</sub>CH<sub>3</sub> & ArOCH<sub>2</sub>CH<sub>2</sub>CH<sub>3</sub>), 1.00 (app. q, <sup>3</sup>*J*<sub>HH</sub> = 7.4, 12H, Ar<sup>P</sup>OCH<sub>2</sub>CH<sub>2</sub>CH<sub>3</sub> & ArOCH<sub>2</sub>CH<sub>2</sub>CH<sub>3</sub>).

**<sup>13</sup>C{<sup>1</sup>H} NMR** (CD<sub>2</sub>Cl<sub>2</sub>, 126 MHz): δ 162.3 (q, <sup>1</sup>*J*<sub>CB</sub> = 50, *i*-Ar<sup>F</sup>), 156.9 (d, <sup>1</sup>*J*<sub>TIC</sub> = 59, *i*-Ar<sup>P</sup>), 154.7 (d, <sup>1</sup>*J*<sub>TIC</sub> = 58, *i*-Ar), 138.1 (dd, 1*J*<sub>PC</sub> = 40, 2*J*<sub>TIC</sub> = 8, *i*-Ph), 136.1 (br d, 1*J*<sub>TIC</sub> = 60, *p*-Ar<sup>P</sup>), 135.4 (s, *o*-Ar<sup>F</sup>), 133.3 (dd, <sup>2</sup>*J*<sub>PC</sub> = 19, <sup>3</sup>*J*<sub>TIC</sub> = 6, *o*-Ph), 131.5 (dd, <sup>1</sup>*J*<sub>TIC</sub> = 58, <sup>3</sup>*J*<sub>PC</sub> = 6, *m*-Ar<sup>P</sup>), 130.9 (d, <sup>1</sup>*J*<sub>TIC</sub> = 57, *m*-Ar), 129.8 (s, *p*-Ph), 129.4 (qq, <sup>2</sup>*J*<sub>FC</sub> = 32, <sup>3</sup>*J*<sub>CB</sub> = 3, *m*-Ar<sup>F</sup>), 129.2 (br. d, <sup>3</sup>*J*<sub>PC</sub> = 5, *m*-Ph), 125.7 (d, <sup>1</sup>*J*<sub>TIC</sub> = 61, *p*-Ar), 125.2 (q, <sup>1</sup>*J*<sub>FC</sub> = 272, CF<sub>3</sub>), 118.0 (sept, <sup>3</sup>*J*<sub>FC</sub> = 4, *p*-Ar<sup>F</sup>), 78.7 – 78.3 (m, Ar<sup>P</sup>OCH<sub>2</sub>CH<sub>2</sub>CH<sub>3</sub> & ArOCH<sub>2</sub>CH<sub>2</sub>CH<sub>3</sub>), 35.2 – 34.7 (m, CH<sub>2</sub>P), 31.5 (d, *J*<sub>TIC</sub> = 19, ArCH<sub>2</sub>Ar<sup>P</sup>), 23.5 (s, Ar<sup>P</sup>OCH<sub>2</sub>CH<sub>2</sub>CH<sub>3</sub> & ArOCH<sub>2</sub>CH<sub>2</sub>CH<sub>3</sub> coincident), 10.4 (s, Ar<sup>P</sup>OCH<sub>2</sub>CH<sub>2</sub>CH<sub>3</sub>), 10.3 (s, ArOCH<sub>2</sub>CH<sub>2</sub>CH<sub>3</sub>). The *o*-Ar<sup>P</sup> and *o*-Ar signals could not be unambiguously located.

**<sup>31</sup>P{<sup>1</sup>H} NMR** (CD<sub>2</sub>Cl<sub>2</sub>, 162 MHz): δ -4.9, (d, <sup>1</sup>*J*<sub>TIP</sub> = 386)

### 6.3.2.6 [Ag(CxP<sub>2</sub>)] [Al(OR<sup>F</sup>)<sub>4</sub>]

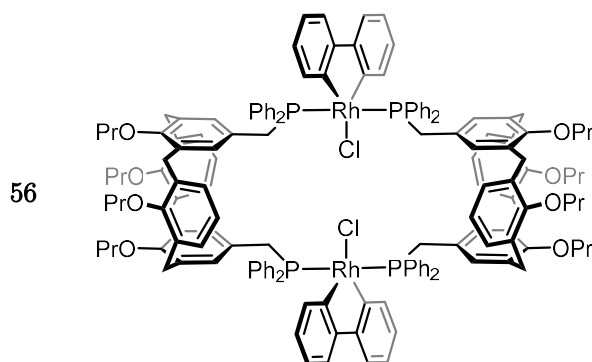


**<sup>1</sup>H NMR** (500 MHz, CD<sub>2</sub>Cl<sub>2</sub>): δ 7.62 (t, <sup>3</sup>*J*<sub>HH</sub> = 7.2, 4H, *p*-Ph), 7.53 (t, <sup>3</sup>*J*<sub>HH</sub> = 7.1, 8H, *m*-Ph), 7.50 – 7.42 (m, 8H, *o*-Ph), 6.86 (t, <sup>3</sup>*J*<sub>HH</sub> = 7.2, 2H, *p*-Ar), 6.79 (d, <sup>3</sup>*J*<sub>HH</sub> = 7.2, 4H, *m*-Ar), 6.30 (s, 4H, *m*-Ar<sup>P</sup>), 4.41 (d, <sup>2</sup>*J*<sub>HH</sub> = 12.6, 4H, ArCH<sub>2(ax)</sub>Ar<sup>P</sup>), 4.09 – 4.02 (m,

4H, ArOCH<sub>2</sub>CH<sub>2</sub>CH<sub>3</sub>), 3.59 (t,  $^3J_{\text{HH}} = 7.2$ , 4H, Ar<sup>P</sup>OCH<sub>2</sub>CH<sub>2</sub>CH<sub>3</sub>), 3.50 (s, 4H, CH<sub>2</sub>P), 3.04 (d,  $^2J_{\text{HH}} = 12.6$ , 4H, ArCH<sub>2</sub>(eq)Ar<sup>P</sup>), 2.08 (app. hept,  $^3J_{\text{HH}} = 7.4$ , 4H, ArOCH<sub>2</sub>CH<sub>2</sub>CH<sub>3</sub>), 1.88 (app. hept,  $^3J_{\text{HH}} = 7.2$ , 4H, Ar<sup>P</sup>OCH<sub>2</sub>CH<sub>2</sub>CH<sub>3</sub>), 1.02 (t,  $^3J_{\text{HH}} = 7.4$ , 6H, Ar<sup>P</sup>OCH<sub>2</sub>CH<sub>2</sub>CH<sub>3</sub>), 0.92 (t,  $^3J_{\text{HH}} = 7.5$ , 6H, ArOCH<sub>2</sub>CH<sub>2</sub>CH<sub>3</sub>). **<sup>13</sup>C{<sup>1</sup>H} NMR** (CD<sub>2</sub>Cl<sub>2</sub>, 126 MHz): δ 157.8 (s, *i*-Ar), 155.6 (s, *i*-Ar<sup>P</sup>), 136.7 (s, *o*-Ar), 134.8 (s, *o*-Ar<sup>P</sup>), 133.5 (t,  $J_{\text{PC}} = 7$ , *o*-Ph), 132.7 (s, *p*-Ph), 130.3 (t,  $J_{\text{PC}} = 5$ , *m*-Ph), 129.4 (s, *m*-Ar<sup>P</sup>), 128.8 (t,  $J_{\text{PC}} = 4$ , *m*-Ar), 128.2 (s, *p*-Ar<sup>P</sup>), 123.1 (s, *p*-Ar), 121.8 (q,  $^1J_{\text{FC}} = 292$ , CF<sub>3</sub>), 78.7 (s, Ar<sup>P</sup>OCH<sub>2</sub>CH<sub>2</sub>CH<sub>3</sub>), 77.0 (s, ArOCH<sub>2</sub>CH<sub>2</sub>CH<sub>3</sub>), 32.2 (t,  $J_{\text{PC}} = 8$ , CH<sub>2</sub>P), 31.4 (s, ArCH<sub>2</sub>Ar<sup>P</sup>), 23.9 (s, Ar<sup>P</sup>OCH<sub>2</sub>CH<sub>2</sub>CH<sub>3</sub>), 23.4 (s, ArOCH<sub>2</sub>CH<sub>2</sub>CH<sub>3</sub>), 10.9 (s, Ar<sup>P</sup>OCH<sub>2</sub>CH<sub>2</sub>CH<sub>3</sub>), 10.1 (s, ArOCH<sub>2</sub>CH<sub>2</sub>CH<sub>3</sub>). The *i*-Ph resonance could not be unambiguously located. **<sup>31</sup>P{<sup>1</sup>H} NMR** (162 MHz, CD<sub>2</sub>Cl<sub>2</sub>): δ 12.2 (app. dd,  $^1J_{107\text{AgP}} = 575$ ,  $^1J_{109\text{AgP}} = 497$ ). **HR ESI-MS** (positive ion): 1097.3989 ([M]<sup>+</sup>, calcd 1097.3782) *m/z*. **Anal.** Calcd for C<sub>82</sub>H<sub>70</sub>AgAlF<sub>36</sub>O<sub>8</sub>P<sub>2</sub> (2064.19 g·mol<sup>-1</sup>): C, 47.71; H, 3.42; N, 0.00. Found: C, 47.83; H, 3.25; N, 0.00.

### 6.3.3 Preparation of dimeric CxP<sub>2</sub> complexes

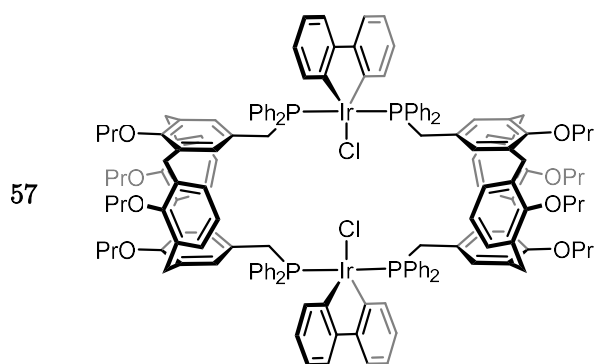
#### 6.3.3.1 [{Rh(2,2'-biphenyl)(CxP<sub>2</sub>)(Cl)}<sub>2</sub>]



A solution of **1** (50.0 mg, 84.0 μmol) and **CxP<sub>2</sub>** (84.1 mg, 85.0 μmol) in CH<sub>2</sub>Cl<sub>2</sub> (5 mL) was stirred at ambient temperature for 3 h. Excess Et<sub>2</sub>O (*ca.* 45 mL) was added with stirring and the resulting precipitate isolated by filtration and dried *in vacuo*. Yield: 78.0 mg (73%, amorphous yellow solid).

**$^1\text{H}$  NMR** (500 MHz,  $\text{CD}_2\text{Cl}_2$ ):  $\delta$  7.33 – 7.28 (m, 12H 6-biph & *p*-Ph), 7.08 (t,  $^3J_{\text{HH}} = 7.6$ , 16H, *o*-Ph), 7.02 – 6.97 (m, 16H, *m*-Ph), 6.80 – 6.76 (m, 8H, 3-biph & 4-biph), 6.72 – 6.67 (m, 4H, 5-biph), 6.21 (s, 8H, *m*-Ar<sup>P</sup>), 6.02 (t,  $^3J_{\text{HH}} = 7.6$ , 4H, *p*-Ar), 5.63 (d,  $^3J_{\text{HH}} = 7.6$ , 8H, *m*-Ar), 4.05 (d,  $^2J_{\text{HH}} = 13.0$ , 8H, ArCH<sub>2(ax)</sub>Ar<sup>P</sup>), 3.78 (br t,  $^3J_{\text{HH}} = 8.2$ , 8H, ArOCH<sub>2</sub>CH<sub>2</sub>CH<sub>3</sub>), 3.64 (br, 8H, CH<sub>2</sub>P), 3.45 (br t, 8H,  $^3J_{\text{HH}} = 6.9$ , Ar<sup>P</sup>OCH<sub>2</sub>CH<sub>2</sub>CH<sub>3</sub>), 2.62 (d,  $^2J_{\text{HH}} = 13.3$ , 8H ArCH<sub>2(eq)</sub>Ar<sup>P</sup>), 1.86 – 1.68 (m, 16H, Ar<sup>P</sup>OCH<sub>2</sub>CH<sub>2</sub>CH<sub>3</sub> & ArOCH<sub>2</sub>CH<sub>2</sub>CH<sub>3</sub>), 0.99 (t,  $^3J_{\text{HH}} = 7.4$ , 12H, Ar<sup>P</sup>OCH<sub>2</sub>CH<sub>2</sub>CH<sub>3</sub>), 0.79 (t,  $^3J_{\text{HH}} = 7.4$ , 12H, ArOCH<sub>2</sub>CH<sub>2</sub>CH<sub>3</sub>).  **$^{13}\text{C}\{^1\text{H}\}$  NMR** ( $\text{CD}_2\text{Cl}_2$ , 126 MHz):  $\delta$  163.7 (dt,  $^1J_{\text{RhC}} = 33$ ,  $^2J_{\text{PC}} = 8$ , 1-biph), 156.9 (s, *i*-Ar<sup>P</sup>), 155.5 (s, *i*-Ar), 152.6 (s, 2-biph), 136.9 (s, *o*-Ar<sup>P</sup>), 135.0 (br, *m*-Ph), 133.4 (s, *o*-Ar), 133.3 (s, 6-biph), 131.0 (s, *m*-Ar<sup>P</sup>), 130.2 (s, *p*-Ph), 129.0 (t,  $J_{\text{PC}} = 22$ , *i*-Ph), 127.9 (br, *o*-Ph), 127.8 (s, *m*-Ar), 127.7 (s, *p*-Ar<sup>P</sup>), 125.0 (s, 3-biph), 123.1 (s, 4-biph), 122.1 (s, 5-biph), 121.8 (s, *p*-Ar), 77.5 (s, Ar<sup>P</sup>OCH<sub>2</sub>CH<sub>2</sub>CH<sub>3</sub>), 76.7 (s, ArOCH<sub>2</sub>CH<sub>2</sub>CH<sub>3</sub>), 31.0 (s, ArCH<sub>2</sub>Ar<sup>P</sup>), 30.1 (t,  $J_{\text{PC}} = 10$ , CH<sub>2</sub>P), 24.0 (s, Ar<sup>P</sup>OCH<sub>2</sub>CH<sub>2</sub>CH<sub>3</sub>), 23.2 (s, ArOCH<sub>2</sub>CH<sub>2</sub>CH<sub>3</sub>), 11.1 (s, Ar<sup>P</sup>OCH<sub>2</sub>CH<sub>2</sub>CH<sub>3</sub>), 10.1 (s, ArOCH<sub>2</sub>CH<sub>2</sub>CH<sub>3</sub>).  **$^{31}\text{P}\{^1\text{H}\}$  NMR** (162 MHz,  $\text{CD}_2\text{Cl}_2$ ):  $\delta$  29.9 (d,  $^1J_{\text{RhP}} = 114$ ). **Anal.** Calcd for  $\text{C}_{156}\text{H}_{156}\text{Cl}_2\text{O}_8\text{P}_4\text{Rh}_2$  (2559.76 g·mol<sup>-1</sup>): C, 73.20; H, 6.14; N, 0.00. Found: C, 73.12; H, 5.99; N, 0.00.

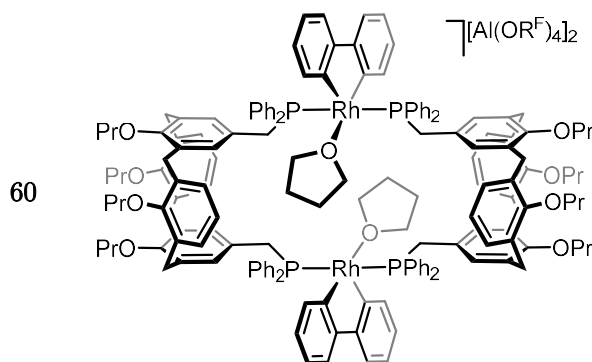
### 6.3.3.2 [ $\{\text{Ir}(2,2'\text{-biphenyl})(\text{C}\mathbf{x}\text{P}_2)(\text{Cl})\}_2$ ]



A solution of **2** (75.0 mg, 76.8  $\mu\text{mol}$ ) and **C $\mathbf{x}$ P<sub>2</sub>** (153 mg, 155  $\mu\text{mol}$ ) in  $\text{CH}_2\text{Cl}_2$  (5 mL) was stirred at ambient temperature for 18 h. Excess  $\text{Et}_2\text{O}$  (ca. 40 mL) was added with stirring and the resulting precipitate isolated by filtration and dried *in vacuo*. Yield: 70.1 mg (66%, red amorphous solid).

**$^1\text{H}$  NMR** (500 MHz,  $\text{CD}_2\text{Cl}_2$ ):  $\delta$  7.32 (t,  $^3J_{\text{HH}} = 7.6$ , 8H, *p*-Ph), 7.25 (d,  $^3J_{\text{HH}} = 7.6$ , 4H, 6-biph), 7.11 (t,  $^3J_{\text{HH}} = 7.4$  Hz, 16H, *m*-Ph), 7.08 – 7.00 (m, 16H, *o*-Ph), 6.79 (d,  $^3J_{\text{HH}} = 7.2$ , 4H, 3-biph), 6.76 (t,  $^3J_{\text{HH}} = 7.2$ , 4H, 5-biph), 6.57 (t,  $^3J_{\text{HH}} = 7.0$ , 4H, 4-biph), 6.19 (s, 8H, *m*-Ar<sup>P</sup>), 6.02 (t,  $^3J_{\text{HH}} = 7.5$ , 4H, *p*-Ar), 5.64 (d,  $^3J_{\text{HH}} = 7.5$ , 8H, *m*-Ar), 4.05 (d,  $^2J_{\text{HH}} = 12.8$ , 8H,  $\text{ArCH}_{2(\text{ax})}\text{Ar}^{\text{P}}$ ), 3.84 – 3.75 (m, 8H,  $\text{ArOCH}_2\text{CH}_2\text{CH}_3$ ), 3.52 (s, 8H,  $\text{CH}_2\text{P}$ ), 3.50 – 3.42 (m, 8H,  $\text{Ar}^{\text{P}}\text{OCH}_2\text{CH}_2\text{CH}_3$ ), 2.61 (d,  $^2J_{\text{HH}} = 13.2$ , 8H,  $\text{ArCH}_{2(\text{eq})}\text{Ar}^{\text{P}}$ ), 1.80 – 1.68 (m, 16H,  $\text{Ar}^{\text{P}}\text{OCH}_2\text{CH}_2\text{CH}_3$  &  $\text{ArOCH}_2\text{CH}_2\text{CH}_3$ ), 0.98 (t,  $^3J_{\text{HH}} = 7.4$ , 12H,  $\text{Ar}^{\text{P}}\text{OCH}_2\text{CH}_2\text{CH}_3$ ), 0.79 (t,  $^3J_{\text{HH}} = 7.4$ , 12H,  $\text{ArOCH}_2\text{CH}_2\text{CH}_3$ ).  **$^{13}\text{C}\{^1\text{H}\}$  NMR** (126 MHz,  $\text{CD}_2\text{Cl}_2$ ):  $\delta$  156.9 (s, *i*-Ar<sup>P</sup>), 155.5 (s, *i*-Ar), 154.6 (s, 2-biph), 138.5 (t,  $^2J_{\text{PC}} = 7$ , 1-biph), 136.9 (s, *o*-Ar<sup>P</sup>), 135.1 (t,  $J_{\text{PC}} = 5$ , *o*-Ph), 133.4 (s, *o*-Ar), 133.2 (s, 6-biph), 131.1 (s, *m*-Ar<sup>P</sup>), 130.2 (s, *p*-Ph), 128.7 (t,  $J_{\text{PC}} = 25$ , *i*-Ph), 128 (HSQC, *m*-Ar), 127.8 (t,  $J_{\text{PC}} = 4$ , *m*-Ph), 127.6 (t,  $J_{\text{PC}} = 4$ , *p*-Ar<sup>P</sup>), 125.1 (s, 4-biph), 122.7 (s, 5-biph), 122.1 (s, *p*-Ar), 121.2 (s, 3-biph), 77.5 (s,  $\text{Ar}^{\text{P}}\text{OCH}_2\text{CH}_2\text{CH}_3$ ), 76.7 (s,  $\text{ArOCH}_2\text{CH}_2\text{CH}_3$ ), 31.1 (s,  $\text{ArCH}_2\text{Ar}^{\text{P}}$ ), 29.0 (t,  $J_{\text{PC}} = 13$ ,  $\text{CH}_2\text{P}$ ), 24.0 (s,  $\text{Ar}^{\text{P}}\text{OCH}_2\text{CH}_2\text{CH}_3$ ), 23.2 (s,  $\text{ArOCH}_2\text{CH}_2\text{CH}_3$ ), 11.1 (s,  $\text{Ar}^{\text{P}}\text{OCH}_2\text{CH}_2\text{CH}_3$ ), 10.1 (s,  $\text{ArOCH}_2\text{CH}_2\text{CH}_3$ ).  **$^{31}\text{P}\{^1\text{H}\}$  NMR** (162 MHz,  $\text{CD}_2\text{Cl}_2$ ):  $\delta$  20.3 (s). **Anal.** Calc. for  $\text{C}_{78}\text{H}_{78}\text{ClIrO}_4\text{P}_2$  (1368.47 g·mol<sup>-1</sup>): C, 68.43; H, 5.74; N, 0.00. Found: C, 68.25; H, 5.77; N, 0.00.

### 6.3.3.3 $[\{\text{Rh}(2,2'\text{-biphenyl})(\text{C}\mathbf{x}\text{P}_2)(\text{thf})\}_2][\text{Al}(\text{OR}^{\text{F}})_4]_2$



THF complex **31** (18.2 mg, 10.0  $\mu\text{mol}$ ) and **CxP<sub>2</sub>** (9.9 mg, 10.0  $\mu\text{mol}$ ) were dissolved in THF (0.5 mL), resulting immediately in the formation of **60** as gauged by  $^{31}\text{P}$  NMR spectroscopy. Characterised *in situ*. Dynamic processes at 298 K preclude any

meaningful assignment of the  $^1\text{H}$  NMR spectrum.  $^{31}\text{P}\{^1\text{H}\}$  NMR (162 MHz, THF):  $\delta$  22.8 (vbr. d, fwhm = 45,  $^1J_{\text{RhP}}$  = 128). **HR ESI-MS** (positive ion): 1243.9422 ( $[\text{M}-2(\text{THF})]^{2+}$ , calcd 1243.9442  $m/z$ ).

### 6.3.4 Substitution reactions

#### 6.3.4.1 Reaction of $[\text{Rh}(2,2'\text{-biphenyl})(\text{PPh}_3)_2(\text{OH}_2)][\text{Al}(\text{OR}^{\text{F}})_4]$ with $\text{CxP}_2$ in THF

In an NMR tube, water complex **30** (11.8 mg, 6.67  $\mu\text{mol}$ ) was dissolved in THF (0.33 mL) resulting in a fast equilibrium mixture of **30** and THF complex **30** (0.15 : 0.85,  $K_{\text{eq}} = 7.8 \times 10^{-3}$ ). The solution was transferred via cannular to a second tube containing  $\text{CxP}_2$  (6.7 mg, 6.7  $\mu\text{mol}$ ) and the reaction monitored by  $^1\text{H}$  and  $^{31}\text{P}$  NMR spectroscopy. Within 5 mins the  $^{31}\text{P}$  spectrum contained a mixture of downfield signal assigned to concentration shifted water complex **30**, calixarene THF complex **60**, calixarene water complex **59** in a 0.4 : 0.4 : 0.2 ratio, with concomitant liberation of 1.2 equivalents of  $\text{PPh}_3$ . Within 5 h the reaction had progressed to contain exclusively **59** and free  $\text{PPh}_3$ .

#### 6.3.4.2 Reaction of $[\text{Rh}(2,2'\text{-biphenyl})(\text{PPh}_3)_2(\text{thf})][\text{Al}(\text{OR}^{\text{F}})_4]$ with $\text{CxP}_2$ in THF

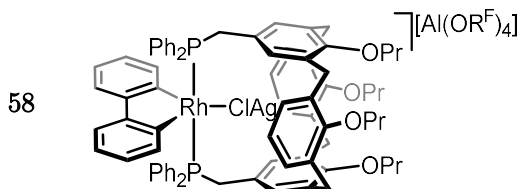
In an NMR tube, THF complex **31** (11.8 mg, 6.67  $\mu\text{mol}$ ) was transferred via cannular to a second tube containing  $\text{CxP}_2$  (6.7 mg, 6.7  $\mu\text{mol}$ ) and the reaction monitored by  $^1\text{H}$  and  $^{31}\text{P}$  NMR spectroscopy. Within 5 mins the  $^{31}\text{P}$  spectrum showed full conversion to calixarene THF complex **60** with concomitant liberation of  $\text{PPh}_3$ .

#### 6.3.4.3 Reaction of $[\text{Rh}(2,2'\text{-biphenyl})(\text{PPh}_3)_2][\text{Al}(\text{OR}^{\text{F}})_4]$ with $\text{CxP}_2$ in $\text{C}_6\text{D}_5\text{F}$

In an NMR tube, to a solution of low-coordinate **29** in  $\text{C}_6\text{D}_5\text{F}$ , prepared from water complex **30** 17.6 mg, 10.0  $\mu\text{mol}$ ) was added  $\text{CxP}_2$  (9.9 mg, 10.0  $\mu\text{mol}$ ). The reaction immediately precipitated a yellow material. The resultant  $^1\text{H}$  and  $^{31}\text{P}$  NMR were broad, consistent with the formation of some oligomeric species.

### 6.3.5 Preparation of monomeric CxP<sub>2</sub> complexes

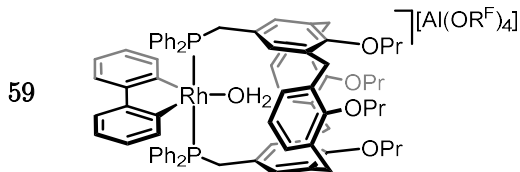
#### 6.3.5.1 [Rh(2,2'-biphenyl)(CxP<sub>2</sub>)(ClAg)][Al(OR<sup>F</sup>)<sub>4</sub>]



A suspension of chloride **56** (29.8 mg, 23.2  $\mu\text{mol}$ ) and  $\text{Ag}[\text{Al}(\text{OR}^{\text{F}})_4]$  (25.1 mg, 23.2  $\mu\text{mol}$ ) in  $\text{CH}_2\text{Cl}_2$  (10 mL) was stirred at ambient temperature for 18 h. In an argon glove box, the solution was passed through a glass microfibre filter pad wedged in a glass pipette (oven dried at 150 °C for 72 h) and directly into a an NMR tube. The solvent was removed *in vacuo* and the residues extracted into  $\text{CD}_2\text{Cl}_2$ . Characterised *in situ*.

**<sup>1</sup>H NMR (400 MHz,  $\text{CD}_2\text{Cl}_2$ ):**  $\delta$  7.62 (d,  $^3J_{\text{HH}} = 8.0$ , 2H, biph), 7.58 – 7.42 (m, 2H, biph), 7.36 (t,  $J=7.7$ , 4H, *p*-Ph), 7.29 (d,  $J=8.4$ , 2H, biph), 7.16 (t,  $J=7.5$ , 8H, *m*-Ph), 7.10 (d,  $^3J_{\text{HH}} = 7.4$ , 4H, *m*-Ar), 6.82 – 6.68 (m, 10H, *o*-Ph & biph), 6.58 – 6.44 (m, 6H, *p*-Ar & *m*-Ar<sup>P</sup>), 6.16 (d,  $^3J_{\text{HH}} = 7.2$ , 2H, biph), 4.52 – 4.42 (m, 8H, Ar<sup>P</sup>OCH<sub>2</sub>CH<sub>2</sub>CH<sub>3</sub> & ArCH<sub>2(ax)</sub>Ar<sup>P</sup>), 3.69 – 3.63 (m, 4H, ArOCH<sub>2</sub>CH<sub>2</sub>CH<sub>3</sub>), 3.29 (br, 4H, CH<sub>2</sub>P), 3.19 (d,  $^2J_{\text{HH}} = 13.1$ , 4H, ArCH<sub>2(eq)</sub>Ar<sup>P</sup>), 2.16 – 2.00 (m, 4H, ArOCH<sub>2</sub>CH<sub>2</sub>CH<sub>3</sub>), 1.98 – 1.83 (m, 4H, Ar<sup>P</sup>OCH<sub>2</sub>CH<sub>2</sub>CH<sub>3</sub>), 1.08 – 0.92 (m, 12H, Ar<sup>P</sup>OCH<sub>2</sub>CH<sub>2</sub>CH<sub>3</sub> & ArOCH<sub>2</sub>CH<sub>2</sub>CH<sub>3</sub>). The biph resonances could not be satisfactorily assigned with the available data. **<sup>31</sup>P{<sup>1</sup>H} NMR (162 MHz,  $\text{CD}_2\text{Cl}_2$ ):**  $\delta$  14.0 (d,  $^1J_{\text{RhP}} = 120$ ).

#### 6.3.5.2 [Rh(2,2'-biphenyl)(CxP<sub>2</sub>)(OH<sub>2</sub>)][Al(OR<sup>F</sup>)<sub>4</sub>]



**Method A:** A suspension of chloride **56** (128.8 mg, 100.0  $\mu\text{mol}$ ) and  $\text{Ag}[\text{Al}(\text{OR}^{\text{F}})_4]$  (107.5 mg, 100.0  $\mu\text{mol}$ ) in  $\text{CH}_2\text{Cl}_2$  (10 mL) was stirred at ambient temperature for 18 h.  $\text{H}_2\text{O}$  (2.7  $\mu\text{L}$ , 150  $\mu\text{mol}$ ) was added, precipitating  $\text{AgCl}$ , and the yellow solution

filtered in air. The solvent was concentrated in vacuo to *ca.* 5 mL and layered in air with wet hexane (*ca.* 45 mL) to afford on diffusion the title compound, along with further AgCl precipitate. The material was extracted into CH<sub>2</sub>Cl<sub>2</sub> (*ca.* 5 mL), filtered, and the crystallisation procedure repeated until no further AgCl was observed. Yield: 171 mg (77%, orange crystalline blocks).

**Method B:** A solution of [Rh(2,2'-biphenyl)(PPh<sub>3</sub>)<sub>2</sub>(OH<sub>2</sub>)] [Al(OR<sup>F</sup>)<sub>4</sub>], **30** (176.5 mg, 100.0 μmol) and **CxP<sub>2</sub>** (100.0 mg, 110.0 μmol) in THF (10 mL) was stirred at ambient temperature for 4 h. H<sub>2</sub>O (18 μL) was added and the reaction stirred for a further 18 h. The solution was then deposited into rapidly stirring hexane, precipitating a yellow material which was isolated by filtration and washed with hexane. The residues were extracted into CH<sub>2</sub>Cl<sub>2</sub> (*ca.* 5 mL) and additional H<sub>2</sub>O added (*ca.* 0.1 mL). Slow diffusion of excess hexane (*ca.* 40 mL), afforded orange crystalline material and a red oily residue. The solid material was isolated by filtration, dried under high vacuum and then, in air, dissolved in *wet* CH<sub>2</sub>Cl<sub>2</sub> and passed through a short plug of Al<sub>2</sub>O<sub>3</sub> (100% CH<sub>2</sub>Cl<sub>2</sub>). The solvent was removed *in vacuo* to afford the title compound. Yield: 97.0 mg (44%, yellow solid).

**Method C:** Any of the compounds **58**, **63**, **64**, **65** or **67** exposed to air for 5 mins, or in an argon-filled glovebox for *ca.* 1 year, or in any way otherwise exposed to adventitious water will cleanly convert to the title compound and may be isolated in near quantitative yield by removal of solvent *in vacuo*.

**<sup>1</sup>H NMR** (600 MHz, C<sub>6</sub>D<sub>5</sub>F, 353 K): δ 7.31 – 7.26 (m, 6H, biph & *p*-Ph), 7.13 (d, <sup>3</sup>*J*<sub>HH</sub> = 7.7, 8H, *o*-Ph), 7.03 (d, <sup>3</sup>*J*<sub>HH</sub> = 7.5, 4H, biph), 6.68 (s, 12H, *m*-Ar & *m*-Ph), 6.43 (s, 4H, *m*-Ar<sup>P</sup>), 6.22 – 6.19 (m, 2H, *p*-Ar), 4.54 (d, <sup>2</sup>*J*<sub>HH</sub> = 12.8, 4H, ArCH<sub>2(ax)</sub>Ar<sup>P</sup>), 4.22 – 4.18 (m, 4H, ArOCH<sub>2</sub>CH<sub>2</sub>CH<sub>3</sub>), 3.61 (t, <sup>3</sup>*J*<sub>HH</sub> = 7.1, 4H, Ar<sup>P</sup>OCH<sub>2</sub>CH<sub>2</sub>CH<sub>3</sub>), 3.23 (t, <sup>2</sup>*J*<sub>PH</sub> = 3.5, 4H CH<sub>2</sub>P), 3.05 (d, <sup>2</sup>*J*<sub>HH</sub> = 12.8, 4H, ArCH<sub>2(eq)</sub>Ar<sup>P</sup>), 2.16 – 2.08 (m, 4H, ArOCH<sub>2</sub>CH<sub>2</sub>CH<sub>3</sub>), 1.85 (app. sex, <sup>3</sup>*J*<sub>HH</sub> = 7.4, 4H, Ar<sup>P</sup>OCH<sub>2</sub>CH<sub>2</sub>CH<sub>3</sub>), 1.00 (t, *J* = 7.4, 6H, Ar<sup>P</sup>OCH<sub>2</sub>CH<sub>2</sub>CH<sub>3</sub>), 0.97 (t, <sup>3</sup>*J*<sub>HH</sub> = 7.5, 6H, ArOCH<sub>2</sub>CH<sub>2</sub>CH<sub>3</sub>), 0.94 (s, 2H, OH<sub>2</sub>). Insufficient data is available to fully assign the biph resonances, one of which could not

be unambiguously located. **<sup>1</sup>H NMR** (600 MHz, C<sub>6</sub>D<sub>5</sub>F):  $\delta$  7.34 (t,  $J = 7.6$ , 3H, Ar), 7.27 (vbr, fwhm = 22, 4H, Ar), 7.05 (vbr, fwhm = 63, 12H, Ar), 6.69 (vbr, fwhm = 85, 10H, Ar), 6.42 (vbr, fwhm = 30, 6H, Ar), 6.20 (vbr, fwhm = 45, 3H, Ar), 4.49 (d,  $^3J_{\text{HH}} = 12.7$ , 4H, ArCH<sub>2(ax)</sub>Ar<sup>P</sup>), 4.15 – 4.07 (m, 4H, Ar<sup>P</sup>OCH<sub>2</sub>CH<sub>2</sub>CH<sub>3</sub>), 3.53 (t,  $^3J_{\text{HH}} = 7.2$ , 4H, Ar<sup>P</sup>OCH<sub>2</sub>CH<sub>2</sub>CH<sub>3</sub>), 3.20 (br, 4H, CH<sub>2</sub>P), 3.03 (br d,  $^2J_{\text{HH}} = 9.1$ , 4H, ArCH<sub>2(eq)</sub>Ar<sup>P</sup>), 2.20 – 2.10 (m, 4H, ArOCH<sub>2</sub>CH<sub>2</sub>CH<sub>3</sub>), 1.84 (app. sex,  $^3J_{\text{HH}} = 7.4$ , 4H, Ar<sup>P</sup>OCH<sub>2</sub>CH<sub>2</sub>CH<sub>3</sub>), 0.99 – 0.93 (m, 14H, ArOCH<sub>2</sub>CH<sub>2</sub>CH<sub>3</sub> & OH<sub>2</sub>). Dynamic exchange at 298 K precludes any meaningful assignment of the aromatic resonances, collectively assigned ‘Ar’. **<sup>1</sup>H NMR** (400 MHz, THF), selected signals:  $\delta$  4.82 (d,  $^2J_{\text{HH}} = 12.6$ , 4H, ArCH<sub>2(ax)</sub>Ar<sup>P</sup>), 3.41 (d,  $^2J_{\text{HH}} = 12.6$ , 4H, ArCH<sub>2(eq)</sub>Ar<sup>P</sup>). **<sup>1</sup>H NMR** (600 MHz, CD<sub>2</sub>Cl<sub>2</sub>):  $\delta$  7.43 (vbr, fwhm = 85, 4H Ar), 7.25 (t,  $J = 7.4$ , 3H, Ar), 7.2 (obsc, 4H, Ar), 7.00 (vbr, fwhm = 44, 6H, Ar), 6.70 (obsc, 2H, Ar), 6.61 (vbr, fwhm = 35, 6H, Ar), 6.53 (obsc, 4H, Ar), 6.36 (vbr, fwhm = 31, 6H, Ar), 6.14 (vbr, fwhm = 44, 3H, Ar), 4.48 (d,  $^2J_{\text{HH}} = 12.7$ , 4H, ArCH<sub>2(ax)</sub>Ar), 4.23 – 4.00 (m, 4H, ArOCH<sub>2</sub>CH<sub>2</sub>CH<sub>3</sub>), 3.63 (t,  $^3J_{\text{HH}} = 7.6$ , 4H, Ar<sup>P</sup>OCH<sub>2</sub>CH<sub>2</sub>CH<sub>3</sub>), 3.27 (br, 4H, CH<sub>2</sub>P), 3.09 (br d,  $^2J_{\text{HH}} = 12.7$ , 4H, ArCH<sub>2(eq)</sub>Ar), 2.16 – 2.08 (m, 4H, ArOCH<sub>2</sub>CH<sub>2</sub>CH<sub>3</sub>), 1.89 (app. sex,  $^3J_{\text{HH}} = 7.4$ , 4H, Ar<sup>P</sup>OCH<sub>2</sub>CH<sub>2</sub>CH<sub>3</sub>), 1.03 (t,  $^3J_{\text{HH}} = 7.4$ , 6H, Ar<sup>P</sup>OCH<sub>2</sub>CH<sub>2</sub>CH<sub>3</sub>), 0.95 (t,  $^3J_{\text{HH}} = 7.5$ , 6H, ArOCH<sub>2</sub>CH<sub>2</sub>CH<sub>3</sub>), 0.84 (s, 2H, OH<sub>2</sub>). Dynamic exchange at 298 K precludes any meaningful assignment of the aromatic resonances, collectively assigned ‘Ar’. **<sup>1</sup>H NMR** (600 MHz, CD<sub>2</sub>Cl<sub>2</sub>, 185 K):  $\delta$  8.06 (t,  $^3J_{\text{HH}} = 7.5$ , 2H, *p*-Ph’), 7.90 (t,  $^3J_{\text{HH}} = 7.7$ , 2H, *p*-Ph), 7.63 – 7.54 (m, 4H, *m*-Ph), 7.40 (d,  $^3J_{\text{HH}} = 7.5$ , 2H, *m*-Ar), 7.34 (t,  $^3J_{\text{HH}} = 7.6$ , 1H, 4- or 5-biph), 7.31 – 7.26 (m, 2H, *m*-Ph’), 7.14 (t,  $^3J_{\text{HH}} = 7.6$ , 1H, 4- or 5-biph), 7.01 (t,  $^3J_{\text{HH}} = 7.3$ , 1H, 4’- or 5’-biph), 6.93 (d,  $^3J_{\text{HH}} = 7.7$ , 1H, 3-biph), 6.87 (t,  $^3J_{\text{HH}} = 7.4$ , 2H, *m*-Ph’), 6.77 (t,  $^3J_{\text{HH}} = 7.6$ , 1H, 4’- or 5’-biph), 6.70 (s, 2H, *m*-Ar<sup>P</sup>), 6.68 (vbr, fwhm = 25, 2H, *o*-Ph), 6.51 (d,  $^3J_{\text{HH}} = 7.6$ , 2H, *m*-Ar), 6.45 (d,  $^3J_{\text{HH}} = 7.5$ , 1H, 3’-biph), 6.39 (vbr t, fwhm = 12,  $^3J_{\text{HH}} = 8.0$ , 2H, *o*-Ph), 6.22 (t,  $^3J_{\text{HH}} = 7.5$ , 1H, *p*-Ar), 5.95 (t,  $^3J_{\text{HH}} = 7.2$ , 1H, *p*-Ar’), 5.85 (s, 2H, *m*-Ar<sup>P</sup>), 5.81 (d,  $^3J_{\text{HH}} = 7.8$ , 1H, 6-biph), 5.71 (vbr, fwhm = 22, 2H, *o*-Ph’), 5.64 (vbr, fwhm = 18, 2H, *o*-Ph’), 5.58 (d,  $^3J_{\text{HH}} = 7.5$ , 1H, 6’-biph), 4.39 (d,  $^2J_{\text{HH}} = 12.4$ , 2H, ArCH<sub>2(ax)</sub>Ar<sup>P</sup>), 4.21 (d,  $^2J_{\text{HH}} = 12.3$ , 2H, ArCH<sub>2(eq)</sub>Ar<sup>P</sup>), 3.96 – 3.89 (m,



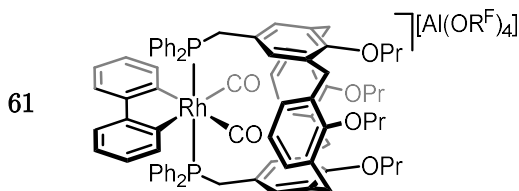
2H, ArOCH<sub>2</sub>CH<sub>2</sub>CH<sub>3</sub>), 3.89 – 3.83 (m, 2H, ArOCH<sub>2</sub>CH<sub>2</sub>CH<sub>3</sub>'), 3.50 – 3.36 (m, 6H, CH<sub>2</sub>P & Ar<sup>P</sup>OCH<sub>2</sub>CH<sub>2</sub>CH<sub>3</sub>), 3.23 (d, <sup>2</sup>J<sub>HH</sub> = 12.5, 2H, ArCH<sub>2(eq)</sub>Ar<sup>P</sup>), 2.98 (d, <sup>2</sup>J<sub>HH</sub> = 15.8, 2H, CH<sub>2</sub>P'), 2.82 (d, <sup>2</sup>J<sub>HH</sub> = 12.4, 2H, ArCH<sub>2(eq)</sub>Ar<sup>P1</sup>), 2.21 (q, <sup>3</sup>J<sub>HH</sub> = 8.2, 2H, ArOCH<sub>2</sub>CH<sub>2</sub>CH<sub>3</sub>), 2.10 (q, <sup>3</sup>J<sub>HH</sub> = 8.2, 2H, ArOCH<sub>2</sub>CH<sub>2</sub>CH<sub>3</sub>'), 1.87 (app. sex, <sup>3</sup>J<sub>HH</sub> = 7.6, 4H, Ar<sup>P</sup>OCH<sub>2</sub>CH<sub>2</sub>CH<sub>3</sub>), 0.91 (t, <sup>3</sup>J<sub>HH</sub> = 7.4, 6H, Ar<sup>P</sup>OCH<sub>2</sub>CH<sub>2</sub>CH<sub>3</sub>), 0.86 (t, <sup>3</sup>J<sub>HH</sub> = 6.6, 3H, ArOCH<sub>2</sub>CH<sub>2</sub>CH<sub>3</sub>), 0.81 (t, <sup>3</sup>J<sub>HH</sub> = 7.1, 3H, ArOCH<sub>2</sub>CH<sub>2</sub>CH<sub>3</sub>'), 0.66 (br, 2H, OH<sub>2</sub>).

**<sup>13</sup>C{<sup>1</sup>H} NMR** (CD<sub>2</sub>Cl<sub>2</sub>, 126 MHz): δ 157.5 (s, *i*-Ar), 156.1 (s, *i*-Ar<sup>P</sup>), 150.3 – 150.2 (m, 1-biph), 148.1 (s, 2-biph), 136.6 (s, *o*-Ar<sup>P</sup>), 136.4 (s, *p*-Ar<sup>P</sup>), 130.3 (s, *m*-Ar), 129.7 (s, 5-biph), 129.0 (s, 6-biph), 128.6 (s, *o*-Ar), 126.3 (s, *p*-Ar), 124.2 (s, 4-biph), 123.7 (s, *m*-Ar<sup>P</sup>), 122.6 (s, 3-biph), 121.8 (d, <sup>1</sup>J<sub>FC</sub> = 294, R<sup>F</sup>). 78.9 (s, Ar<sup>P</sup>OCH<sub>2</sub>CH<sub>2</sub>CH<sub>3</sub>), 77.2 (s, ArOCH<sub>2</sub>CH<sub>2</sub>CH<sub>3</sub>), 32.0 (app. t, <sup>1</sup>J<sub>PC</sub> = <sup>2</sup>J<sub>RhC</sub> = 12.2, ArCH<sub>2</sub>PPh<sub>2</sub>), 31.5 (s, ArCH<sub>2</sub>Ar), 23.9 (s, Ar<sup>P</sup>OCH<sub>2</sub>CH<sub>2</sub>CH<sub>3</sub>), 23.5 (s, ArOCH<sub>2</sub>CH<sub>2</sub>CH<sub>3</sub>), 10.9 (s, Ar<sup>P</sup>OCH<sub>2</sub>CH<sub>2</sub>CH<sub>3</sub>'), 10.0 (s, ArOCH<sub>2</sub>CH<sub>2</sub>CH<sub>3</sub>). Dynamic exchange at 298 K precludes location of the phenyl resonances.

**<sup>13</sup>C{<sup>1</sup>H} NMR** (126 MHz, C<sub>6</sub>D<sub>5</sub>F): δ 157.2 (s, *i*-Ar), 155.8 (s, *i*-Ar<sup>P</sup>), 150.3 – 150.2 (m, 1-biph), 148.0 (s, 2-biph), 136.2 (s, *o*-Ar<sup>P</sup>), 136.1 (s, *o*-Ar), 130.0 (s, *m*-Ar), 129.7 (HSQC, 5-biph), 128.6 (s, 3-biph), 128.2 (s, *p*-Ar<sup>P</sup>), 125.9 (s, *p*-Ar), 123.9 (s, 4-biph), 123.7 (HSQC, *m*-Ar<sup>P</sup>), 122.3 (s, 6-biph), 121.8 (d, <sup>1</sup>J<sub>FC</sub> = 294, R<sup>F</sup>), 78.4 (s, Ar<sup>P</sup>OCH<sub>2</sub>CH<sub>2</sub>CH<sub>3</sub>), 76.8 (s, ArOCH<sub>2</sub>CH<sub>2</sub>CH<sub>3</sub>), 31.4 (t, <sup>1</sup>J<sub>PC</sub> = 12, CH<sub>2</sub>P), 31.0, (s, ArCH<sub>2</sub>Ar), 23.4 (s, Ar<sup>P</sup>OCH<sub>2</sub>CH<sub>2</sub>CH<sub>3</sub>), 23.1 (s, ArOCH<sub>2</sub>CH<sub>2</sub>CH<sub>3</sub>), 10.2 (s, Ar<sup>P</sup>OCH<sub>2</sub>CH<sub>2</sub>CH<sub>3</sub>'), 9.4 (s, ArOCH<sub>2</sub>CH<sub>2</sub>CH<sub>3</sub>). Dynamic exchange at 298 K precludes location of the phenyl resonances.

**<sup>31</sup>P{<sup>1</sup>H} NMR** (CD<sub>2</sub>Cl<sub>2</sub>, 162 MHz): δ 13.2 (d, <sup>1</sup>J<sub>RhP</sub> = 119.9). **<sup>31</sup>P{<sup>1</sup>H} NMR** (162 MHz, THF): δ 13.7 (d, <sup>1</sup>J<sub>RhP</sub> = 119.3). **<sup>31</sup>P{<sup>1</sup>H} NMR** (162 MHz, C<sub>6</sub>D<sub>5</sub>F): δ 13.1 (d, <sup>1</sup>J<sub>RhP</sub> = 120.1). **<sup>19</sup>F{<sup>1</sup>H} NMR** (CD<sub>2</sub>Cl<sub>2</sub>, 377 MHz): δ -75.75 (s). **HR ESI-MS** (positive ion): 1261.4545 ([M]<sup>+</sup>, calcd 1261.4531) *m/z*. **Anal.** Calcd for C<sub>94</sub>H<sub>80</sub>AlF<sub>36</sub>O<sub>9</sub>P<sub>2</sub>Rh (2229.44 g·mol<sup>-1</sup>): C, 50.64; H, 3.62; N, 0.00. Found: C, 50.53; H, 3.58; N, 0.00. **IR** ν(O-H); 3541 cm<sup>-1</sup> (B<sub>1</sub>), 3518 cm<sup>-1</sup> (A<sub>1</sub>).

### 6.3.5.3 $[\text{Rh}(2,2'\text{-biphenyl})(\text{C}_x\text{P}_2)(\text{CO})_2][\text{Al}(\text{OR}^{\text{F}})_4]$

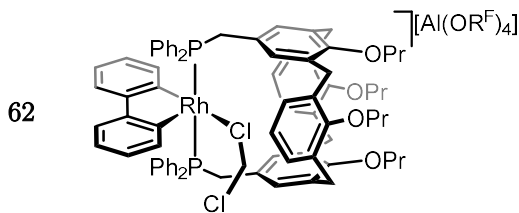


In an NMR tube, a solution of water complex **59** (11.1 mg, 5.00  $\mu\text{mol}$ ) in  $\text{CD}_2\text{Cl}_2$  (0.5 mL) was freeze-pump-thaw degassed three times and placed under an atmosphere of CO (1 bar). The solution became immediately colourless with quantitative conversion to the title compound and liberation of one equivalent of free water. Characterised *in situ* owing to instability of the compound in the absence of CO.

**$^1\text{H}$  NMR** (400 MHz,  $\text{CD}_2\text{Cl}_2$ ):  $\delta$  7.33 (t,  $^3J_{\text{HH}} = 7.4$ , 4H, *p*-Ph), 7.11 (t,  $^3J_{\text{HH}} = 7.6$ , 8H, *o*-Ph), 7.01 - 6.97 (m, 6H, *m*-Ar & *p*-Ar), 6.96 (d,  $^3J_{\text{HH}} = 7.0$ , 2H, 3-biph), 6.85 (t,  $^3J_{\text{HH}} = 7.1$ , 2H, 5-biph), 6.81 (t,  $^3J_{\text{HH}} = 7.1$ , 2H, 4-biph), 6.76 (app. q,  $^3J_{\text{HH}} = 5.6$ , 8H, *m*-Ph), 6.60 (d,  $^3J_{\text{HH}} = 7.0$ , 2H, 6-biph), 6.56 (s, 4H, *m*-Ar<sup>P</sup>), 4.49 (d,  $^2J_{\text{HH}} = 12.6$ , 4H, ArCH<sub>2(ax)</sub>Ar<sup>P</sup>), 4.16 - 4.05 (m, 4H, Ar<sup>P</sup>OCH<sub>2</sub>CH<sub>2</sub>CH<sub>3</sub>), 3.69 - 3.64 (m, 4H, ArOCH<sub>2</sub>CH<sub>2</sub>CH<sub>3</sub>), 3.63 (s, 4H, CH<sub>2</sub>P), 3.15 (d,  $^2J_{\text{HH}} = 12.7$ , 4H, ArCH<sub>2(eq)</sub>Ar<sup>P</sup>), 2.14 (app. h,  $^3J_{\text{HH}} = 7.7$ , 4H, Ar<sup>P</sup>OCH<sub>2</sub>CH<sub>2</sub>CH<sub>3</sub>), 1.91 (app. h,  $^3J_{\text{HH}} = 7.3$ , 4H, ArOCH<sub>2</sub>CH<sub>2</sub>CH<sub>3</sub>), 1.05 (t,  $^3J_{\text{HH}} = 7.4$ , 6H, ArOCH<sub>2</sub>CH<sub>2</sub>CH<sub>3</sub>), 0.96 (t,  $^3J_{\text{HH}} = 7.5$ , 6H, Ar<sup>P</sup>OCH<sub>2</sub>CH<sub>2</sub>CH<sub>3</sub>).

**$^{31}\text{P}\{^1\text{H}\}$  NMR** (162 MHz,  $\text{CD}_2\text{Cl}_2$ ):  $\delta$  15.3 (d,  $^1J_{\text{RhP}} = 97$ ).

### 6.3.5.4 $[\text{Rh}(2,2'\text{-biphenyl})(\text{C}_x\text{P}_2)(\text{dcm})][\text{Al}(\text{OR}^{\text{F}})_4]$

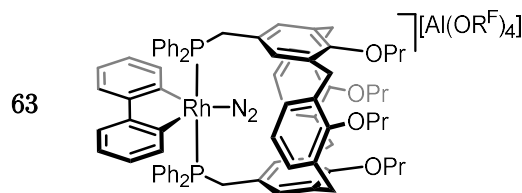


In an NMR tube, a solution of water complex **59** (11.1 mg, 5.00  $\mu\text{mol}$ ) in  $\text{CH}_2\text{Cl}_2$  (0.5 mL) under 3 Å molecular sieves (2000 wt%) segregated by a glass platform was freeze-pump-thaw degassed and placed under an atmosphere of dihydrogen. After inverting the NMR tube at 0.5 Hz for 24 h the solution was cooled to  $-78^\circ\text{C}$ , the volatiles removed

slowly *in vacuo*, the 3 Å molecular sieves replaced (2000 wt%) and the residues dissolved in CH<sub>2</sub>Cl<sub>2</sub> (0.5 mL), twice, affording the title compound.

**<sup>1</sup>H NMR** (500 MHz, CH<sub>2</sub>Cl<sub>2</sub>): δ 7.26 (t, <sup>3</sup>J<sub>HH</sub> = 7.3, 4H, *p*-Ph), 7.13 – 7.06 (m, 4H, 3-biph & 5-biph), 7.04 (t, <sup>3</sup>J<sub>HH</sub> = 7.3, 8H, *m*-Ph), 6.93 (d, <sup>3</sup>J<sub>HH</sub> = 7.4, 2H, 6-biph), 6.77 (t, <sup>3</sup>J<sub>HH</sub> = 7.5, 2H, 4-biph), 6.63 (vbr, fwhm = 22, 8H, *o*-Ph), 6.61 (s, 4H, *m*-Ar<sup>P</sup>), 6.53 (t, <sup>3</sup>J<sub>HH</sub> = 7.3, 4H, *p*-Ar), 6.13 (d, <sup>3</sup>J<sub>HH</sub> = 7.4, 4H, *m*-Ar), 4.48 (d, <sup>2</sup>J<sub>HH</sub> = 12.9, 4H, ArCH<sub>2(ax)</sub>Ar<sup>P</sup>), 4.22 – 4.16 (m, 4H, ArOCH<sub>2</sub>CH<sub>2</sub>CH<sub>3</sub>), 3.82 (br, 4H, CH<sub>2</sub>P), 3.68 (t, <sup>3</sup>J<sub>HH</sub> = 7.3, 4H, Ar<sup>P</sup>OCH<sub>2</sub>CH<sub>2</sub>CH<sub>3</sub>), 3.14 (d, <sup>2</sup>J<sub>HH</sub> = 13.0, 4H, ArCH<sub>2(eq)</sub>Ar<sup>P</sup>), 2.06 – 1.94 (m, 4H, ArOCH<sub>2</sub>CH<sub>2</sub>CH<sub>3</sub>), 1.92 – 1.81 (m, 4H, Ar<sup>P</sup>OCH<sub>2</sub>CH<sub>2</sub>CH<sub>3</sub>), 1.01 (t, <sup>3</sup>J<sub>HH</sub> = 7.4, 6H, Ar<sup>P</sup>OCH<sub>2</sub>CH<sub>2</sub>CH<sub>3</sub>), 0.92 (t, <sup>3</sup>J<sub>HH</sub> = 7.5, 6H, ArOCH<sub>2</sub>CH<sub>2</sub>CH<sub>3</sub>). **<sup>13</sup>C{<sup>1</sup>H} NMR** (126 MHz, CH<sub>2</sub>Cl<sub>2</sub>): δ 157.6 (s, *i*-Ar), 156.1 (s, *i*-Ar<sup>P</sup>), 155.4 – 154.6 (m, 1-biph), 151.0 (s, 2-biph), 135.3 (s, *o*-Ar<sup>P</sup>), 133.1 (br, *o*-Ph), 133.0 (s, *o*-Ar), 131.7 (s, 6-biph), 131.0 (s, *p*-Ph), 130.5 (t, *J*<sub>PC</sub> = 23, *i*-Ph), 130.2 (s, *m*-Ph), 128.0 (s, *p*-Ar), 125.2 (s, 5-biph), 124.3 (s, 4-biph), 123.7 (s, 3-biph), 122.6 (s, *m*-Ar), 121.8 (q, <sup>1</sup>*J*<sub>FC</sub> = 291, R<sup>F</sup>), 78.7 (s, Ar<sup>P</sup>OCH<sub>2</sub>CH<sub>2</sub>CH<sub>3</sub>), 76.5 (s, ArOCH<sub>2</sub>CH<sub>2</sub>CH<sub>3</sub>), 34.3 (t, *J*<sub>PC</sub> = 10, CH<sub>2</sub>P), 31.5 (s, ArCH<sub>2</sub>Ar<sup>P</sup>), 23.5 (s, Ar<sup>P</sup>OCH<sub>2</sub>CH<sub>2</sub>CH<sub>3</sub>), 22.8 (s, ArOCH<sub>2</sub>CH<sub>2</sub>CH<sub>3</sub>), 10.5 (s, Ar<sup>P</sup>OCH<sub>2</sub>CH<sub>2</sub>CH<sub>3</sub>), 9.6 (s, ArOCH<sub>2</sub>CH<sub>2</sub>CH<sub>3</sub>). The *p*-Ar<sup>P</sup> and *m*-Ar<sup>P</sup> resonances could not be unambiguously assigned with the available data. **<sup>31</sup>P{<sup>1</sup>H} NMR** (162 MHz, CD<sub>2</sub>Cl<sub>2</sub>): δ 4.4 (d, <sup>1</sup>*J*<sub>RhP</sub> = 115).

#### 6.3.5.5 [Rh(2,2'-biphenyl)(C<sub>x</sub>P<sub>2</sub>)(N<sub>2</sub>)] [Al(OR<sup>F</sup>)<sub>4</sub>]



**To prepare a sample in CD<sub>2</sub>Cl<sub>2</sub>:** A solution of dihydrogen complex **64** prepared as described in CD<sub>2</sub>Cl<sub>2</sub> was cooled to -78 °C, evaporated slowly to dryness, the 3 Å molecular sieves replaced (2000 wt%) and the residues dissolved in CH<sub>2</sub>Cl<sub>2</sub> (0.1 mL), twice. The solution was evaporated to dryness a third time and the residues dissolved

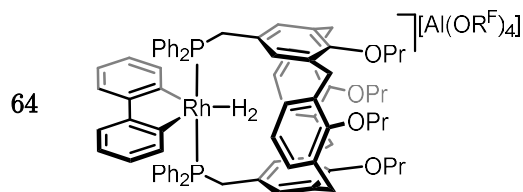
in CD<sub>2</sub>Cl<sub>2</sub>. The resulting solution was freeze-pump-thaw degassed and placed under an atmosphere of dinitrogen affording the title compound as a 5 : 4 equilibrium mixture with CD<sub>2</sub>Cl<sub>2</sub> complex **62**.

**To prepare a sample in C<sub>6</sub>D<sub>5</sub>F**: The above procedure was carried out, followed by cooling the sample to -78 °C and evaporated slowly to dryness. The residues were taken up in C<sub>6</sub>H<sub>5</sub>F, the evaporation procedure repeated, then the residues taken up in C<sub>6</sub>D<sub>5</sub>F. The resulting solution was freeze-pump-thaw degassed and placed under dinitrogen.

Crystals suitable for X-ray diffraction were prepared by slow diffusion of dinitrogen degassed *dry* hexane (*ca.* 19 mL) containing [Me<sub>2</sub>ZrCp<sub>2</sub>] (*ca.* 50 mg) into a dichloromethane solution of a crude reaction mixture from a reaction of water complex **59** with [Me<sub>2</sub>ZrCp<sub>2</sub>] under dinitrogen.

**<sup>1</sup>H NMR** (500 MHz, CD<sub>2</sub>Cl<sub>2</sub>), Selected signals from a 5:4 mixture of **62** and **63**: δ 4.50 – 4.44 (obsc, 4H, ArCH<sub>2(ax)</sub>Ar<sup>P</sup>), 4.10 – 4.05 (m, 4H, ArOCH<sub>2</sub>CH<sub>2</sub>CH<sub>3</sub>), 3.83 (s, 4H, CH<sub>2</sub>P), 3.63 (t, <sup>3</sup>J<sub>HH</sub> = 7.2, 4H, Ar<sup>P</sup>OCH<sub>2</sub>CH<sub>2</sub>CH<sub>3</sub>), 3.15 (d, <sup>2</sup>J<sub>HH</sub> = 13.0, 4H, ArCH<sub>2(eq)</sub>Ar<sup>P</sup>), 2.24 – 2.07 (m, 4H, ArOCH<sub>2</sub>CH<sub>2</sub>CH<sub>3</sub>), 1.89 (h, <sup>3</sup>J<sub>HH</sub> = 6.7, 4H, Ar<sup>P</sup>OCH<sub>2</sub>CH<sub>2</sub>CH<sub>3</sub>), 1.02 (t, <sup>3</sup>J<sub>HH</sub> = 7.4, 6H, Ar<sup>P</sup>OCH<sub>2</sub>CH<sub>2</sub>CH<sub>3</sub>), 0.96 (t, <sup>3</sup>J<sub>HH</sub> = 7.7, 6H, ArOCH<sub>2</sub>CH<sub>2</sub>CH<sub>3</sub>). **<sup>31</sup>P{<sup>1</sup>H} NMR** (162 MHz, CD<sub>2</sub>Cl<sub>2</sub>): δ 16.1 (d, <sup>1</sup>J<sub>RhP</sub> = 116.7). **<sup>31</sup>P{<sup>1</sup>H} NMR** (162 MHz, C<sub>6</sub>D<sub>5</sub>F): δ 16.0 (d, <sup>1</sup>J<sub>RhP</sub> = 116.4).

#### 6.3.5.6 [Rh(2,2'-biphenyl)(C<sub>x</sub>P<sub>2</sub>)(H<sub>2</sub>)] [Al(OR<sup>F</sup>)<sub>4</sub>]

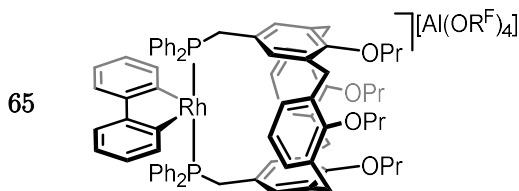


**To prepare a sample in CD<sub>2</sub>Cl<sub>2</sub>**: In an NMR tube, a solution of water complex **59** (11.1 mg, 5.00 μmol) in CD<sub>2</sub>Cl<sub>2</sub> (0.5 mL) under 3 Å molecular sieves (2000 wt%) segregated by a glass platform was freeze-pump-thaw degassed and placed under dihydrogen. The NMR tube was inverted at 0.5 Hz for 12 h.

**To prepare a sample in C<sub>6</sub>H<sub>5</sub>F:** The above procedure was carried out, followed by cooling the sample to -78 °C and evaporated slowly to dryness. The residues were taken up in C<sub>6</sub>H<sub>5</sub>F, the evaporation procedure repeated, then the residues taken up in C<sub>6</sub>D<sub>5</sub>F. The resulting solution was freeze-pump-thaw degassed and placed under dihydrogen affording the title compound.

**<sup>1</sup>H NMR** (500 MHz, CD<sub>2</sub>Cl<sub>2</sub>): δ 8.10 – 5.70 (vbr m, 38H, Ar) 4.47 (br d, <sup>2</sup>J<sub>HH</sub> = 13.1, 4H, ArCH<sub>2(ax)</sub>Ar<sup>P</sup>), 4.18 – 4.06 (m, 4H, ArOCH<sub>2</sub>CH<sub>2</sub>CH<sub>3</sub>), 3.62 (t, <sup>3</sup>J<sub>HH</sub> = 7.1, 4H, Ar<sup>P</sup>OCH<sub>2</sub>CH<sub>2</sub>CH<sub>3</sub>), 3.07 (vbr, fwhm = 100, 4H, ArCH<sub>2(ax)</sub>Ar<sup>P</sup>), 2.25 – 2.10 (m, 4H, ArOCH<sub>2</sub>CH<sub>2</sub>CH<sub>3</sub>), 1.96 (s, 2H), 1.95 – 1.85 (m, <sup>3</sup>J<sub>HH</sub> = 7.3, 4H, Ar<sup>P</sup>OCH<sub>2</sub>CH<sub>2</sub>CH<sub>3</sub>), 1.05 (t, <sup>3</sup>J<sub>HH</sub> = 7.4, 6H, Ar<sup>P</sup>OCH<sub>2</sub>CH<sub>2</sub>CH<sub>3</sub>), 0.96 (t, <sup>3</sup>J<sub>HH</sub> = 7.5, 6H, ArOCH<sub>2</sub>CH<sub>2</sub>CH<sub>3</sub>). **<sup>1</sup>H NMR** (500 MHz, C<sub>6</sub>D<sub>5</sub>F): δ 8.08 – 5.96 (vvbr m, 38H, Ar), 4.90 (vbr, fwhm = 45, 4H, ArCH<sub>2(ax)</sub>Ar<sup>P</sup>), 4.51 (vbr, fwhm = 25, 4H, ArOCH<sub>2</sub>CH<sub>2</sub>CH<sub>3</sub>), 3.93 (t, <sup>3</sup>J<sub>HH</sub> = 7.2, 4H, Ar<sup>P</sup>OCH<sub>2</sub>CH<sub>2</sub>CH<sub>3</sub>), 3.51 (vbr, fwhm = 74, 4H, CH<sub>2</sub>P), 3.41 (vbr, fwhm = 118, 4H, ArCH<sub>2(eq)</sub>Ar<sup>P</sup>), 2.60 (vbr, fwhm = 28, 4H, ArOCH<sub>2</sub>CH<sub>2</sub>CH<sub>3</sub>), 2.24 (app. q, <sup>3</sup>J<sub>HH</sub> = 7.4, 4H, Ar<sup>P</sup>OCH<sub>2</sub>CH<sub>2</sub>CH<sub>3</sub>), 1.36 (t, <sup>3</sup>J<sub>HH</sub> = 7.6, 12H, Ar<sup>P</sup>OCH<sub>2</sub>CH<sub>2</sub>CH<sub>3</sub> & ArOCH<sub>2</sub>CH<sub>2</sub>CH<sub>3</sub>, coincident). Dynamic exchange at 298 K precludes the location of any aromatic signal. **<sup>13</sup>C{<sup>1</sup>H} NMR** (126 MHz, CD<sub>2</sub>Cl<sub>2</sub>): δ 157.8 (s, *i*-Ar<sup>P</sup>), 155.8 (s, *i*-Ar), 137.1 (s, *o*-Ar<sup>P</sup>), 135.6 (br, *p*-Ar<sup>P</sup>), 129.6 (d, <sup>3</sup>J<sub>PC</sub> = 8 *m*-Ar<sup>P</sup>), 127.3 (s, *m*-Ar), 126.5 (s, *o*-Ar) 122.9 (s, *p*-Ar), 121.8 (q, <sup>1</sup>J<sub>FC</sub> = 291, R<sup>F</sup>), 78.7 (s, ArOCH<sub>2</sub>CH<sub>2</sub>CH<sub>3</sub>), 77.2 (s, Ar<sup>P</sup>OCH<sub>2</sub>CH<sub>2</sub>CH<sub>3</sub>), 32.0 (t, <sup>3</sup>J<sub>PC</sub> = 14, CH<sub>2</sub>P), 31.4 (s, ArCH<sub>2</sub>Ar<sup>P</sup>), 24.0 (s, ArOCH<sub>2</sub>CH<sub>2</sub>CH<sub>3</sub>), 23.5 (s, Ar<sup>P</sup>OCH<sub>2</sub>CH<sub>2</sub>CH<sub>3</sub>), 11.0 (s, ArOCH<sub>2</sub>CH<sub>2</sub>CH<sub>3</sub>), 10.1 (s, Ar<sup>P</sup>OCH<sub>2</sub>CH<sub>2</sub>CH<sub>3</sub>). Dynamic exchange at 298 K precludes the location of any phenyl or biph resonance. **<sup>31</sup>P{<sup>1</sup>H} NMR** (162 MHz, CD<sub>2</sub>Cl<sub>2</sub>): δ 25.1 (d, <sup>1</sup>J<sub>RhP</sub> = 112.9). **<sup>31</sup>P{<sup>1</sup>H} NMR** (242 MHz, CD<sub>2</sub>Cl<sub>2</sub>, 185 K): δ 25.4 (d, <sup>1</sup>J<sub>RhP</sub> = 111.9). **<sup>31</sup>P{<sup>1</sup>H} NMR** (162 MHz, C<sub>6</sub>D<sub>5</sub>F): δ 25.1 (d, <sup>1</sup>J<sub>RhP</sub> = 113.3).

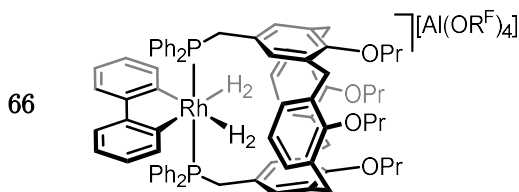
### 6.3.5.7 $[\text{Rh}(2,2'\text{-biphenyl})(\text{C}_x\text{P}_2)][\text{Al}(\text{OR}^{\text{F}})_4]$



A solution of dihydrogen complex **64** prepared as described in  $\text{CD}_2\text{Cl}_2$  was cooled to  $-78^\circ\text{C}$ , evaporated slowly to dryness, the 3 Å MS replaced (2000 wt%) and dissolved in  $\text{CH}_2\text{Cl}_2$  (0.5 mL), twice. The solution was then cooled to  $-78^\circ\text{C}$ , the volatiles removed *in vacuo*, the 3 Å molecular sieves replaced (2000 wt%) and the residues dissolved in  $\text{C}_6\text{H}_5\text{F}$  (0.5 mL), twice. The solution was evaporated to dryness a third time and the residues dissolved in  $\text{C}_6\text{D}_5\text{F}$ , affording the title compound.

**$^1\text{H}$  NMR** (400 MHz,  $\text{C}_6\text{D}_5\text{F}$ ):  $\delta$  7.36 – 7.22 (br m, 6H, Ar), 7.22 – 6.97 (br m, 12H, Ar), 6.76 – 6.55 (br m, 10H, Ar), 6.45 (vbr, fwhm = 51, 4H, Ar), 6.31 (br, 4H, Ar), 6.16 (vbr, fwhm = 97, 2H, Ar), 4.48 (d,  $^2J_{\text{HH}} = 12.7$ , 4H  $\text{ArCH}_{2(\text{ax})}\text{Ar}^{\text{P}}$ ), 4.16 – 4.04 (m, 4H,  $\text{ArOCH}_2\text{CH}_2\text{CH}_3$ ), 3.51 (t,  $^3J_{\text{HH}} = 7.3$ ,  $\text{Ar}^{\text{P}}\text{OCH}_2\text{CH}_2\text{CH}_3$ ), 3.15 (br, 4H,  $\text{CH}_2\text{P}$ ), 3.01 (d,  $^2J_{\text{HH}} = 12.8$ , 4H,  $\text{ArCH}_{2(\text{eq})}\text{Ar}^{\text{P}}$ ), 2.19 (app. hept,  $^3J_{\text{HH}} = 7.7$ , 4H,  $\text{ArOCH}_2\text{CH}_2\text{CH}_3$ ), 1.83 (app. hept,  $^3J_{\text{HH}} = 7.4$ , 4H,  $\text{Ar}^{\text{P}}\text{OCH}_2\text{CH}_2\text{CH}_3$ ), 0.99 – 0.94 (m, 12H,  $\text{Ar}^{\text{P}}\text{OCH}_2\text{CH}_2\text{CH}_3$  &  $\text{ArOCH}_2\text{CH}_2\text{CH}_3$ ). Dynamic exchange at 298 K precludes any meaningful assignment of the ‘Ar’ resonances.  **$^{31}\text{P}\{^1\text{H}\}$  NMR** (162 MHz,  $\text{C}_6\text{D}_5\text{F}$ ):  $\delta$  17.2 (d,  $^1J_{\text{RhP}} = 121.9$ ).

### 6.3.5.8 $[\text{Rh}(2,2'\text{-biphenyl})(\text{C}_x\text{P}_2)(\text{H}_2)_2][\text{Al}(\text{OR}^{\text{F}})_4]$



A solution of dihydrogen complex **64** (*ca.* 10.0  $\mu\text{mol}$ ) in  $\text{CD}_2\text{Cl}_2$  (0.5 mL) under an atmosphere of dihydrogen was cooled below 225 K, resulting in the spontaneous formation of **65**. Characterised *in situ*.  **$^1\text{H}$  NMR** (600 MHz,  $\text{CD}_2\text{Cl}_2$ , 185 K), selected signals:  $\delta$  -0.10 (vbr, fwhm = 177, *exo*- $\text{H}_2$ ), -1.79 (vbr, fwhm = 395, *endo*- $\text{H}_2$ ).  **$^{31}\text{P}\{^1\text{H}\}$  NMR** (242 MHz,  $\text{CD}_2\text{Cl}_2$ , 185 K):  $\delta$  20.3 (d,  $^1J_{\text{RhP}} = 107$ ).

## 6.3.6 Ligand exchange reactions

### 6.3.6.1 Typical procedure for dimethylzirconocene reactions

In an NMR tube, water complex **59** (11.1 mg, 5.00)  $\mu\text{mol}$  and  $[\text{Me}_2\text{ZrCp}_2]$  (3.1 mg, 12.5  $\mu\text{mol}$ ) were dissolved in  $\text{CD}_2\text{Cl}_2$  or  $\text{C}_6\text{H}_5\text{F}$  (0.5 mL). Where desired, the solution was freeze-pump-thaw degassed three times and placed under dihydrogen, dinitrogen, methane or xenon as appropriate. Reactions under argon were not degassed. The reactions were monitored by  $^1\text{H}$  and  $^{31}\text{P}\{^1\text{H}\}$  NMR spectroscopy.

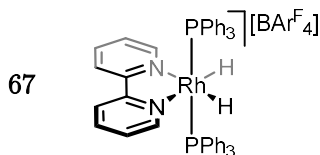
### 6.3.6.2 Typical procedure for 3 Å molecular sieve reactions

In an NMR tube fitted with a glass pedestal supporting *ca.* 250 mg of 3 Å molecular sieves, water complex **59** (11.1 mg, 5.00)  $\mu\text{mol}$  was dissolved in  $\text{CD}_2\text{Cl}_2$  or  $\text{C}_6\text{H}_5\text{F}$  (0.5 mL). Where desired, the solution was freeze-pump-thaw degassed three times and placed under dihydrogen or dinitrogen. The NMR tube was then mounted to a rotating disc, turning at *ca.* 0.5 Hz, to allow the solution to pass over the separated 3 Å molecular sieves. The agitation process was halted intermittently to monitor the reaction by  $^1\text{H}$  and  $^{31}\text{P}\{^1\text{H}\}$  NMR spectroscopy.

## 6.4 Bipyridyl systems

### 6.4.1 Preparation of 2,2'-bipyridyl complexes

#### 6.4.1.1 $[\text{Rh}(2,2'\text{-bipyridyl})(\text{H})_2(\text{PPh}_3)_2][\text{BAr}^{\text{F}}_4]$

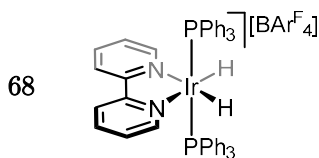


**Method A:** A solution of **69** (31.8 mg, 20.0  $\mu\text{mol}$ ) and 2,2'-bipyridyl (3.1 mg, 20  $\mu\text{mol}$ ) in  $\text{CH}_2\text{Cl}_2$  (1 mL) was freeze-pump-thaw degassed, placed under dihydrogen and stirred at 50 °C for 18 h. The compound was precipitated by the addition of excess hexane (*ca.* 20 mL), which was isolated by filtration. Yield: 17.6 mg (53%, white crystalline solid).

**Method B:** A solution of **76** (100 mg, 81.5  $\mu\text{mol}$ ) and  $\text{PPh}_3$  (42.5 mg, 162  $\mu\text{mol}$ ) in  $\text{CH}_2\text{Cl}_2$  (5 mL) was freeze-pump-thaw degassed and placed under dihydrogen. The solution was stirred for 1 week. Addition of excess pentane (*ca.* 45 mL) afforded the compound on diffusion. Yield: 115 mg (74%, white crystalline solid).

**$^1\text{H}$  NMR** (500 MHz,  $\text{CD}_2\text{Cl}_2$ ):  $\delta$  8.06 (d,  $^3J_{\text{HH}} = 5.2$ , 2H, 6-bipy), 7.75 – 7.70 (m, 8H, *o*-Ar<sup>F</sup>), 7.71 (obsc., 2H, 3-bipy), 7.64 (t,  $^3J_{\text{HH}} = 7.5$ , 2H, 4-bipy), 7.56 (br, 4H, *p*-Ar<sup>F</sup>), 7.39 – 7.29 (m, 18H, *o*-Ph & *p*-Ph), 7.23 (t,  $^3J_{\text{HH}} = 7.4$ , 12H, *m*-Ph), 6.82 (ddd,  $^3J_{\text{HH}} = 7.6$ , 5.5,  $^4J_{\text{HH}} = 1.0$ , 2H, 5-bipy), -15.66 (app. q,  $^1J_{\text{RhH}} \approx ^2J_{\text{PH}} \approx 14.1$ , 2H, RhH).  **$^1\text{H}$  NMR** (400 MHz, THF):  $\delta$  8.17 (br. d,  $^3J_{\text{HH}} = 5.1$ , 2H, 6-bipy), 8.02 (d,  $^3J_{\text{HH}} = 8.1$ , 2H, 3-bipy), 7.78 – 7.73 (m, 8H, *o*-Ar<sup>F</sup>), 7.72 (t,  $^3J_{\text{HH}} = 7.8$ , 2H, 4-bipy), 7.53 (br, 4H, *p*-Ar<sup>F</sup>), 7.34 (app. q,  $^3J_{\text{HH}} = 6.2$ , 12H, *m*-Ph), 7.28 (t,  $J = 7.2$ , 6H, *p*-Ph), 7.20 (t,  $^3J_{\text{HH}} = 7.3$ , 12H, *o*-Ph), 6.89 (t,  $^3J_{\text{HH}} = 6.4$ , 2H, 5-bipy), -15.62 (app. q,  $^1J_{\text{RhH}} \approx ^2J_{\text{PH}} \approx 14.4$ , 2H, RhH).  **$^{13}\text{C}\{^1\text{H}\}$  NMR** (126 MHz,  $\text{CD}_2\text{Cl}_2$ ):  $\delta$  162.3 (q,  $^1J_{\text{CB}} = 50$ , *i*-Ar<sup>F</sup>), 154.5 (s, 6-bipy), 154.3 (s, 2-bipy), 137.8 (s, 4-bipy), 135.4 (s, *o*-Ar<sup>F</sup>), 133.7 (t,  $J_{\text{PC}} = 7$ , *o*-Ph), 132.5 (app t,  $^1J_{\text{PC}} \approx ^2J_{\text{RhC}} \approx 24$ , *i*-Ph), 130.8 (s, *p*-Ph), 129.4 (qq,  $^2J_{\text{FC}} = 32$ ,  $^3J_{\text{CB}} = 3$ , *m*-Ar<sup>F</sup>), 129.0 (t,  $J_{\text{PC}} = 5$ , *m*-Ph), 126.4 (s, 5-bipy), 125.2 (q,  $^3J_{\text{FC}} = 272$ ,  $\text{CF}_3$ ), 122.6 (s, 3-bipy), 118.0 (sept,  $^3J_{\text{FC}} = 4$ , *p*-Ar<sup>F</sup>).  **$^{31}\text{P}\{^1\text{H}\}$  NMR** (162 MHz,  $\text{CD}_2\text{Cl}_2$ ):  $\delta$  47.1 (d,  $^1J_{\text{RhP}} = 115$ ).<sup>†</sup>  **$^{31}\text{P}$  NMR** (162 MHz, THF):  $\delta$  47.3 (d,  $^1J_{\text{RhP}} = 115$ ).<sup>†</sup> **HR ESI-MS** (positive ion): 785.1723  $[\text{M}]^+$  (calcd 785.1716) *m/z*. **Anal.** Calcd for  $\text{C}_{78}\text{H}_{52}\text{BF}_{24}\text{N}_2\text{P}_2\text{Rh}$  (1648.91  $\text{g}\cdot\text{mol}^{-1}$ ): C, 56.82; H, 3.18; N, 1.70. Found: C, 57.04; H, 2.91; N, 1.80.

#### 6.4.1.2 $[\text{Ir}(2,2'\text{-bipyridyl})(\text{H})_2(\text{PPh}_3)_2][\text{BAr}^{\text{F}}_4]$



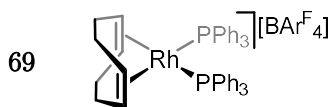
A solution of **70** (33.9 mg, 20.0  $\mu\text{mol}$ ) and 2,2'-bipyridyl (3.1 mg, 20  $\mu\text{mol}$ ) in  $\text{CH}_2\text{Cl}_2$  (1 mL) was freeze-pump-thaw degassed, placed under dihydrogen and agitated at ambient temperature for 10 mins. Addition of excess hexane (*ca.* 20 mL) afforded the



compound on diffusion, which was isolated by filtration and dried *in vacuo*. Yield: 11.2 mg (34%, yellow crystalline solid).

**<sup>1</sup>H NMR** (500 MHz, CD<sub>2</sub>Cl<sub>2</sub>): δ 8.16 (d, <sup>3</sup>J<sub>HH</sub> = 5.3, 2H, 6-bipy), 7.75 – 7.70 (m, 8H, *o*-Ar<sup>F</sup>), 7.71 (obsc., 2H, 3-bipy), 7.64 (t, <sup>3</sup>J<sub>HH</sub> = 7.8, 2H, 4-bipy), 7.56 (br, 4H, *p*-Ar<sup>F</sup>), 7.36 – 7.28 (m, 18H, *o*-Ph & *p*-Ph), 7.22 (t, <sup>3</sup>J<sub>HH</sub> = 7.4, 12H, *m*-Ph), 6.75 (ddd, <sup>3</sup>J<sub>HH</sub> = 7.5, 5.5, <sup>4</sup>J<sub>HH</sub> = 1.0, 2H, 5-bipy), -19.48 (t, <sup>2</sup>J<sub>PH</sub> = 16.6, 2H, IrH). **<sup>1</sup>H NMR** (400 MHz, THF): δ 8.26 (d, <sup>3</sup>J<sub>HH</sub> = 5.5, 2H, 6-nipy), 8.03 (d, <sup>3</sup>J<sub>HH</sub> = 8.2, 2H, 3-bipy), 7.78 – 7.73 (m, 9H, *o*-Ar<sup>F</sup>), 7.73 (t, <sup>3</sup>J<sub>HH</sub> = 8.2, 2H, 4-bipy), 7.53 (s, 4H, *p*-Ar<sup>F</sup>), 7.33 (app. q, <sup>3</sup>J<sub>HH</sub> = 6.3, 12H, *m*-Ph), 7.27 (t, <sup>3</sup>J<sub>HH</sub> = 7.1, 6H, *p*-Ph), 7.19 (t, <sup>3</sup>J<sub>HH</sub> = 7.6, 12H, *o*-Ph), 6.83 (t, <sup>3</sup>J<sub>HH</sub> = 6.7, 2H, 5-bipy), -19.42 (t, <sup>2</sup>J<sub>PH</sub> = 16.8, 2H, IrH). **<sup>13</sup>C{<sup>1</sup>H} NMR** (126 MHz, CD<sub>2</sub>Cl<sub>2</sub>): δ 162.3 (q, <sup>1</sup>J<sub>CB</sub> = 50, *i*-Ar<sup>F</sup>), 156.0 (s, 2-bipy), 155.8 (s, 6-bipy), 137.2 (s, 4-bipy), 135.4 (s, *o*-Ar<sup>F</sup>), 133.6 (t, *J*<sub>FC</sub> = 6, *o*-Ph), 131.8 (t, *J*<sub>FC</sub> = 27, *i*-Ph), 130.9 (s, *p*-Ph), 129.4 (qq, <sup>2</sup>J<sub>FC</sub> = 31, <sup>3</sup>J<sub>CB</sub> = 3, *m*-Ar<sup>F</sup>), 128.9 (t, *J*<sub>FC</sub> = 5, *m*-Ph), 127.3 (s, 5-bipy), 125.2 (q, <sup>1</sup>J<sub>FC</sub> = 272, CF<sub>3</sub>), 123.2 (s, 3-bipy), 118.0 (sept, <sup>3</sup>J<sub>FC</sub> = 4, *p*-Ar<sup>F</sup>). **<sup>31</sup>P{<sup>1</sup>H} NMR** (162 MHz, CD<sub>2</sub>Cl<sub>2</sub>): δ 20.1 (s).<sup>†</sup> **<sup>31</sup>P NMR** (162 MHz, THF): δ 20.2 (s).<sup>†</sup> **HR ESI-MS** (positive ion): 875.2286 [M]<sup>+</sup> (calcd 875.2293) *m/z*. **Anal.** Calcd for C<sub>78</sub>H<sub>52</sub>BF<sub>24</sub>IrN<sub>2</sub>P<sub>2</sub> (1738.22 g·mol<sup>-1</sup>): C, 53.90; H, 3.02; N, 1.61. Found: C, 54.03; H, 2.85; N, 1.69.

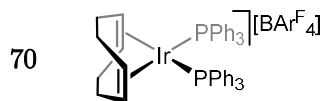
#### 6.4.1.3 [Rh(cod)(PPh<sub>3</sub>)<sub>2</sub>][BAr<sup>F</sup><sub>4</sub>]



A suspension of [{Rh(cod)Cl}<sub>2</sub>] (12.3 mg, 25.0 μmol), PPh<sub>3</sub> (26.2 mg, 100 μmol) and Na[BAr<sup>F</sup><sub>4</sub>] (44.3 mg, 50.0 μmol) in CH<sub>2</sub>Cl<sub>2</sub> (5 ml) was stirred overnight at ambient temperature. Minimal hexane (*ca.* 1 mL) was added with stirring and the solution filtered. The compound was crystallised by slow diffusion of excess hexane (*ca.* 45 mL), and the material isolated by filtration and dried *in vacuo*. Yield: 69.9 mg (87%, orange crystalline solid).

**$^1\text{H}$  NMR** (500 MHz,  $\text{CD}_2\text{Cl}_2$ ):  $\delta$  7.75 – 7.70 (m, 8H, *o*-Ar<sup>F</sup>), 7.56 (br, 4H, *p*-Ar<sup>F</sup>), 7.42 (t,  $^3J_{\text{HH}} = 7.4$ , 6H, *p*-Ph), 7.40 – 7.35 (m, 12H, *o*-Ph), 7.27 (t,  $^3J_{\text{HH}} = 7.2$ , 12H, *m*-Ph), 4.55 (br, 4H, cod CH), 2.54 – 2.42 (m, 4H, cod CH<sub>2</sub>), 2.28 – 2.20 (m, 4H, cod CH<sub>2</sub>).  **$^{13}\text{C}\{^1\text{H}\}$  NMR** (126 MHz,  $\text{CD}_2\text{Cl}_2$ ):  $\delta$  162.3 (q,  $^1J_{\text{CB}} = 50$ , *i*-Ar<sup>F</sup>), 135.4 (s, *o*-Ar<sup>F</sup>), 134.6 (t,  $J_{\text{PC}} = 6$ , *o*-Ph), 131.7 (s, *p*-Ph), 130.5 – 131.3 (m, *i*-Ph), 129.4 (qq,  $^2J_{\text{FC}} = 32$ ,  $^2J_{\text{CB}} = 3$ , *m*-Ar<sup>F</sup>), 129.2 (t,  $J_{\text{PC}} = 5$ , *m*-Ph), 125.2 (q,  $^1J_{\text{FC}} = 272$ , CF<sub>3</sub>), 118.1 (s, *p*-Ar<sup>F</sup>), 99.6 (app. dt,  $^2J_{\text{RhC}} = 8$ ,  $^3J_{\text{PC}} = 5$ , cod CH), 31.2 (s, cod CH<sub>2</sub>).  **$^{31}\text{P}\{^1\text{H}\}$  NMR** (162 MHz,  $\text{CD}_2\text{Cl}_2$ ):  $\delta$  26.5 (d,  $^1J_{\text{RhP}} = 145$ ).<sup>†</sup> **HR ESI-MS** (positive ion): 735.1812 [M]<sup>+</sup> (calcd 735.1811) *m/z*. **Anal.** Calcd for C<sub>78</sub>H<sub>54</sub>BF<sub>24</sub>P<sub>2</sub>Rh (1589.89 g·mol<sup>-1</sup>): C, 57.09; H, 3.40; N, 0.00. Found: C, 57.18; H, 3.56; N, 0.00.

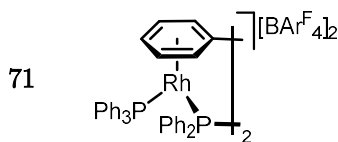
#### 6.4.1.4 [Ir(cod)(PPh<sub>3</sub>)<sub>2</sub>][BAr<sup>F</sup><sub>4</sub>]



A suspension of [ $\{\text{Ir}(\text{cod})\text{Cl}\}_2$ ] (16.8 mg, 25.0  $\mu\text{mol}$ ), PPh<sub>3</sub> (26.2 mg, 100  $\mu\text{mol}$ ) and Na[BAr<sup>F</sup><sub>4</sub>] (44.3 mg, 50.0  $\mu\text{mol}$ ) in CH<sub>2</sub>Cl<sub>2</sub> (5 ml) was stirred overnight at ambient temperature. Minimal hexane (*ca.* 1 mL) was added with stirring and the solution filtered. The compound was crystallised by slow diffusion of excess hexane (*ca.* 45 mL), and the material isolated by filtration and dried *in vacuo*. Yield: 49.0 mg (58%, red crystalline solid).

**$^1\text{H}$  NMR** (400 MHz,  $\text{CD}_2\text{Cl}_2$ ):  $\delta$  7.75 – 7.70 (m, 8H, *o*-Ar<sup>F</sup>), 7.56 (br, 4H, *p*-Ar<sup>F</sup>), 7.42 (t,  $^3J_{\text{HH}} = 7.4$ , 6H, *p*-Ph), 7.40 – 7.35 (m, 12H, *o*-Ph), 7.27 (t,  $^3J_{\text{HH}} = 7.2$ , 12H, *m*-Ph), 4.20 (br, 4H, cod CH), 2.40 – 2.20 (m, 4H, cod CH<sub>2</sub>), 2.06 – 1.85 (m, 4H, cod CH<sub>2</sub>).  **$^{31}\text{P}\{^1\text{H}\}$  NMR** (162 MHz,  $\text{CD}_2\text{Cl}_2$ ):  $\delta$  17.6 (s).<sup>†</sup> **LR ESI-MS** (positive ion): 825.2 [M]<sup>+</sup> (calcd 825.2) *m/z*. Data consistent with previous reports.<sup>385</sup>

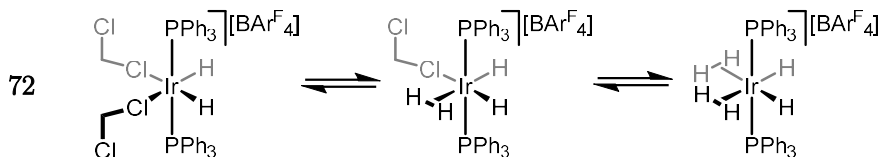
#### 6.4.1.5 $[\{\text{Rh}(\text{PPh}_3)_2\}_2][\text{BAr}^{\text{F}}_4]_2$



A solution of **69** (64.0 mg, 40.0  $\mu\text{mol}$ ) in  $\text{CH}_2\text{Cl}_2$  (5 mL) was freeze-pump-thaw degassed, placed under dihydrogen and stirred for 5 h, after which the solution was freeze-pump-thaw degassed and placed under argon. The compound was crystallised by the slow diffusion of excess hexane (*ca.* 45 mL), which was isolated by filtration and dried *in vacuo*. Yield: 33.7 mg (57%, dark orange crystalline solid).

**$^1\text{H}$  NMR** (500 MHz,  $\text{CD}_2\text{Cl}_2$ ):  $\delta$  7.77 – 7.72 (m, 16H, *o*-Ar<sup>F</sup>), 7.56 (s, 8H, *p*-Ar<sup>F</sup>), 7.50 – 7.41 (m, 4H, Ph), 7.40 – 7.32 (m, 6H, Ph), 7.25 – 7.11 (m, 40H, Ph), 6.87 (t,  $^3J_{\text{HH}} = 6.9$ , 4H,  $\eta$ -*m*-Ph), 6.37 (t,  $^3J_{\text{HH}} = 6.4$ , 4H,  $\eta$ -*o*-Ph), 5.51 (t,  $^3J_{\text{HH}} = 6.5$ , 2H,  $\eta$ -*p*-Ph).  **$^{13}\text{C}\{^1\text{H}\}$  NMR** (126 MHz,  $\text{CD}_2\text{Cl}_2$ ):  $\delta$  162.3 (q,  $^1J_{\text{CB}} = 50$ , *i*-Ar<sup>F</sup>), 135.4 (s, *o*-Ar<sup>F</sup>), 135.1 (d,  $^2J_{\text{PC}} = 12$ , Ph), 134.1 (d,  $^2J_{\text{PC}} = 11$ , Ph), 132.9 (s, Ph), 132.5 (s, Ph), 132.1 (d,  $^4J_{\text{PC}} = 3$ , Ph), 129.5 (d,  $^3J_{\text{PC}} = 8$ , Ph), 129.4 (qq,  $^2J_{\text{FC}} = 32$ ,  $^3J_{\text{CB}} = 3$ , *m*-Ar<sup>F</sup>), 129.2 (d,  $^3J_{\text{PC}} = 11$ , Ph), 129.0 (obsc., Ph), 125.2 (q,  $^1J_{\text{CF}} = 272$ ,  $\text{CF}_3$ ), 123.1 (dd,  $^1J_{\text{PC}} = 33$ ,  $^2J_{\text{RhC}} = 7$ ,  $\eta$ -*i*-Ph), 118.0 (sept,  $^3J_{\text{FC}} = 4$ , *p*-Ar<sup>F</sup>), 106.5 (br d,  $^2J_{\text{PC}} = 10$ ,  $\eta$ -*m*-Ph), 105.4 (s,  $\eta$ -*p*-Ph), 102.6 – 102.4 (m,  $\eta$ -*o*-Ph).  **$^{31}\text{P}\{^1\text{H}\}$  NMR** (162 MHz,  $\text{CD}_2\text{Cl}_2$ ):  $\delta$  45.9 (ddd,  $^1J_{\text{RhP}} = 216$ ,  $^2J_{\text{PP}} = 36$ ,  $^2J_{\text{RhP}} = 7$ ), 43.2 (dd,  $^1J_{\text{RhP}} = 197$ ,  $^2J_{\text{PP}} = 38$ ).<sup>†</sup> **HR ESI-MS** (positive ion): 627.0869 [ $\frac{1}{2}\text{M}$ ]<sup>+</sup> (calcd 627.0872) *m/z*.

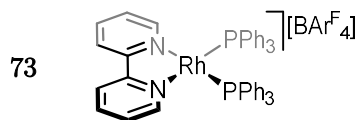
#### 6.4.1.6 $[\text{Ir}(\text{H})_2(\text{PPh}_3)_2\text{L}_2][\text{BAr}^{\text{F}}_4]$ (L = H<sub>2</sub>, $\text{CD}_2\text{Cl}_2$ )



A red solution of **70** (16.9 mg, 10.0  $\mu\text{mol}$ ) in  $\text{CD}_2\text{Cl}_2$  (0.5 mL) was freeze-pump-thaw degassed and placed under dihydrogen, immediately resulting in a colourless solution of **72** and COA on mixing, characterised *in situ*.

**$^1\text{H}$  NMR** (500 MHz,  $\text{CD}_2\text{Cl}_2$ ):  $\delta$  7.76 – 7.71 (m, 8H,  $\text{Ar}^{\text{F}}$ ), 7.56 (s, 4H,  $\text{Ar}^{\text{F}}$ ), 7.58 – 7.47 (m, 30H, Ph), -26.24 (vbr, fwhm = 190 Hz).  **$^1\text{H}$  NMR** (500 MHz,  $\text{CD}_2\text{Cl}_2$ , 185 K):  $\delta$  7.76 – 7.70 (m, 8H,  $\text{Ar}^{\text{F}}$ ), 7.52 (br, 4H,  $\text{Ar}^{\text{F}}$ ), 7.53 – 7.34 (m, 30H, Ph), -1.75 (br,  $T_1 = 54$  ms,  $\text{IrH}_2(\underline{\text{H}}_2)_2$ ), -12.43 (br,  $T_1 = 51$  ms,  $\text{IrH}_2(\underline{\text{H}}_2)(\text{CD}_2\text{Cl}_2)_2$ ), -23.59 (br,  $T_1 = 49$  ms,  $\text{IrH}_2(\text{H}_2)_2$ ), -25.11 (t,  $^2J_{\text{PH}} = 14.6$ ,  $T_1 = 401$  ms,  $\text{IrH}_2(\text{CD}_2\text{Cl}_2)_2$ ), -26.72 (br,  $T_1 = 361$  ms,  $\text{IrH}_2(\text{H}_2)(\text{CD}_2\text{Cl}_2)_2$ ), -28.13 (br,  $T_1 = 358$  ms,  $\text{IrH}_2(\text{H}_2)(\text{CD}_2\text{Cl}_2)_2$ ). The resonance at -23.59 is assigned to a hydride despite the short  $T_1$  value, attributed to chemical exchange on the NMR time scale.  **$^{31}\text{P}\{^1\text{H}\}$  NMR** (202 MHz,  $\text{CD}_2\text{Cl}_2$ ):  $\delta$  23.4 (vbr, fwhm = 130 Hz).<sup>†</sup>  **$^{31}\text{P}\{^1\text{H}\}$  NMR** (202 MHz,  $\text{CD}_2\text{Cl}_2$ , 185 K):  $\delta$  27.0 (s,  $\text{IrH}_2(\text{H}_2)(\text{CD}_2\text{Cl}_2)_2$ ), 23.2 (s,  $\text{IrH}_2(\text{H}_2)_2$ ), 15.7 (s,  $\text{IrH}_2(\text{CD}_2\text{Cl}_2)_2$ ).<sup>†</sup>

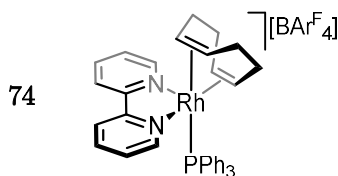
#### 6.4.1.7 $[\text{Rh}(2,2'\text{-bipyridyl})(\text{PPh}_3)_2][\text{BAR}^{\text{F}}_4]$



A solution of **71** (14.9 mg, 5.00  $\mu\text{mol}$ ) and 2,2'-bipyridyl (1.6 mg, 10  $\mu\text{mol}$ ) in  $\text{CH}_2\text{Cl}_2$  (1 mL) and agitated for 10 mins. Slow diffusion of excess hexane (*ca.* 20 mL) deposited the compound as an oil that was isolated by filtration and dried to a solid *in vacuo*. Yield: 2.4 mg (15%, orange-red solid).

**$^1\text{H}$  NMR** (500 MHz,  $\text{CD}_2\text{Cl}_2$ ):  $\delta$  7.97 (d,  $^3J_{\text{HH}} = 8.1$ , 2H, 3-bipy), 7.89 (br d,  $^3J_{\text{HH}} = 5.0$ , 2H, 6-bipy), 7.82 (app t,  $^3J_{\text{HH}} = 7.8$ , 2H, 4-bipy), 7.75 – 7.70 (m, 8H,  $\text{o-Ar}^{\text{F}}$ ), 7.68 – 7.62 (m, 12H,  $\text{o-Ph}$ ), 7.56 (br, 4H,  $\text{p-Ar}^{\text{F}}$ ), 7.30 (t,  $^3J_{\text{HH}} = 7.4$ , 6H,  $\text{p-Ph}$ ), 7.15 (t,  $^3J_{\text{HH}} = 7.5$ , 12H,  $\text{m-Ph}$ ), 6.82 (dd,  $^3J_{\text{HH}} = 6.6$ , 5.8, 2H, 5-bipy).  **$^{13}\text{C}\{^1\text{H}\}$  NMR** (126 MHz,  $\text{CD}_2\text{Cl}_2$ ):  $\delta$  162.3 (q,  $^1J_{\text{CB}} = 50$ ,  $\text{i-Ar}^{\text{F}}$ ), 156.5 (s, 2-bipy), 153.8 (s, 6-bipy), 138.6 (s, 4-bipy), 135.4 (s,  $\text{o-Ar}^{\text{F}}$ ), 135.2 (t,  $J_{\text{PC}} = 6$ ,  $\text{o-Ph}$ ), 134.1 – 133.0 (m,  $\text{i-Ph}$ ), 130.8 (s,  $\text{p-Ph}$ ), 129.4 (qq,  $^2J_{\text{FC}} = 32$ ,  $^3J_{\text{CB}} = 3$ ,  $\text{m-Ar}^{\text{F}}$ ), 128.6 (t,  $J_{\text{PC}} = 5$ ,  $\text{m-Ph}$ ), 126.3 (s, 5-bipy), 125.2 (q,  $^1J_{\text{CF}} = 272$ ,  $\text{CF}_3$ ), 122.5 (s, 3-bipy), 118.0 (sept,  $^3J_{\text{FC}} = 4$ , CH,  $\text{p-Ar}^{\text{F}}$ ).  **$^{31}\text{P}\{^1\text{H}\}$  NMR** (162 MHz,  $\text{CD}_2\text{Cl}_2$ ):  $\delta$  46.6 (d,  $^1J_{\text{RhP}} = 182$ ).<sup>†</sup> **HR ESI-MS** (positive ion): 815.1458  $[\text{M}+\text{MeOH}]^+$  (calcd 815.1458)  $m/z$ .

#### 6.4.1.8 [Rh(2,2'-bipyridyl)(cod)(PPh<sub>3</sub>)] [BAr<sup>F</sup><sub>4</sub>]

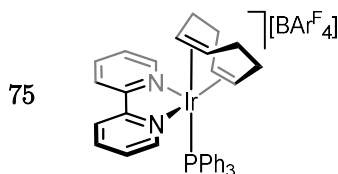


A solution of **76** (24.6 mg, 20.0  $\mu\text{mol}$ ) and PPh<sub>3</sub> (5.2 mg, 20  $\mu\text{mol}$ ) in CH<sub>2</sub>Cl<sub>2</sub> (5 mL) was stirred for 30 mins. The solvent was removed *in vacuo* and the residues washed with hexane (10 mL) and dried *in vacuo*. Yield: 12.0 mg (40%, orange amorphous solid).

Material suitable for X-ray analysis was prepared by slow diffusion of hexane (9 mL) into a CD<sub>2</sub>Cl<sub>2</sub> solution (*ca.* 10 mM) of an equilibrium mixture of the **74** and **73**.

**<sup>1</sup>H NMR** (500 MHz, CD<sub>2</sub>Cl<sub>2</sub>):  $\delta$  9.00 (d,  $^3J_{\text{HH}} = 5.1$ , 2H, 6-bipy), 7.90 (t,  $^3J_{\text{HH}} = 7.4$ , 2H, 4-bipy), 7.77 (d,  $^3J_{\text{HH}} = 8.1$ , 2H, 3-bipy), 7.75 – 7.70 (m, 8H, *o*-Ar<sup>F</sup>), 7.56 (br, 4H, *p*-Ar<sup>F</sup>), 7.55 (obsc., 2H, 5-bipy), 7.38 (t,  $^3J_{\text{HH}} = 7.3$ , 3H, *p*-Ph), 7.26 (br app t,  $J = 8$ , 6H, *o*-Ph), 7.21 (t,  $^3J_{\text{HH}} = 8.4$ , 6H, *m*-Ph), 3.80 (s, 4H, cod CH), 2.67 – 2.55 (m, 4H, cod CH<sub>2</sub>), 2.15 – 2.03 (m, 4H, cod CH<sub>2</sub>). **<sup>13</sup>C{<sup>1</sup>H} NMR** (126 MHz, CD<sub>2</sub>Cl<sub>2</sub>):  $\delta$  162.3 (q,  $^1J_{\text{CB}} = 50$ , *i*-Ar<sup>F</sup>), 154.5 (s, 2-bipy), 151.7 (s, 6-bipy), 139.6 (s, 4-bipy), 135.4 (s, *o*-Ar<sup>F</sup>), 133.9 (d,  $^2J_{\text{PC}} = 12$ , *o*-Ph), 131.3 (d,  $^1J_{\text{PC}} = 28$ , *i*-Ph), 130.8 (s, *p*-Ar<sup>F</sup>), 129.5 (qq,  $^3J_{\text{FC}} = 32$ ,  $^3J_{\text{CB}} = 3$ , *m*-Ar<sup>F</sup>), 129.1 (d,  $^3J_{\text{PC}} = 9$ , *m*-Ph), 127.2 (s, 5-bipy), 125.2 (q,  $^1J_{\text{FC}} = 272$ , CF<sub>3</sub>), 123.4 (s, 3-bipy), 118.0 (sept,  $^3J_{\text{FC}} = 4$ , *p*-Ar<sup>F</sup>), 82.8 (d,  $^1J_{\text{RhC}} = 11$ , cod CH), 31.8 (s, CH<sub>2</sub>, cod CH<sub>2</sub>). **<sup>31</sup>P{<sup>1</sup>H} NMR** (162 MHz, CD<sub>2</sub>Cl<sub>2</sub>):  $\delta$  22.3 (vbr, fwhm = 45 Hz). **<sup>†</sup><sup>31</sup>P{<sup>1</sup>H} NMR** (162 MHz, CD<sub>2</sub>Cl<sub>2</sub>, 200 K):  $\delta$  33.3 (d,  $^1J_{\text{RhP}} = 130$ ). **<sup>†</sup>HR ESI-MS** (positive ion): 367.0679 [M-PPh<sub>3</sub>]<sup>+</sup> (calcd 367.0676) *m/z*. **Anal.** Calcd for C<sub>68</sub>H<sub>47</sub>BF<sub>24</sub>N<sub>2</sub>PRh·CH<sub>2</sub>Cl<sub>2</sub> (1577.72 g·mol<sup>-1</sup>): C, 52.60; H, 3.01; N, 1.78. Found: C, 52.91; H, 3.17; N, 2.15.

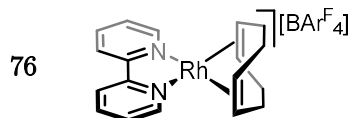
#### 6.4.1.9 [Ir(2,2'-bipyridyl)(cod)(PPh<sub>3</sub>)] [BAr<sup>F</sup><sub>4</sub>]



A solution of **77** (10.0 mg, 7.58  $\mu\text{mol}$ ) and  $\text{PPh}_3$  (2.2 mg, 8.4  $\mu\text{mol}$ ) in  $\text{CH}_2\text{Cl}_2$  (1 mL) was agitated for 10 mins. Slow diffusion of excess hexane (*ca.* 20 mL) crystallised the title compound, which was isolated by filtration and dried *in vacuo*. Yield: 6.7 mg (56%, red crystalline solid).

**$^1\text{H}$  NMR** (500 MHz,  $\text{CD}_2\text{Cl}_2$ ):  $\delta$  9.13 (br, 2H, 6-bipy), 7.89 (t,  $^3J_{\text{HH}} = 7.6$  Hz, 2H, 4-bipy), 7.81 (d,  $^3J_{\text{HH}} = 7.9$  Hz, 2H, 3-bipy), 7.75 – 7.70 (m, 8H, *o*-Ar<sup>F</sup>), 7.56 (br, 4H, *p*-Ar<sup>F</sup>), 7.50 (t,  $^3J_{\text{HH}} = 6.4$ , 2H, 5-bipy), 7.38 (t,  $^3J_{\text{HH}} = 7.3$ , 3H, *p*-Ph), 7.25 (br app t,  $J = 8$ , *o*-Ph), 7.13 (app. t,  $^3J_{\text{HH}} = 8.9$ , 6H, *m*-Ph), 3.23 (br, 4H, cod CH), 2.51 – 2.37 (m, 4H, cod  $\text{CH}_2$ ), 1.94 – 1.81 (m, 4H, cod  $\text{CH}_2$ ).  **$^{13}\text{C}\{^1\text{H}\}$  NMR** (126 MHz,  $\text{CD}_2\text{Cl}_2$ ):  $\delta$  162.3 (q,  $^1J_{\text{CB}} = 50$ , *i*-Ar<sup>F</sup>), 155.6 (HMBC, 2-bipy), 152.5 (s, 6-bipy), 138.9 (s, 4-bipy), 135.4 (s, *o*-Ar<sup>F</sup>), 133.6 (d,  $^3J_{\text{PC}} = 10$ , *m*-Ph), 131.1 (s, *p*-Ph), 130.8 (HMBC, *i*-Ph), 129.4 (qq,  $^2J_{\text{FC}} = 32$ ,  $^3J_{\text{CB}} = 3$ , *m*-Ar<sup>F</sup>), 129.1 (d,  $^2J_{\text{PC}} = 9$ , *o*-Ph), 127.7 (s, 5-bipy), 125.2 (q,  $^1J_{\text{FC}} = 272$ ,  $\text{CF}_3$ ), 123.9 (s, 3-bipy), 118.0 (sept,  $^3J_{\text{FC}} = 5$ , *p*-Ar<sup>F</sup>), 65.2 (br. s, cod CH), 33.0 (s,  $\text{CH}_2$ , cod  $\text{CH}_2$ ).  **$^{31}\text{P}\{^1\text{H}\}$  NMR** (162 MHz,  $\text{CD}_2\text{Cl}_2$ ):  $\delta$  10.1 (s).<sup>†</sup> **HR ESI-MS** (positive ion): 719.2168  $[\text{M}]^+$  (calcd 719.2163) *m/z*. **Anal.** Calcd for  $\text{C}_{68}\text{H}_{47}\text{BF}_{24}\text{N}_2\text{PIr}$  (1582.10  $\text{g}\cdot\text{mol}^{-1}$ ): C, 51.62; H, 2.99; N, 1.77. Found: C, 51.43; H, 2.87; N, 1.84.

#### 6.4.1.10 $[\text{Rh}(2,2'\text{-bipyridyl})(\text{cod})][\text{BAr}^{\text{F}}_4]$

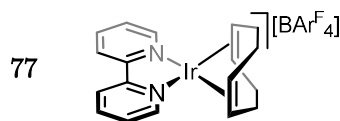


A suspension of  $[\{\text{Rh}(\text{cod})\text{Cl}\}_2]$  (24.6 mg, 50.0  $\mu\text{mol}$ ), 2,2'-bipyridyl (15.6 mg, 100  $\mu\text{mol}$ ) and  $\text{Na}[\text{BAr}^{\text{F}}_4]$  (88.6 mg, 100  $\mu\text{mol}$ ) in  $\text{CH}_2\text{Cl}_2$  (5 mL) was stirred at ambient temperature for 18 h. Minimal hexane (*ca.* 1 mL) was added with stirring and the solution filtered. Slow diffusion of excess hexane (*ca.* 45 mL) crystallised the title compound, which was isolated by filtration and dried *in vacuo*. Yield: 91.9 mg (75%, red crystalline solid).

**$^1\text{H}$  NMR** (500 MHz,  $\text{CD}_2\text{Cl}_2$ ):  $\delta$  8.11 (app. td,  $^3J_{\text{HH}} = 7.9$ ,  $^4J_{\text{HH}} = 1.5$ , 2H, 4-bipy), 8.07 (d,  $^3J_{\text{HH}} = 8.2$ , 2H, 3-bipy), 7.79 (d,  $^3J_{\text{HH}} = 5.5$ , 2H, 6-bipy), 7.75 – 7.70 (m, 8H, *o*-Ar<sup>F</sup>),

7.59 (ddd,  $^3J_{\text{HH}} = 7.7$ , 5.5,  $^4J_{\text{HH}} = 1.4$ , 2H, 5-bipy), 7.55 (br, 4H,  $p\text{-Ar}^{\text{F}}$ ), 4.57 (br, 4H, cod CH), 2.66 – 2.53 (m, 4H, cod CH<sub>2</sub>), 2.24 – 2.12 (m, 4H, cod CH<sub>2</sub>).  **$^{13}\text{C}\{^1\text{H}\}$  NMR** (126 MHz, CD<sub>2</sub>Cl<sub>2</sub>):  $\delta$  162.3 (q,  $^1J_{\text{CB}} = 50$ ,  $i\text{-Ar}^{\text{F}}$ ), 156.8 (s, 2-bipy), 149.1 (s, 6-bipy), 141.7 (s, 4-bipy), 135.4 (s,  $o\text{-Ar}^{\text{F}}$ ), 129.4 (qq,  $^2J_{\text{FC}} = 32$ ,  $^3J_{\text{CB}} = 3$ ,  $m\text{-Ar}^{\text{F}}$ ), 128.1 (s, 5-bipy), 125.2 (q,  $^1J_{\text{FC}} = 272$ , CF<sub>3</sub>), 123.4 (s, 3-bipy), 118.0 (sept,  $^3J_{\text{FC}} = 4$ ,  $p\text{-Ar}^{\text{F}}$ ), 86.5 (d,  $^1J_{\text{RhC}} = 12$ , cod CH), 30.7 (s, cod CH<sub>2</sub>). **HR ESI-MS** (positive ion): 367.0677 [M]<sup>+</sup> (calcd 367.0676) *m/z*. **Anal.** Calcd for C<sub>50</sub>H<sub>32</sub>BF<sub>24</sub>N<sub>2</sub>Rh (1230.50 g·mol<sup>-1</sup>): C, 48.81; H, 2.62; N, 2.28. Found: C, 48.89; H, 2.52; N, 2.46.

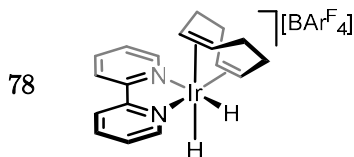
#### 6.4.1.11 [Ir(2,2'-bipyridyl)(cod)][BAR<sup>F</sup><sub>4</sub>]



A suspension of [ $\{\text{Ir}(\text{cod})\text{Cl}\}_2$ ] (24.6 mg, 50.0  $\mu\text{mol}$ ), 2,2'-bipyridyl (15.6 mg, 100  $\mu\text{mol}$ ) and Na[BAR<sup>F</sup><sub>4</sub>] (88.6 mg, 100  $\mu\text{mol}$ ) in CH<sub>2</sub>Cl<sub>2</sub> (5 mL) was stirred at ambient temperature for 18 h. Hexane (*ca.* 1 mL) was added and the solution filtered. Slow diffusion of excess hexane (*ca.* 45 mL) crystallised the title compound, which was isolated by filtration and dried *in vacuo*. Yield: 91.5 mg (67%, dark green solid).

**$^1\text{H}$  NMR** (500 MHz, CD<sub>2</sub>Cl<sub>2</sub>):  $\delta$  8.20 (app. td,  $^3J_{\text{HH}} = 8.2$ ,  $^4J_{\text{HH}} = 1.2$ , 2H, 4-bipy), 8.14 (d,  $^3J_{\text{HH}} = 8.1$ , 2H, 3-bipy), 8.11 (d,  $^3J_{\text{HH}} = 5.6$ , 2H, 6-bipy), 7.75 – 7.70 (m, 8H,  $o\text{-Ar}^{\text{F}}$ ), 7.69 (ddd,  $^3J_{\text{HH}} = 7.8$ , 5.6,  $^4J_{\text{HH}} = 1.0$ , 2H, 5-bipy), 7.55 (br, 4H,  $p\text{-Ar}^{\text{F}}$ ), 4.40 (br, 4H, cod CH), 2.51 – 2.32 (m, 4H, cod CH<sub>2</sub>), 2.14 – 1.97 (m, 4H, cod CH<sub>2</sub>).  **$^{13}\text{C}\{^1\text{H}\}$  NMR** (126 MHz, CD<sub>2</sub>Cl<sub>2</sub>):  $\delta$  162.3 (q,  $^1J_{\text{CB}} = 50$ ,  $i\text{-Ar}^{\text{F}}$ ), 158.4 (s, 2-bipy), 149.6 (s, 6-bipy), 142.6 (s, 4-bipy), 135.4 (s,  $o\text{-Ar}^{\text{F}}$ ), 129.4 (qq,  $^2J_{\text{FC}} = 32$ ,  $^3J_{\text{CB}} = 3$ ,  $m\text{-Ar}^{\text{F}}$ ), 128.9 (s, 5-bipy), 125.2 (q,  $^1J_{\text{FC}} = 272$ , CF<sub>3</sub>), 123.7 (s, 3-bipy), 118.0 (sept,  $^3J_{\text{FC}} = 4$ ,  $p\text{-Ar}^{\text{F}}$ ), 72.2 (s, cod CH), 31.5 (s, cod CH<sub>2</sub>). **HR ESI-MS** (positive ion): 457.1250 [M]<sup>+</sup> (calcd 457.1251) *m/z*. **Anal.** Calcd for C<sub>50</sub>H<sub>32</sub>BF<sub>24</sub>IrN<sub>2</sub> (1319.81 g·mol<sup>-1</sup>): C, 45.50; H, 2.44; N, 2.12. Found: C, 45.83; H, 2.56; N, 2.19.

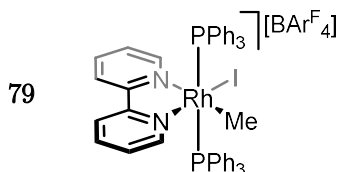
#### 6.4.1.12 [Ir(2,2'-bipyridyl)(cod)(H)<sub>2</sub>][BAr<sup>F</sup><sub>4</sub>]



A solution of **77** (13.2 mg, 10.0  $\mu$ mol) in CD<sub>2</sub>Cl<sub>2</sub> (0.5 mL) was freeze-pump-thaw degassed and placed under dihydrogen immediately resulting in an equilibrium mixture of **77** and **78** on mixing in a 5 : 1 ratio, characterised *in situ*.

<sup>1</sup>H NMR (400 MHz, CD<sub>2</sub>Cl<sub>2</sub>):  $\delta$  9.34 (d, <sup>3</sup>J<sub>HH</sub> = 4.9, 2H, bipy), 9.25 (d, <sup>3</sup>J<sub>HH</sub> = 4.5, 2H, bipy), 8.35 – 8.27 (m, 2H, bipy), 8.11 – 8.04 (m, 2H, bipy), 5.04 – 4.99 (m, 1H, cod CH), 4.96 – 4.89 (m, 1H, cod CH), 4.20 – 4.10 (m, 1H, cod CH), 3.73 – 3.62 (m, 1H, cod CH), 3.52 – 3.44 (m, 2H, cod CH<sub>2</sub>), 2.94 – 2.77 (m, 2H, cod CH<sub>2</sub>), 2.69 – 2.57 (m, 2H, cod CH<sub>2</sub>), 1.83 – 1.70 (m, 2H, cod CH<sub>2</sub>), -11.99 (s, 1H, IrH), -14.31 (s, 1H, IrH).

#### 6.4.1.13 [Rh(2,2'-bipyridyl)(I)(Me)(PPh<sub>3</sub>)<sub>2</sub>][BAr<sup>F</sup><sub>4</sub>]



To a solution of **73** (16.5 mg, 10.0  $\mu$ mol) in CD<sub>2</sub>Cl<sub>2</sub> (0.5 mL) was added MeI (3.1  $\mu$ L, 50.0  $\mu$ mol) and the mixture left to stand for 72 h. Slow diffusion of excess hexane (*ca.* 20 mL) crystallised the title compound, which was isolated by filtration and dried *in vacuo*. Yield: 11.1 mg (62%, orange crystalline solid).

<sup>1</sup>H NMR (500 MHz, CD<sub>2</sub>Cl<sub>2</sub>):  $\delta$  8.85 (d, <sup>3</sup>J<sub>HH</sub> = 5.4, 1H, 6'-bipy), 7.96 (d, <sup>3</sup>J<sub>HH</sub> = 8.1, 1H, 3'-bipy), 7.87 – 7.80 (m, 2H, 5'-bipy & 3-bipy), 7.76 – 7.70 (m, 9H, *o*-Ar<sup>F</sup> & 5-bipy), 7.57 (br, 4H, *p*-Ar<sup>F</sup>), 7.31 (t, <sup>3</sup>J<sub>HH</sub> = 7.2, 6H, *p*-Ph), 7.19 – 7.14 (m, 12H, *m*-Ph), 7.16 (COSY/HSQC, 6-bipy), 7.12 (t, <sup>3</sup>J<sub>HH</sub> = 7.5, 12H, *o*-Ph), 7.07 (t, <sup>3</sup>J<sub>HH</sub> = 6.6, 1H, 4'-bipy), 6.69 (t, <sup>3</sup>J<sub>HH</sub> = 6.7, 1H, 4-bipy), 1.68 (td, <sup>3</sup>J<sub>PH</sub> = 5.7, <sup>2</sup>J<sub>RhH</sub> = 2.0, 3H, Me). <sup>13</sup>C{<sup>1</sup>H} NMR (126 MHz, CD<sub>2</sub>Cl<sub>2</sub>): 162.3 (q, <sup>1</sup>J<sub>CB</sub> = 50, *i*-Ar<sup>F</sup>), 156.6 (s, 2-bipy), 154.9 (s, 6-bipy), 153.0 (s, 2'-bipy), 149.8 (s, 6'-bipy), 139.0 (s, 5-bipy), 138.8 (s, 5'-bipy), 135.4 (s, *o*-Ar<sup>F</sup>), 134.4



(t,  $J_{\text{PC}} = 5$ , *o*-Ph), 131.1 (s, *p*-Ph), 130.0 (t,  $J_{\text{PC}} = 23$ , *i*-Ph), 129.4 (qq,  $^2J_{\text{FC}} = 32$ ,  $^3J_{\text{CB}} = 3$ , *m*-Ar<sup>F</sup>), 128.8 (t,  $J_{\text{PC}} = 5$ , *m*-Ph), 128.7 (s, 4'-bipy), 128.6 (s, 4-bipy), 125.2 (q,  $^1J_{\text{FC}} = 272$ , CF<sub>3</sub>), 123.5 (s, 3-bipy), 122.6 (s, 3'-bipy), 118.0 (sept,  $^3J_{\text{FC}} = 4$ , *p*-Ar<sup>F</sup>), -1.4 (dt,  $^1J_{\text{RhC}} = 20$ ,  $^2J_{\text{PC}} = 7$ , Me). **<sup>31</sup>P{<sup>1</sup>H} NMR** (202 MHz, CD<sub>2</sub>Cl<sub>2</sub>): δ 16.1 (d,  $^1J_{\text{RhP}} = 96$ ).<sup>†</sup> **HR ESI-MS** (positive ion): 925.0823 ([M]<sup>+</sup>, calcd 925.0839) *m/z*.

## 6.4.2 Mechanism probing reactions

### 6.4.2.1 Hydrogenation of [M(cod)(PPh<sub>3</sub>)<sub>2</sub>][BAr<sup>F</sup><sub>4</sub>]

**General procedure:** An NMR tube containing a solution of **69** or **70** (10 μmol) in CD<sub>2</sub>Cl<sub>2</sub> (0.5 mL) was freeze-pump-thaw degassed and placed under dihydrogen. The NMR tube was sealed, inverted several times, and left to stand at the appropriate temperature while being monitored by <sup>1</sup>H and <sup>31</sup>P{<sup>1</sup>H} NMR spectroscopy.

**Hydrogenation of 69 at 25 °C:** Smooth conversion to **71** is observed ( $t_{1/2} = 0.8$  h) with exclusive formation of COA as the only hydrocarbon product.

**Hydrogenation of 69 at 50 °C:** Smooth conversion to **71** is observed ( $t_{1/2} = 0.6$  h) with exclusive formation of COA as the only hydrocarbon product.

**Hydrogenation of 70 at 25 °C:** Full conversion to **72** within 5 min with exclusive formation of COA as the only hydrocarbon product.

### 6.4.2.2 Reaction of [{Rh(PPh<sub>3</sub>)<sub>2</sub>}<sub>2</sub>][BAr<sup>F</sup>]<sub>2</sub>, **71** with 2,2'-bipyridyl

Addition of 2,2'-bipyridyl (1.6 mg, 10.0 μmol) to a solution of **71** (14.9 mg, 5.0 μmol) in CD<sub>2</sub>Cl<sub>2</sub> (0.5 mL) in an NMR tube resulted in quantitative formation of **73** within 5 mins as gauged by <sup>1</sup>H and <sup>31</sup>P{<sup>1</sup>H} NMR spectroscopy.

### 6.4.2.3 Reaction of [IrH<sub>2</sub>(PPh<sub>3</sub>)<sub>2</sub>L<sub>2</sub>][BAr<sup>F</sup><sub>4</sub>] (L = H<sub>2</sub>, CD<sub>2</sub>Cl<sub>2</sub>) with 2,2'-bipyridyl

A solution of **72** was transferred to an NMR tube containing 2,2'-bipyridyl (1.6 mg, 10 μmol) under dihydrogen resulting immediately in the quantitative formation of **70**.

#### 6.4.2.4 Hydrogenation of $[M(\text{cod})(\text{PPh}_3)_2][\text{BAr}^{\text{F}}_4]$ in the presence of 2,2'-bipyridyl

**General procedure:** **69** or **70** (10  $\mu\text{mol}$ ) and 2,2'-bipyridyl (1.6 mg, 10  $\mu\text{mol}$ ) cooled in liquid nitrogen, then thawed under an atmosphere of dihydrogen. The NMR tube was sealed, inverted several times, then left to stand at the appropriate reaction temperature with *in situ* monitoring by  $^1\text{H}$  spectroscopy. At the conclusion of the reaction, the mixture was passed through a short plug of  $\text{SiO}_2$  ( $\text{CH}_2\text{Cl}_2$ ) and analysed by gas chromatography.

**Hydrogenation of 69 and 2,2'-bipyridyl at 25 °C:** After 2 h, **69** was consumed with concomitant formation of **67** (*ca.* 58% [Rh]) and **74** (*ca.* 42% [Rh]). Complete conversion to **67** was observed after 8 days with a hydrocarbon distribution of: COA (14%), COE (23%), COD (63%).

**Hydrogenation of 69 and 2,2'-bipyridyl at 50 °C:** After 1 h, **69** was consumed with concomitant formation of **67** (*ca.* 58% [Rh]) and **74** (*ca.* 42% [Rh]). Complete conversion to **67** was observed after 18 h with a hydrocarbon distribution of: COA (6%), COE (36%), COD (58%).

**Hydrogenation of 70 and 2,2'-bipyridyl at 25 °C:** The red solution became immediately pale yellow, with quantitative conversion to **68** and a hydrocarbon distribution of: COA (14%), COE (86%), COD (0%).

#### 6.4.2.5 Reaction of $[\text{Rh}(2,2'\text{-bipyridyl})(\text{cod})][\text{BAr}^{\text{F}}_4]$ with 2.0 equivalents of $\text{PPh}_3$

In an NMR tube, **76** (12.3 mg, 10.0  $\mu\text{mol}$ ) and  $\text{PPh}_3$  (5.2 mg, 20  $\mu\text{mol}$ ) was dissolved in  $\text{CD}_2\text{Cl}_2$  (0.5 mL) resulting in the immediate formation of a fast exchanging mixture of  $[\text{Rh}(2,2'\text{-bipyridyl})(\text{cod})(\text{PPh}_3)][\text{BAr}^{\text{F}}_4]$ , **74** and free  $\text{PPh}_3$ , which was analysed by VT-NMR spectroscopy.  $^{31}\text{P}\{^1\text{H}\}$  NMR (202 MHz,  $\text{CD}_2\text{Cl}_2$ ):  $\delta$  10.6 (vbr, fwhm = 55 Hz, **74** &  $\text{PPh}_3$ ).<sup>†</sup>  $^{31}\text{P}\{^1\text{H}\}$  NMR (202 MHz,  $\text{CD}_2\text{Cl}_2$ , 200 K):  $\delta$  33.3 (d,  $^1J_{\text{RhP}} = 129$ , **74**), -8.3 (s,  $\text{PPh}_3$ ).<sup>†</sup>

#### 6.4.2.6 Reaction of $[\text{Ir}(\text{2,2'-'bipyridyl})(\text{cod})][\text{BAr}^{\text{F}}_4]$ , **77** with 2.0 equivalents of $\text{PPh}_3$

In an NMR tube, **77** (10.0 mg, 7.6  $\mu\text{mol}$ ) and  $\text{PPh}_3$  (4.2 mg, 15  $\mu\text{mol}$ ) was dissolved in  $\text{CD}_2\text{Cl}_2$  (0.5 mL) resulting in the immediate formation of **75** and free  $\text{PPh}_3$ .

#### 6.4.2.7 Reaction of $[\text{M}(\text{cod})(\text{PPh}_3)_2][\text{BAr}^{\text{F}}_4]$ with 2,2'-bipyridyl

**General procedure:** An NMR tube containing  $[\text{M}(\text{cod})(\text{PPh}_3)_2][\text{BAr}^{\text{F}}_4]$  ( $\text{M} = \text{Rh}$ , **69**;  $\text{M} = \text{Ir}$ , **70**; 10  $\mu\text{mol}$ ) dissolved in  $\text{CD}_2\text{Cl}_2$  (0.5 mL) was added 2,2'-bipyridyl (1.6 mg, 10  $\mu\text{mol}$ ). The NMR tube was sealed, inverted several times, then left to stand at the appropriate reaction temperature.

**Reaction of 69 with 2,2'-bipyridyl at 25 °C:** Full initial conversion to **74** ( $t_{1/2} = 1.3$  h), with subsequent slow equilibrium formation of **73** alongside liberation of COD. Modelling the kinetics of the approach to equilibrium over 8 days,<sup>431</sup> enabled the determination of the reaction rate ( $t_{1/2} = 107$  h) and equilibrium constant ( $K_{\text{eq}} = 2.41$ ).

**Reaction of 69 with 2,2'-bipyridyl at 50 °C:** Full initial conversion to **74** ( $t_{1/2} \approx 0.47$  h), with subsequent equilibrium formation of **73** alongside liberation of COD. The equilibrium is fully established in *ca.* 8 h ( $t_{1/2} = 1.81$  h,  $K_{\text{eq}} = 2.07$ ).

**Reaction of 70 with 2,2'-bipyridyl at 25 °C:** Slow conversion to **75** ( $t_{1/2} = 34$  h) with no subsequent reaction observed.

#### 6.4.2.8 Hydrogenation of $[\text{M}(\text{2,2'-'bipyridyl})(\text{cod})][\text{BAr}^{\text{F}}_4]$

**General procedure:** In an NMR tube, a solution of **76** or **77** (10.0  $\mu\text{mol}$ ) in  $\text{CD}_2\text{Cl}_2$  (0.5 mL) was freeze-pump-thaw degassed and placed under dihydrogen (1 atm). The tube was sealed, inverted several times, then left to stand at ambient temperature for 24 h and at 50 °C for a further 72 h with periodic monitoring by  $^1\text{H}$  and  $^{31}\text{P}\{^1\text{H}\}$  NMR spectroscopy.

**Hydrogenation of 78:** No reaction was observed.

**Hydrogenation of 79:** Immediate conversion to an 1:5 equilibrium mixture of **77** and  $[\text{Ir}(2,2'\text{-bipyridyl})(\text{cod})\text{H}_2][\text{BAr}^{\text{F}}_4]$ , **78**. No appreciable change in the constituency of the mixture is detected upon extended heating, and upon a subsequent freeze-pump-thaw degas **77** is the only species of observed in solution.

#### 6.4.2.9 Hydrogenation of $[\text{Rh}(2,2'\text{-bipyridyl})(\text{PPh}_3)_2][\text{BAr}^{\text{F}}_4]$

An NMR tube containing a solution of **73** (16.5 mg, 10.0  $\mu\text{mol}$ ) in  $\text{CD}_2\text{Cl}_2$  (0.5 mL) was freeze-pump-thaw degassed and placed under dihydrogen resulting in quantitative formation of **67** within 5 mins as gauged by  $^1\text{H}$  and  $^{31}\text{P}\{^1\text{H}\}$  NMR spectroscopy.

### 6.4.3 Dehydrogenation reactions

#### 6.4.3.1 Reactions of $[\text{M}(2,2'\text{-bipyridyl})\text{H}_2(\text{PPh}_3)_2][\text{BAr}^{\text{F}}_4]$ with COD

**General procedure:** An NMR tube containing a solution of  $[\text{M}(2,2'\text{-bipyridyl})\text{H}_2(\text{PPh}_3)_2][\text{BAr}^{\text{F}}_4]$  ( $\text{M} = \text{Rh}$ , **67**;  $\text{M} = \text{Ir}$ , **68**; 10  $\mu\text{mol}$ ) in  $\text{CD}_2\text{Cl}_2$  (0.5 mL) was freeze-pump-thaw degassed and placed under dihydrogen. Under a flow of dihydrogen, COD (1.2  $\mu\text{L}$ , 10  $\mu\text{mol}$ ) was added and the tube sealed. After heating at 50  $^\circ\text{C}$  for 18 h (**67**) or immediately (**68**) a  $^1\text{H}$  and  $^{31}\text{P}\{^1\text{H}\}$  NMR spectrum was recorded and the sample passed through a short plug of  $\text{SiO}_2$  ( $\text{CH}_2\text{Cl}_2$ ) for analysis by gas chromatography.

**Reaction of 67 with COD:** No COA or COE was observed by NMR. GC analysis indicated hydrocarbon ratios of COA (0%), COE (1%), COD (99%).

**Reaction of 68 with COD:** No COA or COE was observed by NMR or GC analysis.

#### 6.4.3.2 Reaction of $[\text{M}(2,2'\text{-bipyridyl})\text{H}_2(\text{PPh}_3)_2][\text{BAr}^{\text{F}}_4]$ with TBE

**General procedure:** To an NMR tube containing a solution of **67** or **68** (10  $\mu\text{mol}$ ) in  $\text{CD}_2\text{Cl}_2$  (0.5 mL) was added TBE (12.9  $\mu\text{L}$ , 100  $\mu\text{mol}$ ). The tube was sealed and the reaction mixture heated at 50  $^\circ\text{C}$  with intermittent monitoring by  $^1\text{H}$  and  $^{31}\text{P}\{^1\text{H}\}$  NMR spectroscopy.

**Reaction of 67 with TBE:** After 6 days 15% conversion to  $[\text{Rh}(2,2'\text{-bipyridyl})(\text{PPh}_3)_2][\text{BAr}^{\text{F}}_4]$  **73** was observed.

**Reaction of 68 with TBE:** No reaction was observed after 42 days.

#### 6.4.4 Oxidative addition reactions

##### 6.4.4.1 Reaction of $[\text{Rh}(2,2'\text{-bipyridyl})(\text{PPh}_3)_2][\text{BAr}^{\text{F}}_4]$ with MeI

To an NMR tube containing a solution of **73** (16.5 mg, 10.0  $\mu\text{mol}$ ) in  $\text{CD}_2\text{Cl}_2$  (0.5 mL) was added MeI (3.1  $\mu\text{L}$ , 50  $\mu\text{mol}$ ). The tube was sealed and the reaction monitored by  $^1\text{H}$  and  $^{31}\text{P}\{^1\text{H}\}$  NMR spectroscopy. The reaction was complete in 24 h ( $t_{1/2} = 6.0$  h).

##### 6.4.4.2 Reaction of $[\text{Rh}(2,2'\text{-bipyridyl})(\text{PPh}_3)_2][\text{BAr}^{\text{F}}_4]$ with methane

In an NMR tube, a solution of **73** (16.5 mg, 10.0  $\mu\text{mol}$ ) in  $\text{CD}_2\text{Cl}_2$  (0.5 mL) was freeze-pump-thaw degassed three times and placed under an atmosphere of methane. The tube was sealed and heated to 50  $^\circ\text{C}$  and the reaction monitored by  $^1\text{H}$  and  $^{31}\text{P}\{^1\text{H}\}$  NMR spectroscopy. No reaction was observed after 1 week. Over the subsequent 3 weeks decomposition to several unidentified compounds was observed, attributed to a leak of the NMR tube rather than any reaction with methane.

#### 6.4.5 Substitution reactions

##### 6.4.5.1 Reaction of $[\text{M}(2,2'\text{-bipyridyl})\text{H}_2(\text{PPh}_3)_2][\text{BAr}^{\text{F}}_4]$ with $\text{PCy}_3$ in THF

**General procedure:** A solution of **67** or **68** (10  $\mu\text{mol}$ ) in THF (0.5 mL) was transferred via cannula to an NMR tube containing  $\text{PCy}_3$  (14.0 mg, 50  $\mu\text{mol}$ ). The tube was sealed, and the reaction monitored by  $^1\text{H}$  and  $^{31}\text{P}\{^1\text{H}\}$  NMR spectroscopy at ambient temperature for 6 days. The reaction was then heated to 50  $^\circ\text{C}$  with intermittent monitoring by  $^1\text{H}$  and  $^{31}\text{P}\{^1\text{H}\}$  NMR spectroscopy.

**Reaction of 67 with  $\text{PCy}_3$ :** No reaction was observed after 6 days at ambient temperature. Heating to 50  $^\circ\text{C}$  **67** gave rise over a period of 16 weeks to an equilibrium

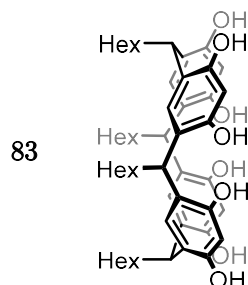
mixture of **67** (26%),  $[\text{Rh}(2,2'\text{-bipyridyl})(\text{H})_2(\text{PPh}_3)(\text{PCy}_3)][\text{BAr}^{\text{F}}_4]$  (**80**, 68%) and  $[\text{Rh}(2,2'\text{-bipyridyl})(\text{H})_2(\text{PCy}_3)_2][\text{BAr}^{\text{F}}_4]$  (**81**, 6%). Selected data for **80**:  $^1\text{H}$  NMR (400 MHz, THF):  $\delta$  -16.69 (app. q,  $^1J_{\text{RhH}} \approx {}^2J_{\text{PH}} \approx 15.0$ ).  $^{31}\text{P}\{^1\text{H}\}$  NMR (162 MHz, THF):  $\delta$  46.9 (d,  $^1J_{\text{RhP}} = 111$ ),<sup>†</sup> LR ESI-MS (positive ion): 803.4 ( $[\text{M-H}]^+$ , calcd 803.4)  $m/z$ . Selected data for **81**:  $^1\text{H}$  NMR (400 MHz, THF):  $\delta$  -17.71 (app. q,  $^1J_{\text{RhH}} \approx {}^2J_{\text{PH}} \approx 15.45$ ),  $^{31}\text{P}\{^1\text{H}\}$  NMR (162 MHz, THF):  $\delta$  42.1 (d,  $^1J_{\text{RhP}} = 108$ ).<sup>†</sup>

**Reaction of 69 with PCy<sub>3</sub>**: No reaction was observed after 2 weeks at 50 °C.

## 6.5 RcPOP

### 6.5.1 Ligand Synthesis

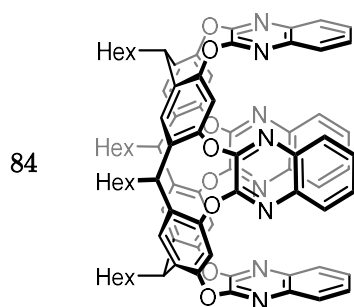
#### 6.5.1.1 2,8,14,20-tetrahexyl-4,6,10,12,16,18,22,24-octahydroxyresorcin[4]arene



In air, to a solution of resorcinol (11.0 g, 0.10 mol) in EtOH/H<sub>2</sub>O (70 mL, 19:1) was added HCl<sub>(aq)</sub> (37%, 20 mL). The solution was cooled to 0 °C and heptanal (14.0 mL, 0.10 mol) added dropwise over 1 h, after which the reaction was allowed to warm to ambient temperature and then heated at 80 °C for 18 h with vigorous stirring. After cooling the red suspension to ambient temperature, the precipitated material was collected by filtration and washed with ice cold EtOH/H<sub>2</sub>O (*ca.* 500 mL, 1:1) until the washings were of neutral pH. The resulting orange solid was dissolved in EtOH (*ca.* 100 mL) and reprecipitated from slow diffusion into H<sub>2</sub>O (*ca.* 900 mL). The solid material was washed with H<sub>2</sub>O (*ca.* 200 mL) and dried under high vacuum at 100 °C for 18 h. Yield: 17.5 g (85%, tan solid).

**$^1\text{H}$  NMR** (400 MHz,  $d_6$ -DMSO):  $\delta$  8.86 (s, 8H, OH), 7.14 (s, 4H, *ex*-Ar), 6.14 (s, 4H, *en*-Ar), 4.21 (t,  $^3J_{\text{HH}} = 7.7$ , 4H, CH), 2.01 (app. q,  $^3J_{\text{HH}} = 7$ , 8H 1-CH<sub>2</sub>), 1.35 – 1.10 (m, 32H, CH<sub>2</sub>), 0.84 (t,  $^3J_{\text{HH}} = 6.8$ , 12H, CH<sub>3</sub>). **LR ESI-MS** (negative ion): 823.5 ([M-H]<sup>-</sup>, calcd 823.5)  $m/z$ . Data consistent with previous reports.<sup>405,432</sup>

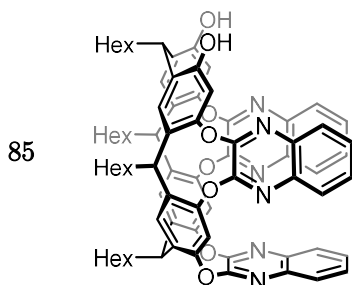
#### 6.5.1.2 RcQ<sub>4</sub>



To a suspension of resorcinarene **83** (17.5 g, 21.2 mmol) and 2,3-dichloroquinoxaline (19.0 g, 95.4 mmol) in DMSO (250 mL) heated to 60 °C was added K<sub>2</sub>CO<sub>3</sub> (23.44 g, 169.6 mmol). The reaction was heated at 60 °C for 18 h, then cooled to ambient temperature and poured onto H<sub>2</sub>O (*ca.* 1 L). The precipitated material was collected by filtration, washed with H<sub>2</sub>O (*ca.* 500 mL) and dried under high vacuum. The orange solid was dissolved in CH<sub>2</sub>Cl<sub>2</sub> (100 mL) and crystallised by slow diffusion into EtOAc (900 mL). The resulting white crystalline solid was collected by filtration and washed with EtOAc (100 mL) with further material obtained by concentrating the supernatant. Yield: 17.5 g (62%, white crystalline solid).

**$^1\text{H}$  NMR** (400 MHz, CDCl<sub>3</sub>):  $\delta$  8.14 (s, 4H, *ex*-Ar), 7.82 – 7.77 (m, 8H, 5,8-Q), 7.50 – 7.44 (m, 8H, 6,7-Q), 7.21 (s, 4H, *en*-Ar), 5.55 (t,  $^3J_{\text{HH}} = 7.9$ , 4H, CH), 2.26 (app. q,  $^3J_{\text{HH}} = 8$ , 8H, 1-CH<sub>2</sub>), 1.53 – 1.30 (m, 32H, CH<sub>2</sub>), 0.93 (t,  $^3J_{\text{HH}} = 6.7$ , 12H, CH<sub>3</sub>). Data consistent with previous reports.<sup>405,433</sup>

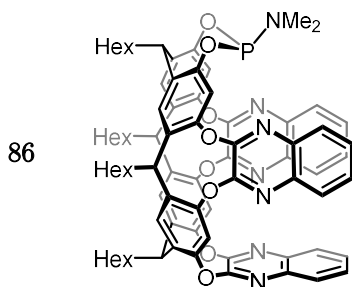
### 6.5.1.3 RcQ<sub>3</sub>H<sub>2</sub>



To a suspension of tetra-walled resorcinarene **84** (13.3 g, 10.0 mmol) and CsF (30.4 g, 200 mmol) in DMF (2 L) heated to 80 °C was added pyrocatechol (1.21 g, 11.0 mmol). The reaction was stirred at 80 °C for 1 h, then quenched by pouring onto iced brine (4 L). The precipitated material was collected by filtration, washed with H<sub>2</sub>O (2 L) and dried in air. The compound was purified by flash column chromatography (SiO<sub>2</sub>, gradient; 100% CH<sub>2</sub>Cl<sub>2</sub> to 9:1 CH<sub>2</sub>Cl<sub>2</sub>/EtOAc) and dried under high vacuum. Yield: 6.00 g (50%, white solid).

**<sup>1</sup>H NMR** (400 MHz, CDCl<sub>3</sub>): δ 8.24 (s, 2H, *ex*-Ar<sup>Q</sup>), 7.94 (d, <sup>3</sup>*J*<sub>HH</sub> = 8.4, 2H, 8-Q'), 7.88 – 7.78 (m, 2H, 5,8-Q), 7.68 (d, <sup>3</sup>*J*<sub>HH</sub> = 8.1, 2H, 5-Q'), 7.56 (t, <sup>3</sup>*J*<sub>HH</sub> = 7.6, 2H, 7-Q'), 7.52 – 7.44 (m, 4H, 6,7-Q & 6-Q'), 7.28 (s, 2H, *en*-Ar<sup>Q</sup>), 7.13 (s, 2H, *en*-Ar), 7.09 (s, 2H, *ex*-Ar), 5.60 (t, <sup>3</sup>*J*<sub>HH</sub> = 8.4, 1H, CH<sup>Q</sup>), 5.52 (t, <sup>3</sup>*J*<sub>HH</sub> = 7.7, 2H, CH<sup>Q'</sup>), 4.26 (t, <sup>3</sup>*J*<sub>HH</sub> = 6.7, 1H, CH), 2.49 – 2.12 (m, 8H, 1-CH<sub>2</sub>), 1.52 – 1.18 (m, 32H, CH<sub>2</sub>), 0.99 – 0.84 (m, 12H, CH<sub>3</sub>). **LR ESI-MS** (negative ion): 1201.4 ([M-H]<sup>-</sup>, calcd 1201.6) *m/z*. Data consistent with previous reports.<sup>434,435</sup>

### 6.5.1.4 RcQ<sub>3</sub>PNMe<sub>2</sub>

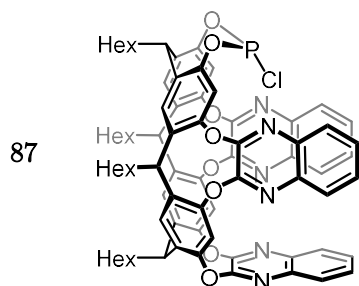




To a solution of tris-walled resorcinarene **85** (6.00 g, 5.00 mmol) in toluene (60 mL) heated to 75 °C was added NEt<sub>3</sub> (1.74 mL, 12.5 mmol) and P(NMe<sub>2</sub>)<sub>3</sub> (1.36 mL, 7.50 mmol) and the reaction stirred for 1.5 h at ambient temperature. The solvent was then removed *in vacuo*. The crude material purified by column chromatography (SiO<sub>2</sub>, 3:17 hexane/CH<sub>2</sub>Cl<sub>2</sub>, 1% NEt<sub>3</sub>) and the compound dried under high vacuum. Yield: 2.01 g (32%, white solid).

**<sup>1</sup>H NMR** (400 MHz, CDCl<sub>3</sub>): δ 8.31 (s, 2H, *ex*-Ar<sup>Q</sup>), 8.01 (d, <sup>3</sup>*J*<sub>HH</sub> = 8.2, 2H, 8-Q'), 7.78 – 7.68 (m, 4H, 5,8-Q & 5-Q'), 7.59 (t, <sup>3</sup>*J*<sub>HH</sub> = 7.8, 2H, 7-Q'), 7.49 (t, <sup>3</sup>*J*<sub>HH</sub> = 7.8, 2H, 6-Q'), 7.43 – 7.36 (m, 2H, 6,7-Q), 7.23 (s, 2H, *en*-Ar<sup>Q</sup>), 7.21 (s, 2H, *en*-Ar<sup>P</sup>), 7.20 (s, 2H, *ex*-Ar<sup>P</sup>), 5.69 (t, <sup>3</sup>*J*<sub>HH</sub> = 8.2, 3H CH<sup>Q</sup> & CH<sup>Q'</sup>), 4.55 (t, <sup>3</sup>*J*<sub>HH</sub> = 8.2, 1H, CH<sup>P</sup>), 2.78 (d, <sup>3</sup>*J*<sub>PH</sub> = 10.5, 6H, NMe), 2.28 (app. q, <sup>3</sup>*J*<sub>HH</sub> = 7.5, 4H, 1-CH<sub>2</sub><sup>Q</sup> & 1-CH<sub>2</sub><sup>Q'</sup>), 2.20 (app. q, <sup>3</sup>*J*<sub>HH</sub> = 7.6, 2H, 1-CH<sub>2</sub><sup>P</sup>), 1.64 – 1.17 (m, 32H, CH<sub>2</sub>), 1.00 – 0.85 (m, 12H, CH<sub>3</sub>). **<sup>31</sup>P{<sup>1</sup>H} NMR** (162 MHz, CDCl<sub>3</sub>): δ 142.0 (s).<sup>†</sup> **LR ESI-MS** (positive ion, Ag<sup>+</sup> doped): 1382.5 ([M+Ag]<sup>+</sup>, calcd 1382.5) *m/z*. Data in good agreement with a closely related variant with undecyl groups in place of hexyl.<sup>436</sup>

#### 6.5.1.5 RcQ<sub>3</sub>PCl



To a solution of phosphoramidite **86** (1.60 g, 1.25 mmol) in THF (40 mL) was added HCl (1M in Et<sub>2</sub>O, 3.75 mmol) and the reaction stirred for 1 h at ambient temperature. The resulting suspension was filtered and dried *in vacuo*. Yield: 1.55 g (98%, white solid).

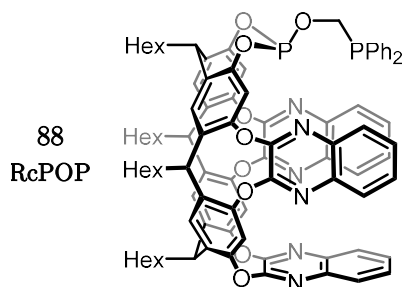
**<sup>1</sup>H NMR** (500 MHz, CD<sub>2</sub>Cl<sub>2</sub>): δ 8.24 (s, 2H, *ex*-Ar<sup>Q</sup>), 7.93 (d, <sup>3</sup>*J*<sub>HH</sub> = 8.4, 2H, 8-Q'), 7.86 – 7.79 (m, 2H, 5,8-Q), 7.67 (d, <sup>3</sup>*J*<sub>HH</sub> = 8.2, 2H, 5-Q'), 7.58 (t, <sup>3</sup>*J*<sub>HH</sub> = 7.6, 2H, 7-Q'), 7.55

– 7.51 (m, 2H, 6,7-Q), 7.50 (t,  $^3J_{\text{HH}} = 7.4$ , 2H, 6-Q'), 7.29 (s, 2H, *en*-Ar<sup>Q</sup>), 7.25 (s, 2H, *en*-Ar<sup>P</sup>), 7.22 (s, 2H, *ex*-Ar<sup>P</sup>), 5.72 (t,  $^3J_{\text{HH}} = 8.1$ , 1H, CH<sup>Q</sup>), 5.66 (t,  $^3J_{\text{HH}} = 8.2$ , 2H, CH<sup>Q'</sup>), 4.49 (t,  $^3J_{\text{HH}} = 7.9$ , 1H, CH<sup>P</sup>), 2.39 – 2.18 (m, 8H, 1-CH<sub>2</sub>), 1.57 – 1.42 (m, 8H, 3-CH<sub>2</sub>), 1.42 – 1.28 (m, 24H, 2-CH<sub>2</sub> & 4-CH<sub>2</sub> & 5-CH<sub>2</sub>), 1.01 – 0.87 (m, 12H, CH<sub>3</sub>).

**<sup>13</sup>C{<sup>1</sup>H} NMR** (126 MHz, CD<sub>2</sub>Cl<sub>2</sub>): δ 153.3 (s, ArO<sup>Q</sup>), 153.2 (s, ArO<sup>Q'Q'</sup>), 153.07 (2-Q'), 152.94 (2,3-Q), 152.87 (3-Q'), 152.5 (d,  $^4J_{\text{PC}} = 1$ , ArO<sup>PQ'</sup>), 148.6 (d,  $^2J_{\text{PC}} = 16$ , ArO<sup>P</sup>), 140.31 (s, 1-Q'), 140.25 (s, 1,4-Q), 140.19 (s, 4-Q'), 136.7 (s, ArC<sup>Q</sup>), 136.6 (s, ArC<sup>Q'Q'</sup>), 136.4, (s, ArC<sup>PQ'</sup>), 135.9 (d,  $^3J_{\text{PC}} = 1$ , ArC<sup>P</sup>), 130.1 (s, 6,7-Q), 129.74 (s, 8-Q'), 129.66 (s, 5-Q'), 128.44 (s, 7-Q'), 128.39 (s, (6-Q')), 128.3 (s, 5,8-Q), 124.4 (s, *en*-Ar<sup>Q</sup>), 123.1 (s, *en*-Ar<sup>P</sup>), 119.7 (s, *ex*-Ar<sup>Q</sup>), 118.7 (d,  $^4J_{\text{PC}} = 2$ , *ex*-Ar<sup>P</sup>), 37.1 (s, CH<sup>Q</sup>), 34.9 (s, CH<sup>Q'</sup>), 34.7 (s, CH<sup>P</sup>), 33.1 (s, 1-CH<sub>2</sub><sup>Q</sup>), 32.9 (s, 1-CH<sub>2</sub><sup>Q'</sup>), 32.5 (s, 2-CH<sub>2</sub><sup>Q</sup>), 32.44 (s, 2-CH<sub>2</sub><sup>Q'</sup>), 32.42 (s, 2-CH<sub>2</sub><sup>P</sup>), 31.5 (s, 1-CH<sub>2</sub><sup>P</sup>), 29.98 (s, 3-CH<sub>2</sub><sup>Q</sup>), 29.96 (s, 3-CH<sub>2</sub><sup>Q'</sup>), 29.91 (s, 3-CH<sub>2</sub><sup>P</sup>), 28.6 (s, 4-CH<sub>2</sub><sup>Q</sup>), 28.5 (s, 4-CH<sub>2</sub><sup>Q'</sup>), 28.4 (s, 4-CH<sub>2</sub><sup>P</sup>), 23.27 (s, 5-CH<sub>2</sub><sup>Q</sup>), 23.25 (s, 5-CH<sub>2</sub><sup>Q'</sup>), 23.23 (s, 5-CH<sub>2</sub><sup>P</sup>), 14.44 (s, CH<sub>3</sub><sup>Q</sup>), 14.42 (s, CH<sub>3</sub><sup>Q'</sup>), 14.40 (s, CH<sub>3</sub><sup>P</sup>).

**<sup>31</sup>P{<sup>1</sup>H} NMR** (162 MHz, CD<sub>2</sub>Cl<sub>2</sub>): δ 121.3 (s).<sup>†</sup> **Anal.** Calcd for C<sub>76</sub>H<sub>76</sub>ClN<sub>6</sub>O<sub>8</sub>P (1267.90 g·mol<sup>-1</sup>): C, 72.00; H, 6.04; N, 6.63. Found: C, 71.81; H, 5.92; N, 6.47.

#### 6.5.1.6 RcQ<sub>3</sub>POCH<sub>2</sub>PPh<sub>2</sub>



A solution of (hydroxymethyl)diphenylphosphine was first prepared by the reaction of paraformaldehyde (23.7 mg, 0.790 mmol) with neat diphenylphosphine (137.4  $\mu$ L, 0.7895 mmol) at 120 °C for 1 h. The resulting colourless oil was extracted into CH<sub>2</sub>Cl<sub>2</sub> (1 mL) and filtered onto a solution of chlorophosphite **87** (1.000 g, 0.7895 mmol) in CH<sub>2</sub>Cl<sub>2</sub> (10 mL). To the reaction mixture was added NEt<sub>3</sub> (121  $\mu$ L, 0.869 mmol). The reaction was stirred for 1 h then the solvent removed *in vacuo*. The crude material was

extracted into toluene (10 mL), filtered, the solvent removed *in vacuo*, and the material triturated with hexane ( $2 \times 10$  mL). The resulting solid was isolated by filtration and dried *in vacuo*. Additional material was obtained through concentration of the hexane washes. Yield: 1.005 g (88%, white solid).

Material suitable for crystallographic analysis was obtained by diffusion of ethanol (*ca.* 20 mL) into a dichloromethane solution of **RcPOP** (1 mL, 5 mM). **Note:** cleavage of the aryl-phosphite linkage of compound **RcPOP** results if the crude reaction mixture described above is exposed to methanol or ethanol, giving rise to a deep purple solution from which analytically pure tris-walled resorcinarene **85** may be precipitated by the addition of excess hexane. Isolated **RcPOP** appears to be stable to anhydrous alcohols, and so the triethylamine hydrochloride generated in the reaction is likely critical to the decomposition reaction, a reaction which is sufficiently slow to allow for crystallisation of **RcPOP**, though the yield of material obtained in this way is low, typically < 30%.

**<sup>1</sup>H NMR** (500 MHz, CD<sub>2</sub>Cl<sub>2</sub>):  $\delta$  8.24 (s, 2H, *ex*-Ar<sup>Q</sup>), 7.96 (d,  $^3J_{\text{HH}} = 8.2$ , 2H, 8-Q'), 7.79 – 7.73 (m, 4H, 5,8-Q & 5-Q'), 7.62 (t,  $^3J_{\text{HH}} = 7.5$ , 2H, 7-Q'), 7.59 – 7.54 (m, 4H, *o*-Ph), 7.53 (t,  $^3J_{\text{HH}} = 7.9$ , 2H, 6-Q'), 7.51 – 7.47 (m, 2H, 6,7-Q), 7.44 – 7.38 (m, 6H, *m*-Ph & *p*-Ph), 7.31 (s, 2H, *en*-Ar<sup>Q</sup>), 7.29 (s, 2H, *en*-Ar<sup>P</sup>), 7.22 (s, 2H, *ex*-Ar<sup>P</sup>), 5.68 (t,  $^3J_{\text{HH}} = 8.2$ , 3H, CH<sup>Q</sup> & CH<sup>Q'</sup>), 5.03 (app. t,  $^2J_{\text{PH}} \approx ^3J_{\text{PH}} = 5.9$ , 2H, CH<sub>2</sub>P), 4.51 (t,  $^3J_{\text{HH}} = 7.9$ , 1H, CH<sup>P</sup>), 2.37 – 2.28 (m, 6H, 1-CH<sub>2</sub><sup>Q</sup> & 1-CH<sub>2</sub><sup>Q'</sup>), 2.23 (q,  $^3J_{\text{HH}} = 8.0$ , 2H, 1-CH<sub>2</sub><sup>P</sup>), 1.54 – 1.47 (m, 6H, 3-CH<sub>2</sub>), 1.47 – 1.40 (m, 8H, CH<sub>2</sub>), 1.40 – 1.33 (m, 12H, CH<sub>2</sub>), 1.33 – 1.27 (m, 6H, CH<sub>2</sub>), 0.99 – 0.87 (m, 12H, CH<sub>3</sub>). **<sup>13</sup>C{<sup>1</sup>H} NMR** (126 MHz, CD<sub>2</sub>Cl<sub>2</sub>):  $\delta$  153.3 (s, 2-Q'), 153.1 (s, ArO<sup>Q</sup>), 152.98 (s, ArO<sup>QQ'</sup>), 152.95 (s, 2,3-Q), 152.92 (s, 3-Q'), 152.85 (s, ArO<sup>PQ'</sup>), 147.39 (d,  $^2J_{\text{PC}} = 5$ , ArO<sup>P</sup>), 140.25 (s, 1-Q'), 140.23 (s, 1,4-Q), 140.21 (s, 4-Q'), 137.9 (d,  $^3J_{\text{PC}} = 3$ , ArC<sup>P</sup>), 136.8 (d,  $^1J_{\text{PC}} = 21$ , *i*-Ph), 136.0 (s, ArC<sup>Q</sup>), 135.9 (s, ArC<sup>QQ'</sup>), 135.8 (s, ArC<sup>PQ'</sup>), 133.8 (d,  $^2J_{\text{PC}} = 19$ , *o*-Ph), 130.0 (s, 6-Q'), 129.8 (s, 6,7-Q), 129.7 (s, *p*-Ph), 129.6 (s, 7-Q'), 129.1 (d,  $^3J_{\text{PC}} = 7$ , *m*-Ph), 128.5 (s, 5-Q'), 128.4 (s, 5,8-Q), 128.3 (s, 8-Q'), 124.1 (s, *en*-Ar<sup>Q</sup>), 123.2 (s, *en*-Ar<sup>P</sup>), 119.6 (s, *ex*-Ar<sup>Q</sup>), 118.1 (d,  $^4J_{\text{PC}} = 2$ , *ex*-Ar<sup>P</sup>), 63.0 (dd,  $^1J_{\text{PC}} = 15$ ,  $^2J_{\text{PC}} = 5$ , CH<sub>2</sub>P), 36.4 (s, CH<sup>P</sup>), 34.9 (s, CH<sup>Q</sup>), 34.8 (s, CH<sup>Q'</sup>), 33.2 (s, 1-CH<sub>2</sub><sup>Q</sup>), 32.7 (s, 1-CH<sub>2</sub><sup>Q'</sup>), 32.48 (s, 2-CH<sub>2</sub><sup>Q</sup>), 32.46

(s, 2-CH<sub>2</sub><sup>Q'</sup>), 32.39 (s, 2-CH<sub>2</sub><sup>P</sup>), 32.1 (s, 1-CH<sub>2</sub><sup>P</sup>), 30.0 (s, 3-CH<sub>2</sub><sup>Q</sup> & 3-CH<sub>2</sub><sup>Q'</sup>), 29.9 (s, 3-CH<sub>2</sub><sup>P</sup>), 28.60 (s, 4-CH<sub>2</sub><sup>Q</sup>), 28.57 (s, 4-CH<sub>2</sub><sup>Q'</sup>), 28.4 (s, 4-CH<sub>2</sub><sup>P</sup>), 23.27 (s, 5-CH<sub>2</sub><sup>Q</sup>), 23.26 (s, 5-CH<sub>2</sub><sup>Q'</sup>), 23.25 (s, 5-CH<sub>2</sub><sup>P</sup>), 14.44 (s, CH<sub>3</sub><sup>Q</sup>), 14.43 (s, CH<sub>3</sub><sup>Q'</sup>), 14.41 (s, CH<sub>3</sub><sup>P</sup>). **<sup>31</sup>P{<sup>1</sup>H}** NMR (162 MHz, CD<sub>2</sub>Cl<sub>2</sub>): δ 127.5 (d, <sup>3</sup>J<sub>PP</sub> = 5, PO), -14.5 (d, <sup>3</sup>J<sub>PP</sub> = 5, PC).<sup>†</sup> **Anal.** Calcd for C<sub>89</sub>H<sub>88</sub>N<sub>6</sub>O<sub>9</sub>P<sub>2</sub> (1447.66 g·mol<sup>-1</sup>): C, 73.84; H, 6.13; N, 5.81. Found: C, 73.66; H, 6.16; N, 5.71.

## 6.5.2 Preparation of [Rh(alkene)(RcPOP)][anion]

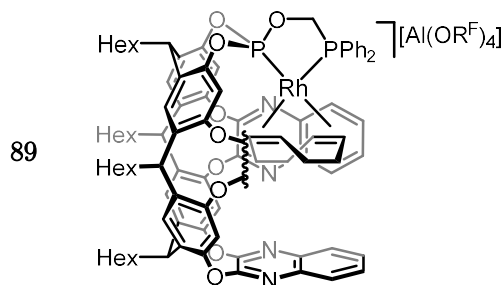
### 6.5.2.1 General procedure

**Method A:** A suspension of metal salt ([{Rh(cod)Cl}<sub>2</sub>] or [{Rh(nbd)Cl}<sub>2</sub>]), M[anion] (Li[Al(OR<sup>F</sup>)<sub>4</sub>], Na[BAr<sup>F</sup><sub>4</sub>], Cs[HCB<sub>11</sub>Me<sub>5</sub>I<sub>6</sub>] or Ag[SbF<sub>6</sub>]), and RcPOP in CH<sub>2</sub>Cl<sub>2</sub> was stirred at ambient temperature for 18 h. The compound of interest was precipitated by the addition of excess hexane (*ca.* 10× the reaction volume), isolated by filtration, extracted into a minimal amount of CH<sub>2</sub>Cl<sub>2</sub>, filtered, and the solvent removed *in vacuo*.

**Method B:** A solution of [Rh(diene)<sub>2</sub>][anion] and RcPOP in CH<sub>2</sub>Cl<sub>2</sub> was stirred at ambient temperature for 18 h. The compound of interest was precipitated by the addition of excess pentane or hexane (*ca.* 10× the reaction volume), isolated by filtration with further alkane washes, and dried *in vacuo*. Alternatively, where the metal precursor was used in excess and the diene is COD, the compound was purified by passing through a short plug of Al<sub>2</sub>O<sub>3</sub> (100% CH<sub>2</sub>Cl<sub>2</sub>) and the solvent removed *in vacuo*.

**Crystals** suitable for X-ray analysis were prepared by slow diffusion of hexane into concentrated solutions of the particular compound in dichloromethane or fluorobenzene. In crystallisation from fluorobenzene, the material co-crystallised with one to two equivalents of fluorobenzene.

### 6.5.2.2 [Rh(cod)(RcPOP)][Al(OR<sup>F</sup>)<sub>4</sub>]



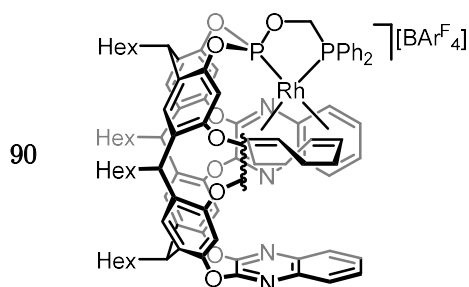
Prepared per Method A with [ $\{\text{Rh}(\text{cod})\text{Cl}\}_2$ ] (4.9 mg, 10  $\mu\text{mol}$ ),  $\text{Li}[\text{Al}(\text{OR}^{\text{F}})_4]$  (21.9 mg, 22.0  $\mu\text{mol}$ ) and RcPOP (28.9 mg, 20.0  $\mu\text{mol}$ ) in  $\text{CH}_2\text{Cl}_2$  (5 mL). Yield: 36.6 mg (70%, yellow-orange solid).

Prepared per Method B with  $[\text{Rh}(\text{cod})_2][\text{Al}(\text{OR}^{\text{F}})_4]$  (24.7 mg, 20.0  $\mu\text{mol}$ ) and RcPOP (28.9 mg, 20.0  $\mu\text{mol}$ ) in  $\text{CH}_2\text{Cl}_2$  (5 mL). Purified via precipitation from hexane. Yield: 29.5 mg (56%, yellow-orange solid).

**$^1\text{H}$  NMR** (500 MHz,  $\text{CD}_2\text{Cl}_2$ ):  $\delta$  8.21 (d,  $^3J_{\text{HH}} = 7.4$ , 2H, 8-Q'), 8.20 (s, 2H, *ex*-Ar<sup>Q</sup>), 7.84 – 7.76 (m, 4H, *p*-Ph & 7-Q'), 7.76 – 7.72 (m, 4H, *m*-Ph), 7.61 (d,  $^3J_{\text{HH}} = 8.0$ , 2H, 5-Q'), 7.59 – 7.52 (m, 4H, 6-Q' & 5,8-Q), 7.48 (s, 2H, *en*-Ar<sup>Q</sup>), 7.46 (d,  $^3J_{\text{HH}} = 7.9$ , 2H, *o*-Ph), 7.44 (d,  $^3J_{\text{HH}} = 7.9$ , 2H, *o*-Ph), 7.42 (s, 2H, *ex*-Ar<sup>P</sup>), 7.39 (s, 2H, *en*-Ar<sup>P</sup>), 7.35 – 7.31 (m, 4H, 6,7-Q), 5.80 (t,  $^3J_{\text{HH}} = 8.1$ , 2H, CH<sup>Q</sup>'), 5.61 (t,  $^3J_{\text{HH}} = 8.1$ , 1H, CH<sup>Q</sup>), 4.52 (d,  $^2J_{\text{PH}} = 24.6$ , 2H, CH<sub>2</sub>P), 4.46 (t,  $^3J_{\text{HH}} = 7.7$ , 1H, CH<sup>P</sup>), 3.65 (s, 2H, cod *ex*-CH), 2.50 – 2.39 (m, 6H, 1-CH<sub>2</sub> & cod *en*-CH), 2.35 – 2.19 (m, 4H, 1-CH<sub>2</sub>), 1.58 – 1.19 (m, 32H, CH<sub>2</sub>), 1.00 – 0.87 (m, 12H CH<sub>3</sub>), -0.79 – -0.98 (m, 2H, cod *ex*-CH<sub>2</sub>(eq)), -0.97 – -1.10 (m, 2H, cod *ex*-CH<sub>2</sub>(ax)), -1.47 – -1.66 (m, 4H, cod *en*-CH<sub>2</sub>(ax) & cod *en*-CH<sub>2</sub>(eq)).  **$^{13}\text{C}\{^1\text{H}\}$  NMR** (126 MHz,  $\text{CD}_2\text{Cl}_2$ ):  $\delta$  153.6 (s, ArO<sup>Q</sup>), 153.23 (s, 3-Q'), 153.19 (s, ArO<sup>QQ</sup>'), 152.9 (s, 2-Q'), 152.7 (s, 2,3-Q), 152.3 (s, ArO<sup>PQ</sup>'), 146.1 (s, ArO<sup>P</sup>), 140.6 (s, 1,4-Q), 140.2 (s, 1-Q'), 140.0 (s, 4-Q'), 139.0 (s, ArC<sup>PQ</sup>'), 137.3 (s, ArC<sup>QQ</sup>'), 137.1 (s, ArC<sup>Q</sup>), 135.7 (d,  $^3J_{\text{PC}} = 2$ , ArC<sup>P</sup>), 133.9 (d,  $^4J_{\text{PC}} = 2$ , *p*-Ph), 133.3 (d,  $^2J_{\text{PC}} = 11$  *o*-Ph), 131.1 (s, 6-Q'), 130.84 (d,  $^3J_{\text{PC}} = 11$ , *m*-Ph), 130.82 (s, 7-Q'), 130.2 (s, 6,7-Q), 128.9 (s, 8-Q'), 128.2, (s, 5-Q'), 128.0 (s, 5,8-Q), 127.2 (d,  $^1J_{\text{PC}} = 47$ , *i*-Ph), 124.9 (s, *en*-Ar<sup>Q</sup>), 124.2 (s, *en*-Ar<sup>P</sup>), 121.8 (q,  $^1J_{\text{FC}} = 293$ , R<sup>F</sup>), 118.9 (s, *ex*-Ar<sup>P</sup>), 116.9 (d,  $^3J_{\text{PC}} = 4$ , *ex*-Ar<sup>P</sup>), 105.5 (dd,

$^1J_{\text{RhC}} = 12$ ,  $^2J_{\text{PC}} = 6$ , cod *ex*-CH), 103.1 (dd,  $^1J_{\text{RhC}} = 7$ ,  $^2J_{\text{PC}} = 6$ , cod *en*-CH), 67.3 (dd,  $^1J_{\text{PC}} = 31$ ,  $^2J_{\text{PC}} = 17$ , CH<sub>2</sub>P), 36.8 (s, CH<sup>P</sup>), 35.3 (s, CH<sup>Q'</sup>), 35.0 (s, CH<sup>Q</sup>), 33.9 (s, 1-CH<sub>2</sub><sup>Q</sup>), 33.1 (s, 1-CH<sub>2</sub><sup>P</sup>), 32.5 (s, 2-CH<sub>2</sub><sup>Q'</sup>), 32.4 (s, 1-CH<sub>2</sub><sup>Q'</sup>), 32.3 (s, 2-CH<sub>2</sub><sup>Q</sup>), 31.5 (s, 2-CH<sub>2</sub><sup>P</sup>), 29.88 (s, 3-CH<sub>2</sub><sup>Q'</sup>), 29.87 (s, 3-CH<sub>2</sub><sup>Q</sup>), 29.7 (s, 3-CH<sub>2</sub><sup>P</sup>), 28.51 (s, 4-CH<sub>2</sub><sup>Q'</sup>), 28.46 (s, 4-CH<sub>2</sub><sup>Q</sup>), 28.2 (s, 4-CH<sub>2</sub><sup>P</sup>), 27.6 (br, cod *ex*-CH<sub>2</sub>), 26.8 (br, cod *en*-CH<sub>2</sub>), 23.2 (s, 5-CH<sub>2</sub><sup>Q</sup> & 5-CH<sub>2</sub><sup>Q'</sup>), 23.1 (s, 5-CH<sub>2</sub><sup>P</sup>), 14.41 (s, CH<sub>3</sub><sup>Q</sup> & CH<sub>3</sub><sup>Q'</sup>), 14.35 (s, CH<sub>3</sub><sup>P</sup>).  **$^{31}\text{P}\{^1\text{H}\}$  NMR** (162 MHz, CD<sub>2</sub>Cl<sub>2</sub>):  $\delta$  153.8 (dd,  $^1J_{\text{RhP}} = 254$ ,  $^2J_{\text{PP}} = 40$ , PO), 66.7 (dd,  $^1J_{\text{RhP}} = 149$ ,  $^2J_{\text{PP}} = 40$ , PC).  **$^{31}\text{P}\{^1\text{H}\}$  NMR** (162 MHz, C<sub>6</sub>H<sub>5</sub>F):  $\delta$  154.15 (dd,  $^1J_{\text{RhP}} = 254$ ,  $^2J_{\text{PP}} = 40$ , PO), 66.54 (dd,  $^1J_{\text{RhP}} = 149$ ,  $^2J_{\text{PP}} = 40$ , PC).  **$^{31}\text{P}\{^1\text{H}\}$  NMR** (162 MHz, C<sub>6</sub>H<sub>4</sub>F<sub>2</sub>):  $\delta$  153.9 (dd,  $^1J_{\text{RhP}} = 252$ ,  $^2J_{\text{PP}} = 41$ , PO), 67.6 (dd,  $^1J_{\text{RhP}} = 149$ ,  $^2J_{\text{PP}} = 40$ , PC).  **$^{19}\text{F}\{^1\text{H}\}$  NMR** (376 MHz, CD<sub>2</sub>Cl<sub>2</sub>):  $\delta$  -75.72 (s). **HR ESI-MS** (positive ion): 1631.5678 ([M-(cod)+2(MeCN)]<sup>+</sup>, calcd 1631.5669) *m/z*. **Anal.** Calcd for C<sub>113</sub>H<sub>100</sub>AlF<sub>36</sub>N<sub>6</sub>O<sub>13</sub>P<sub>2</sub>Rh (2625.85 g·mol<sup>-1</sup>): C, 51.69; H, 3.84; N, 3.20. Found: C, 51.62; H, 3.74; N, 3.17.

#### 6.5.2.3 [Rh(cod)(RcPOP)][BAr<sup>F</sup><sub>4</sub>]

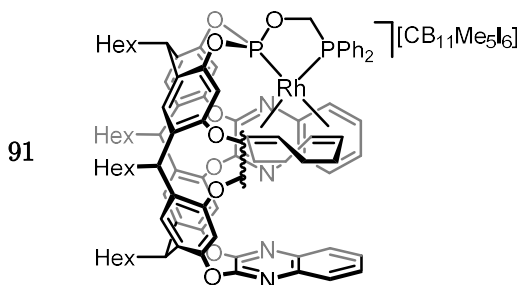


Prepared per Method A with [{Rh(cod)Cl}<sub>2</sub>] (4.9 mg, 10  $\mu\text{mol}$ ), Na[BAr<sup>F</sup><sub>4</sub>] (21.9 mg, 22.0  $\mu\text{mol}$ ) and RcPOP (28.9 mg, 20.0  $\mu\text{mol}$ ) in CH<sub>2</sub>Cl<sub>2</sub> (5 mL). Yield: 26.6 mg (53%, yellow-orange solid).

Prepared per Method B with [Rh(cod)<sub>2</sub>][BAr<sup>F</sup><sub>4</sub>] (26.0 mg, 22.0  $\mu\text{mol}$ ) and RcPOP (28.9 mg, 20.0  $\mu\text{mol}$ ) in CH<sub>2</sub>Cl<sub>2</sub> (5 mL). Purified by Al<sub>2</sub>O<sub>3</sub> and precipitation from pentane. Yield: 31.0 mg (61%, yellow-orange solid).

**$^1\text{H}$  NMR** (500 MHz,  $\text{CD}_2\text{Cl}_2$ ):  $\delta$  8.21 (d,  $^3J_{\text{HH}} = 7.0$ , 2H, 8-Q'), 8.20 (s, 2H, *ex*-Ar<sup>Q</sup>), 7.82 – 7.75 (m, 4H, *m*-Ph), 7.75 – 7.67 (m, 12H, 7-Q' & *p*-Ph & *o*-Ar<sup>F</sup>), 7.63 (d,  $^3J_{\text{HH}} = 8.1$ , 2H, 5-Q'), 7.60 – 7.52 (m, 8H, 5,8-Q & 6-Q' & *p*-Ar<sup>F</sup>), 7.48 (s, 2H, *en*-Ar<sup>P</sup>), 7.46 (dd,  $^3J_{\text{HH}} = 7.8$ , 2H *o*-Ph), 7.44 (dd,  $^3J_{\text{HH}} = 7.8$ , 2H *o*-Ph), 7.42 (s, 2H, *ex*-Ar<sup>P</sup>), 7.39 (s, 2H, *en*-Ar<sup>Q</sup>), 7.34 – 7.27 (m, 2H, 6,7-Q), 5.80 (t,  $^3J_{\text{HH}} = 8.1$ , 2H, CH<sup>Q'</sup>), 5.60 (t,  $^3J_{\text{HH}} = 8.1$ , 1H, CH<sup>Q</sup>), 4.52 (d,  $^2J_{\text{PH}} = 24.7$ , 2H, CH<sub>2</sub>P), 4.46 (t,  $J = 7.6$ , 1H, CH<sup>P</sup>), 3.64 (s, 2H, *ex*-CH), 2.50 – 2.42 (m, 4H, 1-CH<sub>2</sub>), 2.42 (s, 2H, *en*-CH), 2.32 – 2.20 (m, 4H, 1-CH<sub>2</sub>), 1.60 – 1.19 (m, 32H, CH<sub>2</sub>), 1.00 – 0.85 (m, 12H, CH<sub>3</sub>), -0.81 – -0.96 (m, 2H, cod *ex*-CH<sub>2(eq)</sub>), -0.96 – -1.07 (m, 2H, cod *ex*-CH<sub>2(ax)</sub>), -1.44 – -1.67 (m, 4H, cod *en*-CH<sub>2(ax)</sub> & cod *en*-CH<sub>2(eq)</sub>).  **$^{13}\text{C}\{^1\text{H}\}$  NMR** (126 MHz,  $\text{CD}_2\text{Cl}_2$ ):  $\delta$  162.3 (q,  $^1J_{\text{CB}} = 50$ , *i*-Ar<sup>F</sup>), 153.6 (s, ArO<sup>Q</sup>), 153.22 (s, 3-Q'), 153.20 (s, ArO<sup>QQ'</sup>), 152.9 (s, 2-Q'), 152.8 (s, 2,3-Q), 152.3 (s, ArO<sup>PQ'</sup>), 146.1 (s, ArO<sup>P</sup>), 140.6 (s, 1,4-Q), 140.2 (s, 1-Q'), 140.0 (s, 4-Q'), 139.0 (s, ArC<sup>PQ'</sup>), 137.3 (s, ArC<sup>QQ'</sup>), 137.2 (s, ArC<sup>Q</sup>), 135.7 (d,  $^3J_{\text{PC}} = 2$ , ArC<sup>P</sup>), 135.4 (s, *o*-Ar<sup>F</sup>), 133.9 (d,  $^4J_{\text{PC}} = 2$ , *p*-Ph), 133.4 (d,  $^2J_{\text{PC}} = 11$  *o*-Ph), 131.1 (s, 6-Q'), 130.83 (d,  $^3J_{\text{PC}} = 11$ , *m*-Ph), 130.82 (s, 7-Q'), 130.2 (s, 6,7-Q), 129.4 (qq,  $^2J_{\text{FC}} = 32$ ,  $^3J_{\text{CB}} = 3$ , *m*-Ar<sup>F</sup>), 128.9 (s, 8-Q'), 128.2 (s, 5-Q'), 128.0 (s, 5,8-Q), 127.2 (d,  $^1J_{\text{PC}} = 47$ , *i*-Ph), 125.2 (q,  $^1J_{\text{FC}} = 272$ , CF<sub>3</sub>), 124.9 (s, *en*-Ar<sup>Q</sup>), 124.2 (s, *en*-Ar<sup>P</sup>), 118.8 (s, *ex*-Ar<sup>P</sup>), 118.0 (sept,  $^3J_{\text{FC}} = 4$ , *p*-Ar<sup>F</sup>), 116.9 (d,  $^3J_{\text{PC}} = 4$ , *ex*-Ar<sup>P</sup>), 105.5 (dd,  $^1J_{\text{RhC}} = 12$ ,  $^2J_{\text{PC}} = 6$ , cod *ex*-CH), 103.1 (dd,  $^1J_{\text{RhC}} = 7$ ,  $^2J_{\text{PC}} = 6$ , cod *en*-CH), 67.3 (dd,  $^1J_{\text{PC}} = 32$ ,  $^2J_{\text{PC}} = 16$ , CH<sub>2</sub>P), 36.8 (s, CH<sup>P</sup>), 35.3 (s, CH<sup>Q'</sup>), 35.0 (s, CH<sup>Q</sup>), 33.9 (s, 1-CH<sub>2</sub><sup>Q</sup>), 33.1 (s, 1-CH<sub>2</sub><sup>P</sup>), 32.5 (s, 2-CH<sub>2</sub><sup>Q'</sup>), 32.4 (s, 1-CH<sub>2</sub><sup>Q'</sup>), 32.3 (2-CH<sub>2</sub><sup>Q</sup>), 31.5 (s, 2-CH<sub>2</sub><sup>P</sup>), 29.88 (s, 3-CH<sub>2</sub><sup>Q'</sup>), 29.86 (s, 3-CH<sub>2</sub><sup>Q</sup>), 29.7 (s, 3-CH<sub>2</sub><sup>P</sup>), 28.51 (s, 4-CH<sub>2</sub><sup>Q'</sup>), 28.46 (s, 4-CH<sub>2</sub><sup>Q</sup>), 28.2 (s, 4-CH<sub>2</sub><sup>P</sup>), 27.6 (s, cod *en*-CH<sub>2</sub>), 26.9 (s, cod *ex*-CH<sub>2</sub>), 23.24 (s, 5-CH<sub>2</sub><sup>Q</sup> & 5-CH<sub>2</sub><sup>Q'</sup>), 23.15 (s, 5-CH<sub>2</sub><sup>P</sup>), 14.41 (s, CH<sub>3</sub><sup>Q</sup> & CH<sub>3</sub><sup>Q'</sup>), 14.35 (s, CH<sub>3</sub><sup>P</sup>).  **$^{31}\text{P}\{^1\text{H}\}$  NMR** (162 MHz,  $\text{CD}_2\text{Cl}_2$ ):  $\delta$  153.8 (dd,  $^1J_{\text{RhP}} = 254$ ,  $^2J_{\text{PP}} = 41$ , PO), 66.8 (dd,  $^1J_{\text{RhP}} = 149$ ,  $^2J_{\text{PP}} = 41$ , PC).  **$^{19}\text{F}\{^1\text{H}\}$  NMR** (376 MHz,  $\text{CD}_2\text{Cl}_2$ ):  $\delta$  -62.85 (s).  **$^{11}\text{B}\{^1\text{H}\}$  NMR** (96 MHz,  $\text{CD}_2\text{Cl}_2$ ):  $\delta$  -6.6 (s). **Anal.** Calcd for  $\text{C}_{129}\text{H}_{112}\text{BF}_{24}\text{N}_6\text{O}_{13}\text{P}_2\text{Rh}$  (2521.97 g·mol<sup>-1</sup>): C, 61.44; H, 4.48; N, 3.33. Found: C, 60.58; H, 4.29; N, 3.19.

#### 6.5.2.4 [Rh(cod)(RcPOP)][CB<sub>11</sub>I<sub>6</sub>Me<sub>5</sub>]



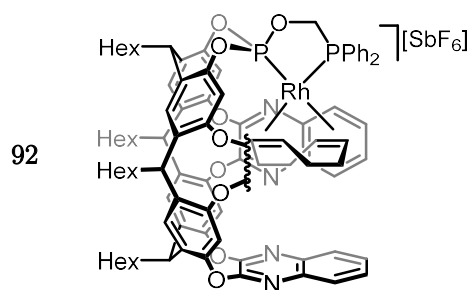
Prepared per Method A with  $[\{\text{Rh}(\text{cod})\text{Cl}\}_2]$  (4.9 mg, 10  $\mu\text{mol}$ ),  $\text{Cs}[\text{HCB}_{11}\text{Me}_5\text{I}_6]$  (24.2 mg, 22.0  $\mu\text{mol}$ ) and RcPOP (28.9 mg, 20.0  $\mu\text{mol}$ ) in  $\text{CH}_2\text{Cl}_2$  (5 mL). Yield: 17.7 mg (34%, yellow-orange solid).

**$^1\text{H}$  NMR** (500 MHz,  $\text{CD}_2\text{Cl}_2$ ):  $\delta$  8.21 (d,  $^3J_{\text{HH}} = 7.0$ , 2H, 8-Q'), 8.20 (s, 2H, *ex*-Ar<sup>Q</sup>), 7.88 – 7.81 (m, 4H, 6-Q' & 7-Q'), 7.79 (t,  $^3J_{\text{HH}} = 7.0$ , 4H, *m*-Ph), 7.61 (t,  $^3J_{\text{HH}} = 7.7$ , 2H, *p*-Ph), 7.58 – 7.53 (m, 4H, 5-Q' & 5,8-Q), 7.52 – 7.46 (m, 8H, 6,7-Q & *o*-Ph & *en*-Ar<sup>Q</sup>), 7.42 (s, 2H, *ex*-Ar<sup>P</sup>), 7.38 (s, 2H, *en*-Ar<sup>P</sup>), 5.80 (t,  $^3J_{\text{HH}} = 8.1$ , 2H, CH<sup>Q'</sup>), 5.62 (t,  $^3J_{\text{HH}} = 8.2$ , 1H, CH<sup>Q</sup>), 4.54 (d,  $^2J_{\text{PH}} = 24.7$ , 2H, CH<sub>2</sub>P), 4.46 (t,  $^3J_{\text{HH}} = 7.6$ , 1H CH<sup>P</sup>), 3.70 (s, 2H, *ex*-CH), 2.70 (s, 1H, HCB), 2.52 – 2.43 (m, 4H, 1-CH<sub>2</sub>), 2.41 (s, 2H, *en*-CH), 2.27 (q,  $^3J_{\text{HH}} = 8.0$ , 2H, 1-CH<sub>2</sub>), 2.25 (q,  $^3J_{\text{HH}} = 8.0$ , 2H, 1-CH<sub>2</sub>), 1.58 – 1.18 (m, 32H, CH<sub>2</sub>), 0.99 – 0.84 (m, 12H, CH<sub>3</sub>), 0.28 (s, 15H, BMe), -0.81 – -0.95 (m, 2H, cod *ex*-CH<sub>2</sub>(eq)), -1.00 – -1.12 (m, 2H, cod *ex*-CH<sub>2</sub>(ax)), -1.53 – -1.61 (m, 2H, cod *en*-CH<sub>2</sub>(eq)), -1.61 – -1.71 (m, 2H, cod *en*-CH<sub>2</sub>(ax)).  **$^{13}\text{C}\{^1\text{H}\}$  NMR** (126 MHz,  $\text{CD}_2\text{Cl}_2$ ):  $\delta$  153.6 (s, ArO<sup>Q</sup>), 153.2 (s, 3-Q'), 153.1 (s, ArO<sup>Q'</sup>), 152.8 (s, 2-Q'), 152.7 (s, 2,3-Q), 152.3 (s, ArO<sup>P'</sup>), 146.1 (s, ArO<sup>P</sup>), 140.6 (s, 1,4-Q), 140.1 (s, 1-Q'), 139.9 (s, 4-Q'), 139.0 (s, ArC<sup>P'</sup>), 137.3 (s, ArC<sup>Q'</sup>), 137.1 (s, ArC<sup>Q</sup>), 135.7 (d,  $^3J_{\text{PC}} = 2$ , ArC<sup>P</sup>), 134.0 (d,  $^4J_{\text{PC}} = 2$ , *p*-Ph), 133.4 (d,  $^2J_{\text{PC}} = 11$  *o*-Ph), 131.4 (s, 6-Q'), 131.2 (s, 7-Q'), 131.0 (d,  $^3J_{\text{PC}} = 11$ , *m*-Ph), 130.9 (s, 6,7-Q), 128.8 (s, 8-Q'), 128.0 (s, 5-Q'), 127.9 (s, 5,8-Q), 127.4 (d,  $^1J_{\text{PC}} = 47$ , *i*-Ph), 124.8 (s, *en*-Ar<sup>Q</sup>), 124.2 (s, *en*-Ar<sup>P</sup>), 118.9 (s, *ex*-Ar<sup>P</sup>), 116.9 (d,  $^3J_{\text{PC}} = 4$ , *ex*-Ar<sup>P</sup>), 105.5 (dd,  $^1J_{\text{RhC}} = 11$ ,  $^2J_{\text{PC}} = 6$ , cod *ex*-CH), 103.1 (app. t,  $^1J_{\text{RhC}} \approx ^2J_{\text{PC}} \approx 6$ , cod *en*-CH), 67.1 (dd,  $^1J_{\text{PC}} = 31$ ,  $^2J_{\text{PC}} = 17$ , CH<sub>2</sub>P), 62.06 – 61.80 (m, CB), 36.8 (s, CH<sup>P</sup>), 35.2 (s, CH<sup>Q'</sup>), 34.9 (s, CH<sup>Q</sup>), 33.9 (s, 1-CH<sub>2</sub><sup>Q</sup>), 33.1 (s, 1-CH<sub>2</sub><sup>P</sup>), 32.5 (s, 2-CH<sub>2</sub><sup>Q'</sup>), 32.4 (s, 1-CH<sub>2</sub><sup>Q'</sup>), 32.3 (s, 2-CH<sub>2</sub><sup>Q</sup>), 31.5 (s, 2-CH<sub>2</sub><sup>P</sup>), 29.89 (s, 3-CH<sub>2</sub><sup>Q'</sup>),



29.87 (s, 3-CH<sub>2</sub><sup>Q</sup>), 29.7 (s, 3-CH<sub>2</sub><sup>P</sup>), 28.52 (s, 4-CH<sub>2</sub><sup>Q'</sup>), 28.47 (s, 4-CH<sub>2</sub><sup>Q</sup>), 28.2 (s, 4-CH<sub>2</sub><sup>P</sup>), 27.5 (br, cod *ex*-CH<sub>2</sub>), 26.9 (br, cod *en*-CH<sub>2</sub>), 23.24 (s, 5-CH<sub>2</sub><sup>Q</sup> & 5-CH<sub>2</sub><sup>Q'</sup>), 23.15 (s, 5-CH<sub>2</sub><sup>P</sup>), 14.44 (s, CH<sub>3</sub><sup>Q</sup>), 14.42 (s, CH<sub>3</sub><sup>Q'</sup>), 14.37 (s, CH<sub>3</sub><sup>P</sup>), 0 (HSQC, BMe). **<sup>31</sup>P{<sup>1</sup>H} NMR** (162 MHz, CD<sub>2</sub>Cl<sub>2</sub>): δ 153.8 (dd, <sup>1</sup>J<sub>RhP</sub> = 254, <sup>2</sup>J<sub>PP</sub> = 40, PO), 66.5 (dd, <sup>1</sup>J<sub>RhP</sub> = 149, <sup>2</sup>J<sub>PP</sub> = 40, PC). **<sup>11</sup>B{<sup>1</sup>H} NMR** (96 MHz, CD<sub>2</sub>Cl<sub>2</sub>): δ -8.71 (br, fwhm = 153, 6B, BI), -16.38 (br, fwhm = 77, 5B, BMe). **Anal.** Calcd for C<sub>103</sub>H<sub>116</sub>B<sub>11</sub>I<sub>6</sub>N<sub>6</sub>O<sub>13</sub>P<sub>2</sub>Rh (2627.28 g·mol<sup>-1</sup>): C, 47.09; H, 4.45; N, 3.20. Found: C, 40.44; H, 3.58; N, 2.48.

#### 6.5.2.5 [Rh(cod)(RcPOP)][SbF<sub>6</sub>]

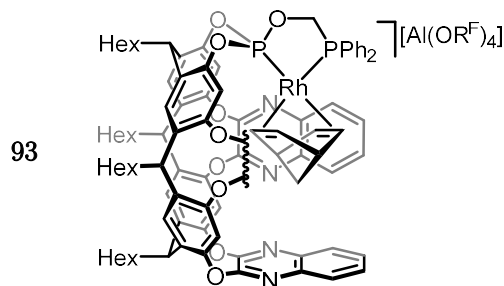


Prepared per Method B with [Rh(cod)<sub>2</sub>][SbF<sub>6</sub>] (14.5 mg, 10.0 μmol) and RcPOP (5.5 mg, 10 μmol) in CD<sub>2</sub>Cl<sub>2</sub> (0.5 mL). Purified by precipitation from hexane. Yield: 10.0 mg (53%, yellow-orange solid).

**<sup>1</sup>H NMR** (500 MHz, CD<sub>2</sub>Cl<sub>2</sub>): δ 8.20 (s, 2H, *ex*-Ar<sup>Q</sup>), 8.19 (d, <sup>3</sup>J<sub>HH</sub> = 7.0, 2H, 8-Q'), 7.86 – 7.78 (m, 4H, 6-Q' & 7-Q'), 7.76 (t, <sup>3</sup>J<sub>HH</sub> = 6.9, 4H, *m*-Ph), 7.63 (d, <sup>3</sup>J<sub>HH</sub> = 8.0, 2H, 5-Q'), 7.59 (t, <sup>3</sup>J<sub>HH</sub> = 8.0, 2H, *p*-Ph), 7.57 – 7.53 (m, 2H, 5,8-Q), 7.49 (s, 2H, *en*-Ar<sup>Q</sup>), 7.48 (d, <sup>3</sup>J<sub>HH</sub> = 8.0, *o*-Ph), 7.46 (d, <sup>3</sup>J<sub>HH</sub> = 8.0, *o*-Ph), 7.42 (s, 2H, *ex*-Ar<sup>P</sup>), 7.40 (s, 2H, *en*-Ar<sup>P</sup>), 7.39 – 7.35 (m, 2H, 6,7-Q), 5.81 (t, <sup>3</sup>J<sub>HH</sub> = 8.1, 2H, CH<sup>Q'</sup>), 5.61 (t, <sup>3</sup>J<sub>HH</sub> = 8.1, 1H, CH<sup>Q</sup>), 4.54 (d, <sup>2</sup>J<sub>PH</sub> = 24.8, 2H, CH<sub>2</sub><sup>P</sup>), 4.46 (t, <sup>3</sup>J<sub>HH</sub> = 7.7, 1H CH<sup>P</sup>), 3.66 (s, 2H, *ex*-CH), 2.51 – 2.41 (m, 4H, 1-CH<sub>2</sub>), 2.36 (s, 2H, *en*-CH), 2.27 (q, <sup>3</sup>J<sub>HH</sub> = 8.0, 2H, 1-CH<sub>2</sub>), 2.27 (q, <sup>3</sup>J<sub>HH</sub> = 8.0, 2H, 1-CH<sub>2</sub>), 1.60 – 1.18 (m, 32H, CH<sub>2</sub>), 0.98 – 0.87 (m, 12H, CH<sub>3</sub>), -0.86 – -0.98 (m, 2H, cod *ex*-CH<sub>2</sub>(eq)), -1.00 – -1.13 (m, 2H, cod *ex*-CH<sub>2</sub>(ax)), -1.50 – -1.72 (m, 4H, cod *en*-CH<sub>2</sub>(ax) & cod *en*-CH<sub>2</sub>(eq)). **<sup>13</sup>C{<sup>1</sup>H} NMR** (126 MHz, CD<sub>2</sub>Cl<sub>2</sub>): δ 153.6 (s, ArO<sup>Q</sup>), 153.19 (s, 3-Q'), 153.15 (s, ArO<sup>QQ'</sup>), 152.9 (s, 2-Q'), 152.7 (s, 2,3-Q), 152.3 (s, ArO<sup>PQ'</sup>), 146.2 (s, ArO<sup>P</sup>), 140.6 (s, 1,4-Q), 140.2 (s, 1-Q'), 140.0 (s, 4-Q'), 139.0

(s, ArC<sup>PQ</sup>), 137.3 (s, ArC<sup>Q'</sup>), 137.2 (s, ArC<sup>Q</sup>), 135.8 (d, <sup>3</sup>J<sub>PC</sub> = 3, ArC<sup>P</sup>), 133.9 (d, <sup>4</sup>J<sub>PC</sub> = 2, *p*-Ph), 133.4 (d, <sup>2</sup>J<sub>PC</sub> = 11 *o*-Ph), 131.2 (s, 6-Q'), 131.1 (s, 7-Q'), 130.8 (d, <sup>3</sup>J<sub>PC</sub> = 11, *m*-Ph), 130.5 (s, 6,7-Q), 128.8 (s, 8-Q'), 128.1, (s, 5-Q'), 128.0 (s, 5,8-Q), 127.2 (d, <sup>1</sup>J<sub>PC</sub> = 47, *i*-Ph), 124.9 (s, *en*-Ar<sup>Q</sup>), 124.3 (s, *en*-Ar<sup>P</sup>), 118.9 (s, *ex*-Ar<sup>P</sup>), 116.9 (d, <sup>3</sup>J<sub>PC</sub> = 4, *ex*-Ar<sup>P</sup>), 105.8 (dd, <sup>1</sup>J<sub>RhC</sub> = 12, <sup>2</sup>J<sub>PC</sub> = 6, cod *ex*-CH), 103.1 (dd, <sup>1</sup>J<sub>RhC</sub> = 7, <sup>2</sup>J<sub>PC</sub> = 6, cod *en*-CH), 67.3 (dd, <sup>1</sup>J<sub>PC</sub> = 31, <sup>2</sup>J<sub>PC</sub> = 16, CH<sub>2</sub>P), 36.8 (s, CH<sup>P</sup>), 35.3 (s, CH<sup>Q</sup>), 35.0 (s, CH<sup>Q</sup>), 33.9 (s, 1-CH<sub>2</sub><sup>Q</sup>), 33.0 (s, 1-CH<sub>2</sub><sup>P</sup>), 32.5 (s, 2-CH<sub>2</sub><sup>Q'</sup>), 32.4 (s, 1-CH<sub>2</sub><sup>Q'</sup>), 32.3 (s, 2-CH<sub>2</sub><sup>Q</sup>), 31.5 (s, 2-CH<sub>2</sub><sup>P</sup>), 29.9 (s, 3-CH<sub>2</sub><sup>Q'</sup> & 3-CH<sub>2</sub><sup>Q</sup>), 29.7 (s, 3-CH<sub>2</sub><sup>P</sup>), 28.53 (s, 4-CH<sub>2</sub><sup>Q'</sup>), 28.48 (s, 4-CH<sub>2</sub><sup>Q</sup>), 28.2 (s, 4-CH<sub>2</sub><sup>P</sup>), 27.6 (br, cod *ex*-CH<sub>2</sub>), 26.8 (br, cod *en*-CH<sub>2</sub>), 23.24 (s, 5-CH<sub>2</sub><sup>Q</sup> & 5-CH<sub>2</sub><sup>Q'</sup>), 23.15 (s, 5-CH<sub>2</sub><sup>P</sup>), 14.42 (s, CH<sub>3</sub><sup>Q</sup> & CH<sub>3</sub><sup>Q'</sup>), 14.37 (s, CH<sub>3</sub><sup>P</sup>). **<sup>31</sup>P{<sup>1</sup>H} NMR** (162 MHz, CD<sub>2</sub>Cl<sub>2</sub>): δ 153.5 (dd, <sup>1</sup>J<sub>RhP</sub> = 255, <sup>2</sup>J<sub>PP</sub> = 40, PO), 66.2 (dd, <sup>1</sup>J<sub>RhP</sub> = 148, <sup>2</sup>J<sub>PP</sub> = 40, PC).<sup>†</sup> **<sup>19</sup>F{<sup>1</sup>H} NMR** (376 MHz, CD<sub>2</sub>Cl<sub>2</sub>): δ -82.0 (s). **HR ESI-MS** (positive ion): 1631.5668 ([M-COD+2(MeCN)]<sup>+</sup>, calcd 1631.5669) *m/z*. **Anal.** Calcd for C<sub>97</sub>H<sub>100</sub>F<sub>6</sub>N<sub>6</sub>O<sub>13</sub>P<sub>2</sub>RhSb (1894.50 g·mol<sup>-1</sup>): C, 61.50; H, 5.32; N, 4.44. Found: C, 61.37; H, 5.17; N, 4.24.

#### 6.5.2.6 [Rh(nbd)(RcPOP)][Al(OR<sup>F</sup>)<sub>4</sub>]

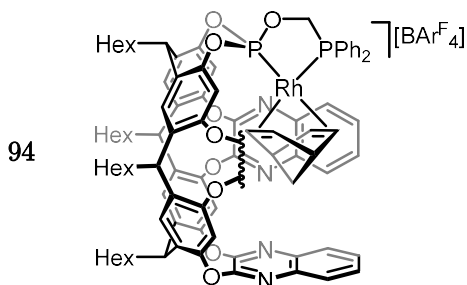


Prepared per Method A with [Rh(nbd)Cl]<sub>2</sub> (23.0 mg, 50.0 μmol), Li[Al(OR<sup>F</sup>)<sub>4</sub>] (97.4 mg, 110 μmol) and RcPOP (144.8 mg, 100.0 μmol) in CH<sub>2</sub>Cl<sub>2</sub> (5 mL). Yield: 227.4 mg (87%, orange solid).

Prepared per Method B with [Rh(nbd)<sub>2</sub>][Al(OR<sup>F</sup>)<sub>4</sub>] (125.4 mg, 100.0 μmol) and RcPOP (144.8 mg, 100.0 μmol) in CH<sub>2</sub>Cl<sub>2</sub> (5 mL). Purified via precipitation from hexane. Yield: 172.9 mg (70%, orange solid).

**<sup>1</sup>H NMR** (500 MHz, CD<sub>2</sub>Cl<sub>2</sub>): δ 8.21 (s, 2H, *ex*-Ar<sup>Q</sup>), 8.06 (d, <sup>3</sup>J<sub>HH</sub> = 8.3, 2H, 8-Q'), 7.87 – 7.79 (m, 4H, *p*-Ph & 5,8-Q), 7.76 (t, <sup>3</sup>J<sub>HH</sub> = 6.7, 4H, *m*-Ph), 7.67 (t, <sup>3</sup>J<sub>HH</sub> = 7.6, 2H, 7-Q'), 7.55 (s, 1H, *ex*-Ar<sup>P</sup>), 7.54 – 7.51 (m, 2H, 6,7-Q), 7.48 (d, <sup>3</sup>J<sub>HH</sub> = 6.7, 2H, 5-Q'), 7.47 (s, 2H, *en*-Ar<sup>Q</sup>), 7.42 (t, <sup>3</sup>J<sub>HH</sub> = 7.6, 2H, 6-Q'), 7.42 – 7.33 (m, 6H, *ex*-Ar<sup>Q</sup> & *o*-Ph), 7.39 (s, 2H, *en*-Ar<sup>P</sup>), 5.78 (t, <sup>3</sup>J<sub>HH</sub> = 8.1, 2H, CH<sup>Q'</sup>), 5.62 (t, <sup>3</sup>J<sub>HH</sub> = 8.1, 1H, CH<sup>Q</sup>), 4.58 (d, <sup>2</sup>J<sub>PH</sub> = 23.5, 2H, CH<sub>2</sub><sup>P</sup>), 4.46 (t, <sup>3</sup>J<sub>HH</sub> = 7.4, 1H, CH<sup>P</sup>), 3.64 (br, 2H, nbd *ex*-CH), 2.43 – 2.36 (m, 4H, 1-CH<sub>2</sub><sup>Q'</sup>), 2.34 (app q, <sup>3</sup>J<sub>HH</sub> = 8.5, 2H, 1-CH<sub>2</sub><sup>Q</sup>), 2.28 (app q, <sup>3</sup>J<sub>HH</sub> = 7.9, 2H, 1-CH<sub>2</sub><sup>P</sup>), 1.91 (br, 2H, nbd *en*-CH), 1.59 – 1.15 (m, 32H, (2-5)-CH<sub>2</sub>), 0.98 – 0.84 (m, 12H, CH<sub>3</sub>), -0.31 (s, 2H, nbd CH), -2.15 – -2.29 (br. m, 1H, nbd CH<sub>2(exo)</sub>), -2.61 – -2.71 (br. m, 1H, nbd CH<sub>2(endo)</sub>). **<sup>13</sup>C{<sup>1</sup>H} NMR** (126 MHz, CD<sub>2</sub>Cl<sub>2</sub>): δ 153.38 (2-Q'), 153.36 (s, 2,3-Q), 153.3 (s, 3-Q'), 153.2 (s, 1-Q'), 152.8 (s, 4-Q'), 152.7 (s, 1,4-Q), 146.3 (s, ArO<sup>P</sup>), 140.5 (s, ArO<sup>PQ'</sup>), 140.23 (s, ArO<sup>QQ'</sup>), 140.16 (s, ArO<sup>Q</sup>), 139.3 (s, ArC<sup>PQ'</sup>), 137.3 (s, ArC<sup>QQ'</sup>), 136.8 (s, ArC<sup>Q</sup>), 136.3 (d, <sup>3</sup>J<sub>PC</sub> = 3, ArC<sup>P</sup>), 134.0 (d, <sup>4</sup>J<sub>PC</sub> = 2, *p*-Ph), 133.0 (d, <sup>2</sup>J<sub>PC</sub> = 11, *o*-Ph), 131.0 (d, <sup>3</sup>J<sub>PC</sub> = 11, *m*-Ph), 130.9 (6,7-Q), 130.7 (s, 7-Q'), 130.3 (s, 6-Q'), 128.7 (s, 5,8-Q), 128.1 (s, 8-Q'), 127.9 (s, 5-Q'), 126.3 (d, <sup>1</sup>J<sub>PC</sub> = 47, *i*-Ph), 125.0 (s, *en*-Ar<sup>Q</sup>), 124.0 (s, *en*-Ar<sup>P</sup>), 121.8 (q, <sup>1</sup>J<sub>FC</sub> = 291, CF<sub>3</sub>), 118.8 (s, *ex*-Ar<sup>Q</sup>), 117.9 (d, <sup>3</sup>J<sub>PC</sub> = 4, *ex*-Ar<sup>P</sup>), 97.3 – 96.8 (m, nbd *ex*-CH), 96.2 – 95.7 (m, nbd *en*-CH), 70.1 – 69.9 (m, nbd CH<sub>2</sub>), 68.3 (dd, <sup>2</sup>J<sub>PC</sub> = 30, <sup>2</sup>J<sub>PC</sub> = 16, CH<sub>2</sub><sup>P</sup>), 53 (obsc., nbd CH), 36.7 (s, CH<sup>P</sup>), 35.1 (s, CH<sup>Q</sup> & CH<sup>Q'</sup>), 33.0 (s, 1-CH<sub>2</sub><sup>Q</sup>), 32.5 (s, 1-CH<sub>2</sub><sup>P</sup>), 32.4 (s, 2-CH<sub>2</sub><sup>Q</sup> & 2-CH<sub>2</sub><sup>Q'</sup>), 32.33 (s, 1-CH<sub>2</sub><sup>Q'</sup>), 32.31 (s, 2-CH<sub>2</sub><sup>P</sup>), 29.88 (s, 3-CH<sub>2</sub><sup>Q</sup>), 29.86 (s, 3-CH<sub>2</sub><sup>Q'</sup>), 29.7 (s, 3-CH<sub>2</sub><sup>P</sup>), 28.5 (s, 4-CH<sub>2</sub><sup>Q</sup> & 4-CH<sub>2</sub><sup>Q'</sup>), 28.2 (s, 4-CH<sub>2</sub><sup>P</sup>), 23.2 (s, 5-CH<sub>2</sub><sup>Q</sup> & 5-CH<sub>2</sub><sup>Q'</sup>), 23.1 (s, 5-CH<sub>2</sub><sup>P</sup>), 14.4 (s, CH<sub>3</sub><sup>Q</sup> & CH<sub>3</sub><sup>Q'</sup>), 14.3 (s, CH<sub>3</sub><sup>P</sup>). **<sup>31</sup>P{<sup>1</sup>H} NMR** (162 MHz, CD<sub>2</sub>Cl<sub>2</sub>): δ 161.4 (dd, <sup>1</sup>J<sub>RhP</sub> = 263, <sup>2</sup>J<sub>PP</sub> = 51, PO), 66.2 (dd, <sup>1</sup>J<sub>RhP</sub> = 154, <sup>2</sup>J<sub>PP</sub> = 51, PC). **HR ESI-MS** (positive ion): 1631.5635 ([M-NBD+2(MeCN)]<sup>+</sup>, calcd 1631.5669) *m/z*. **Anal.** Calcd for C<sub>112</sub>H<sub>95</sub>AlF<sub>36</sub>N<sub>6</sub>O<sub>13</sub>P<sub>2</sub>Rh (2608.80 g·mol<sup>-1</sup>): C, 51.57; H, 3.67; N, 3.22. Found: C, 51.45; H, 3.63; N, 3.19.

### 6.5.2.7 [Rh(nbd)(RcPOP)][BAR<sup>F</sup><sub>4</sub>]

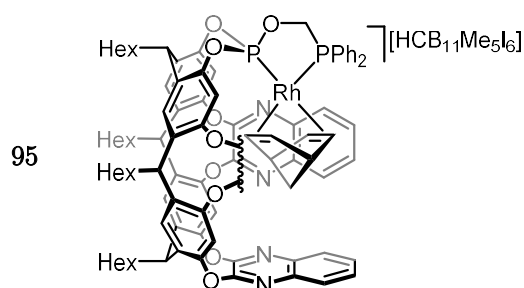


Prepared per Method A with [ $\{\text{Rh}(\text{nbd})\text{Cl}\}_2$ ] (11.5 mg, 25.0  $\mu\text{mol}$ ), Na[ $\text{BAR}^{\text{F}}_4$ ] (44.3 mg, 50  $\mu\text{mol}$ ) and RcPOP (77.4 mg, 50.0  $\mu\text{mol}$ ) in  $\text{CH}_2\text{Cl}_2$  (5 mL). Yield: 42.5 mg (34%, orange solid).

**$^1\text{H}$  NMR** (500 MHz,  $\text{CD}_2\text{Cl}_2$ ):  $\delta$  8.20 (s, 2H, *ex*-Ar<sup>Q</sup>), 8.06 (d,  $^3J_{\text{HH}} = 8.3$ , 2H, 8-Q'), 7.83 – 7.77 (m, 4H, 5,8-Q & *p*-Ph), 7.77 – 7.71 (m, 12H, *m*-Ph & *o*-Ar<sup>F</sup>), 7.65 (t,  $^3J_{\text{HH}} = 7.7$ , 2H, 7-Q'), 7.55 (br, 6H, *ex*-Ar<sup>P</sup> & *p*-Ar<sup>F</sup>), 7.54 – 7.49 (m, 4H, 5-Q' & 6,7-Q), 7.47 (s, 2H, *en*-Ar<sup>Q</sup>), 7.44 – 7.33 (m, 8H, 6-Q' & *en*-Ar<sup>P</sup> & *o*-Ph), 5.77 (t,  $^3J_{\text{HH}} = 8.1$ , 2H, CH<sup>Q</sup>), 5.61 (t,  $^3J_{\text{HH}} = 8.1$ , 1H, CH<sup>Q</sup>), 4.58 (d,  $^2J_{\text{PH}} = 23.7$ , 2H, CH<sub>2</sub>P), 4.46 (t,  $^3J_{\text{HH}} = 7.3$ , 1H, CH<sup>P</sup>), 3.63 (s, 2H, nbd *ex*-CH), 2.45 – 2.38 (m, 4H, 1-CH<sub>2</sub><sup>Q'</sup>), 2.34 (app. q,  $^3J_{\text{HH}} = 7.1$ , 2H, 1-CH<sub>2</sub><sup>Q</sup>), 2.28 (app. q,  $^3J_{\text{HH}} = 7.1$ , 2H, 1-CH<sub>2</sub><sup>P</sup>), 1.90 (s, 2H, nbd *en*-CH), 1.58 – 1.21 (m, 32H, CH<sub>2</sub>), 1.00 – 0.86 (m, 12H, CH<sub>3</sub>), -0.30 (s, 2H, nbd CH), -2.22 – -2.18 (m, 1H, nbd CH<sub>2</sub>(*exo*)), -2.66 – -2.62 (m, 1H, nbd CH<sub>2</sub>(*endo*)).  **$^{13}\text{C}\{^1\text{H}\}$  NMR** (126 MHz,  $\text{CD}_2\text{Cl}_2$ ):  $\delta$  162.3 (q,  $^1J_{\text{CB}} = 50$ , *i*-Ar<sup>F</sup>), 153.40 (2-Q'), 153.35 (s, 2,3-Q), 153.3 (s, 3-Q'), 153.2 (s, 1-Q'), 152.83 (s, 4-Q'), 152.76 (s, 1,4-Q), 146.3 (s, ArO<sup>P</sup>), 140.5 (s, ArO<sup>PQ'</sup>), 140.3 (s, ArO<sup>QQ'</sup>), 140.2 (s, ArO<sup>Q</sup>), 139.3 (s, ArC<sup>PQ'</sup>), 137.3 (s, ArC<sup>QQ'</sup>), 136.7 (s, ArC<sup>Q</sup>), 136.3 (d,  $^3J_{\text{PC}} = 3$ , ArC<sup>P</sup>), 135.4 (s, *o*-Ar<sup>F</sup>), 134.0 (d,  $^4J_{\text{PC}} = 2$ , *p*-Ph), 133.0 (d,  $^2J_{\text{PC}} = 11$ , *o*-Ph), 131.0 (d,  $^3J_{\text{PC}} = 11$ , *m*-Ph), 130.9 (6,7-Q), 130.7 (s, 7-Q'), 130.2 (s, 6-Q'), 129.4 (qq,  $^2J_{\text{FC}} = 32$ ,  $^3J_{\text{CB}} = 3$ , *m*-Ar<sup>F</sup>), 128.7 (s, 5,8-Q), 128.1 (s, 8-Q'), 127.9 (s, 5-Q'), 126.3 (d,  $^1J_{\text{PC}} = 47$ , *i*-Ph), 125.2 (q,  $^1J_{\text{FC}} = 272$ , CF<sub>3</sub>), 125.0 (s, *en*-Ar<sup>Q</sup>), 124.0 (s, *en*-Ar<sup>P</sup>), 118.8 (s, *ex*-Ar<sup>Q</sup>), 118.0 (sept,  $^3J_{\text{FC}} = 4$ , *p*-Ar<sup>F</sup>), 117.9 (d,  $^3J_{\text{PC}} = 4$ , *ex*-Ar<sup>P</sup>), 97.3 – 96.8 (m, nbd *ex*-CH), 96.2 – 95.7 (m, nbd *en*-CH), 70.1 – 69.9 (m, nbd CH<sub>2</sub>), 68.3 (dd,  $^2J_{\text{PC}} = 30$ ,  $^2J_{\text{PC}} = 16$ , CH<sub>2</sub>P), 53 (obsc., nbd CH), 36.7 (s, CH<sup>P</sup>), 35.1 (s, CH<sup>Q</sup> & CH<sup>Q'</sup>), 33.0 (s, 1-CH<sub>2</sub><sup>Q</sup>), 32.5 (s, 1-CH<sub>2</sub><sup>P</sup>), 32.4 (s, 2-CH<sub>2</sub><sup>Q</sup> & 2-CH<sub>2</sub><sup>Q'</sup>), 32.33 (s, 1-CH<sub>2</sub><sup>Q'</sup>), 32.31

(s, 2-CH<sub>2</sub><sup>P</sup>), 29.88 (s, 3-CH<sub>2</sub><sup>Q</sup>), 29.85 (s, 3-CH<sub>2</sub><sup>Q'</sup>), 29.7 (s, 3-CH<sub>2</sub><sup>P</sup>), 28.5 (s, 4-CH<sub>2</sub><sup>Q</sup> & 4-CH<sub>2</sub><sup>Q'</sup>), 28.2 (s, 4-CH<sub>2</sub><sup>P</sup>), 23.2 (s, 5-CH<sub>2</sub><sup>Q</sup> & 5-CH<sub>2</sub><sup>Q'</sup>), 23.1 (s, 5-CH<sub>2</sub><sup>P</sup>), 14.4 (s, CH<sub>3</sub><sup>Q</sup> & CH<sub>3</sub><sup>Q'</sup>), 14.3 (s, CH<sub>3</sub><sup>P</sup>). **<sup>31</sup>P{<sup>1</sup>H} NMR** (162 MHz, CD<sub>2</sub>Cl<sub>2</sub>): δ 161.5 (dd, <sup>1</sup>J<sub>RhP</sub> = 262, <sup>2</sup>J<sub>PP</sub> = 51, PO), 66.2 (dd, <sup>1</sup>J<sub>RhP</sub> = 153, <sup>2</sup>J<sub>PP</sub> = 51, PC). **<sup>19</sup>F{<sup>1</sup>H} NMR** (376 MHz, CD<sub>2</sub>Cl<sub>2</sub>): δ -62.86 (s). **<sup>11</sup>B{<sup>1</sup>H} NMR** (128 MHz, CD<sub>2</sub>Cl<sub>2</sub>): δ -6.61 (s). **HR ESI-MS** (positive ion): 1631.5629 ([M-NBD+2(MeCN)]<sup>+</sup>, calcd 1631.5669) *m/z*. **Anal.** Calcd for C<sub>128</sub>H<sub>107</sub>BF<sub>24</sub>N<sub>6</sub>O<sub>13</sub>P<sub>2</sub>Rh (2504.92 g·mol<sup>-1</sup>): C, 61.38; H, 4.31; N, 3.36. Found: C, 60.51; H, 4.11; N, 3.47.

#### 6.5.2.8 [Rh(nbd)(RcPOP)][CB<sub>11</sub>I<sub>6</sub>Me<sub>5</sub>]



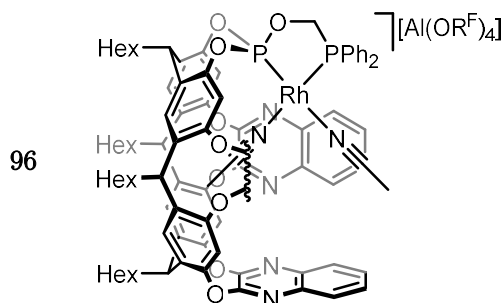
Prepared per Method A with [{Rh(nbd)Cl}<sub>2</sub>] (23.0 mg, 50.0 μmol), Cs[CB<sub>11</sub>Me<sub>5</sub>I<sub>6</sub>] (121.2 mg, 110.0 μmol) and RcPOP (144.8 mg, 100.0 μmol) in CH<sub>2</sub>Cl<sub>2</sub> (5 mL). Yield: 121.9 mg (47%, orange solid).

**<sup>1</sup>H NMR** (500 MHz, CD<sub>2</sub>Cl<sub>2</sub>): δ 8.21 (s, 2H, *ex*-Ar<sup>Q</sup>), 8.06 (d, <sup>3</sup>J<sub>HH</sub> = 8.2, 2H, 8-Q'), 7.85 (app. td, <sup>3</sup>J<sub>HH</sub> = 7.6, <sup>4</sup>J<sub>HH</sub> = 1.4, 2H, *m*-Ph), 7.81 – 7.77 (m, 6H & *p*-Ph & 5,8-Q), 7.74 (app. td, <sup>3</sup>J<sub>HH</sub> = 7.6, <sup>4</sup>J<sub>HH</sub> = 0.9, 2H, *m*-Ph), 7.64 – 7.58 (m, 2H, 6,7-Q), 7.55 (s, 2H, *ex*-Ar<sup>P</sup>), 7.50 (t, <sup>3</sup>J<sub>HH</sub> = 8.0, 2H, 6-Q'), 7.46 (s, 2H, *en*-Ar<sup>Q</sup>), 7.46 (d, <sup>3</sup>J<sub>HH</sub> = 7.2, 2H, 5-Q'), 7.42 (d, <sup>3</sup>J<sub>HH</sub> = 7.4, 2H, *o*-Ph), 7.40 (d, <sup>3</sup>J<sub>HH</sub> = 7.4, 2H, *o*-Ph), 7.38 (s, 2H, *en*-Ar<sup>P</sup>), 5.77 (t, <sup>3</sup>J<sub>HH</sub> = 8.1, 2H, CH<sup>Q'</sup>), 5.63 (t, <sup>3</sup>J<sub>HH</sub> = 8.2, 1H, CH<sup>Q</sup>), 4.61 (d, <sup>2</sup>J<sub>PH</sub> = 23.4, 2H, CH<sub>2</sub><sup>P</sup>), 4.46 (t, <sup>3</sup>J<sub>HH</sub> = 7.4, 1H, CH<sup>P</sup>), 3.78 – 3.58 (m, 2H, nbd *ex*-CH), 2.70 (s, 1H, HCB), 2.45 – 2.35 (m, 4H, 1-CH<sub>2</sub><sup>Q'</sup>), 2.35 – 2.31 (m, 2H, 1-CH<sub>2</sub><sup>Q</sup>), 2.31 – 2.24 (m, 2H, 1-CH<sub>2</sub><sup>P</sup>), 1.92 (br, 2H, nbd *en*-CH), 1.58 – 1.17 (m, 32H, CH<sub>2</sub>), 1.00 – 0.85 (m, 12H, CH<sub>3</sub>), 0.29 (s, 15H, BMe), -0.32 (s, 2H, nbd CH), -2.21 (s, 1H, nbd CH<sub>2(exo)</sub>), -2.70 (s, 1H, nbd CH<sub>2(endo)</sub>). **<sup>13</sup>C{<sup>1</sup>H} NMR** (126 MHz, CD<sub>2</sub>Cl<sub>2</sub>): δ 153.36 (2-Q'), 153.34

(s, 2,3-Q), 153.2 (s, 3-Q'), 153.1 (s, 1-Q'), 152.8 (s, 4-Q'), 152.7 (s, 1,4-Q), 146.3 (s, ArO<sup>P</sup>), 140.4 (s, ArO<sup>PQ'</sup>), 140.2 (s, ArO<sup>QQ'</sup>), 140.1 (s, ArO<sup>Q</sup>), 139.2 (s, ArC<sup>PQ'</sup>), 137.2 (s, ArC<sup>QQ'</sup>), 136.8 (s, ArC<sup>Q</sup>), 136.3 (d, <sup>3</sup>J<sub>PC</sub> = 3, ArC<sup>P</sup>), 134.0 (d, <sup>4</sup>J<sub>PC</sub> = 2, *p*-Ph), 133.1 (d, <sup>2</sup>J<sub>PC</sub> = 11, *o*-Ph), 131.2 (d, <sup>3</sup>J<sub>PC</sub> = 11, *m*-Ph), 131.12 (6,7-Q), 131.10 (s, 7-Q'), 130.7 (s, 6-Q'), 128.6 (s, 5,8-Q), 128.0 (s, 8-Q'), 127.9 (s, 5-Q'), 126.3 (d, <sup>1</sup>J<sub>PC</sub> = 47, *i*-Ph), 124.9 (s, *en*-Ar<sup>Q</sup>), 123.9 (s, *en*-Ar<sup>P</sup>), 118.9 (s, *ex*-Ar<sup>Q</sup>), 117.9 (d, <sup>3</sup>J<sub>PC</sub> = 4, *ex*-Ar<sup>P</sup>), 97.3 – 96.8 (m, nbd *ex*-CH), 96.2 – 95.7 (m, nbd *en*-CH), 70.1 – 69.9 (m, nbd CH<sub>2</sub>), 68.3 (dd, <sup>2</sup>J<sub>PC</sub> = 31, <sup>2</sup>J<sub>PC</sub> = 16, CH<sub>2</sub>P), 62.1 – 61.8 (m, CB), 53 (obsc., nbd CH), 36.7 (s, CH<sup>P</sup>), 35.03 (s, CH<sup>Q'</sup>), 35.01 (s, CH<sup>Q</sup>), 33.0 (s, 1-CH<sub>2</sub><sup>Q</sup>), 32.5 (s, 1-CH<sub>2</sub><sup>P</sup>), 32.4 (s, 2-CH<sub>2</sub><sup>Q</sup> & 2-CH<sub>2</sub><sup>Q'</sup>), 32.33 (s, 1-CH<sub>2</sub><sup>Q'</sup>), 32.31 (s, 2-CH<sub>2</sub><sup>P</sup>), 29.88 (s, 3-CH<sub>2</sub><sup>Q</sup>), 29.86 (s, 3-CH<sub>2</sub><sup>Q'</sup>), 29.7 (s, 3-CH<sub>2</sub><sup>P</sup>), 28.5 (s, 4-CH<sub>2</sub><sup>Q</sup> & 4-CH<sub>2</sub><sup>Q'</sup>), 28.2 (s, 4-CH<sub>2</sub><sup>P</sup>), 23.23 (s, 5-CH<sub>2</sub><sup>Q</sup> & 5-CH<sub>2</sub><sup>Q'</sup>), 23.15 (s, 5-CH<sub>2</sub><sup>P</sup>), 14.41 (s, CH<sub>3</sub><sup>Q'</sup>), 14.41 (s, CH<sub>3</sub><sup>Q</sup>), 14.37 (s, CH<sub>3</sub><sup>P</sup>). 0 (HSQC, BMe). **<sup>31</sup>P{<sup>1</sup>H} NMR** (162 MHz, CD<sub>2</sub>Cl<sub>2</sub>): δ 160.5 (dd, <sup>1</sup>J<sub>RhP</sub> = 263, <sup>2</sup>J<sub>PP</sub> = 51, PO), 65.4 (dd, <sup>1</sup>J<sub>RhP</sub> = 153, <sup>2</sup>J<sub>PP</sub> = 51, PC). **<sup>11</sup>B{<sup>1</sup>H} NMR** (128 MHz, CD<sub>2</sub>Cl<sub>2</sub>): δ -8.75 (br, fwhm = 166, 6B, BI), -16.37 (br, fwhm = 79, 5B, BMe). **LR ESI-MS** (positive ion): 1631.7 ([M-NBD+2(MeCN)]<sup>+</sup>, calcd 1631.6) *m/z*. **Anal.** Calcd for C<sub>102</sub>H<sub>111</sub>B<sub>11</sub>I<sub>6</sub>N<sub>6</sub>O<sub>13</sub>P<sub>2</sub>Rh (2610.23 g·mol<sup>-1</sup>): C, 46.94; H, 4.29; N, 3.22. Found: C, 44.29; H, 3.92; N, 3.04.

### 6.5.3 Preparation of other RcPOP complexes

#### 6.5.3.1 [Rh(NCMe)<sub>2</sub>(RcPOP)][Al(OR<sup>F</sup>)<sub>4</sub>]

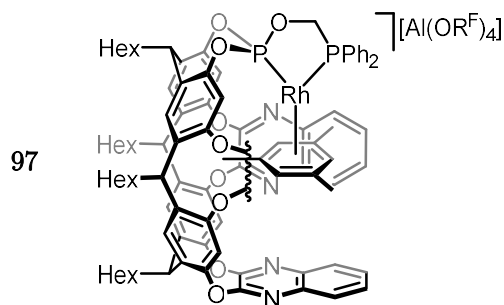


[Rh(nbd)(RcPOP)][Al(OR<sup>F</sup>)<sub>4</sub>] **96** (39.1 mg, 15.0 μmol) was dissolved in MeCN (0.5 mL). After 5 mins the solvent was removed *in vacuo*. The residues were extracted into CH<sub>2</sub>Cl<sub>2</sub>

(1 mL) and the title compound precipitated with the addition of excess hexane (ca. 20 mL). Yield: 11.4 mg (29%, appearance).

**$^1\text{H}$  NMR** (500 MHz,  $\text{CD}_2\text{Cl}_2$ ):  $\delta$  8.25 (s, 2H, *ex*-Ar<sup>Q</sup>), 8.14 – 8.06 (m, 2H, 5,8-Q), 7.91 – 7.84 (m, 6H, *p*-Ph & *o*-Ph), 7.81 (d,  $^3J_{\text{HH}} = 8.3$ , 2H, 8-Q'), 7.79 – 7.75 (m, 2H, 6,7-Q), 7.73 (br, 4H *m*-Ph), 7.59 (s, 2H, *ex*-Ar<sup>P</sup>), 7.58 (d,  $^3J_{\text{HH}} = 8.3$ , 2H, 5-Q'), 7.51 (t,  $^3J_{\text{HH}} = 7.1$ , 2H, 7-Q'), 7.36 (s, 2H, *en*-Ar<sup>Q</sup>), 7.35 (s, *en*-Ar<sup>P</sup>), 7.32 (t,  $^3J_{\text{HH}} = 7.7$ , 2H, 6-Q'), 5.73 – 5.67 (m, 3H, CH<sup>Q'</sup> & CH<sup>Q</sup>), 4.73 (t,  $^3J_{\text{HH}} = 7.0$ , 1H CH<sup>P</sup>), 4.61 (d,  $^2J_{\text{PH}} = 22.5$ , 2H, CH<sub>2</sub>P), 2.50 – 2.17 (m, 8H, 1-CH<sub>2</sub>), 1.58 – 1.14 (m, 32H, CH<sub>2</sub>), 1.05 (s, 3H, *ex*-NCMe), 1.02 – 0.75 (m, 12H, CH<sub>3</sub>), -2.55 (s, 3H, *en*-NCMe).  **$^{13}\text{C}\{^1\text{H}\}$  NMR** (126 MHz,  $\text{CD}_2\text{Cl}_2$ ):  $\delta$  153.5 (s, 2-Q'), 153.2 (s, 2,3-Q), 152.8 (s, 3-Q'), 152.75 (s, 1-Q'), 152.73 (s, 1,4-Q), 152.70 (s, 4-Q'), 146.4 (s, ArO<sup>P</sup>), 140.32 (s, ArO<sup>PQ'</sup>), 140.28 (s, ArO<sup>QQ'</sup>), 140.1, (s, ArO<sup>Q</sup>), 137.5 (s, ArC<sup>P</sup>), 137.0 (s, ArC<sup>QQ'</sup>), 136.9 (s, ArC<sup>Q</sup>), 136.6 (s, ArC<sup>PQ'</sup>), 134.0 (d,  $^2J_{\text{PC}} = 12$ , *o*-Ph), 133.1 (d,  $^4J_{\text{PC}} = 1$ , *p*-Ph), 130.7 (s, 6,7-Q), 130.1 (d,  $^3J_{\text{PC}} = 11$ , *m*-Ph), 130.0, (s, 7-Q'), 129.5 (s, 6-Q'), 129.2 (d,  $^1J_{\text{RHP}} = 50$ , *i*-Ph), 128.8 (s, 8-Q'), 128.7 (s, 5,8-Q), 128.3, 5-Q'), 124.5 (s, *en*-Ar<sup>Q</sup>), 123.2 (s, *en*-Ar<sup>P</sup>), 121.81 (q,  $^1J_{\text{FC}} = 291$ , CF<sub>3</sub>), 121.0 (br, *ex*-CN), 120.0 (br d,  $^3J_{\text{PC}} = 1$ , *ex*-Ar<sup>P</sup>), 119.6 (s, *ex*-Ar<sup>Q</sup>), 118.5 (m, *en*-CN), 69.8 (dd,  $^1J_{\text{PC}} = 34$ ,  $^2J_{\text{PC}} = 18$ , CH<sub>2</sub>P), 36.5 (s, CH<sup>P</sup>), 35.3 (s, CH<sup>Q'</sup>), 34.9 (s, CH<sup>Q</sup>), 33.0 (s, 1-CH<sub>2</sub><sup>Q'</sup>), 32.44 (s, 3-CH<sub>2</sub><sup>P</sup>), 32.41 (s, 2-CH<sub>2</sub><sup>Q'</sup>), 32.37 (s, 2-CH<sub>2</sub><sup>Q</sup>), 31.7 (s, 2-CH<sub>2</sub><sup>P</sup>), 31.0 (s, 1-CH<sub>2</sub><sup>P</sup>), 29.92 (s, 1-CH<sub>2</sub><sup>Q</sup>), 29.88 (s, 3-CH<sub>2</sub><sup>Q</sup>), 29.8 (s, 3-CH<sub>2</sub><sup>Q'</sup>), 28.39 (s, 4-CH<sub>2</sub><sup>Q</sup>), 28.37 (s, 4-CH<sub>2</sub><sup>Q'</sup>), 28.35 (s, 4-CH<sub>2</sub><sup>P</sup>), 23.23 (s, 5-CH<sub>2</sub><sup>Q</sup>), 23.22 (s, 5-CH<sub>2</sub><sup>Q'</sup>), 23.19 (s, 5-CH<sub>2</sub><sup>P</sup>), 14.41 (s, CH<sub>3</sub><sup>P</sup>), 14.39 (s, CH<sub>3</sub><sup>Q</sup> & CH<sub>3</sub><sup>Q'</sup>), 2.5 (s, *ex*-Me), -4.6 (s, *en*-Me).  **$^{31}\text{P}\{^1\text{H}\}$  NMR** (162 MHz,  $\text{CD}_2\text{Cl}_2$ ):  $\delta$  159.9 (dd,  $^1J_{\text{RHP}} = 294$ ,  $^2J_{\text{PP}} = 63$ , PO), 83.4 (dd,  $^1J_{\text{RHP}} = 165$ ,  $^2J_{\text{PP}} = 63$ , PC). **HR ESI-MS** (positive ion): 1631.5635 ( $[\text{M}]^+$ , calcd 1631.5669) *m/z*.

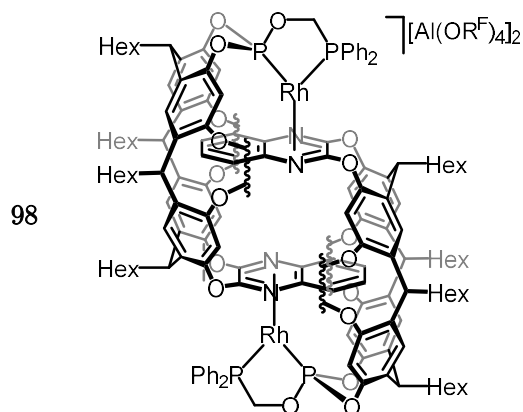
### 6.5.3.2 $[\text{Rh}(1,3,5\text{-C}_6\text{H}_3\text{Me}_3)(\text{RcPOP})][\text{Al}(\text{OR}^{\text{F}})_4]$



A solution of NBD complex **96** (13.0 mg, 5.0 0  $\mu\text{mol}$ ) in mesitylene (0.5 mL) was freeze-pump-thaw degassed three times and placed under an atmosphere of dihydrogen. After 1 h the reaction was freeze-pump-thaw degassed and placed under an atmosphere of argon. Addition of excess hexane precipitated the title compound as orange blocks.

$^{31}\text{P}\{^1\text{H}\}$  NMR (162 MHz, mesitylene):  $\delta$  152.8 (dd,  $^1J_{\text{RhP}} = 329$ ,  $^2J_{\text{PP}} = 57$ , PO), 84.1 (dd,  $^1J_{\text{RhP}} = 194$ ,  $^2J_{\text{PP}} = 58$ ).  $^{31}\text{P}\{^1\text{H}\}$  NMR (162 MHz, 1,2- $\text{C}_6\text{H}_4\text{F}_2$ ):  $\delta$  153.8 (dd,  $^1J_{\text{RhP}} = 328$ , 59), 84.2 (dd,  $J = 193.9$ , 59).

### 6.5.3.3 $[\{\text{Rh}(\text{RcPOP})\}_2][\text{Al}(\text{OR}^{\text{F}})_4]_2$

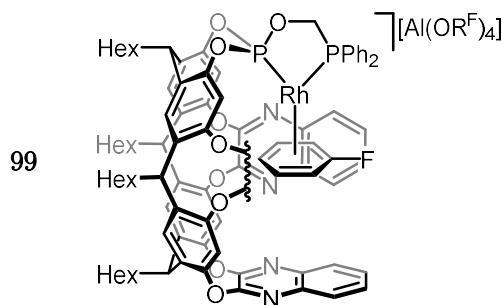


A solution of NBD complex **96** (13.0 mg, 5.0 0  $\mu\text{mol}$ ) in MTBE (0.5 mL) was freeze-pump-thaw degassed three times and placed under an atmosphere of dihydrogen. The reaction was left to stand for 1 week, resulting in an orange precipitate, which was isolated by filtration, washed with MTBE (*ca.* 2 mL) and dried under high vacuum.

**Anal.** Calcd for  $\text{C}_{210}\text{H}_{176}\text{Al}_2\text{F}_{72}\text{N}_{12}\text{O}_{26}\text{P}_2\text{Rh}$  (2517.67  $\text{g}\cdot\text{mol}^{-1}$ ): C, 50.09; H, 3.52; N, 3.34. Found: C, 50.24; H, 3.38; N, 3.23.



#### 6.5.3.4 [Rh(C<sub>6</sub>H<sub>5</sub>F)(RcPOP)][Al(OR<sup>F</sup>)<sub>4</sub>]

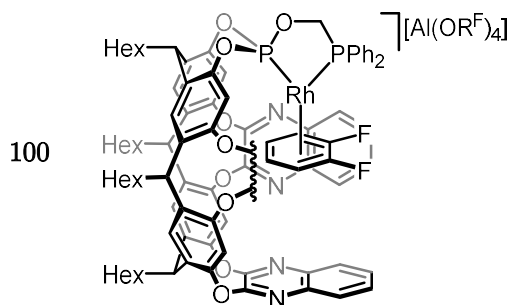


A solution of **96** (60.0 mg, 25.0  $\mu$ mol) in C<sub>6</sub>H<sub>5</sub>F (1 mL) was freeze-pump-thaw degassed three times and placed under an atmosphere of dihydrogen. After 1 h the solution was freeze-pump-thaw degassed three times and placed under an atmosphere of argon. The compound was precipitated by the addition of excess hexane (*ca.* 19 mL), isolated by filtration and dried *in vacuo*. Characterised in CD<sub>2</sub>Cl<sub>2</sub> with the addition of 10 equivalents of fluorobenzene. Yield: 44.8 mg (69%, pale yellow solid).

**<sup>1</sup>H NMR** (500 MHz, CD<sub>2</sub>Cl<sub>2</sub>):  $\delta$  8.23 (d,  $^3J_{\text{HH}} = 8.3$ , 2H, 8-Q'), 7.91 – 7.85 (m, 4H, *m*-Ph), 7.83 – 7.76 (m, 4H, *p*-Ph & Q), 7.76 – 7.68 (m, 8H, 5-Q' & 5,8-Q & *o*-Ph), 7.46 (s, 2H, *ex*-Ar<sup>Q</sup>), 7.4 (HSQC, *ex*-Ar<sup>P</sup>), 7.21 (s, 2H, *en*-Ar<sup>Q</sup>), 7.0 (HSQC, *en*-Ar<sup>P</sup>), 5.55 (vbr, fwhm = 24, 2H, CH<sup>Q'</sup>), 5.02 (vbr, fwhm = 22, 1H, CH<sup>Q</sup>), 4.54 (d,  $^2J_{\text{PH}} = 25.7$ , 2H, CH<sub>2</sub>P), 4.40 (t,  $^3J_{\text{HH}} = 8.2$ , 1H, CH<sup>P</sup>), 3.81 (vbr, fwhm = 31, *o*-FB), 3.43 (vbr, fwhm = 36, 2H, *m*-FB), 2.47 – 2.37 (m, 5H, *p*-Fb & 1-CH<sub>2</sub>), 2.23 (app. q,  $^3J_{\text{HH}} = 7.8$ , 4H, 1-CH<sub>2</sub>), 1.50 – 1.20 (m, 32H), 0.99 – 0.81 (m, 12H, CH<sub>3</sub>). The 6-Q', 7-Q', and 6,7-Q resonances could not be unambiguously located. **<sup>1</sup>H NMR** (500 MHz, C<sub>6</sub>H<sub>5</sub>F):  $\delta$  8.44 (s, 2H, *ex*-Ar<sup>Q</sup>), 8.17 (d,  $^3J_{\text{HH}} = 8.5$ , 2H, 8-Q'), 7.78 (s, 2H, *en*-Ar<sup>Q</sup>), 7.69 (s, 2H, *en*-Ar<sup>P</sup>), 7.67 – 7.60 (m, 4H, 7-Q' & *p*-Ph), 7.55 – 7.50 (m, 2H, 6-Q'), 7.50 – 7.43 (m, 6H, *m*-Ph & 5-Q'), 7.36 (s, 2H, *ex*-Ar<sup>P</sup>), 7.12 (COSY, *o*-Ph), 6.00 (t,  $^3J_{\text{HH}} = 8.0$ , 2H, CH<sup>Q'</sup>), 5.66 (t,  $^3J_{\text{HH}} = 8.2$ , 1H, CH<sup>Q</sup>), 4.43 (t,  $^3J_{\text{HH}} = 7.8$ , 1H, CH<sup>P</sup>), 4.07 (d,  $^2J_{\text{PH}} = 26.2$ , 2H, CH<sub>2</sub>P), 3.29 (t,  $^3J_{\text{HH}} = 5.2$ , 2H, *o*-FB), 2.84 (q,  $^3J_{\text{HH}} = 6.4$ , 2H, *m*-FB), 2.53 – 2.38 (m, 4H, 1-CH<sub>2</sub>), 2.33 – 2.23 (m, 4H, 1-CH<sub>2</sub>), 2.01 (t,  $^3J_{\text{HH}} = 6.1$ , *p*-FB), 1.51 – 1.43 (m, 4H, CH<sub>2</sub>), 1.37 – 1.28 (m, 6H, CH<sub>2</sub>), 1.28 – 1.16 (m, 20H, CH<sub>2</sub>), 1.16 – 1.10 (m, 2H, CH<sub>2</sub>), 0.89 – 0.80 (m, 12H, CH<sub>3</sub>). The 5,8-Q and 6,7-Q resonances could not be

unambiguously located.  $^{13}\text{C}\{^1\text{H}\}$  NMR (126 MHz,  $\text{CD}_2\text{Cl}_2$ ):  $\delta$  153.9 (s, Q or Q'), 152.7 (s, Q or Q'), 152.6 (s, Q or Q'), 151.4 (s, Q or Q'), 146.4 (s,  $\text{ArO}^{\text{P}}$ ), 140.4 (s,  $\text{ArO}^{\text{PQ}'}$ ), 140.0 (s,  $\text{ArO}^{\text{QQ}'}$ ), 139.2 (s,  $\text{ArO}^{\text{Q}}$ ), 136.6 – 136.39 (m,  $\text{ArC}^{\text{Q}}$  &  $\text{ArC}^{\text{QQ}'}$  &  $\text{ArC}^{\text{PQ}'}$ ), 136.3 – 136.0 (m  $\text{ArC}^{\text{P}}$ ), 133.8 (s, *p*-Ph), 132.6 (d,  $J=11.9$ , *o*-Ph), 131.1 (s, Q or Q'), 131.0 (s, Q or Q'), 130.5 (obsc. *m*-Ph), 130.0 (d,  $^1J_{\text{PC}} = 52$ , *i*-Ph), 129.6 (s, Q or Q'), 129.2 (s, Q or Q'), 128.1 (s, Q or Q'), 127.9 (s, Q or Q'), 124.8 (s, *ex*- $\text{Ar}^{\text{Q}}$ ), 124.1 (s, *ex*- $\text{Ar}^{\text{P}}$ ), 121.8 (q,  $^1J_{\text{FC}} = 294$ ), 118.8 (s, *en*- $\text{Ar}^{\text{Q}}$ ), 117.6 (s, *en*- $\text{Ar}^{\text{P}}$ ), 101.7 (br, *m*-FB), 95.0 (br, *p*-FB), 93.4 (br, *o*-FB), 70.5 – 70.0 (br. m,  $\text{CH}_2\text{P}$ ), 36.7 (s,  $\text{CH}^{\text{P}}$ ), 35.9 (s,  $\text{CH}^{\text{Q}}$ ), 35.8 (s,  $\text{CH}^{\text{Q}'}$ ), 33.5 (s,  $1\text{-CH}_2^{\text{P}}$ ), 32.8 (s,  $2\text{-CH}_2^{\text{P}}$ ), 32.4 (s,  $2\text{-CH}_2^{\text{Q}'}$ ), 32.34 (s,  $1\text{-CH}_2^{\text{Q}}$ ), 32.30 (s,  $2\text{-CH}_2^{\text{Q}}$ ), 31.5 (s,  $1\text{-CH}_2^{\text{Q}'}$ ), 29.78 (s,  $3\text{-CH}_2^{\text{Q}'}$ ), 29.75 (s,  $3\text{-CH}_2^{\text{Q}}$ ), 29.71 (s,  $3\text{-CH}_2^{\text{P}}$ ), 28.3 (s,  $4\text{-CH}_2^{\text{Q}'}$ ), 28.21 (s,  $4\text{-CH}_2^{\text{Q}}$ ), 28.16 (s,  $4\text{-CH}_2^{\text{P}}$ ), 23.22 (s,  $5\text{-CH}_2^{\text{Q}'}$ ), 23.19 (s,  $5\text{-CH}_2^{\text{Q}}$ ), 23.15 (s,  $5\text{-CH}_2^{\text{P}}$ ), 14.38 (s,  $\text{CH}_3^{\text{Q}'}$ ), 14.37 (s,  $\text{CH}_3^{\text{Q}}$ ), 14.35 (s,  $\text{CH}_3^{\text{P}}$ ). The *i*-FB resonance could not be unambiguously located, the quinoxaline carbons could not be unambiguously assigned. Anomalous signals in the  $^{13}\text{C}\{^1\text{H}\}$  NMR spectrum recorded in  $\text{C}_6\text{H}_4\text{F}$  precluded any reasonable assignment.  $^{31}\text{P}\{^1\text{H}\}$  NMR (121 MHz,  $\text{CD}_2\text{Cl}_2$ ):  $\delta$  163.5 (dd,  $^1J_{\text{RhP}} = 324$ ,  $^2J_{\text{PP}} = 54$ , PO), 82.5 (dd,  $^1J_{\text{RhP}} = 193$ ,  $^2J_{\text{PP}} = 56$ , PC).<sup>†</sup>  $^{31}\text{P}\{^1\text{H}\}$  NMR (162 MHz,  $\text{C}_6\text{H}_5\text{F}$ ):  $\delta$  164.5 (dd,  $^1J_{\text{RhP}} = 323$ ,  $^2J_{\text{PP}} = 54$ , PO), 82.5 (dd,  $^1J_{\text{RhP}} = 194$ ,  $^2J_{\text{PP}} = 56$ , PC).  $^{19}\text{F}\{^1\text{H}\}$  NMR (282 MHz,  $\text{CD}_2\text{Cl}_2$ ):  $\delta$  -74.96 (s,  $\text{R}^{\text{F}}$ ), -116.96 (s,  $\eta^6\text{-FB}$ ).  $^{19}\text{F}\{^1\text{H}\}$  NMR (376 MHz,  $\text{C}_6\text{H}_5\text{F}$ ):  $\delta$  -74.95 (s, 36F,  $\text{R}^{\text{F}}$ ), -117.30 (s, 1F,  $\eta^6\text{-FB}$ ). **HR ESI-MS** (positive ion): 1631.5655 ( $[\text{M-FB}+2\text{MeCN}]^+$ , calcd 1631.5669) *m/z*. **Anal.** Calcd for  $\text{C}_{111}\text{H}_{93}\text{AlF}_{37}\text{N}_6\text{O}_{13}\text{P}_2\text{Rh}$  (2613.77  $\text{g}\cdot\text{mol}^{-1}$ ): C, 51.01; H, 3.59; N, 3.22. Found: C, 50.66; H, 3.43; N, 3.16.

#### 6.5.3.5 $[\text{Rh}(1,2\text{-C}_6\text{H}_4\text{F}_2)(\text{RcPOP})][\text{Al}(\text{OR}^{\text{F}})_4]$



A solution of **96** (26.1 mg, 10.0  $\mu$ mol) in 1,2-C<sub>6</sub>H<sub>4</sub>F<sub>2</sub> (1 mL) was freeze-pump-thaw degassed three times and placed under an atmosphere of dihydrogen. After 1 h the solution was freeze-pump-thaw degassed three times and placed under an atmosphere of argon. The compound was precipitated by the addition of excess hexane (*ca.* 19 mL), isolated by filtration and dried *in vacuo*. The compound is appreciably contaminated (*ca.* 20%) by a compound seemingly featuring a different coordinated fluoroarene.

**<sup>1</sup>H NMR** (500 MHz, C<sub>6</sub>D<sub>2</sub>F<sub>2</sub>):  $\delta$  8.24 (s, 2H, *ex*-Ar<sup>Q</sup>), 8.16 (d, <sup>3</sup>*J*<sub>HH</sub> = 8.3, 2H, 8-Q'), 7.72 (t, *J*=7.2, 6H, 7-Q' & *p*-Ph & *en*-Ar<sup>Q</sup>), 7.62 (s, 2H, *en*-Ar<sup>P</sup>), 7.59 – 7.54 (m, 4H, 5-Q' & 6-Q'), 7.54 – 7.49 (m, 4H, *m*-Ph), 7.25 (s, 2H, *ex*-Ar<sup>P</sup>), 7.23 (d, <sup>3</sup>*J*<sub>HH</sub> = 7.9, 2H, *o*-Ph), 7.21 (d, <sup>3</sup>*J*<sub>HH</sub> = 7.8, 2H, *o*-Ph), 7.17 (br, 4H, 5,8-Q & 6,7-Q), 5.86 (t, *J*=7.8, 2H, CH<sup>Q'</sup>), 5.54 (t, *J*=8.0, 1H, CH<sup>Q</sup>), 4.35 (t, <sup>3</sup>*J*<sub>HH</sub> = 8.3, 1H, CH<sup>P</sup>), 4.34 (d, <sup>2</sup>*J*<sub>PH</sub> = 26.1, 2H, CH<sub>2</sub><sup>P</sup>), 3.47 – 3.38 (m, 2H, 4,5-DiFB), 2.50 – 2.35 (m, 8H, 1-CH<sub>2</sub>), 2.27 (app. q, <sup>3</sup>*J*<sub>HH</sub> = 8.0, 2H, 1-CH<sub>2</sub>), 2.06 – 2.01 (m, 2H, 3,6-DiFB), 1.44 – 1.35 (m, 4H, CH<sub>2</sub>), 1.32 – 1.23 (m, 8H, CH<sub>2</sub>), 1.20 – 1.10 (m, 20H, CH<sub>2</sub>), 0.81 – 0.71 (m, 12H, CH<sub>3</sub>). Anomalous signals in the <sup>13</sup>C{<sup>1</sup>H} NMR spectrum recorded in 1,2-C<sub>6</sub>H<sub>4</sub>F<sub>2</sub> precluded a reasonable assignment of the data. **<sup>31</sup>P{<sup>1</sup>H} NMR** (162 MHz, C<sub>6</sub>D<sub>4</sub>F<sub>2</sub>):  $\delta$  161.9 (dd, <sup>1</sup>*J*<sub>RhP</sub> = 328, <sup>2</sup>*J*<sub>PP</sub> = 58, PO), 82.6 (dd, <sup>1</sup>*J*<sub>RhP</sub> = 195, <sup>2</sup>*J*<sub>PP</sub> = 57, PC). **<sup>19</sup>F{<sup>1</sup>H} NMR** (471 MHz, C<sub>6</sub>D<sub>4</sub>F<sub>2</sub>):  $\delta$  -75.44 (s, R<sup>F</sup>), -139.60 (s, DiFB) -141.45 (s,  $\eta^6$ -DiFB). **HR ESI-MS** (positive ion): 1631.5654 ([M-C<sub>6</sub>H<sub>4</sub>F<sub>2</sub>+2(MeCN)]<sup>+</sup>, calcd 1631.5669) *m/z*.

## References

---

- 1 A. Cowan and M. W. George, *Coord. Chem. Rev.*, 2008, **252**, 2504–2511.
- 2 C. Hall and R. N. Perutz, *Chem. Rev.*, 1996, **96**, 3125–3146.
- 3 R. D. Young, *Chem. Eur. J.*, 2014, **20**, 12704–12718.
- 4 A. S. Weller, F. M. Chadwick and A. I. McKay, *Adv. Organomet. Chem.*, 2016, **66**, 223–276.
- 5 R. N. Perutz and S. Sabo-Etienne, *Angew. Chem. Int. Ed.*, 2007, **46**, 2578–2592.
- 6 M. Lersch and M. Tilset, *Chem. Rev.*, 2005, **105**, 2471–2526.
- 7 J. A. Labinger and J. E. Bercaw, *Nature*, 2002, **417**, 507–514.
- 8 R. H. Crabtree, *Chem. Rev.*, 1995, **95**, 987–1007.
- 9 R. H. Crabtree, M. Lavin, E. M. Holt and S. M. Morehouse, *Inorg. Chem.*, 1985, **24**, 1986–1992.
- 10 Q. Lu, F. Neese and G. Bistoni, *Angew. Chem. Int. Ed.*, 2018, **57**, 4760–4764.
- 11 Q. Lu, F. Neese and G. Bistoni, *Phys. Chem. Chem. Phys.*, 2019, **21**, 11569–11577.
- 12 M. Brookhart, M. L. H. Green and G. Parkin, *Proc. Natl. Acad. Sci.*, 2007, **104**, 6908–6914.
- 13 H. Urtel, C. Meier, F. Eisenträger, F. Rominger, J. P. Joschek and P. Hofmann, *Angew. Chem. Int. Ed.*, 2001, **40**, 781–784.
- 14 A. B. Chaplin, A. I. Poblador-Bahamonde, H. A. Sparkes, J. A. K. Howard, S. A. Macgregor and A. S. Weller, *Chem. Commun.*, 2009, **91**, 244–246.
- 15 Y. Wang, C. Qin, X. Jia, X. Leng and Z. Huang, *Angew. Chem. Int. Ed.*, 2017, **56**, 1614–1618.
- 16 V. Lavallo, Y. Canac, A. DeHope, B. Donnadiou and G. Bertrand, *Angew. Chem. Int. Ed.*, 2005, **44**, 7236–7239.
- 17 D. M. Speckman, C. B. Knobler and M. F. Hawthorne, *Organometallics*, 1985, **4**, 1692–1694.
- 18 K. I. Galkin, S. E. Lubimov, I. A. Godovikov, F. M. Dolgushin, A. F. Smol'yakov, E. A. Sergeeva, V. A. Davankov and I. T. Chizhevsky, *Organometallics*, 2012, **31**, 6080–6084.
- 19 A. V. Safronov, T. V. Zinevich, F. M. Dolgushin, O. L. Tok, E. V. Vorontsov and I. T. Chizhevsky, *Organometallics*, 2004, **23**, 4970–4979.
- 20 S. K. Brayshaw, E. L. Sceats, J. C. Green and A. S. Weller, *Proc. Natl. Acad. Sci.*, 2007, **104**, 6921–6926.
- 21 A. B. Chaplin, J. C. Green and A. S. Weller, *J. Am. Chem. Soc.*, 2011, **133**, 13162–13168.
- 22 S. K. Brayshaw, J. C. Green, G. Kociok-Koehn, E. L. Sceats and A. S. Weller, *Angew. Chem. Int. Ed.*, 2006, **45**, 452–456.
- 23 H. A. Sparkes, T. Krämer, S. K. Brayshaw, J. C. Green, A. S. Weller and J. A. K. Howard, *Dalton Trans.*, 2011, **40**, 10708.
- 24 A. B. Chaplin and A. S. Weller, *J. Organomet. Chem.*, 2013, **730**, 90–94.

- 25 N. M. Scott, R. Dorta, E. D. Stevens, A. Correa, L. Cavallo and S. P. Nolan, *J. Am. Chem. Soc.*, 2005, **127**, 3516–3526.
- 26 R. Dorta, E. D. Stevens and S. P. Nolan, *J. Am. Chem. Soc.*, 2004, **126**, 5054–5055.
- 27 N. M. Scott, V. Pons, E. D. Stevens, D. M. Heinekey and S. P. Nolan, *Angew. Chem. Int. Ed.*, 2005, **44**, 2512–2515.
- 28 C. Y. Tang, A. L. Thompson and S. Aldridge, *J. Am. Chem. Soc.*, 2010, **132**, 10578–10591.
- 29 T. M. Douglas, A. B. Chaplin and A. S. Weller, *Organometallics*, 2008, **27**, 2918–2921.
- 30 L. J. Sewell, A. B. Chaplin, J. A. B. Abdalla and A. S. Weller, *Dalton Trans.*, 2010, **39**, 7437–7439.
- 31 A. C. Cooper, E. Clot, J. C. Huffman, W. E. Streib, F. Maseras, O. Eisenstein and K. G. Caulton, *J. Am. Chem. Soc.*, 1999, **121**, 97–106.
- 32 I. W. Stolz, G. R. Dobson and R. K. Sheline, *J. Am. Chem. Soc.*, 1962, **84**, 3589–3590.
- 33 I. W. Stolz, G. R. Dobson and R. K. Sheline, *J. Am. Chem. Soc.*, 1963, **85**, 1013–1014.
- 34 A. J. Rest, J. R. Sodeau and D. J. Taylor, *J. Chem. Soc. Dalton Trans.*, 1978, 651–656.
- 35 J. D. Black and P. S. Braterman, *J. Organomet. Chem.*, 1973, **63**, C19–C20.
- 36 M. Poliakoff and J. J. Turner, *J. Chem. Soc. Dalton Trans.*, 1974, 2276.
- 37 J. M. Kelly, D. V. Bent, H. Hermann, D. Schultefrohlinde and E. K. von Gustorf, *J. Organomet. Chem.*, 1974, **69**, 259–269.
- 38 J. M. Kelly, H. Hermann and E. K. von Gustorf, *J. Chem. Soc. Chem. Commun.*, 1973, 105.
- 39 J. Nasielski, P. Kirsch and L. Wilputte-Steinert, *J. Organomet. Chem.*, 1971, **29**, 269–274.
- 40 A. G. Joly and K. A. Nelson, *Chem. Phys.*, 1991, **152**, 69–82.
- 41 R. N. Perutz and J. J. Turner, *J. Am. Chem. Soc.*, 1975, **97**, 4791–4800.
- 42 A. J. Cowan, P. Portius, H. K. Kawanami, O. S. Jina, D. C. Grills, X.-Z. X.-Z. Sun, J. McMaster and M. W. George, *Proc. Natl. Acad. Sci.*, 2007, **104**, 6933–6938.
- 43 J. M. Morse, G. H. Parker and T. J. Burkey, *Organometallics*, 1989, **8**, 2471–2474.
- 44 P. M. Hodges, S. A. Jackson, J. Jacke, M. Poliakoff, J. J. Turner and F. W. Grevels, *J. Am. Chem. Soc.*, 1990, **112**, 1234–1244.
- 45 G. Leu and T. J. Burkey, *J. Coord. Chem.*, 1995, **34**, 87–97.
- 46 E. F. Walsh, V. K. Popov, M. W. George and M. Poliakoff, *J. Phys. Chem.*, 1995, **99**, 12016–12020.
- 47 C. J. Breheny, J. M. Kelly, C. Long, S. O’Keeffe, M. T. Pryce, G. Russell and M. M. Walsh, *Organometallics*, 1998, **17**, 3690–3695.
- 48 G. R. Dobson, P. M. Hodges, M. A. Healy, M. Poliakoff, J. J. Turner, S. Firth and K. J. Asali, *J. Am. Chem. Soc.*, 1987, **109**, 4218–4224.

- 49 Y. Ishikawa, C. E. Brown, P. A. Hackett and D. M. Rayner, *Chem. Phys. Lett.*, 1988, **150**, 506–510.
- 50 C. E. Brown, Y. Ishikawa, P. A. Hackett and D. M. Rayner, *J. Am. Chem. Soc.*, 1990, **112**, 2530–2536.
- 51 M. Brookhart, W. Chandler, R. J. Kessler, Y. Liu, N. J. Pienta, C. C. Santini, C. Hall, R. N. Perutz and J. A. Timney, *J. Am. Chem. Soc.*, 1992, **114**, 3802–3815.
- 52 S. T. Belt, D. W. Ryba and P. C. Ford, *Inorg. Chem.*, 1990, **29**, 3633–3634.
- 53 M. W. George, M. T. Haward, P. A. Hamley, C. Hughes, F. P. A. Johnson, V. K. Popov and M. Poliakoff, *J. Am. Chem. Soc.*, 1993, **115**, 2286–2299.
- 54 F. P. A. Johnson, V. K. Popov, M. W. George, V. N. Bagratashvili, M. Poliakoff and J. J. Turner, *Mendeleev Commun.*, 1991, **1**, 145–148.
- 55 J. A. Calladine, S. B. Duckett, M. W. George, S. L. Matthews, R. N. Perutz, O. Torres and K. Q. Vuong, *J. Am. Chem. Soc.*, 2011, **133**, 2303–2310.
- 56 G. I. Childs, C. S. Colley, J. Dyer, D. C. Grills, X. Sun, J. Yang and M. W. George, *J. Chem. Soc. Dalton Trans.*, 2000, **2**, 1901–1906.
- 57 B. S. Creaven, A. J. Dixon, J. M. Kelly, C. Long and M. Poliakoff, *Organometallics*, 1987, **6**, 2600–2605.
- 58 M. K. Kuimova, W. Z. Alsindi, J. Dyer, D. C. Grills, O. S. Jina, P. Matousek, A. W. Parker, P. Portius, X. Zhong Sun, M. Towrie, C. Wilson, J. Yang and M. W. George, *Dalton Trans.*, 2003, 3996.
- 59 X.-Z. Sun, D. C. Grills, S. M. Nikiforov, M. Poliakoff and M. W. George, *J. Am. Chem. Soc.*, 1997, **119**, 7521–7525.
- 60 J. A. Calladine, O. Torres, M. Anstey, G. E. Ball, R. G. Bergman, J. Curley, S. B. Duckett, M. W. George, A. I. Gilson, D. J. Lawes, R. N. Perutz, X.-Z. Sun and K. P. C. Vollhardt, *Chem. Sci.*, 2010, **1**, 622.
- 61 E. F. Walsh, M. W. George, S. Goff, S. M. Nikiforov, V. K. Popov, X. Sun and M. Poliakoff, *J. Phys. Chem.*, 1996, **100**, 19425–19429.
- 62 R. D. Young, A. F. Hill, W. Hillier and G. E. Ball, *J. Am. Chem. Soc.*, 2011, **133**, 13806–13809.
- 63 S. B. Duckett, M. W. George, O. S. Jina, S. L. Matthews, R. N. Perutz, X.-Z. Sun and K. Q. Vuong, *Chem. Commun.*, 2009, 1401.
- 64 S. Geftakis and G. E. Ball, *J. Am. Chem. Soc.*, 1998, **120**, 9953–9954.
- 65 G. E. Ball, C. M. Brookes, A. J. Cowan, T. A. Darwish, M. W. George, H. K. Kawanami, P. Portius and J. P. Rourke, *Proc. Natl. Acad. Sci.*, 2007, **104**, 6927–6932.
- 66 D. J. Lawes, S. Geftakis and G. E. Ball, *J. Am. Chem. Soc.*, 2005, **127**, 4134–4135.
- 67 H. M. Yau, A. I. McKay, H. Hesse, R. Xu, M. He, C. E. Holt and G. E. Ball, *J. Am. Chem. Soc.*, 2015, **138**, 281–288.
- 68 I. Krossing, *Chem. Eur. J.*, 2001, **7**, 490–502.
- 69 I. Krossing and A. Reisinger, *Coord. Chem. Rev.*, 2006, **250**, 2721–2744.
- 70 D. J. Lawes, T. A. Darwish, T. Clark, J. B. Harper and G. E. Ball, *Angew. Chem. Int. Ed.*, 2006, **45**, 4486–4490.
- 71 J. S. Yeston, B. K. McNamara, R. G. Bergman and C. B. Moore, *Organometallics*,

- 2000, **19**, 3442–3446.
- 72 A. A. Bengali, R. H. Schultz, C. B. Moore and R. G. Bergman, *J. Am. Chem. Soc.*, 1994, **116**, 9585–9589.
  - 73 S. Brough, C. Hall, A. McCamley, R. N. Perutz, S. Stahl, U. Wecker and H. Werner, *J. Organomet. Chem.*, 1995, **504**, 33–46.
  - 74 M. W. George, M. B. Hall, P. Portius, A. L. Renz, X.-Z. Z. Sun, M. Towrie and X. Yang, *Dalton Trans.*, 2011, **40**, 1751–1757.
  - 75 M. W. George, M. B. Hall, O. S. Jina, P. Portius, X.-Z. Sun, M. Towrie, H. Wu, X. Yang and S. D. Zarić, *Proc. Natl. Acad. Sci.*, 2010, **107**, 20178–20183.
  - 76 A. J. Blake, M. W. George, M. B. Hall, J. McMaster, P. Portius, X. Z. Sun, M. Towrie, C. E. Webster, C. Wilson and S. D. Zarić, *Organometallics*, 2008, **27**, 189–201.
  - 77 J. B. Asbury, H. N. Ghosh, J. S. Yeston, R. G. Bergman and T. Lian, *Organometallics*, 1998, **17**, 3417–3419.
  - 78 R. H. Schultz, A. A. Bengali, M. J. Tauber, B. H. Weiller, E. P. Wasserman, K. R. Kyle, C. B. Moore and R. G. Bergman, *J. Am. Chem. Soc.*, 1994, **116**, 7369–7377.
  - 79 A. L. Pitts, A. Wriglesworth, X. Z. Sun, J. A. Calladine, S. D. Zarić, M. W. George and M. B. Hall, *J. Am. Chem. Soc.*, 2014, **136**, 8614–8625.
  - 80 S. E. Bromberg, H. Yang, M. C. Asplund, T. Lian, B. K. McNamara, K. T. Kotz, J. S. Yeston, M. Wilkens, H. Frei, R. G. Bergman and C. B. Harris, *Science*, 1997, **278**, 260–263.
  - 81 T. Lian, S. E. Bromberg, H. Yang, G. Proulx, R. G. Bergman and C. B. Harris, *J. Am. Chem. Soc.*, 1996, **118**, 3769–3770.
  - 82 W. H. Bernskoetter, C. K. Schauer, K. I. Goldberg and M. Brookhart, *Science*, 2009, **326**, 553–556.
  - 83 M. D. Walter, P. S. White, C. K. Schauer and M. Brookhart, *J. Am. Chem. Soc.*, 2013, **135**, 15933–15947.
  - 84 W. H. Bernskoetter, S. K. Hanson, S. K. Buzak, Z. Davis, P. S. White, R. Swartz, K. I. Goldberg and M. Brookhart, *J. Am. Chem. Soc.*, 2009, **131**, 8603–8613.
  - 85 D. R. Evans, T. Drovetskaya, R. Bau, C. A. Reed and P. D. W. Boyd, *J. Am. Chem. Soc.*, 1997, **119**, 3633–3634.
  - 86 I. Castro-Rodriguez, H. Nakai, P. Gantzel, L. N. Zakharov, A. L. Rheingold and K. Meyer, *J. Am. Chem. Soc.*, 2003, **125**, 15734–15735.
  - 87 N. R. Andreychuk and D. J. H. Emslie, *Angew. Chem. Int. Ed.*, 2013, **52**, 1696–1699.
  - 88 S. D. Pike and A. S. Weller, *Philos. Trans. Royal Soc. A*, 2015, **373**, 20140187.
  - 89 S. D. Pike, A. L. Thompson, A. G. Algarra, D. C. Apperley, S. A. Macgregor and A. S. Weller, *Science*, 2012, **337**, 1648–1651.
  - 90 S. D. Pike, F. M. Chadwick, N. H. Rees, M. P. Scott, A. S. Weller, T. Krämer and S. A. Macgregor, *J. Am. Chem. Soc.*, 2015, **137**, 820–833.
  - 91 F. M. Chadwick, N. H. Rees, A. S. Weller, T. Krämer, M. Iannuzzi and S. A. Macgregor, *Angew. Chem. Int. Ed.*, 2016, **55**, 3677–3681.
  - 92 A. I. McKay, T. Krämer, N. H. Rees, A. L. Thompson, K. E. Christensen, S. A.

- Macgregor and A. S. Weller, *Organometallics*, 2017, **36**, 22–25.
- 93 A. J. Martínez-Martínez, B. E. Tegner, A. I. McKay, A. J. Bukvic, N. H. Rees, G. J. Tizzard, S. J. Coles, M. R. Warren, S. A. Macgregor and A. S. Weller, *J. Am. Chem. Soc.*, 2018, **140**, 14958–14970.
- 94 A. I. McKay, A. J. Bukvic, B. E. Tegner, A. L. Burnage, A. J. Martínez-Martínez, N. H. Rees, S. A. Macgregor and A. S. Weller, *J. Am. Chem. Soc.*, 2019, **141**, 11700–11712.
- 95 S. D. Pike, T. Krämer, N. H. Rees, S. A. Macgregor and A. S. Weller, *Organometallics*, 2015, **34**, 1487–1497.
- 96 F. M. Chadwick, A. I. McKay, A. J. Martinez-Martinez, N. H. Rees, T. Krämer, S. A. Macgregor and A. S. Weller, *Chem. Sci.*, 2017, **8**, 6014–6029.
- 97 A. I. McKay, A. J. Martínez-Martínez, H. J. Griffiths, N. H. Rees, J. B. Waters, A. S. Weller, T. Krämer and S. A. Macgregor, *Organometallics*, 2018, **37**, 3524–3532.
- 98 F. M. Chadwick, T. Krämer, T. Gutmann, N. H. Rees, A. L. Thompson, A. J. Edwards, G. Buntkowsky, S. A. Macgregor and A. S. Weller, *J. Am. Chem. Soc.*, 2016, **138**, 13369–13378.
- 99 O. Eisenstein, J. Milani and R. N. Perutz, *Chem. Rev.*, 2017, **117**, 8710–8753.
- 100 J. L. Kiplinger, T. G. Richmond and C. E. Osterberg, *Chem. Rev.*, 1994, **94**, 373–431.
- 101 E. Clot, O. Eisenstein, N. Jasim, S. A. MacGregor, J. E. McGrady and R. N. Perutz, *Acc. Chem. Res.*, 2011, **44**, 333–348.
- 102 S. D. Pike, M. R. Crimmin and A. B. Chaplin, *Chem. Commun.*, 2017, **53**, 3615–3633.
- 103 M. Reinhold, J. E. McGrady and R. N. Perutz, *J. Am. Chem. Soc.*, 2004, **126**, 5268–5276.
- 104 J. Choi, D. Y. Wang, S. Kundu, Y. Choliy, T. J. Emge, K. Krogh-Jespersen and A. S. Goldman, *Science*, 2011, **332**, 1545–1548.
- 105 M. Su and S. Chu, *J. Am. Chem. Soc.*, 1997, **119**, 10178–10185.
- 106 M. Su and S. Chu, *J. Am. Chem. Soc.*, 1999, **121**, 1045–1058.
- 107 M. W. Bouwkamp, P. H. M. Budzelaar, J. Gercama, I. Del Hierro Morales, J. de Wolf, A. Meetsma, S. I. Troyanov, J. H. Teuben and B. Hessen, *J. Am. Chem. Soc.*, 2005, **127**, 14310–14319.
- 108 M. W. Bouwkamp, J. de Wolf, I. del Hierro Morales, J. Gercama, A. Meetsma, S. I. Troyanov, B. Hessen and J. H. Teuben, *J. Am. Chem. Soc.*, 2002, **124**, 12956–12957.
- 109 F. Basuli, H. Aneetha, J. C. Huffman and D. J. Mindiola, *J. Am. Chem. Soc.*, 2005, **127**, 17992–17993.
- 110 V. C. Gibson, C. Redshaw, L. J. Sequeira, K. B. Dillon, W. Clegg and M. R. J. Elsegood, *Chem. Commun.*, 1996, **835**, 2151–2152.
- 111 W. Lee and L. Liang, *Inorg. Chem.*, 2008, **47**, 3298–3306.
- 112 T. Ritter, M. W. Day and R. H. Grubbs, *J. Am. Chem. Soc.*, 2006, **128**, 11768–11769.
- 113 P. S. Engl, A. Fedorov, C. Copéret and A. Togni, *Organometallics*, 2016, **35**, 887–



- 893.
- 114 S. D. Perera, B. L. Shaw and M. Thornton-Pett, *Inorganica Chim. Acta*, 2001, **325**, 151–154.
  - 115 R. M. R. M. Catala, D. Cruz-Garritz, A. Hills, L. Hug, R. L. R. L. Richards, P. Sosap, H. Torrens, D. L. Hughes, R. L. R. L. Richards, P. Sosa and H. Torrens, *J. Chem. Soc. Chem. Commun.*, 1987, **489**, 261–262.
  - 116 R.-M. Catalá, D. Cruz-Garritz, P. Sosa, P. Terreros, H. Torrens, A. Hills, D. L. Hughes and R. L. Richards, *J. Organomet. Chem.*, 1989, **359**, 219–232.
  - 117 R. J. Kulawiec, E. M. Holt, M. Lavin and R. H. Crabtree, *Inorg. Chem.*, 1987, **26**, 2559–2561.
  - 118 A. Scharf, I. Goldberg and A. Vigalok, *J. Am. Chem. Soc.*, 2013, **135**, 967–970.
  - 119 K. Stanek, B. Czarniecki, R. Aardoom, H. Rüegger and A. Togni, *Organometallics*, 2010, **29**, 2540–2546.
  - 120 I. G. Phillips, R. G. Ball and R. G. Cavell, *Inorg. Chem.*, 1987, **26**, 4074–4079.
  - 121 I. Klopsch, E. Y. Yuzik-Klimova and S. Schneider, *Top. Organomet. Chem.*, 2017, **60**, 71–112.
  - 122 N. Khoenkhoen, B. de Bruin, J. N. H. Reek and W. I. Dzik, *Eur. J. Inorg. Chem.*, 2015, **2015**, 567–598.
  - 123 A. W. Pierpont and T. R. Cundari, *J. Coord. Chem.*, 2011, **64**, 3123–3135.
  - 124 V. Krewald, *Dalton Trans.*, 2018, **47**, 10320–10329.
  - 125 I. Haiduc, *J. Coord. Chem.*, 2018, **71**, 3139–3179.
  - 126 Y. Nishibayashi, *Dalton Trans.*, 2018, **47**, 11290–11297.
  - 127 Y. Roux, C. Duboc and M. Gennari, *ChemPhysChem*, 2017, **18**, 2606–2617.
  - 128 R. J. Burford and M. D. Fryzuk, *Nat. Rev. Chem.*, 2017, **1**, 0026.
  - 129 C. Köthe and C. Limberg, *Anorg. Allg. Chem.*, 2015, **641**, 18–30.
  - 130 C. C. Lu and S. D. Prinslow, in *Transition Metal-Dinitrogen Complexes*, ed. Y. Nishibayashi, Wiley-VCH Verlag GmbH & Co. KGaA, Weinheim, Germany, 2019, vol. 60, pp. 337–402.
  - 131 P. L. Holland, *Dalton Trans.*, 2010, **39**, 5415.
  - 132 S. Donovan-Mtunzi, R. L. Richards and J. Mason, *J. Chem. Soc. Dalton Trans.*, 1984, 469.
  - 133 P. R. Hoffman, T. Yoshida, T. Okano, S. Otsuka and J. A. Ibers, *Inorg. Chem.*, 1976, **15**, 2462–2466.
  - 134 T. Yoshida, T. Okano, D. L. Thorn, T. H. Tulip, S. Otsuka and J. A. Ibers, *J. Organomet. Chem.*, 1979, **181**, 183–201.
  - 135 O. V. Zenkina, E. C. Keske, R. Wang and C. M. Crudden, *Angew. Chem. Int. Ed.*, 2011, **50**, 8100–8104.
  - 136 J. M. Praetorius, R. Wang and C. M. Crudden, *Eur. J. Inorg. Chem.*, 2009, **2009**, 1746–1751.
  - 137 M. D. Millard, C. E. Moore, A. L. Rheingold and J. S. Figueroa, *J. Am. Chem. Soc.*, 2010, **132**, 8921–8923.
  - 138 N. Zhang, R. S. Sherbo, G. S. Bindra, D. Zhu and P. H. M. Budzelaar, *Organometallics*, 2017, **36**, 4123–4135.
  - 139 J. D. Masuda and D. W. Stephan, *Can. J. Chem.*, 2005, **83**, 324–327.

- 140 W. H. Bernskoetter, E. Lobkovsky and P. J. Chirik, *Chem. Commun.*, 2004, **4**, 764–765.
- 141 S. Gatard, C. Guo, B. M. Foxman and O. V. Ozerov, *Organometallics*, 2007, **26**, 6066–6075.
- 142 M. G. Scheibel, Y. Wu, A. C. Stückl, L. Krause, E. Carl, D. Stalke, B. de Bruin and S. Schneider, *J. Am. Chem. Soc.*, 2013, **135**, 17719–17722.
- 143 M. Hasegawa, Y. Segawa, M. Yamashita and K. Nozaki, *Angew. Chem. Int. Ed.*, 2012, **51**, 6956–6960.
- 144 R. Cohen, B. Rybtchinski, M. Gandelman, H. Rozenberg, J. M. L. Martin and D. Milstein, *J. Am. Chem. Soc.*, 2003, **125**, 6532–6546.
- 145 A. Vigalok, Y. Ben-David and D. Milstein, *Organometallics*, 1996, **15**, 1839–1844.
- 146 A. Vigalok, H. Kraatz, L. Konstantinovsky and D. Milstein, *Chem. Eur. J.*, 1997, **3**, 253–260.
- 147 R. Cohen, B. Rybtchinski, M. Gandelman, L. J. W. Shimon, J. M. L. Martin and D. Milstein, *Angew. Chem. Int. Ed.*, 2003, **42**, 1949–1952.
- 148 H. Salem, Y. Ben-David, L. J. W. Shimon and D. Milstein, *Organometallics*, 2006, **25**, 2292–2300.
- 149 M. E. Van Der Boom, S. Y. Liou, Y. Ben-David, L. J. W. Shimon and D. Milstein, *J. Am. Chem. Soc.*, 1998, **120**, 6531–6541.
- 150 S. K. Hanson, D. M. Heinekey and K. I. Goldberg, *Organometallics*, 2008, **27**, 1454–1463.
- 151 C. Rebreyend, Y. Gloaguen, M. Lutz, J. I. van der Vlugt, I. Siewert, S. Schneider and B. de Bruin, *Chem. Eur. J.*, 2017, **23**, 17438–17443.
- 152 M. Feller, Y. Diskin-Posner, L. J. W. Shimon, E. Ben-Ari and D. Milstein, *Organometallics*, 2012, **31**, 4083–4101.
- 153 G. M. Adams, F. M. Chadwick, S. D. Pike and A. S. Weller, *Dalton Trans.*, 2015, **44**, 6340–6342.
- 154 J. Schöffel, N. Šušnjar, S. Nüchel, D. Sieh and P. Burger, *Eur. J. Inorg. Chem.*, 2010, **2010**, 4911–4915.
- 155 M. T. Whited and R. H. Grubbs, *J. Am. Chem. Soc.*, 2008, **130**, 16476–16477.
- 156 M. G. Scheibel, B. Askevold, F. W. Heinemann, E. J. Reijerse, B. de Bruin and S. Schneider, *Nat. Chem.*, 2012, **4**, 552–558.
- 157 J. Abbeneth, M. Finger, C. Würtele, M. Kasanmascheff and S. Schneider, *Inorg. Chem. Front.*, 2016, **3**, 469–477.
- 158 A. Y. Verat, M. Pink, H. Fan, J. Tomaszewski and K. G. Caulton, *Organometallics*, 2008, **27**, 166–168.
- 159 J. M. Goldberg, S. D. T. Cherry, L. M. Guard, W. Kaminsky, K. I. Goldberg and D. M. Heinekey, *Organometallics*, 2016, **35**, 3546–3556.
- 160 D. W. Lee, W. C. Kaska and C. M. Jensen, *Organometallics*, 1998, **17**, 1–3.
- 161 R. Ghosh, M. Kanzelberger, T. J. Emge, G. S. Hall and A. S. Goldman, *Organometallics*, 2006, **25**, 5668–5671.
- 162 A. Arunachalampillai, D. Olsson and O. F. Wendt, *Dalton Trans.*, 2009, 8626.
- 163 Z. Huang, P. S. White and M. Brookhart, *Nature*, 2010, **465**, 598–601.
- 164 I. Göttker-Schnetmann, P. S. White and M. Brookhart, *Organometallics*, 2004,

- 23**, 1766–1776.
- 165 M. T. Whited, N. P. Mankad, Y. Lee, P. F. Oblad and J. C. Peters, *Inorg. Chem.*, 2009, **48**, 2507–2517.
  - 166 W. Yang, S. Zhang, Y. Ding, L. Shi and Q. Song, *Chem. Commun.*, 2011, **47**, 5310.
  - 167 E. Gutierrez, A. Monge, M. C. Nicasio, M. L. Poveda and E. Carmona, *J. Am. Chem. Soc.*, 1994, **116**, 791–792.
  - 168 E. Gutiérrez-Puebla, Á. Monge, M. C. Nicasio, P. J. Pérez, M. L. Poveda and E. Carmona, *Chem. Eur. J.*, 1998, **4**, 2225–2236.
  - 169 S. Conejero, A. C. Esqueda, J. E. V. Valpuesta, E. Álvarez, C. Maya and E. Carmona, *Inorganica Chim. Acta*, 2011, **369**, 165–172.
  - 170 D. M. Tellers and R. G. Bergman, *J. Am. Chem. Soc.*, 2000, **122**, 954–955.
  - 171 D. M. Tellers and R. G. Bergman, *Organometallics*, 2001, **20**, 4819–4832.
  - 172 H. Fang, Y.-K. Choe, Y. Li and S. Shimada, *Chem. Asian J.*, 2011, **6**, 2512–2521.
  - 173 J. R. Wells and E. Weitz, *J. Am. Chem. Soc.*, 1992, **114**, 2783–2787.
  - 174 S. A. Fairhurst, J. R. Morton, R. N. Perutz and K. F. Preston, *Organometallics*, 1984, **3**, 1389–1391.
  - 175 M. Brookhart, W. Chandler, R. J. Kessler, Y. Liu, N. J. Pienta, C. C. Santini, C. Hall, R. N. Perutz and J. A. Timney, *J. Am. Chem. Soc.*, 1992, **114**, 3802–3815.
  - 176 Z. Zhou and Y. Zhao, *J. Phys. Chem. A*, 2019, **123**, 556–564.
  - 177 W. B. Maier, M. Poliakoff, M. B. Simpson and J. J. Turner, *J. Chem. Soc. Chem. Commun.*, 1980, 587.
  - 178 J. J. Turner, M. B. Simpson, M. Poliakoff, W. B. Maier and M. A. Graham, *Inorg. Chem.*, 1983, **22**, 911–920.
  - 179 M. B. Simpson, M. Poliakoff, J. J. Turner, W. B. Maier and J. G. McLaughlin, *J. Chem. Soc. Chem. Commun.*, 1983, 1355.
  - 180 B. H. Weiller, *J. Am. Chem. Soc.*, 1992, **114**, 10910–10915.
  - 181 X. Sun, M. W. George, S. G. Kazarian, S. M. Nikiforov and M. Poliakoff, *J. Am. Chem. Soc.*, 1996, **118**, 10525–10532.
  - 182 D. C. Grills, G. I. Childs and M. W. George, *Chem. Commun.*, 2000, **3**, 1841–1842.
  - 183 Y. Zhao, Y. Gong and M. Zhou, *J. Phys. Chem. A*, 2006, **110**, 10777–10782.
  - 184 A. Horton-Mastin, M. Poliakoff and J. J. Turner, *Organometallics*, 1986, **5**, 405–408.
  - 185 D. C. Grills, X. Z. Sun, G. I. Childs and M. W. George, *J. Phys. Chem. A*, 2000, **104**, 4300–4307.
  - 186 G. E. Ball, T. A. Darwish, S. Geftakis, M. W. George, D. J. Lawes, P. Portius and J. P. Rourke, *Proc. Natl. Acad. Sci.*, 2005, **102**, 1853–1858.
  - 187 M. Besora, J.-L. Carreón-Macedo, A. J. Cowan, M. W. George, J. N. Harvey, P. Portius, K. L. Ronayne, X.-Z. Sun and M. Towrie, *J. Am. Chem. Soc.*, 2009, **131**, 3583–3592.
  - 188 P. Portius, J. Yang, X.-Z. Sun, D. C. Grills, P. Matousek, A. W. Parker, M. Towrie and M. W. George, *J. Am. Chem. Soc.*, 2004, **126**, 10713–10720.
  - 189 R. J. Mawby, R. N. Perutz and M. K. Whittlesey, *Organometallics*, 1995, **14**,

- 3268–3274.
- 190 M. K. Whittlesey, R. N. Perutz, I. G. Virrels and M. W. George, *Organometallics*, 1997, **16**, 268–274.
- 191 B. H. Weiller, E. P. Wasserman, C. B. Moore and R. G. Bergman, *J. Am. Chem. Soc.*, 1993, **115**, 4326–4330.
- 192 B. H. Weiller, E. P. Wasserman, R. G. Bergman, C. B. Moore and G. C. Pimentel, *J. Am. Chem. Soc.*, 1989, **111**, 8288–8290.
- 193 O. S. Jina, X. Z. Sun and M. W. George, *Dalton Trans.*, 2003, **2**, 1773–1778.
- 194 J. McMaster, P. Portius, G. E. Ball, J. P. Rourke and M. W. George, *Organometallics*, 2006, **25**, 5242–5248.
- 195 A. W. Ehlers, G. Frenking and E. J. Baerends, *Organometallics*, 1997, **16**, 4896–4902.
- 196 T. Kégl, *J. Quantum Chem.*, 2014, **2014**, 1–5.
- 197 S. A. Bartlett, N. A. Besley, A. J. Dent, S. Diaz-Moreno, J. Evans, M. L. Hamilton, M. W. D. Hanson-Heine, R. Horvath, V. Manici, X. Sun, M. Towrie, L. Wu, X. Zhang and M. W. George, *J. Am. Chem. Soc.*, 2019, **141**, 11471–11480.
- 198 K. Seppelt, *Anorg. Allg. Chem.*, 2003, **629**, 2427–2430.
- 199 D. Schröder, H. Schwarz, J. Hrušák and P. Pykkö, *Inorg. Chem.*, 1998, **37**, 624–632.
- 200 I. Hwang and K. Seppelt, *Anorg. Allg. Chem.*, 2002, **628**, 765.
- 201 S. Seidel, *Science*, 2000, **290**, 117–118.
- 202 T. Drews, S. Seidel and K. Seppelt, *Angew. Chem. Int. Ed.*, 2002, **41**, 454–456.
- 203 I. Hwang, S. Seidel and K. Seppelt, *Angew. Chem. Int. Ed.*, 2003, **42**, 4392–4395.
- 204 Y. Chauvin, N. Marchal, H. Olivier and L. Saussine, *J. Organomet. Chem.*, 1993, **445**, 93–97.
- 205 L. Wang, J. Cheng and L. Deng, *Inorganica Chim. Acta*, 2017, **460**, 49–54.
- 206 L. Liu, M. Zhu, H.-T. Yu, W.-X. Zhang and Z. Xi, *J. Am. Chem. Soc.*, 2017, **139**, 13688–13691.
- 207 P. Buchalski, I. Grabowska, E. Kamińska and K. Suwińska, *Organometallics*, 2008, **27**, 2346–2349.
- 208 L. Nilakantan, D. R. McMillin and P. R. Sharp, *Organometallics*, 2016, **35**, 2339–2347.
- 209 B. David, U. Monkowius, J. Rust, C. W. Lehmann, L. Hyzak and F. Mohr, *Dalton Trans.*, 2014, **43**, 11059–11066.
- 210 M. A. Bennett, T. Dirnberger, D. C. R. Hockless, E. Wenger and A. C. Willis, *J. Chem. Soc. Dalton Trans.*, 1998, 271–278.
- 211 C. Sieck, M. G. Tay, M. H. Thibault, R. M. Edkins, K. Costuas, J. F. Halet, A. S. Batsanov, M. Haehnel, K. Edkins, A. Lorbach, A. Steffen and T. B. Marder, *Chem. Eur. J.*, 2016, **22**, 10523–10532.
- 212 D. A. Laviska, T. Zhou, A. Kumar, T. J. Emge, K. Krogh-Jespersen and A. S. Goldman, *Organometallics*, 2016, **35**, 1613–1623.
- 213 D. a Laviska, C. Guan, T. J. Emge, M. Wilklow-Marnell, W. W. Brennessel, W. D. Jones, K. Krogh-Jespersen and A. S. Goldman, *Dalton Trans.*, 2014, **43**, 16354–16365.

- 214 J. M. Racowski, N. D. Ball and M. S. Sanford, *J. Am. Chem. Soc.*, 2011, **133**, 18022–18025.
- 215 A. Maleckis, J. W. Kampf and M. S. Sanford, *J. Am. Chem. Soc.*, 2013, **135**, 6618–6625.
- 216 S. Bin Zhao, R. Y. Wang, H. Nguyen, J. J. Becker and M. R. Gagné, *Chem. Commun.*, 2012, **48**, 443–445.
- 217 G. Dong, *Topics in Current Chemistry: C-C Bond Activation*, 2014, vol. 346.
- 218 J. J. Eisch, A. M. Piotrowski, K. I. Han, C. Krüger and Y. H. Tsay, *Organometallics*, 1985, **4**, 224–231.
- 219 H. Takano, T. Ito, K. S. Kanyiva and T. Shibata, *Eur. J. Org. Chem.*, 2019, **2019**, 2871–2883.
- 220 C. Perthuisot, B. L. Edelbach, D. L. Zubris, N. Simhai, C. N. Iverson, C. Mueller, T. Satoh and W. D. Jones, *J. Mol. Catal. A Chem.*, 2002, **189**, 157–168.
- 221 M. Murakami and N. Ishida, *J. Am. Chem. Soc.*, 2016, **138**, 13759–13769.
- 222 J. M. Darmon, S. C. E. Stieber, K. T. Sylvester, I. Fernández, E. Lobkovsky, S. P. Semproni, E. Bill, K. Wieghardt, S. Debeer and P. J. Chirik, *J. Am. Chem. Soc.*, 2012, **134**, 17125–17137.
- 223 J. R. Bour, N. M. Camasso, E. A. Meucci, J. W. Kampf, A. J. Canty and M. S. Sanford, *J. Am. Chem. Soc.*, 2016, **138**, 16105–16111.
- 224 P. Buchalski, R. Pacholski, K. Chodkiewicz, W. Buchowicz, K. Suwińska and A. Shkurenko, *Dalton Trans.*, 2015, **44**, 7169–7176.
- 225 H. Schwager, S. Spyroudis and K. P. C. Vollhardt, *J. Organomet. Chem.*, 1990, **382**, 191–200.
- 226 R. Beck and S. A. Johnson, *Chem. Commun.*, 2011, **47**, 9233–9235.
- 227 A. L. Keen, M. Doster and S. A. Johnson, *J. Am. Chem. Soc.*, 2007, **129**, 810–819.
- 228 T. Schaub and U. Radius, *Chem. Eur. J.*, 2005, **11**, 5024–5030.
- 229 T. Schaub, M. Backes and U. Radius, *Organometallics*, 2006, **25**, 4196–4206.
- 230 D. Suter, L. T. C. G. van Summeren, O. Blacque and K. Venkatesan, *Inorg. Chem.*, 2018, **57**, 8160–8168.
- 231 J. DePriest, G. Y. Zheng, N. Goswami, D. M. Eichhorn, C. Woods and D. P. Rillema, *Inorg. Chem.*, 2000, **39**, 1955–1963.
- 232 X. Zhang, G. B. Carpenter and D. A. Sweigart, *Organometallics*, 1999, **18**, 4887–4888.
- 233 K. Yu, H. Li, E. J. Watson, K. L. Virkaitis, G. B. Carpenter and D. A. Sweigart, *Organometallics*, 2001, **20**, 3550–3559.
- 234 B. L. Edelbach, R. J. Lachicotte and W. D. Jones, *J. Am. Chem. Soc.*, 1998, **120**, 2843–2853.
- 235 T. Debaerdemaeker, R. Hohenadel and H.-A. Brune, *J. Organomet. Chem.*, 1991, **410**, 265–275.
- 236 B. L. Edelbach, D. A. Vicic, R. J. Lachicotte and W. D. Jones, *Organometallics*, 1998, **17**, 4784–4794.
- 237 N. Simhai, C. N. Iverson, B. L. Edelbach and W. D. Jones, *Organometallics*, 2001, **20**, 2759–2766.

- 238 D. A. Vicic and W. D. Jones, *J. Am. Chem. Soc.*, 1999, **121**, 7606–7617.
- 239 D. P. Rillema, *Inorg. Chem.*, 1999, **38**, 794–797.
- 240 C. Y. Wu, T. Horibe, C. B. Jacobsen and F. D. Toste, *Nature*, 2015, **517**, 449–454.
- 241 P. T. Bohan and F. Dean Toste, *J. Am. Chem. Soc.*, 2017, **139**, 11016–11019.
- 242 J. Chu, D. Munz, R. Jazzar, M. Melaimi and G. Bertrand, *J. Am. Chem. Soc.*, 2016, **138**, 7884–7887.
- 243 M. Joost, L. Estévez, K. Miqueu, A. Amgoune and D. Bourissou, *Angew. Chem. Int. Ed.*, 2015, **54**, 5236–5240.
- 244 L. Rocchigiani, J. Fernandez-Cestau, I. Chambrier, P. Hrobárik and M. Bochmann, *J. Am. Chem. Soc.*, 2018, **140**, 8287–8302.
- 245 I. Chambrier, L. Rocchigiani, D. L. Hughes, P. M. H. Budzelaar and M. Bochmann, *Chem. Eur. J.*, 2018, **24**, 11467–11474.
- 246 A. V. Zhukhovitskiy, I. J. Kobylanskii, C. Y. Wu and F. D. Toste, *J. Am. Chem. Soc.*, 2018, **140**, 466–474.
- 247 C. Perthuisot, B. L. Edelbach, D. L. Zubris and W. D. Jones, *Organometallics*, 2002, **16**, 2016–2023.
- 248 C. Perthuisot and W. D. Jones, *J. Am. Chem. Soc.*, 1994, **116**, 3647–3648.
- 249 J. Graeupner, T. P. Brewster, J. D. Blakemore, N. D. Schley, J. M. Thomsen, G. W. Brudvig, N. Hazari and R. H. Crabtree, *Organometallics*, 2012, **31**, 7158–7164.
- 250 C. N. Iverson and W. D. Jones, *Organometallics*, 2001, **20**, 5745–5750.
- 251 Z. Lu, C.-H. Jun, S. R. de Gala, M. P. Sigalas, O. Eisenstein and R. H. Crabtree, *J. Chem. Soc. Chem. Commun.*, 1993, **2**, 1877–1880.
- 252 Z. Lu, C.-H. Jun, S. R. de Gala, M. P. Sigalas, O. Eisenstein and R. H. Crabtree, *Organometallics*, 1995, **14**, 1168–1175.
- 253 G. Ujaque, F. Maseras, O. Eisenstein, L. Liable-Sands, A. L. Rheingold, W. Yao and R. H. Crabtree, *New J. Chem.*, 1998, **15**, 1493–1498.
- 254 A. B. Chaplin, R. Tonner and A. S. Weller, *Organometallics*, 2010, **29**, 2710–2714.
- 255 F. L. Taw, H. Mellows, P. S. White, F. J. Hollander, R. G. Bergman, M. Brookhart and D. M. Heinekey, *J. Am. Chem. Soc.*, 2002, **124**, 5100–5108.
- 256 B. K. Corkey, F. L. Taw, R. G. Bergman and M. Brookhart, *Polyhedron*, 2004, **23**, 2943–2954.
- 257 T. Wang, J. L. Niu, S. L. Liu, J. J. Huang, J. F. Gong and M. P. Song, *Adv. Synth. Catal.*, 2013, **355**, 927–937.
- 258 P. Ren, S. D. Pike, I. Pernik, A. S. Weller and M. C. Willis, *Organometallics*, 2015, **34**, 711–723.
- 259 J. Campos and E. Carmona, *Organometallics*, 2015, **34**, 2212–2221.
- 260 A. R. Chianese, M. J. Drance, K. H. Jensen, S. P. McCollom, N. Yusufova, S. E. Shaner, D. Y. Shopov and J. A. Tendler, *Organometallics*, 2014, **33**, 457–464.
- 261 S. Gruber, M. Neuburger and A. Pfaltz, *Organometallics*, 2013, **32**, 4702–4711.
- 262 E. Piras, F. Läng, H. Rüegger, D. Stein, M. Wörle and H. Grützmacher, *Chem. Eur. J.*, 2006, **12**, 5849–5858.
- 263 D. Huang, J. C. Huffman, J. C. Bollinger, O. Eisenstein and K. G. Caulton, *J.*

- Am. Chem. Soc.*, 1997, **119**, 7398–7399.
- 264 P. L. Arnold, A. Prescimone, J. H. Farnaby, S. M. Mansell, S. Parsons and N. Kaltsoyannis, *Angew. Chem. Int. Ed.*, 2015, **54**, 6735–6739.
- 265 M. Lein, *Coord. Chem. Rev.*, 2009, **253**, 625–634.
- 266 X. Fradera, M. A. Austen and R. F. W. Bader, *J. Phys. Chem. A*, 1999, **103**, 304–314.
- 267 P. L. . Popelier and G. Logothetis, *J. Organomet. Chem.*, 1998, **555**, 101–111.
- 268 M. Lein, J. A. Harrison and A. J. Nielson, *Dalton Trans.*, 2013, **42**, 10939–10951.
- 269 T. S. Thakur and G. R. Desiraju, *J. Mol. Struct. Theochem*, 2007, **810**, 143–154.
- 270 U. Koch and P. L. A. Popelier, *J. Phys. Chem.*, 1995, **99**, 9747–9754.
- 271 R. R. Schrock and J. A. Osborn, *Inorg. Chem.*, 1970, **9**, 2339–2343.
- 272 A. Rifat, N. J. Patmore, M. F. Mahon and A. S. Weller, *Organometallics*, 2002, **21**, 2856–2865.
- 273 S. Jin, Y. Hao, Z. Zhu, N. Muhammad, Z. Zhang, K. Wang, Y. Guo, Z. Guo and X. Wang, *Inorg. Chem.*, 2018, **57**, 11135–11145.
- 274 S. Kumaraswamy, S. S. Jalisatgi, A. J. Matzger, O. Miljanić and K. P. C. Vollhardt, *Angew. Chem. Int. Ed.*, 2004, **43**, 3711–3715.
- 275 W. Y. Yeh, S. C. N. Hsu, S. M. Peng and G. H. Lee, *Organometallics*, 1998, **17**, 2477–2483.
- 276 A. Galan and P. Ballester, *Chem. Soc. Rev.*, 2016, **45**, 1720–1737.
- 277 S. Kumar, S. Chawla and M. C. Zou, *J. Incl. Phenom. Macro.*, 2017, **88**, 129–158.
- 278 K. E. Chaffee, H. A. Fogarty, T. Brotin, B. M. Goodson and J.-P. Dutasta, *J. Phys. Chem. A*, 2009, **113**, 13675–13684.
- 279 J. Nakazawa, Y. Sakae, M. Aida and Y. Naruta, *J. Org. Chem.*, 2007, **72**, 9448–9455.
- 280 C. Gropp, B. L. Quigley and F. Diederich, *J. Am. Chem. Soc.*, 2018, **140**, 2705–2717.
- 281 Y. Yu and J. Rebek Jr., *Acc. Chem. Res.*, 2018, **51**, 3031–3040.
- 282 D. Ajami and J. Rebek Jr., *Acc. Chem. Res.*, 2013, **46**, 990–999.
- 283 H. Gan, C. J. Benjamin and B. C. Gibb, *J. Am. Chem. Soc.*, 2011, **133**, 4770–4773.
- 284 A. Scarso, L. Trembleau and J. Rebek Jr., *J. Am. Chem. Soc.*, 2004, **126**, 13512–13518.
- 285 A. Asadi, D. Ajami and J. Rebek Jr., *J. Am. Chem. Soc.*, 2011, **133**, 10682–10684.
- 286 K.-D. Zhang, D. Ajami, J. V. Gavette and J. Rebek Jr., *J. Am. Chem. Soc.*, 2014, **136**, 5264–5266.
- 287 A. Scarso, L. Trembleau and J. Rebek, *Angew. Chem. Int. Ed.*, 2003, **42**, 5499–5502.
- 288 S. V. V. Velpuri, H. M. Gade and P. P. Wanjari, *Chem. Phys.*, 2019, **521**, 100–107.
- 289 R. M. Fairchild, A. I. Joseph, K. T. Holman, H. A. Fogarty, T. Brotin, J.-P. Dutasta, C. Boutin, G. Huber and P. Berthault, *J. Am. Chem. Soc.*, 2010, **132**, 15505–15507.
- 290 M. El Haouaj, Y. Ho Ko, M. Luhmer, K. Kim and K. Bartik, *J. Chem. Soc. Perkin*

- Trans. 2*, 2001, 2104–2107.
- 291 G. Huber, T. Brotin, L. Dubois, H. Desvaux, J. P. Dutasta and P. Berthault, *J. Am. Chem. Soc.*, 2006, **128**, 6239–6246.
  - 292 P. A. Hill, Q. Wei, R. G. Eckenhoff and I. J. Dmochowski, *J. Am. Chem. Soc.*, 2007, **129**, 9262–9263.
  - 293 N. Branda, R. M. Grotzfeld, C. Valdes and J. Rebek Jr., *J. Am. Chem. Soc.*, 1995, **117**, 85–88.
  - 294 E. B. Brouwer, G. D. Enright and J. A. Ripmeester, *Chem. Commun.*, 1997, 939–940.
  - 295 C. D. Gutsche, B. Dhawan, K. H. No and R. Muthukrishnan, *J. Am. Chem. Soc.*, 1981, **103**, 3782–3792.
  - 296 C. D. Gutsche and J. A. Levine, *J. Am. Chem. Soc.*, 1982, **104**, 2652–2653.
  - 297 C. D. Gutsche and P. F. Pagoria, *J. Org. Chem.*, 1985, **123**, 5795–5802.
  - 298 C. D. Gutsche, J. A. Levine and P. K. Sujeeth, *J. Org. Chem.*, 1985, **50**, 5802–5806.
  - 299 C. D. Gutsche and L.-G. Lin, *Tetrahedron*, 1986, **42**, 1633–1640.
  - 300 P. Neri, J. L. Sessler and M. X. Wang, *Calixarenes and beyond*, 2016.
  - 301 G. E. Arnott, *Chem. Eur. J.*, 2018, **24**, 1744–1754.
  - 302 J. Rebek Jr., *Chem. Commun.*, 2000, 637–643.
  - 303 V. Böhmer, *Angew. Chem. Int. Ed.*, 1995, **34**, 713–745.
  - 304 A. Ikeda, S. Shinkai and A. I. Analysis, *J. Chem. Soc. Perkin Trans.*, 1994, **2**, 2073–2080.
  - 305 J. Matousek, M. Cajan, P. Kulhanek and J. Koca, *J. Phys. Chem. A*, 2008, **112**, 1076–1084.
  - 306 S. Simaan and S. E. Biali, *J. Org. Chem.*, 2003, **68**, 7685–7692.
  - 307 M. Conner, V. Janout and S. L. Regen, *J. Am. Chem. Soc.*, 1991, **113**, 9670–9671.
  - 308 C. D. Gutsche and L. J. Bauer, *J. Am. Chem. Soc.*, 1985, **107**, 6052–6059.
  - 309 D. M. Homden and C. Redshaw, *Chem. Rev.*, 2008, **108**, 5086–5130.
  - 310 D. Sémeril and D. Matt, *Coord. Chem. Rev.*, 2014, **279**, 58–95.
  - 311 J. W. Steed, R. K. Juneja and J. L. Atwood, *Angew. Chem. Int. Ed.*, 1995, **33**, 2456–2457.
  - 312 Y. Ishii, K. Onaka, H. Hirakawa and K. Shiramizu, *Chem. Commun.*, 2002, 1150–1151.
  - 313 R. Gramage-Doria, D. Armspach and D. Matt, *Coord. Chem. Rev.*, 2013, **257**, 776–816.
  - 314 C. Wieser, C. B. Dieleman and D. Matt, *Coord. Chem. Rev.*, 1997, **165**, 93–161.
  - 315 T. Iwasawa, *Tetrahedron Lett.*, 2017, **58**, 4217–4226.
  - 316 H. Ren, B. Ourri, E. Jeanneau, T. Tu, I. Bonnamour and U. Darbost, *Transit. Met. Chem.*, 2016, **41**, 827–834.
  - 317 H. Ren, Y. Xu, E. Jeanneau, I. Bonnamour, T. Tu and U. Darbost, *Tetrahedron*, 2014, **70**, 2829–2837.
  - 318 E. K. Bullough, M. A. Little and C. E. Willans, *Organometallics*, 2013, **32**, 570–577.
  - 319 M. Vézina, J. Gagnon, K. Villeneuve, M. Drouin and P. D. Harvey, *Chem.*



- Commun.*, 2000, 1073–1074.
- 320 T. Fahlbusch, M. Frank, G. Maas and J. Schatz, *Organometallics*, 2009, **28**, 6183–6193.
- 321 I. Dinarès, C. G. De Miguel, M. Font-Bardia, X. Solans and E. Alcalde, *Organometallics*, 2007, **26**, 5125–5128.
- 322 M. Frank, G. Maas and J. Schatz, *Eur. J. Org. Chem.*, 2004, 607–613.
- 323 E. Brenner, D. Matt, M. Henrion, M. Teci and L. Toupet, *Dalton Trans.*, 2011, **40**, 9889.
- 324 N. Khiri-Meribout, E. Bertrand, J. Bayardon, M. J. Eymin, Y. Rousselin, H. Cattey, D. Fortin, P. D. Harvey and S. Jugé, *Organometallics*, 2013, **32**, 2827–2839.
- 325 T. Brendgen, M. Frank and J. Schatz, *Eur. J. Org. Chem.*, 2006, 2378–2383.
- 326 R. Patchett and A. B. Chaplin, *Dalton Trans.*, 2016, **45**, 8945–8955.
- 327 R. Patchett, R. C. Knighton, J. D. Mattock, A. Vargas and A. B. Chaplin, *Inorg. Chem.*, 2017, **56**, 14345–14350.
- 328 L. Monnereau, D. Sémeril, D. Matt and L. Toupet, *Chem. Eur. J.*, 2010, **16**, 9237–9247.
- 329 L. Monnereau, D. Sémeril, D. Matt and C. Gourlaouen, *Eur. J. Inorg. Chem.*, 2017, **2017**, 581–586.
- 330 S. Sameni, M. Lejeune, C. Jeunesse, D. Matt and R. Welter, *Dalton Trans.*, 2009, 7912–7923.
- 331 N. Khiri, E. Bertrand, M. J. Ondel-Eymin, Y. Rousselin, J. Bayardon, P. D. Harvey and S. Jugé, *Organometallics*, 2010, **29**, 3622–3631.
- 332 F. Elaieb, D. Sémeril, D. Matt, M. Pfeffer, P.-A. Bouit, M. Hissler, C. Gourlaouen and J. Harrowfield, *Dalton Trans.*, 2017, **46**, 9833–9845.
- 333 F. Elaieb, A. Hedhli, D. Sémeril and D. Matt, *Eur. J. Lipid Sci. Technol.*, 2016, **2016**, 1867–1873.
- 334 F. Elaieb, A. Hedhli, D. Sémeril, D. Matt and J. Harrowfield, *Eur. J. Org. Chem.*, 2016, **2016**, 3103–3108.
- 335 F. Elaieb, D. Sémeril, C. Bauder, D. Matt, C. Bailly and L. Karmazin, *Polyhedron*, 2018, **139**, 172–177.
- 336 K. Hirasawa, S. Tanaka, T. Horiuchi, T. Kobayashi, T. Sato, N. Morohashi and T. Hattori, *Organometallics*, 2016, **35**, 420–427.
- 337 S. D. Alexandratos and S. Natesan, *Ind. Eng. Chem. Res.*, 2000, **39**, 3998–4010.
- 338 P. Maji, L. Mahalakshmi, S. S. Krishnamurthy and M. Nethaji, *J. Organomet. Chem.*, 2011, **696**, 3169–3179.
- 339 P. Maji, *Inorganica Chim. Acta*, 2011, **372**, 120–125.
- 340 M. Stolzmar, C. Floriani, A. Chiesi-Villa and C. Rizzoli, *Inorg. Chem.*, 1997, **36**, 1694–1701.
- 341 P. Maji, S. S. Krishnamurthy and M. Nethaji, *Polyhedron*, 2008, **27**, 3519–3527.
- 342 C. Wieser, D. Matt, J. Fischer and A. Harriman, *J. Chem. Soc. Dalton Trans.*, 1997, **1**, 2391–2402.
- 343 C. Wieser, D. Matt, L. Toupet, H. Bourgeois and J. P. Kintzinger, *J. Chem. Soc. Dalton Trans.*, 1996, **66**, 4041–4043.

- 344 C. Jeunesse, C. Dieleman, S. Steyer and D. Matt, *J. Chem. Soc. Dalton Trans.*, 2001, 881–892.
- 345 M. Lejeune, C. Jeunesse, D. Matt, N. Kyritsakas, R. Welter and J.-P. Kintzinger, *J. Chem. Soc. Dalton Trans.*, 2002, 1642–1650.
- 346 S. Sameni, C. Jeunesse, M. Awada, D. Matt and R. Welter, *Eur. J. Inorg. Chem.*, 2010, 4917–4923.
- 347 M. Lejeune, D. Sémeril, C. Jeunesse, D. Matt, F. Peruch, P. J. Lutz and L. Ricard, *Chem. Eur. J.*, 2004, **10**, 5354–5360.
- 348 M. Lejeune, D. Sémeril, C. Jeunesse, D. Matt, P. Lutz and L. Toupet, *Adv. Synth. Catal.*, 2006, **348**, 881–886.
- 349 K. Takenaka, Y. Obora, L. H. Jiang and Y. Tsuji, *Organometallics*, 2002, **21**, 1158–1166.
- 350 C. Wieser-Jeunesse, D. Matt and A. De Cian, *Angew. Chem. Int. Ed.*, 1998, **37**, 2861–2864.
- 351 D. R. Evans, M. Huang, J. C. Fettingner and T. L. Williamst, *Inorg. Chem.*, 2002, **41**, 5986–6000.
- 352 I. A. Bagatin, D. Matt, H. Thonnessen and P. G. Jones, *Inorg. Chem.*, 1999, **38**, 1585–1591.
- 353 X. Fang, B. L. Scott, J. G. Watkin, C. A. G. Carter and G. J. Kubas, *Inorganica Chim. Acta*, 2001, **317**, 276–281.
- 354 N. Natarajan, M. C. Pierrevelcin, D. Sémeril, C. Bauder, D. Matt and R. Ramesh, *Catal. Commun.*, 2019, **118**, 70–75.
- 355 D. S. Lee, M. R. J. Elsegood, C. Redshaw and S. Zhan, *Acta Crystallogr. C*, 2009, **65**, 291–295.
- 356 J. A. Marsella, J. C. Huffman, K. Folting and K. G. Caulton, *Inorganica Chim. Acta*, 1985, **96**, 161–170.
- 357 W. E. Hunter, D. C. Hrnčir, R. V. Bynum, R. A. Penttilä and J. L. Atwood, *Organometallics*, 1983, **2**, 750–755.
- 358 P. C. Wailes, H. Weigold and A. P. Bell, *J. Organomet. Chem.*, 1972, **34**, 155–164.
- 359 A. D. Phillips, R. J. Wright, M. M. Olmstead and P. P. Power, *J. Am. Chem. Soc.*, 2002, **124**, 5930–5931.
- 360 J. S. Johnson and R. G. Bergman, *J. Am. Chem. Soc.*, 2001, **123**, 2923–2924.
- 361 G. Proulx and R. G. Bergman, *Organometallics*, 1996, **15**, 684–692.
- 362 D. A. Dobbs and R. G. Bergman, *Organometallics*, 1994, **13**, 4594–4605.
- 363 N. A. Yakelis and R. G. Bergman, *Organometallics*, 2005, **24**, 3579–3581.
- 364 H. Lee, P. J. Desrosiers, I. Guzei, A. L. Rheingold and G. Parkin, *J. Am. Chem. Soc.*, 1998, **120**, 3255–3256.
- 365 D. R. McAlister, D. K. Erwin and J. E. Bercaw, *J. Am. Chem. Soc.*, 1978, **100**, 5966–5968.
- 366 H. H. Brintzinger, *J. Organomet. Chem.*, 1979, **171**, 337–344.
- 367 K. I. Gell, B. Posin, J. Schwartz and G. M. Williams, *J. Am. Chem. Soc.*, 1982, **104**, 1846–1855.
- 368 J. Halpern, *J. Phys. Chem.*, 1959, **63**, 398–403.

- 369 P. T. Wolczanski and J. E. Bercaw, *Organometallics*, 1982, **1**, 793–799.
- 370 S. Couturier and B. Gautheron, *J. Organomet. Chem.*, 1978, **157**, 63–65.
- 371 R. F. Jordan, C. S. Bajgur, W. E. Dasher and A. L. Rheingold, *Organometallics*, 1987, **6**, 1041–1051.
- 372 R. Lin, A. Ladshaw, Y. Nan, J. Liu, S. Yiacoumi, C. Tsouris, D. W. DePaoli and L. L. Tavlarides, *Ind. Eng. Chem. Res.*, 2015, **54**, 10442–10448.
- 373 P. C. W. Leung, K. B. Kunz, K. Seff and I. E. Maxwell, *J. Phys. Chem.*, 1975, **79**, 2157–2162.
- 374 L. E. Sutton, *Tables of Interatomic Distances and Configuration in Molecules & Ions*, The Chemical Society, London, 1965.
- 375 P. Alam, C. Climent, G. Kaur, D. Casanova, A. Roy Choudhury, A. Gupta, P. Alemany and I. R. Laskar, *Cryst. Growth Des.*, 2016, **16**, 5738–5752.
- 376 B. D. Alexander, B. J. Johnson, S. M. Johnson, A. L. Casalnuovo and L. H. Pignolet, *J. Am. Chem. Soc.*, 1986, **108**, 4409–4417.
- 377 A. Macchioni, C. Zuccaccia, E. Clot, K. Gruet and R. H. Crabtree, *Organometallics*, 2001, **20**, 2367–2373.
- 378 B. D. Alexander, B. J. Johnson, S. M. Johnson, P. D. Boyle, N. C. Kann, A. M. Mueting and L. H. Pignolet, *Inorg. Chem.*, 1987, **26**, 3506–3513.
- 379 I. A. Guzei, A. L. Rheingold, D.-H. Lee and R. H. Crabtree, *Z. Allg. Krist. NSC*, 1998, **213**, 585–587.
- 380 I. I. Bhayat and W. R. McWhinnie, *J. Organomet. Chem.*, 1972, **46**, 159–165.
- 381 C. Cocevar, G. Mestroni and A. Camus, *J. Organomet. Chem.*, 1972, **35**, 389–395.
- 382 Á. Álvarez, R. Macías, M. J. Farba, M. L. Martín, F. J. Lahoz and L. A. Oro, *Inorg. Chem.*, 2007, **46**, 6811–6826.
- 383 T. Yoshida, T. Okano and S. Otsuka, *J. Am. Chem. Soc.*, 1980, **102**, 5966–5967.
- 384 G. L. Moxham, S. K. Brayshaw and A. S. Weller, *Dalton Trans.*, 2007, 1759–1761.
- 385 A. Rifat, G. Kociok-ko, J. W. Steed and A. S. Weller, *Organometallics*, 2004, **2**, 428–432.
- 386 R. R. Schrock and J. A. Osborn, *J. Am. Chem. Soc.*, 1971, **93**, 2397–2407.
- 387 J. R. Shapley, R. R. Schrock and J. A. Osborn, *J. Am. Chem. Soc.*, 1969, **91**, 2816–2817.
- 388 M. J. Ingleson, S. K. Brayshaw, M. F. Mahon, G. O. Ruggiero and A. S. Weller, *Inorg. Chem.*, 2005, **44**, 3162–3171.
- 389 G. L. Moxham, T. M. Douglas, S. K. Brayshaw, G. Kociok-Köhn, J. P. Lowe and A. S. Weller, *Dalton Trans.*, 2006, 5492–5505.
- 390 R. H. Crabtree, J. W. Faller, M. F. Mellea and J. M. Quirk, *Organometallics*, 1982, **2**, 1361–1366.
- 391 R. H. Crabtree, P. C. Demou, D. Eden, J. M. Mihelcic, C. A. Parnell, J. M. Quirk and G. E. Morris, *J. Am. Chem. Soc.*, 1982, **104**, 6994–7001.
- 392 R. H. Crabtree, H. Felkin and G. E. Morris, *J. Organomet. Chem.*, 1977, **141**, 205–215.
- 393 E. P. Shestakova, Y. S. Varshavsky, V. N. Khrustalev, S. N. Smirnov, I. S.

- Podkorytov, M. V. Borisova and A. B. Nikolskii, *J. Organomet. Chem.*, 2011, **696**, 3214–3222.
- 394 I. C. Douek and G. Wilkinson, *J. Chem. Soc. A Inorganic, Phys. Theor.*, 1969, 2604.
- 395 A. R. Siedle, R. A. Newmark and L. H. Plgnolet, *Organometallics*, 1984, **3**, 855–859.
- 396 J. B. Niederl and H. J. Vogel, *J. Am. Chem. Soc.*, 1940, **62**, 2512–2514.
- 397 A. G. Sverker Högberg, *J. Am. Chem. Soc.*, 1980, **102**, 6046–6050.
- 398 A. G. S. Hogberg, *J. Org. Chem.*, 1980, **45**, 4498–4500.
- 399 J. Rebek Jr., *Acc. Chem. Res.*, 2009, **42**, 1660–1668.
- 400 T. Gottschalk, B. Jaun and F. Diederich, *Angew. Chem. Int. Ed.*, 2007, **46**, 260–264.
- 401 A. Asadi, D. Ajami and J. Rebek Jr., *Chem. Sci.*, 2013, **4**, 1212.
- 402 N. Natarajan, E. Brenner, D. Sémeril, D. Matt and J. Harrowfield, *Eur. J. Org. Chem.*, 2017, **2017**, 6100–6113.
- 403 C. Gibson and J. Rebek, *Org. Lett.*, 2002, **4**, 1887–1890.
- 404 M. P. Schramm, M. Kanaura, K. Ito, M. Ide and T. Iwasawa, *Eur. J. Org. Chem.*, 2016, **2016**, 813–820.
- 405 R. C. Knighton and A. B. Chaplin, *Tetrahedron*, 2017, **73**, 4591–4596.
- 406 M. Cacciarini, V. A. Azov, P. Seiler, H. Künzer and F. Diederich, *Chem. Commun.*, 2005, **2**, 5269–5271.
- 407 G. Farkas, S. Balogh, J. Madarász, Á. Szöllősy, F. Darvas, L. Üрге, M. Gouygou and J. Bakos, *Dalton Trans.*, 2012, **41**, 9493.
- 408 P. Kleman, M. Vaquero, I. Arribas, A. Suárez, E. Álvarez and A. Pizzano, *Tetrahedron Asymmetry*, 2014, **25**, 744–749.
- 409 C. G. Arena, F. Faraone, C. Graiff and A. Tiripicchio, *Eur. J. Inorg. Chem.*, 2002, 711–716.
- 410 G. E. Ball, W. R. Cullen, M. D. Fryzuk, B. R. James and S. J. Rettig, *Organometallics*, 1991, **10**, 3767–3769.
- 411 S. D. Pike, I. Pernik, R. Theron, J. S. Mcindoe and A. S. Weller, *J. Organomet. Chem.*, 2015, **784**, 75–83.
- 412 I. Pernik, J. F. Hooper, A. B. Chaplin, A. S. Weller and M. C. Willis, *ACS Catal.*, 2012, **2**, 2779–2786.
- 413 J. L. Herde, J. C. Lambert and C. V. Senoff, *Inorg. Synth.*, 1974, **15**, 18–20.
- 414 P. Hofmann, C. Meiera, U. Englertb and M. U. Schmidt, *Chem. Ber.*, 1992, **125**, 353–365.
- 415 A. van der Ent and A. L. Onderdelinden, *Inorg. Synth.*, 1990, **28**, 90–92.
- 416 G. Giordano and R. H. Crabtree, *Inorg. Synth.*, 1990, **28**, 88–90.
- 417 A. B. Chaplin, J. F. Hooper, A. S. Weller and M. C. Willis, *J. Am. Chem. Soc.*, 2012, **134**, 4885.
- 418 W. E. Buschmann and J. S. Miller, *Inorg. Synth.*, 2002, **83**, 83.
- 419 J. G. Park, I. Jeon and T. D. Harris, *Inorg. Chem.*, 2015, **54**, 359–369.
- 420 D. Stasko and C. A. Reed, *J. Am. Chem. Soc.*, 2002, **124**, 1148–1149.
- 421 D. Peral, D. Herrera, J. Real, T. Flor and J. C. Bayón, *Catal. Sci. Technol.*, 2016,

- 6, 800–808.
- 422 T. K. Panda, M. T. Gamer and P. W. Roesky, *Organometallics*, 2003, **22**, 877–878.
- 423 E. Neumann and A. Pfaltz, *Organometallics*, 2005, **24**, 2008–2011.
- 424 G. R. Fulmer, A. J. M. Miller, N. H. Sherden, H. E. Gottlieb, A. Nudelman, B. M. Stoltz, J. E. Bercaw and K. I. Goldberg, *Organometallics*, 2010, **29**, 2176–2179.
- 425 R. Streck and A. J. Barnes, *Spectrochim. Acta Part A Mol. Biomol. Spectrosc.*, 2002, **55**, 1049–1057.
- 426 T. E. Stennett, J. Pahl, H. S. Zijlstra, F. W. Seidel and S. Harder, *Organometallics*, 2016, **35**, 207–217.
- 427 A. Dondoni, C. Ghiglione, A. Marra and M. Scoponi, *Macromol. Chem. Phys.*, 1999, **86**, 77–86.
- 428 M. Larsen and M. Jørgensen, *J. Org. Chem.*, 1996, **61**, 6651–6655.
- 429 M. H. Düker, F. Kutter, T. Dülcks and V. a. Azov, *Supramol. Chem.*, 2014, **26**, 552–560.
- 430 A. Marra, M.-C. Scherrmann, A. Dondoni, R. Ungaro, A. Casnati and P. Minari, *Angew. Chem. Int. Ed.*, 1995, **33**, 2479–2481.
- 431 J. W. Moore and R. G. Pearson, *Kinetics and Mechanism*, John Wiley & Sons, New York, 3rd edn., 1981.
- 432 L. Abis, E. Dalcanale, A. Du Vosel and S. Spera, *J. Chem. Soc. Perkin Trans. 2*, 1990, 2075–2080.
- 433 E. Dalcanale, P. Soncini, G. Bacchilega and F. Ugozzoli, *J. Chem. Soc. Chem. Commun.*, 1989, 500–502.
- 434 P. Soncini, S. Bonsignore, E. Dalcanale and F. Ugozzoli, *J. Org. Chem.*, 1992, **57**, 4608–4612.
- 435 P. P. Castro, G. Zhao, G. A. Masangkay, C. Hernandez and L. M. Gutierrez-Tunstad, *Org. Lett.*, 2004, **6**, 333–336.
- 436 T. Iwasawa, Y. Nishimoto, K. Hama, T. Kamei, M. Nishiuchi and Y. Kawamura, *Tetrahedron Lett.*, 2008, **49**, 4758–4762.

## Index of compounds

---

<b>1</b>	[Rh(2,2'-biphenyl)(dtbpm)Cl]	33	147
<b>2</b>	[{Ir(2,2'-biphenyl)(cod)Cl} <sub>2</sub> ]	33	148
<b>3</b>	[Rh(2,2'-biphenyl)(PPh <sub>3</sub> ) <sub>2</sub> Cl]	34	149
<b>4</b>	[Rh(2,2'-biphenyl)(PCy <sub>3</sub> ) <sub>2</sub> Cl]	34	149
<b>5</b>	[Rh(2,2'-biphenyl)(P <sup>i</sup> Pr <sub>3</sub> ) <sub>2</sub> Cl]	34	150
<b>6</b>	[Rh(2,2'-biphenyl)(P <sup>i</sup> Bu <sub>3</sub> ) <sub>2</sub> Cl]	34	151
<b>7</b>	[Ir(2,2'-biphenyl)(PPh <sub>3</sub> ) <sub>2</sub> Cl]	34	151
<b>8</b>	[Ir(2,2'-biphenyl)(PCy <sub>3</sub> ) <sub>2</sub> Cl]	34	152
<b>9</b>	[Ir(2,2'-biphenyl)(P <sup>i</sup> Pr <sub>3</sub> ) <sub>2</sub> Cl]	34	153
<b>10</b>	[Ir(2,2'-biphenyl)(P <sup>i</sup> Bu <sub>3</sub> ) <sub>2</sub> Cl]	34	153
<b>11</b>	[Rh(2,2'-biphenyl)(PPh <sub>3</sub> ) <sub>2</sub> ][BAr <sup>F</sup> <sub>4</sub> ]	34	154
<b>12</b>	[Rh(2,2'-biphenyl)(PCy <sub>3</sub> ) <sub>2</sub> ][BAr <sup>F</sup> <sub>4</sub> ]	34	155
<b>13</b>	[Rh(2,2'-biphenyl)(P <sup>i</sup> Pr <sub>3</sub> ) <sub>2</sub> ][BAr <sup>F</sup> <sub>4</sub> ]	34	156
<b>14</b>	[Rh(2,2'-biphenyl)(P <sup>i</sup> Bu <sub>3</sub> ) <sub>2</sub> ][BAr <sup>F</sup> <sub>4</sub> ]	34	156
<b>15</b>	[Rh(2,2'-biphenyl)(P <sup>i</sup> Bu <sub>3</sub> ) <sub>2</sub> ][Al(OR <sup>F</sup> ) <sub>4</sub> ]	34	157
<b>16</b>	[Ir(2,2'-biphenyl)(PPh <sub>3</sub> ) <sub>2</sub> ][BAr <sup>F</sup> <sub>4</sub> ]	34	157
<b>17</b>	[Ir(2,2'-biphenyl)(PCy <sub>3</sub> ) <sub>2</sub> ][BAr <sup>F</sup> <sub>4</sub> ]	34	158
<b>18</b>	[Ir(2,2'-biphenyl)(P <sup>i</sup> Pr <sub>3</sub> ) <sub>2</sub> ][BAr <sup>F</sup> <sub>4</sub> ]	34	159
<b>19</b>	[Ir(2,2'-biphenyl)(P <sup>i</sup> Bu <sub>3</sub> ) <sub>2</sub> ][BAr <sup>F</sup> <sub>4</sub> ]	34	159
<b>20</b>	[Ir(2,2'-biphenyl)(P <sup>i</sup> Bu <sub>3</sub> ) <sub>2</sub> ][Al(OR <sup>F</sup> ) <sub>4</sub> ]	34	160
<b>21</b>	[{Rh(2,2'-biphenyl)(PPh <sub>2</sub> Tol <sup>F</sup> )Cl} <sub>2</sub> ]	45	160
<b>22</b>	[Rh(2,2'-biphenyl)(PPh <sub>2</sub> Tol <sup>F</sup> ) <sub>2</sub> ][Cl]	45	161
<b>23</b>	[Rh(2,2'-biphenyl)(PPh <sub>2</sub> Tol <sup>F</sup> ) <sub>2</sub> ][BAr <sup>F</sup> <sub>4</sub> ]	45	162
<b>24</b>	[Rh(2,2'-biphenyl)(2,2'-bipyridyl)(PPh <sub>2</sub> Tol <sup>F</sup> )][BAr <sup>F</sup> <sub>4</sub> ]	45	163
<b>25</b>	[Rh(acac)(2,2'-biphenyl)(PPh <sub>2</sub> Tol <sup>F</sup> )]	45	164
<b>26</b>	[Rh(2,2'-biphenyl)(Cp)(PPh <sub>2</sub> Tol <sup>F</sup> )]	45	165
<b>27</b>	[Rh(2,2'-biphenyl)(PPh <sub>3</sub> ) <sub>2</sub> (OH <sub>2</sub> )][BAr <sup>F</sup> <sub>4</sub> ]	51	166
<b>28</b>	[Ir(2,2'-biphenyl)(PPh <sub>3</sub> ) <sub>2</sub> (OH <sub>2</sub> )][BAr <sup>F</sup> <sub>4</sub> ]	51	167
<b>29</b>	[Rh(2,2'-biphenyl)(PPh <sub>3</sub> ) <sub>2</sub> ][Al(OR <sup>F</sup> ) <sub>4</sub> ]	53	167
<b>30</b>	[Rh(2,2'-biphenyl)(PPh <sub>3</sub> ) <sub>2</sub> (OH <sub>2</sub> )][Al(OR <sup>F</sup> ) <sub>4</sub> ]	53	168
<b>31</b>	[Rh(2,2'-biphenyl)(PPh <sub>3</sub> ) <sub>2</sub> (thf)][Al(OR <sup>F</sup> ) <sub>4</sub> ]	55	169
<b>32</b>	[Rh(η <sup>6</sup> -biphenyl)(PPh <sub>3</sub> ) <sub>2</sub> ][Al(OR <sup>F</sup> ) <sub>4</sub> ]	56	170
<b>33</b>	[Rh(2,2'-biphenyl)(PPh <sub>3</sub> ) <sub>2</sub> (CO) <sub>2</sub> ][Al(OR <sup>F</sup> ) <sub>4</sub> ]	57	171
<b>34</b>	[Rh(2,2'-biphenyl)(PPh <sub>3</sub> ) <sub>2</sub> (CO)][Al(OR <sup>F</sup> ) <sub>4</sub> ]	58	174

---

35	[Rh( $\alpha$ ,2-fluorenyl)(CO)(PPh <sub>3</sub> ) <sub>2</sub> ][Al(OR <sup>F</sup> ) <sub>4</sub> ]	58	174
36	[Rh( $\kappa^1$ -O-fluorenone)(CO)(PPh <sub>3</sub> ) <sub>2</sub> ][Al(OR <sup>F</sup> ) <sub>4</sub> ]	58	171
37	[Rh(2,2'-biphenyl)(PPh <sub>3</sub> ) <sub>2</sub> (OCH <sub>2</sub> CH <sub>2</sub> CH <sub>2</sub> CH <sub>2</sub> PPh <sub>3</sub> )] [Al(OR <sup>F</sup> ) <sub>4</sub> ]	60	174
38	[Rh(2,2'-biphenyl)(PPh <sub>3</sub> ) <sub>2</sub> (O <sub>2</sub> CCH <sub>2</sub> CH <sub>2</sub> CH <sub>2</sub> PPh <sub>3</sub> )] [Al(OR <sup>F</sup> ) <sub>4</sub> ]	60	172
39	[Ir(2,2'-biphenyl)(PPh <sub>3</sub> )(PCy <sub>3</sub> )] [BAr <sup>F</sup> <sub>4</sub> ]	61	175
40	[Rh(2,2'-biphenyl)(PPh <sub>3</sub> )(PCy <sub>3</sub> )Cl]	61	175
41	[{Rh(2,2'-biphenyl)(PPh <sub>3</sub> ) <sub>3</sub> }]	63	-
42	25,26,27,28-tetrahydroxycalix[4]arene	72	176
43	25,26,27,28-tetrapropoxycalix[4]arene	72	176
44	5,11,17,23-tetrabromo-25,26,27,28-tetrapropoxycalix[4]arene	72	177
45	5,17-dibromo-25,26,27,28-tetrapropoxycalix[4]arene	72	178
46	5,17-diformyl-25,26,27,28-tetrapropoxycalix[4]arene	72	178
47	5,17-bis(hydroxymethyl)-25,26,27,28-tetrapropoxycalix[4]arene	72	179
48	5,17-bis(chloromethyl)-25,26,27,28-tetrapropoxycalix[4]arene	72	180
49	5,17-bis(bromomethyl)-25,26,27,28-tetrapropoxycalix[4]arene	72	180
50	CxP <sub>2</sub>	72	181
51	[Li <sub>2</sub> (CxP <sub>2</sub> )] [Al(OR <sup>F</sup> ) <sub>4</sub> ] <sub>2</sub>	73	183
52	[Na(CxP <sub>2</sub> )] [BAr <sup>F</sup> <sub>4</sub> ]	73	183
53	[K(CxP <sub>2</sub> )] [BAr <sup>F</sup> <sub>4</sub> ]	73	184
54	[Tl(CxP <sub>2</sub> )] [BAr <sup>F</sup> <sub>4</sub> ]	73	185
55	[Ag(CxP <sub>2</sub> )] [Al(OR <sup>F</sup> ) <sub>4</sub> ]	73	186
56	[{Rh(2,2'-biphenyl)(CxP <sub>2</sub> )(Cl)} <sub>2</sub> ]	77	187
57	[{Ir(2,2'-biphenyl)(CxP <sub>2</sub> )(Cl)} <sub>2</sub> ]	77	188
58	[Rh(2,2'-biphenyl)(CxP <sub>2</sub> )(ClAg)] [Al(OR <sup>F</sup> ) <sub>4</sub> ]	80	190
59	[Rh(2,2'-biphenyl)(CxP <sub>2</sub> )(OH <sub>2</sub> )] [Al(OR <sup>F</sup> ) <sub>4</sub> ]	81	191
60	[{Rh(2,2'-biphenyl)(CxP <sub>2</sub> )(thf)} <sub>2</sub> ] [Al(OR <sup>F</sup> ) <sub>4</sub> ] <sub>2</sub>	87	189
61	[Rh(2,2'-biphenyl)(CxP <sub>2</sub> )(CO) <sub>2</sub> ] [Al(OR <sup>F</sup> ) <sub>4</sub> ]	89	194
62	[Rh(2,2'-biphenyl)(CxP <sub>2</sub> )(dcm)] [Al(OR <sup>F</sup> ) <sub>4</sub> ]	90	195
63	[Rh(2,2'-biphenyl)(CxP <sub>2</sub> )(N <sub>2</sub> )] [Al(OR <sup>F</sup> ) <sub>4</sub> ]	91	196
64	[Rh(2,2'-biphenyl)(CxP <sub>2</sub> )(H <sub>2</sub> )] [Al(OR <sup>F</sup> ) <sub>4</sub> ]	92	197
65	[Rh(2,2'-biphenyl)(CxP <sub>2</sub> )] [Al(OR <sup>F</sup> ) <sub>4</sub> ]	93	198
66	[Rh(2,2'-biphenyl)(CxP <sub>2</sub> )(H <sub>2</sub> ) <sub>2</sub> ] [Al(OR <sup>F</sup> ) <sub>4</sub> ]	99	199
67	[Rh(2,2'-bipyridyl)(H) <sub>2</sub> (PPh <sub>3</sub> ) <sub>2</sub> ] [BAr <sup>F</sup> <sub>4</sub> ]	106	200
68	[Ir(2,2'-bipyridyl)(H) <sub>2</sub> (PPh <sub>3</sub> ) <sub>2</sub> ] [BAr <sup>F</sup> <sub>4</sub> ]	106	201
69	[Rh(cod)(PPh <sub>3</sub> ) <sub>2</sub> ] [BAr <sup>F</sup> <sub>4</sub> ]	106	202
70	[Ir(cod)(PPh <sub>3</sub> ) <sub>2</sub> ] [BAr <sup>F</sup> <sub>4</sub> ]	106	202
71	[{Rh(PPh <sub>3</sub> ) <sub>2</sub> } <sub>2</sub> ] [BAr <sup>F</sup> <sub>4</sub> ] <sub>2</sub>	109	203
72	[Ir(H) <sub>2</sub> (PPh <sub>3</sub> ) <sub>2</sub> L <sub>2</sub> ] [BAr <sup>F</sup> <sub>4</sub> ]	111	204

<b>73</b>	$[\text{Rh}(2,2'\text{-bipyridyl})(\text{PPh}_3)_2][\text{BAr}^{\text{F}}_4]$	111	204
<b>74</b>	$[\text{Rh}(2,2'\text{-bipyridyl})(\text{cod})(\text{PPh}_3)][\text{BAr}^{\text{F}}_4]$	112	205
<b>75</b>	$[\text{Ir}(2,2'\text{-bipyridyl})(\text{cod})(\text{PPh}_3)][\text{BAr}^{\text{F}}_4]$	112	206
<b>76</b>	$[\text{Rh}(2,2'\text{-bipyridyl})(\text{cod})][\text{BAr}^{\text{F}}_4]$	112	207
<b>77</b>	$[\text{Ir}(2,2'\text{-bipyridyl})(\text{cod})][\text{BAr}^{\text{F}}_4]$	112	207
<b>78</b>	$[\text{Ir}(2,2'\text{-bipyridyl})(\text{cod})(\text{H})_2][\text{BAr}^{\text{F}}_4]$	114	208
<b>79</b>	$[\text{Rh}(2,2'\text{-bipyridyl})(\text{I})(\text{Me})(\text{PPh}_3)_2][\text{BAr}^{\text{F}}_4]$	116	208
<b>80</b>	$[\text{Rh}(2,2'\text{-bipyridyl})(\text{H})_2(\text{PPh}_3)(\text{PCy}_3)][\text{BAr}^{\text{F}}_4]$	118	213
<b>81</b>	$[\text{Rh}(2,2'\text{-bipyridyl})(\text{H})_2(\text{PCy}_3)_2][\text{BAr}^{\text{F}}_4]$	118	213
<b>82</b>	$[\text{Ir}(\text{cod})(\text{RcQ}_3\text{PNMe}_2)\text{Cl}]$	125	-
<b>83</b>	$\text{RcH}_8$	126	215
<b>84</b>	$\text{RcQ}_4$	126	216
<b>85</b>	$\text{RcQ}_3\text{H}_2$	126	216
<b>86</b>	$\text{RcQ}_3\text{PNMe}_2$	126	217
<b>87</b>	$\text{RcQ}_3\text{PCl}$	126	218
<b>88</b>	$\text{RcPOP}$	126	219
<b>89</b>	$[\text{Rh}(\text{cod})(\text{RcPOP})][\text{Al}(\text{OR}^{\text{F}})_4]$	128	221
<b>90</b>	$[\text{Rh}(\text{cod})(\text{RcPOP})][\text{BAr}^{\text{F}}_4]$	128	223
<b>91</b>	$[\text{Rh}(\text{cod})(\text{RcPOP})][\text{CB}_{11}\text{I}_6\text{Me}_5]$	128	224
<b>92</b>	$[\text{Rh}(\text{cod})(\text{RcPOP})][\text{SbF}_6]$	128	226
<b>93</b>	$[\text{Rh}(\text{nbd})(\text{RcPOP})][\text{Al}(\text{OR}^{\text{F}})_4]$	128	227
<b>94</b>	$[\text{Rh}(\text{nbd})(\text{RcPOP})][\text{BAr}^{\text{F}}_4]$	128	228
<b>95</b>	$[\text{Rh}(\text{nbd})(\text{RcPOP})][\text{CB}_{11}\text{I}_6\text{Me}_5]$	128	230
<b>96</b>	$[\text{Rh}(\text{NCMe})_2(\text{RcPOP})][\text{Al}(\text{OR}^{\text{F}})_4]$	132	231
<b>97</b>	$[\text{Rh}(1,3,5\text{-C}_6\text{H}_3\text{Me}_3)(\text{RcPOP})][\text{Al}(\text{OR}^{\text{F}})_4]$	133	232
<b>98</b>	$[\{\text{Rh}(\text{RcPOP})\}_2][\text{Al}(\text{OR}^{\text{F}})_4]_2$	135	233
<b>99</b>	$[\text{Rh}(\text{C}_6\text{H}_5\text{F})(\text{RcPOP})][\text{Al}(\text{OR}^{\text{F}})_4]$	135	234
<b>100</b>	$[\text{Rh}(1,2\text{-C}_6\text{H}_4\text{F}_2)(\text{RcPOP})][\text{Al}(\text{OR}^{\text{F}})_4]$	135	235